M. Phil. Thesis

Investigation Into the Sea Level Rise as Fallout of Climatic Change: Case Study of the Coast of Bangladesh

Submitted By

Md. Masudur Rahman

Registration No: 081

Session: 2012-2013

Under the Supervision of

Prof. Dr. Mohammad Abdur Rob

Department of Geography and Environment

University of Dhaka

Declaration

I do hereby declare that the work presented in this M. Phil. Thesis entitled **Investigation Into the Sea Level Rise as Fallout of Climatic Change: Case Study of the Coast of Bangladesh** is an original work done by me under the supervision of Dr. Mohammad Abdur Rob, Professor, Department of Geography and Environment, University of Dhaka.

No part of this Thesis has been previously submitted to any other University/College/Institution or Organization for any academic certificate/degree/diploma or qualification. The work I have presented does not breach any existing copyright law and no portion of this thesis is copied from any work done by anyone without citation.

I further undertake to assure the Department and the authority of Dhaka University against any loss or damage arising from breach of the forgoing obligations, if any.

Md. Masudur Rahman
Registration No: 081
Session: 2012-2013
Department of Geography and Environment
University of Dhaka

Supervisor's Certificate

This is to certify that an empirical M. Phil. Thesis entitled **Investigation Into the Sea Level Rise as Fallout of Climatic Change: Case Study of the Coast of Bangladesh** is done by Md. Masudur Rahman, Registration No: 081, Session: 2012-2013 in partial fulfillment of the requirements of M. Phil. Degree from the Department of Geography and Environment, University of Dhaka.

The Thesis has been prepared under my supervision and guidance and is a record of the bona fide work carried out by the author.

Dr. Mohammad Abdur Rob
Professor
Department of Geography and Environment
University of Dhaka

Acknowledgement

Firstly, I add a special note of gratitude to the almighty Allah for making me able with a view to complete this thesis successfully. Words will never be enough to express my level best acknowledgement towards my honorable supervisor Dr. Mohammad Abdur Rob, Professor, Department of Geography and Environment, University of Dhaka, for his guidance and supervision in every steps of this thesis. I will remain ever grateful to him for his help and cooperation in this research effort, along with Prof. Dr. AQM Mahbub, Prof. Dr. Hafiza Khatun and course teacher Prof. Dr. Md. Humayun Kabir whose sincere guidance as well as heartfelt advice help me acquiring knowledge in various relevant courses and in consequently, I reach at this stage and have completed my M. Phil. program fruitfully.

I especially thankful to Prof. Dr. Ashraf Mahmud Dewan in many ways from his ideas of research professionals, providing topographic map (1910s, 1940s, 1950s and 1960s) data and ArcGIS 10.3 licensed software, intensive care and guidance for the fulfillment of my M. Phil. program.

I would like to thank ICT Division, Ministry of Posts, Telecommunications and Information Technology, Government of the People's Republic of Bangladesh, providing ICT research fellowship for Master of Philosophy (M. Phil.) Degree.

I am grateful to The International Global Change Institute (IGCI), The University of Waikato, Hamilton, New Zealand, for software sponsorship (SimCLIM 2013), providing licensed software and Global and Bangladesh Spatial AR5 Dataset for future climate change projections of my M. Phil. research.

I never fail to recall talented individuals including my friends, seniors, juniors and well-wisher.

A note of my gratefulness must be extended to all the office stuffs of the Department of Geography and Environment, University of Dhaka, for their cooperation in order to complete my M. Phil. session.

Above all, I am likewise in the debt of my beloved family members for their inspiration towards me to continue my study still now. My sincere thanks and gratitude are due to my beloved father Md. Abdul Karim and Mother Mrs. Nurzahan Begum for their affectionate encouragements and *doa* for my success in this pursuit of academic endeavor.

Any demerits and deficiencies remaining in this thesis must be attributed solely for me.

This thesis is dedicated to my parents who have given me their unstinting supports in every steps of this academic effort

Abstract

Several thousands of years have so far been elapsed since its emergence as an alluvial land, the today's land of Bangladesh exhibits the experiences almost all the natural calamities, hazards and disasters in its geographical perspectives. Magnitudes of occurrences of the natural disasters have always been inversed and exemplified now a days due to the immense multiplications of the human population in a comparatively smaller area. Needless to say, that the pressure of ever-increasing population in Bangladesh has exerted innumerable adverse effects on the natural settings of the region and often worsening the situation appearing as some complex and intricate anthropogenic hazards and disasters in Bangladesh. To evaluate regional and local climate settings and its trend is a complicated task and should give due consideration to the consistency, homogeneity and continuity of data, unequal length of available data, outliers and extreme values in available records and appropriate statistical and mapping tools. Most of the CMIP5 and earth system model simulations for AR5 WRI were performed with prescribed CO_2 concentrations reaching 421 ppm (RCP2.6), 538 ppm (RCP4.5), 670 ppm (RCP6.0) and 936 ppm (RCP 8.5) by the year 2100. In this research I found RCP4.5 a strong correlation regression $R^2 = 0.917$ with temperature and sea level rise in Bangladesh among RCPs. Annual average mean, maximum (mean) and minimum (mean) temperature found increasing trend during 1948-2016 is 0.82 ^{0}C, 0.96 ^{0}C and 1.41 ^{0}C per century whereas in the period of 1987-2016 is 0.85 ^{0}C, 2.38 ^{0}C and 1.24 ^{0}C per century respectively; but in seasonal, period of 1948-2016 is increasing trend and period of 1987-2016 increasing and decreasing both trends are present. During 1948-2016 SNHT showed that out of 35 stations, there are 22, 21 and 19 common stations in annual average mean, maximum (mean) and minimum (mean) temperature increasing trend respectively with high significant. Decadal variation of pre-monsoon, monsoon, post-monsoon and winter rainfall showed that increasing trends are 52.32 mm, 210.02 mm, 26.06 mm and 4.13 mm per climatic period respectively. The annual seasonal increasing trend in the pre-monsoon, monsoon, post-monsoon and winter were found 5.21 mm, 20.93 mm, 2.61 mm and 0.39 mm/yr respectively, at the same time most of the monthly normal rainfall having the same trends. A SimCLIM simulation based on baseline 1995 temperature that, the global temperature showed the lowest and height temperature are -44.52 ^{0}C and 30.27 ^{0}C. In Bangladesh average mean, maximum (mean) and minimum (mean) temperature from baseline varied 19.00 ^{0}C-29.10 ^{0}C, 25.80 ^{0}C-34.40 ^{0}C and 12.20 ^{0}C-26.20 ^{0}C respectively and precipitation is 7.00 mm - 381.00 mm. Annual average mean, maximum (mean) and minimum (mean) temperature for observed and model projected values are 25.90 ^{0}C (baseline), 26.58 ^{0}C,

27.20 ^{0}C, 27.81 ^{0}C and 28.46 ^{0}C; 30.67 ^{0}C (baseline), 31.33 ^{0}C, 31.93 ^{0}C, 32.55 ^{0}C and 33.16 ^{0}C; 21.18 ^{0}C (baseline), 21.88 ^{0}C, 22.53 ^{0}C, 23.22 ^{0}C and 23.92 ^{0}C respectively by the year of baseline, 2025, 2050, 2075 and 2100. In this research I found overall mainland shoreline and island shoreline net loss/gain are -14.79 km and 579.20 km respectively. Island shoreline (positive value) bigger than mainland shoreline (negative value). 1910s-2015 mainland and island area in total net gain 1178.55 km^2 and 288.75 km^2 respectively. Overall Bangladesh coastal zone obtain 1467.30 km^2 area in this 105 year. In this research I also found the average sea level rise rate in Bangladesh is 2.72 mm/yr whereas global average 5.87 mm/yr which is about two times more than Bangladesh average. Khepupara is the height increasing rate by 13.32 mm/yr and Sonapur is the lowest decreasing rate by -11.59 mm/yr. Three regions, Eastern rate is 2.80 mm/yr, Central rate is -1.04 mm/yr and Western rate is 6.39 mm/yr. Eastern and Western region is higher rate than Central region where Central region is negative in trend. Except Teknaf, the trend in Bangladesh average, only 1.63 mm/yr, this rate is very little compare to the global average. In this study the rise in Global Mean Sea Level for the period of 2025-2100, based on process-based models is likely to be in the range 10.33-53.33 cm for RCP 4.5, 10.00-55.33 cm for RCP 6.0 and 10.00-75.00 for RCP 8.5. If we encompass 2015 is the base year and its trend go through the same rate then in the year of 2025 Bangladesh will be reach 27.20 mm from 2015; and 2050, 2075 and 2100 will be 95.20 mm, 163.20 mm and 231.20 mm respectively. Calculate the global rate, in the year of 2025 world will reach 63.90 mm from 2015; and 2050, 2075 and 2100 will be 223.65 mm, 383.40 mm and 543.15 mm respectively.

CONTENTS

Chapter Five

Analysis of Observed Maximum Temperature

Chapter Six

Analysis of Observed Minimum Temperature

Chapter Seven

Analysis of Observed Rainfall

Chapter Eight

Spatial Pattern of Future Climate Change Scenario

Chapter Nine

Bangladesh Coastal Dynamics and Shoreline Change Detection

Chapter Ten

Correlation with Temperature and Sea Level Rise: Future Perspectives

Chapter Eleven

Conclusion and Recommendation

List of Figures

List of Tables

List of Flowchart

Acronyms and Abbreviations

%	Percentage
^0C	Degree Celsius
AMS	American Meteorological Society
AR5	Fifth Assessment Report
BBS	Bangladesh Bauru of Statistics
BIWTA	Bangladesh Inland Water Transport Authority
BMD	Bangladesh Meteorological Department
BWDB	Bangladesh Water Development Board
Char	Island (Local Name)
cm	centimeter
CMIP5	Coupled Model Intercomparison Project Phase 5
CO_2	Carbon Dioxide
COP	Conference of the Parties
DEM	Digital Elevation Model
DN	Digital Number
DOE	Department of Environment
DSAS	Digital Shoreline Analysis System
ECI	Confidence of End Point Rate
EPR	End Point Rate
ESM	Earth System Model
ESRI	Environmental Systems Research Institute
ETM	Enhance Thematic Mapper
FLAASH	Fast Line of Sight Atmospheric Analysis of Spectral Hyper Cubes
GBM	Ganges-Brahmaputra-Meghna
GCM	General Circulation Model
GHG	Green House Gas
GIS	Geographic Information System
GMSL	Global Mean Sea Level
GW	Global Warming
ICZMP	Integrated Coastal Zone Management Plan
IDW	Inverse Distance Weight
IPCC	Intergovernmental Panel on Climate Change
km^2	squire kilometer
LCI	Confidence Interval of Linear Regression
LMS	Least Median of Squares
LR2	R-squired of Linear Regression
LRR	Linear Regression Rate
LSE	Standard Error of Linear Regression
LWI	Land Water Index
m	meter
MK	Mann Kendall
mm	millimeter

MNDWI	Modified Normalized Difference Water Index
MOEF	Ministry of Environment and Forests
MSS	Multi Spectral Scanner
mt	metrics ton
NAPA	National Adaption Program of Action
NCA	National Climate Assessment
NDWI	Normalized Difference Water Index
NIR	Near Infrared
NSM	Net Shoreline Movement
OECD	Organization for Economic Cooperation and Development
OIF	Optimum Index Factor
OLI	Operational Land Imager
OLS	Ordinary Least Squares
ppm	parts per milli
PSMSL	Permanent Service for Mean Sea Level
RCM	Regional Climate Model
RCP	Representative Concentration Pathway
RMSE	Root Mean Square Error
RS	Remote Sensing
SAARC	South Asian Association for Regional Cooperation
SEC	Shoreline Change Envelope
SLC	Scan Line Corrector
SLR	Sea Level Rise
SMRC	SAARC Meteorological Research Centre
SNHT	Standard Normal Homogeneity Tests
SOB	Survey of Bangladesh
SRTM	Shuttle Radar Topography Mission
SST	Sea Surface Temperature
SWIR	Short Wave Infrared
TIRS	Thermal Infrared Sensor
TM	Thematic Mapper
TOA	Top of Atmosphere
UHSLC	University of Hawaii Sea Level Center
UN	United Nations
UNEP	United Nations Environment Program
UNFCCC	United Nations Framework Convention on Climate Change
USA	United States of America
USGS	United States Geological Survey
UTM	Universal Transverse Mercator
WB	World Bank
WCI	Confidence Interval of Weighted Linear Regression
WLR	Weighted Linear Regression Rate
WR2	R-squired of Linear Regression
WSE	Standard Error of Weighted Linear Regression

Chapter One
Introduction

1.1 Background

In Bangladesh, natural hazard a common phenomenon and climate change risk is a future alarming condition which very much depends on its physiographic units and global climatic settings. To assess such kind of risk must have need of credible information of climatic data variability and its trend, sometimes remote sensing data also be used to assess this. Future climatic condition and its inconsistency may obtain from General Circulation Model (GCM) and Regional Climate Model (RCM) projection. The information of existing climatic condition and its trend is resultant either from the analysis of the observed historical data or from the community perception and experience. Such kind of information on base climate and its trend when conveyed to an influential people, community people, risk analysts, policy and decision makers, and elite society can better assess the intensity of community risk and formulate better mitigation and adaptation strategies and plans. To checking the reliability of climate model projections this information can also be useful.

However, in Bangladesh long term or average information about the climatic trends is scarce and inadequate. The spatial coverage in terms of the number of stations, the parameter coverage in terms of the number of climatic variables, the temporal coverage in terms of annual, seasonal, monthly, or 15-days, etc., and the analytical soundness in terms of availability of clear records are often inadequate and not characterize for the entire country. In addition, only 35 weather stations which have 30 years or more climatic information is available at entire country and absence in community level which is at union or lower level. It is required to fulfill this information and knowledge gap in order to formulate appropriate policy and strategic measures and action plan.

To produce the regional and local climate settings and its trends is a complicated task and should give due consideration to the consistency, homogeneity and continuity of data, unequal length of available data, outliers and extreme values in available records, and appropriate statistical and mapping tools. Furthermore, all available data sets including maximum temperature, minimum temperature, rainfall, evaporation, humidity, sunshine wind speed, etc., should be analyzed. Earlier studies (Climate Change Cell, 2009) suggest that, the evaporation data of Bangladesh Water Development Board (BWDB) is not very reliable source and Bangladesh Meteorological Department (BMD) data should be considered. The analysis of the data and subsequent generation of climate and its trend maps would provide important information on geographical areas and time periods of concerns due to climate change. Climate change resulting drought and desertification, polar ice melting and permafrost, storm surge, changing Sea Surface Temperature (SST) and Sea Level Rise (SLR). This study tries to reveal why the climate change is responsible for sea level rise.

Sea level rise along the coastal area of Bangladesh is another serious issue that may increase the vulnerability to global climate change (Karim, M.F., Mimura, N., 2008). A study carried out by the meteorological research council of the South Asian Association for Regional Cooperation on relative sea level rise in the Bay of Bengal based on 22 years (1977-1998) calculated sea-level data and observed that sea levels at Hiron Point, Char Changa and Cox's Bazar have been rising by 4.0, 6.0 and 7.8 mm/yr, respectively (SMRC, 2003). Resulting, the rate of sea level rise along the coast of Bangladesh is much higher than the global rate of 1.0-2.0 mm/yr in the last century. However, local factors such as tectonic setting, sediment load and deltaic subsidence is influenced the relative sea level in the Bay of Bengal (Warrick *et al.*, 1996). Ganges-Brahmaputra delta is subsiding at a rate of 2-4mm/year (Alam, 1996). The Bangladesh country study (Agrawala *et. al.*, 2003) put the range at 30-100 cm by 2100, while IPCC projected 26-59 cm global SLR under scenario A1F1 (Meehl *et. al.*, 2007). In an earlier study, potential SLR in Bangladesh was predicted as 30-150 cm by 2050 (DOE, 1993). Based on IPCC reports and available SLR studies, the NAPA for Bangladesh recommended SLRs of 14, 32 and 88 cm for the years 2030, 2050 and 2100, respectively (MOEF, 2005).

1.2 Aim and Objectives

The relation between climate change and sea level rise is extremely involved over there. This study was undertaken to characterize the spatial and temporal changes and trends in long-term climatic conditions of Bangladesh using the measured data available with the Bangladesh Meteorological Department (BMD) all 35 weather stations. With the availability of 10 tidal level station from Bangladesh Water Development Board (BWDB), Permanent Service for Mean Sea Level (PSMSL) (website http://www.psmsl.org/data/), the University of Hawaii Sea Level Center (UHSLC) (website https://uhslc.soest.hawaii.edu/data/?rq#uh138a), Survey of Bangladesh (SOB) and Bangladesh Inland Water Transport Authority (BIWTA) data with Shuttle Radar Topography Mission (SRTM), Digital Elevation Model (DEM) satellite imagery in different locations of Bangladesh. From the British Library, Library to Texas and Survey of Bangladesh (SOB) 4 sets of historical topographic map in different sources, Landsat Satellite imagery (website https://glovis.usgs.gov), Shuttle Radar Topography Mission (SRTM) and Digital Elevation Model (DEM) satellite imagery (website https://earthexplorer.usgs.gov[1]) data were collected and generated vector data to characterize the special and temporal changes, trends and future scenario of inundation along the coast. This information will be very much useful for the assessment of community risk and serve as baseline information for calibration and validation of Regional Climate Models (RCM) and local sea level change.

1.3 Specific Objectives

1. Homogenization of long-term climatic data (BMD 1948-2016) by adjusted series and applied corrections to produce actual climate change and predict the future climate change scenario using IPCC AR5 40 GCM ensemble data by SimCLIM simulations.

2. Produce coastal shoreline from historical topographic map (1910s-1960s) and Landsat Satellite Imagery (1974-2015) to determine rate of shoreline change using DSAS and erosion/accretion using ArcGIS a Geographic Information System (GIS) and Remote Sensing (RS) techniques.

3. Examine the Sea Level Rise (SLR) rate in different locations, 1 to 5 meters sea level rise scenario and total inundated coastal area by 2025, 2050, 2075 and 2100.

1.4 Scope of Work

- Spatial and temporal changes and its trend in long-term climate of Bangladesh by the measured data available from the BMD (1948-2016). Time series analysis of Standard Normal Homogeneity Tests (SNHT) was applied by XLSTAT to interpolate adjusted series and applied corrections for all stations from beginning to present. Mann-Kendall' trend test and SNHT tests find out 95% and 90% significant level *P*-value examine whether H0-nul hypothesis and H1-aulternative hypothesis is accepted or rejected.

- To evaluate long-term climate changes and its trend in dry bulb air temperatures (maximum, minimum and mean) at different stations of the BMD data. Annual, seasonal

[1] 2011 is the baseline year for special Digital Elevation Model (DEM)

(monsoon, pre-monsoon, post-monsoon and winter) and monthly trends were assessed. Trends in annual maximum, minimum and mean temperatures were also evaluated.

- To evaluate long-term climate changes and its trend in rainfall at different stations of the BMD climatic data. Annual, seasonal (monsoon, pre-monsoon, post-monsoon and winter) and monthly trend were assessed.

- To characterize regional and all-Bangladesh changes in air temperature pattern and its trend at different temporal resolutions.

- To characterize regional and all-Bangladesh changes in rainfall patterns and its trend at different temporal resolutions.

- To develop base map of changes and trends in mean air temperatures at different temporal resolutions to identify the geographical regions where the likelihood of changes in temperatures is high and low.

- To develop base map of changes and trends in minimum air temperatures at different temporal resolutions to identify the geographical regions where the likelihood of changes in temperatures is high and low.

- To develop base map of changes and trends in maximum air temperatures at different temporal resolutions to identify the geographical regions where the likelihood of changes in temperatures is high and low.

- To develop base map of changes and trends in rainfalls at different temporal resolutions to identify the geographical regions where the likelihood of changes in rainfalls is high and low.

- Computer cartography and Geographic Information System (GIS) technology used to produce 4 sets of scanned raster to vector data (1910s-1960s) by digitizing with 1:5000 scales from the then British Survey, Survey of India and Survey of Pakistan period toposheets.

- Landsat satellite imagery (1974-2015) processed by single operator digitize for Land Water Index (LWI) in ENVI 5.1, ERDAS imagine 2015 and ArcGIS 10.5 to create standard shore line in respective temporal date.

- From the standard base line, coastal shoreline also measured.

- From the tidal gauge data, sea level rise rates were computed from BWDB, PSMSL, UHSLC, BIWTA and SOB data at Hatiya, Sonapur, Moheshkhali, Rayenda, Charchanga, Cox's Bazar, Hiron point, Khepupara, Chittagong and Teknaf stations in Bangladesh.

- Different types of tests, maps, graphs, charts were produced in ENVI 5.1, ERDAS Imagine 2015, ArcGIS 10.5, QGIS 3.0.0, Surfer 10, TerrSet, SimCLIM 3.4.0.0, SPSS Statistics 17.0, ILWIS 3.8.5, Microsoft Excel 2016, Microsoft access 2016, XLSTAT 2016 and web GIS.

Though I had an initial plan to analyze temperature and precipitation data of Bangladesh and to assess temporal and spatial change patterns in these variables by PRECIS software from Hedley Center, United Kingdom, but I could not obtain the high-resolution data, the data were much low resolution and give up the PRECIS simulation plan. Later, I obtained 1 arc second 30-meter climatic high-resolution data sponsored by IGCI, The University of Waikato, Hamilton, New Zealand, SimCLIM 2013 software and data for this research. This data verified by IPCC AR5 where 40 regional climate model(s) were accumulated in a single platform.

Local climatic data and regional climate model express how much climate change influence on local and global sea level rise. Sea level rise is not responsible for coastal erosion or accretion rather than high tide, tidal surge and tropical cyclone increase the volume of water and affect the coastal shoreline. How many people will be undergoing or migrating due to sea level rise? To know this question, a series of coastal inundation map produced to understand how far and how many areas and people will be trapped if 1 to 5 meters sea level rise and what will be the next scenario by 2025, 2050, 2075 and 2100.

1.5 Limitations of the Study

Climate change and Sea Level Rise (SLR) is a common phenomenon nowadays. Floodplain and low laying country like, Bangladesh faced different types of natural hazard; sea level rise is one of the most upcoming events. Due to polar ice melting and permafrost, rising Green House Gas (GHG) and different types of anthropogenic factors affecting climate change and sea level rise. International community and national level try to reveal this upcoming event that what will be the adverse situations. But to doing this investigation, researchers sometimes facing critical problems. In this study have some limitation which is unanticipated, but in this research sometimes avoid this situation due to lacking data, tools and techniques.

- Bangladesh long term or average information about the climatic trends is scarce and inadequate.

- The spatial coverage of stations, parameter coverage of climatic variables, temporal coverage in terms of annual, seasonal, monthly clear records and the analytical soundness are often inadequate and not characterize for the entire country.

- 35 weather stations which have 30 years or more climatic information is available at entire country and absence in community level which is at union or lower level.

- Lacking in consideration to the consistency, homogeneity and continuity of climatic data.

- Unequal length of available data, outliers and extreme values in available records, appropriate statistical and mapping tools.

- For future climate change this research only have minimum temperature, maximum temperature, mean temperature and precipitation in Regional Climate Model (RCM) but absent in Sea Level Rise which only have General Circulation Model (GCM).

- Discontinuous and inadequate data in BWDB and BIWTA of tidal gauge and sea level rise stations.

- Influencing of seasonal flood in tidal gauge and SLR data was not considered.

- An additional dynamic factor is land subsidence under natural conditions was counteracted by sedimentation from the rivers at high tide was not considered.

- Local factors such as tectonic setting, sediment load and deltaic subsidence is influenced the relative sea level was not measured.

- High resolution satellite imageries were not used in this research.

- Based on 30-meter Landsat satellite and 90-meter STRM DEM were used which have 15% uncertainty in the result. Analysis several errors happened because of the flashy quality of the image.

- Coastal inundation assuming the output result which varying in the credible data.

- Shoreline change and erosion/accretion varying different temporal date.

- Shoreline baseline and transects casting method was selected by researcher.

- Based on BBS 2011 population census the actual population affecting in the coastal inundation were not reflecting in the new era.

- On an average SRTM DEM have 2-3-meter RMSE, as a result real picture was not reflected in five sets of maps in SLR scenario in 2011, 2025, 2050,2075 and 2100.

- Mainly quantitative research is applying in this research and qualitative research gap could be influence the actual reflection of the full scenario in this study area.

Studying in an empirical research, researchers followed some rules and regulations. None of the researchers fulfill the entire result without any limitations. But to writing a thesis with this problem need a reliable source of data for output. Providing credible information and presentation of data must be follow according to the previous literature review. References and sources of information should have cleared view and state of the art.

Chapter Two
Literature Review

2.1 Climate Change

The Fifth Assessment Report (AR5) of the United Nations (UN) Intergovernmental Panel on Climate Change (IPCC) is the fifth in a series of reports was finalized in 2014. The outline of the AR5 was developed through a scoping process which involved climate change experts from all relevant disciplines and users of IPCC reports; in particular representatives from governments. AR5 relies on the Coupled Model Intercomparison Project Phase 5 (CMIP5), an international effort among the climate modeling community to coordinate climate change experiments.[2] Most of the CMIP5 and Earth System Model (ESM) simulations for AR5 WRI were performed with prescribed CO_2 concentrations reaching 421 ppm (RCP2.6), 538 ppm (RCP4.5), 670 ppm (RCP6.0) and 936 ppm (RCP 8.5) by the year 2100.[2]

From the IPCC CMIP5 simulations, predictions of the future climate of Bangladesh are available based on regional climate models (RCM), atmospheric and coupled atmospheric-oceanic general circulation models (GCM). Both the resolution and the accuracy of these models are improving; however, there are a number of uncertainties in predicted climates, especially in regional climates for its low regulation where it is perfect for high regulation. There are large differences among inter-model forecasts. To overcome the uncertainties as well as to apprehend the magnitude and direction of future changes, it is necessary to evaluate the spatial and temporal changes that have already occurred in our past climate of Bangladesh.

However, relatively few studies have been done in this respect though a vast body of literature is available on future climates from model predictions. Ahmed *et al.*, (1992) studied the trends in annual rainfalls of Bangladesh. They concluded that there was no significant trend in the annual rainfall over the country. Ahmad *et. al.,* (1996) reported an increase of 0.5 ^{0}C in temperature over Bangladesh during past 100 years. Rahman *et. al.,* (1997) studied the long-term monsoonal rainfall pattern at 12 stations of Bangladesh. Though they found no overall trend in seasonal total rainfall, they detected some trends in monthly rainfalls of the two highly urbanized stations (Dhaka and Chittagong). Mondal and Wasimi (2004), analyzed the

[2] "CMIP5 Coupled Model Intercomparison Project". WCRP World Climate Research Program. (IPCC AR5 WGI, page 22).

temperatures and rainfalls of the Ganges Delta within Bangladesh and found an increasing trend of 0.5 ^{0}C and 1.1 ^{0}C per century in day-time maximum and night-time minimum temperatures, respectively. They also analyzed seasonal rainfalls of the delta. Though their results show increasing trends in winter, pre-monsoon and summer rainfalls, there is no appreciable overall trend in critical period rainfall. Based on regional trends in temperatures and rainfalls, they concluded that the water scarcity in the dry season might increase and the critical period could become more critical in future. SAARC Meteorological Research Centre (SMRC, 2003) studied surface climatological data on monthly and annual mean maximum and minimum temperatures, and monthly and annual rainfalls for the period of 1961-1990. The study shows an increasing trend of mean maximum and minimum temperatures in some seasons and decreasing trend in some others.

Overall, the trend of the annual mean maximum temperature has shown a significant increase over the period of 1961-1990. Rahman and Alam (2003), found that the temperature is generally increasing in the June-August period. Average maximum and minimum temperatures show an increasing trend of 5 ^{0}C and 3 ^{0}C per century, respectively. On the other hand, average maximum and minimum temperatures of December-February period show, respectively, a decreasing and an increasing trend of 0.1 ^{0}C and 1.6 ^{0}C per century. Regional variations have also been observed around the average trend (SMRC, 2003). In a recent study, Climate Change Cell (2009) has analyzed the temperature and sunshine duration at all BMD stations of Bangladesh. It has also analyzed rainfall trend at eight stations. Rainfall data at other stations could not be analyzed due to time and budgetary limitations and also, the rainfall data after the year of 2001 were not available for the study. Islam and Neelim (2010), analyzed the maximum and minimum temperatures of four months (January, April, May and December) and two seasons only. The two months of April-May were considered as the summer season and the two months of December-January as the winter season in the study. The study found in general an increasing trend in both summer and winter temperatures. The rainfall data of some selected locations were also studied by Islam and Neelim (2010).

However, they did not make any complete assessment of trend in rainfall in different time scales. Most of their analyses are on simple distribution of rainfall in a form of bar graphs. The spatial distribution of trends is not available. More importantly, the statistical significance of the trends, in either rainfall or temperature, was not reported. I have reasons to doubt whether a proper statistical technique was followed in the study.

The studies that have been done so far on long-term changes in observed climates are not comprehensive enough in spatial coverage, temporal resolution and number of variables. In most studies, appropriate statistical techniques and tools were not used. None of these studies provides collective information for the country as a whole at a glance. The only exception could be the study by the Climate Change Cell (2009) on temperature and sunshine.

In this study I include four climatic variables, recent climatic data and IPCC CMIP5 RCP data simulations. It will generate baseline maps of local climatic trends and evaluate the impacts of climate. According to Ahmed, (2005a & b) water resources and associated sectors compound the vulnerability of vast masses of the country's poor by significantly affecting their lives and livelihoods. Ahmed, (2005a & b) also reported the population of the country has been coping with extreme water-related events since ages. Bangladesh is already highly prone to water-related extreme events where Sea Level Rise is one of them. Brammer, H. *et.al,* (1996) presents possible impacts of global warming and sea-level rise on Bangladesh's water, agricultural, forestry, fisheries and livestock resources. In earlier Brammer, H., (1989) a rise in sea-level would raise low-flow and flood-season river levels in the southern half of Bangladesh. He also reported that the effects which slowly-rising sea and river levels might have on adjoining land areas are difficult to predict precisely. The most serious effects probably would not occur in coastal areas where sedimentation from tidal flooding would continue to build up land levels. Interior floodplain regions which do not receive regular deposits consequences for agricultural production. Monitoring of such changes would be very difficult.

2.2 Sea Level Rise

The Bangladesh delta is dynamic not static, considerable hydrological, geomorphological, infrastructural and land use changes would be expected to occur, in the next 50 years, irrespective of any change in sea-level. Additionally, the considerable regional diversity and local complexity of the physical and agricultural environments imply that a rising sea-level might produce different effects in different areas. Consequently, several impact monitoring sites might be needed.

The projected worldwide rise of sea level during the next 100 years will be particularly hard-felt in deltaic areas where substantial areas are barely above sea level studied by Broadus *et. al.* (1986). Regional subsidence will increase the relative rate of sea level rise; and damming of large rivers could prevent sediment influx from compensating for regional subsidence, increasing coastal erosion. These effects will be felt most in developing countries, where the rivers are large, deltas extensive and inhabited, and proposed damming of large rivers may dramatically increase coastal erosion. To help understand the potential consequences of sea level rise in the deltaic regions of the world, this study concentrated on the delta of the complex Ganges-Brahmaputra-Meghna River system in Bangladesh, in which river damming has begun and is expected to increase during the next 15 years. Erosion and deposition statistics of the Ganges indicate that 57 km^2 of land was lost along the right bank whereas around 59 km^2 has been gained along the left bank during the assessment period studied by Dewan *et.al.,* (2017a).

Sea level rise along the coastal area of Bangladesh is a serious issue that may increase the vulnerability to global climate change (Karim, M.F., Mimura, N., 2008). A study carried out by the meteorological research council of the South Asian Association for Regional Cooperation on relative sea level rise in the Bay of Bengal based on 22 years (1977-1998) calculated sea-level data and observed that sea levels at Hiron Point, Char Changa and Cox's Bazar have been rising by 4.0, 6.0 and 7.8 mm/year, respectively (SMRC, 2003). Resulting, the rate of sea level rise along the coast of Bangladesh is much higher than the global rate of 1.0-2.0 mm/year in the last century.

However, local factors such as tectonic setting, sediment load and deltaic subsidence is influenced the relative sea level in the Bay of Bengal (Warrick *et al.,* 1996). Ganges-Brahmaputra delta is subsiding at a rate of 2-4 mm/year (Alam, 1996). The Bangladesh country study (Agrawala *et. al.*, 2003) put the range at 30-100 cm by 2100, while IPCC projected 26-59 cm global SLR under scenario A1F1 (Meehl *et. al.*, 2007). In an earlier study, potential SLR in Bangladesh was predicted as 30-150 cm by 2050 (DOE, 1993). Based on IPCC reports and available SLR studies, the NAPA for Bangladesh recommended SLRs of 14, 32 and 88 cm for the years 2030, 2050 and 2100, respectively (MOEF, 2005).

Vulnerability assessment of coastal regions includes two major areas: the first considers physical variables to evaluate the locational vulnerability of a particular coast (Gornitz, 1990; Gornitz *et al.*, 1994; Shaw et al., 1998; Thieler and Hammar-Klose, 1999; Pendleton *et. al.,* 2004; Doukakis, 2005; Hegde and Reju, 2007; Nageswara Rao *et. al*., 2008; Yin *et. al*., 2012; Kumar and Kunte, 2012; Bagdanaviciute *et. al*., 2015) whereas the second one includes socioeconomic variables such as population density together with physical parameters to estimate socioeconomic vulnerability of a particular coast (Boruff *et. al.*, 2005; Szlafsztein and

Sterr, 2007; Devoy, 2008; Murali *et. al.*, 2013; Kunte *et. al.*, 2014; Mahapatra *et. al.*, 2015). However, because of regular variableness and lack of authentic data regarding dwellers and more or less analogous economic conditions, particularly in a data scarce country like Bangladesh, this paper puts particular emphasis on the calculation of physical vulnerability of the Bangladesh coast. A number of techniques have been used to study coastal erosion and accretion, sea shore line change detection and so forth. The major intention of these works is to generate information on the impacts of sea level rise, climate change and non-climatic drivers on a coastline that may be of significant value for community members, coastal managers and other stakeholders for informed decision making.

2.3 Shoreline Change Detection

Shorelines subjected to erosion are considered as high vulnerability (Islam, M. A. *et. al.,* 2016) whereas shorelines prone to accretion are considered to be less vulnerable. They examined Linear Regression Rate (LRR) along 1047 transects, covering the entire study area, to assess vulnerable shorelines where it is estimated that 774 transects are retreated through erosion whilst 273 transects experienced accretion (Islam, M. A. *et. al.,* 2016) where the maximum erosion is 96.9 m/y and the minimum erosion rate is 0.04 m/y, in case of accretion, the maximum rate was 69.54 m/y as opposed to 0.01 m/y minimum accretion. In general, the whole shoreline is dominated by erosion but the rate of erosion is < 15 m/y for a good number of transects (more than 550 among 1047 transects) (Islam, M. A. *et. al.,* 2016) spatially, maximum erosion was observed in the southern tip of Patharghata with an erosion rate ~97 m/y whereas accretion is dominant along the coast near Nilkomal, north west of Dublar Char, near Kochikhali, east coast of Patharghata, west coast of Barabagi, east coast of Kuakata, east coast of Rangabali and south-east coast of Bhola off-shore island.

Shorelines, being dynamic in nature, are always subject to change temporally as well as spatially due to various coastal processes (Carter, 1988; Bird, 1993; Kumar *et. al*., 2010a). Statistics pertaining to shoreline change gives a better understanding and measure of direct response to sea level rise (Nageswara Rao *et. al.*, 2008; Yin *et. al*., 2012). To assess hazard vulnerability of the shoreline, coastal scientists, engineers and others, involved in coastal zone planning, often include shoreline changes as part of their common measurement and planning process (Savage and Foster, 1989). However, it is the single physical parameter directly discerned in the field; hence a clear insight of vulnerability is possible to map for a particular shoreline. Linear regression rate (LRR) was taken along the transects, covering the entire study area, to assess vulnerable shorelines. It is essential to estimate that whether transects are retreated through erosion or transects experienced accretion.

2.3.1 Digital Shoreline Analysis System (DSAS)

The Digital Shoreline Analysis System (DSAS) is a freely available software application that works within the Environmental Systems Research Institute (ESRI) Geographic Information System (ArcGIS) software (Thieler *et. al*., 2009). DSAS computes rate-of-change statistics for a time series of shoreline vector data. Version 4.3 was released in April 2012 and is only compatible with ArcGIS v.10.5. It is supported on Windows XP, Vista, Windows 7, Windows 8 and Windows 10 operating systems. DSAS user guide describes the system requirements, installation procedures, and necessary inputs to establish measurement locations with transects and compute rate-of-change calculations using DSAS.

The DSAS software was developed in the early 1990s. Updates have focused on improving the rate-of-change statistics as well as the user interface and are designed to be compatible with the current version of ESRI ArcView software. Although the nomenclature for this software utility is based on use in a coastal environment, the DSAS application is also useful for computing rates of change for any boundary-change problem that incorporates a clearly-identified feature position at discrete times, such as glacier limits, river banks, or land use/cover boundaries. A sample dataset for DSAS 4.3 is available for download on the DSAS.[3]

The calculated rates of change provided by DSAS are only as reliable as the shoreline data. To better quantify the statistical reliability of the computed rates, users must account for measurement and sampling errors when compiling each shoreline position (Anders and Byrnes, 1991; Crowell *et. al*., 1991; Thieler and Danforth 1994; and Moore 2000). Users have the option of specifying for each shoreline an overall uncertainty value, which should account for both positional and measurement uncertainties. Refer to (Morton *et. al*., 2004; Morton and Miller, 2005; Hapke *et. al*., 2006; and Hapke and Reid, 2007) for examples of how to calculate an overall shoreline uncertainty.

The shoreline uncertainty will be incorporated into the calculations for the standard error, correlation coefficient, and confidence intervals, which are provided for the simple and

[3] http://pubs.usgs.gov/of/2008/1278/

weighted linear regression methods. For any shoreline vectors assigned a value of zero or null, DSAS will use the value specified by the user in the Set Default parameters window.

2.4 Land subsidence

Subsidence is the motion of a surface (usually, the earth's surface) as it shifts downward relative to a datum such as sea level, the opposite of subsidence is uplift, which results in an increase in elevation (Wikipedia, 2018).[4] Land subsidence occurred in natural conditions responsible for sedimentation from the river at high tide. The construction of embankments cut off this natural sediment accretion within polders (Brammer, 2014). Few studies have been made to-date to measure actual subsidence rates or determine its causes and the situation is complicated by the breaching of embankments in some areas for shrimp farming and by storm surges which periodically enable new (but probably irregular) sedimentation on the land (Brammer, 2014). Using high resolution satellite altimetric data unsupported by ground truthing Syvitski *et. al.,* (2009) included the Ganges delta with a stated rate of 18 mm/yr among 33 ‘sinking deltas’ world-wide, grouping it with deltas experiencing large subsidence rates attributed to human activities such as embankment construction and water or gas abstraction. The Ganges delta also includes the Ganges River Floodplain, not just the tidal floodplain assumed by Brammer (2014), there is no field evidence that either of this region is subsiding at such a very high rate and subsidence rates are not uniform within the area as implied by the single figure of 18 mm/yr. Measurements of plinth levels of a 15th century mosque at Bagerhat in the north of the tidal floodplain, a 400- year-old Hindu temple in the Sundarbans forest in the south and a 200-year-old temple 25 km north-east of Khepupara in the south-east show that long-term subsidence rates in those areas have not exceeded 1-2.5 mm/yr (Sarker *et. al.,* 2012). If subsidence had occurred at the 18 mm/yr rate given by Syvitski *et. al.,* (2009), these buildings would now be 2.4-7.6 m below sea-level. Calculation of depths to radio-carbon-dated organic materials in this region (mainly in the Sundarbans mangrove forest where embankments have not interfered with sedimentation) show subsidence rates of 1.3-7.1 mm/yr (Table 10.9), from which probably 1.3 mm/yr can be subtracted for global sea-level rise, dating of exposed 300-year-old salt kilns on the coast in the east of the Sundarbans about 35 km west of Kuakata suggests subsidence rates in that area of 5.2 ± 1.1 mm/yr (Hanebuth *et. al.,* 2013). Therefore, the balance of available evidence suggests that most of the region is currently subsiding at less than 2 mm/yr except near the coast where rates may be up to 6 mm/yr.

---

[4] https://en.wikipedia.org/wiki/Subsidence

Chapter Three
Methodology

3.1 Methodological Approach

In my research I have followed both qualitative and quantitate methods and incorporated with interpretive case study approach. This methodological approach essentially aims to understand the subjective and changing human experience (Fitzgerald, 2012). The assessment of these understandings acknowledges in advance that there is a level of subjectivity inherent in the interpretation and in making meaning from the data (Fitzgerald, 2012). This study was quantitative in nature and generally associated with positivist paradigm. This study involves a set of collection of data which is converting into numerical forms and produced different statistical test and calculation.

3.2 Quantitative Research

In quantitative research, researchers taken one or more hypothesis. The researchers try to address the predictions about possible relationships between what they want or investigate. The researchers also used different types instrument (e.g. old maps, software, device, tests, check lists etc.) and define what they want. Researchers collect data in different source and produce various types of statistical analysis.

Researchers nowadays, used sophisticated software package to drawn different types of graphs, charts, maps and data table. They want to find what relationship between two or more variables. Computer based statistical analysis results complex causal relationship which is determine how one variable influence on another. The researchers find out the end result carried out a *P* value. *P* value is the output of a probability that results a particular finding. The *P* value is a scale between 0 and 1 (Alzheimer Europe, 2009). Closer result of 0 less important for an observation and 1 is higher likelihood for observation that find out a standard result. Since this calculation or result is not too much familiar for general people that’s why researchers explain the whole process about the result in the result section and how this result will be implemented properly in a society. When researcher need a future scenario or forecast about a variable, quantitative research is more useful than qualitative research. Though statistical analysis doesn’t meet 100% accurate but it provides height probability about the result.

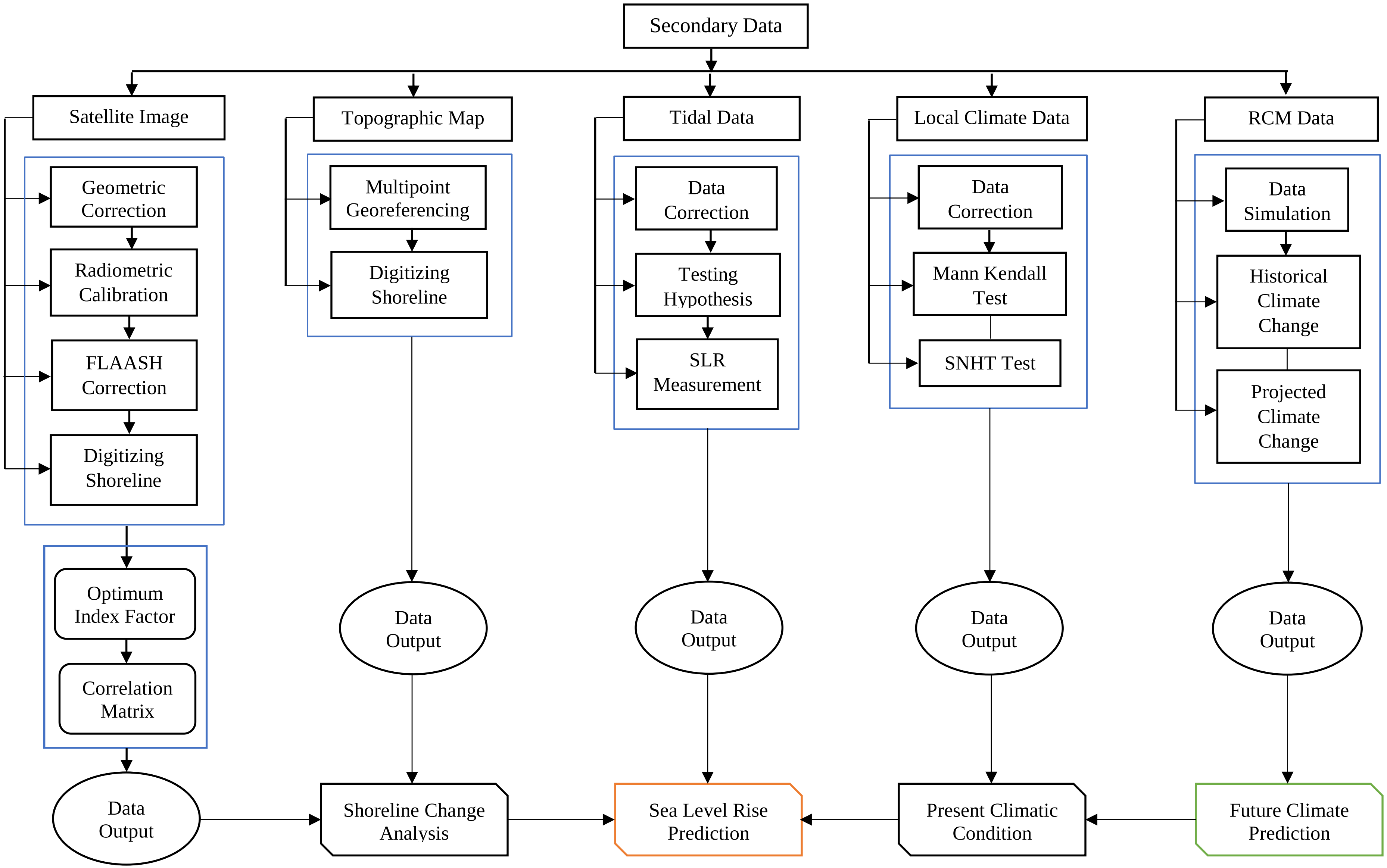

Flowchart 3.1: Basic flowchart of the total process of this research indicating the direction of the sea level rise (SLR) result

3.3 Linear Trend Analysis

The trend of temporal change can be linear or non-linear and monotonic or non-monotonic. Linear monotonic change is expressed by the following form:

$$y = a + bt + \varepsilon$$

where, y is the dependent variable such as temperature and rainfall; t is the independent variable which is time (year) in this case; ε is the random variation (noise) in the dependent variable; (a and b) are, respectively, the intercept and slope of the linear trend line. The estimate of b is the change in the variable per unit time and is the linear trend.

The two parameters (a and b) can be estimated by the parametric or non-parametric method. Parametric method is commonly used and is robust in case of normally distributed residuals (noise) and in absence of outliers and extremes in the data set. Otherwise, a non-parametric method becomes more suitable. In parametric method, the parameters are estimated by an ordinary least-squares regression (OLS) technique. It is required in such estimation that the residuals be normally, independently and identically distributed. It is to be noted that the above requirements are for the residuals, and no assumptions are made concerning the distribution of either the explanatory or the response variable.

The trends in different climatic and hydrologic variables, reported in IPCC (2007), are mostly based on this method. In non-parametric method, the parameters are estimated by comparing each data pair to all others in a pair-wise fashion. The fitted line passes through the median point. It has been found that when the departures from the true linear relationship (true residuals) are normally distributed, OLS is more efficient than the non-parametric line. However, when residuals depart from normality (are skewed or prone to outliers and extremes), then the non-parametric trend is more efficient than the OLS trend. Thus, the appropriateness of a technique depends on the given set of data to be analyzed.

For testing the statistical significance of trend, the most commonly used statistic in parametric method is Pearson's r. Pearson's r measures the linear monotonic association between two variables and most widely used. Kendall's τ and Spearman's ρ are usually used to measure both linear and non-linear monotonic associations between two variables. Both τ and ρ are rank-based procedures-the latter being dependent on the actual magnitudes of the two variables, while the former being not dependent on them. The values of these three correlation coefficients indicate the presence or absence of the trend and its direction (I = increasing or D

= decreasing). However, the coefficient in itself does not indicate whether the trend is statistically significant or not at a given confidence level. For that purpose, a t -test for Pearson's r and a z -test for Kendall's τ can be used (Helsel and Hirsch, 2002). Bhattacharyya and Johnson (1977), present the exact and large sample approximation versions of the significance testing for Spearman's ρ. By this way, one can know whether there is any significant increasing or decreasing trend in a data set.

In this study, the temporal trend in a variable at a place is estimated using a parametric technique. Climatic data of Bangladesh (Climate Change Cell, 2009a; Mondal and Wasimi, 2004; Mondal *et. al.*, 2009; Nasrin and Mondal, 2011; Zaman and Mondal, 2011) testing both the methods in a number of cases and in this study indicated that there would not be any significant gain in using a nonparametric technique.

The study made use of the BMD data on temperature rainfall (1948-2015) incorporated all the available stations of this organization. The stations for which data are reliable were identified by checking the length of available periods of records, continuity and consistency of data. Continuity and consistency of data was checked by calculating of available records within the period of records (for detail added in appendix). The homogeneity of measuring stations was checked by standard procedure and the missing data were filled in based on the available data according to Standard Normal Homogeneity Test (SNHT).

3.4 Spatial Trend Analysis

The main purpose of this study was to generate information about the change of climate at local level. As mentioned in the preceding section, temporal trends were generated for each meteorological station using time series data. To obtain spatial distribution of such trends, the value of such trend for each station was plotted in a point shape map. An interpolation surface was generated using the interpolation techniques.

Inverse Distance Weight (IDW), Thin Plate Spline and Kriging are the three commonly used interpolation techniques for the geo-spatial data. Kriging (Van Beers and Kleijnen, 2004) is the geostatistical interpolation technique which has been widely used because it can provide error prediction maps. The results from each of the interpolation techniques were compared and the technique which produced the least root mean square error (RMSE) was selected.

3.5 Prediction of Future Climate

3.5.1 Pattern Scaling

Pattern scaling is based on the theory that, firstly, a simple climate model can accurately represent the global responses of a GCM, even when the response is non-linear (Raper *et. al.,* 2001), and secondly, a wide range of climatic variables represented by a GCM are a linear function of the global annual mean temperature change represented by the same GCM at different spatial and/or temporal scales (Mitchell, 2003, Whetton *et. al*., 2005). Pattern-scaling does not seem to be a very large source of error in constructing regional climate projections for extreme scenarios (Ruosteenoja, *et. al*., 2007), however, in applying pattern-scaling, two fundamental sources of error related to its underlying theory need to be addressed: (1) Nonlinearity error: the local responses of climate variables, precipitation in particular, may not be inherently linear functions of the global mean temperature change; and (2) Noise due to the internal variability of the GCM. Based on the pattern scaling theory, for a given GCM, the linear response change pattern of a climate variable to global mean temperature change represented by the GCM, should be obtained from any one of its GHG emission simulation outputs. Pattern scaling may be described as follows: for a given climate variable *V*, its anomaly ΔV^* for a particular grid, cell (*i*), month (*j*) and year or period (*y*) under a representative concentration pathway (RCP) 4.5:

$$\Delta V^*_{yij} = \Delta T_y * \Delta V_{ij} \qquad \text{------------------------} (1)$$

ΔT being the annual global mean temperature change.

The local change pattern value ($\Delta V'_{ij}$) was calculated from the GCM simulation anomaly (ΔV_{yij}) using linear least squares regression, that is, the slope of the fitted linear line.

$$\Delta V'_{ij} = \frac{\sum_{y=1}^{m} \Delta T_y \cdot \Delta V_{yij}}{\sum_{y=1}^{m} (\Delta T_y)\, 2} \qquad \text{------------------------} (2)$$

where *m* is the number of future sample periods used, from 2006-2100, 19 periods in total. The average of 5 years represents a period.

The RCP4.5 runs were used for generating the patterns for the SimCLIM 2013 default pattern dataset, regarding the compatibility with IPCC (2013), other patterns generated from other RCP runs are also available on request. The global patterns are in 0.5^0 latitude X longitude grids interpolated from GCM original resolution, using a bilinear interpolation method. Global pattern for other variable, include wind, solar radiation, relative humidity, sea surface temperature, all use the same methodology. See table 2 for the list of GCMs used in SimCLIM 2013 monthly precipitation and temperature patterns.

According to the IPCC AR5 global climate models are used to predict plausible future climate based on 40 GCM patterns are ACCESS1-0, BCC-CSM1-1, CANESM2, ACCESS1-3, BCC-CSM1-1-M, BNU-ESM, CCSM4, CESM1-BGC, CESM1-CAM5, CMCC-CM, CMCC-CMS, CNRM-CM5, CSIRO-MK3-6-0, EC-EARTH, FGOALS-G2, FGOALS-S2, GFDL-CM3, FGDL-ESM2G, FGDL-ESM2M, GISS-E2-H, GISS-E2-H-CC, GISS-E2-R, GISS-E2-R-CC, HADCM3, HADGEM2-AO, HADGEM2-CC, HADGEM2-ES, INMCM4, IPSL-CM5A-LR, IPSL-CM5A-MR, IPSL-CM5B-LR, MIROC-ESM, MIROC-ESM-CHEM, MIROC4H, MIROC5, MPI-ESM-LR, MPI-ESM-MR, MRI-CGCM3, NorESM1-M and NorESM1-ME which model were used ensemble where first three model for both global and Bangladesh rest of thirty seven only for Bangladesh in this study. Since SimCLIM always follows the IPCC (currently the Fifth Assessment Report), SimCLIM 2013 mainly focuses on the IPCC CMIP5 datasets and the baseline period generally ranges from 1986 to 2005 (centered on 1995).

In SimCLIM 2013, the most basic spatial dataset (baseline and future) is run at the global scale of 0.5^0 X 0.5^0 resolution. Higher spatial resolution study areas for other regions are generally derived from this dataset through nonlinear/linear interpolation methods. Mean, maximum and minimum temperatures for the land area are extracted from the CRU_ts3.20 (1981-2010) dataset with a spatial resolution of 0.5^0. It can check the details on (website http://badc.nerc.ac.uk/view/badc.nerc.ac.uk_ATOM_ACTIVITY_3ec0d1c6-4616-11e2-a3-00163e251233).

Mean temperature data for the ocean area were derived from NASA reanalysis data (website http://disc.sci.gsfc.nasa.gov/daac-bin/FTPSubset.pl), and the diurnal temperature range were calculated from multiple GCMs, then maximum and minimum temperatures were derived. Land precipitation: CRU_ts3.20 with a spatial resolution of 0.5^0 degrees (1981-2010). Ocean precipitation is from Xie Arkin (1981-2002), plus GPCP (2003-2010) (1.0^0).

A regional climate model (RCM) is a downscaling tool that adds fine scale (high-resolution) information to the large-scale projections of a Global Circulation Model (GCM). Regional models can resolve the GCM features down to 30-meter horizontal resolution in SimCLIM. This makes for a more accurate representation of many surface features, such as complex mountain topographies and coastlines. It also allows small islands and peninsulas to be represented realistically, whereas in a global model their size (relative to the model grid-box) would mean their climate would be that of the surrounding ocean. A Regional Climate Model, SimCLIM (Providing Regional Climates for Impact Studies), was run at the researcher simulation computer from which the primary climate prediction data were collected in different temporal date. Simulation with a regional model, such as SimCLIM, is computationally expensive and requires lateral boundary data from a GCM. It was, therefore, not possible to carry out simulations with a number of regional climate models.

I obtained 30-meter horizontal resolution data which had sponsored and has been developed by the CLIMsystems, SimCLIM 3.4.0.0 (website http://www.climsystems.com), Hamilton, New Zealand, is a physically based model which helped generate high-resolution climate change information for Bangladesh. It is a mathematical model of the atmosphere and land surface and sea level data for the ocean. It contains representations of most of the important physical processes within the climate system including mean temperature, minimum temperature, maximum temperature, rainfall and global sea level rise.

Table 3.1: Overview of representative concentration pathways (RCPs)

	Description[5]	**CO_2 Equivalent**	**SRES Equivalent**	**Publication-IA Model**
RCP8.5	Rising radiative forcing pathway leading to 8.5 W/m^2 in 2100.	1370	A1FI	Raiahi *et. al.*, 2007-MESSAGE
RCP6.0	Stabilization without overshoot pathway to 6 W/m^2 at 2100	850	B2	Fujino *et. al.*, 2006; Hijioka *et. al.*, 2007-AIM
RCP4.5	Stabilization without overshoot pathway to 4.5 W/m^2 2100	650	B1	Clark *et. al.*, 2006; Smith and Wigley, 2006; Wise *et. al.*, 2009-GCAM
RCP2.6	Peak in radiative forcing at ~ 3 W/m^2 before 2100 and decline	490	None	Van Vuuren *et. al.*, 2007; Van Vuuren *et. al.*, 2006-IMAGE

Source: Van Vuuren *et. al.*, 2011; Moss *et. al.*, 2010; Rojeli *et. al.*, 2012

[5] Approximate radiative forcing levels were defined as ±5% of the stated level in W/m2 relative to pre-industrial levels. Radiative forcing values include the net effect of all anthropogenic GHGs and other forcing agents

Above (Table 3.1) describe about 4 RCPs that the carbon dioxide concentration in different pathway changed its characteristics in 2100. This table express the CO_2 and SRES equivalent in different unit where peak in radiative forcing at ~ 3, stabilization without overshoot pathway to 4.5, stabilization without overshoot pathway to 6 and rising radiative forcing pathway leading to 8.5 by 2100.

3.6 Assessment of Shoreline Change using (DSAS) and Erosion/Accretion

3.6.1 Satellite Data and Historical Topographic Map

In this study, I used 8 sets of Landsat Satellite images in the year of 1974, 1980, 1990, 1995, 2000, 2005, 2010 and 2015 in this research (Table 3.3). All these scenes were acquired from the freely available Landsat archive of the United States Geological Survey (USGS) (https://glovis.usgs.gov). I also used 4 sets of 1: 253,440, 1: 250,000 and 1: 50,000 scales of historical topographic maps in the year of 1910s, 1940s, 1950s and 1960s (covering coastal area) (Table 3.2) acquired from the British Library (BL), Texas Library (TL) and Survey of Bangladesh (SOB). All topographic maps of (BL) and (SOB) were purchased from this two organizations. Satellite images were already georeferenced to the Universal Transverse Mercator (UTM), map projection (Zone 45N and 46N) with WGS84 datum and ellipsoid, except two scenes WRS path 147 and row 045 in 1974 scene ID LM11470451974010AAA04 and 1980 scene ID LM31470451980015AAA08 were then georeferenced manually in the same projection. Some of the images which had cloud cover 0.08% to 37.05% but in my study area fully free from cloud cover. Yet, I did atmospheric correction for haze and aerosol removal using by Fast Line-of-Sight Atmospheric Analysis of Spectral Hyper Cubes (FLAASH) tools in ENVI 5.1. The Shuttle Radar Topography Mission (SRTM) (https://glovis.usgs.gov) Digital Elevation Model (DEM) were used to generate sea level rise. The original SRTM elevations were calculated relative to the WGS84 ellipsoid and then the EGM96 geoid separation values were added to convert to heights relative to the geoid for all the released products (Hirt, C. *et. al.*, 2010).

Table 3.2: Details of the Topographic Map used in this study

Topographic Map	Date Period	Scale (Inch)	Surveyed By	Data Source
Toposheet	1910s	1:253,440	Survey of India	British Library
Toposheet	1940s	1:253,440	Survey of India	SOB
Toposheet	1950s	1:250,000	US Army	Texas Library
Toposheet	1960s	1:50,000	Survey of Pakistan	SOB

Table 3.3: Details of the Landsat Images used in this study

Spacecraft & Sensor	Acquisition Date	Data Type/ L0RP	Station	Path/ Row	Quality	Cell Size (m)	Cloud Cover (%)
Landsat-1 MSS	1) 10/01/1974	L1T/MSSX	XXX	147/044	0	60	0%
	2) 27/01/1974	L1T/MSSX	XXX	146/044	0	60	0%
	3) 10/01/1974	L1G/MSSX	XXX	147/045	0	60	0%
	4) 27/01/1974	L1T/MSSX	XXX	146/045	0	60	0%
	5) 26/01/1974	L1T/MSSX	XXX	145/046	0	60	0%
Landsat-2 MSS	6) 10/03/1975	L1T/MSSR	XXX	148/045	0	60	0%
Landsat-3 MSS	1) 15/01/1980	L1T/TMR	KHC	137/044	9	60	0%
	2) 14/01/1980	L1T/MSSR	AAA	146/044	0	60	0%
	3) 15/01/1980	L1G/MSSR	AAA	147/045	0	60	0%
	4) 14/01/1980	L1T/MSSR	AAA	146/045	0	60	0%
	5) 31/01/1980	L1T/MSSR	AAA	145/046	0	60	0%
	6) 16/01/1980	L1T/MSSR	AAA	148/045	0	60	*2%
Landsat-5 TM	1) 24/02/1990	L1T/TMR	BKT	137/044	7	30	*8%
	2) 05/03/1990	L1T/TMR	BKT	136/044	9	30	*2%
	3) 24/02/1990	L1T/TMR	BKT	137/045	7	30	*1%
	4) 05/03/1990	L1T/TMR	BKT	136/045	9	30	0%
	5) 10/02/1990	L1T/TMR	BKT	135/046	7	30	0%
Landsat-5 TM	1) 21/01/1995	L1T/TMR	ISP	137/044	7	30	0%
	2) 14/01/1995	L1T/TMR	BKT	136/044	9	30	*11%
	3) 21/01/1995	L1T/TMR	ISP	137/045	7	30	0%
	4) 14/01/1995	L1T/TMR	BKT	136/045	9	30	*5%
	5) 23/01/1995	L1T/TMR	BKT	135/046	9	30	0%
	6) 28/01/1995	L1T/TMR	ISP	138/045	7	30	0%
Landsat-5 TM	1) 19/01/2000	L1T/TMR	BKT	137/044	9	30	0%
	2) 28/01/2000	L1T/TMR	BKT	136/044	9	30	0%
	3) 19/01/2000	L1T/TMR	BKT	137/045	7	30	0%
	4) 28/01/2000	L1T/TMR	BKT	136/045	9	30	0%
	5) 21/01/2000	L1T/TMR	BKT	135/046	7	30	0%
Landsat-5 TM	1) 16/01/2005	L1T/TMR	BKT	137/044	7	30	0%
	2) 10/02/2005	L1T/TMR	BKT	136/044	7	30	0%
	3) 16/01/2005	L1T/TMR	BKT	137/045	7	30	0%
	4) 10/02/2005	L1T/TMR	BKT	136/045	7	30	0%
	5) 18/01/2005	L1T/TMR	BKT	135/046	7	30	0%
	6) 07/01/2005	L1T/TMR	BKT	138/045	7	30	0%
Landsat-5 TM	1) 30/01/2010	L1T/TMR	KHC	137/044	9	30	0%
	2) 23/01/2010	L1T/TMR	KHC	136/044	9	30	0%
	3) 30/01/2010	L1T/TMR	KHC	137/045	9	30	0%
	4) 23/01/2010	L1T/TMR	BKT	136/045	7	30	0%
	5) 16/01/2010	L1T/TMR	BKT	135/046	7	30	0%
	6) 21/01/2010	L1T/TMR	KHC	138/045	9	30	0%
Landsat-8 OLI	1) 28/01/2015	L1T	LGN	137/044	9	30	*22.64%
	2) 10/03/2015	L1T	LGN	136/044	9	30	*5.20%
	3) 28/01/2015	L1T	LGN	137/045	9	30	*3.59%
	4) 10/03/2015	L1T	LGN	136/045	9	30	*0.08%
	5) 30/01/2015	L1T	LGN	135/046	9	30	*0.31%
	6) 19/01/2015	L1T	LGN	138/045	9	30	*37.05%

Note: *Cloud cover was not present in the study area

3.7 Image Pre-Processing

Before analyzing data, it is essential to avoid different types data distortion or manipulation from pre-processing satellite image. Pre-processing is also needed to establish direct linkage between data and biophysical phenomena (Coppin *et. al.,* 2004). In my research there was no any scan-line corrector (SLC) off image from Landsat 7, that's why no description included about SLC. Atmospheric correction and topographic normalization are required to improve the classification results (Song *et. al.,* 2001 and Hale *et. al.,* 2003). Atmospheric correction primarily includes the removal of haze, which originates from fractions of water vapor, fog, dust, smoke, or other minute atmospheric particles (Makarau *et. al.,* 2014). The topographic normalization is important for mountainous areas such as KV, because the presence of slopes can cause variations in illumination of identical features (Tan *et. al.,* 2013 and Vanonckelen *et. al.,* 2013). I used Atmospheric correction (FLAASH) feature in ENVI 5.1 for haze, aerosol removal and topographic normalization. For historical topographic map I used manual georeferenced proses based on Latitude and Longitude and more precisely used physical object like benchmark and historical monument by special adjustment in ArcGIS 10.5. As my research area is a flood plain land with slight variation in topography, I used SRTM Global DEM with 90-meter spatial resolution for Sea Level Rise (SLR) analysis.

The spectral information sensed by each Landsat MSS, Landsat-4/5 TM and Landsat-7 ETM+ sensors are stored as 8-bit digital number (DN) (Markham *et. al.,* 2006) and Landsat-8 OLI sensor as 16-bit DN with 12-bit radiometric resolution (Roy *et. al.,* 2014) in the L1T and L1G products. DNs of each scene were converted to top of atmospheric (TOA) spectral radiance following equations (Eq) adopted by Chander *et. al.,* (2009) and USGS (Eq-1 for MSS/TM images, Eq-2 for OLI images) using sensor specific calibration parameters derived from the image L1T and L1G metadata file. The radiance of the reflective bands of each scene was then converted to the TOA reflectance using the standard equations (Eq-3 for MSS/TM images, Eq-4 for OLI images) formulated by Roy *et. al.,* (2010) and USGS.

$$L_\lambda = \frac{(Lmax - Lmin)}{(QCALmax - QCALmin)} * (QCAL - QCALmin) + Lmin \quad (1)$$

$$L_\lambda = M_L * QCAL + A_L \quad (2)$$

$$p_\lambda = \frac{\Pi * L_\lambda * d^2}{ESUN_\lambda * cos\theta_s} \quad (3)$$

$$p_\lambda = M_p * QCAL + A_p \quad (4)$$

In the above equations L_λ is the TOA spectral radiance (W m^{-2} sr^{-1}μm^{-1}), *QCALmax* and *QCALmin* are maximum and minimum quantized calibrated pixel values typically as 255 and 1, *QCAL* is the DN values, *Lmax* and *Lmin* are spectral radiances scaled to *QCALmax* and *QCALmin*, M_L and A_L are band specific multiplicative and additive radiance rescaling factors obtained from the image L1T and L1G metadata file, ρ_λ is the unitless TOA reflectance, *d* is the earth-sun distance in astronomical units, $ESUN_\lambda$ is the mean solar exoatmospheric irradiances (W m^{-2} μm^{-1}), $cos\theta_s$ is the solar zenith angle (radians) calculated from the solar elevation angle stored in the image L1T and L1G metadata file, ρ_λ is the TOA spectral reflectance, M_p and A_p are band specific multiplicative and additive reflectance rescaling factors obtained from the image L1T and L1G metadata file. The $ESUN_\lambda$ and *d* values were used from Chander *et al.* (2009).

After completing the image pre-processing part, "the operation calculates correlation coefficients of raster maps in a map list. Correlation coefficients characterize the distribution of pixel values in two raster maps. Analyzing satellite data, the images often show a degree of correlation. This means that when spectral values in one band are high the values in another band are expected to be high as well. Plotting values from highly correlated bands in a feature space will result in an ellipsoid denoting that the two bands contain dependent information. From a set of highly correlated bands only one adds real value whilst the other ones may be derived or estimated.

Calculating a correlation matrix helps to detect the redundancy and identifies possible reductions in the number of bands, *e.g.*, to be used in a color composite. Correlation coefficients are normalized covariance values. A correlation coefficient range from -1 to +1. Diagonal elements are always 1. A correlation close to +1 indicates a direct relationship between two bands. This suggests that if the reflectance (DN) of a pixel in one band is known, the reflectance of that pixel in the other band can be derived or estimated. A correlation close to -1 indicates an inverse relationship between the reflectance values of one band and the reflectance values in the other one"[6]. All the operation of Optimum Index Factor (OIF) and correlation matrix done by ILWIS 3.8.5 software. The following example (Table 3.4) shows a correlation matrix for 7 input bands. Bands 1 and 2 are highly correlated with a correlation coefficient of 0.999 (orange color box). Bands 2 and 6 seem independent with a correlation coefficient of 0.836

[6] http://spatial-analyst.net/ILWIS/htm/ilwisapp/correlation_matrix_functionality.htm

(green color box) where diagonal element a direct relationship between two bands indicate +1 (ash color box). Based on rank 1 (Table 3.5) band b1, b2 and b5 image then composite and digitized manually according to first second and third order.

Table 3.4: Optimum Index Factor (OIF) correlation matrix based on Landsat 8 OLI

Bands	b1	b2	b3	b4	b5	b6	b7
b1	1.000	0.999	0.994	0.985	0.845	0.839	0.899
b2	0.999	1.000	0.996	0.988	0.841	0.836	0.898
b3	0.994	0.996	1.000	0.995	0.852	0.847	0.905
b4	0.985	0.988	0.995	1.000	0.866	0.868	0.922
b5	0.845	0.841	0.852	0.866	1.000	0.964	0.944
b6	0.839	0.836	0.847	0.868	0.964	1.000	0.987
b7	0.899	0.898	0.905	0.922	0.944	0.987	1.000

Note: OIF correlation matrix generated from Landsat 8 OLI 28/01/2015 ID=LC81370452015028LGN00[7]

Table 3.5: Optimum Index Factor (OIF) highest ranking

Rank	First Order	Second Order	Third Order	Rank Value
1	b1	b2	b5	5191.45
2	b1	b3	b5	5023.80
3	b1	b5	b6	4949.41
4	b1	b2	b6	4932.01
5	b2	b3	b5	4911.54
6	b1	b4	b5	4884.64

3.8 Classification Procedure and Accuracy Assessment

There are several methods for image classification and indexing in Landsat satellite image like NDWI, MNDWI and Land Water Masking. Initial stage I used all methods and found excellent result, but my research area is a mostly flood plain land. Every year huge amount of sediment carried out by Ganges-Brahmaputra-Meghna (GBM). The basin includes one of the largest deltas of the world (Coleman 1981), the Bengal delta, and is situated at the confluence of the Ganges-Brahmaputra-Meghna (GBM) river system (the Bangladesh part of the Ganges and Brahmaputra are called the Padma and Jamuna, respectively) the world's largest sediment dispersal system (Kuehl *et. al.* 1989) encompassing its total lower drainage. It accounts for about 9.2% (Rasid and Paul 1987) of the total drainage area of the GBM system (about $1.64X10^6$ km^2; Milliman *et. al.* 1995). The GBM river system offers the passage of an estimated sediment load of more than 1060 million tons annually to the Bay of Bengal, which ranks first in sediment flux to the oceans on a global scale (Milliman *et. al.* 1995). For that reason, islands of the Bay of Bengal fluctuate every year, sometimes disappear or submerged some are newly

[7] Total 47 Landsat satellite scenes is generated for OIF index highest ranking and one real example given above

born or newly shaped. Some island looks like as mud flat and those are not characterized or recognized as an island. It is very difficult to calculate/identify vast area of shoreline or islands using different types of indexing. The basic principle of change detection through remote sensing is that the changes in spectral signatures commensurate with the change in land cover (Rahman, 2013). There are several methods such as water indices (McFeeters, 1996 and Xu, 2006) and manual digitizing at fixed zoom-in level by single operator (Dewan *et. al.,* 2017a) already established for extraction of land-water boundary from satellite images. Water indices yields the best output in respect of specific Landsat sensor. I have used 5000 scale fixed zoom-in level in ArcGIS 10.5 by myself as a single operator for extracting raster to vector data.

Table 3.6: Accuracy Assessment for 2015 (one example explains)

Land/Water Class	Land	Water	Total (User's)
Land	76	4	80
Water	3	77	80
Total (Producer's)	79	81	160

3.8.1 Overall Accuracy

$$\text{Overall Accuracy} = \frac{\text{Total Number of Correctly Classified Pixels (diagonal)}}{\text{Total Number of Referenced Pixels}} \text{ X } 100$$

$$= \frac{76 + 77}{160} \text{ X } 100$$

$$= \frac{153}{160} \text{ X } 100$$

$$= 95.63\%$$

3.8.2 User's Accuracy Land

$$\text{User's Accuracy} = \frac{\text{Number of Correctly Classified pixels in each Category}}{\text{Total Number of Classified Pixels in that Category (row total)}} \text{ X } 100$$

$$= \frac{76}{80} \text{ X } 100$$

$$= 95.00\%$$

3.8.3 User's Accuracy Water

$$\text{User's Accuracy} = \frac{\text{Number of Correctly Classified pixels in each Category}}{\text{Total Number of Classified Pixels in that Category (row total)}} \text{ X } 100$$

$$= \frac{77}{80} \text{ X } 100$$

$$= 96.25\%$$

3.8.4 Producer's Accuracy Land

$$\text{Producer's Accuracy} = \frac{\text{Number of Correctly Classified pixels in each Category}}{\text{Total Number of Classified Pixels in that Category (column total)}} \text{ X } 100$$

$$= \frac{76}{79} \text{ X } 100$$

= 96.20%

3.8.5 Producer's Accuracy Water

$$\text{Producer's Accuracy} = \frac{\text{Number of Correctly Classified pixels in each Category}}{\text{Total Number of Classified Pixels in that Category (column total)}} \text{ X } 100$$

$$= \frac{77}{81} \text{ X } 100$$

= 95.06%

3.8.6 Kappa Coefficient

$$\text{Kappa Coefficient (T)} = \frac{(\text{TS X TCS}) - \sum (\text{CT X RT})}{\text{TS}^2 - \sum (\text{CT X RT})} \text{ X } 100$$

Where,
TS = Total Sample
TCS = Total Corrected Sample (diagonal)
CT = Column Total
RT = Row Total

$$= \frac{(160 \text{ X } 153) - \{(79 \text{ X } 80) + (81 \text{ X } 80)\}}{25600 - \{(79 \text{ X } 80) + (81 \text{ X } 80)\}} \text{ X } 100$$

$$= \frac{24480 - (6320 + 6480)}{25600 - (6320 + 6480)} \text{ X } 100$$

$$= \frac{24480 - 12800}{25600 - 12800} \text{ X } 100$$

$$= \frac{11680}{12800} \text{ X } 100$$

= 0.9125 X 100

= 91.25

= 0.91%

Table 3.7a: Summary of classification accuracies (in %)*

Land Water Class	1910s		1940s		1950s		1960s		1974		1980	
	Producer's	**User's**	**Producer's**	**User's**	**Producer's**	**User's**	**Producer's**	**User's**	**Producer's**	**User's**	**Producer's**	**User's**
Land	91.14	90.00	90.36	93.75	91.36	92.50	92.50	92.50	92.59	93.75	96.10	92.50
Water	90.12	91.25	93.51	90.00	92.41	91.25	92.50	92.50	93.67	92.50	92.77	96.25
Overall Accuracy	90.63		91.88		91.88		92.50		93.13		94.38	
Kappa Coefficient	81.25		83.75		83.75		85.00		86.25		88.75	
Tau Coefficient *(Equal probability)*	0.81		0.84		0.84		0.85		0.86		0.89	
Correlation Matrix	-		-		-		-		100		100	

Note: *Table continued…...

Table 3.7b: Summary of classification accuracies (in %)

Land Water Class	1990		1995		2000		2005		2010		2015	
	Producer's	**User's**	**Producer's**	**User's**	**Producer's**	**User's**	**Producer's**	**User's**	**Producer's**	**User's**	**Producer's**	**User's**
Land	97.44	95.00	93.75	93.75	94.94	93.75	96.25	96.25	97.47	96.25	96.20	95.00
Water	95.12	97.50	93.75	93.75	93.83	95.00	96.25	96.25	96.30	97.50	95.06	96.25
Overall Accuracy	96.25		93.75		94.38		96.25		96.88		95.63	
Kappa Coefficient	92.50		87.50		88.75		92.50		93.75		91.00	
Tau Coefficient *(Equal probability)*	0.93		0.88		0.89		0.93		0.94		0.91	
Correlation Matrix	100		100		100		100		100		100	

Shoreline positions can reference several different features such as the vegetation line, the high-water line, the low-water line, or the wet/dry line. It can be digitized from a variety of sources (for example, satellite imagery, digital orthophotos, historical coastal-survey maps), collected by global-positioning-system field surveys, or extracted from lidar surveys. It is strongly recommended that initial data-preparation steps be taken to reference all shoreline vectors to the same feature (for example, mean high water) before using Digital Shoreline Analysis System (DSAS) to compute change statistics. Each shoreline vector represents a specific position in time and must be assigned a date in the shoreline feature-class attribute table. The measurement transects that are cast by DSAS from the baseline will intersect the shoreline vectors. The points of intersection provide location and time information used to calculate rates of change. The distances from the baseline to each intersection point along a transects are used to compute the selected statistics.

The calculated rates of change provided by DSAS are only as reliable as the shoreline data. To better quantify the statistical reliability of the computed rates, users must account for measurement and sampling errors when compiling each shoreline position (Anders and Byrnes, 1991; Crowell *et. al.,* 1991; Thieler and Danforth, 1994 and Moore, 2000). Users have the option of specifying for each shoreline an overall uncertainty value, which should account for both positional and measurement uncertainties. Refer to Morton *et. al.,* 2004; Morton and Miller, 2005; Hapke *et. al.,* 2006; and Hapke and Reid, 2007 for examples of how to calculate an overall shoreline uncertainty. The shoreline uncertainty will be incorporated into the calculations for the standard error, correlation coefficient, and confidence intervals, which are provided for the simple and weighted linear regression methods. For any shoreline vectors assigned a value of zero or null, DSAS will use the value specified by the user in the Set Default parameters window.

3.9 Set Casting Method

- **Simple Baseline Cast:** Each simple transect is cast at a 90^0 angle from the baseline segment at which it originates. Transects are generated at user-specified intervals along the baselines.
- **Smoothed Baseline Cast:** This option is used to orient transects along curved sections of baseline. A supplemental baseline is temporarily created to determine the orientation of the measurement transect.
- **Smoothing Distance:** The specified length of a supplemental baseline, with the transect location at the midpoint. The user-specified smoothing value creates a straighter

orthogonal reference for casting transects. Larger values result in a longer reference line and produce more uniform transect orientations. Instead of transects fanning around a curve, as in a simple cast, transects will be oriented more parallel to each other. There will be little to no difference in the orientations of transects along straight sections of baseline.

- **Flip Baseline Orientation:** DSAS creates transects sequentially along each segment of baseline (starting with baseline ID=1). Each baseline segment has a starting-point vertex and an ending-point vertex that describe the order in which the line segments were drawn. In some cases, sequential baseline segments may have been digitized in opposite directions alongshore. Transect casting order will be determined by the direction described as “start to finish” for the baseline segment with an ID=1.

Coastal morphology has gone through significant changes due to erosion and accretion (Thomas *et. al.,* 2014). The coastline morphology change can be analyzed from two aspects: the change of coastline *i.e.* shoreline length and geometry, area and the change of coastline types *i.e.* erosion-accretion (Sun, *et. al.*, 2011).

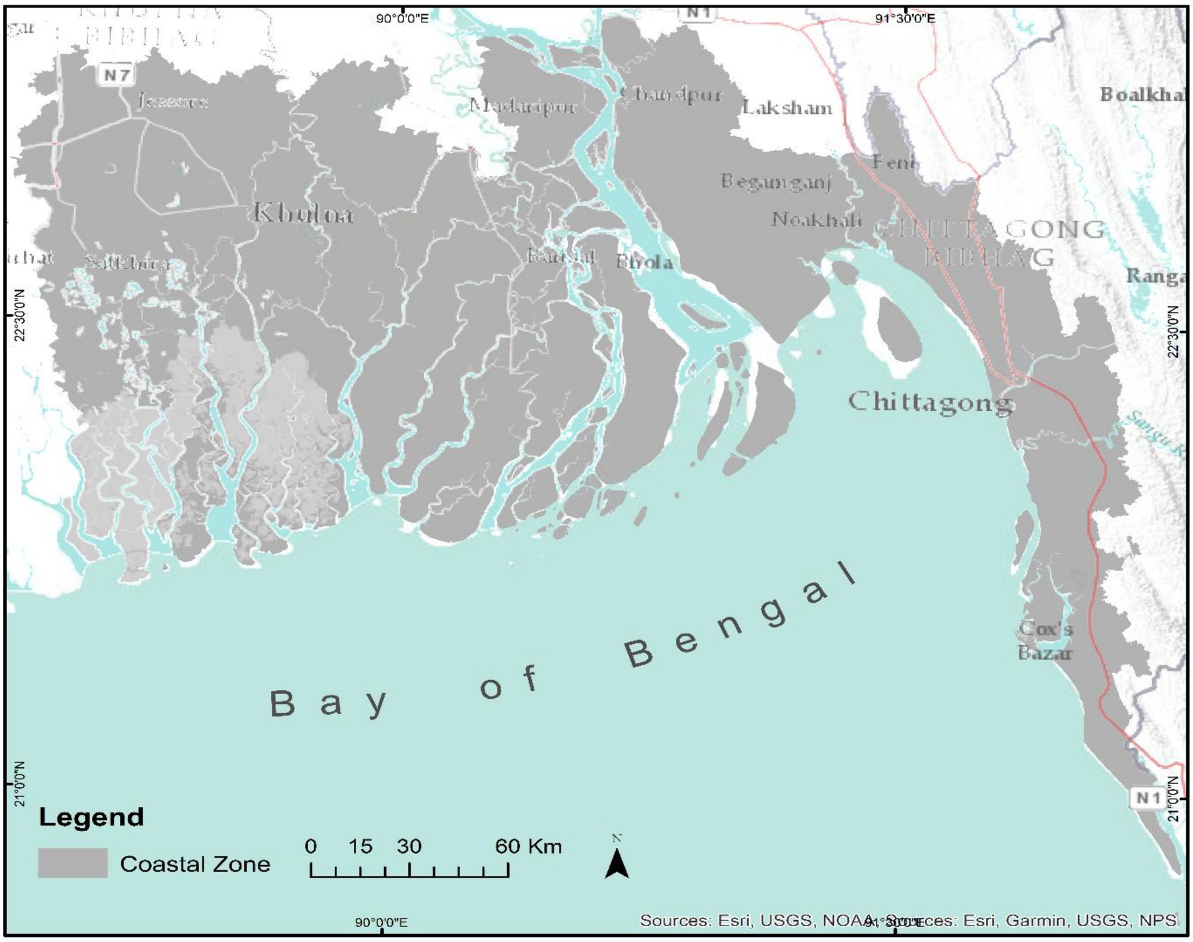

Figure 3.1: Study Area, Coastal Zone of Bangladesh

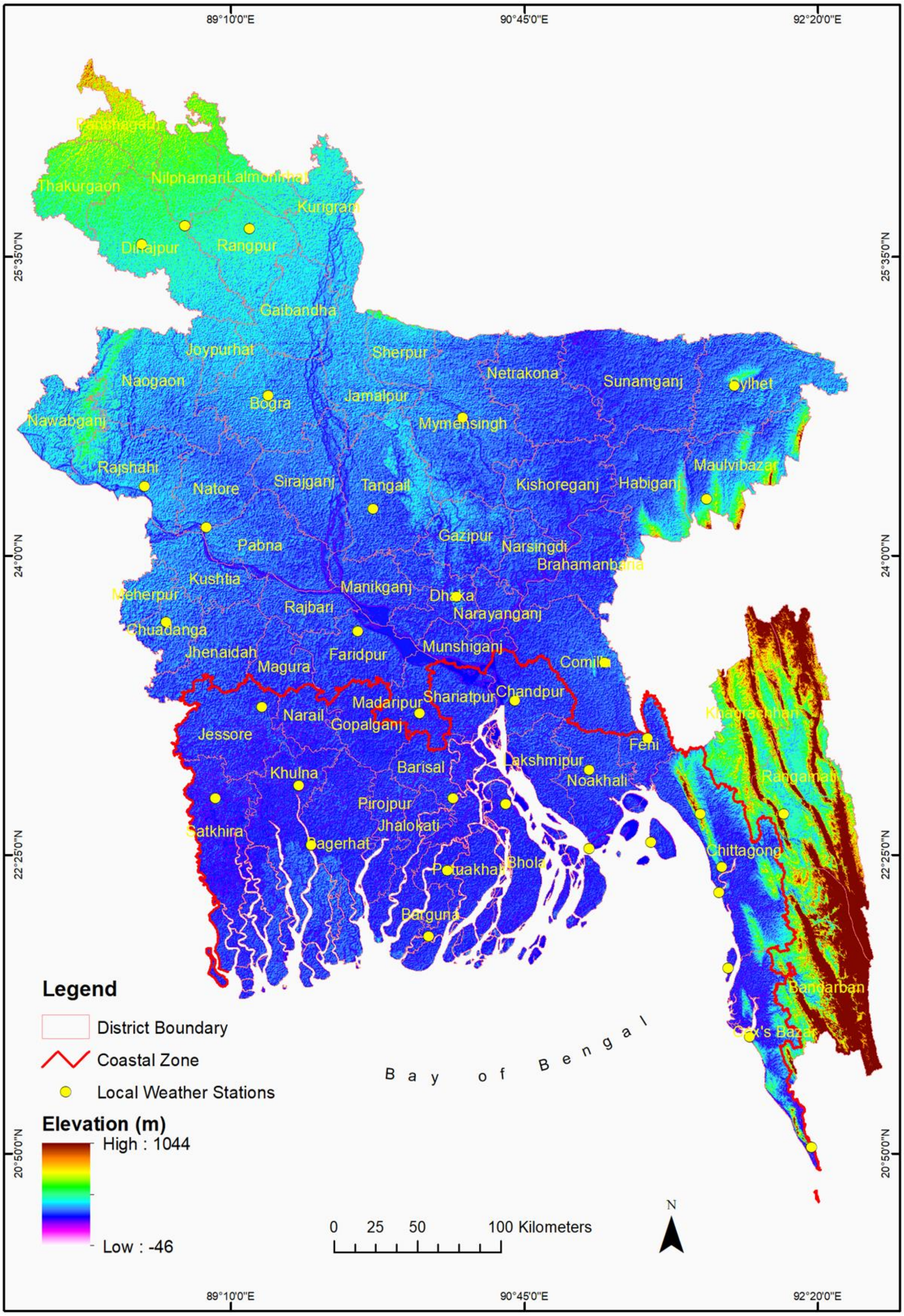

Figure 3.2: Location of the local weather stations in Bangladesh (elevation source: SRTM)

Chapter Four
Analysis of Observed Mean Temperature

4.1 Introduction

Temperature is a measure of a quality of a state of a material (Bryan, 1907). The quality may be regarded as a more abstract entity than any particular temperature scale that measures it and is called *hotness* by some writers (Pippard, 1957/1966**).** The average temperature of the dry bulb air temperature as indicated by a properly exposed thermometer during a given period, usually a day, a month, or a year. For climatological tables, the mean temperature is generally calculated for each month and for the year. For charts, the observed mean values at station level are reduced to sea level by adding a correction for elevation, usually taken as 0.5 ^{0}C for each 100 m (1^{0}F for 360 ft), but in some mountainous countries different rates are used, based on local observations[8].

4.2 Local Data Analysis

For local data daily maximum and minimum temperatures were available at 35 locations for a period of 69 years (1948-2016). From these two temperatures, mean temperatures were calculated by Bangladesh Meteorological Department (BMD). The estimated trends in mean annual temperatures for 35 stations are given in (Table 4.1). It is seen from the bellow table that almost all the stations in Bangladesh exhibit increasing trends in mean annual temperatures. In fact, 9 stations seen decreasing trend where 5 stations are not enough for negative trend (Table 4.1). In my analysis including all 35 stations suggests that the trend is 0.82 ^{0}C per century (100 years) (Table 4.3). The corresponding pre-monsoon (March-May), monsoon (June-September), post-monsoon (October-November) and winter (December-February) trends are 0.13, 1.07, 1.28 and 0.86 ^{0}C per century respectively (Table 4.3).

4.3 Time Series Analysis

Kendall's τ and Spearman's ρ used to measure linear monotonic associations between year and observed data. Both τ and ρ are rank-based procedures – the latter being dependent on the actual magnitudes of the two variables, while the former being not dependent on them. The values of these correlation coefficients indicate the presence or absence of the trend and its direction I = increasing and D = decreasing (Table 4.1). However, the coefficient does not indicate whether the trend is statistically significant or not at a given confidence level.

[8] http://glossary.ametsoc.org/wiki/Mean_temperature

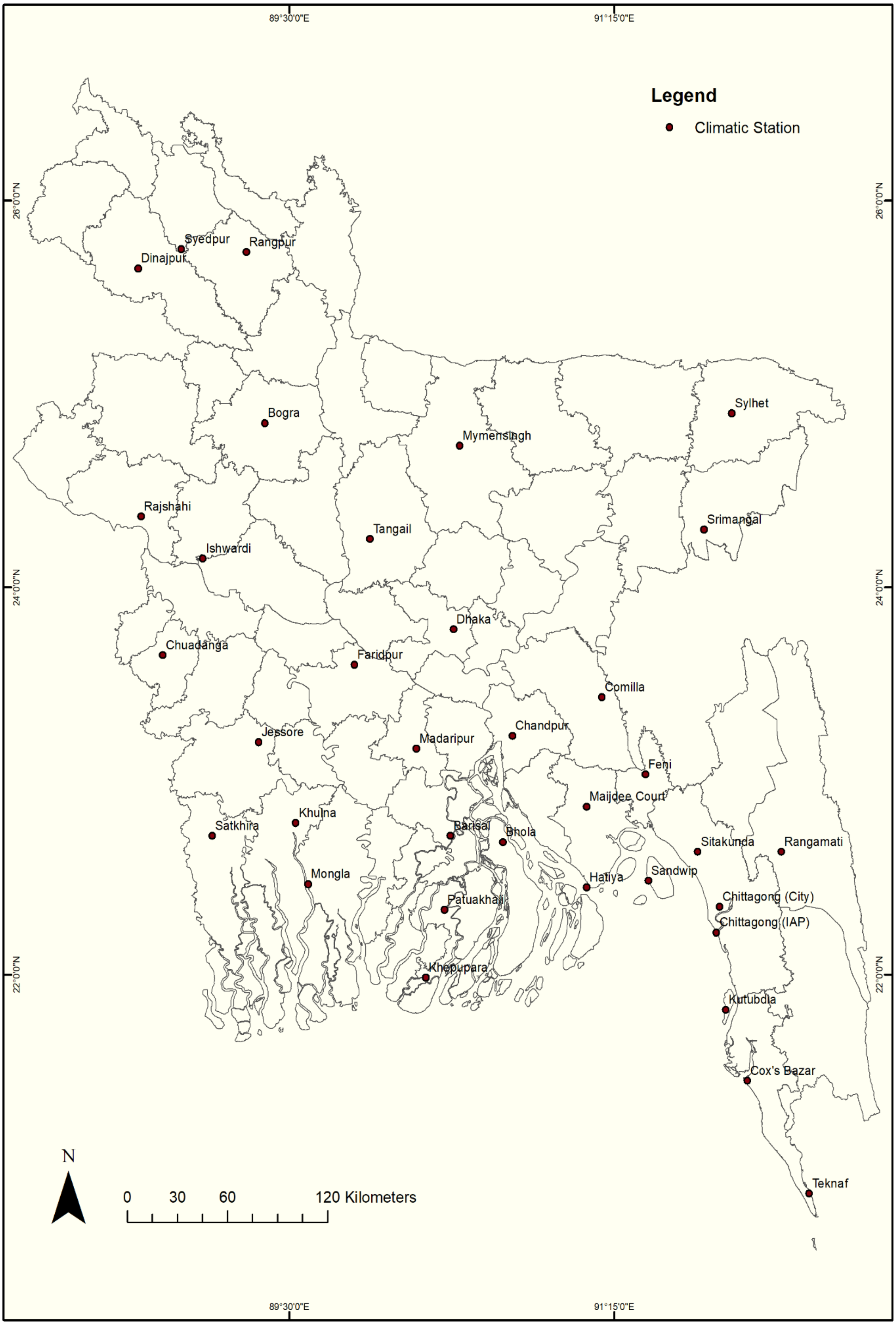

Figure 4.1: Locations of the BMD climatic stations used in the study (average temperature)

Table 4.1: Results of the Mann-Kendall test for annual mean temperature data for all-Bangladesh (1948-2016)

Stations	Available Year	Kendall's tau	S	Var(S)	*P* (Two-tailed)	alpha	Test Int.	Trend ^{0}C/100 y	Sig.
Ambagan Ctg	18	0.072	11.00	0.00	0.709	0.05	A	1.05	NS
Barisal	66	-0.035	-75.00	32651.67	0.682	0.05	A	-0.62	NS
Bhola	50	0.264	323.00	14291.67	0.007	0.05	R	0.55	**I
Bogra	65	0.148	308.00	31200.00	0.082	0.05	A	0.25	*
Chandpur	48	0.238	268.00	0.00	0.017	0.05	R	0.79	**I
Chittagong	63	0.359	701.00	28427.00	< 0.0001	0.05	R	1.07	**I
Chuadanga	18	-0.176	-27.00	0.00	0.330	0.05	R	0.08	NS
Comilla	65	0.121	252.00	31200.00	0.155	0.05	R	0.11	NS
Cox's Bazar	69	0.501	1176.00	37275.33	< 0.0001	0.05	R	1.33	**I
Dhaka	63	0.568	1109.00	28427.00	< 0.0001	0.05	R	1.72	**I
Dinajpur	61	-0.005	-10.00	25823.33	0.955	0.05	A	0.03	NS
Faridpur	69	0.414	972.00	37275.33	< 0.0001	0.05	R	1.17	**I
Feni	43	0.030	27.00	0.00	0.787	0.05	A	0.21	NS
Hatiya	49	-0.088	-104.00	0.00	0.377	0.05	A	-1.09	NS
Ishurdi	56	0.108	166.00	20020.00	0.244	0.05	A	0.32	NS
Jessore	64	0.443	894.00	29792.00	< 0.0001	0.05	R	1.19	**I
Khepupara	43	-0.276	-249.00	0.00	0.009	0.05	R	-1.32	**D
Khulna	65	0.243	506.00	31200.00	0.004	0.05	R	0.54	**I
Kutubdia	32	0.363	180.00	0.00	0.003	0.05	R	1.79	**I
M.Court	64	0.438	882.00	29792.00	< 0.0001	0.05	R	1.91	**I
Madaripur	39	-0.350	-259.00	0.00	0.002	0.05	R	-2.66	**D
Mongla	26	0.077	25.00	0.00	0.601	0.05	A	0.79	NS
Mymensingh	68	0.067	152.00	35688.67	0.424	0.05	A	0.21	NS
Patuakhali	42	-0.175	-151.00	0.00	0.104	0.05	A	-0.84	NS
Rajshahi	53	0.010	14.00	16995.33	0.921	0.05	A	-0.32	NS
Rangamati	58	0.187	309.00	22223.67	0.039	0.05	R	1.1	**I
Rangpur	58	0.383	633.00	22223.67	< 0.0001	0.05	R	1.57	**I
Sandwip	49	-0.017	-20.00	0.00	0.871	0.05	A	-0.51	NS
Satkhira	67	0.214	473.00	34147.67	0.011	0.05	R	0.95	**I
Sitakunda	40	-0.297	-232.00	0.00	0.007	0.05	R	-2.36	**D
Srimangal	68	0.442	1006.00	35688.67	< 0.0001	0.05	R	2.08	**I
Sydpur	17	0.544	74.00	0.00	0.002	0.05	R	4.26	**I
Sylhet	60	0.342	606.00	24583.33	0.00	0.05	R	0.65	**I
Tangail	30	0.246	107.00	0.00	0.058	0.05	A	0.79	*
Teknaf	39	-0.298	-221.00	0.00	0.007	0.05	R	-2.17	**D

Note: **Significant at the 95% level of confidence; *Significant at the 90% level of confidence; NS-Not Significant at the 90% level of confidence; A-Accepted at the p>0.05; R-Rejected at the p<0.05; I-Increased; D-Decreases

Table 4.2: Results of the Standard Normal Homogeneity Test (SNHT) for annual mean temperature data for all-Bangladesh (1948-2016)

Sl. No.	Stations	T0	t	*P* (Two-tailed)	alpha	Test Int.	Sig.
1	Ambagan(Ctg)	36.079	1999	< 0.0001	0.05	R	**
2	Barisal	19.997	1996	0.034	0.05	R	**
3	Bhola	58.931	1966	< 0.0001	0.05	R	**
4	Bogra	8.764	2015	0.082	0.05	A	*
5	Chandpur	26.798	1966	< 0.0001	0.05	R	**
6	Chittagong	25.182	1993	< 0.0001	0.05	R	**
7	Chuadanga	25.070	1999	< 0.0001	0.05	R	**
8	Comilla	4.445	1956	0.366	0.05	A	NS
9	Cox's Bazar	29.175	1977	< 0.0001	0.05	R	**
10	Dhaka	14.700	1984	0.051	0.05	A	*
11	Dinajpur	4.859	1981	0.355	0.05	A	NS
12	Faridpur	15.831	1971	0.040	0.05	R	**
13	Feni	40.399	1975	< 0.0001	0.05	R	**
14	Hatiya	32.811	2015	< 0.0001	0.05	R	**
15	Ishurdi	16.607	1961	0.001	0.05	R	**
16	Jessore	16.748	1971	0.001	0.05	R	**
17	Khepupara	31.320	1984	< 0.0001	0.05	R	**
18	Khulna	10.860	1963	0.054	0.05	A	*
19	Kutubdia	42.181	1985	< 0.0001	0.05	R	**
20	M.Court	24.488	1971	< 0.0001	0.05	R	**
21	Madaripur	35.643	1978	< 0.0001	0.05	R	**
22	Mongla	31.191	2015	0.016	0.05	R	**
23	Mymensingh	16.072	1963	0.006	0.05	R	**
24	Patuakhali	39.265	1983	< 0.0001	0.05	R	**
25	Rajshahi	21.481	1965	0.000	0.05	R	**
26	Rangamati	47.993	1961	< 0.0001	0.05	R	**
27	Rangpur	39.470	1957	< 0.0001	0.05	R	**
28	Sandwip	24.951	1982	< 0.0001	0.05	R	**
29	Satkhira	20.125	1971	0.032	0.05	R	**
30	Sitakunda	51.117	1988	< 0.0001	0.05	R	**
31	Srimangal	32.735	1978	< 0.0001	0.05	R	**
32	Sydpur	51.446	2004	< 0.0001	0.05	R	**
33	Sylhet	41.967	1956	< 0.0001	0.05	R	**
34	Tangail	59.603	1988	< 0.0001	0.05	R	**
35	Teknaf	40.428	1988	< 0.0001	0.05	R	**

Note: **Significant at the 95% level of confidence; *Significant at the 90% level of confidence; NS-Not Significant at the 90% level of confidence; A-Accepted at the p>0.05; R-Rejected at the p<0.05

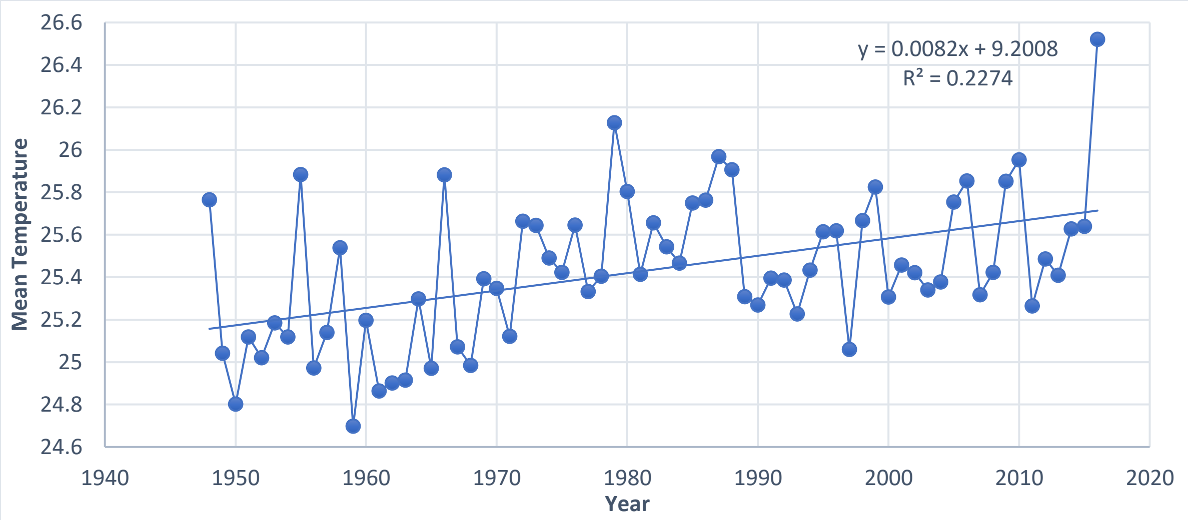

Figure 4.2: Time series of all-Bangladesh annual mean temperatures (1948-2016)

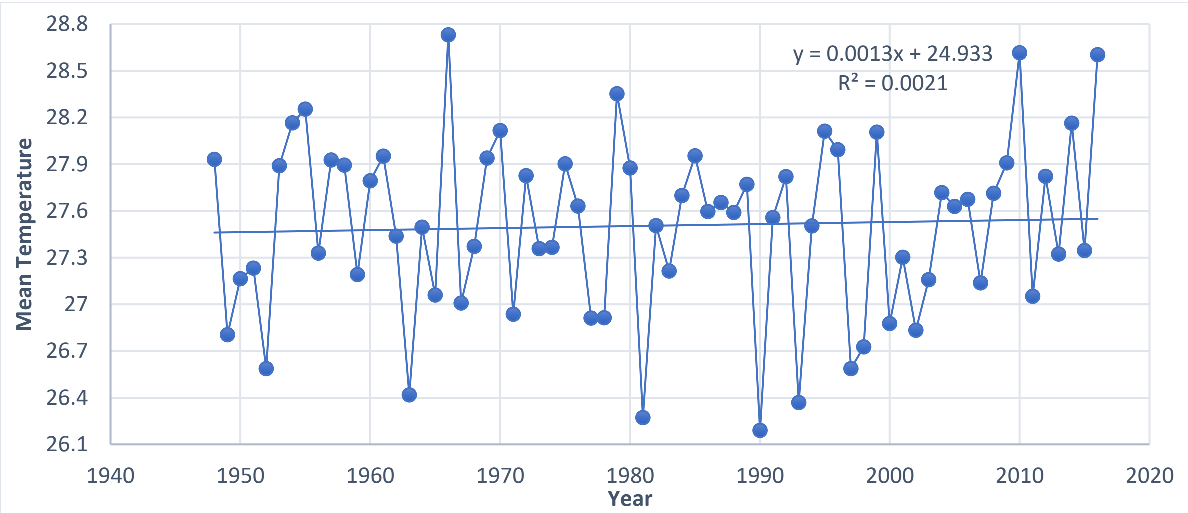

Figure 4.3: Time series of all-Bangladesh pre-monsoon mean temperatures (1948-2016)

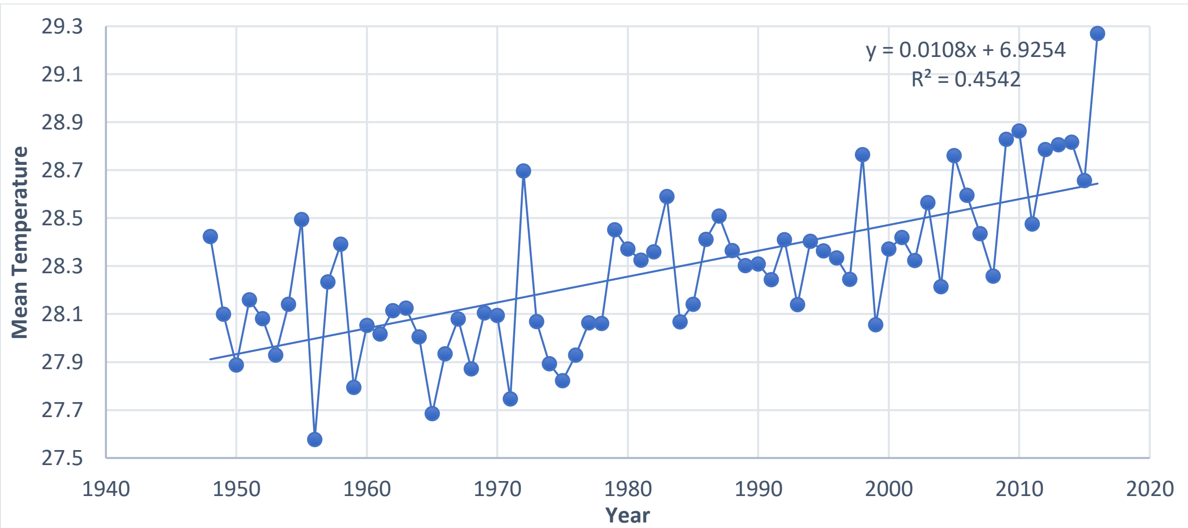

Figure 4.4: Time series of all-Bangladesh monsoon mean temperatures (1948-2016)

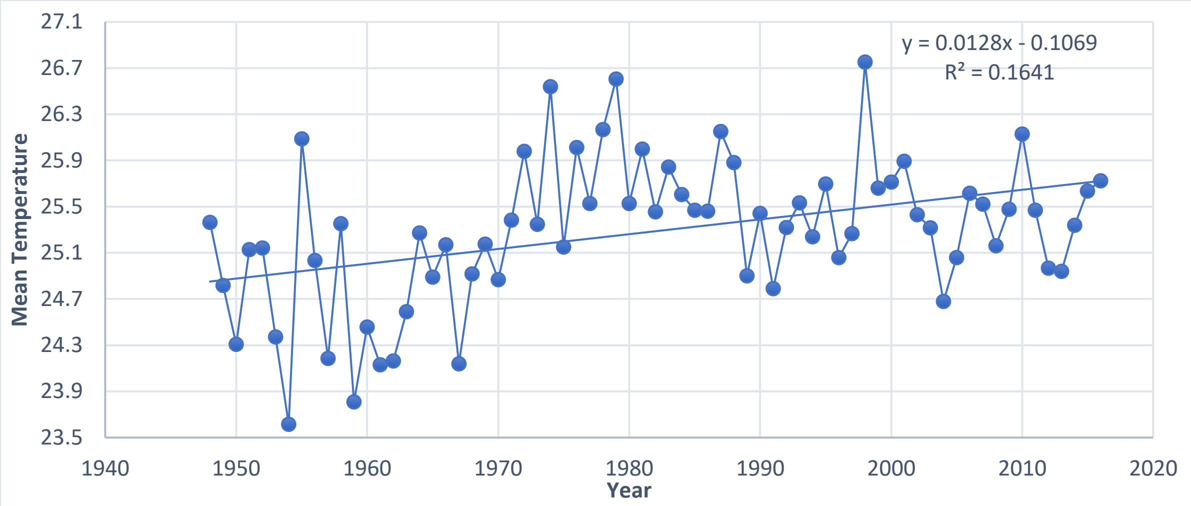

Figure 4.5: Time series of all-Bangladesh post-monsoon mean temperatures (1948-2016)

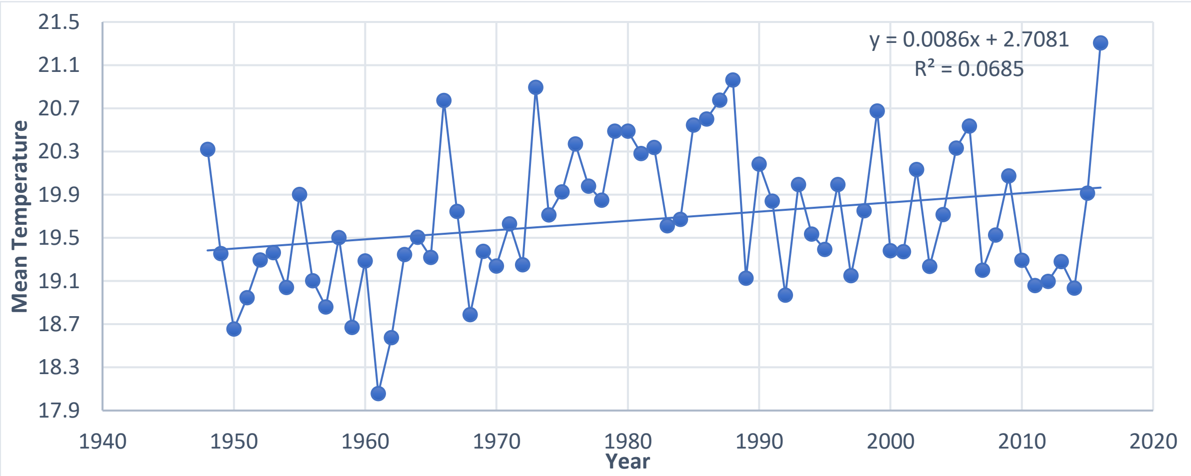

Figure 4.6: Time series of all-Bangladesh winter mean temperatures (1948-2016)

Normal average temperature is expressed as most recent 30 years data compilation. From the normal data another situation is calculated either average temperature will be increase or decrease. It is seen from the above figures that the trends would be quite different during the period of 1987-2016 than that in the entire period (1948-2016). This is particularly evident in the post-monsoon, winter and annual temperatures (Table 4.3). Therefore, the all-Bangladesh trends in seasonal and annual mean temperatures are also calculated using the data from 1987-2016 are shone in (Table 4.3). The trends in annual mean temperatures at different stations using recent normal data (1987-2016) were also evaluated. The trends were found to be increasing in maximum stations. The magnitude at individual stations varied between -0.15% to 0.25% of normal annual temperature per year. The spatial distribution of trends, expressed as % of normal annual temperature, is shown in (Figure 4.7). It is seen from the figure that the northern part of the country has a higher rate of increase in average temperatures compared to the mid and mid-western and south eastern hilly regions.

Table 4.3: All-Bangladesh trends in seasonal and annual mean temperatures (1948-2016)

Seasons	Trend[1] (^{0}C/century)	Significance[1]	Trend[2] (^{0}C/century)	Significance[2]
Pre-monsoon (Mar-May)	0.13	NS	2.05	NS
Monsoon (Jun-Sep)	1.08	**	2.00	**
Post-monsoon (Oct-Nov)	1.28	**	-1.17	NS
Winter (Dec-Feb)	0.86	*	-1.08	NS
Annual (Jan-Dec)	0.82	**	0.85	NS

Note: [1]using data of all stations from 1948 to 2016; [2]using data of all stations from 1987 to 2016; **Significant at the 95% level of confidence; *Significant at the 90% level of confidence; NS-Not Significant at the 90% level of confidence

It is seen from the (Table 4.3) that the increasing trend in annual average temperatures during the 1987-2016 period is about 0.85 ^{0}C per century. This value is about same of the value computed using the data for the entire time period (1948-2016). The rise in mean annual temperatures projected by IPCC (2007) for South Asia is 3.3 ^{0}C with a range of 2.7 ^{0}C in JJA to 3.6 ^{0}C in DJF. Thus, the current trend is far from the IPCC projection. However, it is clear that the use of the recent data, or the historical data, differ from to the IPCC projection. In this study all BMD data were used hence, some anomaly affected calculating the data. Sometimes researchers are ignoring or avoid such kind of unexpected data where one or two days represent the whole month.

The monsoon and post-monsoon trends have become stronger and significant indeed and the pre-monsoon trend has become weaker where winter is significant at the 90% level of confidence. But in recent period only monsoon is only stronger than others. The IPCC (2007) median projections for quarterly temperatures are increases of 3.6, 3.5, 2.7 and 3.1 ^{0}C in December-February, March-May, June-August, and September-November, respectively, by the end of the 21st century. The IPCC projections of seasonal temperatures are also higher than the present seasonal trends.

However, the projection is not unrealistic in that the recent trends are higher than the past and it may further strengthen in the future. Trends in all-Bangladesh annual and seasonal temperatures are given in (Figure 4.2, 4.3, 4.4, 4.5 and 4.6). On the other hand, two values are reported in the (Table 4.3) one using the data since 1948 and the other using the recent data since 1987. In figure 5 it is seen that pre-monsoon increase rate is very much slow and nearly steady. From the bellow (Figure 4.7) showing north-western part is hotter region and it's become hotter. Overall situation of the central region quite normal though the lower Meghna basin is negative trend. Global mean temperature shown in (Figure 4.8).

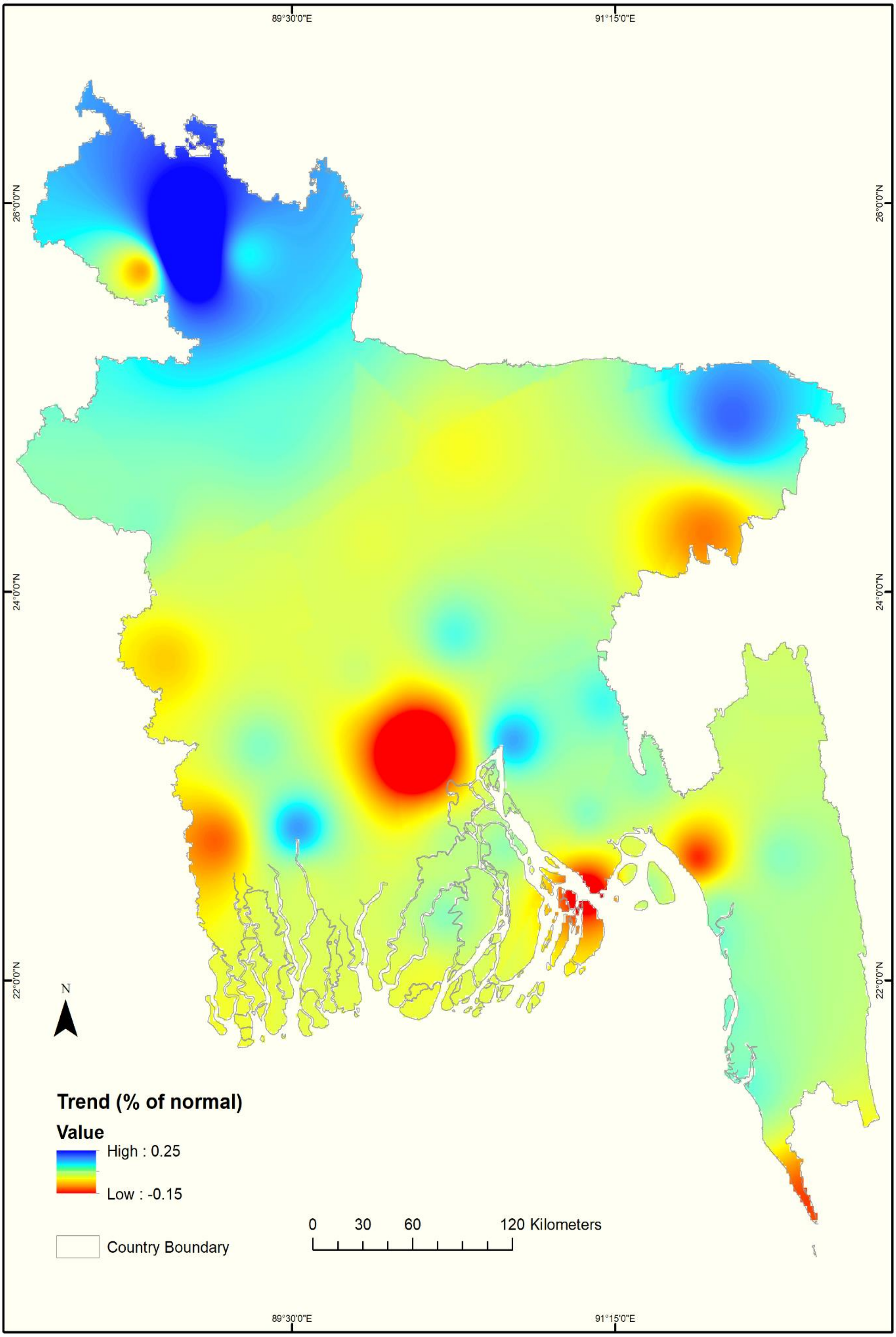

Figure 4.7: Spatial pattern of trends in annual mean temperatures (% of normal) (1987-2016)

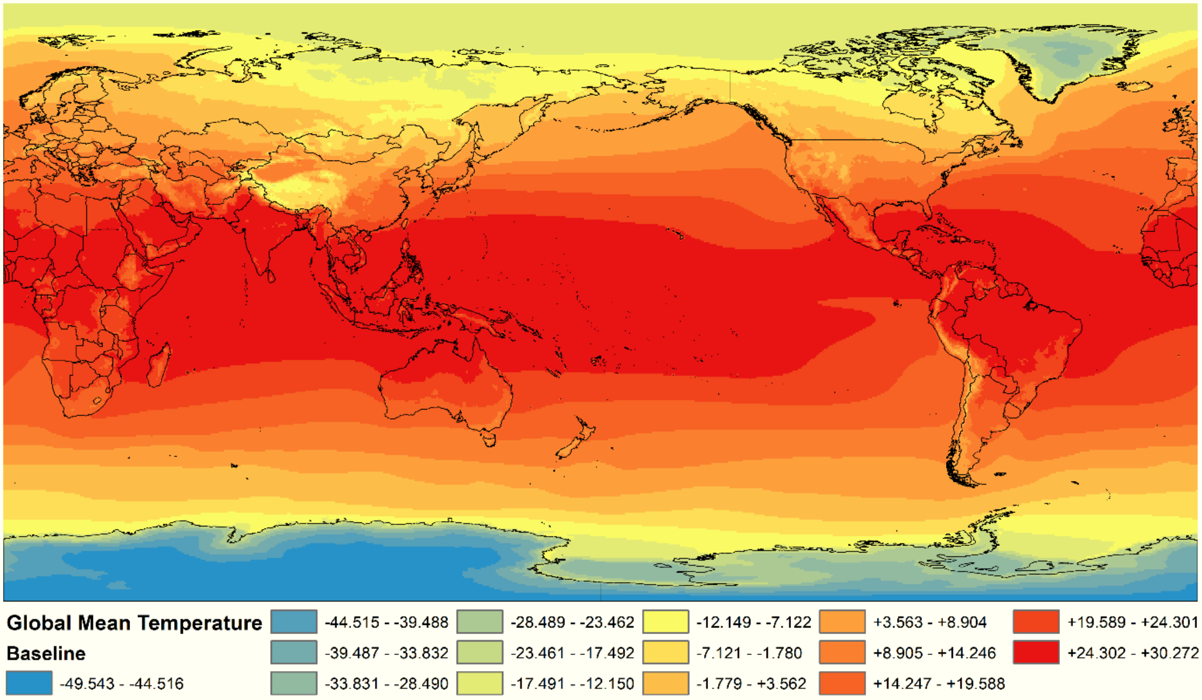

Figure 4.8: Global mean temp (^{0}C) mid sensitivity from SimCLIM simulation, baseline 1995

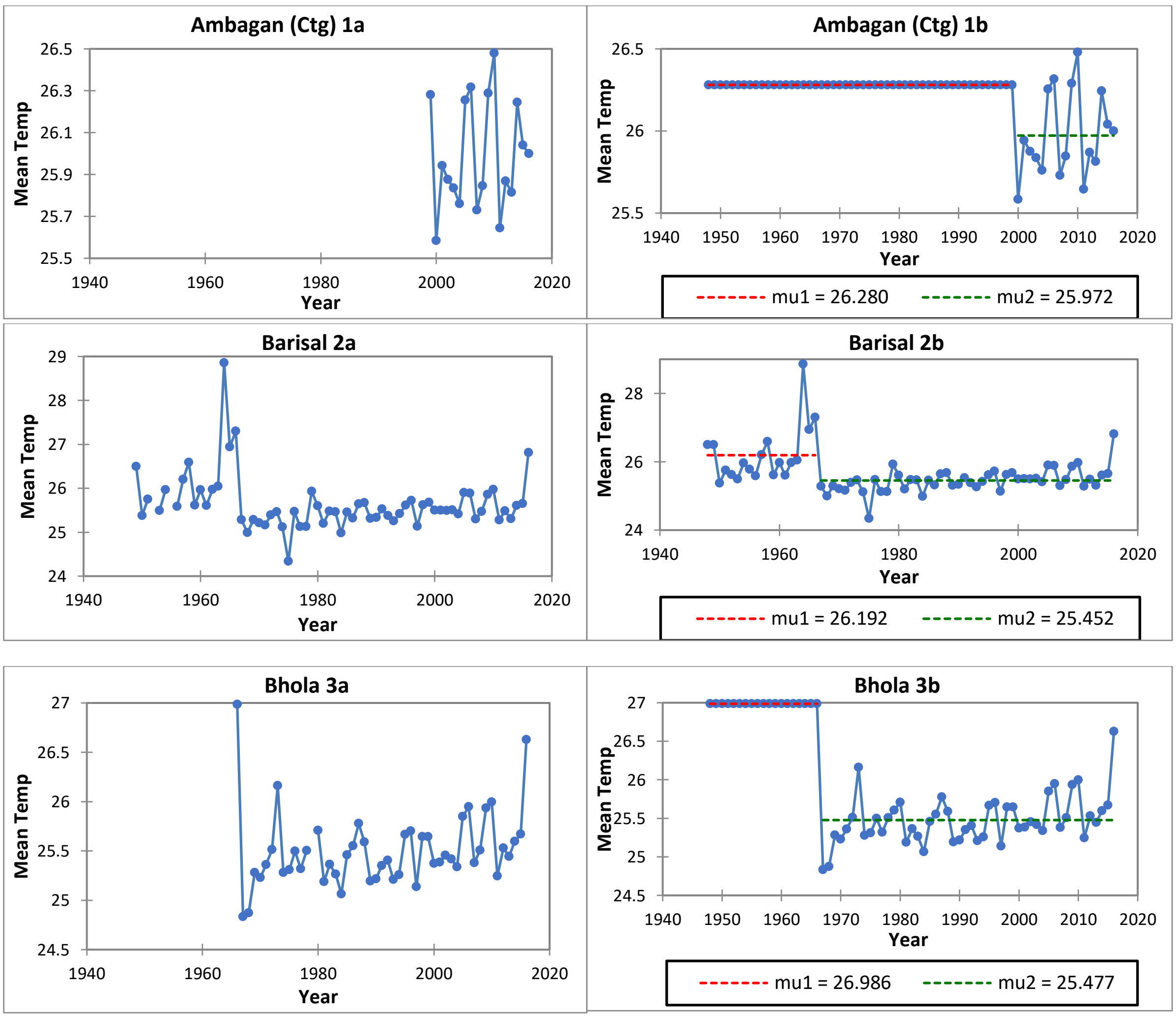

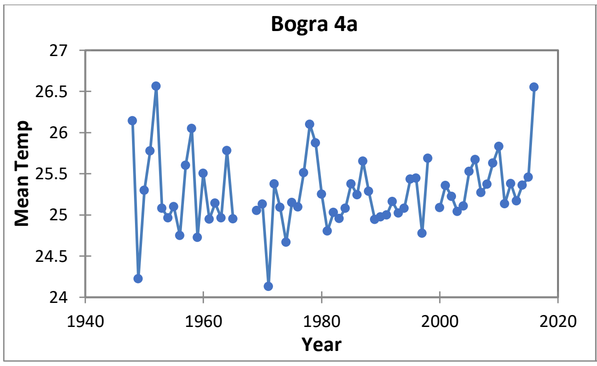
Bogra 4a
Mean Temp
Year

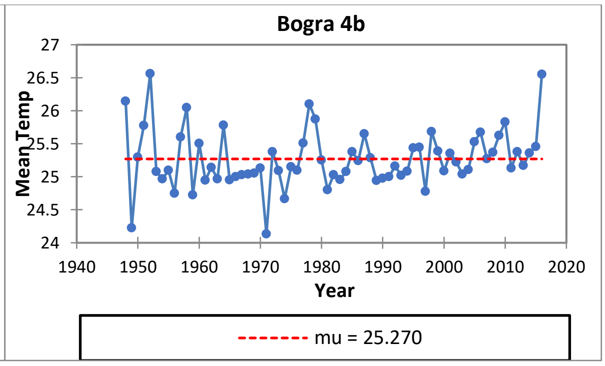
Bogra 4b
Mean Temp
Year
mu = 25.270

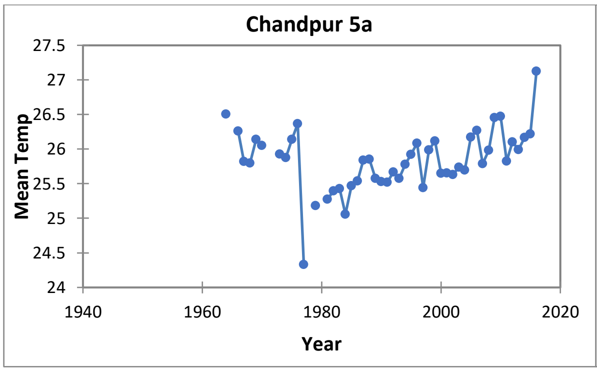
Chandpur 5a
Mean Temp
Year

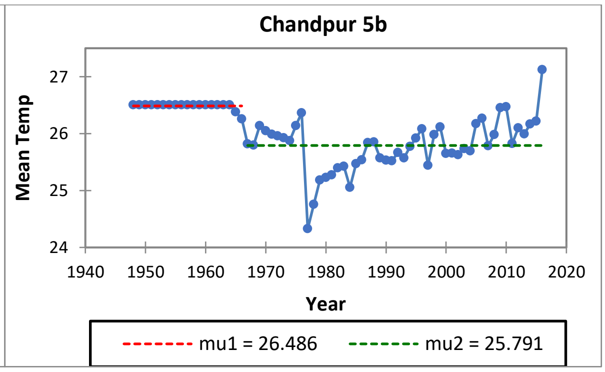
Chandpur 5b
Mean Temp
Year
mu1 = 26.486
mu2 = 25.791

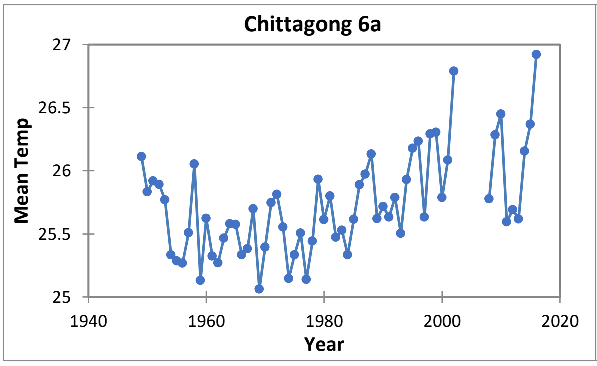
Chittagong 6a
Mean Temp
Year

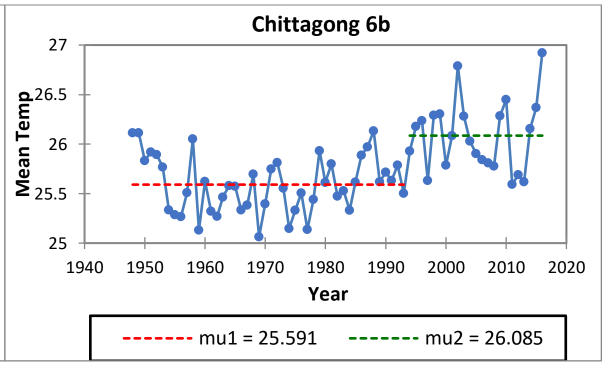
Chittagong 6b
Mean Temp
Year
mu1 = 25.591
mu2 = 26.085

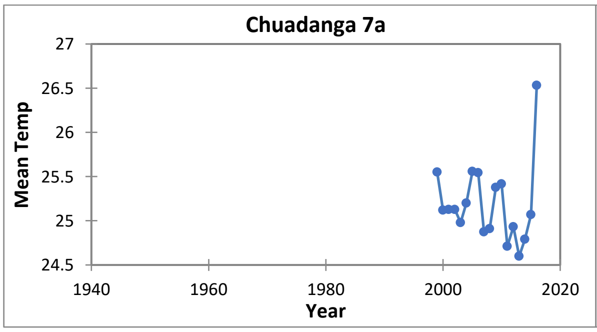
Chuadanga 7a
Mean Temp
Year

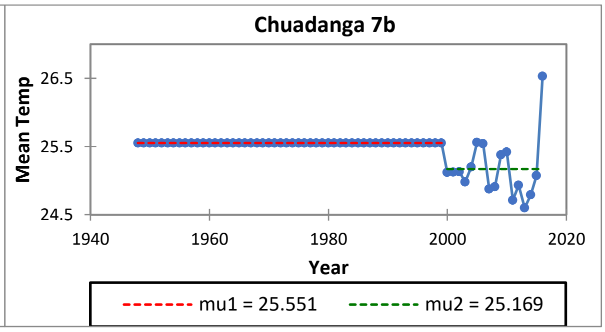
Chuadanga 7b
Mean Temp
Year
mu1 = 25.551
mu2 = 25.169

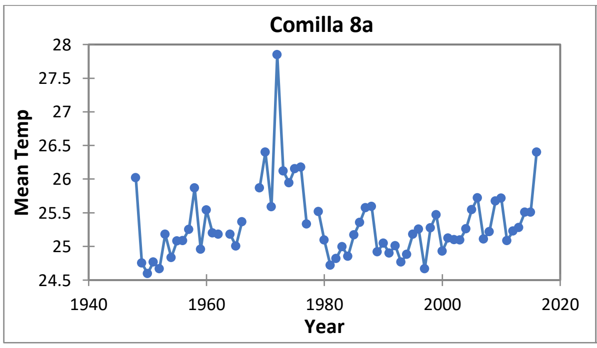
Comilla 8a
Mean Temp
Year

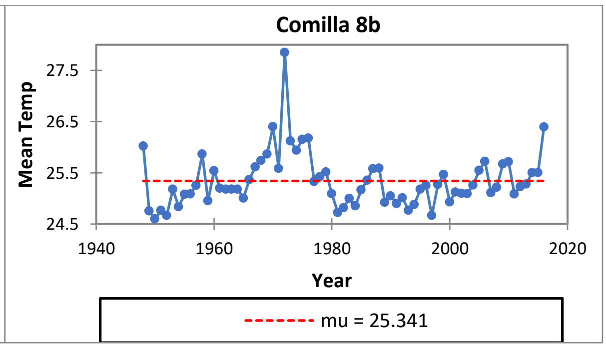
Comilla 8b
Mean Temp
Year
mu = 25.341

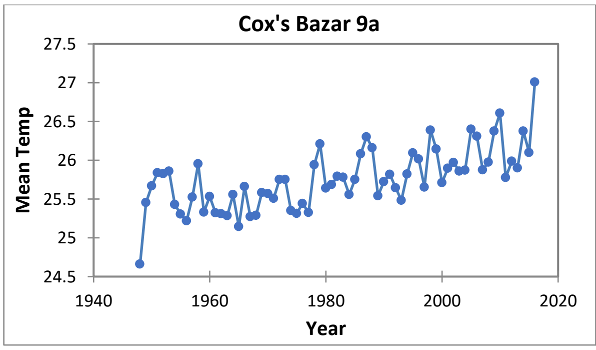
Cox's Bazar 9a
Mean Temp
27.5
27
26.5
26
25.5
25
24.5
1940
1960
1980
2000
2020
Year

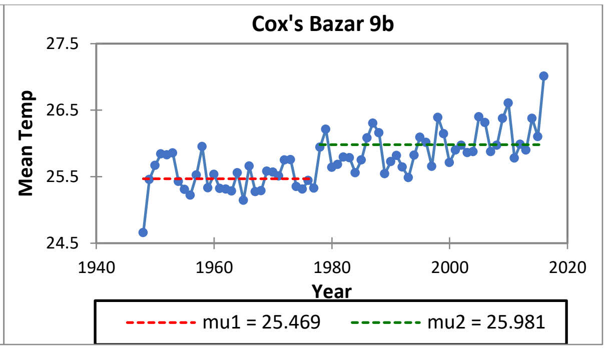
Cox's Bazar 9b
Mean Temp
27.5
26.5
25.5
24.5
1940
1960
1980
2000
2020
Year
mu1 = 25.469
mu2 = 25.981

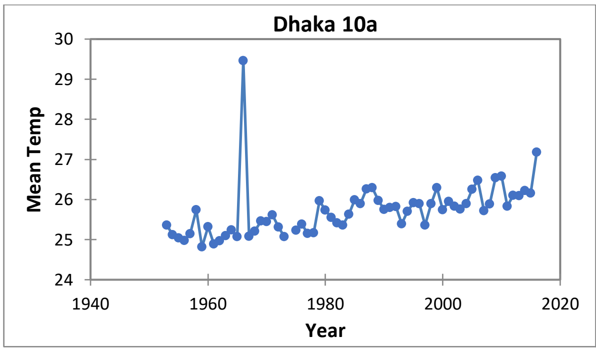
Dhaka 10a
Mean Temp
30
29
28
27
26
25
24
1940
1960
1980
2000
2020
Year

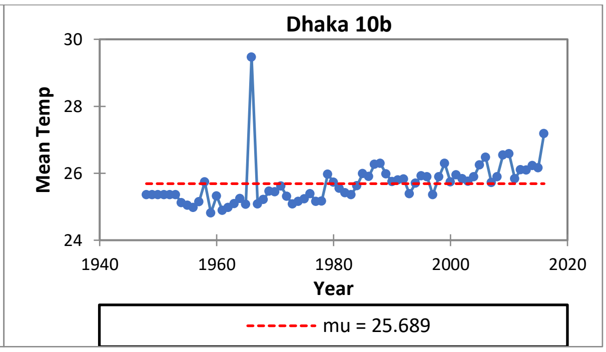
Dhaka 10b
Mean Temp
30
28
26
24
1940
1960
1980
2000
2020
Year
mu = 25.689

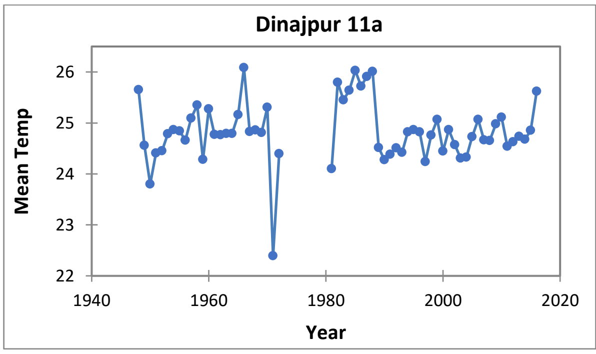
Dinajpur 11a
Mean Temp
26
25
24
23
22
1940
1960
1980
2000
2020
Year

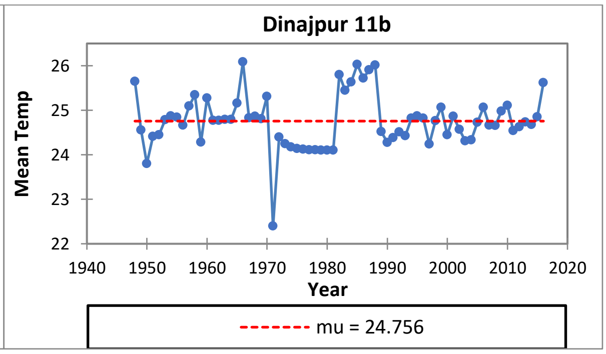
Dinajpur 11b
Mean Temp
26
25
24
23
22
1940
1950
1960
1970
1980
1990
2000
2010
2020
Year
mu = 24.756

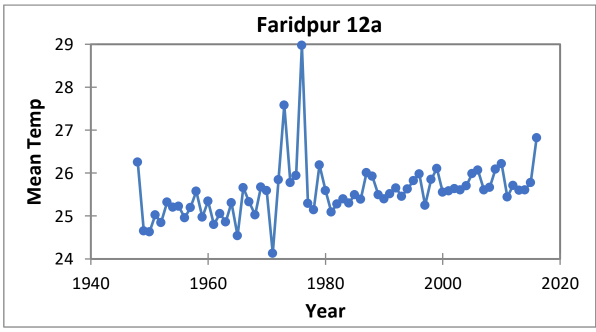
Faridpur 12a
Mean Temp
29
28
27
26
25
24
1940
1960
1980
2000
2020
Year

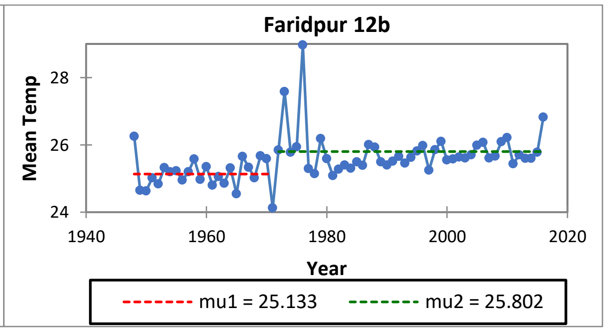
Faridpur 12b
Mean Temp
28
26
24
1940
1960
1980
2000
2020
Year
mu1 = 25.133
mu2 = 25.802

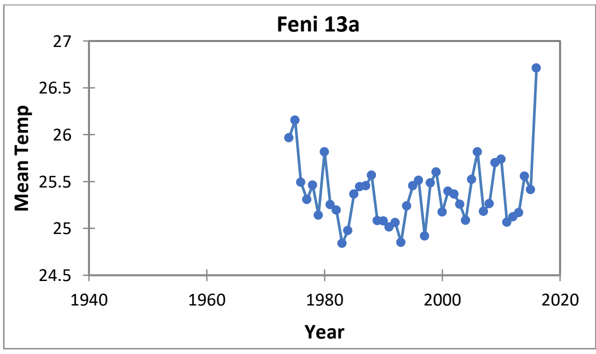
Feni 13a
Mean Temp
27
26.5
26
25.5
25
24.5
1940
1960
1980
2000
2020
Year

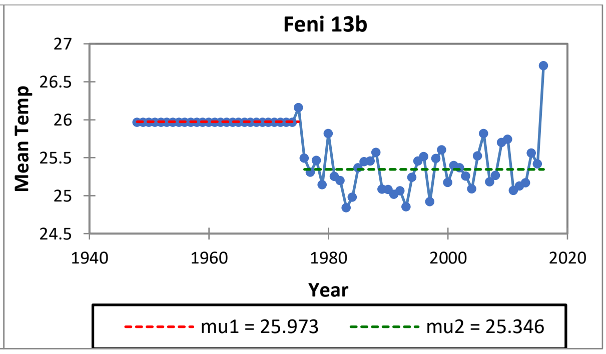
Feni 13b
Mean Temp
27
26.5
26
25.5
25
24.5
1940
1960
1980
2000
2020
Year
mu1 = 25.973
mu2 = 25.346

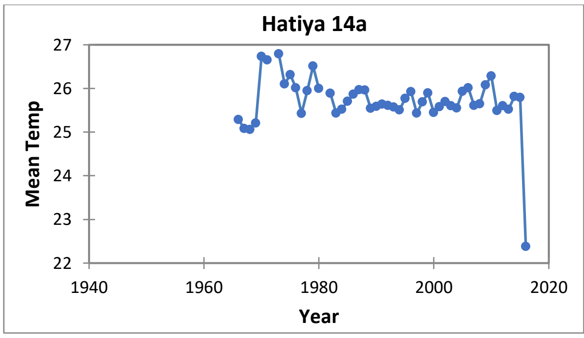
Hatiya 14a
Mean Temp
27
26
25
24
23
22
1940
1960
1980
2000
2020
Year

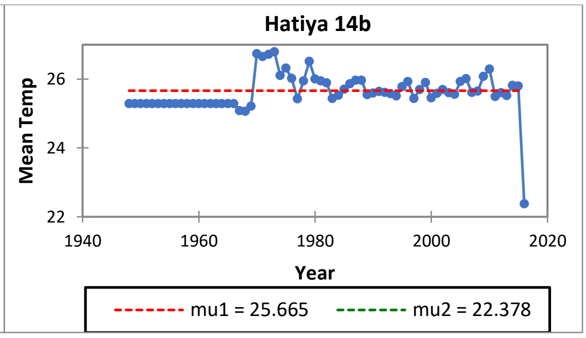
Hatiya 14b
Mean Temp
26
24
22
1940
1960
1980
2000
2020
Year
mu1 = 25.665
mu2 = 22.378

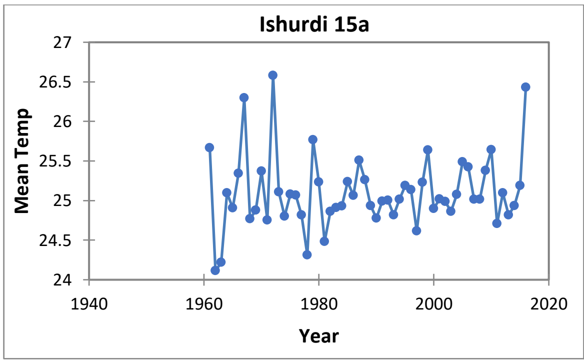
Ishurdi 15a
Mean Temp
27
26.5
26
25.5
25
24.5
24
1940
1960
1980
2000
2020
Year

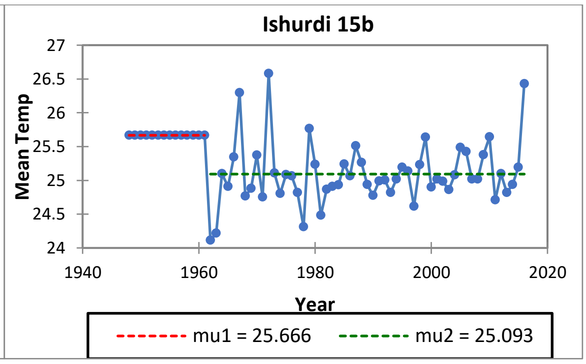
Ishurdi 15b
Mean Temp
27
26.5
26
25.5
25
24.5
24
1940
1960
1980
2000
2020
Year
mu1 = 25.666
mu2 = 25.093

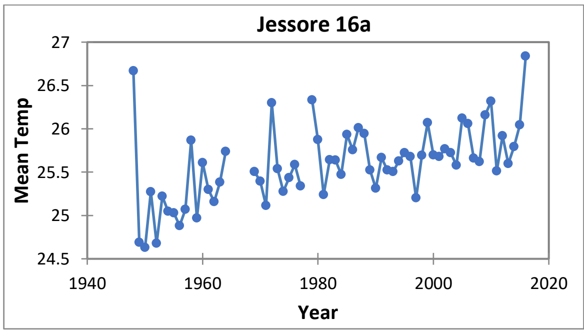
Jessore 16a
Mean Temp
27
26.5
26
25.5
25
24.5
1940
1960
1980
2000
2020
Year

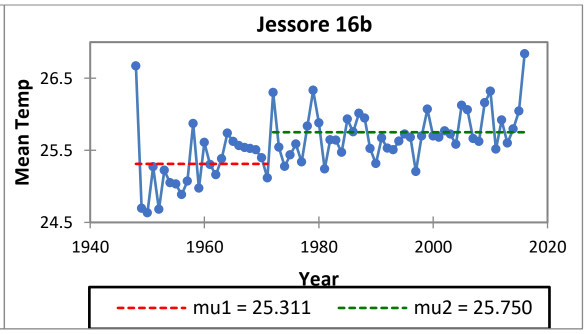
Jessore 16b
Mean Temp
26.5
25.5
24.5
1940
1960
1980
2000
2020
Year
mu1 = 25.311
mu2 = 25.750

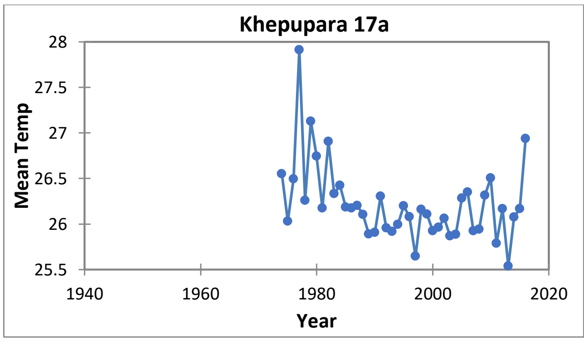
Khepupara 17a
Mean Temp
28
27.5
27
26.5
26
25.5
1940
1960
1980
2000
2020
Year

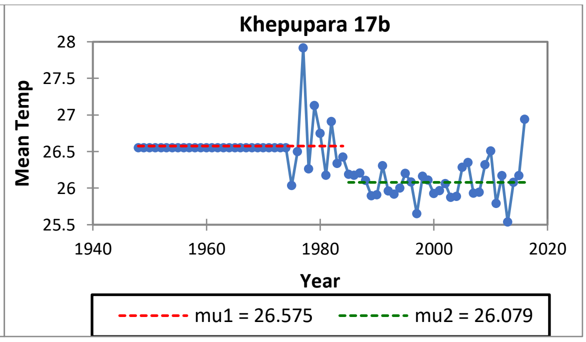
Khepupara 17b
Mean Temp
28
27.5
27
26.5
26
25.5
1940
1960
1980
2000
2020
Year
mu1 = 26.575
mu2 = 26.079

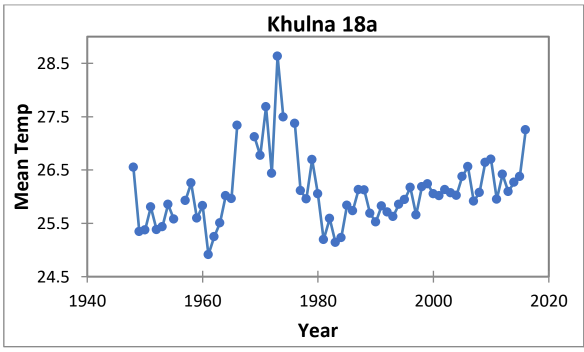
Khulna 18a
Mean Temp
28.5
27.5
26.5
25.5
24.5
1940
1960
1980
2000
2020
Year

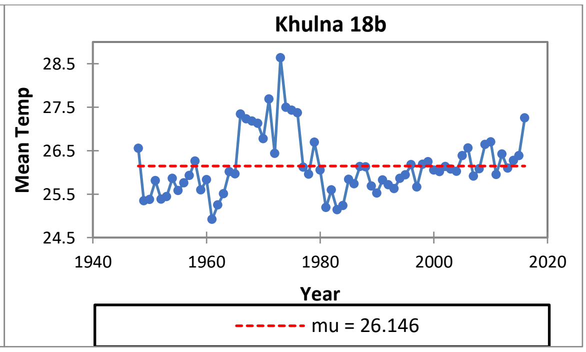
Khulna 18b
Mean Temp
28.5
27.5
26.5
25.5
24.5
1940
1960
1980
2000
2020
Year
mu = 26.146

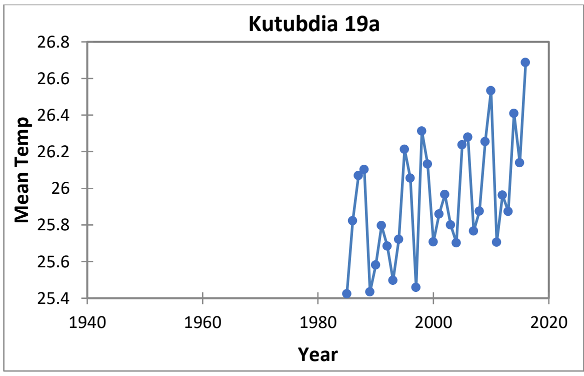
Kutubdia 19a
Mean Temp
26.8
26.6
26.4
26.2
26
25.8
25.6
25.4
1940
1960
1980
2000
2020
Year

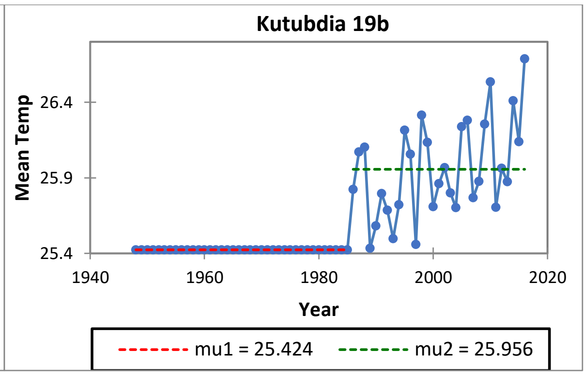
Kutubdia 19b
Mean Temp
26.4
25.9
25.4
1940
1960
1980
2000
2020
Year
mu1 = 25.424
mu2 = 25.956

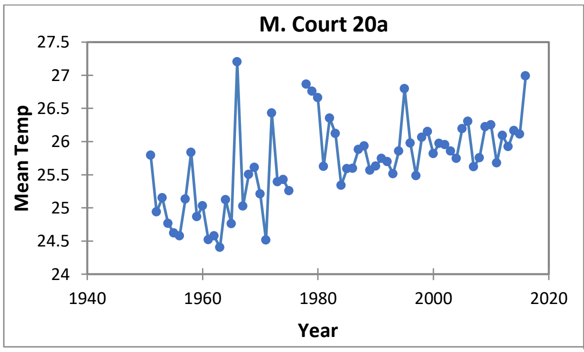
M. Court 20a
Mean Temp
27.5
27
26.5
26
25.5
25
24.5
24
1940
1960
1980
2000
2020
Year

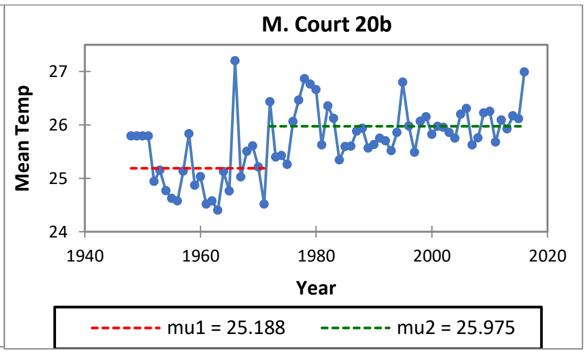
M. Court 20b
Mean Temp
27
26
25
24
1940
1960
1980
2000
2020
Year
mu1 = 25.188
mu2 = 25.975

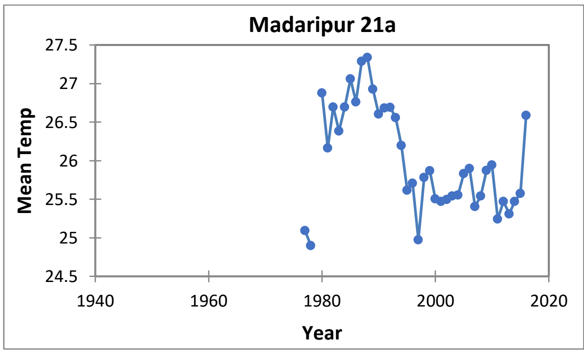
Madaripur 21a
Mean Temp
27.5
27
26.5
26
25.5
25
24.5
1940
1960
1980
2000
2020
Year

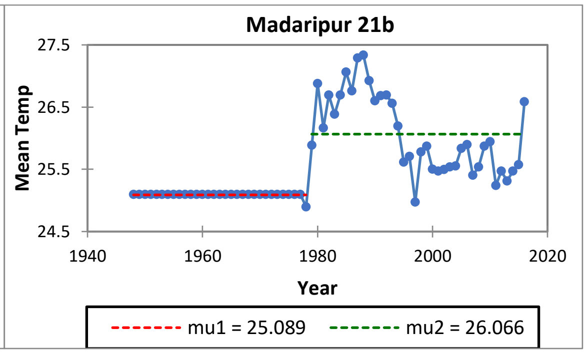
Madaripur 21b
Mean Temp
27.5
26.5
25.5
24.5
1940
1960
1980
2000
2020
Year
mu1 = 25.089
mu2 = 26.066

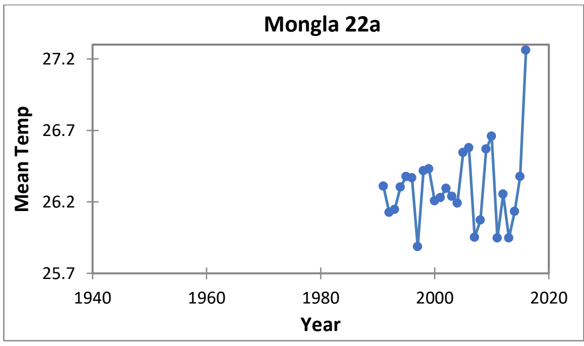
Mongla 22a
Mean Temp
27.2
26.7
26.2
25.7
1940
1960
1980
2000
2020
Year

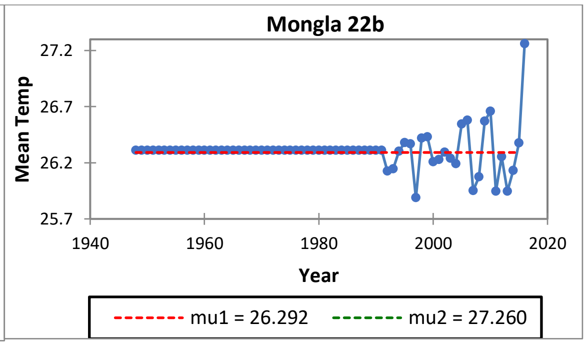
Mongla 22b
Mean Temp
27.2
26.7
26.2
25.7
1940
1960
1980
2000
2020
Year
mu1 = 26.292
mu2 = 27.260

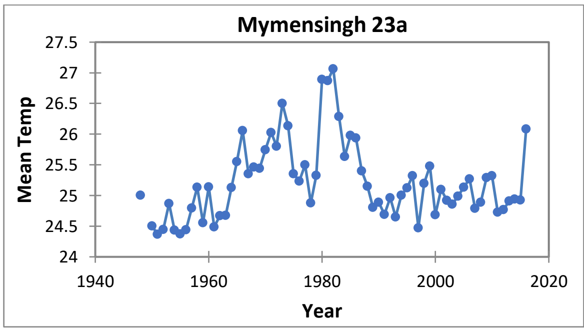
Mymensingh 23a
Mean Temp
27.5
27
26.5
26
25.5
25
24.5
24
1940
1960
1980
2000
2020
Year

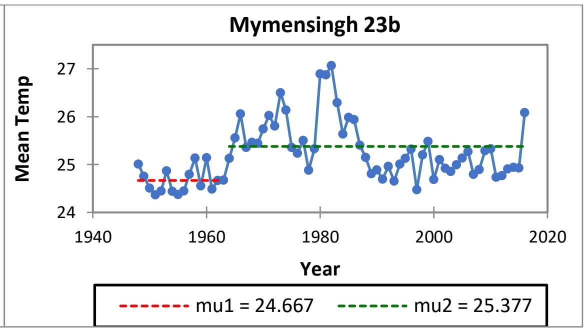
Mymensingh 23b
Mean Temp
27
26
25
24
1940
1960
1980
2000
2020
Year
mu1 = 24.667
mu2 = 25.377

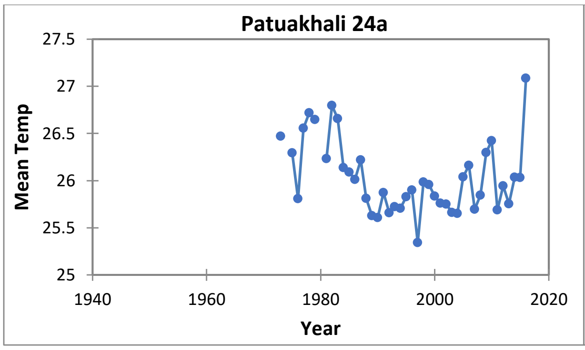
Patuakhali 24a
Mean Temp
27.5
27
26.5
26
25.5
25
1940
1960
1980
2000
2020
Year

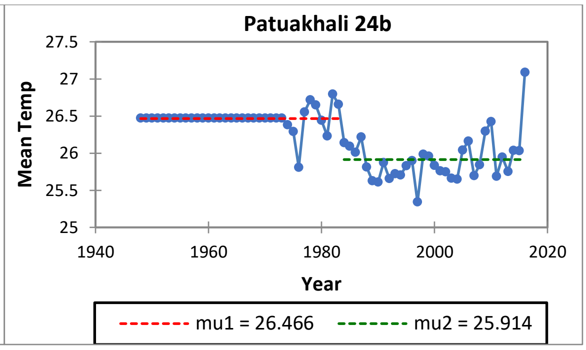
Patuakhali 24b
Mean Temp
27.5
27
26.5
26
25.5
25
1940
1960
1980
2000
2020
Year
mu1 = 26.466
mu2 = 25.914

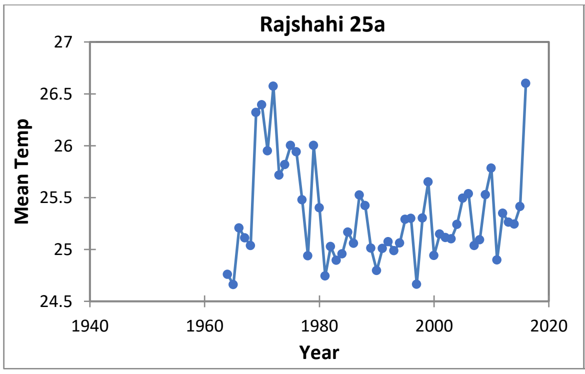
Rajshahi 25a
Mean Temp
27
26.5
26
25.5
25
24.5
1940
1960
1980
2000
2020
Year

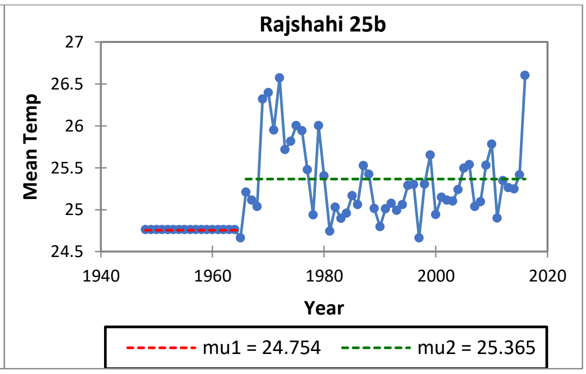
Rajshahi 25b
Mean Temp
27
26.5
26
25.5
25
24.5
1940
1960
1980
2000
2020
Year
mu1 = 24.754
mu2 = 25.365

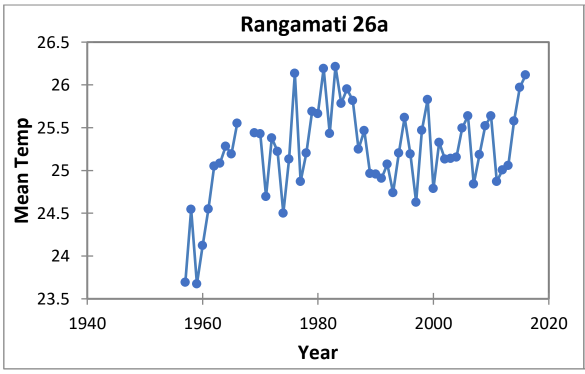
Rangamati 26a
Mean Temp
26.5
26
25.5
25
24.5
24
23.5
1940
1960
1980
2000
2020
Year

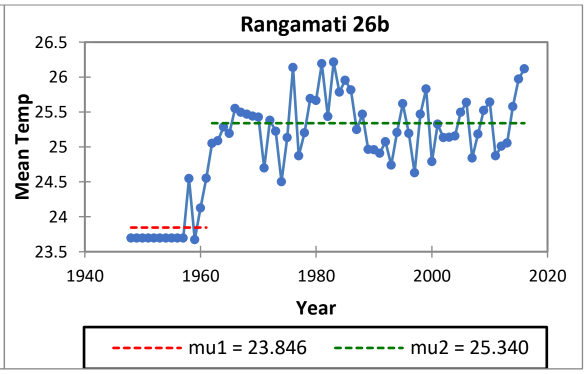
Rangamati 26b
Mean Temp
26.5
26
25.5
25
24.5
24
23.5
1940
1960
1980
2000
2020
Year
mu1 = 23.846
mu2 = 25.340

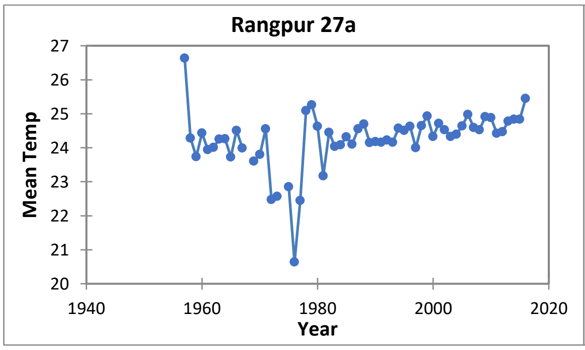
Rangpur 27a
Mean Temp
27
26
25
24
23
22
21
20
1940
1960
1980
2000
2020
Year

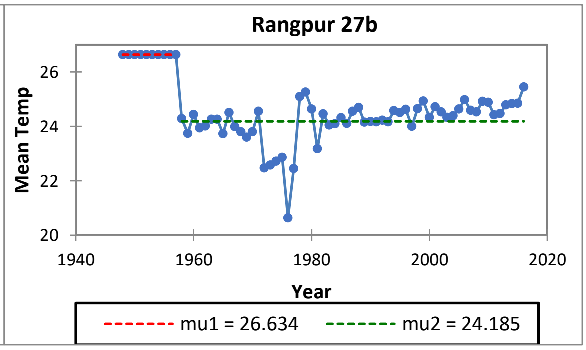
Rangpur 27b
Mean Temp
26
24
22
20
1940
1960
1980
2000
2020
Year
mu1 = 26.634
mu2 = 24.185

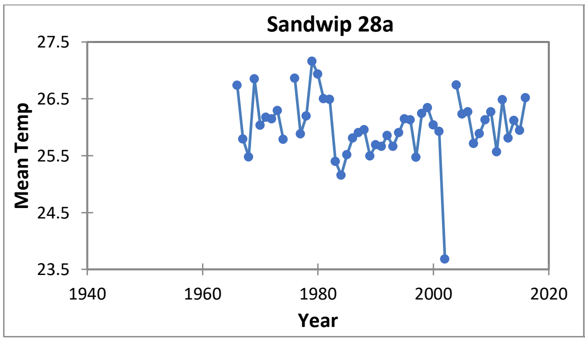
Sandwip 28a
Mean Temp
27.5
26.5
25.5
24.5
23.5
1940
1960
1980
2000
2020
Year

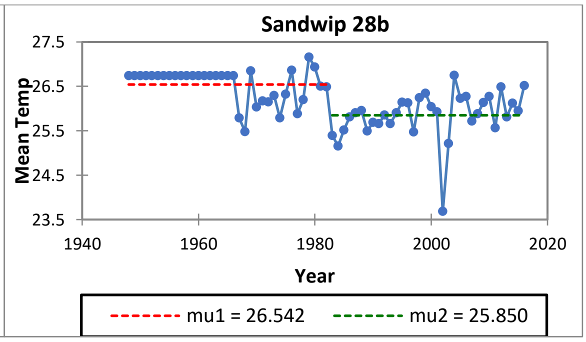
Sandwip 28b
Mean Temp
27.5
26.5
25.5
24.5
23.5
1940
1960
1980
2000
2020
Year
mu1 = 26.542
mu2 = 25.850

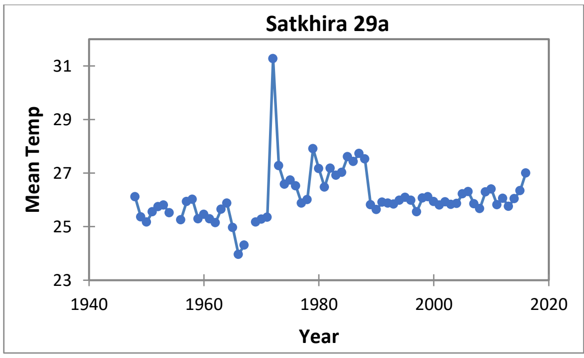
Satkhira 29a
Mean Temp
31
29
27
25
23
1940
1960
1980
2000
2020
Year

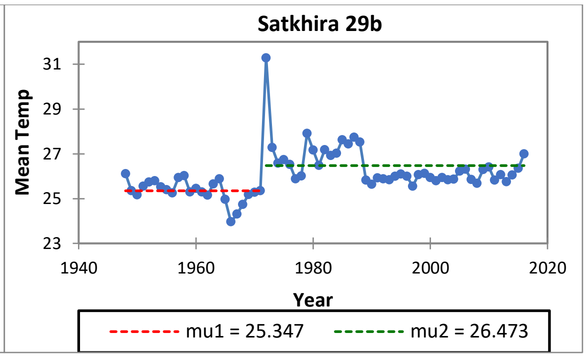
Satkhira 29b
Mean Temp
31
29
27
25
23
1940
1960
1980
2000
2020
Year
mu1 = 25.347
mu2 = 26.473

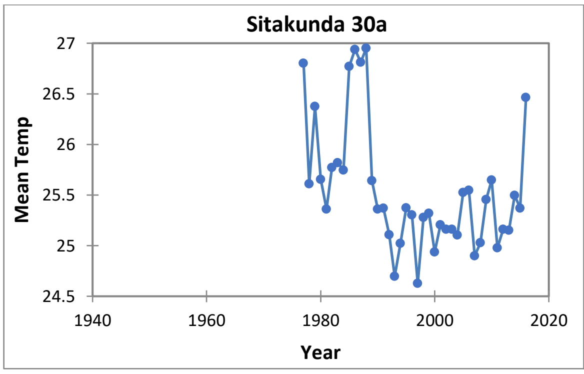
Sitakunda 30a
Mean Temp
27
26.5
26
25.5
25
24.5
1940
1960
1980
2000
2020
Year

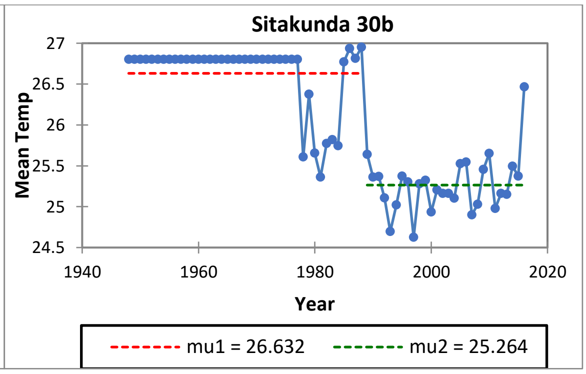
Sitakunda 30b
Mean Temp
27
26.5
26
25.5
25
24.5
1940
1960
1980
2000
2020
Year
mu1 = 26.632
mu2 = 25.264

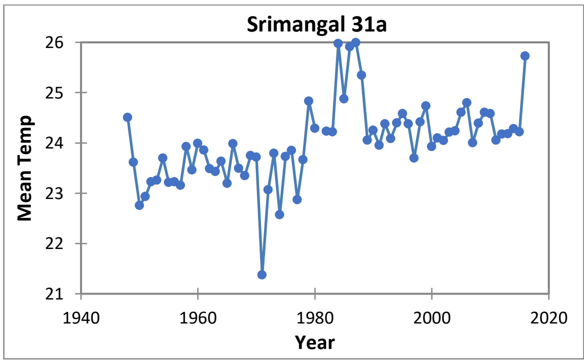
Srimangal 31a
Mean Temp
26
25
24
23
22
21
1940
1960
1980
2000
2020
Year

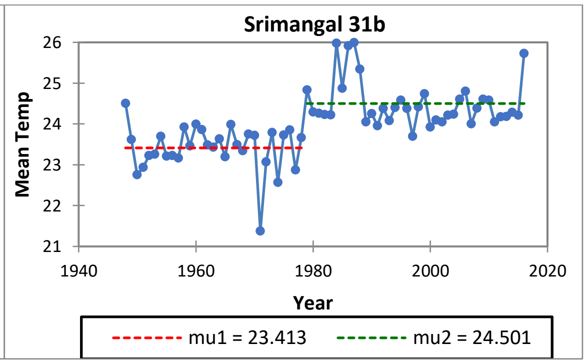
Srimangal 31b
Mean Temp
26
25
24
23
22
21
1940
1960
1980
2000
2020
Year
mu1 = 23.413
mu2 = 24.501

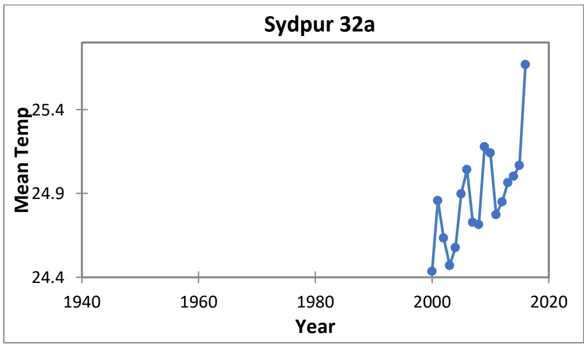
Sydpur 32a
Mean Temp
25.4
24.9
24.4
1940
1960
1980
2000
2020
Year

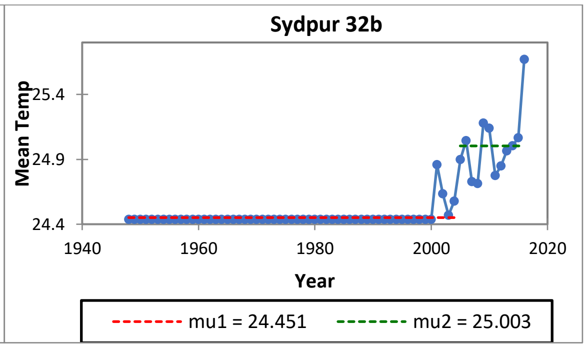
Sydpur 32b
Mean Temp
25.4
24.9
24.4
1940
1960
1980
2000
2020
Year
mu1 = 24.451
mu2 = 25.003

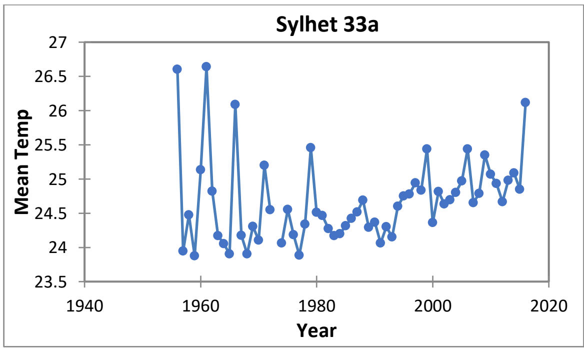
Sylhet 33a
Mean Temp
27
26.5
26
25.5
25
24.5
24
23.5
1940
1960
1980
2000
2020
Year

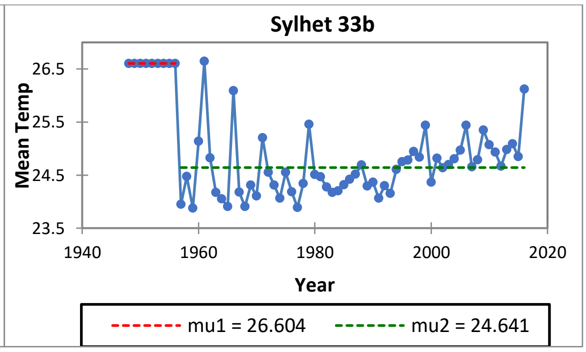
Sylhet 33b
Mean Temp
26.5
25.5
24.5
23.5
1940
1960
1980
2000
2020
Year
mu1 = 26.604
mu2 = 24.641

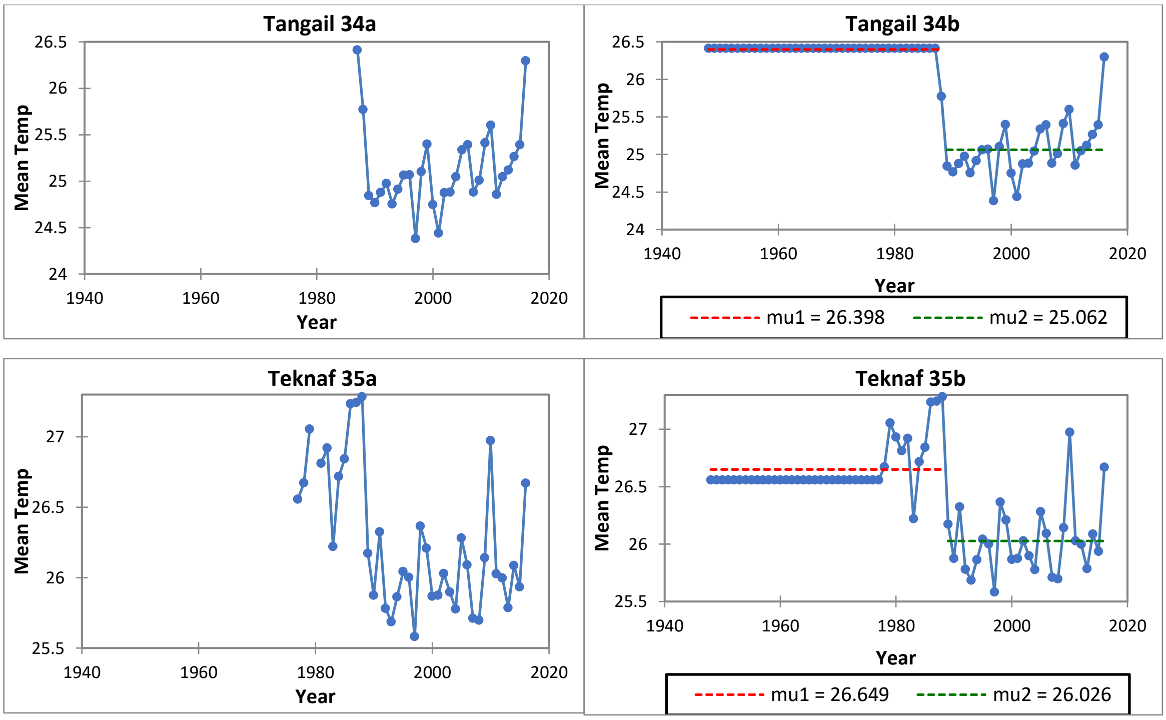

Figure 4.9: Changing year in annual average temperature all stations MK(a) & SNHT(b) test

4.4 Homogeneity tests *P*-value Approximation

The tests presented in this tool correspond to the alternative hypothesis of a single shift. For all tests, XLSTAT provides p-values using Monte Carlo resampling. Exact calculations are either impossible or too costly in computing time.

Homogeneity analysis shows that 35 annual mean temperature series (station wise) are heterogeneous around the year 1948-2016, it means there is a significant change in the mean before and after the detected change point. SNHT test is known to find change point towards find the changes in the middle of a series (Mart´ınez *et. al.*, 2009). The results given in (Table 4.2) are showing most of the series homogenous.

An analysis across the tests shows that there are 22 common stations where all the tests are in about to same change point year with high significant. The changes in the mean of these series along with the mean temperature plots are shown in (Figure 4.9). Of these 13 stations, 9 stations show less significant, 2 stations are 90% significant and 2 stations are not significant the change point. The figures clearly show that there is a noticeable change in the temperature mean of the series before and after the change point in all the stations.

Chapter Five
Analysis of Observed Maximum Temperature

5.1 Introduction
From the American Meteorological Society (AMS) Glossary of Meteorology (the second edition in 2000, http://amsglossary.allenpress.com/glossary/), the daily maximum temperature is defined as 'the maximum temperature in the course of a continuous time interval of 24 h', in which the maximum temperature is defined as 'the highest temperature reported for a given location during a given period'. The maximum temperature of the dry bulb air temperature as indicated by a properly exposed thermometer during a given period, usually a day, a month, or a year. For climatological tables, the maximum temperature is generally calculated for each month and for the year.

5.2 Local Data Analysis
For local data daily, maximum temperatures were available at 35 locations for a period of 69 years (1948-2016). The estimated trends in mean maximum annual temperatures for 35 stations are given in (Table 5.1). It is seen from the bellow table that almost all the stations in Bangladesh exhibit increasing trends in mean maximum annual temperatures. In fact, 3 stations seen decreasing trend where 2 stations are not enough for negative trend (Table 5.1). In my analysis including all the 35 stations suggests that the trend is 0.96 ^{0}C per century (100 years) (Table 5.3). The corresponding pre-monsoon (March-May), monsoon (June-September), post-monsoon (October-November) and winter (December-February) trends are 0.06, 1.77, 2.33 and 0.02 ^{0}C per century respectively (Table 5.3).

5.3 Time Series Analysis
Kendall's τ and Spearman's ρ used to measure linear monotonic associations between year and observed data. Both τ and ρ are rank-based procedures-the latter being dependent on the actual magnitudes of the two variables, while the former being not dependent on them. The values of these correlation coefficients indicate the presence or absence of the trend and its direction I = increasing and D = decreasing (Table 5.1). However, the coefficient does not indicate whether the trend is statistically significant or not at a given confidence level. At 5% significance level, 6 stations which hypothesis of homogeneity of trends is accepted and 29 stations of trends is rejected during 1948-2016. It means the overall the trends of series for this duration are significant for increasing and decreasing in the entire area.

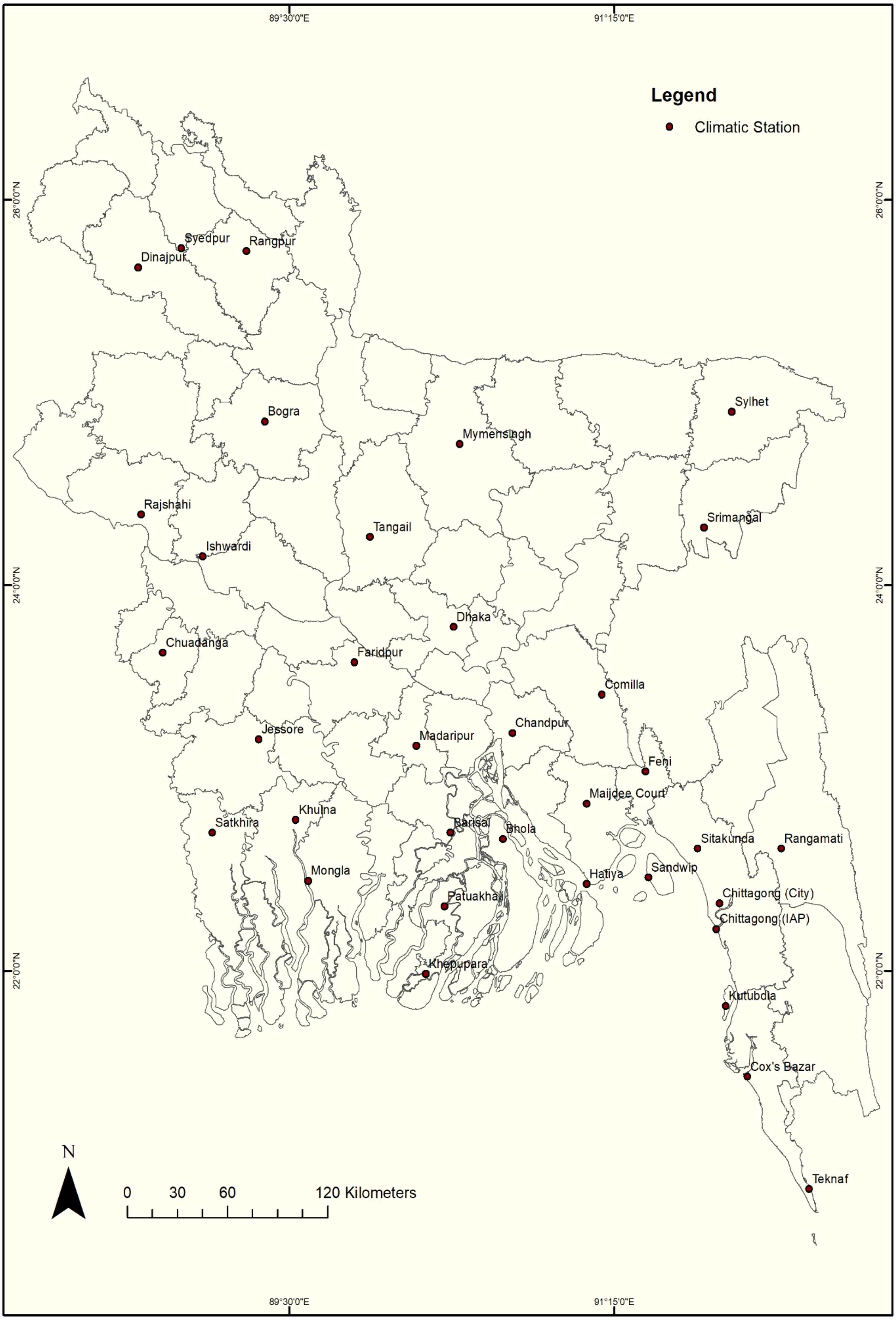

Figure 5.1: Locations of the BMD climatic stations used in the study (maximum temperature)

Table 5.1: Results of the Mann-Kendall test for annual mean maximum temperature data for all-Bangladesh (1948-2016)

Stations	**Available Year**	**Kendall's tau**	**S**	**Var(S)**	***P* (Two-tailed)**	**alpha**	**Test Int.**	**Trend ^{0}C/100 y**	**Sig.**
Ambagan(Ctg)	18	0.221	30.00	0.00	0.236	0.05	A	1.61	NS
Barisal	64	0.332	670.00	29792.00	0.000	0.05	R	1.05	**I
Bhola	50	0.399	489.00	14291.67	< 0.0001	0.05	R	1.76	**I
Bogra	65	0.181	376.00	31200.00	0.034	0.05	R	1.30	**I
Chandpur	49	0.425	500.00	0.00	< 0.0001	0.05	R	2.51	**I
Chittagong	63	0.323	631.00	28427.00	0.000	0.05	R	1.11	**I
Chuadanga	41	0.063	24.00	0.00	0.653	0.05	A	0.41	NS
Comilla	65	0.138	288.00	31200.00	0.104	0.05	A	0.62	NS
Cox's Bazar	69	0.552	1294.00	37275.33	< 0.0001	0.05	R	3.04	**I
Dhaka	63	0.323	631.00	28427.00	0.000	0.05	R	1.35	**I
Dinajpur	61	-0.243	-444.00	25823.33	0.006	0.05	R	-1.27	**D
Faridpur	69	0.575	1348.00	37275.33	< 0.0001	0.05	R	2.84	**I
Feni	44	0.171	162.00	0.00	0.104	0.05	A	1.71	NS
Hatiya	44	0.575	544.00	0.00	< 0.0001	0.05	R	2.59	**I
Ishurdi	55	0.212	315.00	18975.00	0.023	0.05	R	0.74	**I
Jessore	68	0.443	1010.00	35688.67	< 0.0001	0.05	R	1.60	**I
Khepupara	42	0.584	503.00	0.00	< 0.0001	0.05	R	3.39	**I
Khulna	66	0.193	415.00	32651.67	0.022	0.05	R	0.62	**I
Kutubdia	32	0.480	238.00	0.00	< 0.0001	0.05	R	2.82	**I
M.Court	64	0.492	992.00	29792.00	< 0.0001	0.05	R	2.08	**I
Madaripur	39	0.142	105.00	0.00	0.210	0.05	A	0.84	NS
Mongla	28	0.571	216.00	0.00	< 0.0001	0.05	R	3.15	**I
Mymensingh	67	-0.139	-307.00	34147.67	0.098	0.05	A	-0.50	*D
Patuakhali	42	0.619	533.00	0.00	< 0.0001	0.05	R	3.70	**I
Rajshahi	52	0.253	336.00	16059.33	0.008	0.05	R	1.57	**I
Rangamati	60	0.121	214.00	24583.33	0.174	0.05	A	0.61	NS
Rangpur	54	-0.166	-237.00	17967.00	0.078	0.05	A	-1.55	*D
Sandwip	48	0.323	364.00	0.00	0.001	0.05	R	2.32	**I
Satkhira	67	0.106	235.00	34147.67	0.205	0.05	A	0.47	NS
Sitakunda	40	0.669	522.00	0.00	< 0.0001	0.05	R	5.27	**I
Srimangal	67	0.196	433.00	34147.67	0.019	0.05	R	0.78	**I
Sydpur	26	0.446	145.00	0.000	0.001	0.05	R	3.75	**I
Sylhet	60	0.496	878.00	24583.33	< 0.0001	0.05	R	2.62	**I
Tangail	30	0.393	171.00	0.00	0.002	0.05	R	2.92	**I
Teknaf	40	0.410	320.00	0.00	0.000	0.05	R	2.04	**I

Note: **Significant at the 95% level of confidence; *Significant at the 90% level of confidence; NS-Not Significant at the 90% level of confidence; A-Accepted at the p>0.05; R-Rejected at the p<0.05; I-Increased; D-Decreases

Table 5.2: Results of the Standard Normal Homogeneity Test (SNHT) for annual mean maximum temperature data for all-Bangladesh (1948-2016)

Sl. No.	Stations	T0	t	*P* (Two-tailed)	alpha	Test Int.	Sig.
1	Ambagan(Ctg)	5.718	2004	0.336	0.05	A	NS
2	Barisal	12.443	1995	0.008	0.05	R	**
3	Bhola	10.500	2008	0.024	0.05	R	**
4	Bogra	17.208	1951	0.036	0.05	R	**
5	Chandpur	13.764	2005	0.044	0.05	R	**
6	Chittagong	15.251	1984	0.002	0.05	R	**
7	Chuadanga	26.774	1990	< 0.0001	0.05	R	**
8	Comilla	15.751	1953	0.002	0.05	R	**
9	Cox's Bazar	48.794	1993	< 0.0001	0.05	R	**
10	Dhaka	19.499	1984	< 0.0001	0.05	R	**
11	Dinajpur	24.770	1966	< 0.0001	0.05	R	**
12	Faridpur	31.676	1951	< 0.0001	0.05	R	**
13	Feni	66.219	1973	< 0.0001	0.05	R	**
14	Hatiya	40.680	2004	< 0.0001	0.05	R	**
15	Ishurdi	5.166	2004	0.336	0.05	A	NS
16	Jessore	24.800	1998	< 0.0001	0.05	R	**
17	Khepupara	47.771	1977	< 0.0001	0.05	R	**
18	Khulna	6.176	1950	0.217	0.05	A	NS
19	Kutubdia	59.212	1985	< 0.0001	0.05	R	**
20	M.Court	33.710	1994	< 0.0001	0.05	R	**
21	Madaripur	47.499	1978	< 0.0001	0.05	R	**
22	Mongla	45.726	1998	< 0.0001	0.05	R	**
23	Mymensingh	6.807	1980	0.180	0.05	A	NS
24	Patuakhali	47.490	1994	< 0.0001	0.05	R	**
25	Rajshahi	10.409	1978	0.104	0.05	A	NS
26	Rangamati	15.089	2000	0.001	0.05	R	**
27	Rangpur	38.209	1974	< 0.0001	0.05	R	**
28	Sandwip	36.012	2000	< 0.0001	0.05	R	**
29	Satkhira	7.266	1983	0.128	0.05	A	NS
30	Sitakunda	54.495	1997	< 0.0001	0.05	R	**
31	Srimangal	10.525	2008	0.017	0.05	R	**
32	Sydpur	41.238	1993	< 0.0001	0.05	R	**
33	Sylhet	33.744	1993	< 0.0001	0.05	R	**
34	Tangail	35.997	1987	< 0.0001	0.05	R	**
35	Teknaf	47.986	1983	< 0.0001	0.05	R	**

Note: **Significant at the 95% level of confidence; *Significant at the 90% level of confidence; NS-Not Significant at the 90% level of confidence; A-Accepted at the p>0.05; R-Rejected at the p<0.05

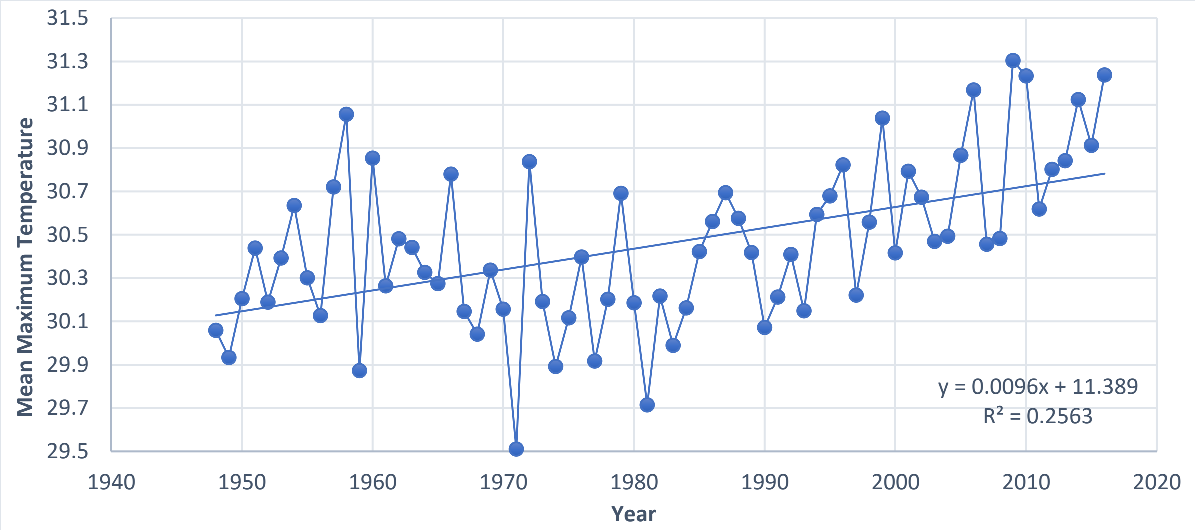

Figure 5.2: Time series of all-Bangladesh annual mean maximum temperatures (1948-2016)

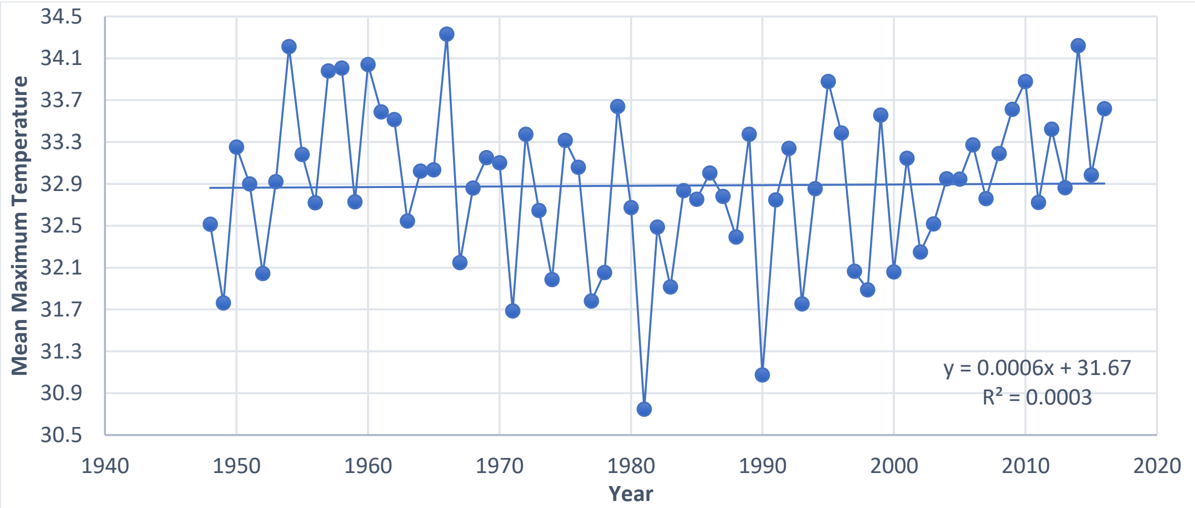

Figure 5.3: Time series of all-Bangladesh pre-monsoon mean maximum temperatures (1948-2016)

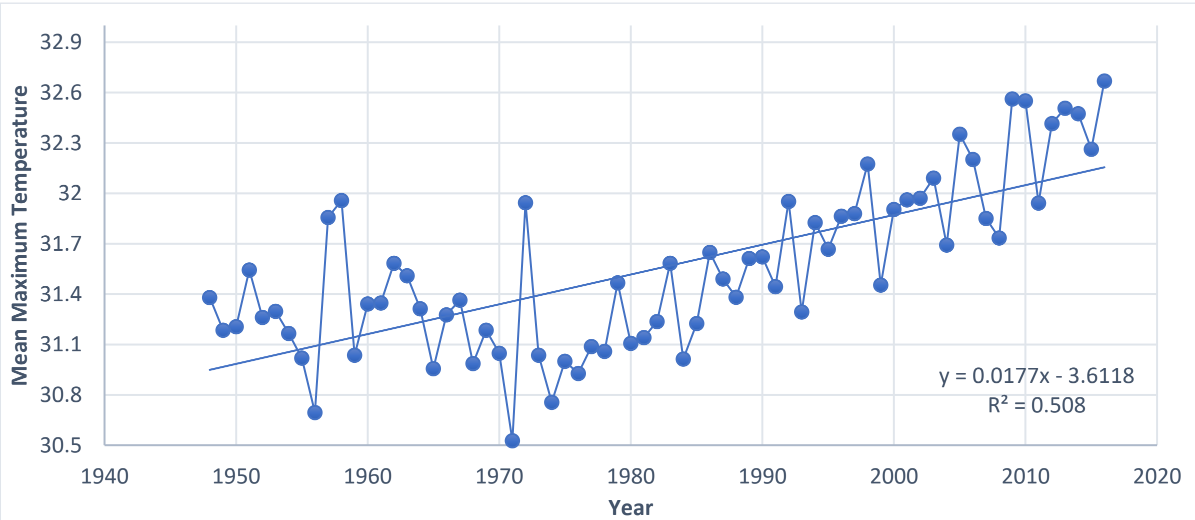

Figure 5.4: Time series of all-Bangladesh monsoon mean maximum temperatures (1948-2016)

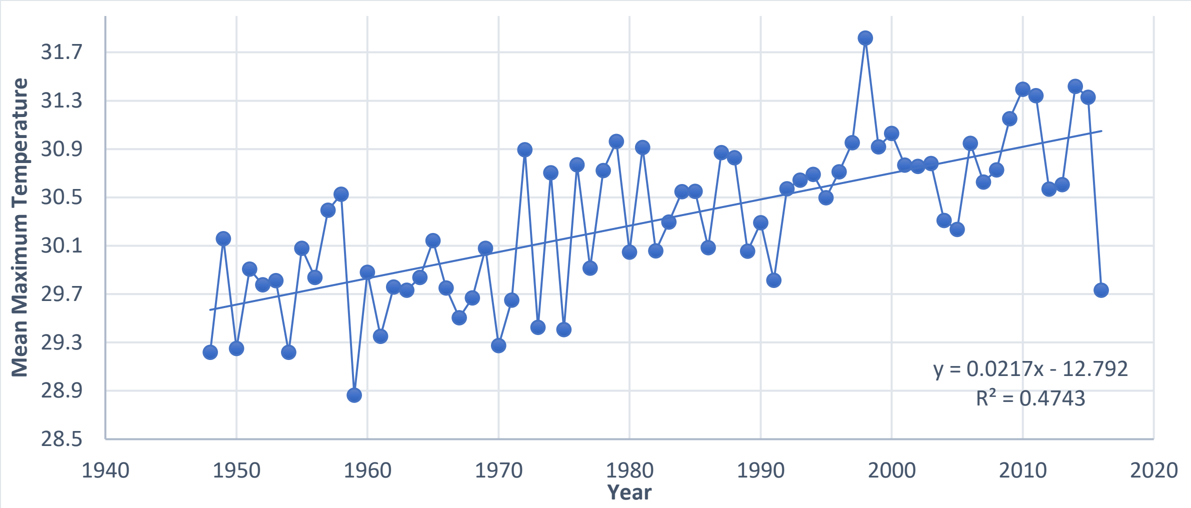

Figure 5.5: Time series of all-Bangladesh post-monsoon mean max temp (1948-2016)

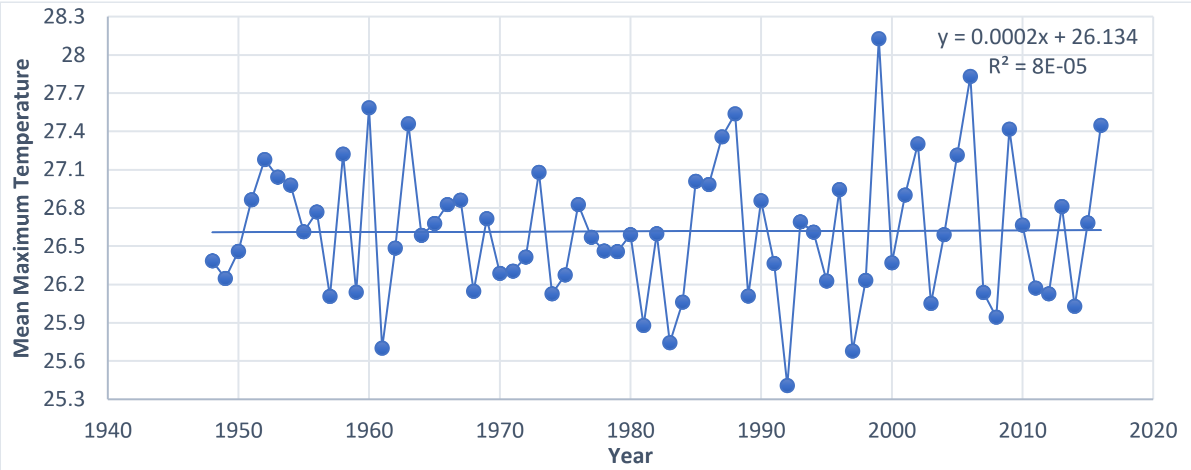

Figure 5.6: Time series of all-Bangladesh winter mean max temperatures (1948-2016)

Normal maximum temperature is expressed as most recent 30 years data compilation. From the normal data, another situation is calculated either maximum temperature will be increase or decrease. It is seen from the above figures that the trends would be quite different during the period of 1987-2016 than that in the entire period (1948-2016). This is particularly evident in the pre-monsoon temperatures (Table 5.3). Therefore, the all-Bangladesh trends in seasonal and annual mean maximum temperatures are also calculated using the data from 1987-2016 are shone in (Table 5.3). The trends in annual maximum temperatures at different stations using recent normal data (1987-2016) were also evaluated. The trends were found to be increasing in maximum stations. The magnitude at individual stations varied between -0.06% to 0.24% of normal annual maximum temperature per year. The spatial distribution of trends expressed as % of normal annual temperature is shown in (Figure 5.7). It is seen from the figure that the north and south-eastern and central part of coastal zone of the country has a higher rate of increase in maximum temperatures compared to the mid to mid-western and mid northern part.

Table 5.3: All-Bangladesh trends in seasonal and annual mean maximum temperatures (1948-2016)

Seasons	**Trend[1] (^{0}C/century)**	**Significance[1]**	**Trend[2] (^{0}C/century)**	**Significance[2]**
Pre-monsoon (Mar-May)	0.06	NS	3.44	**
Monsoon (Jun-Sep)	1.77	**	3.54	**
Post-monsoon (Oct-Nov)	2.33	**	2.05	**
Winter (Dec-Feb)	0.02	NS	-1.53	NS
Annual (Jan-Dec)	0.96	**	2.38	**

Note: [1]using data of all stations from 1948 to 2016; [2]using data of all stations from 1987 to 2016; **Significant at the 95% level of confidence; *Significant at the 90% level of confidence; NS-Not Significant at the 90% level of confidence

It is seen from the (Table 5.3) that the increasing trend in annual maximum temperatures during the 1987-2016 period is about 2.38 ^{0}C per century. This value is two and quarter time higher the value computed using the data for the entire time period (1948-2016). In this study all BMD data were used hence, some anomaly affected calculating the data. Sometimes researchers are ignoring or avoid such kind of unexpected data where one or two days represent the whole month.

In the (Figure 5.4 and 5.5) shows that seasonal maximum temperature trends are high positive relation 0.0177 ^{0}C and 0.0217 ^{0}C per year respectively. But in per-monsoon and winter seasons there are no any relation in increasing and decreasing rate 0.0006 ^{0}C and 0.0002 ^{0}C per year where 0.06 and 0.02 ^{0}C/century respectively.

From the (Table 5.3) the monsoon and post-monsoon trends have become stronger and significant indeed and the pre-monsoon and winter trend have become weaker with not significant at 95% and 90% level of confidence. But in recent period 1987-2016 all seasons are stronger accept winter which is negative trend with not significant. Trends in all-Bangladesh annual and seasonal temperatures are given in (Figure 5.2, 5.3, 5.4, 5.5 and 5.6).

On the other hand, two values are reported in the (Table 5.3) one using the data since 1948 and the other using the recent data since 1987. In (Figure 5.3) it is seen that pre-monsoon increase rate is very much slow and nearly steady. From the bellow (Figure 5.7) showing north-eastern part is hotter region and it’s become hotter. Overall situation of the central region quite normal though the upper Sundarbans region is negative trend.

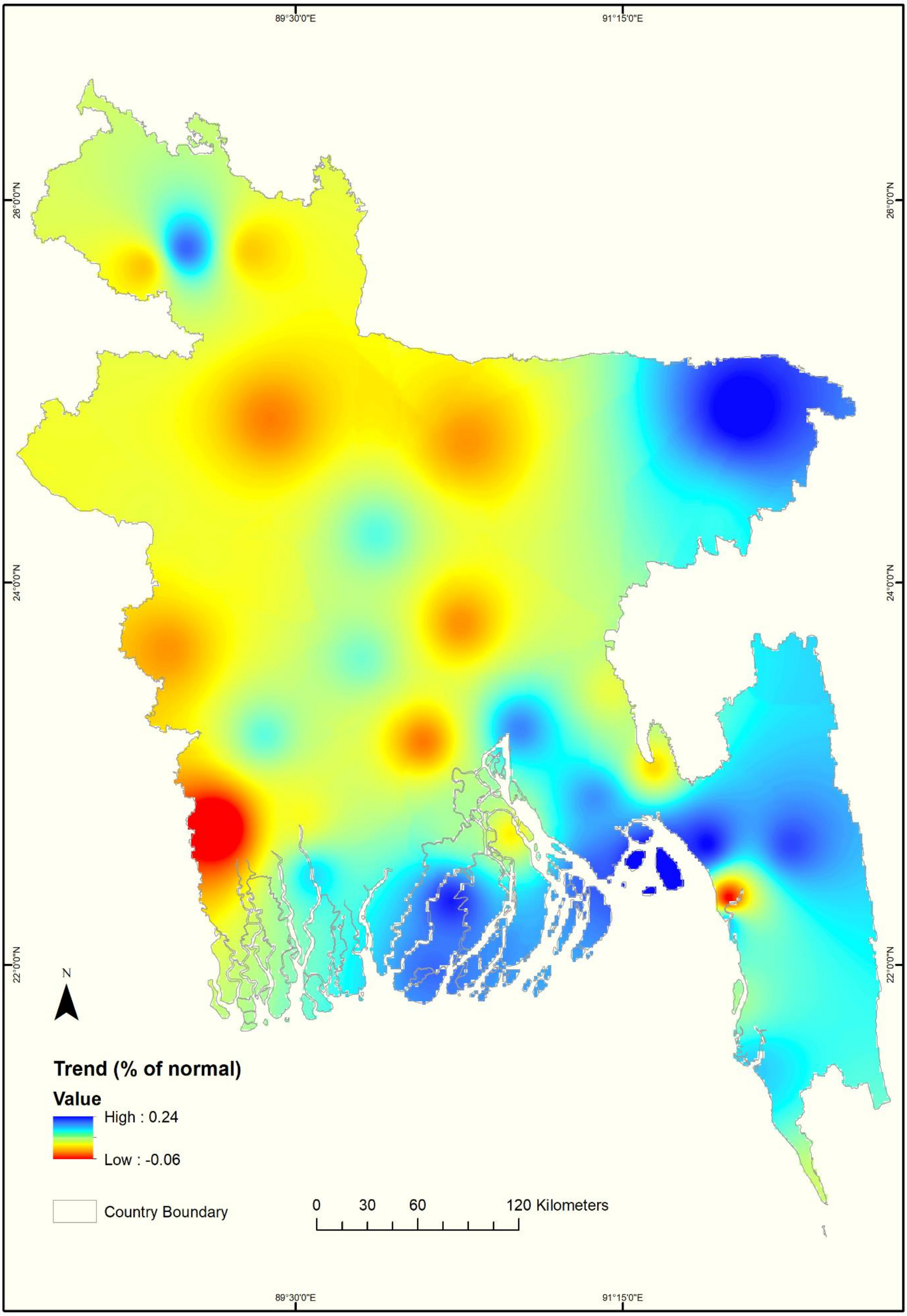

Figure 5.7: Spatial pattern of trends in annual mean maximum temperatures (% of normal) (1987-2016)

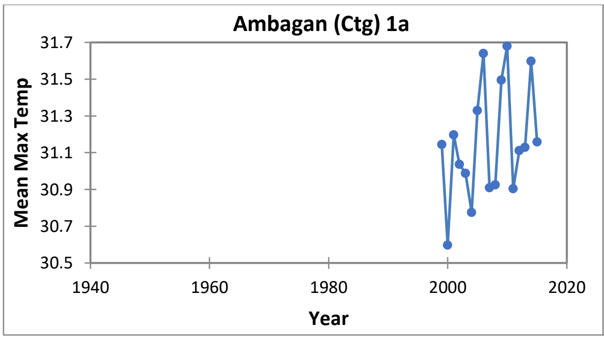
Ambagan (Ctg) 1a
Mean Max Temp
Year

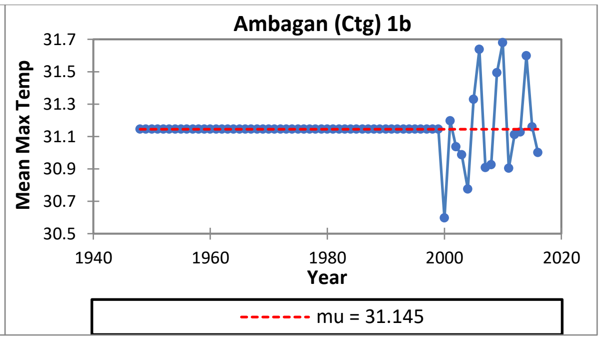
Ambagan (Ctg) 1b
Mean Max Temp
Year
mu = 31.145

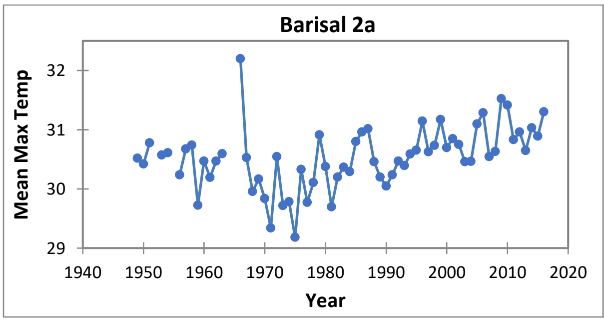
Barisal 2a
Mean Max Temp
Year

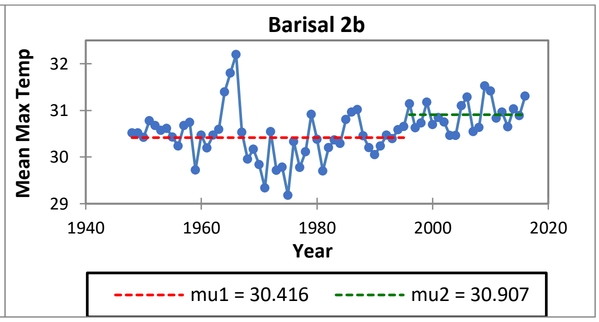
Barisal 2b
Mean Max Temp
Year
mu1 = 30.416
mu2 = 30.907

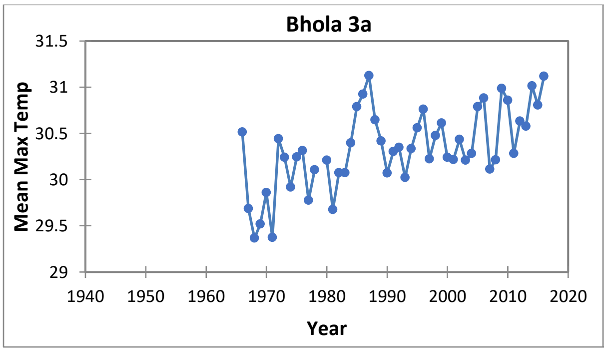
Bhola 3a
Mean Max Temp
Year

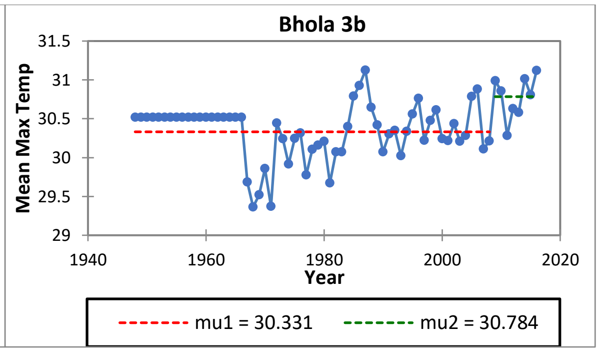
Bhola 3b
Mean Max Temp
Year
mu1 = 30.331
mu2 = 30.784

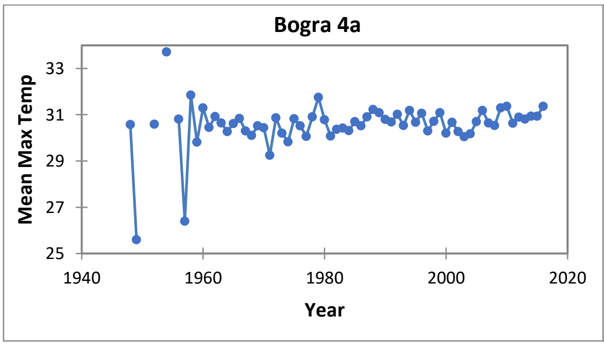
Bogra 4a
Mean Max Temp
Year

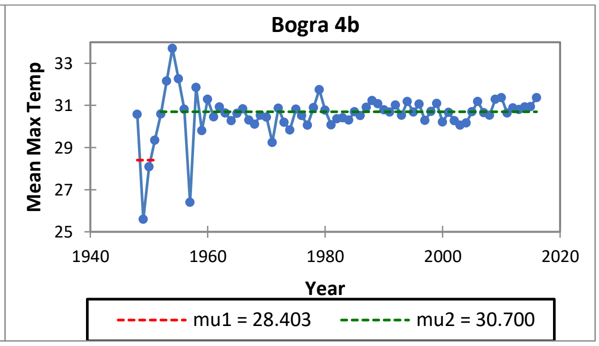
Bogra 4b
Mean Max Temp
Year
mu1 = 28.403
mu2 = 30.700

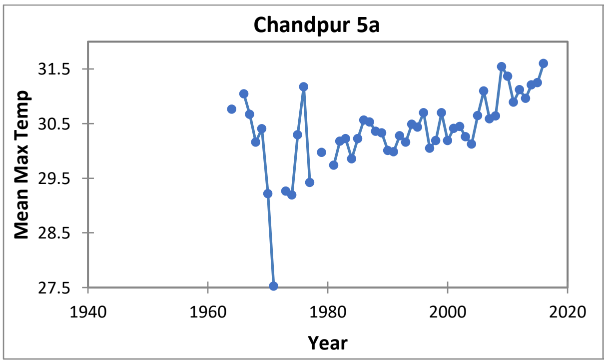
Chandpur 5a
Mean Max Temp
Year

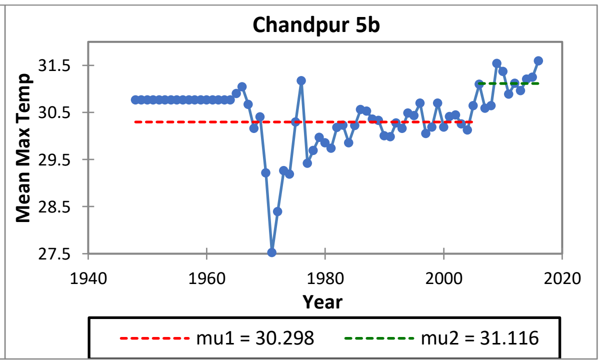
Chandpur 5b
Mean Max Temp
Year
mu1 = 30.298
mu2 = 31.116

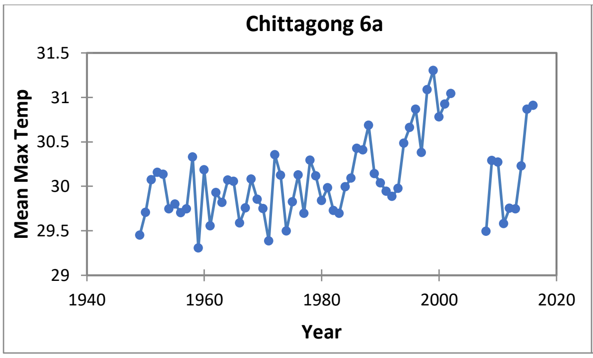
Chittagong 6a
Mean Max Temp
Year

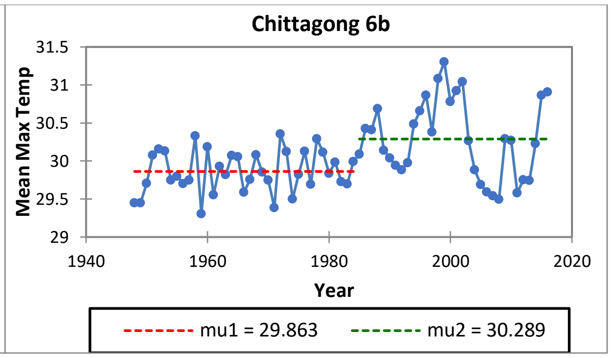
Chittagong 6b
Mean Max Temp
Year
mu1 = 29.863
mu2 = 30.289

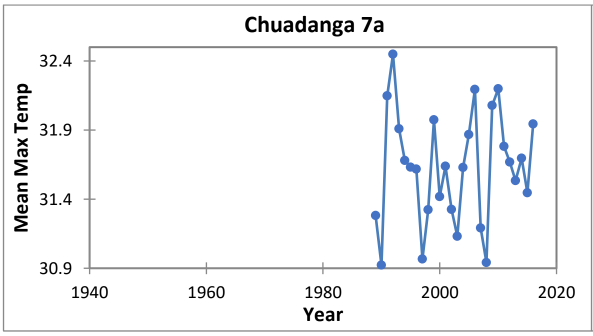
Chuadanga 7a
Mean Max Temp
Year

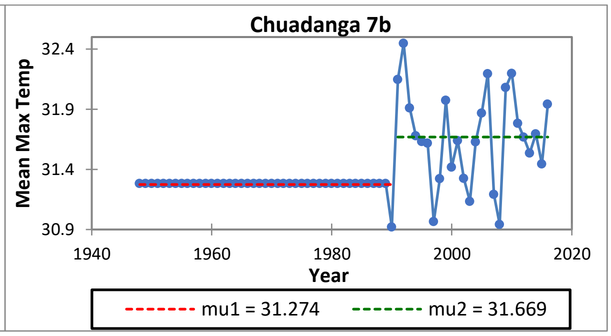
Chuadanga 7b
Mean Max Temp
Year
mu1 = 31.274
mu2 = 31.669

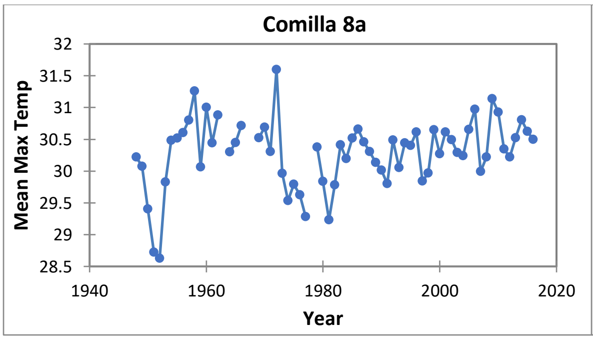
Comilla 8a
Mean Max Temp
Year

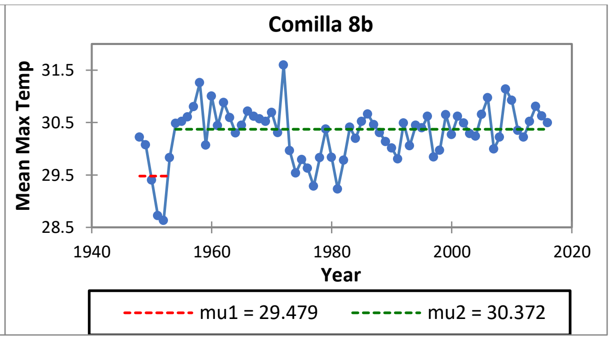
Comilla 8b
Mean Max Temp
Year
mu1 = 29.479
mu2 = 30.372

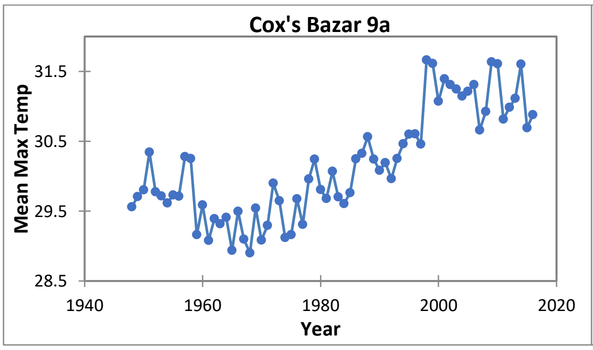
Cox's Bazar 9a
Mean Max Temp
Year

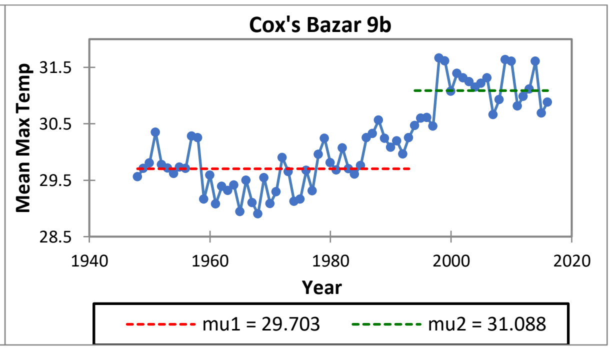
Cox's Bazar 9b
Mean Max Temp
Year
mu1 = 29.703
mu2 = 31.088

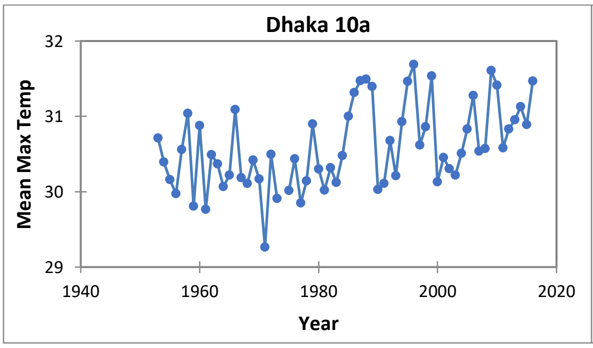
Dhaka 10a
Mean Max Temp
Year

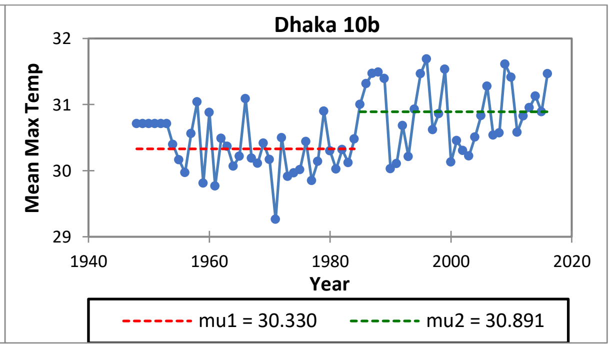
Dhaka 10b
Mean Max Temp
Year
mu1 = 30.330
mu2 = 30.891

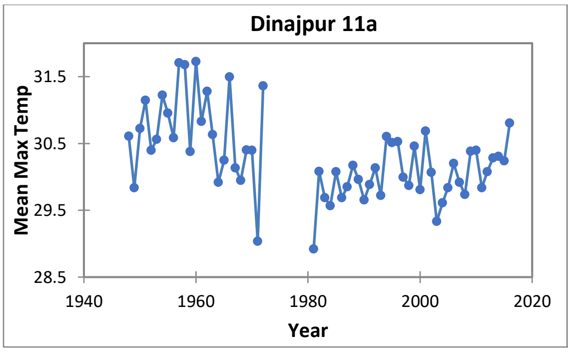
Dinajpur 11a
Mean Max Temp
31.5
30.5
29.5
28.5
1940
1960
1980
2000
2020
Year

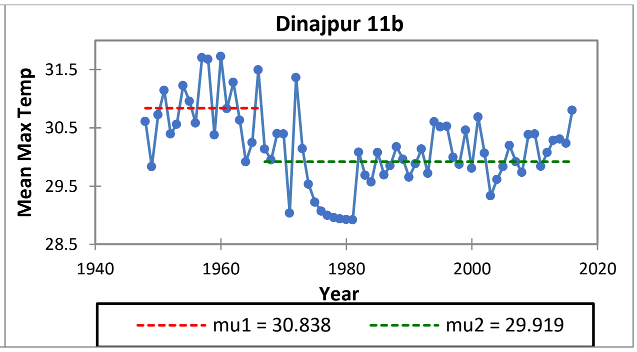
Dinajpur 11b
Mean Max Temp
31.5
30.5
29.5
28.5
1940
1960
1980
2000
2020
Year
mu1 = 30.838
mu2 = 29.919

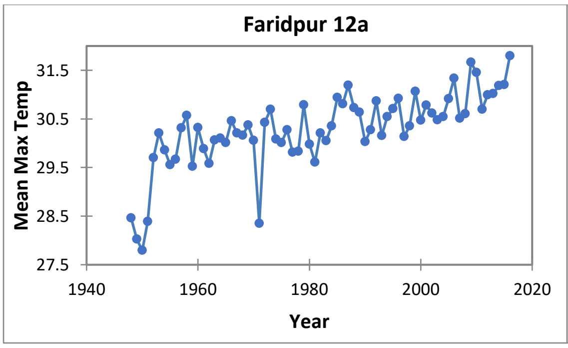
Faridpur 12a
Mean Max Temp
31.5
30.5
29.5
28.5
27.5
1940
1960
1980
2000
2020
Year

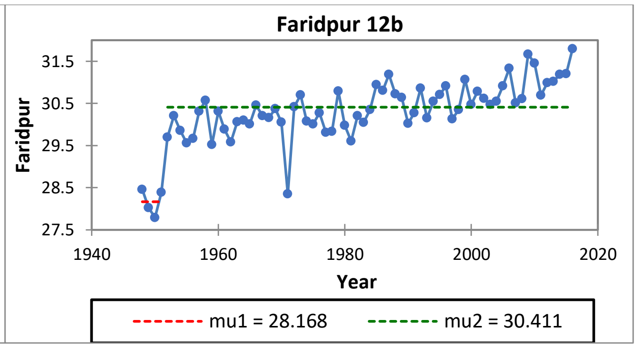
Faridpur 12b
Faridpur
31.5
30.5
29.5
28.5
27.5
1940
1960
1980
2000
2020
Year
mu1 = 28.168
mu2 = 30.411

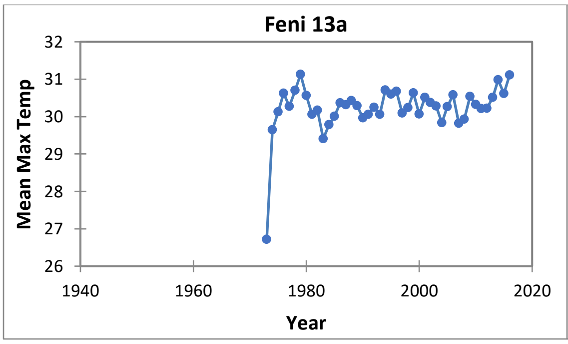
Feni 13a
Mean Max Temp
32
31
30
29
28
27
26
1940
1960
1980
2000
2020
Year

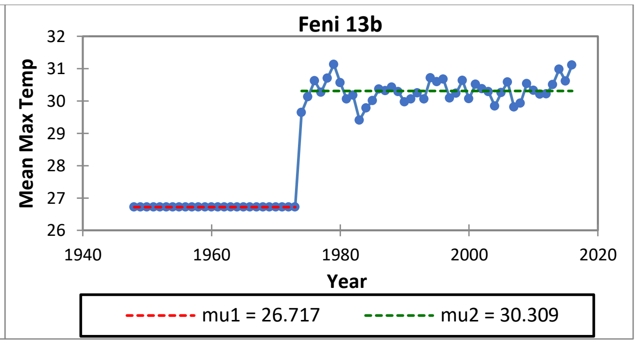
Feni 13b
Mean Max Temp
32
31
30
29
28
27
26
1940
1960
1980
2000
2020
Year
mu1 = 26.717
mu2 = 30.309

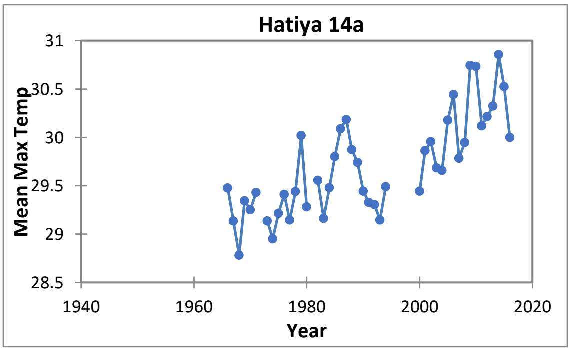
Hatiya 14a
Mean Max Temp
31
30.5
30
29.5
29
28.5
1940
1960
1980
2000
2020
Year

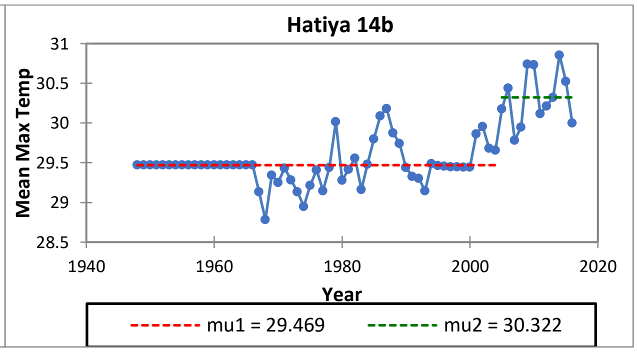
Hatiya 14b
Mean Max Temp
31
30.5
30
29.5
29
28.5
1940
1960
1980
2000
2020
Year
mu1 = 29.469
mu2 = 30.322

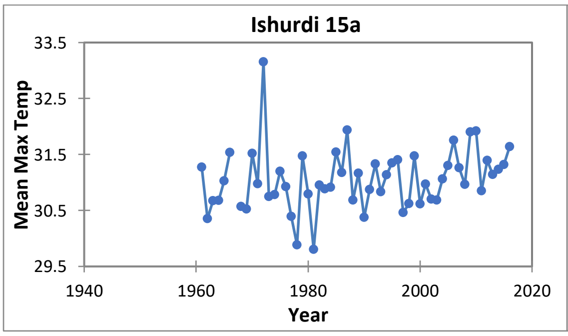
Ishurdi 15a
Mean Max Temp
33.5
32.5
31.5
30.5
29.5
1940
1960
1980
2000
2020
Year

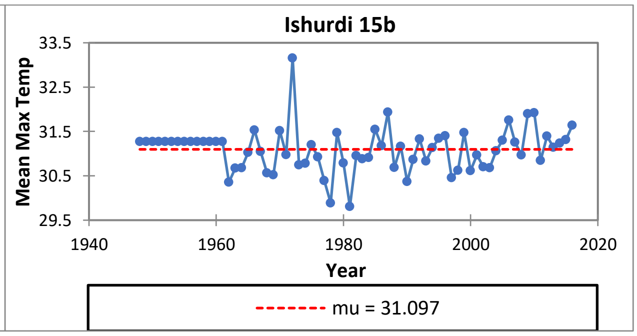
Ishurdi 15b
Mean Max Temp
33.5
32.5
31.5
30.5
29.5
1940
1960
1980
2000
2020
Year
mu = 31.097

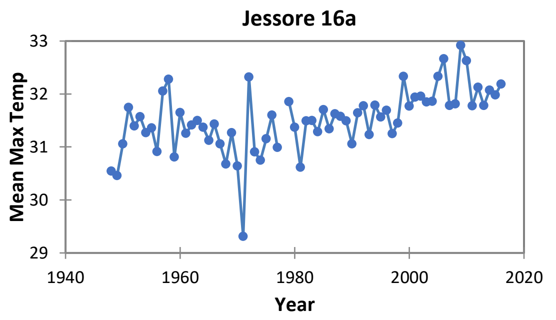
Jessore 16a
Mean Max Temp
33
32
31
30
29
1940
1960
1980
2000
2020
Year

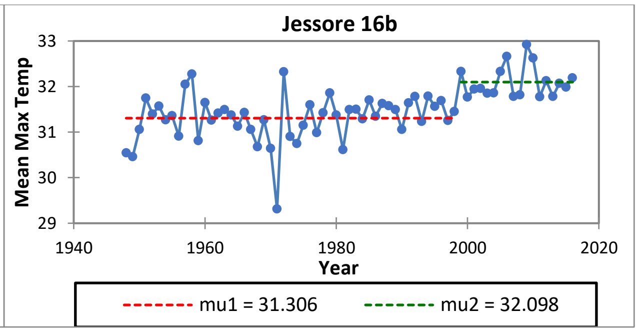
Jessore 16b
Mean Max Temp
33
32
31
30
29
1940
1960
1980
2000
2020
Year
mu1 = 31.306
mu2 = 32.098

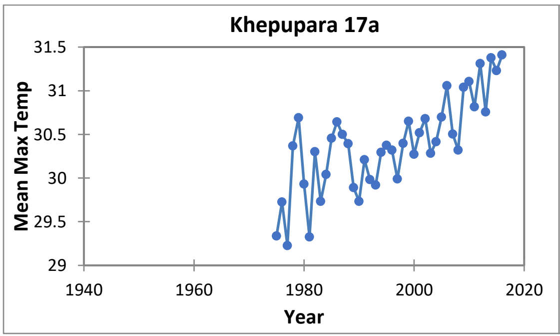
Khepupara 17a
Mean Max Temp
31.5
31
30.5
30
29.5
29
1940
1960
1980
2000
2020
Year

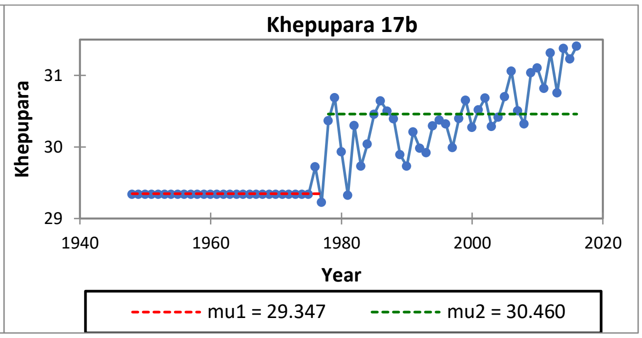
Khepupara 17b
Khepupara
31
30
29
1940
1960
1980
2000
2020
Year
mu1 = 29.347
mu2 = 30.460

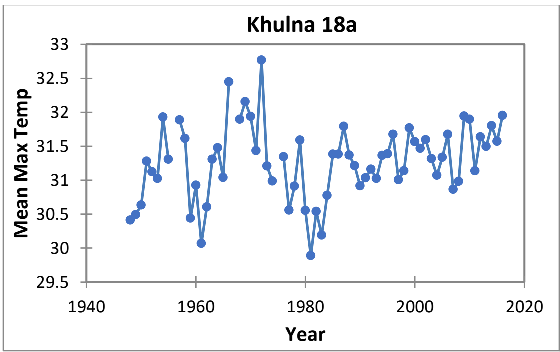
Khulna 18a
Mean Max Temp
33
32.5
32
31.5
31
30.5
30
29.5
1940
1960
1980
2000
2020
Year

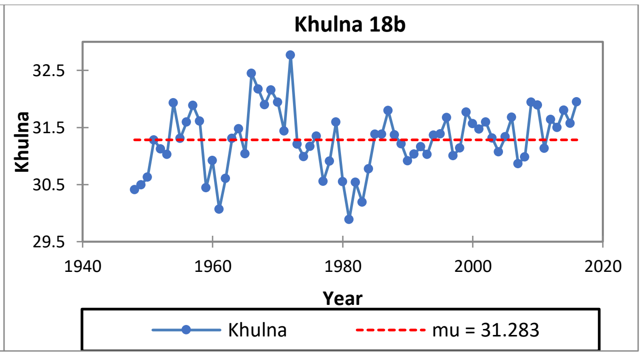
Khulna 18b
Khulna
32.5
31.5
30.5
29.5
1940
1960
1980
2000
2020
Year
Khulna
mu = 31.283

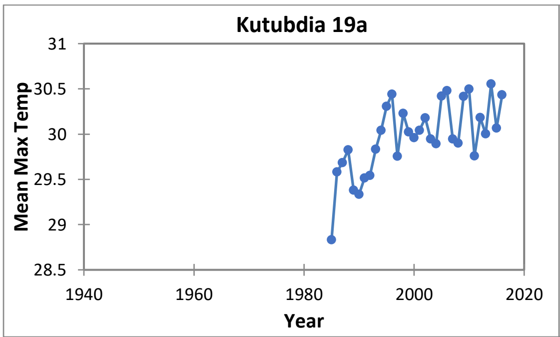
Kutubdia 19a
Mean Max Temp
31
30.5
30
29.5
29
28.5
1940
1960
1980
2000
2020
Year

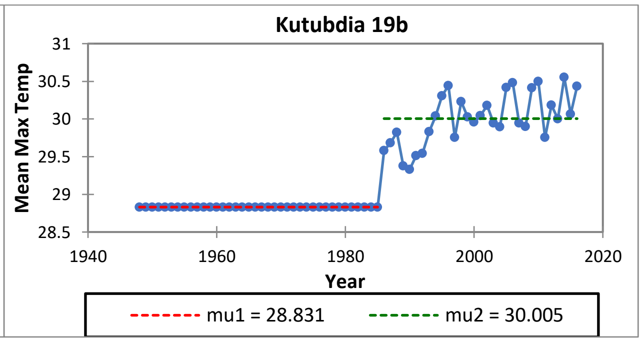
Kutubdia 19b
Mean Max Temp
31
30.5
30
29.5
29
28.5
1940
1960
1980
2000
2020
Year
mu1 = 28.831
mu2 = 30.005

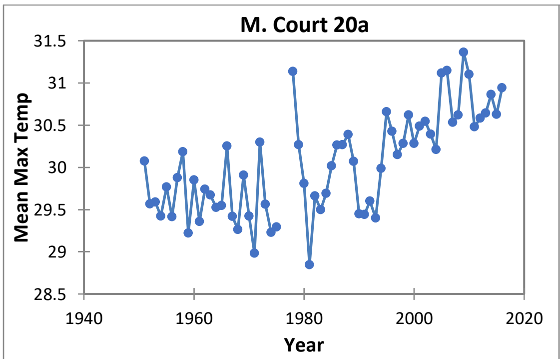
M. Court 20a
Mean Max Temp
31.5
31
30.5
30
29.5
29
28.5
1940
1960
1980
2000
2020
Year

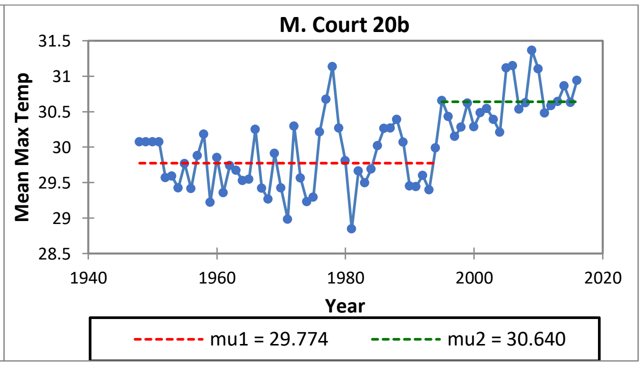
M. Court 20b
Mean Max Temp
31.5
31
30.5
30
29.5
29
28.5
1940
1960
1980
2000
2020
Year
mu1 = 29.774
mu2 = 30.640

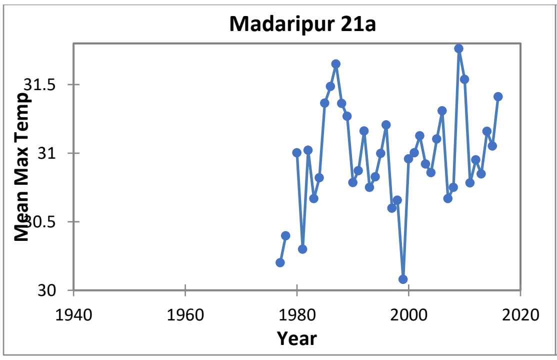
Madaripur 21a
Mean Max Temp
31.5
31
30.5
30
1940
1960
1980
2000
2020
Year

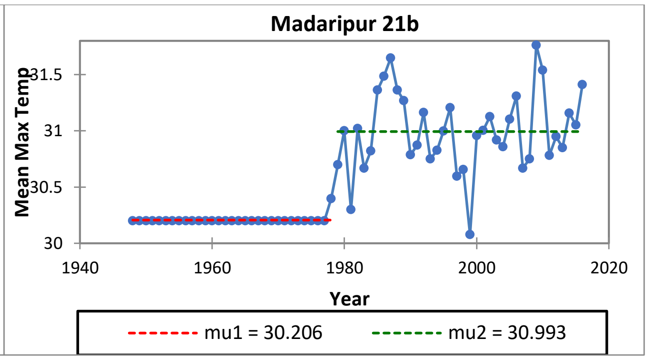
Madaripur 21b
Mean Max Temp
31.5
31
30.5
30
1940
1960
1980
2000
2020
Year
mu1 = 30.206
mu2 = 30.993

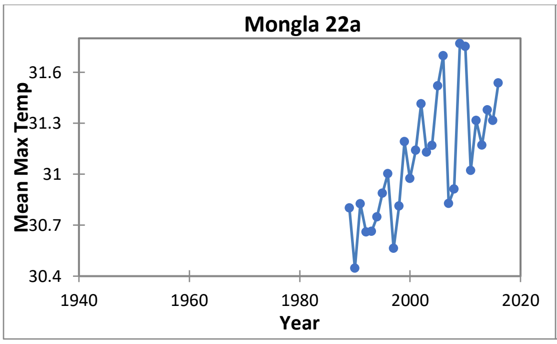
Mongla 22a
Mean Max Temp
31.6
31.3
31
30.7
30.4
1940
1960
1980
2000
2020
Year

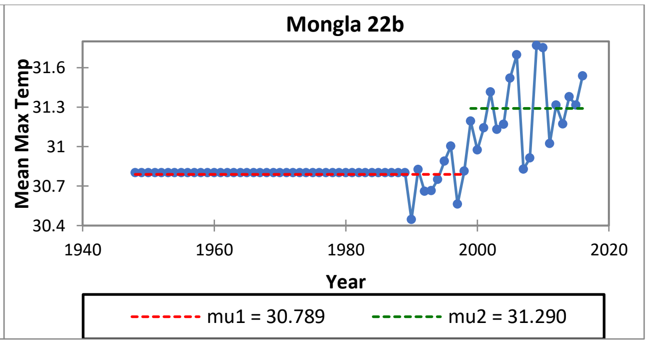
Mongla 22b
Mean Max Temp
31.6
31.3
31
30.7
30.4
1940
1960
1980
2000
2020
Year
mu1 = 30.789
mu2 = 31.290

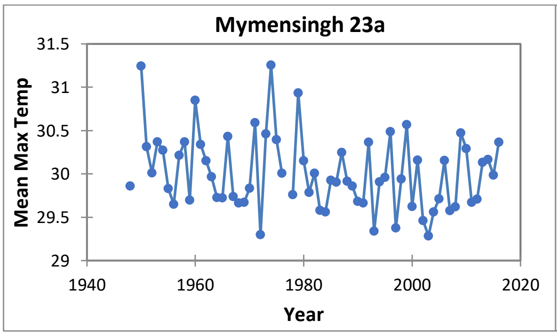
Mymensingh 23a
Mean Max Temp
31.5
31
30.5
30
29.5
29
1940
1960
1980
2000
2020
Year

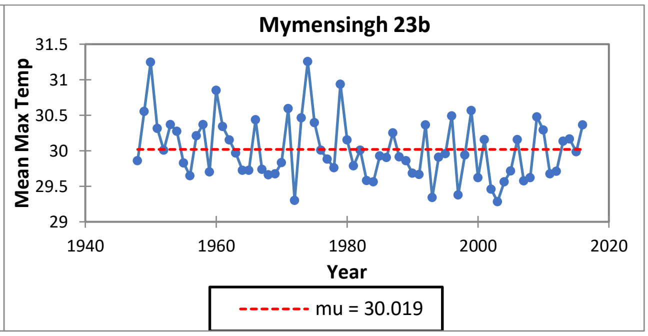
Mymensingh 23b
Mean Max Temp
31.5
31
30.5
30
29.5
29
1940
1960
1980
2000
2020
Year
mu = 30.019

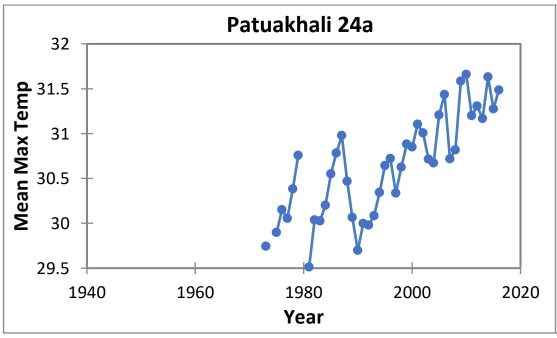
Patuakhali 24a
Mean Max Temp
32
31.5
31
30.5
30
29.5
1940
1960
1980
2000
2020
Year

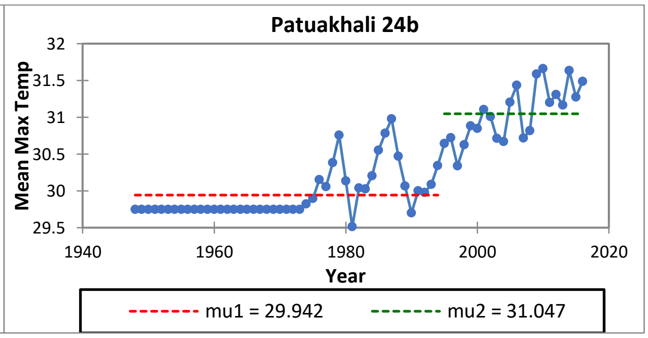
Patuakhali 24b
Mean Max Temp
32
31.5
31
30.5
30
29.5
1940
1960
1980
2000
2020
Year
mu1 = 29.942
mu2 = 31.047

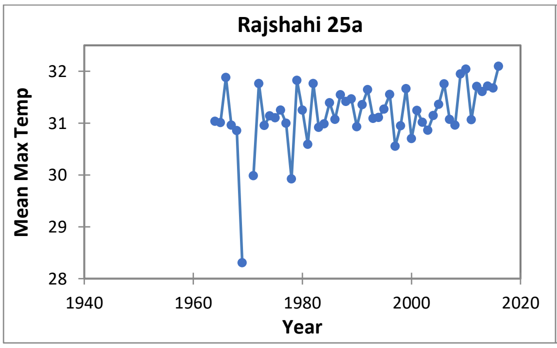
Rajshahi 25a
Mean Max Temp
32
31
30
29
28
1940
1960
1980
2000
2020
Year

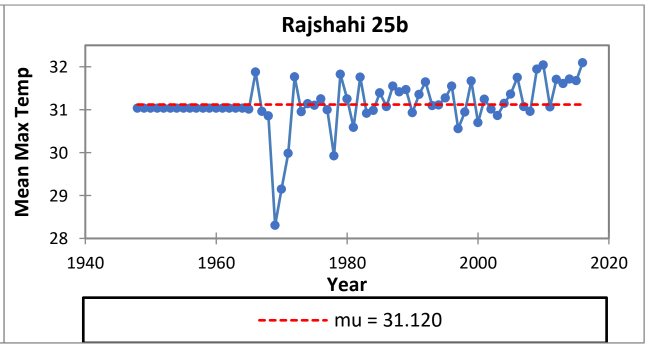
Rajshahi 25b
Mean Max Temp
32
31
30
29
28
1940
1960
1980
2000
2020
Year
mu = 31.120

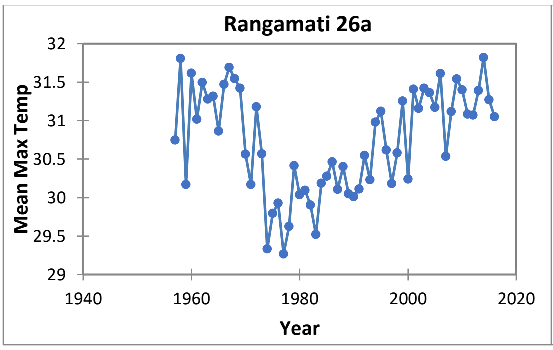
Rangamati 26a
Mean Max Temp
Year

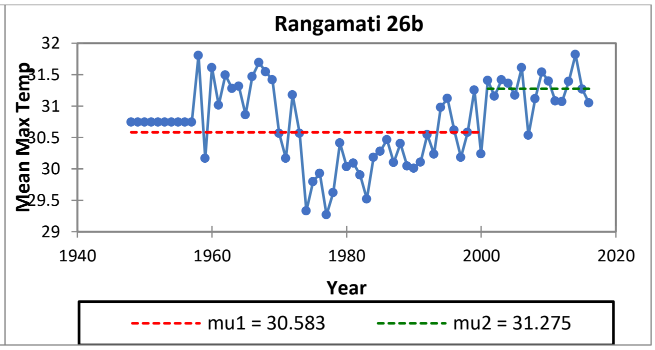
Rangamati 26b
Mean Max Temp
Year
mu1 = 30.583
mu2 = 31.275

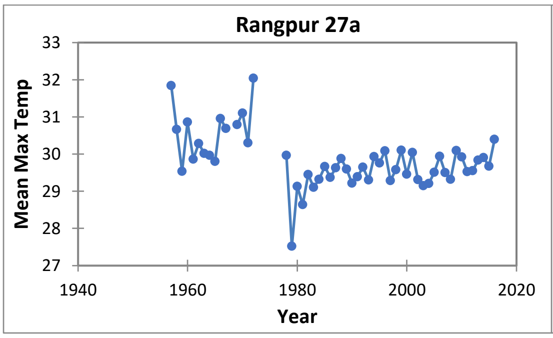
Rangpur 27a
Mean Max Temp
Year

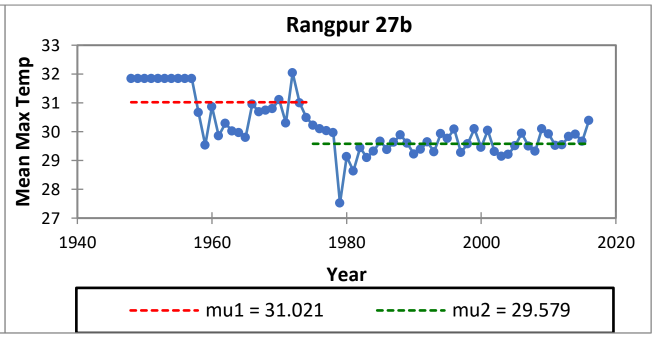
Rangpur 27b
Mean Max Temp
Year
mu1 = 31.021
mu2 = 29.579

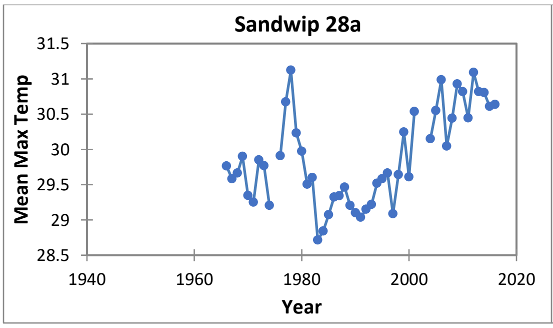
Sandwip 28a
Mean Max Temp
Year

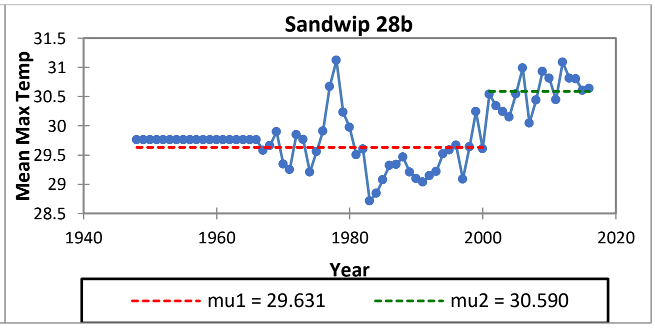
Sandwip 28b
Mean Max Temp
Year
mu1 = 29.631
mu2 = 30.590

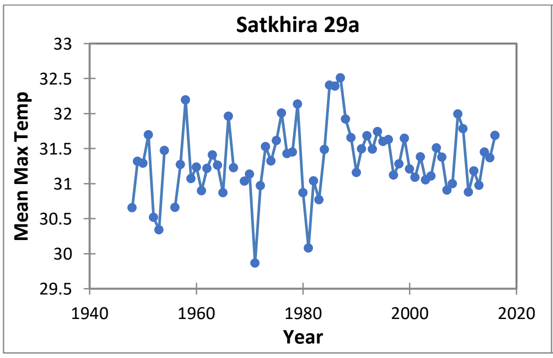
Satkhira 29a
Mean Max Temp
Year

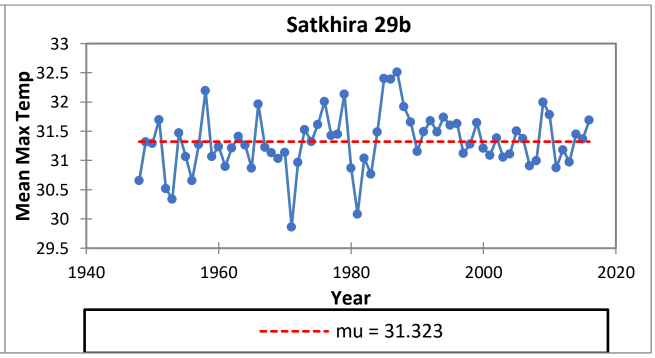
Satkhira 29b
Mean Max Temp
Year
mu = 31.323

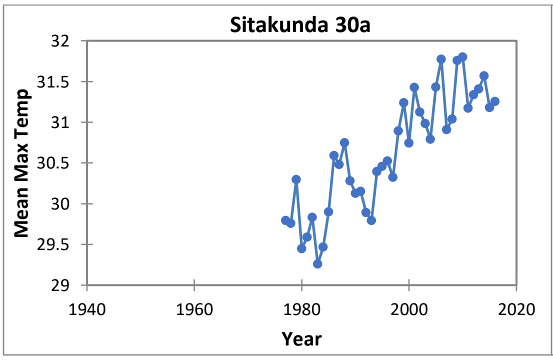
Sitakunda 30a
Mean Max Temp
Year

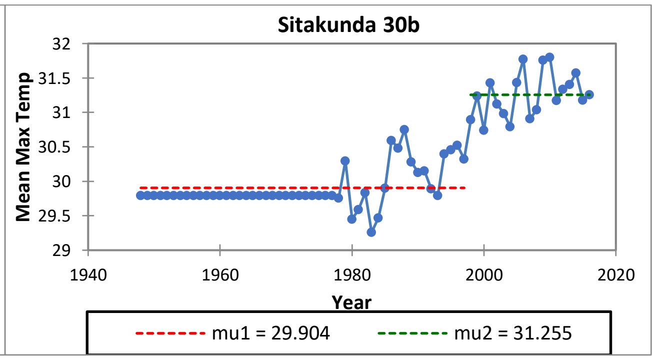
Sitakunda 30b
Mean Max Temp
Year
mu1 = 29.904
mu2 = 31.255

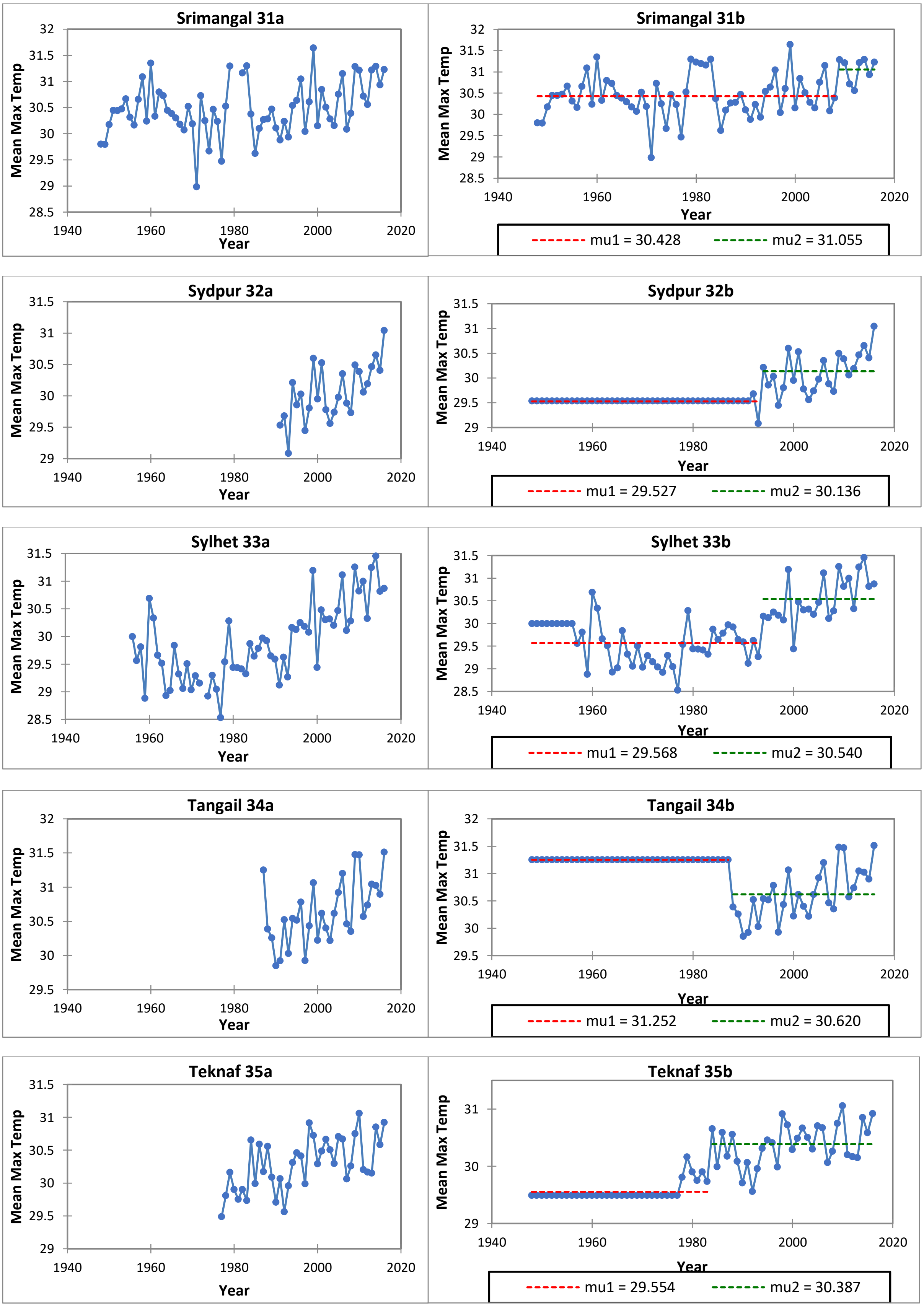

Figure 19(5.8): Changing year in annual maximum temperature all stations MK(a) & SNHT(b) test

Compering with the Mann-Kendall and Standard Normal Homogeneity Test (SNHT) defer a little bit. Mainly MK(a) and SNHT(b) comparing two side (Figure 5.8) filling gape year (b) with average value. Value shows the same (average value) if the gape year started from beginning and value is quite well when it is in the middle. Hence, trend curve should be different from MK to SNHT because trend curve is measured entire data beginning to present where data is filled by average with before and after but beginning data is plotted based on before value. It was not possible to interpolate beginning year by XLSTAT that's why only average value was added in the beginning year where it is required an individual station.

Kendall's tau test is widely used to testing the hypothesis. In (Table 5.1) clearly shows that whether the station is significant or not. In that table 25 stations were increased 3 stations were decreased where 2 stations were decreased with 90% level of confidence and 7 stations change were not significant.

4.4 Homogeneity tests *P*-value Approximation

From homogeneity test *P*-value (two-tailed) was calculated (Table 5.1). For all tests, XLSTAT provides *p*-values using Monte Carlo resampling. Exact calculations are either impossible or too costly in computing time. From SNHT (Table 5.2) is generated where *p*-value and significant values were measured.

In this chapter homogeneity analysis shows that 35 annual maximum temperature series (station wise) are merely same as mean temperature (Table 4.2) and look like as heterogeneous around the year 1948-2016, it means there is a significant change in the mean before and after the detected change point. SNHT test is known to find change point towards find the changes in the middle of a series (Mart´ınez *et. al.,* 2009). The results given in (Table 5.2) are showing most of the series homogenous.

SNHT tests shows that there are 21 common stations where all the tests are in about to same change point year with high significant same as mean temperature. The changes in the mean of these series along with the temperature plots are shown in figure 19. Of these 14 stations, 8 stations show also significant with 95% level of confidence and 6 stations are not significant at the change point. The figures clearly show that there is a noticeable change in the maximum temperature mean of the series before and after the change point in all the stations. In (Figure 5.8) no data were manipulated and ignored triple star sign in raw data.

Chapter Six

Analysis of Observed Minimum Temperature

6.1 Introduction

The lowest temperature recorded-diurnally, monthly, seasonally, or annually, or the lowest temperature of the entire record (Encyclopedia, 1998)[9]. Daily dry bulb air temperature minima are recorded by the screen minimum thermometer. The Approved Code of Practice (2015) suggests the minimum temperature in a workplace should normally be at least 16 degrees Celsius, if the work involves rigorous physical effort, the temperature should be at least 13 degrees Celsius.[10]

6.2 Local Data Analysis

In this chapter local data daily, minimum temperatures were available at 35 locations for a period of 69 years (1948-2016). The estimated trends in mean minimum annual temperatures for 35 stations are given in (Table 6.1). It is seen from the bellow table that almost all the stations one third of Bangladesh exhibit increasing trends in mean minimum annual temperatures. In fact, 4 stations seen decreasing trend where 9 stations are not enough for negative trend (Table 6.1). In my analysis including all 35 stations suggests that the trend is 1.41 ^{0}C per century (100 years) (Table 6.3). The corresponding pre-monsoon (March-May), monsoon (June-September), post-monsoon (October-November) and winter (December-February) trends are 1.55, 0.97, 1.13 and 1.97 ^{0}C per century respectively (Table 6.3).

6.3 Time Series Analysis

Kendall's τ and Spearman's ρ used to measure linear monotonic associations between year and observed data. Both τ and ρ are rank-based procedures-the latter being dependent on the actual magnitudes of the two variables, while the former being not dependent on them. The values of these correlation coefficients indicate the presence or absence of the trend and its direction I = increasing and D = decreasing (Table 6.1). However, the coefficient does not indicate whether the trend is statistically significant or not at a given confidence level. At 5% significance level, 6 stations which hypothesis of homogeneity of trends is accepted and 29 stations of trends is rejected during 1948-2016.

[9] http://www.encyclopedia.com/science/dictionaries-thesauruses-pictures-and-press-releases/minimum-emperature-1
[10] http://www.hse.gov.uk/temperature/law.htm

Figure 6.1: Locations of the BMD climatic stations used in the study (minimum temperature)

Table 6.1: Results of the Mann-Kendall test for annual mean minimum temperature data for all-Bangladesh (1948-2016)

Stations	Available Year	Kendall's tau	S	Var(S)	*P* (Two-tailed)	alpha	Test Int.	Trend ^{0}C/100 y	Sig.
Ambagan(Ctg)	18	0.072	11.00	0.000	0.709	0.05	A	0.69	NS
Barisal	64	-0.032	-64.00	29792.00	0.715	0.05	A	-0.66	NS
Bhola	50	0.402	493.00	14291.67	< 0.0001	0.05	R	1.67	**I
Bogra	65	0.372	774.00	31200.00	< 0.0001	0.05	R	3.46	**I
Chandpur	49	0.233	274.00	31200.00	0.018	0.05	R	1.34	**I
Chittagong	63	0.345	673.00	28427.00	< 0.0001	0.05	R	1.22	**I
Chuadanga	28	-0.016	-6.00	28427.00	0.922	0.05	A	0.00	NS
Comilla	65	0.201	418.00	31200.00	0.018	0.05	R	0.49	**I
Cox's Bazar	69	0.594	1394.00	37275.33	< 0.0001	0.05	R	2.17	**I
Dhaka	63	0.634	1239.00	28427.00	< 0.0001	0.05	R	2.48	**I
Dinajpur	61	0.367	672.00	25823.33	< 0.0001	0.05	R	1.29	**I
Faridpur	69	0.384	900.00	37275.33	< 0.0001	0.05	R	1.87	**I
Feni	44	0.304	288.00	37275.33	0.003	0.05	R	2.63	**I
Hatiya	44	-0.207	-196.00	37275.33	0.048	0.05	R	-1.56	**D
Ishurdi	55	0.305	453.00	18975.00	0.001	0.05	R	0.52	**I
Jessore	68	0.293	668.00	35688.67	0.000	0.05	R	0.81	**I
Khepupara	42	0.013	11.00	35688.67	0.914	0.05	A	0.12	NS
Khulna	66	0.030	65.00	32651.67	0.723	0.05	A	0.14	NS
Kutubdia	32	0.274	136.00	32651.67	0.028	0.05	R	1.90	**I
M.Court	64	0.481	970.00	29792.00	< 0.0001	0.05	R	2.28	**I
Madaripur	39	0.358	265.00	29792.00	0.001	0.05	R	2.81	**I
Mongla	28	0.138	52.00	29792.00	0.317	0.05	A	0.62	NS
Mymensingh	65	0.360	748.00	31200.00	< 0.0001	0.05	R	0.97	**I
Patuakhali	42	0.110	95.00	31200.00	0.311	0.05	A	1.88	NS
Rajshahi	52	0.060	80.00	16059.33	0.533	0.05	A	0.46	NS
Rangamati	60	-0.255	-452.00	24583.33	0.004	0.05	R	-1.66	**D
Rangpur	54	0.442	633.00	17967.00	< 0.0001	0.05	R	2.52	**I
Sandwip	48	-0.218	-246.00	17967.00	0.029	0.05	R	-1.64	**D
Satkhira	67	0.342	757.00	34147.67	< 0.0001	0.05	R	1.28	**I
Sitakunda	40	-0.208	-162.00	34147.67	0.060	0.05	R	-1.93	*D
Srimangal	67	0.423	935.00	34147.67	< 0.0001	0.05	R	2.04	**I
Sydpur	26	0.268	87.00	34147.67	0.058	0.05	R	1.62	*I
Sylhet	60	0.329	582.00	24583.33	0.000	0.05	R	1.23	**I
Tangail	30	-0.071	-31.00	24583.33	0.596	0.05	A	-1.38	NS
Teknaf	40	0.346	270.00	24583.33	0.001	0.05	R	1.79	**I

Note: **Significant at the 95% level of confidence; *Significant at the 90% level of confidence; NS-Not Significant at the 90% level of confidence; A-Accepted at the p>0.05; R-Rejected at the p<0.05; I-Increased; D-Decreases

Table 6.2: Results of the Standard Normal Homogeneity Test (SNHT) for annual mean minimum temperature data for all-Bangladesh (1948-2016)

Sl. No.	Stations	T0	t	p-value (Two-tailed)	alpha	Test Int.	Sig.
1	Ambagan(Ctg)	31.413	1999	< 0.0001	0.05	R	**
2	Barisal	17.853	1966	0.039	0.05	R	**
3	Bhola	14.852	1966	0.004	0.05	R	**
4	Bogra	20.637	1957	0.066	0.05	A	*
5	Chandpur	40.781	1965	< 0.0001	0.05	R	**
6	Chittagong	25.982	1994	< 0.0001	0.05	R	**
7	Chuadanga	29.483	1989	< 0.0001	0.05	R	**
8	Comilla	8.687	2004	0.124	0.05	A	NS
9	Cox's Bazar	41.218	1982	< 0.0001	0.05	R	**
10	Dhaka	34.215	1983	< 0.0001	0.05	R	**
11	Dinajpur	17.259	1984	0.002	0.05	R	**
12	Faridpur	21.188	1976	0.004	0.05	R	**
13	Feni	66.666	1973	< 0.0001	0.05	R	**
14	Hatiya	23.117	1982	< 0.0001	0.05	R	**
15	Ishurdi	20.372	1961	0.033	0.05	R	**
16	Jessore	17.215	1952	0.001	0.05	R	**
17	Khepupara	6.624	1977	0.232	0.05	A	NS
18	Khulna	3.487	1971	0.449	0.05	A	NS
19	Kutubdia	28.800	1997	< 0.0001	0.05	R	**
20	M.Court	29.534	1989	< 0.0001	0.05	R	**
21	Madaripur	40.816	1987	< 0.0001	0.05	R	**
22	Mongla	15.506	2014	0.008	0.05	R	**
23	Mymensingh	11.795	1978	0.017	0.05	R	**
24	Patuakhali	11.804	1973	0.097	0.05	A	*
25	Rajshahi	9.641	1964	0.086	0.05	A	*
26	Rangamati	26.387	1960	< 0.0001	0.05	R	**
27	Rangpur	28.941	1957	< 0.0001	0.05	R	**
28	Sandwip	25.265	2000	< 0.0001	0.05	R	**
29	Satkhira	16.526	1972	0.003	0.05	R	**
30	Sitakunda	56.723	1977	< 0.0001	0.05	R	**
31	Srimangal	34.732	1975	< 0.0001	0.05	R	**
32	Sydpur	55.798	1993	< 0.0001	0.05	R	**
33	Sylhet	17.433	1956	0.048	0.05	R	**
34	Tangail	66.269	1987	< 0.0001	0.05	R	**
35	Teknaf	54.292	1978	< 0.0001	0.05	R	**

Note: **Significant at the 95% level of confidence; *Significant at the 90% level of confidence; NS-Not Significant at the 90% level of confidence; A-Accepted at the p>0.05; R-Rejected at the p<0.05

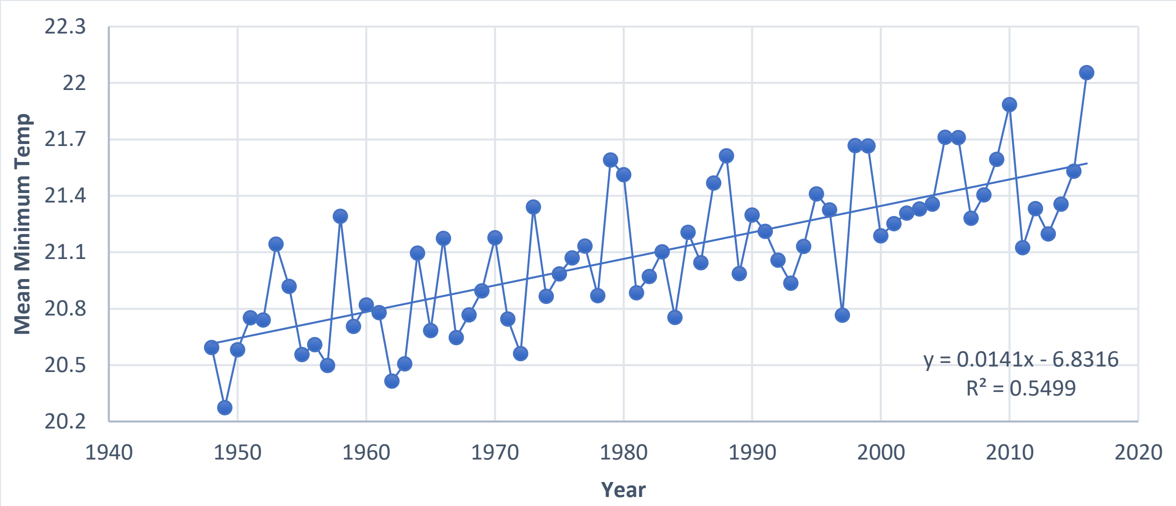

Figure 6.2: Time series of all-Bangladesh annual mean minimum temperatures (1948-2016)

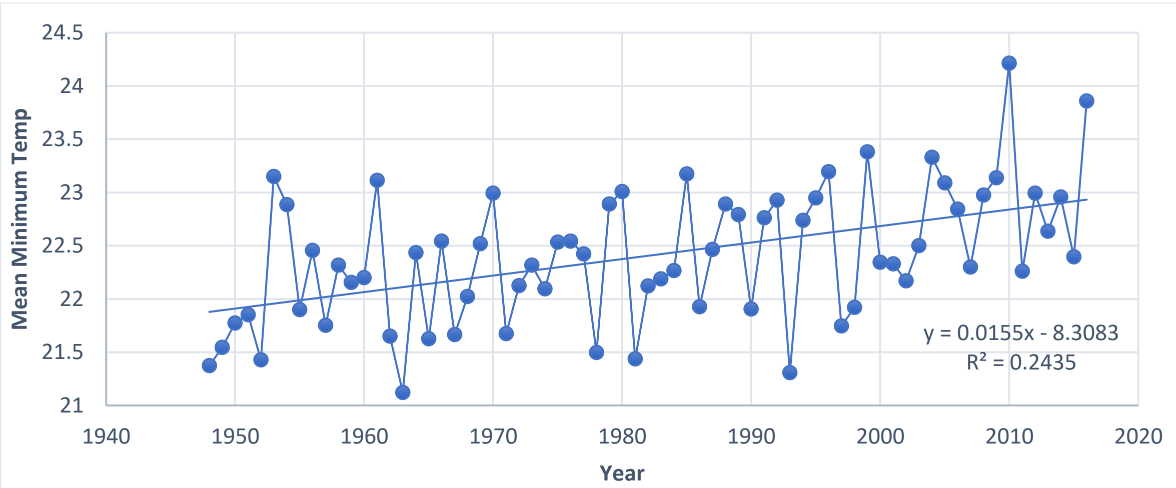

Figure 6.3: Time series of all-Bangladesh pre-monsoon mean minimum temperatures (1948-2016)

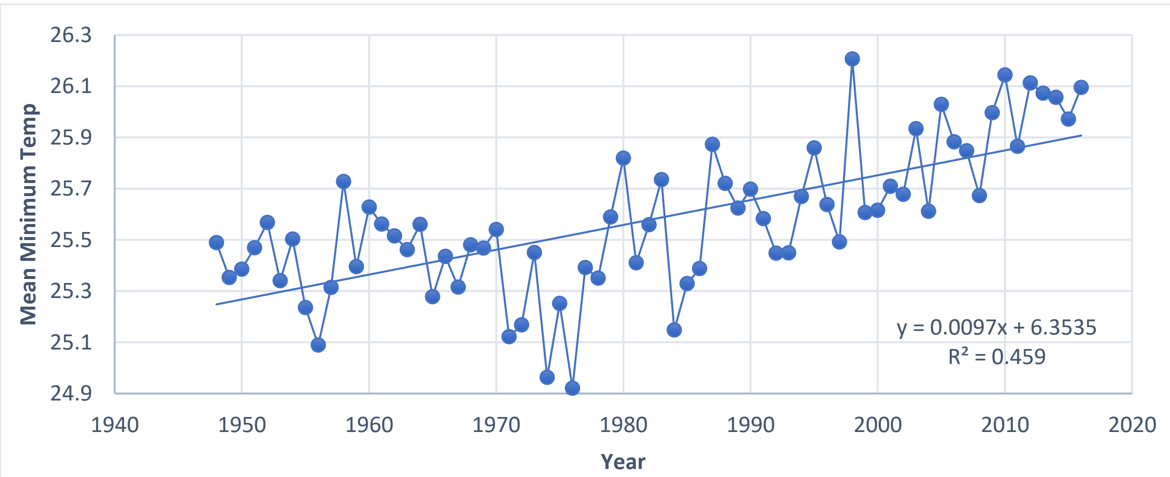

Figure 6.4: Time series of all-Bangladesh monsoon mean minimum temperatures (1948-2016)

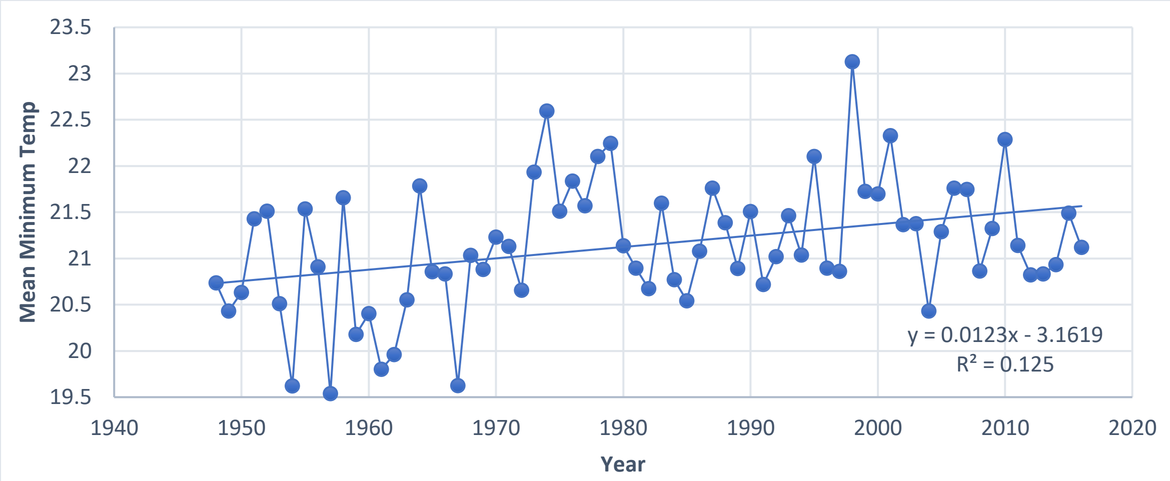

Figure 6.5: Time series of all-Bangladesh post-monsoon mean minimum temperatures (1948-2016)

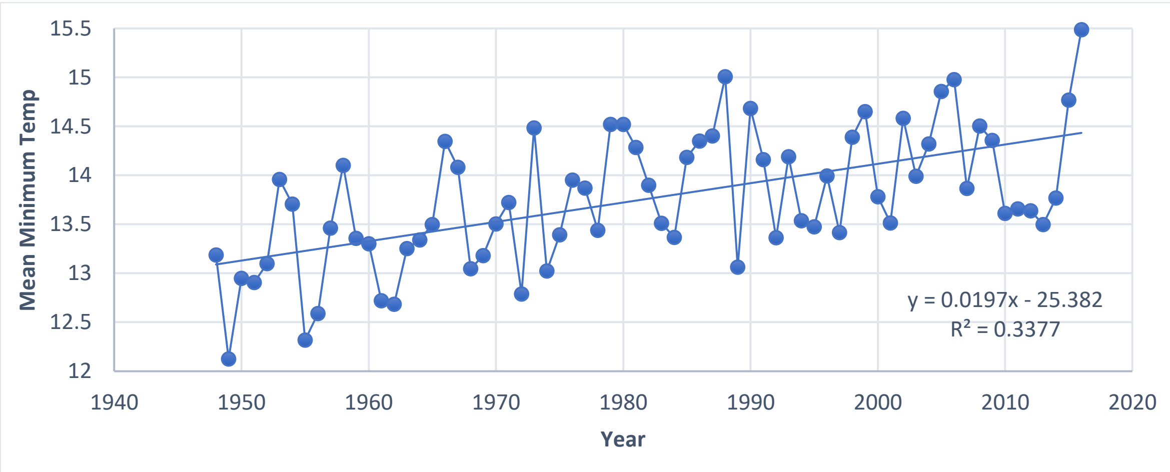

Figure 6.6: Time series of all-Bangladesh winter mean minimum temperatures (1948-2016)

Normal minimum temperature is expressed as most recent 30 years data compilation. From the normal data, another situation is calculated either minimum temperature will be increase or decrease. It is seen from the above figures that the trends would be quite different during the period of 1987-2016 than that in the entire period (1948-2016). This is particularly evident in the pre-monsoon and winter temperatures (Table 6.3). Therefore, the all-Bangladesh trends in seasonal and annual mean minimum temperatures are also calculated using the data from 1987-2016 are shone in (Table 6.3). The trends in annual minimum temperatures at different stations using recent normal data (1987-2016) were also evaluated. The trends were found to be increasing in maximum stations. The magnitude at individual stations varied between -0.12% to 0.24% of normal annual minimum temperature per year (Figure 6.7). The spatial distribution of trends expressed as % of normal annual temperature is shown in (Figure 6.7). It is seen from the figure that the north-eastern part of the country has a higher rate of increase and middle to Meghna estuary has a higher rate of decrease in minimum temperatures.

Table 6.3: All-Bangladesh trends in seasonal and annual mean minimum temperatures (1948-2016)

Seasons	**Trend[1] (^{0}C/century)**	**Significance[1]**	**Trend[2] (^{0}C/century)**	**Significance[2]**
Pre-monsoon (Mar-May)	1.55	**	2.32	NS
Monsoon (Jun-Sep)	0.97	**	1.59	**
Post-monsoon (Oct-Nov)	1.13	**	-0.61	**
Winter (Dec-Feb)	1.97	**	0.93	NS
Annual (Jan-Dec)	1.41	**	1.24	**

Note: [1]using data of all stations from 1948 to 2016; [2]using data of all stations from 1987 to 2016; **Significant at the 95% level of confidence; *Significant at the 90% level of confidence; NS-Not Significant at the 90% level of confidence

It is seen from the (Table 6.3) that the increasing trend in annual minimum temperatures during the 1987-2016 period is about 1.24 ^{0}C per century. This value is about to similar with the value computed using the data for the entire time period (1948-2016). In this study all BMD data were used hence, some anomaly affected calculating the data. Sometimes researchers are ignoring or avoid such kind of unexpected data where one or two days represent the whole month.

In the (Figure 6.3 and 6.6) shows that seasonal minimum temperature trends are high positive relation 0.0155 ^{0}C and 0.0197 ^{0}C per year respectively. But in monsoon and post-monsoon seasons are not negligible because both are relation in increasing rate 0.0097 ^{0}C and 0.0123 ^{0}C per year where 0.97 and 1.13 ^{0}C/century respectively.

From the (Table 6.3) the pre-monsoon and winter trends have become stronger and significant indeed and the monsoon and post-monsoon trend have become weaker but have significant at 95% level of confidence. But in recent period 1987-2016 monsoon and post-monsoon seasons are stronger with post-monsoon is negative trend on the other hand, pre-monsoon and winter which have not significant either 95% or 90% level of confidence.

Trends in all-Bangladesh annual and seasonal temperatures are given in (Figure 6.2, 6.3, 6.4, 6.5 and 6.6). On the contrary two values are reported in the (Table 6.3) one using the data since 1948 and the other using the recent data since 1987. In (Figure 6.2, 6.3, 6.4, 6.5 and 6.6) is seen that all seasonal and annual increase rate are positive. From the bellow (Figure 6.7) showing north-eastern part is hotter region and it's become hotter. Overall situation of the north Bengal quite normal though the central part and Meghna estuary region is negative trend and south-eastern hilly region and mid-western region also a little bit negative trend.

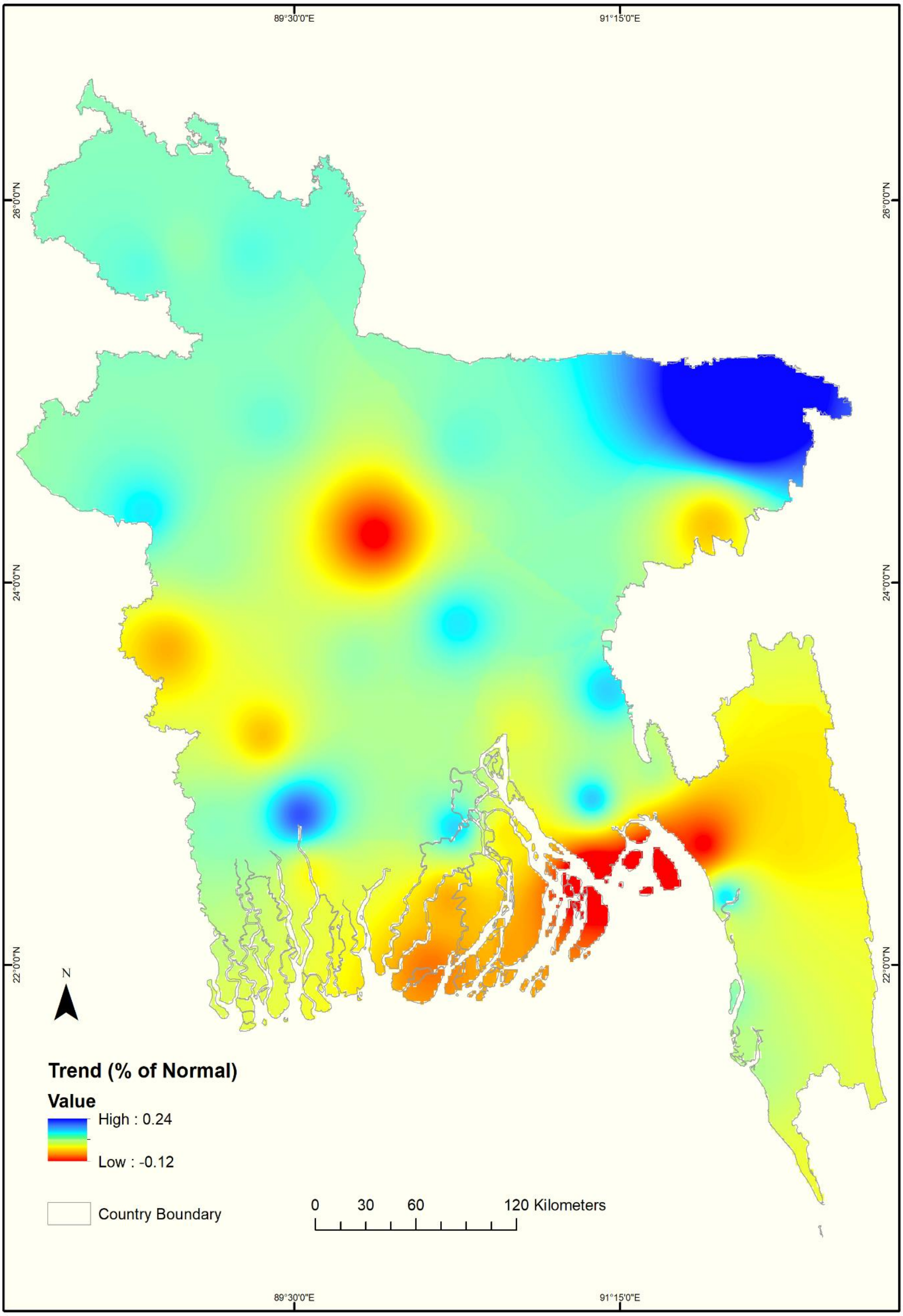

Figure 6.7: Spatial pattern of trends in annual mean minimum temperatures (% of normal) (1987-2016)

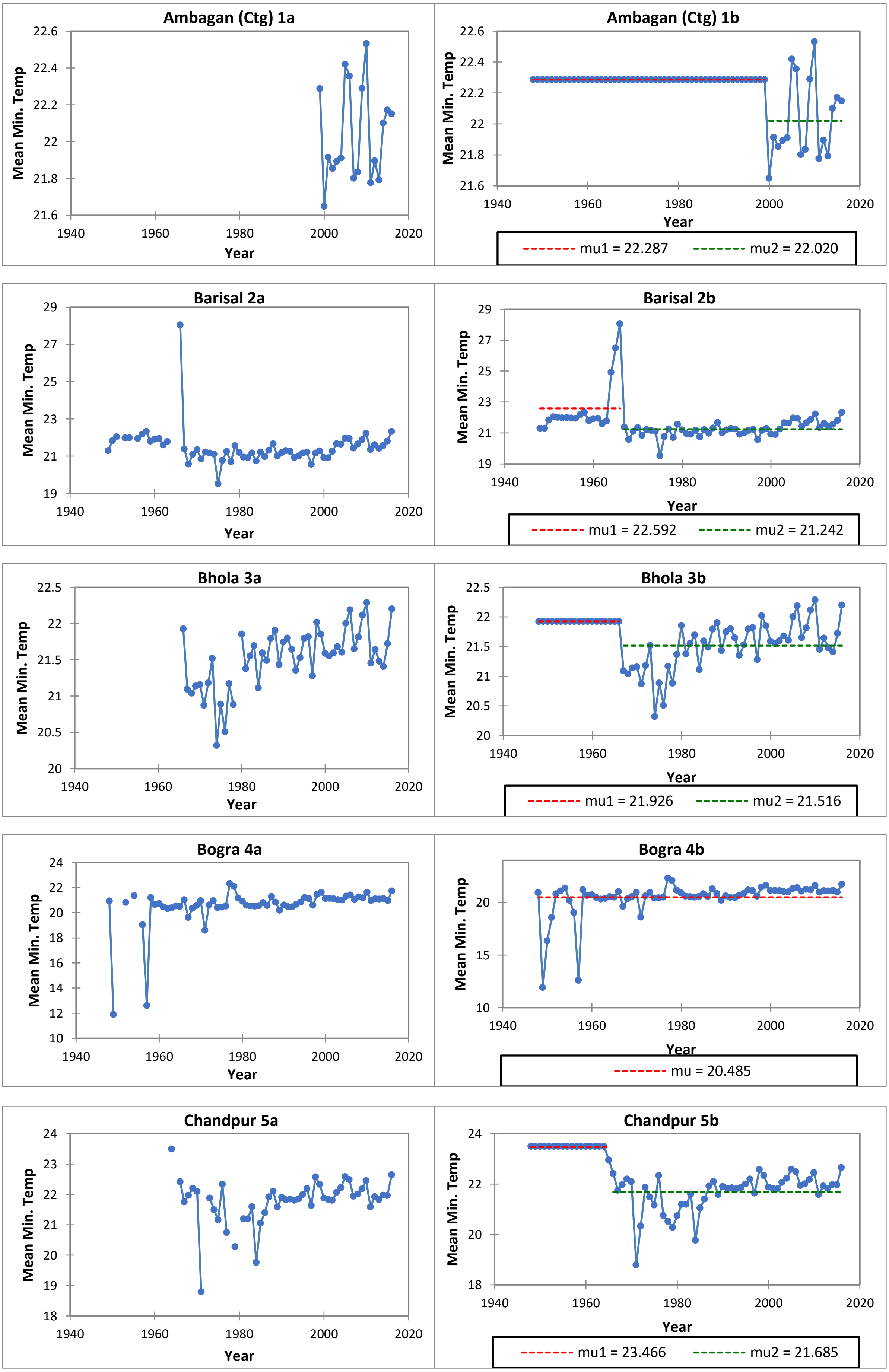
Ambagan (Ctg) 1a
Mean Min. Temp
Year
Ambagan (Ctg) 1b
Mean Min. Temp
Year
mu1 = 22.287
mu2 = 22.020
Barisal 2a
Mean Min. Temp
Year
Barisal 2b
Mean Min. Temp
Year
mu1 = 22.592
mu2 = 21.242
Bhola 3a
Mean Min. Temp
Year
Bhola 3b
Mean Min. Temp
Year
mu1 = 21.926
mu2 = 21.516
Bogra 4a
Mean Min. Temp
Year
Bogra 4b
Mean Min. Temp
Year
mu = 20.485
Chandpur 5a
Mean Min. Temp
Year
Chandpur 5b
Mean Min. Temp
Year
mu1 = 23.466
mu2 = 21.685

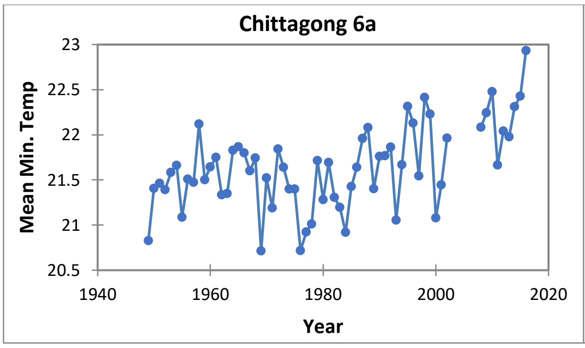
Chittagong 6a
Mean Min. Temp
Year
23
22.5
22
21.5
21
20.5
1940
1960
1980
2000
2020

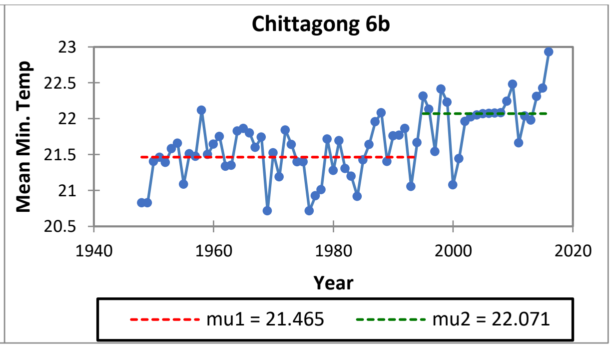
Chittagong 6b
Mean Min. Temp
Year
23
22.5
22
21.5
21
20.5
1940
1960
1980
2000
2020
mu1 = 21.465
mu2 = 22.071

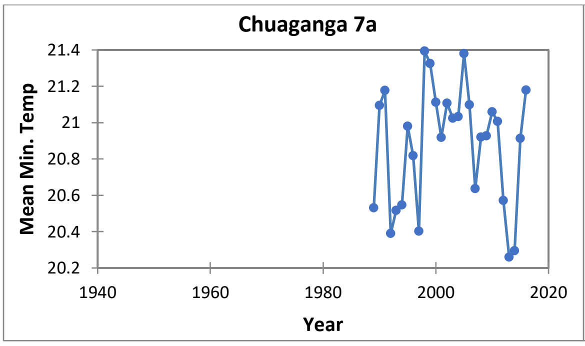
Chuaganga 7a
Mean Min. Temp
Year
21.4
21.2
21
20.8
20.6
20.4
20.2
1940
1960
1980
2000
2020

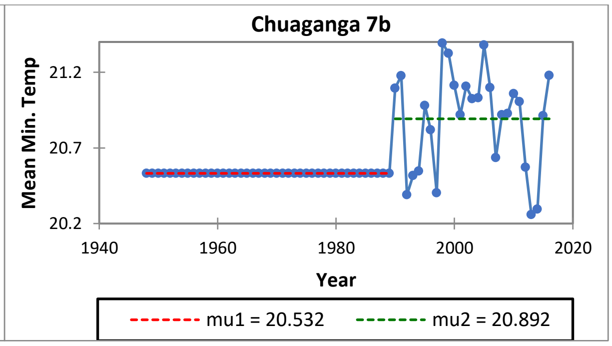
Chuaganga 7b
Mean Min. Temp
Year
21.2
20.7
20.2
1940
1960
1980
2000
2020
mu1 = 20.532
mu2 = 20.892

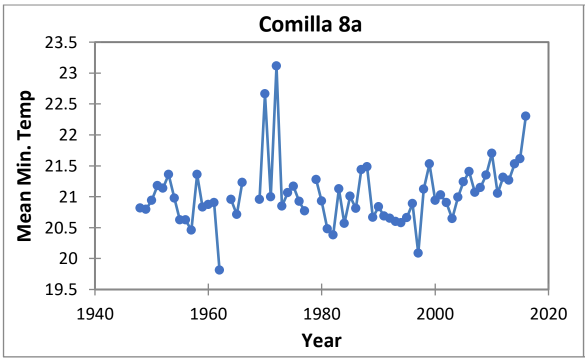
Comilla 8a
Mean Min. Temp
Year
23.5
23
22.5
22
21.5
21
20.5
20
19.5
1940
1960
1980
2000
2020

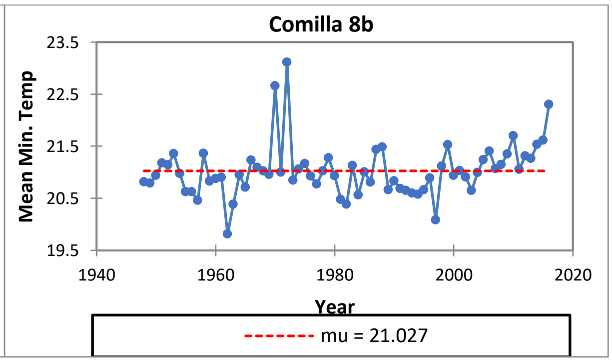
Comilla 8b
Mean Min. Temp
Year
23.5
22.5
21.5
20.5
19.5
1940
1960
1980
2000
2020
mu = 21.027

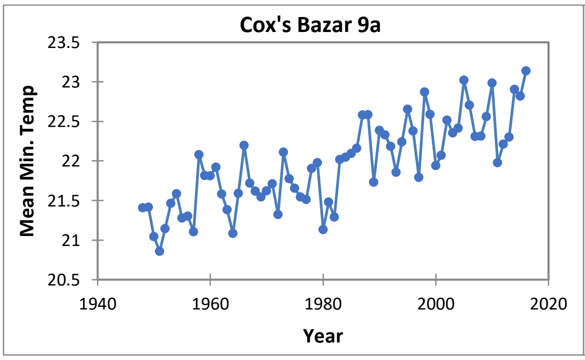
Cox's Bazar 9a
Mean Min. Temp
Year
23.5
23
22.5
22
21.5
21
20.5
1940
1960
1980
2000
2020

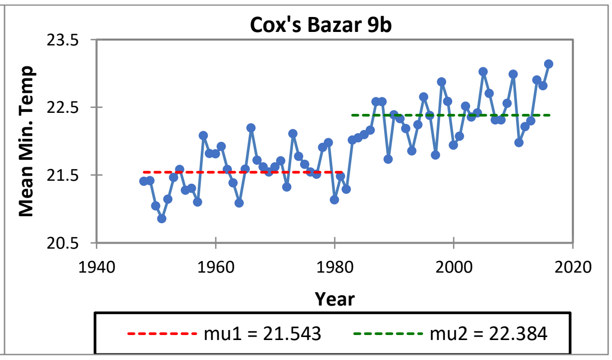
Cox's Bazar 9b
Mean Min. Temp
Year
23.5
22.5
21.5
20.5
1940
1960
1980
2000
2020
mu1 = 21.543
mu2 = 22.384

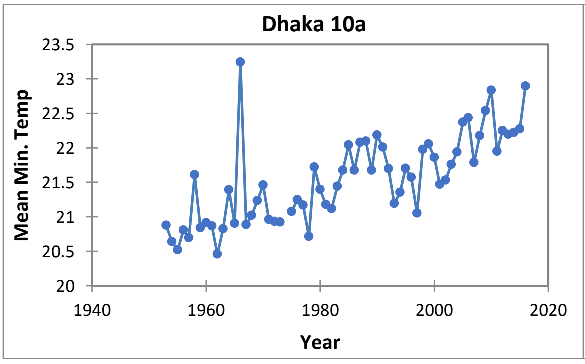
Dhaka 10a
Mean Min. Temp
Year
23.5
23
22.5
22
21.5
21
20.5
20
1940
1960
1980
2000
2020

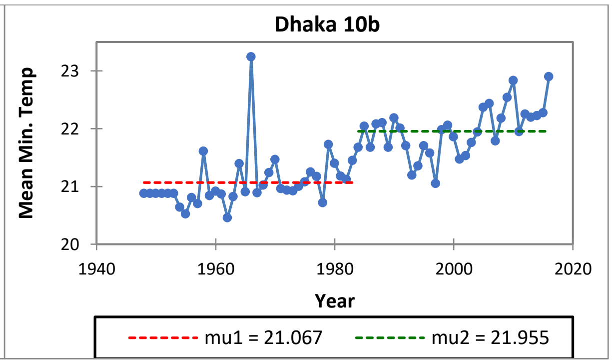
Dhaka 10b
Mean Min. Temp
Year
23
22
21
20
1940
1960
1980
2000
2020
mu1 = 21.067
mu2 = 21.955

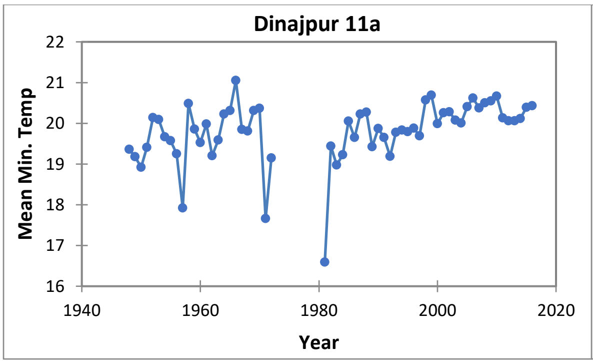
Dinajpur 11a
Mean Min. Temp
Year

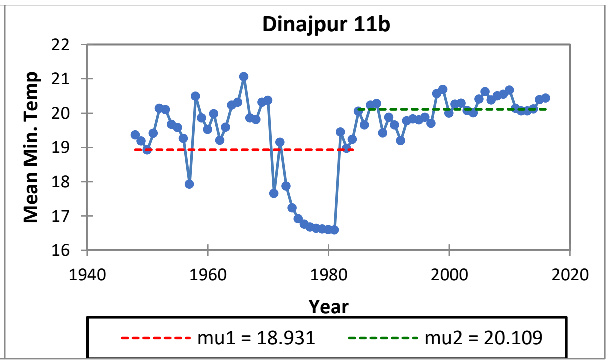
Dinajpur 11b
Mean Min. Temp
Year
mu1 = 18.931
mu2 = 20.109

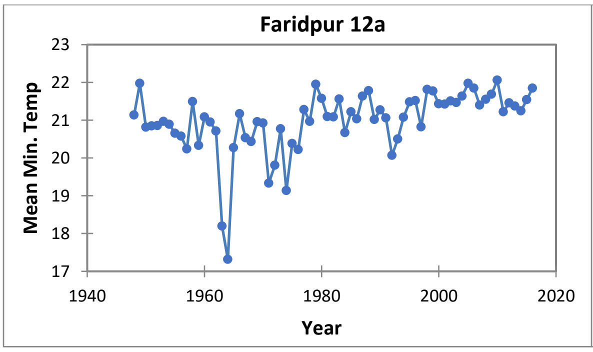
Faridpur 12a
Mean Min. Temp
Year

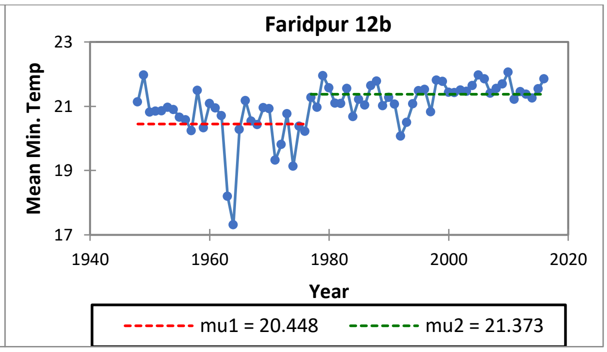
Faridpur 12b
Mean Min. Temp
Year
mu1 = 20.448
mu2 = 21.373

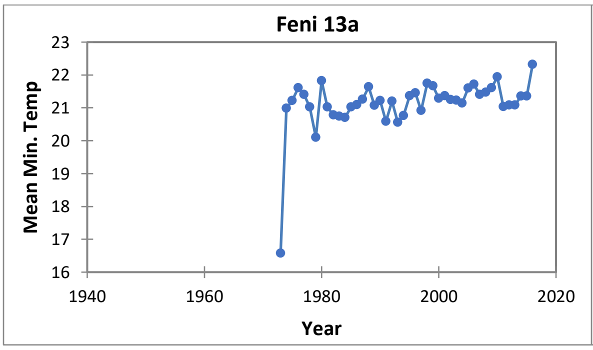
Feni 13a
Mean Min. Temp
Year

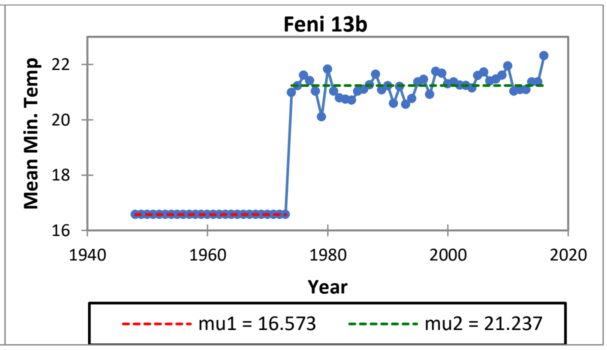
Feni 13b
Mean Min. Temp
Year
mu1 = 16.573
mu2 = 21.237

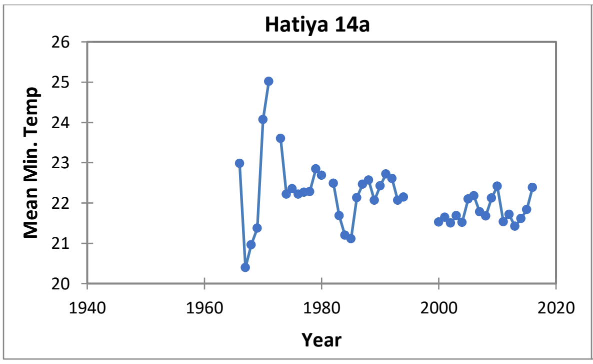
Hatiya 14a
Mean Min. Temp
Year

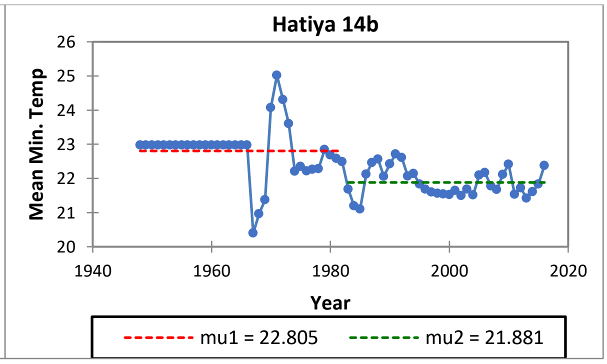
Hatiya 14b
Mean Min. Temp
Year
mu1 = 22.805
mu2 = 21.881

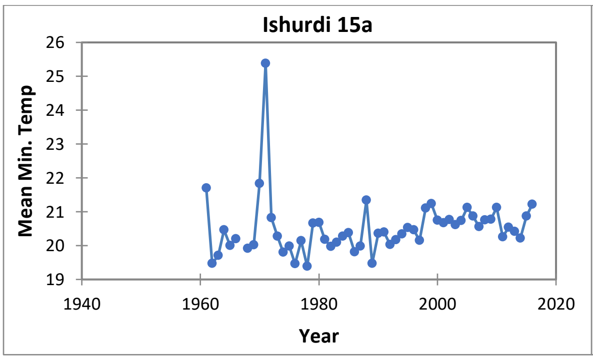
Ishurdi 15a
Mean Min. Temp
Year

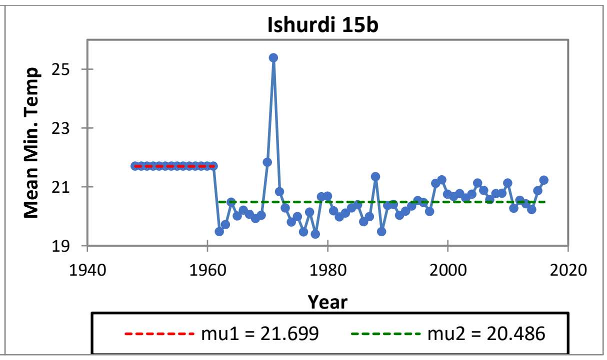
Ishurdi 15b
Mean Min. Temp
Year
mu1 = 21.699
mu2 = 20.486

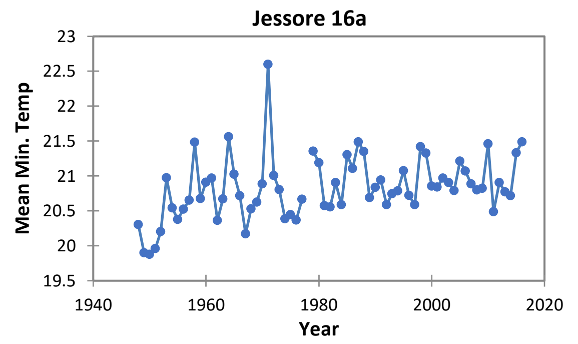
Jessore 16a
Mean Min. Temp
23
22.5
22
21.5
21
20.5
20
19.5
1940
1960
1980
2000
2020
Year

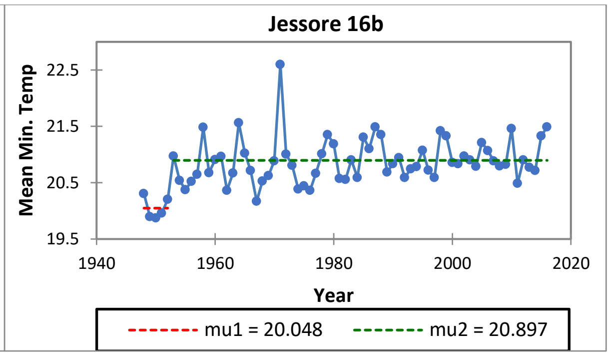
Jessore 16b
Mean Min. Temp
22.5
21.5
20.5
19.5
1940
1960
1980
2000
2020
Year
mu1 = 20.048
mu2 = 20.897

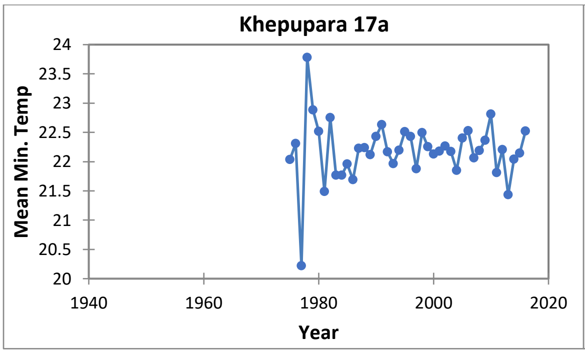
Khepupara 17a
Mean Min. Temp
24
23.5
23
22.5
22
21.5
21
20.5
20
1940
1960
1980
2000
2020
Year

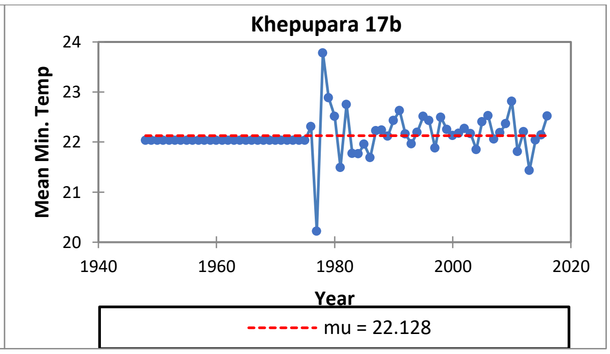
Khepupara 17b
Mean Min. Temp
24
23
22
21
20
1940
1960
1980
2000
2020
Year
mu = 22.128

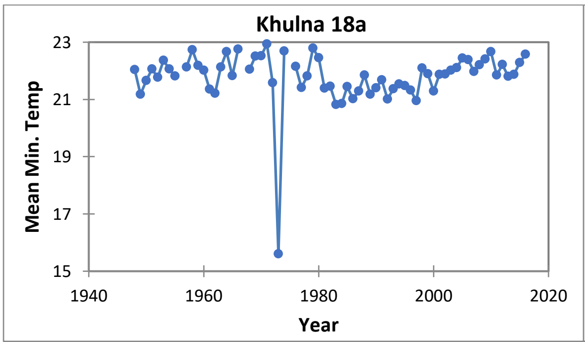
Khulna 18a
Mean Min. Temp
23
21
19
17
15
1940
1960
1980
2000
2020
Year

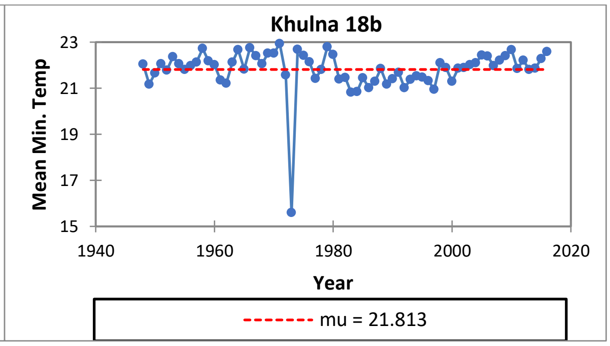
Khulna 18b
Mean Min. Temp
23
21
19
17
15
1940
1960
1980
2000
2020
Year
mu = 21.813

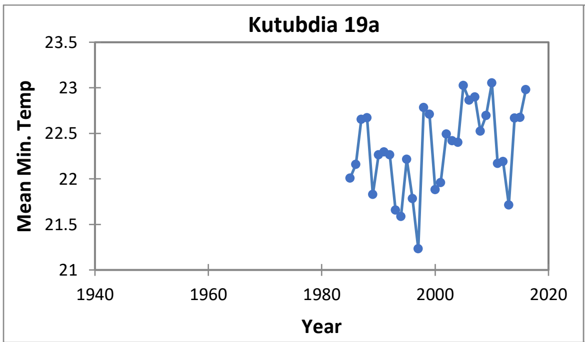
Kutubdia 19a
Mean Min. Temp
23.5
23
22.5
22
21.5
21
1940
1960
1980
2000
2020
Year

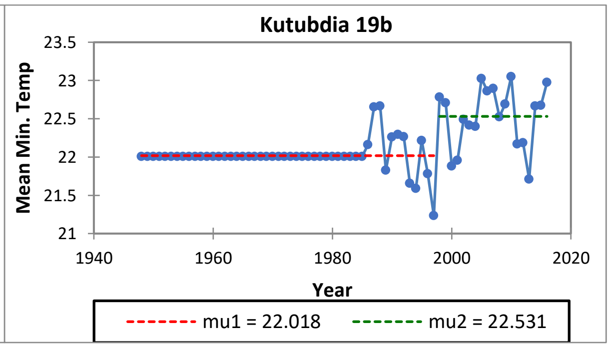
Kutubdia 19b
Mean Min. Temp
23.5
23
22.5
22
21.5
21
1940
1960
1980
2000
2020
Year
mu1 = 22.018
mu2 = 22.531

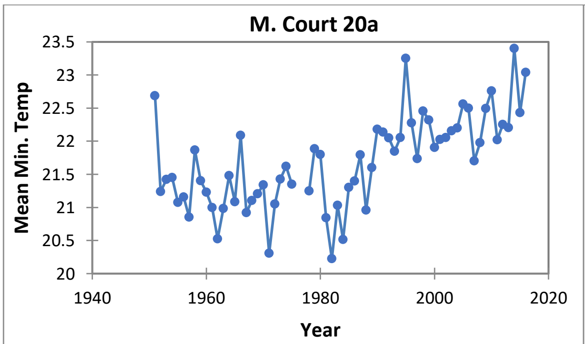
M. Court 20a
Mean Min. Temp
23.5
23
22.5
22
21.5
21
20.5
20
1940
1960
1980
2000
2020
Year

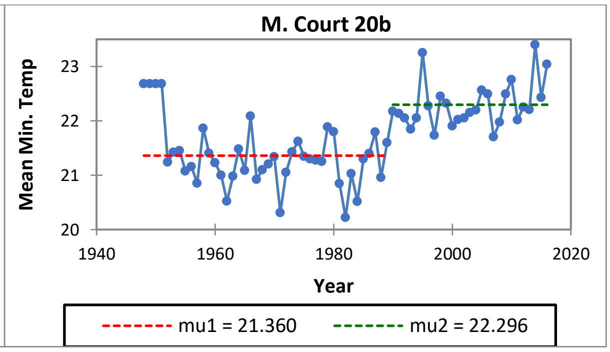
M. Court 20b
Mean Min. Temp
23
22
21
20
1940
1960
1980
2000
2020
Year
mu1 = 21.360
mu2 = 22.296

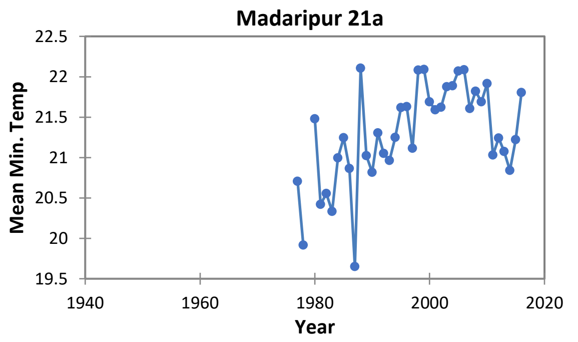
Madaripur 21a
Mean Min. Temp
22.5
22
21.5
21
20.5
20
19.5
1940
1960
1980
2000
2020
Year

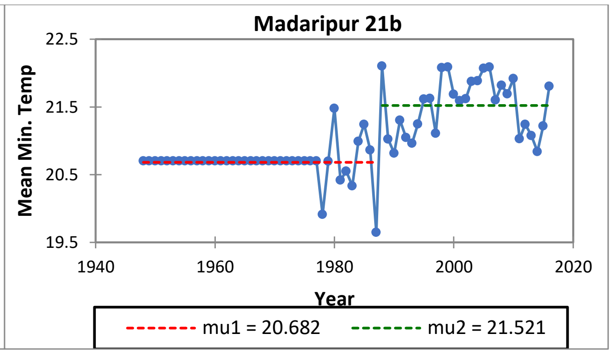
Madaripur 21b
Mean Min. Temp
22.5
21.5
20.5
19.5
1940
1960
1980
2000
2020
Year
mu1 = 20.682
mu2 = 21.521

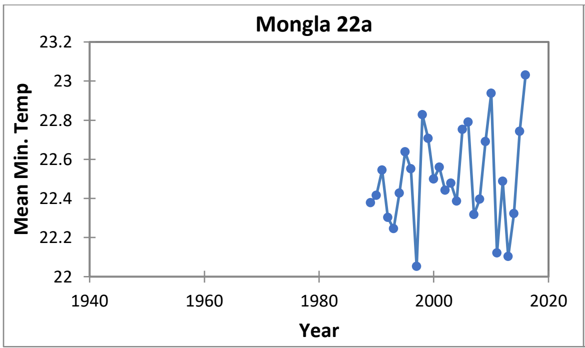
Mongla 22a
Mean Min. Temp
23.2
23
22.8
22.6
22.4
22.2
22
1940
1960
1980
2000
2020
Year

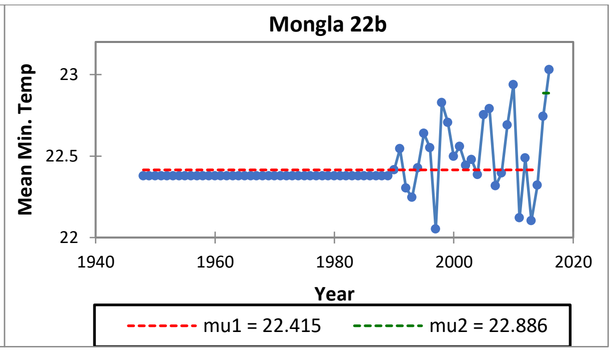
Mongla 22b
Mean Min. Temp
23
22.5
22
1940
1960
1980
2000
2020
Year
mu1 = 22.415
mu2 = 22.886

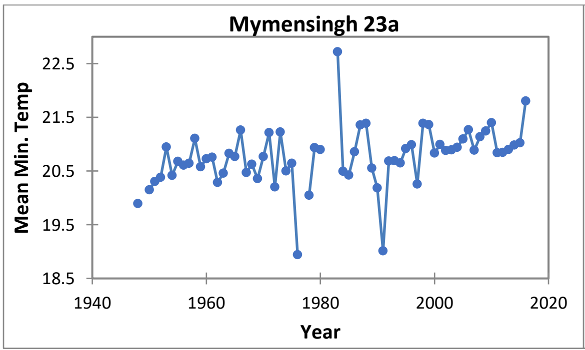
Mymensingh 23a
Mean Min. Temp
22.5
21.5
20.5
19.5
18.5
1940
1960
1980
2000
2020
Year

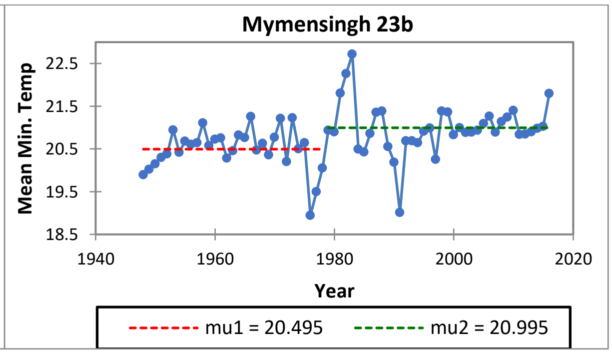
Mymensingh 23b
Mean Min. Temp
22.5
21.5
20.5
19.5
18.5
1940
1960
1980
2000
2020
Year
mu1 = 20.495
mu2 = 20.995

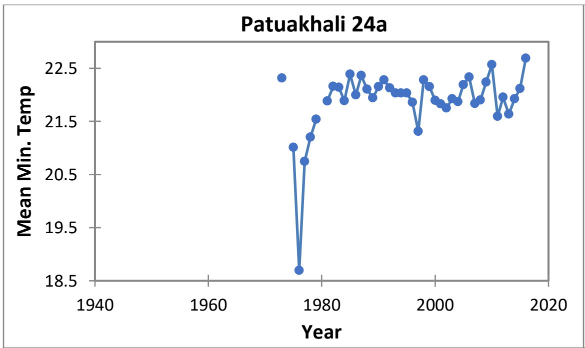
Patuakhali 24a
Mean Min. Temp
22.5
21.5
20.5
19.5
18.5
1940
1960
1980
2000
2020
Year

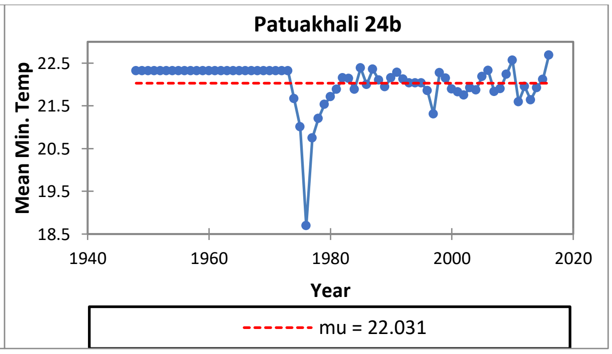
Patuakhali 24b
Mean Min. Temp
22.5
21.5
20.5
19.5
18.5
1940
1960
1980
2000
2020
Year
mu = 22.031

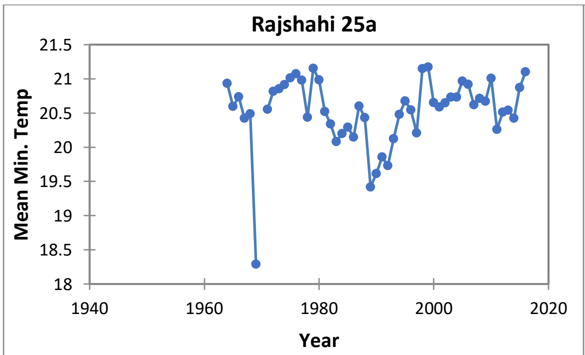
Rajshahi 25a
Mean Min. Temp
21.5
21
20.5
20
19.5
19
18.5
18
1940
1960
1980
2000
2020
Year

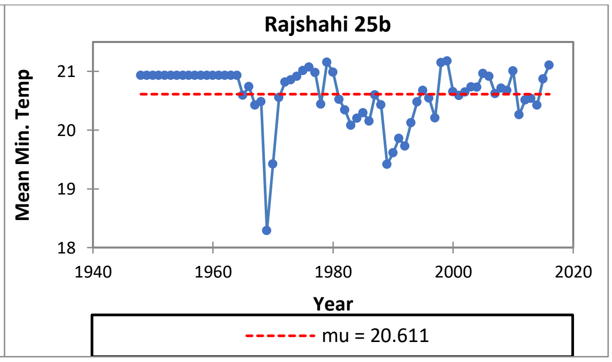
Rajshahi 25b
Mean Min. Temp
21
20
19
18
1940
1960
1980
2000
2020
Year
mu = 20.611

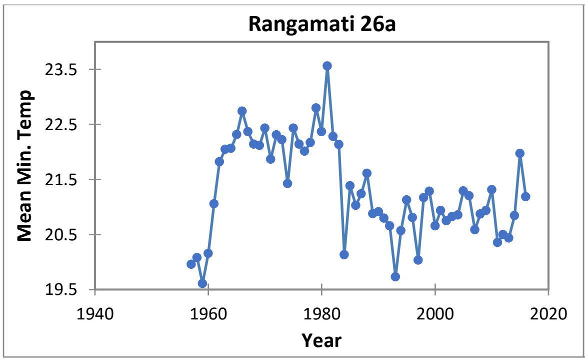
Rangamati 26a
Mean Min. Temp
Year

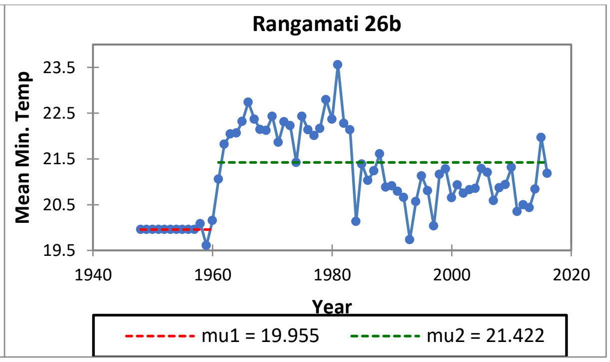
Rangamati 26b
Mean Min. Temp
Year
mu1 = 19.955
mu2 = 21.422

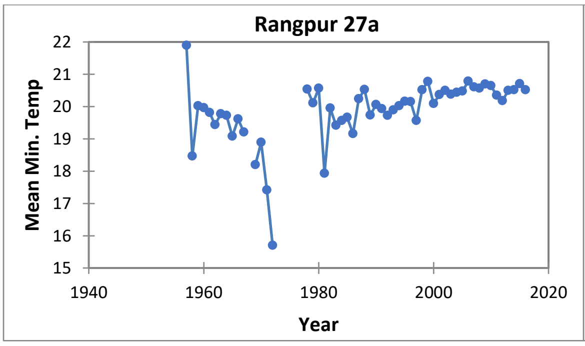
Rangpur 27a
Mean Min. Temp
Year

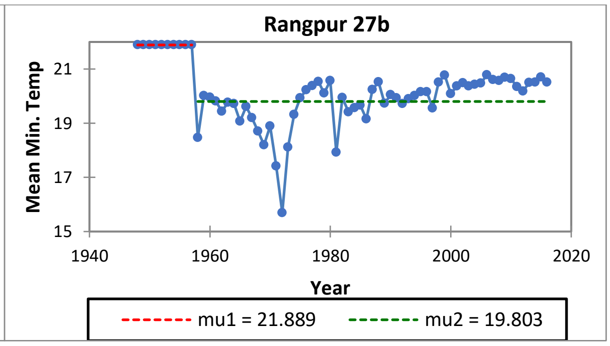
Rangpur 27b
Mean Min. Temp
Year
mu1 = 21.889
mu2 = 19.803

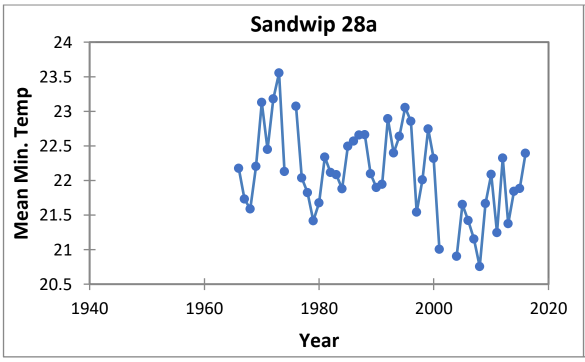
Sandwip 28a
Mean Min. Temp
Year

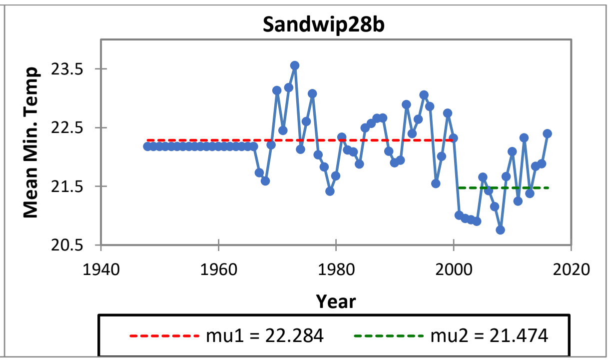
Sandwip28b
Mean Min. Temp
Year
mu1 = 22.284
mu2 = 21.474

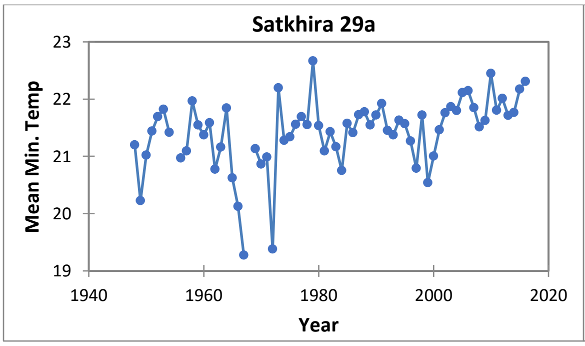
Satkhira 29a
Mean Min. Temp
Year

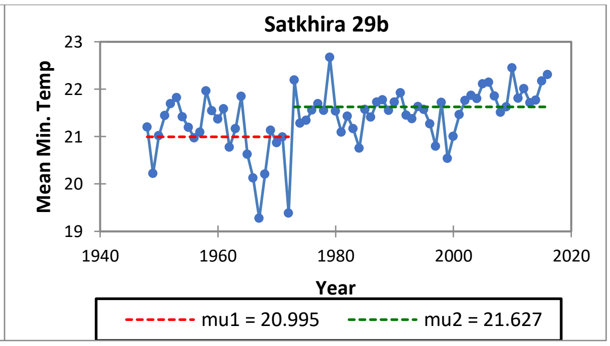
Satkhira 29b
Mean Min. Temp
Year
mu1 = 20.995
mu2 = 21.627

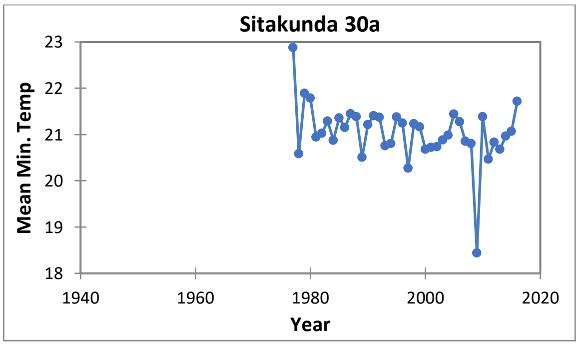
Sitakunda 30a
Mean Min. Temp
Year

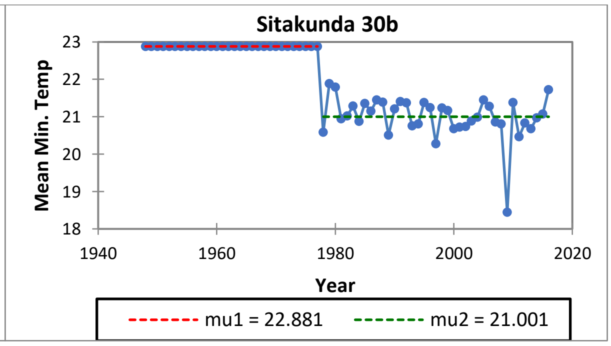
Sitakunda 30b
Mean Min. Temp
Year
mu1 = 22.881
mu2 = 21.001

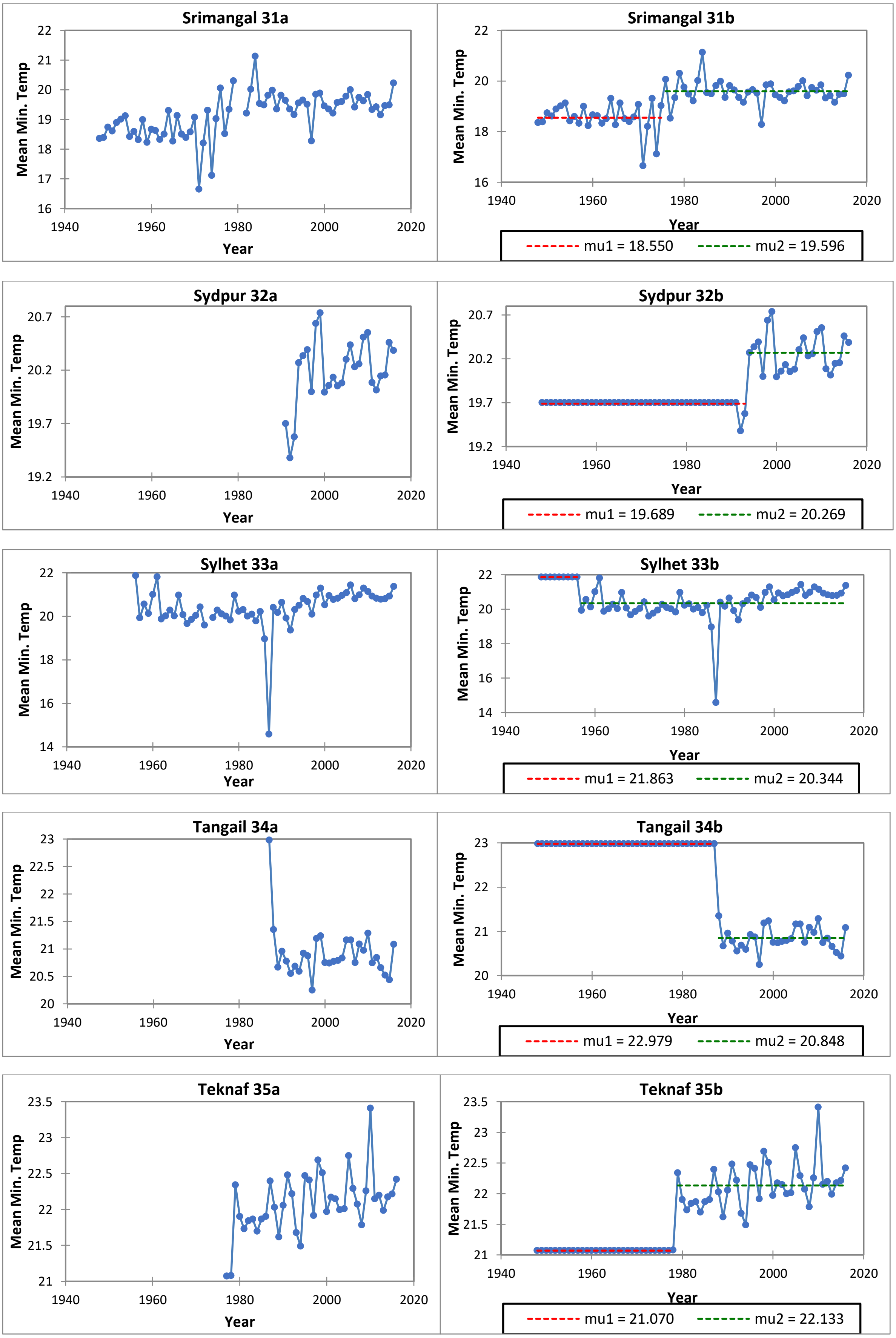

Figure 27(6.8): Changing year in annual minimum temperature all stations MK(a) & SNHT(b) test

Compering with the Mann-Kendall and Standard Normal Homogeneity Test (SNHT) defer a little bit. Mainly MK(*a*) and SNHT(*b*) comparing with the two-side (*a* and *b*) (Figure 6.8) filling gape year (*b*) with average value. Value shows the same (average value) if the gape year started from beginning and value is quite well when it is in the middle. Hence, trend curve should be different from MK to SNHT because trend curve is measured entire data beginning to present where data is filled by average with before and after but beginning data is plotted based on before value. It was not possible to interpolate beginning year by XLSTAT that's why only average value was added in the beginning year where it is required an individual station. Kendall's tau test is widely used to testing the hypothesis. In (Table 6.1) clearly shows that whether the station is significant or not. In that table, 22 stations were increased, 4 stations were decreased where 1 station was decreased with 90% level of confidence and 9 stations change were not significant at all.

6.4 Homogeneity tests *P*-value Approximation

From homogeneity test *P*-value (two-tailed) was calculated (Table 6.2). For all tests, XLSTAT provides *P*-values using Monte Carlo resampling. Exact calculations are either impossible or too costly in computing time. From SNHT (Table 6.2) is generated where *p*-value and significant level were measured.

In this chapter homogeneity analysis shows that 35 annual minimum temperature series (station wise) are merely same as mean temperature and maximum temperature (Table 4.2 and 5.2) and look like as heterogeneous around the year 1948-2016, it means there is a significant change in the mean before and after the detected change point. SNHT test is known to find change point towards find the changes in the middle of a series (Mart´ınez *et. al.*, 2009). The results given in (Table 6.2) are showing most of the series homogenous in nature.

SNHT tests shows that there are 19 common stations where all the tests are in about to same change point year {p-value (Two-tailed)} with high significant same as mean temperature and maximum temperature. The changes in the mean of these series along with the temperature plots are shown in (Figure 6.8). Rest of these 16 stations, 10 stations show also significant with 95% level of confidence and 3 stations are 90% level of confidence on the other hand 3 stations are not significant at the change point. The figures clearly show that there is a noticeable change in the minimum temperature mean of the series before and after the change point in all the stations. In (Figure 6.8) no data were manipulated and ignored triple star sign in raw data.

Chapter Seven
Analysis of Observed Rainfall

7.1 Introduction

Rainfall water that is condensed from the aqueous vapor in the atmosphere and falls in drops from the sky to the earth is called rain; and the total amount of rain that falls in a particular area within a certain time is called rainfall (Banglapedia, 2015). Winter season (December-February) is very much dry with less than 4% of annual rainfall (Banglapedia, 2015). It varies from 20 mm in the west and south to 40 mm in the north-east, which is caused by the westerly disturbances that enter the country from the northwestern part of India (Banglapedia, 2015). In pre-monsoon season 10-20% of the total annual rainfall occurred. June through October mainly counted as rainy season in Bangladesh when 70-85% rainfall was counted. The average annual rainfall in Bangladesh varies from 1500 mm in the west-central part to over 3000 mm in the northeast and southeast (Banglapedia, 2015). In (Figure 7.1) shows that the mean annual rainfall variation in Bangladesh.

To evaluate and calculate the amount of normal rainfall a vast database must be needed. To calculate daily rainfall data at different stations data requisition is necessary from collected from either BMD or BWDB. BWDB have 284 stations which is precisely/clearly evaluate whole Bangladesh. But in this study BMD data were used to evaluate and calculate to generate a scenario of the present condition of Bangladesh. The data were available for 35 stations but not homogeneous for time duration. Missing data were filled by SNHT test (whenever possible) (see Appendix). The data for this study were available for a maximum period of 69 years (1948-2016).

However, most of the stations had available record lengths more than 30 years. Locations of the stations is given in (Figure 7.2). From the daily values, monthly total rainfall was calculated for each month, for station and for each year. Seasonal and annual rainfalls were calculated from the monthly values. The all-Bangladesh rainfall series for a given month, season or year was calculated from the average rainfall of different stations. Since the stations spread all-over the country, and the available periods of record and the missing values at different stations do not follow any spatial pattern, the averaging from all available stations is justified. In this study also calculated normal rainfall most recent 30 years basis.

7.2 Annual Rainfall

All-Bangladesh annual normal rainfall for a period of 30 years (1987-2016) is found to be 2360.37 mm. Such rainfalls were 1068.17, 1460.57, 1845.10 and 2215.20 mm during 1948-1976, 1957-1986, 1967-1996, 1977-2006 respectively. It thus appears that the annual normal rainfalls have changed in Bangladesh. All-Bangladesh decadal (10 years) rainfalls are shown in (Figure 7.3). It is seen from the figure that the rainfalls increased gradually over the first six decades and then decreased. The highest rainfall was observed during the 1997-2006.

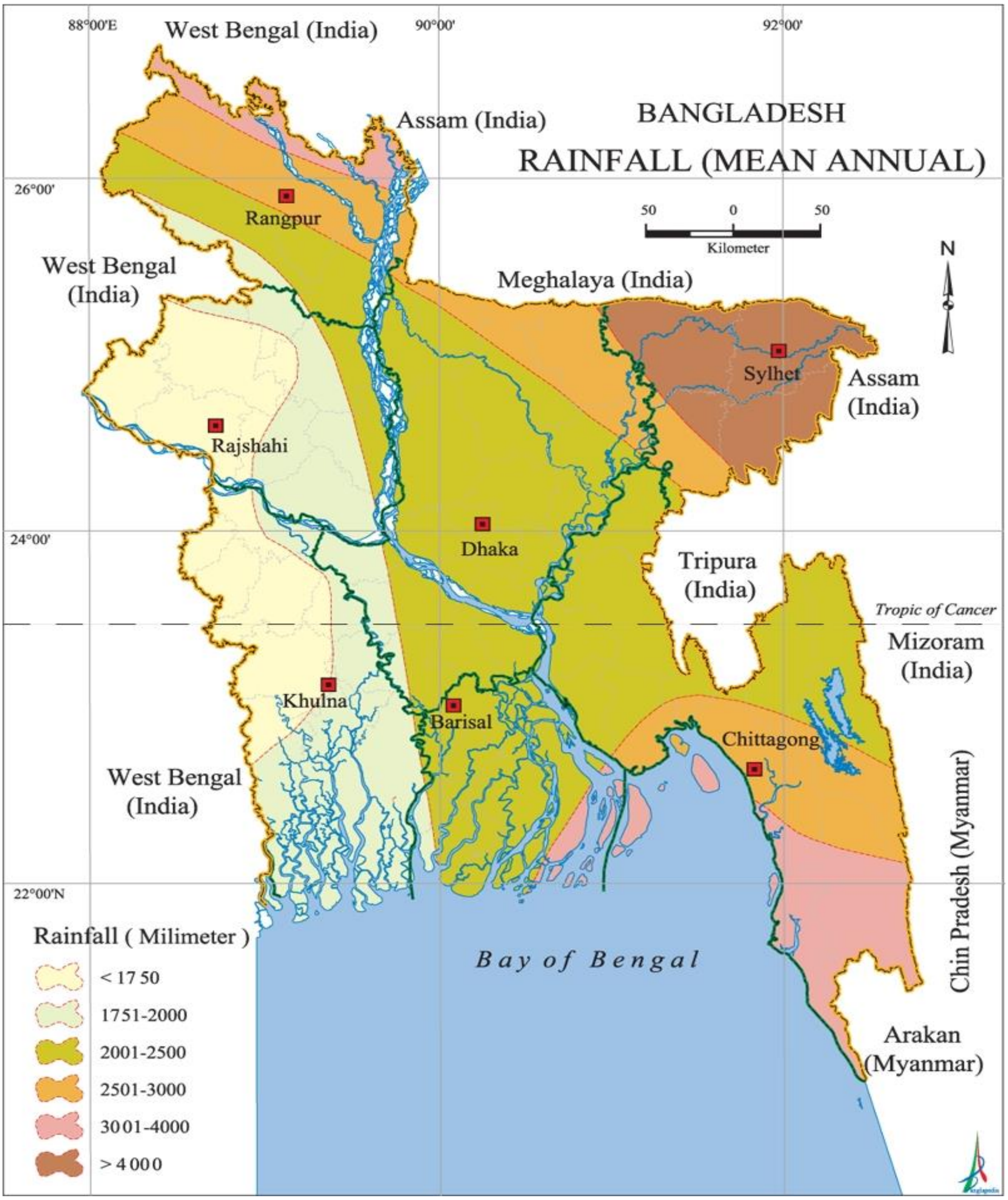

Figure 7.1: Mean annual rainfall variation in Bangladesh (Source: Banglapedia, 2015)

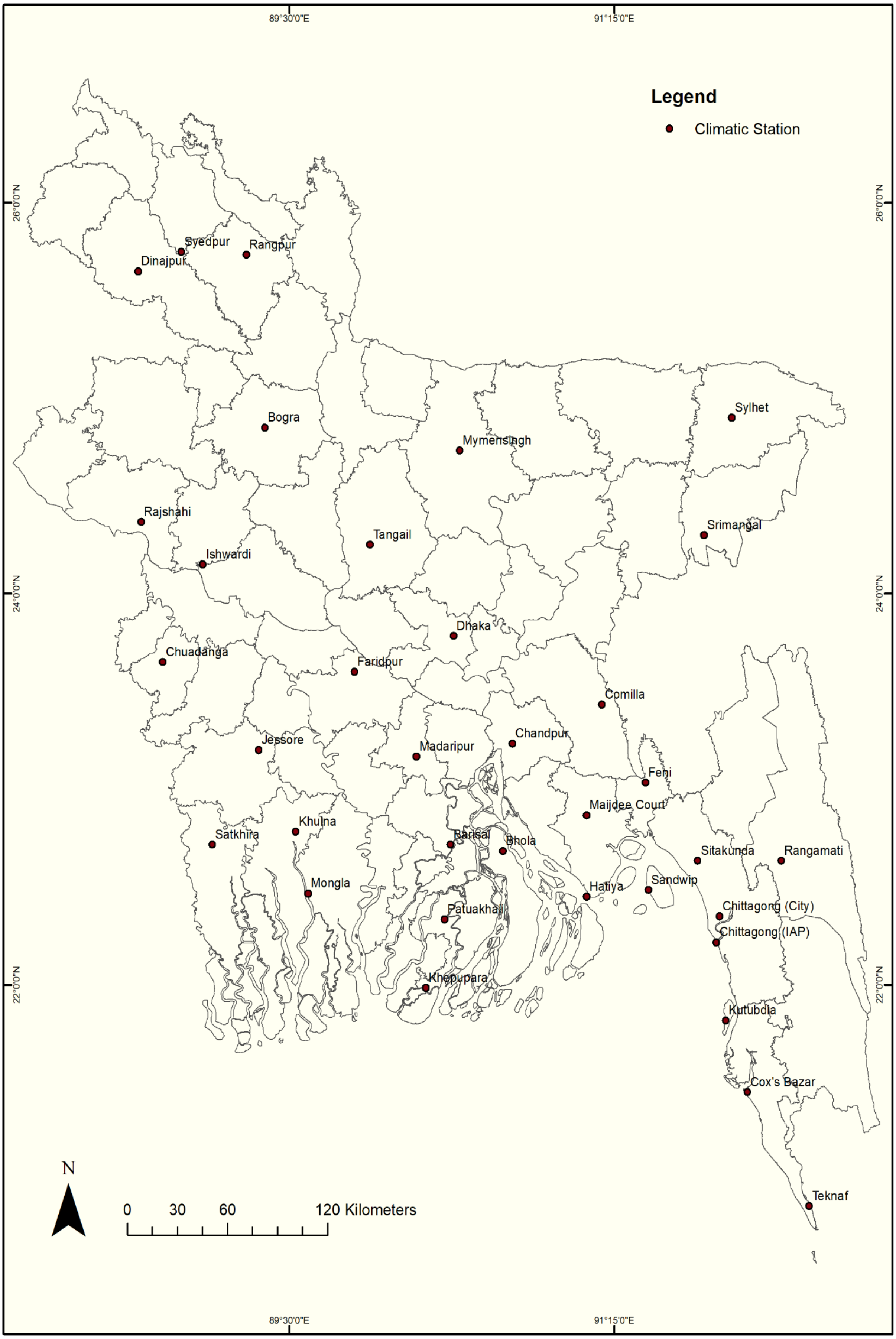

Figure 7.2: Locations of the BMD climatic stations used in the study (rainfall)

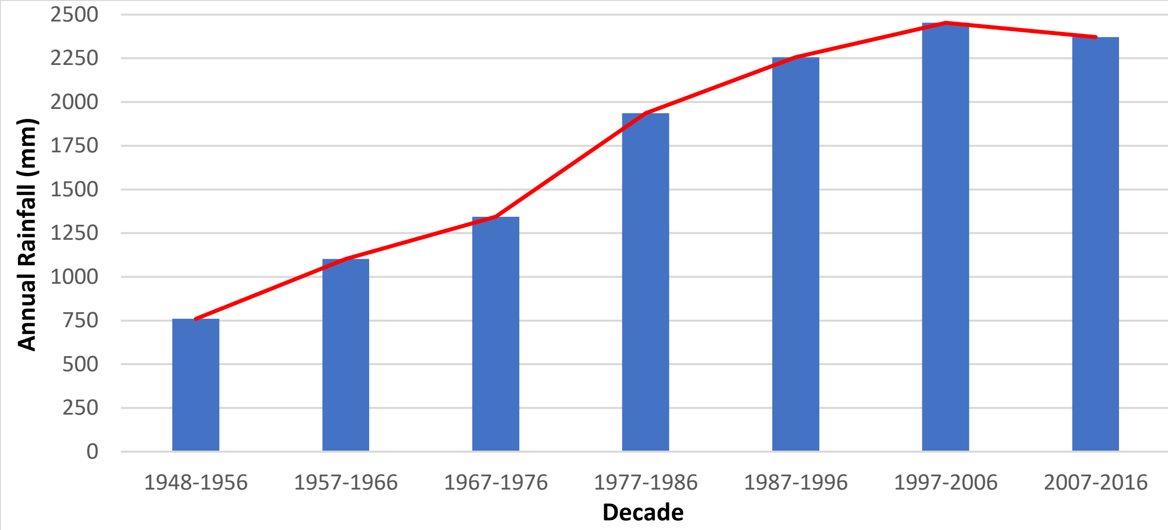

Figure 7.3: All-Bangladesh annual rainfalls during different decades

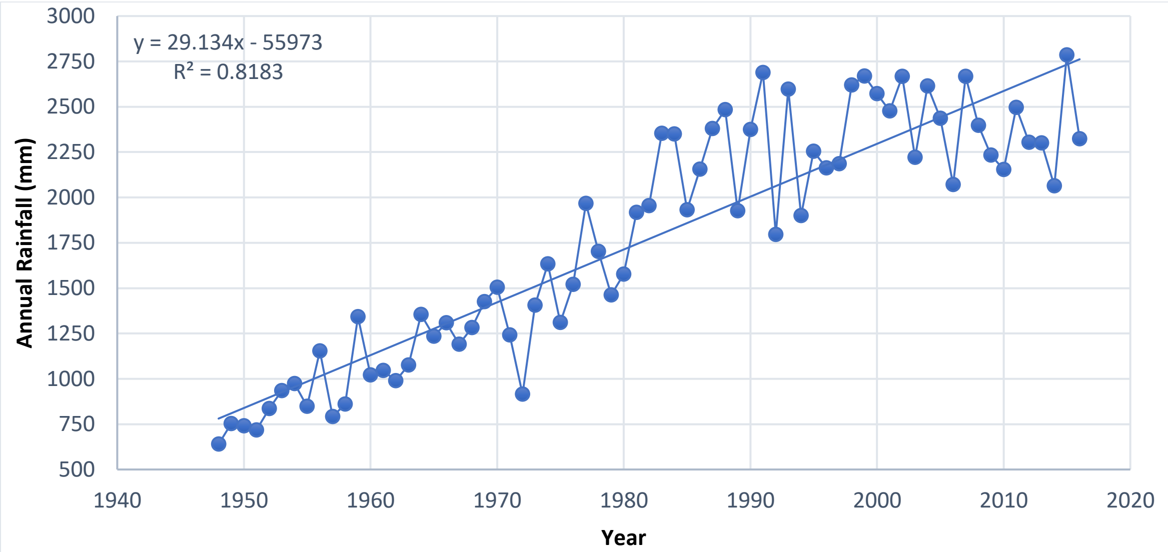

Figure 7.4: All-Bangladesh annual rainfall time series 1948-2016

7.3 Seasonal Normal Rainfall

In pre-monsoon season mean monthly total rain corelate strong positive association with monthly lightning flashes (Dewan *et. al.*, 2017b, Dewan *et. al.*, 2017c and Dewan *et. al.*, 2017d) but less rainfall than monsoon. Rainy season mainly counted in monsoon and maximum rainfall was recorded in this season. All-Bangladesh normal rainfalls in different seasons are given in (Table 7.1). It is seen from the table that the monsoon (June-September), post-monsoon (October-November) and winter (December-February) normal rainfalls have increased decadal climatic period; and the pre-monsoon (March-May) normal rainfall has increased in the last four decadal climatic periods and then decreased (negligible) over the fifth period (1987-2016). However, these increasing changes in different seasons would be statistically highly significant.

Table 7.1: Decadal variation all-Bangladesh normal rainfalls in different seasons per climate

Season	**Normal Rainfall (mm)**					**Trend**
	1948-1976	**1957-1986**	**1967-1996**	**1977-2006**	**1987-2016**	
Pre-monsoon	174	257	336	417	412	52.32
Monsoon	808	1054	1316	1568	1693	210.02
Post-monsoon	109	127	162	194	220	26.06
Winter	14	22	31	36	62	4.13

The decadal rainfalls in different seasons are given in (Figure 7.5, 7.6, 7.7 and 7.8). It is seen that the rainfalls in the pre-monsoon increased and decreased. Decadal variation of pre-monsoon, monsoon, post-monsoon and winter rainfall shows that the increasing trends are 52.32 mm, 210.02 mm, 26.06 mm and 4.13 mm per climate respectively.

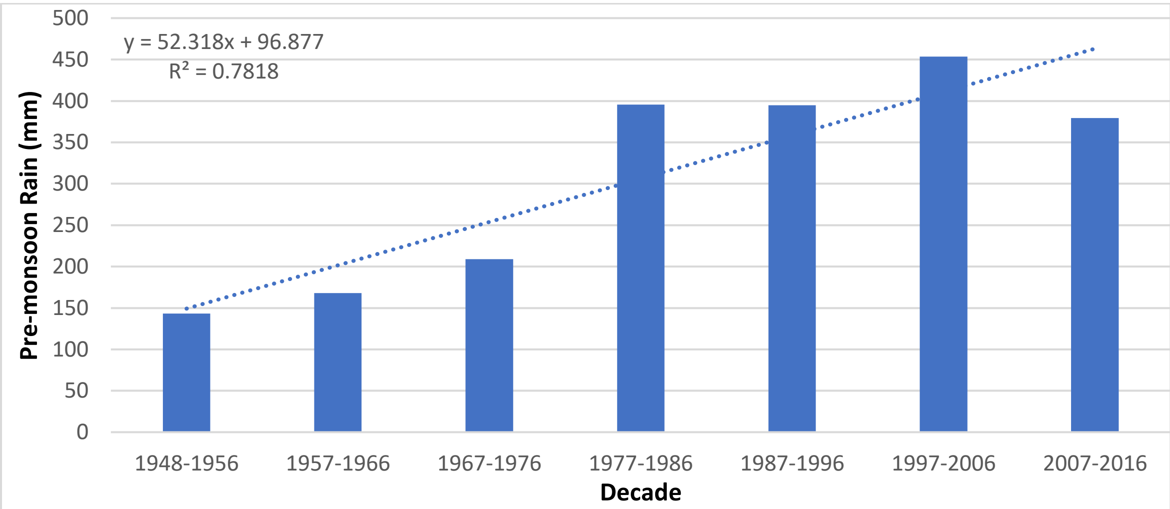

Figure 7.5: All-Bangladesh pre-monsoon rainfalls during different decades

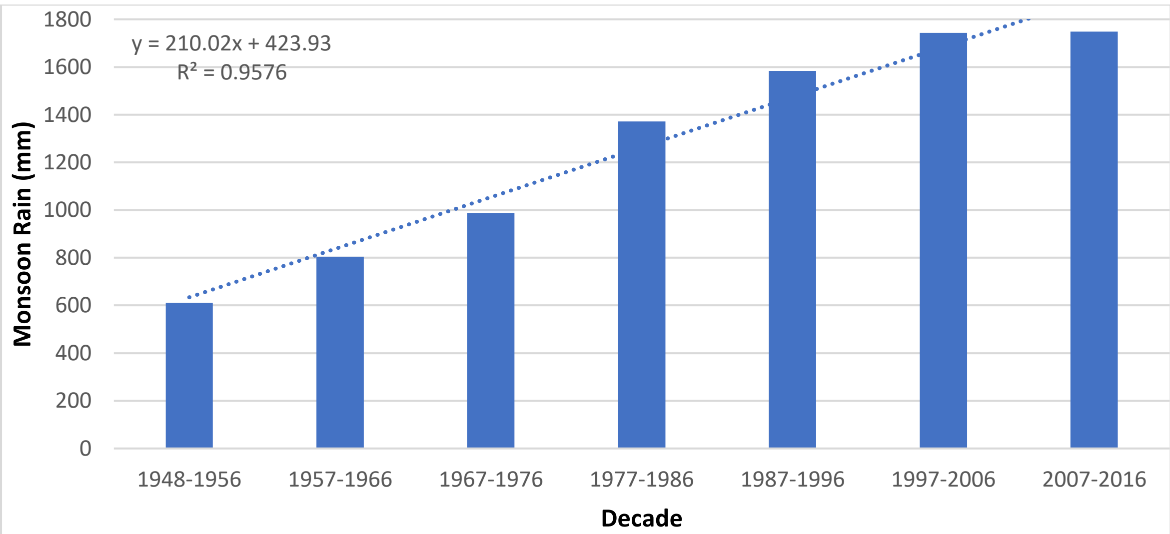

Figure 7.6: All-Bangladesh monsoon rainfalls during different decades

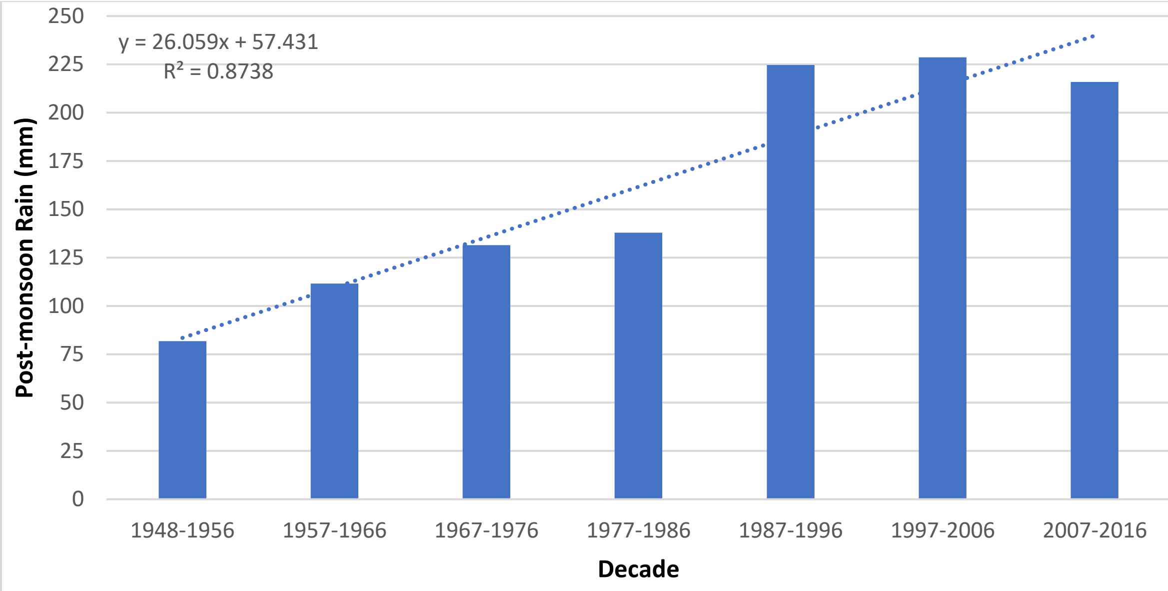

Figure 7.7: All-Bangladesh post-monsoon rainfalls during different decades

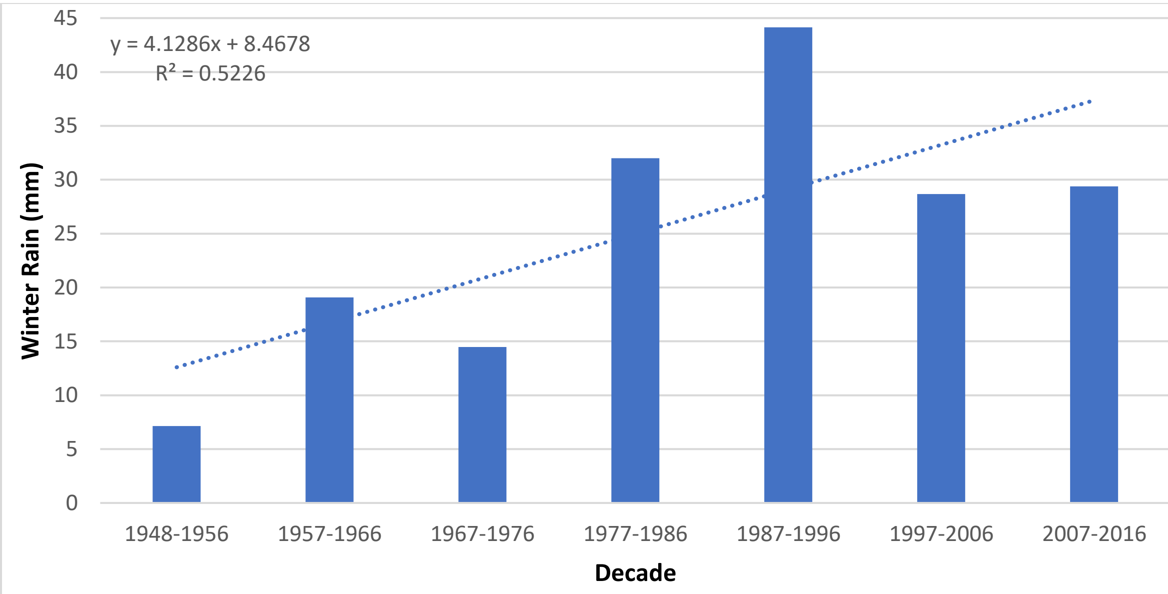

Figure 7.8: All-Bangladesh winter rainfalls during different decades

Table 7.2: Results of the Mann-Kendall trends test for all Bangladesh seasonal rainfall (1948-2016)

Season	Kendall's tau	S	Var(S)	*P*-value (Two-tailed)	Alpha	Test Int.	Sig.
Pre-monsoon	0.500	1172	37275.33	< 0.0001	0.05	R	**I
Monsoon	0.719	1686	37275.33	< 0.0001	0.05	R	**I
Post-monsoon	0.383	898	37275.33	< 0.0001	0.05	R	**I
Winter	0.265	622	37273.33	0.001	0.05	R	**I

Note: **Significant at the 95% level of confidence; *Significant at the 90% level of confidence; NS-Not Significant at the 90% level of confidence; A-Accepted at the p>0.05; R-Rejected at the p<0.05; I-Increased; D-Decreased

Form the Mann-Kendall's tau test it is seen that all seasons are very much significant and increasing trend too. In the (Figure 7.5, 7.6, 7.7 and 7.8) also proved the Kendall's tau test.

7.4 Rainfall Time Series Analysis

Time series plots of all-Bangladesh rainfalls for different seasons are shown in (Figure 7.9, 7.10, 7.11 and 7.12). It is seen from the figure that the rainfalls in all seasons have increasing trends. The increasing trend in the pre-monsoon, monsoon, post-monsoon and winter were found 5.21, 20.93, 2.61 and 0.39 mm/year respectively where annual rate is 29.13 (Figure 7.4). There was a significant trend in different seasons. But Shahid (2010), did not find any significant trends in monsoon and post-monsoon rainfalls at country level.

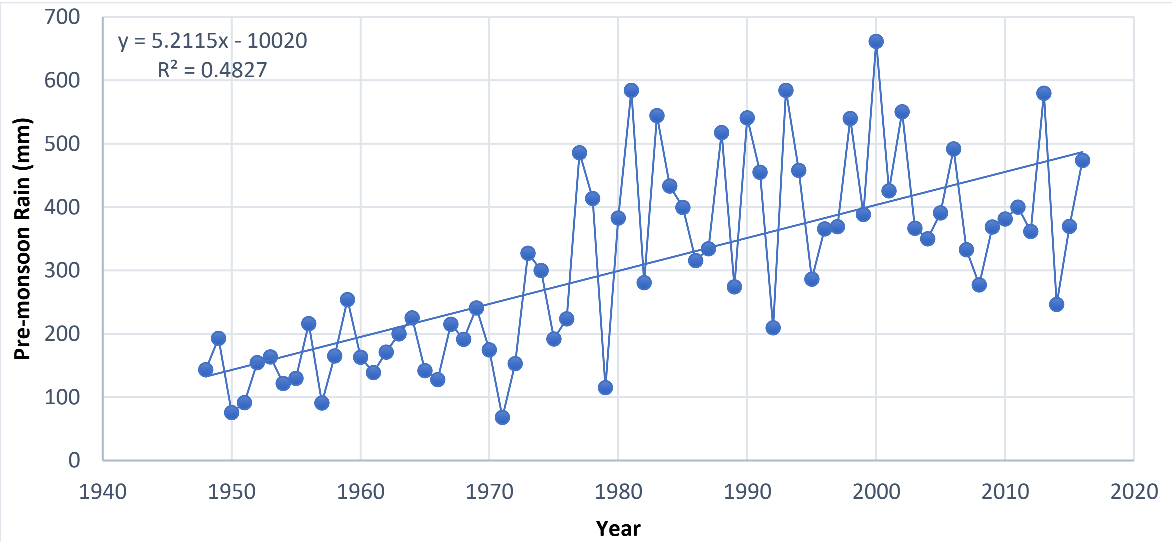

Figure 7.9: Trends in all-Bangladesh pre-monsoon season rainfall time series

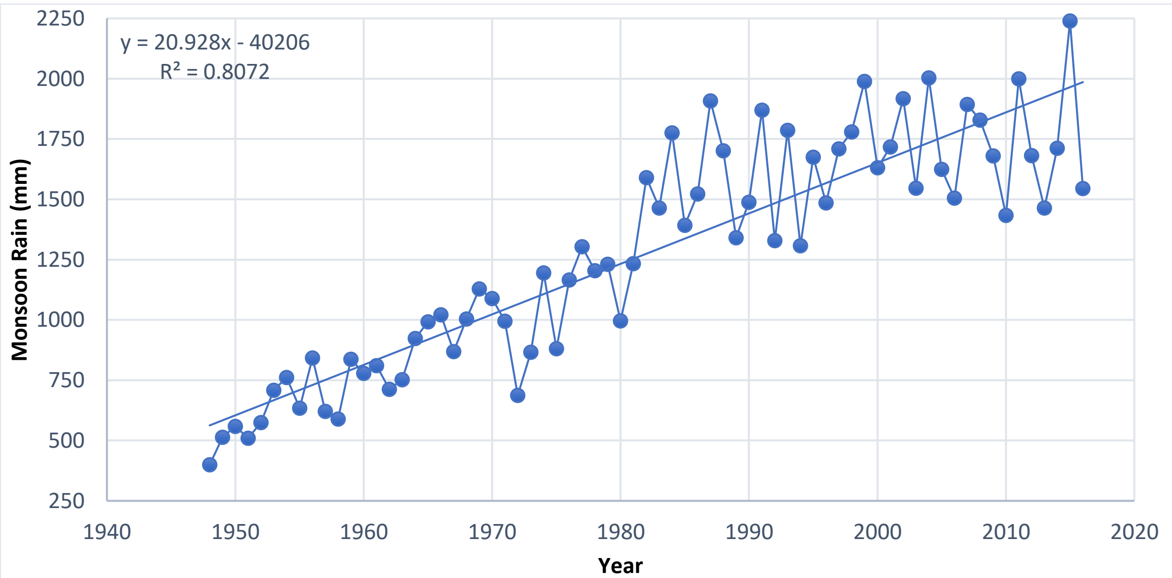

Figure 7.10: Trends in all-Bangladesh monsoon season rainfall time series

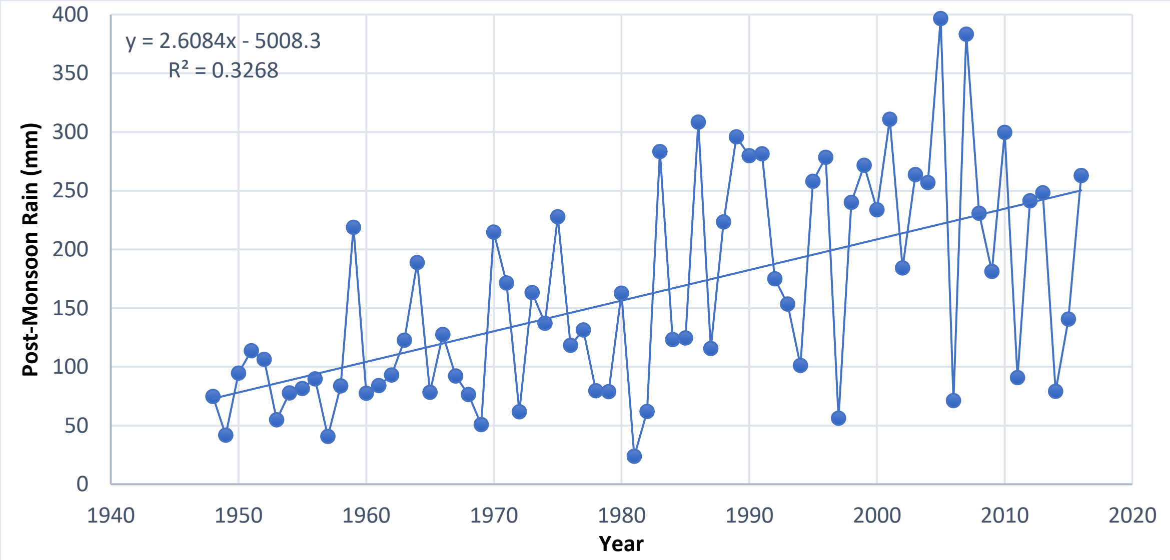

Figure 7.11: Trends in all-Bangladesh post-monsoon season rainfall time series

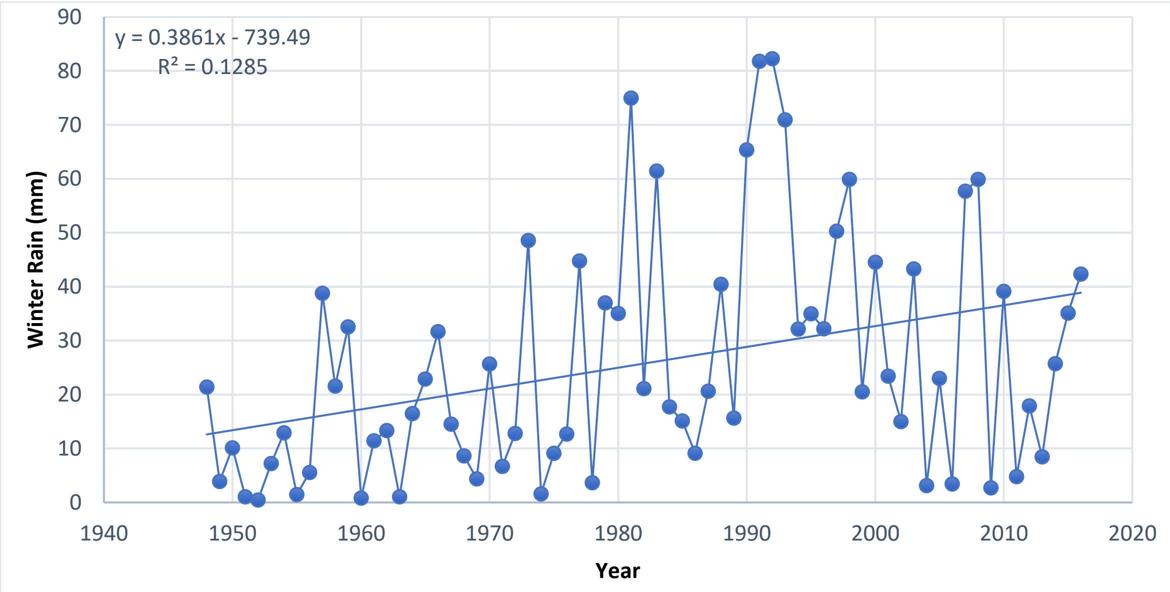

Figure 7.12: Trends in all-Bangladesh winter season rainfall time series

7.5 Monthly Normal Rainfall

All-Bangladesh monthly normal rainfall variations are given in (Figure 7.13). It is seen from the figure that, the normal rainfalls in the months of May (pre-monsoon); July and September (monsoon) have increased, while the normal rainfalls in the months of December, January and February (winter) has nearly stable position on the other hand, in the month of March and April (pre-monsoon) and the month in the October and November (post-monsoon) have increased and decreased situation. All the normal rainfall data classified into five set 30 years basis from 1948-2016 and calculated in monthly normal rainfall. A pyramid layer shows in the month of July higher increasing rate.

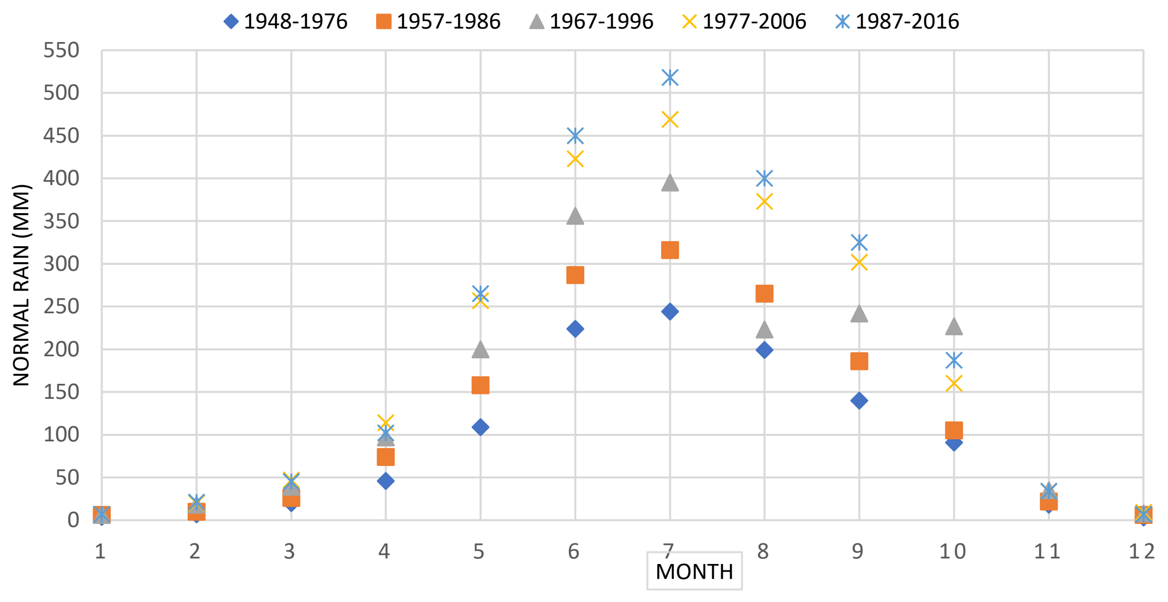

Figure 7.13: All-Bangladesh normal rainfall variation in different months

Table 7.3: All-Bangladesh normal rainfalls in different months

Month	Normal Rain (mm)				
	1948-1976	1957-1986	1967-1996	1977-2006	1987-2016
January	3.90	5.66	5.54	6.96	7.03
February	6.98	10.43	18.25	20.23	21.00
March	20.21	25.84	38.95	46.82	45.29
April	45.59	73.81	96.77	113.96	101.53
May	108.54	157.74	199.97	256.51	265.00
June	224.33	287.05	356.29	423.29	449.57
July	244.03	316.11	395.38	469.11	518.45
August	199.32	265.00	322.98	372.69	400.33
September	140.05	186.25	241.57	302.49	324.73
October	91.04	104.66	126.96	159.94	186.68
November	18.11	22.27	34.87	34.29	33.56
December	2.90	5.75	7.58	8.91	7.21

The decadal variation of all-Bangladesh monthly rainfalls is given in (Figure 7.14-7.25). It is seen from the figures that the rainfalls in the monsoon months, except for July, have decreased in recent decades compared to the past. Rainfalls have significantly increased in October and decreased in November of the post-monsoon season in the last decade compared to the past decades. There is no definite pattern in variations of monthly rainfalls in other seasons. Though May to October risk of increase is not noticeable but they have much significant in trend. The trends in all-Bangladesh monthly rainfalls are given in (Figure 7.26). It is seen from the figure that the rainfalls in the months of December 0.08 mm, January 0.07 mm and February 0.24 mm of the winter season have near stable increasing trends. The month of March of the pre-monsoon season also about to same as winter like 0.47 mm and the months of April and May of the pre-monsoon season have slightly increasing trends with 1.13 and 3.61 mm respectively in rainfalls. The months of June, July, August and September of the monsoon season have a high increasing trend with 5.27, 6.56, 4.84 and 4.27 mm respectively. However, the trends of October post-monsoon season also slightly increasing trend 2.27 mm and November of post-monsoon season was found to be near stable trend with 0.34 mm.

The trends in monthly rainfalls for each individual station were also calculated. For, January, 35 stations have been calculated and 21 stations were found to have negative trends, 13 stations were found positive trends and 1 station was found stable in trend. The spatial variation of trends is shown in (Figure 7.27). It is seen from the figure that the north-western part and north-eastern hilly region of the country has increasing trends while the south-eastern hilly region and central to south-western part have decreasing trends. Since there is no strong correlation among the rainfall trends at different stations, they can be considered as independent observations from a continuous probability distribution. However, the mathematical form of this distribution is not known. In absence of such knowledge, an empirical technique based on probability plotting can be used to estimate the probability of increase or decrease in rainfall. It is found that the overall chance of decreasing in rainfall in January is about 0.20%. The expected change, which is expressed by a median change with an exceedance probability of 50%, is found to be decreasing at a rate of 0.02% per year (Figure 7.27). This means that, over a period of 10 years, the rainfall in the month of January has decreased by 0.20%.

For, February, 35 stations have been calculated and 31 stations were found to have negative trends and 4 stations were found positive trends. The spatial variation of trends is shown in (Figure 7.28). It is seen from the figure that the north-western part and south to south-eastern hilly region of the country has increasing trends while the north to north-eastern hilly region and central part have decreasing trends. Since there is a strong correlation among the rainfall trends at different stations. It is found that the overall chance of decreasing in rainfall in February is about 26.54%. The expected change, which is expressed by a median change with an exceedance probability of 50%, is found to be decreasing at a rate of 0.86% per year (Figure 7.28). This means that, over a period of 10 years, the rainfall in the month of February has decreased by 8.60%.

For, March, 35 stations have been calculated and 31 stations were found to have negative trends and 4 stations were found positive trends. The spatial variation of trends is shown in (Figure 7.29). It is seen from the figure that the half of the country of the south has increasing trends while half of the country of the north has decreasing trends. Since there is a strong correlation among the rainfall trends at different stations. It is found that the overall chance of decreasing in rainfall in March is about 49.93%. The expected change, which is expressed by a median change with an exceedance probability of 50%, is found to be decreasing at a rate of 1.60% per year (Figure 7.29). This means that, over a period of 10 years, the rainfall in the month of March has decreased by 16.00%.

For, April, 35 stations have been calculated and 25 stations were found to have negative trends and 10 stations were found positive trends. The spatial variation of trends is shown in (Figure 7.30). It is seen from the figure that the changes over the country is discontinuity and decreasing in CHT, north-western, north-eastern and mid-southern part of the country while Meghna estuary of the country upper part of Sundarbans and central part of the country have increasing trends. Since there is a strong correlation among the rainfall trends at different stations. It is found that the overall chance of decreasing in rainfall in April is about 44.29%. The expected change, which is expressed by a median change with an exceedance probability of 50%, is found to be decreasing at a rate of 1.58% per year (Figure 7.30). This means that, over a period of 10 years, the rainfall in the month of April has decreased by 15.80%.

For, May, 35 stations have been calculated and 12 stations were found to have negative trends and 23 stations were found positive trends. The spatial variation of trends is shown in (Figure 7.31). It is seen from the figure that the half of the country of the south has increasing trends and slightly decreasing in CHT while half of the country of the north has decreasing trends. Since there is a strong correlation among the rainfall trends at different stations. It is found that the overall chance of increasing in rainfall in May is about 19.64%. The expected change, which is expressed by a median change with an exceedance probability of 50%, is found to be increasing at a rate of 0.72% per year (Figure 7.31). This means that, over a period of 10 years, the rainfall in the month of May has increased by 7.20%.

For, June, 35 stations have been calculated and 16 stations were found to have negative trends and 19 stations were found positive trends. The spatial variation of trends is shown in (Figure 7.32). It is seen from the figure that the central part to Chittagong Division have increasing trends while Ganges-Padma basin and Sylhet, Mymensingh, Jamalpur, Rangpur and Rajshahi

Thakorgaon region have decreasing trends. Since there is a strong correlation among the rainfall trends at different stations. It is found that the overall chance of increasing in rainfall in June is about 20.38%. The expected change, which is expressed by a median change with an exceedance probability of 50%, is found to be increasing at a rate of 0.24% per year (Figure 7.32). This means that, over a period of 10 years, the rainfall in the month of June has increased by 2.40%.

For, July, 35 stations have been calculated and 16 stations were found to have negative trends and 19 stations were found positive trends. The spatial variation of trends is shown in (Figure 7.33). It is seen from the figure that the Dhaka and Mymensingh Division and slightly in Chittagong district have decreasing trends while rest of the country has increasing trends. Since there is a strong correlation among the rainfall trends at different stations. It is found that the overall chance of increasing in rainfall in July is about 10.10%. The expected change, which is expressed by a median change with an exceedance probability of 50%, is found to be increasing at a rate of 0.62% per year (Figure 7.33). This means that, over a period of 10 years, the rainfall in the month of July has increased by 6.20%.

For, August, 35 stations have been calculated and 16 stations were found to have negative trends and 19 stations were found positive trends. The spatial variation of trends is shown in (Figure 7.34). It is seen from the figure that the North Bengal, western part, north-eastern part and slightly in Chittagong district have increasing trends while central part of the country to central and western coastal zone and slightly in Cox's Bazar district have decreasing trends. Since there is a strong correlation among the rainfall trends at different stations. It is found that the overall chance of increasing in rainfall in August is about 32.85%. The expected change, which is expressed by a median change with an exceedance probability of 50%, is found to be increasing at a rate of 0.93% per year (Figure 7.34). This means that, over a period of 10 years, the rainfall in the month of August has increased by 9.30%.

For, September, 35 stations have been calculated and 18 stations were found to have negative trends and 17 stations were found positive trends. The spatial variation of trends is shown in (Figure 7.35). It is seen from the figure that the western to northern half of the country and slightly in Teknaf have increasing trend and other half of the country has decreasing trends. Since there is not strong correlation among the rainfall trends at different stations. It is found that the overall chance of decreasing in rainfall in September is about 24.98%. The expected change, which is expressed by a median change with an exceedance probability of 50%, is found to be decreasing at a rate of 0.06% per year (Figure 7.35). This means that, over a period of 10 years, the rainfall in the month of September has decreased by 0.60%.

For, October, 35 stations have been calculated and 15 stations were found to have negative trends, 19 stations were found positive trends and 1 station has stable in trend. The spatial variation of trends is shown in (Figure 7.36). It is seen from the figure that Tangail and Sylhet district and whole coastal zone except slightly in Chittagong district region have decreasing trends while rest of the country has increasing trends. Since there is not strong correlation among the rainfall trends at different stations. It is found that the overall chance of increasing in rainfall in October is about 6.59%. The expected change, which is expressed by a median change with an exceedance probability of 50%, is found to be increasing at a rate of 0.16% per year (Figure 7.36). This means that, over a period of 10 years, the rainfall in the month of October has increased by 1.60%.

For, November, 35 stations have been calculated and 33 stations were found to have negative trends and 2 stations were found positive trends. The spatial variation of trends is shown in (Figure 7.37). It is seen from the figure that Ganges Padma basin except Jessore region has increasing trends while rest of the country has decreasing trends. Since there is a strong correlation among the rainfall trends at different stations. It is found that the overall chance of decreasing in rainfall in November is about 38.52%. The expected change, which is expressed by a median change with an exceedance probability of 50%, is found to be decreasing at a rate of 0.86% per year (Figure 7.37). This means that, over a period of 10 years, the rainfall in the month of November has decreased by 8.60%.

For, December, 35 stations have been calculated and 33 stations were found to have negative trends and 2 stations were found positive trends. The spatial variation of trends is shown in (Figure 7.38). It is seen from the figure that Sundarbans region and Teknaf have increasing trends while rest of the country has decreasing trends. Since there is a strong correlation among the rainfall trends at different stations. It is found that the overall chance of decreasing in rainfall in December is about 14.17%. The expected change, which is expressed by a median change with an exceedance probability of 50%, is found to be decreasing at a rate of 0.37% per year (Figure 7.38). This means that, over a period of 10 years, the rainfall in the month of December has decreased by 3.70%.

Table 7.4: Summary of monthly rainfall trends and risk for different months

Month	Trend Per Decade	Risk of Increase (%)	Significance
January	0.83	6.90	*
February	2.56	6.90	*
March	4.78	13.61	NS
April	11.82	23.89	NS
May	36.00	1.07	**
June	51.70	0.04	**
July	66.85	0.04	**
August	49.11	0.04	**
September	42.57	0.28	**
October	22.58	1.07	**
November	3.18	77.26	NS
December	0.87	23.89	NS

Note: **Significant at the 95% level of confidence; *Significant at the 90% level of confidence; NS-Not Significant at the 90% level of confidence

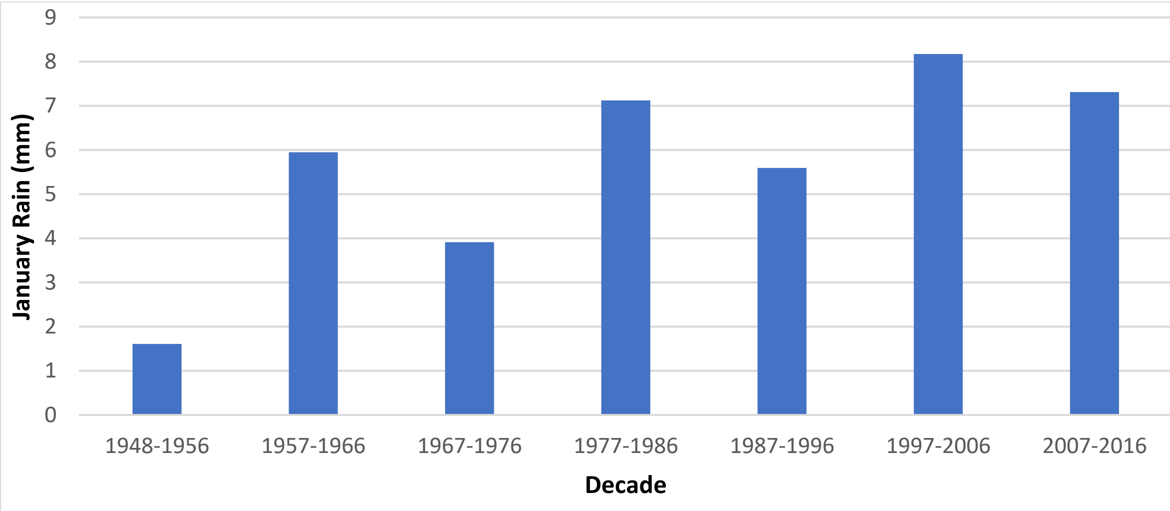

Figure 7.14: Decadal variation in all-Bangladesh January rainfalls

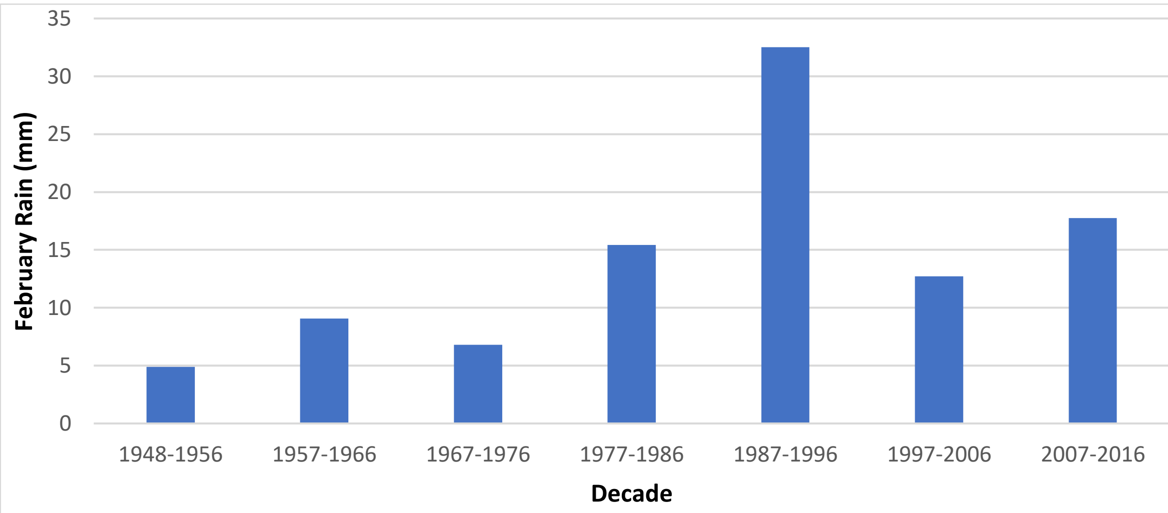

Figure 7.15: Decadal variation in all-Bangladesh February rainfalls

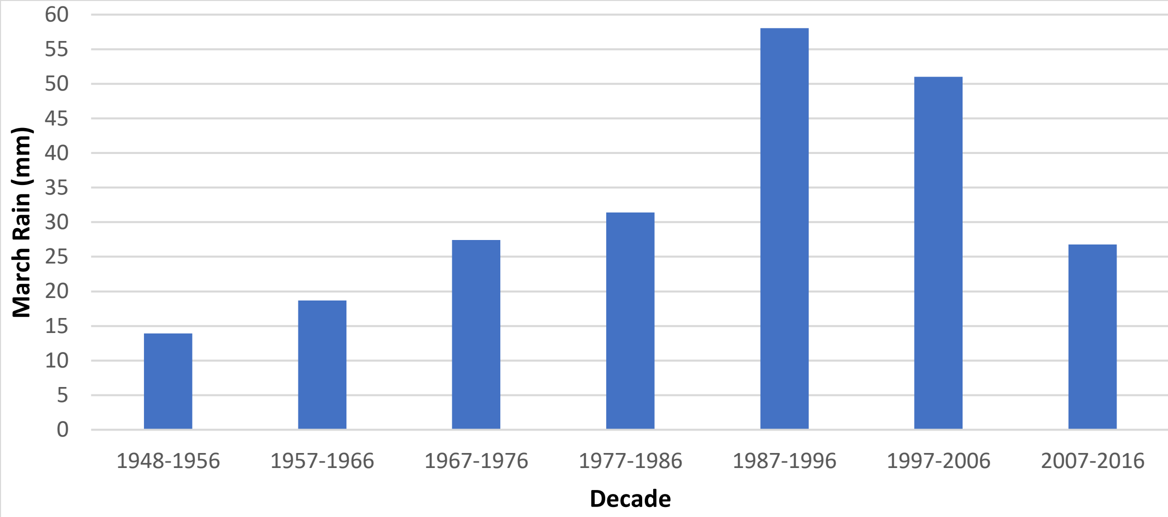

Figure 7.16: Decadal variation in all-Bangladesh March rainfalls

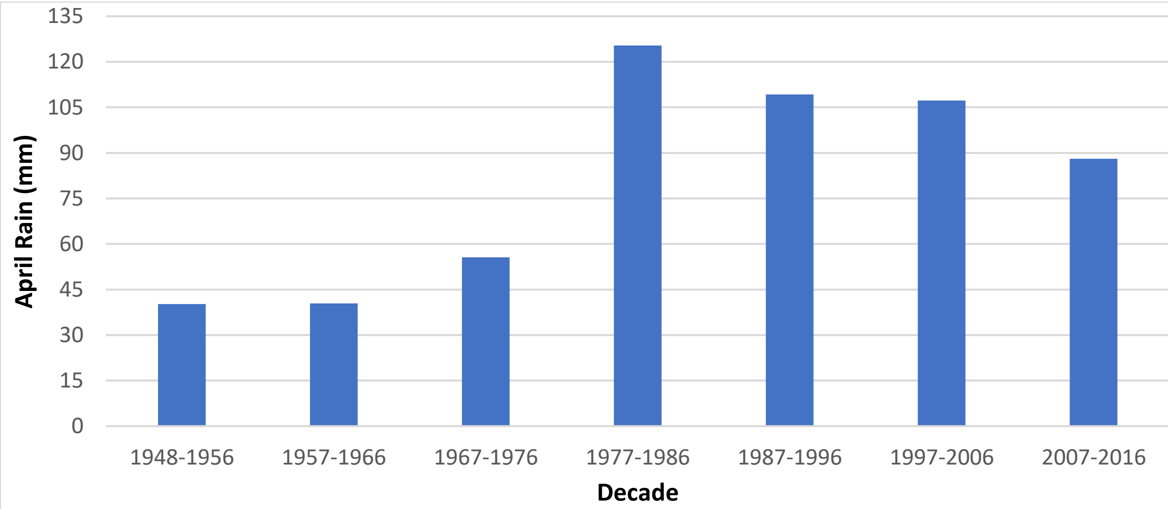

Figure 7.17: Decadal variation in all-Bangladesh April rainfalls

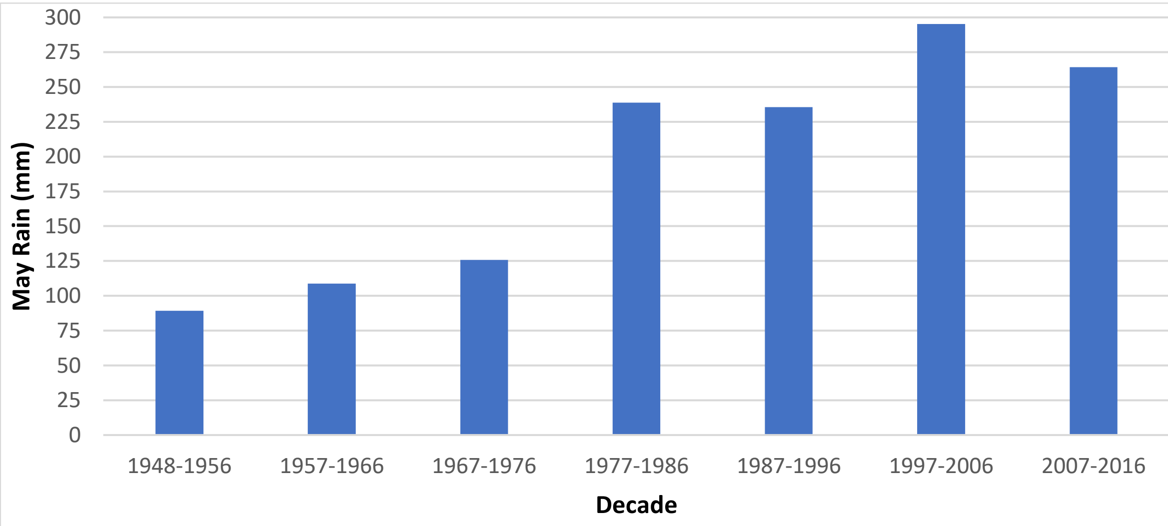

Figure 7.18: Decadal variation in all-Bangladesh May rainfalls

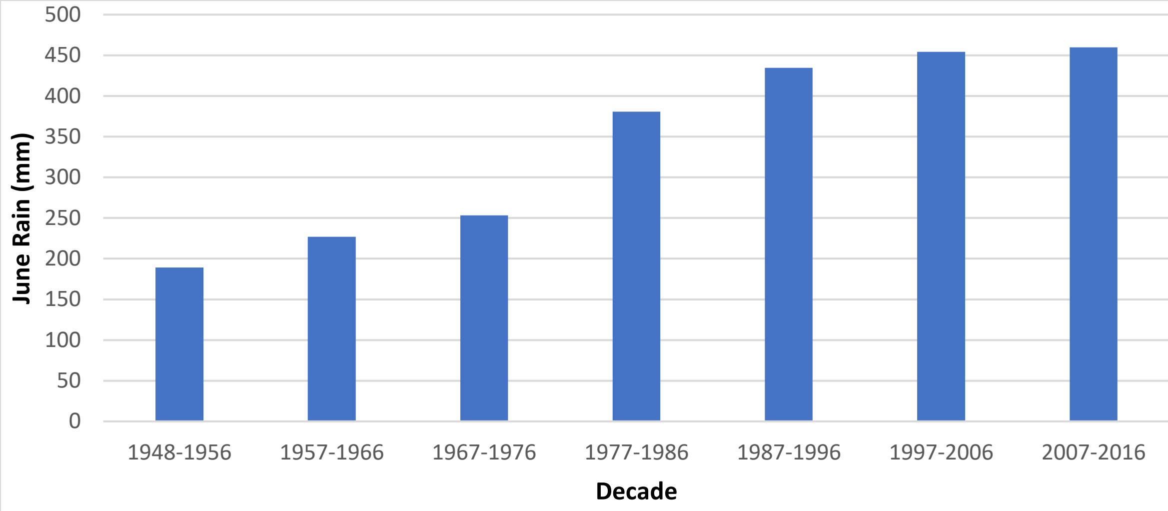

Figure 7.19: Decadal variation in all-Bangladesh June rainfalls

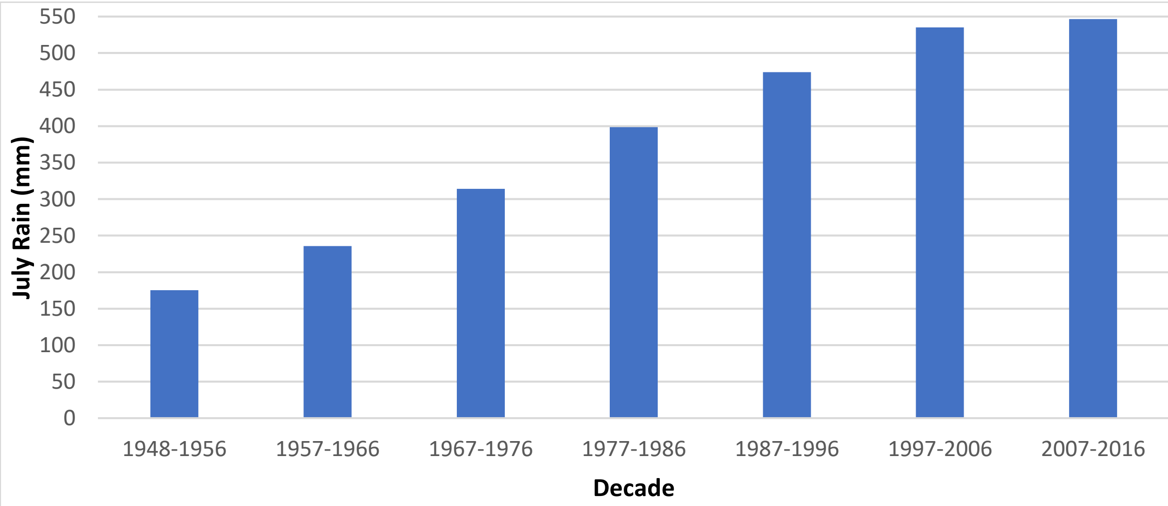

Figure 7.20: Decadal variation in all-Bangladesh July rainfalls

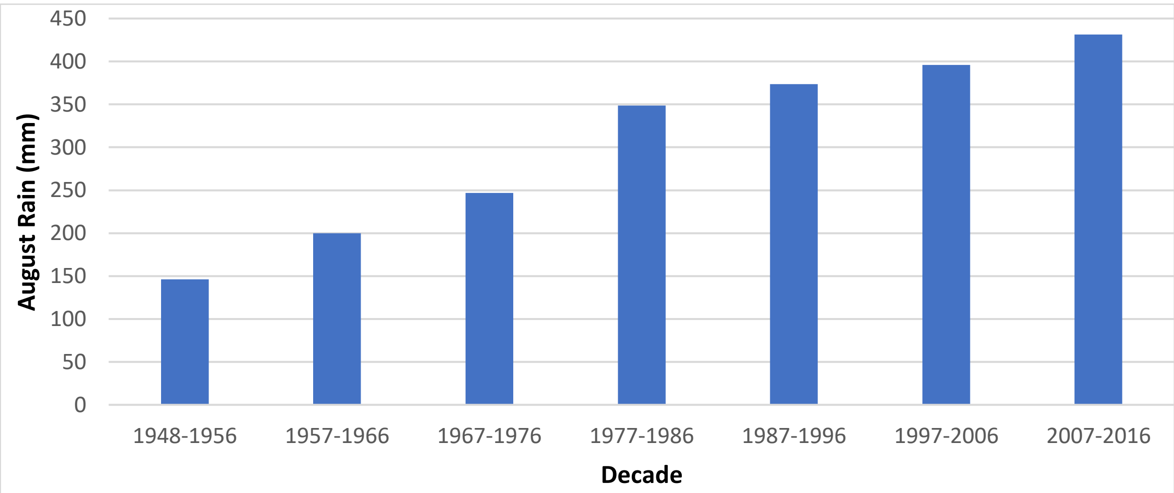

Figure 7.21: Decadal variation in all-Bangladesh August rainfalls

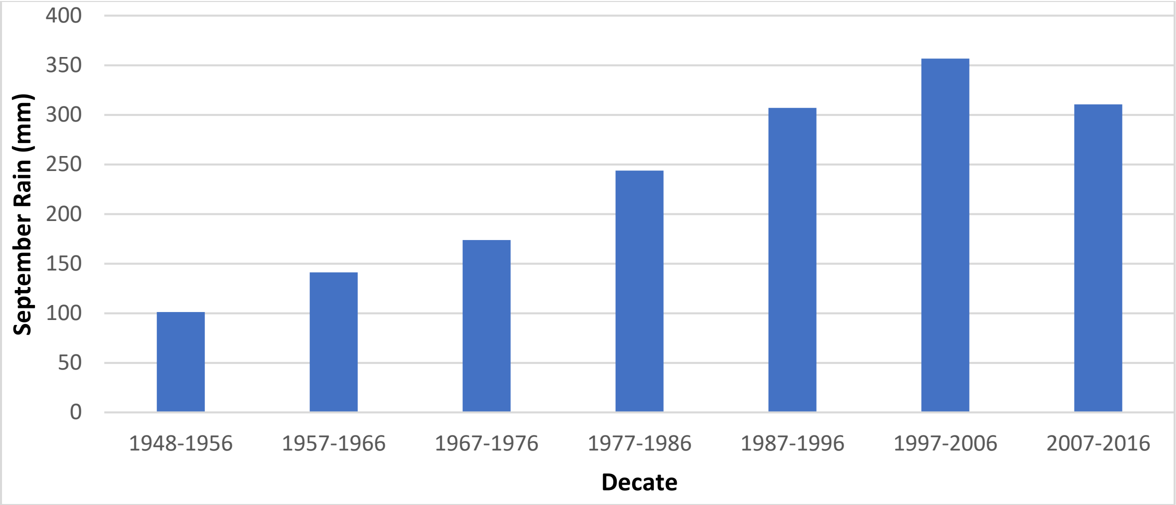

Figure 7.22: Decadal variation in all-Bangladesh September rainfalls

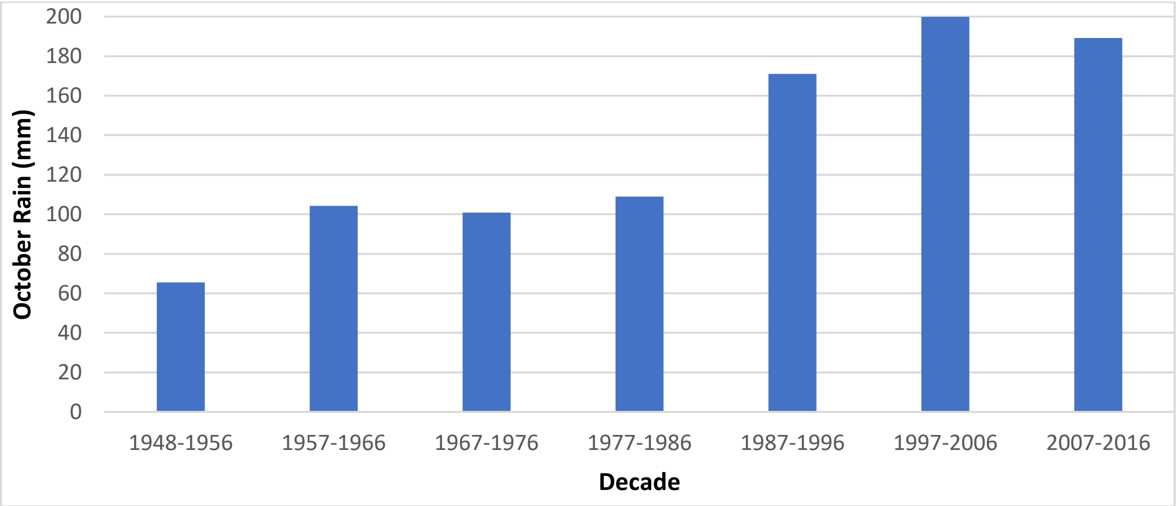

Figure 7.23: Decadal variation in all-Bangladesh October rainfalls

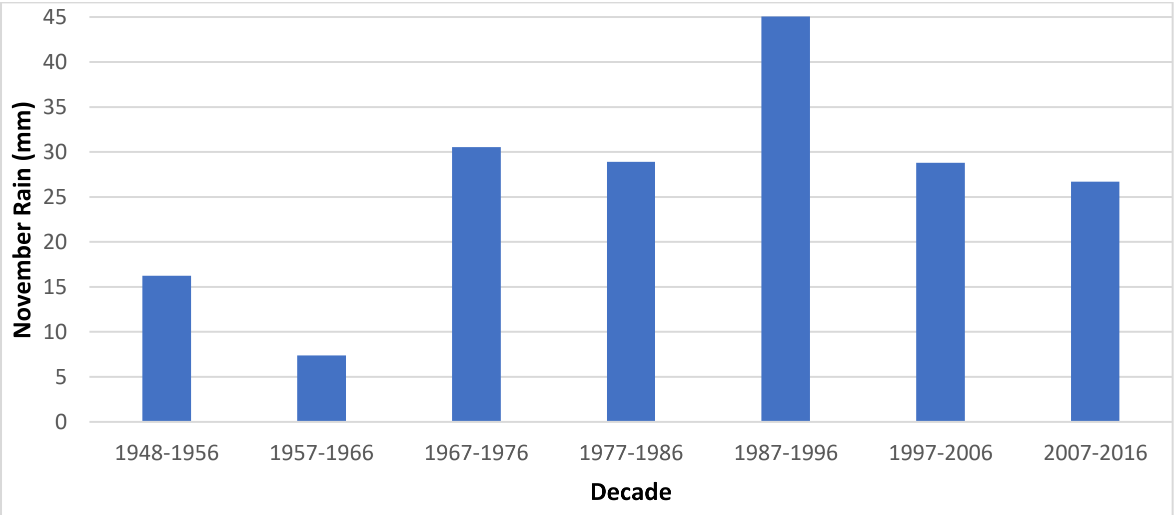

Figure 7.24: Decadal variation in all-Bangladesh November rainfalls

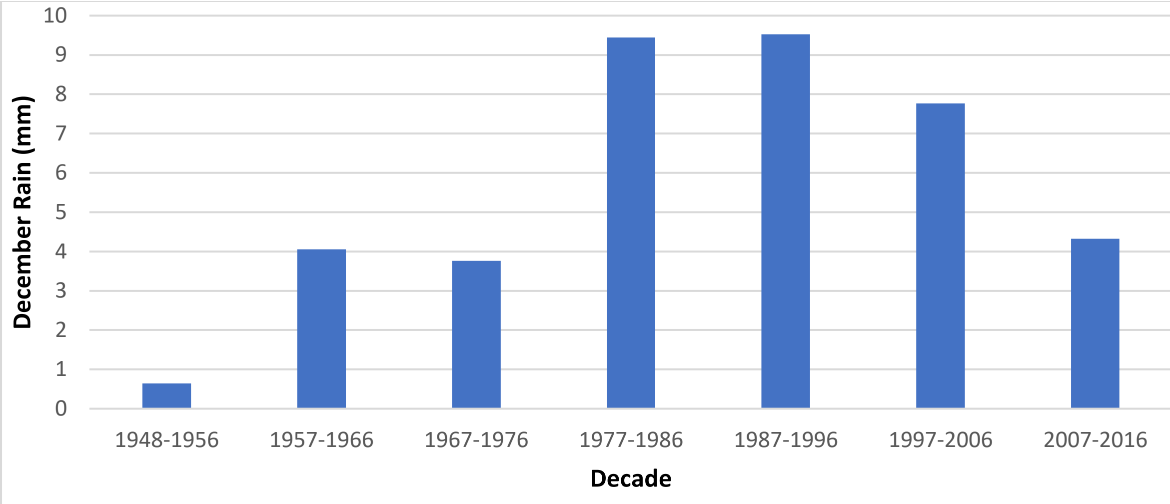

Figure 7.25: Decadal variation in all-Bangladesh December rainfalls

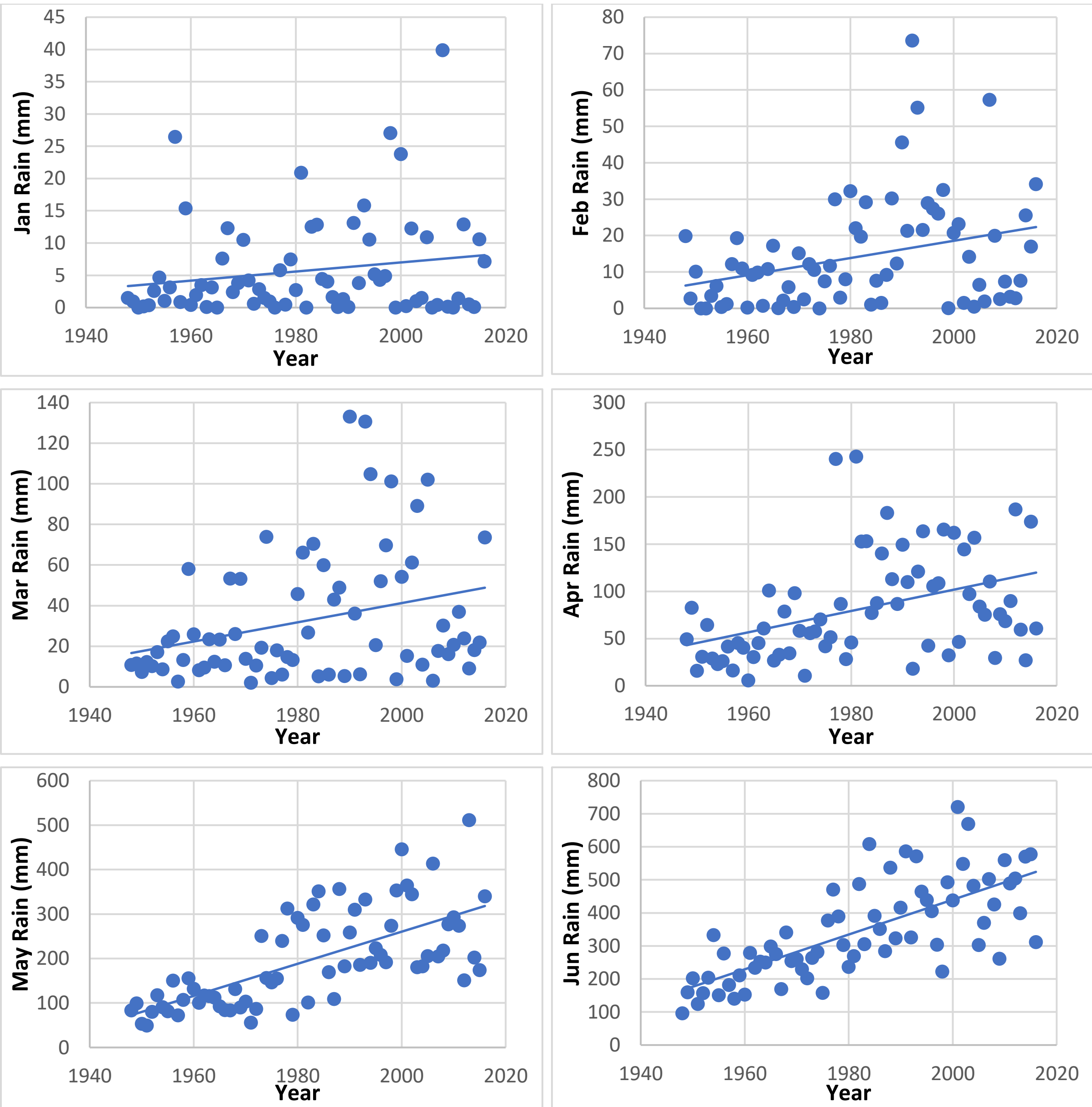

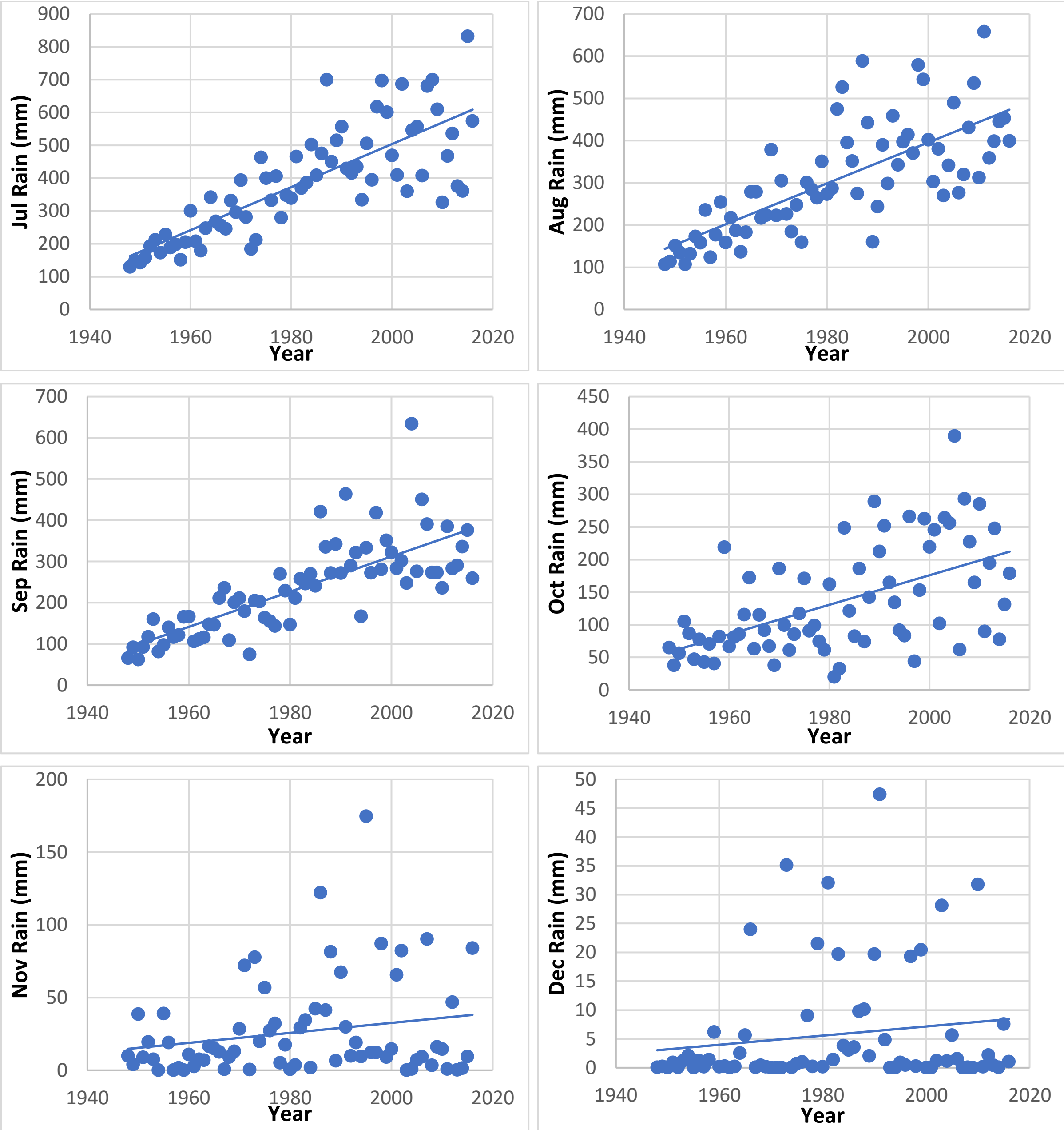

Figure 7.26: Trends in all-Bangladesh monthly rainfalls

The above scatter plot (Figure 7.26) shows the trends in all Bangladesh monthly rainfall. Since there is no strong correlation among the rainfall trends in all Bangladesh at different Months, they can be considered as independent observations from a continuous probability distribution. Based on scatter plot a probability plotting can be used to estimate the probability of increase or decrease in rainfall.

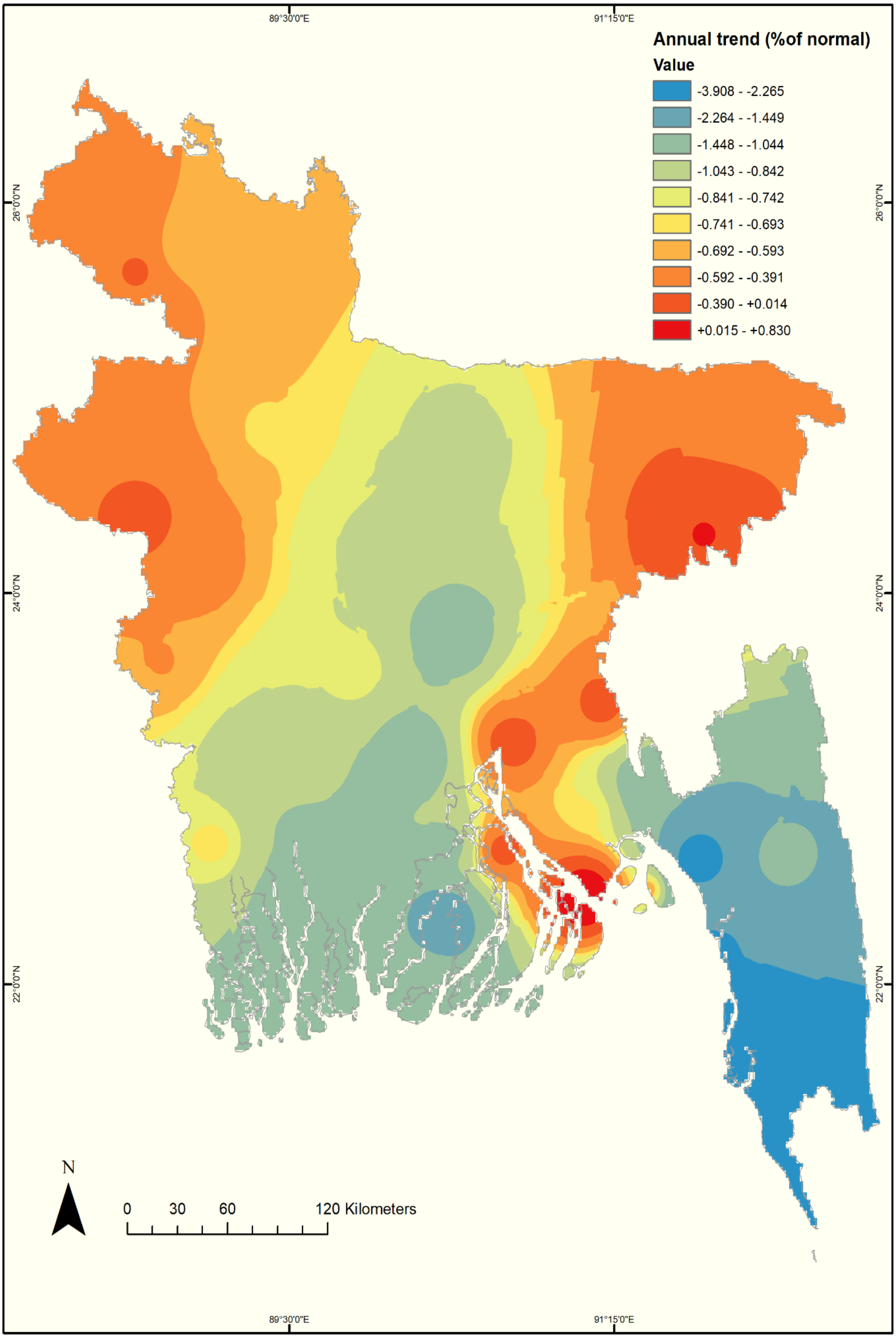

Figure 7.27: Spatial variation of trends in January rainfall (% of normal rainfall)

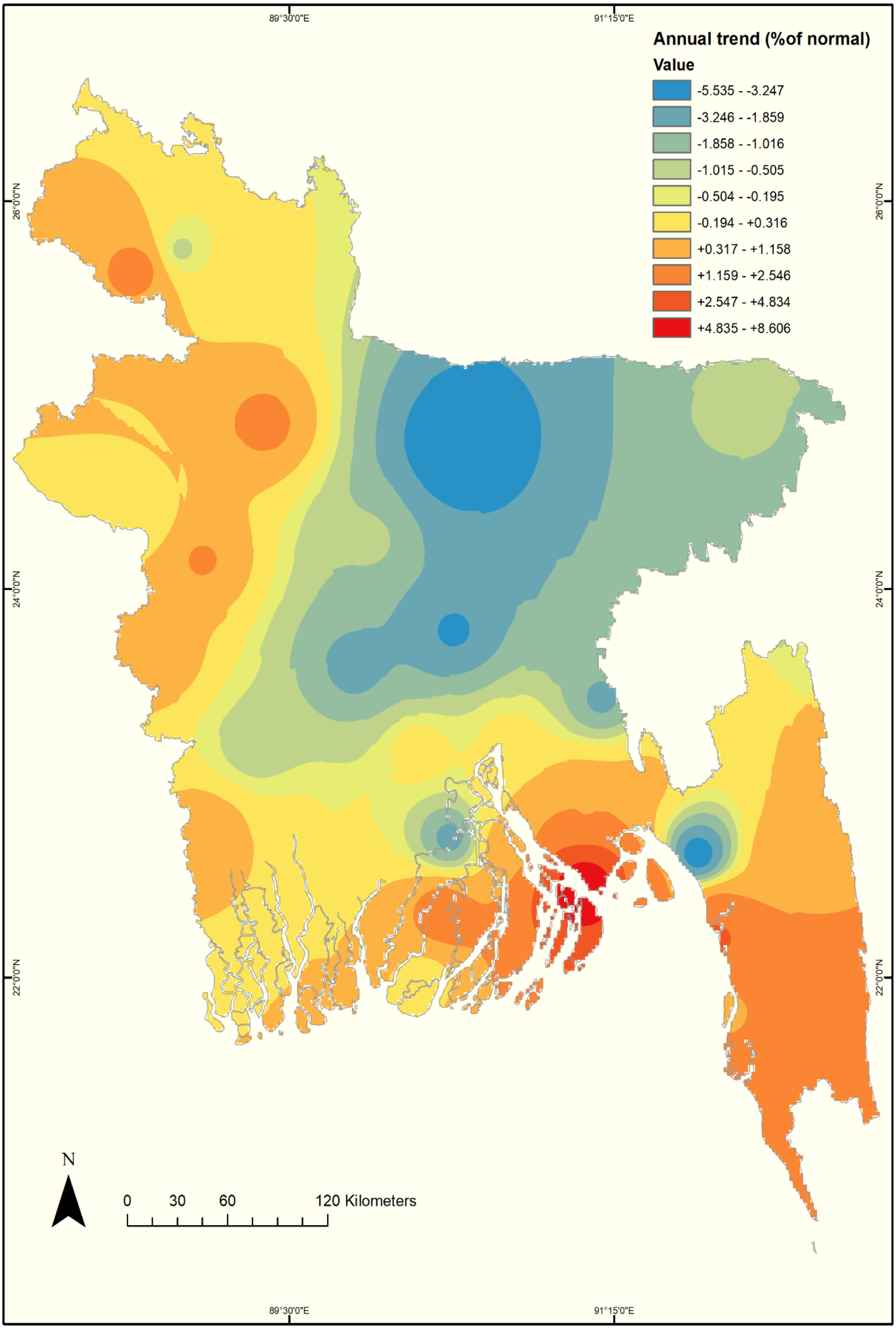

Figure 7.28: Spatial variation of trends in February rainfall (% of normal rainfall)

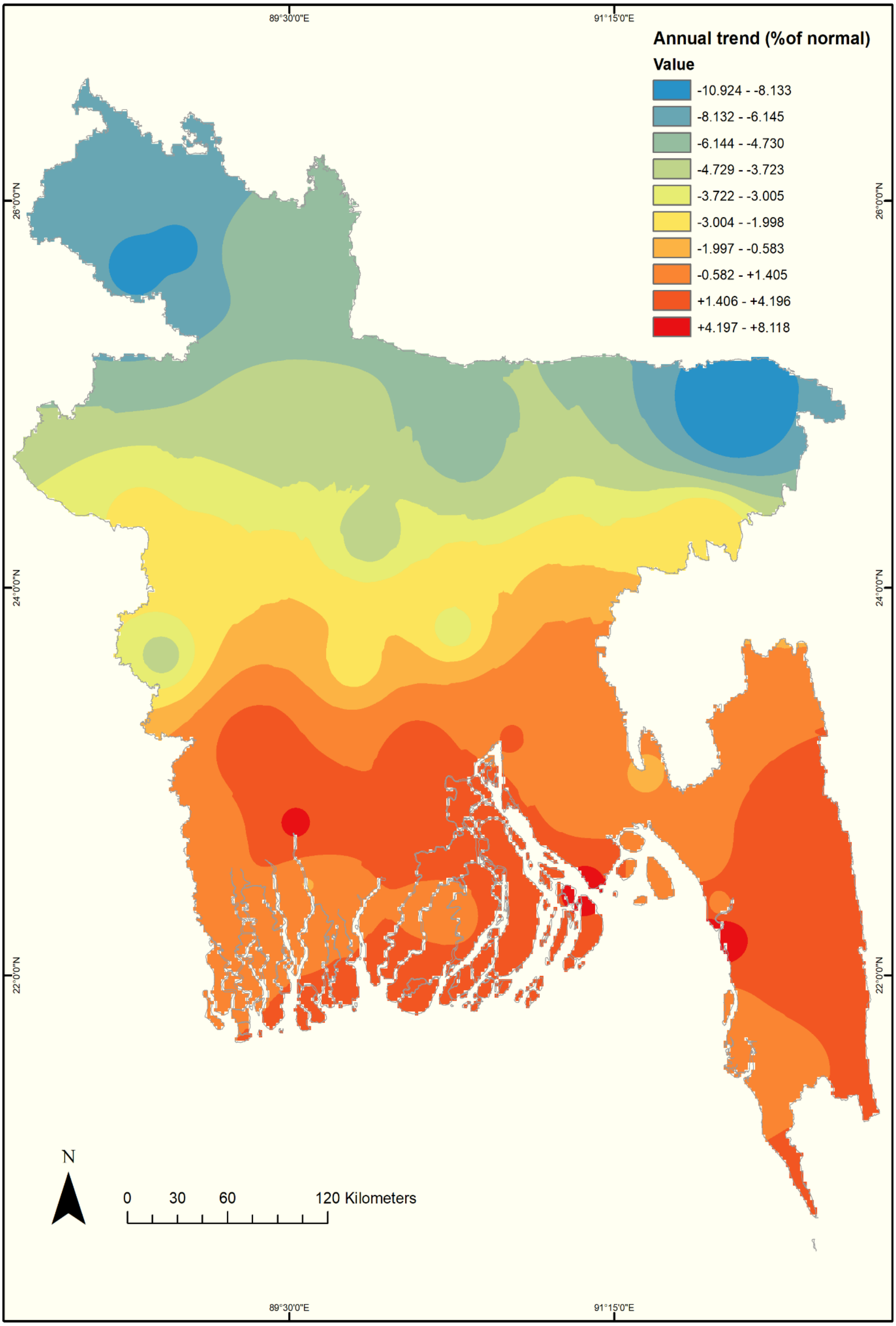

Figure 7.29: Spatial variation of trends in March rainfall (% of normal rainfall)

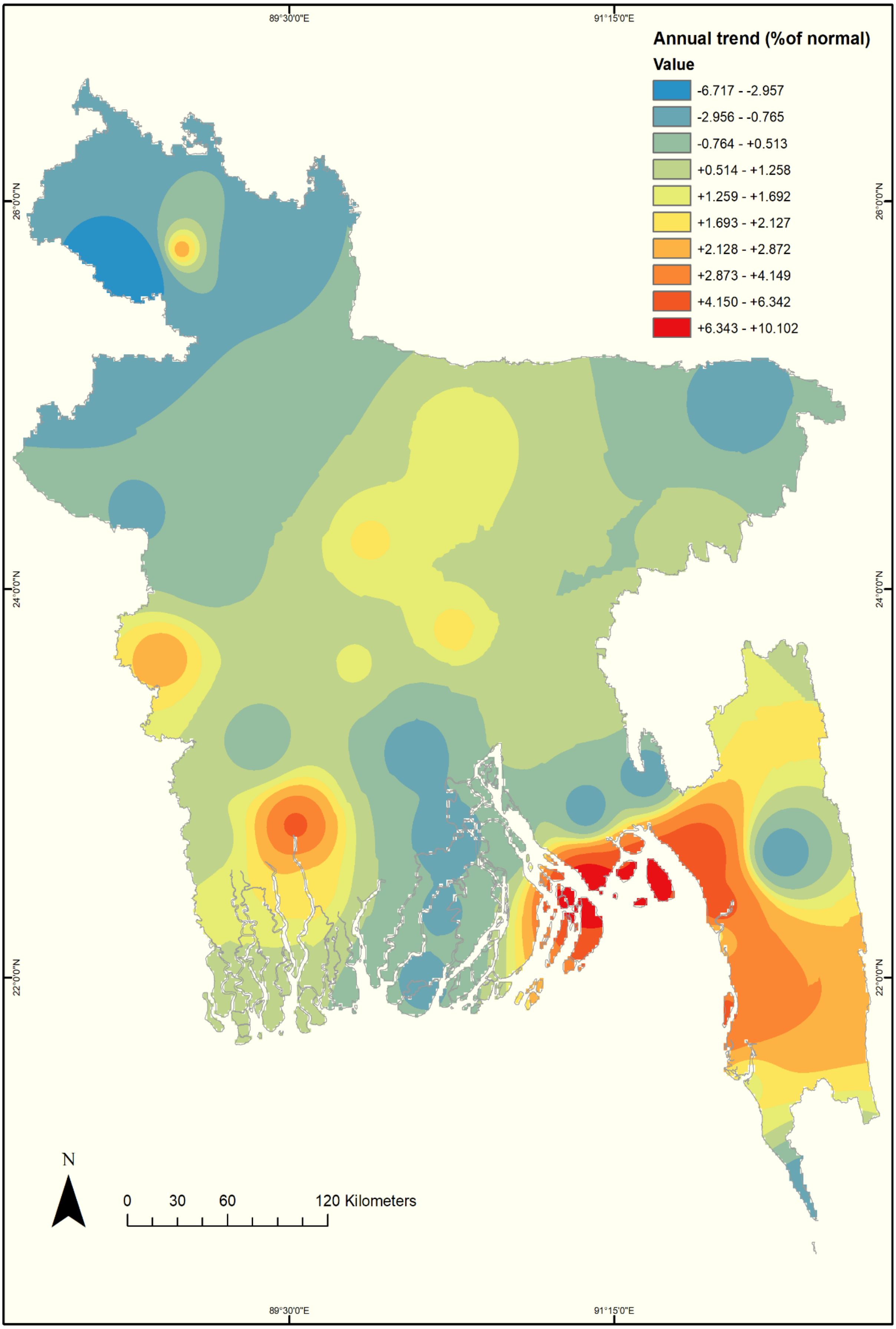

Figure 7.30: Spatial variation of trends in April rainfall (% of normal rainfall)

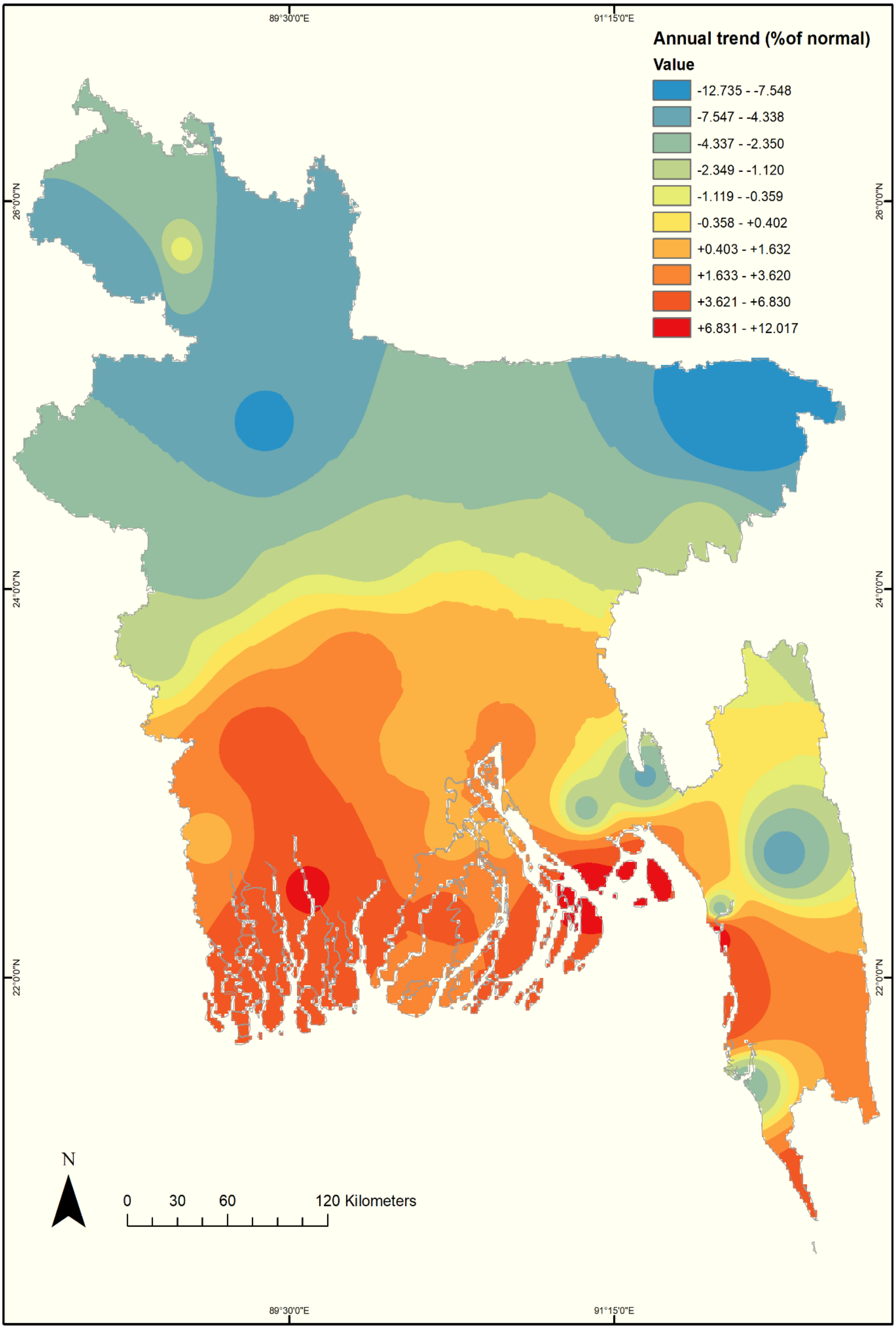

Figure 7.31: Spatial variation of trends in May rainfall (% of normal rainfall)

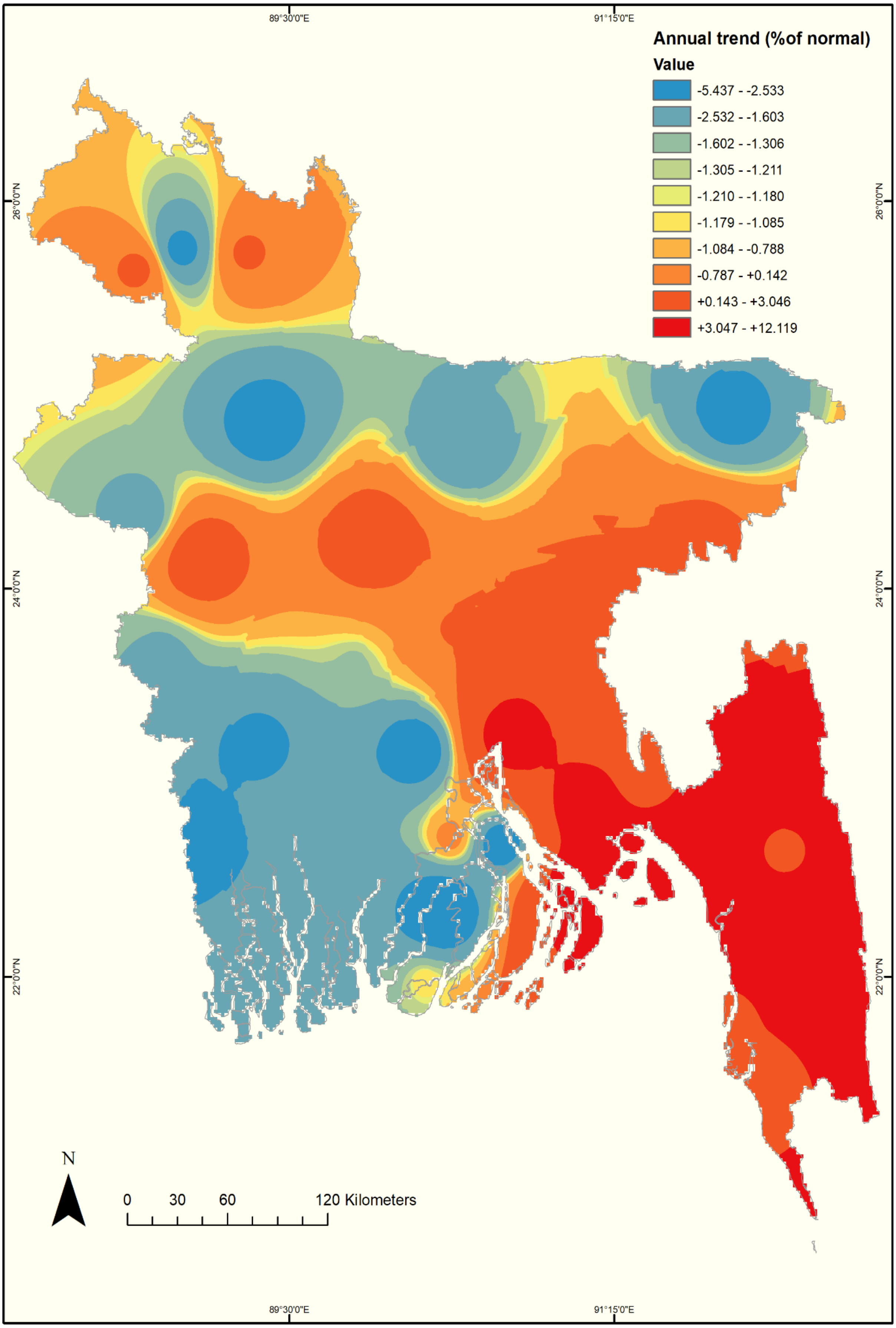

Figure 7.32: Spatial variation of trends in June rainfall (% of normal rainfall)

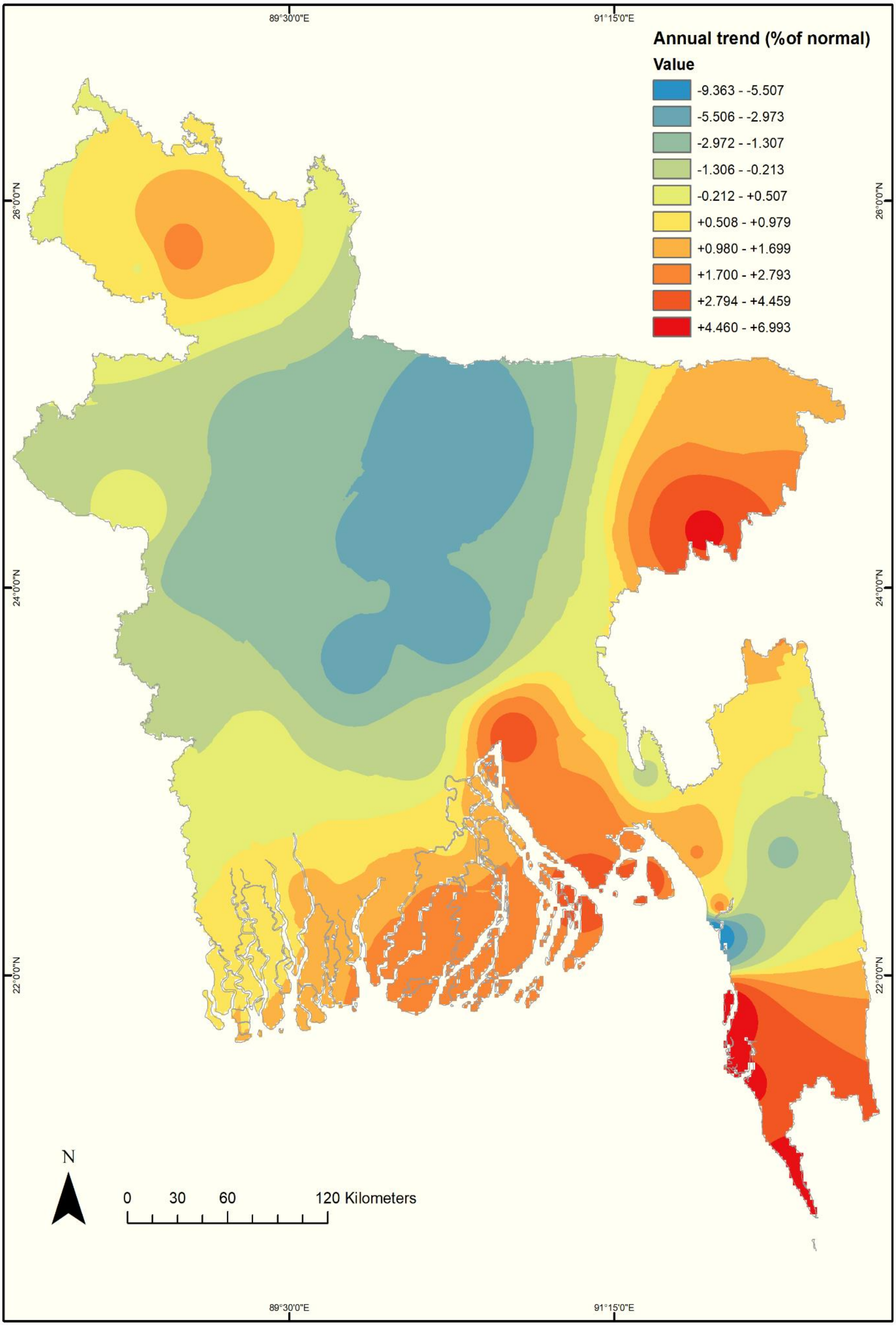

Figure 7.33: Spatial variation of trends in July rainfall (% of normal rainfall)

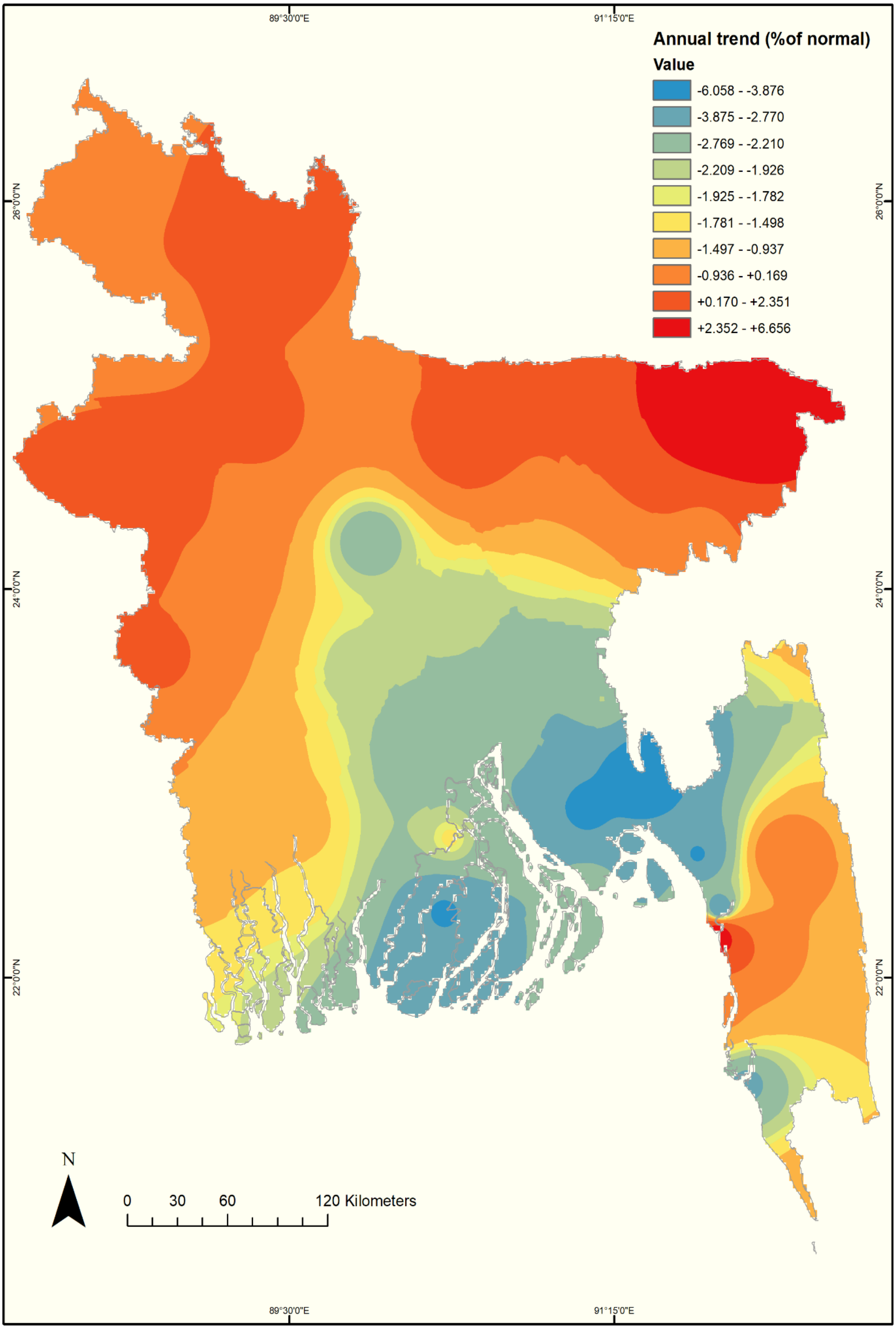

Figure 7.34: Spatial variation of trends in August rainfall (% of normal rainfall)

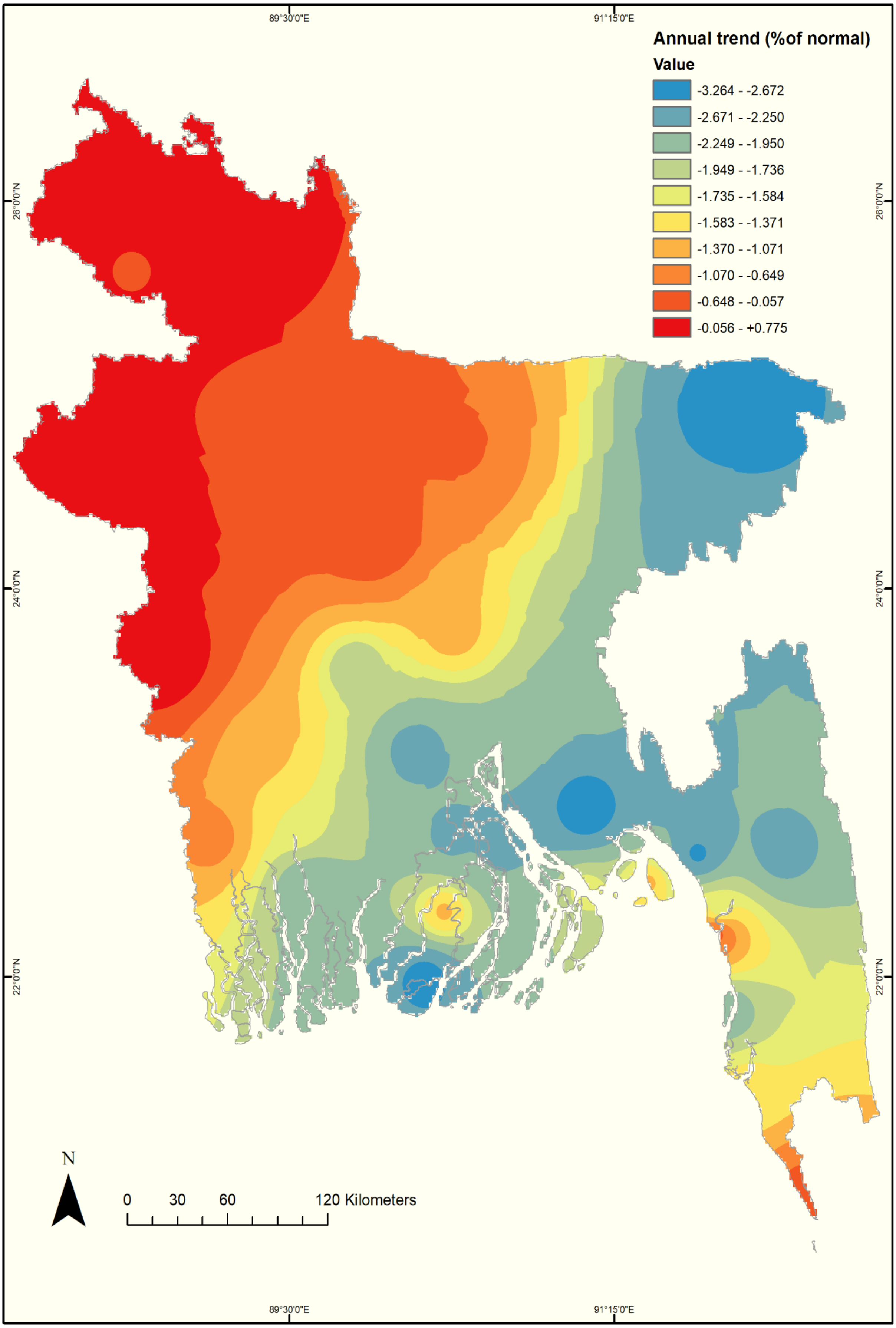

Figure 7.35: Spatial variation of trends in September rainfall (% of normal rainfall)

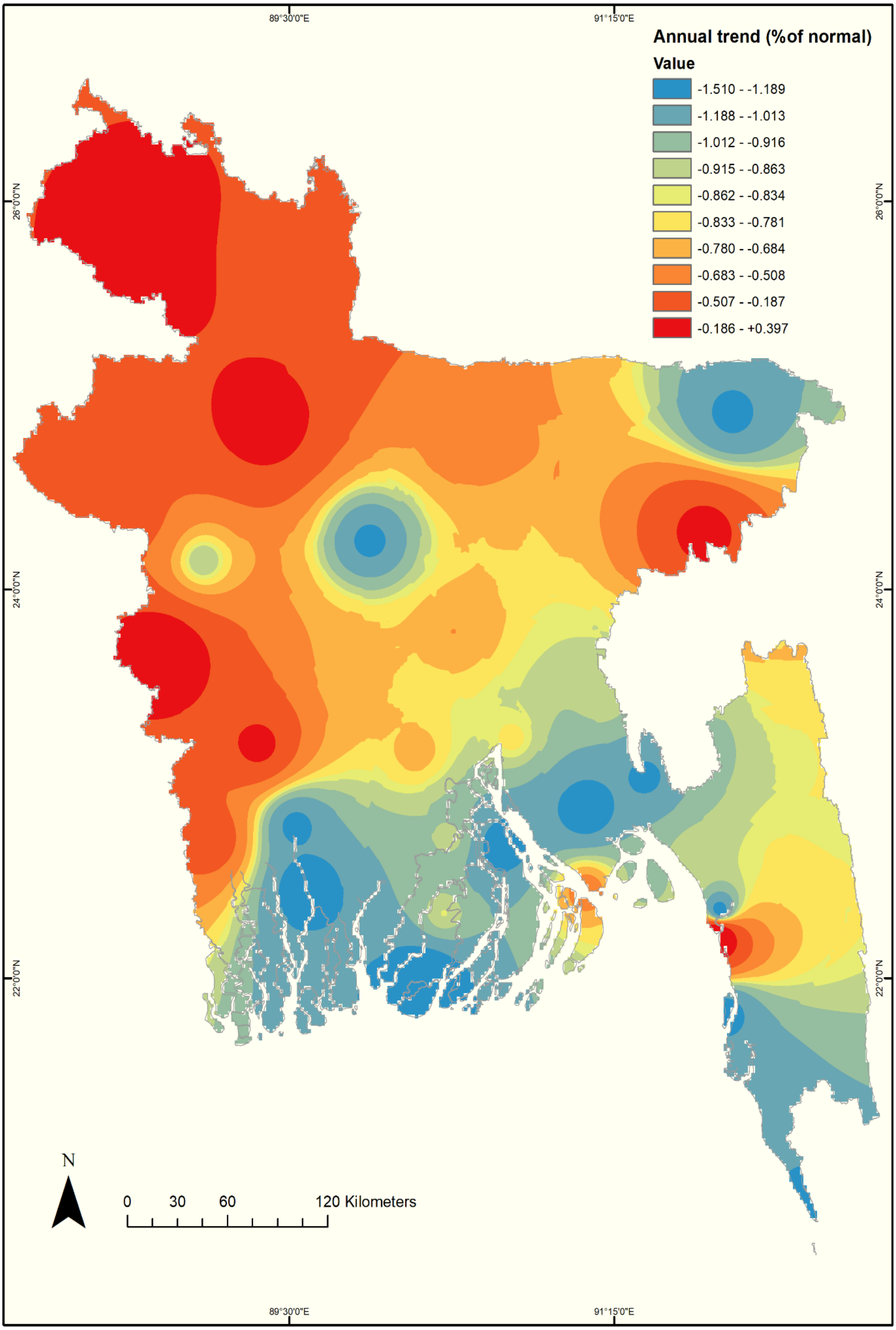

Figure 7.36: Spatial variation of trends in October rainfall (% of normal rainfall)

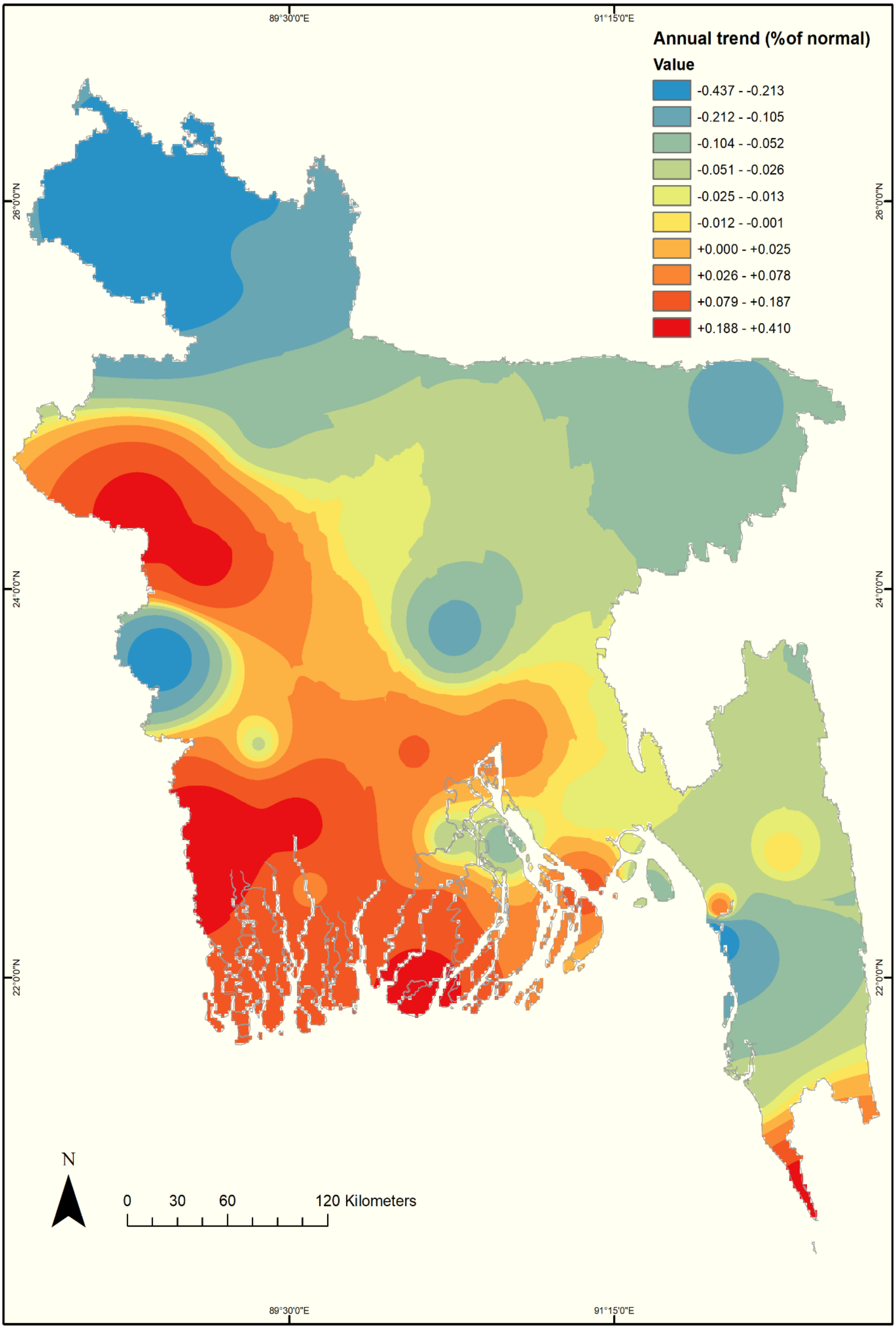

Figure 7.37: Spatial variation of trends in November rainfall (% of normal rainfall)

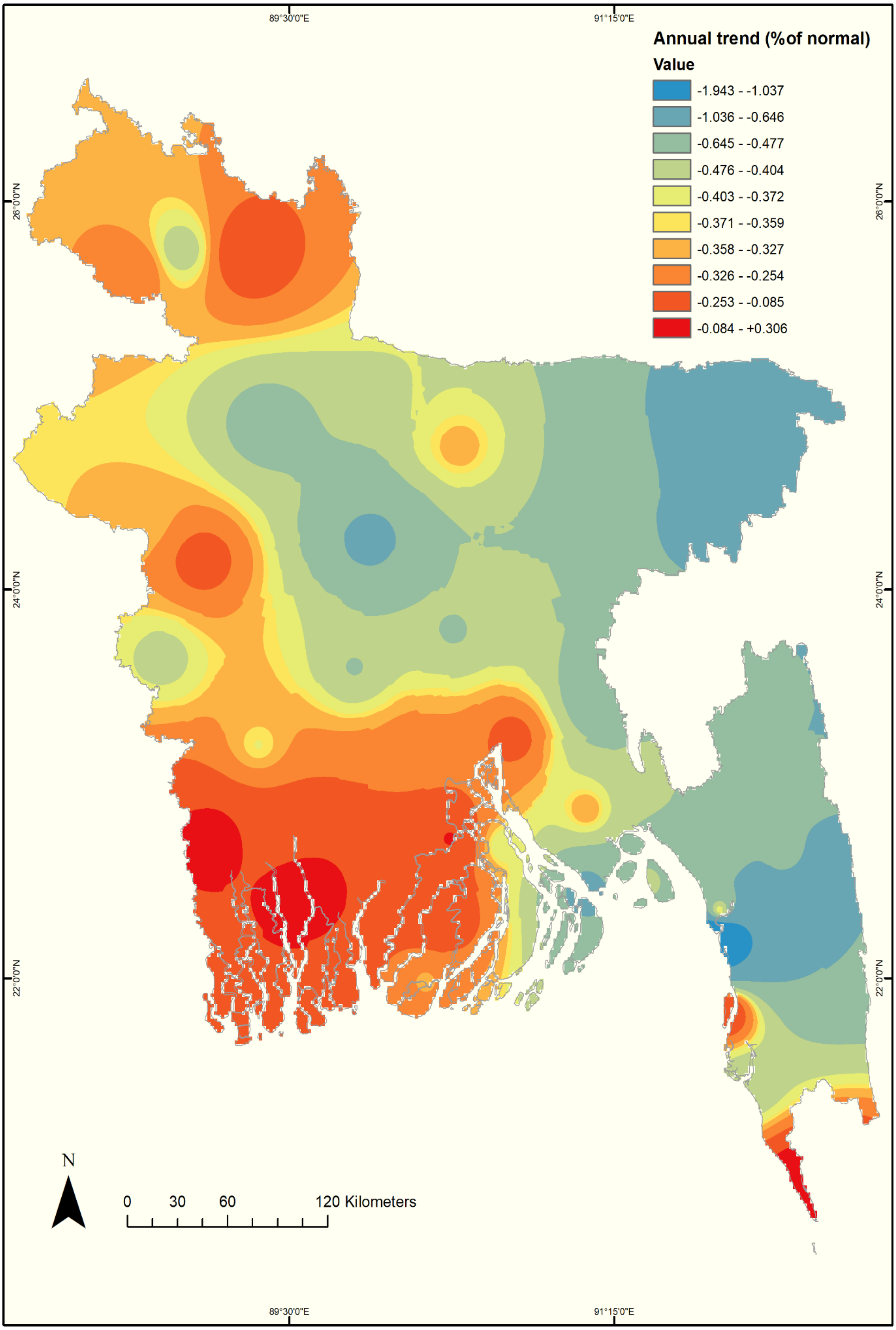

Figure 7.38: Spatial variation of trends in December rainfall (% of normal rainfall)

7.6 Variability of Monthly Rainfall

The variability, measured in terms of standard deviation, in all-Bangladesh monthly rainfalls is given in (Figure 7.39). It is seen from the figure that the variability in rainfalls in the months of January, February, March, April, May, June, August and October have increased, while that in the months of July and September have decreased. It thus appears that the interannually variability in rainfalls in most months has increased. This indicates that the rainfall is becoming increasingly more uncertain and unpredictable.

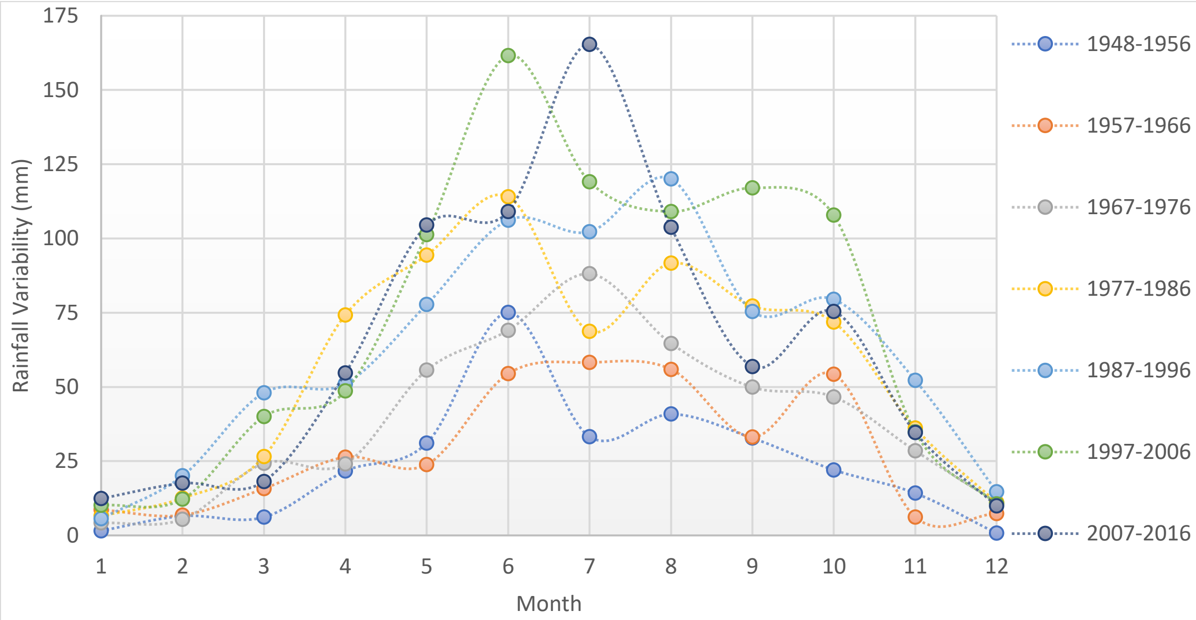

Figure 7.39: All-Bangladesh variability in monthly rainfalls

Chapter Eight

Spatial Pattern of Future Climate Change Scenario

8.1 Introduction

Future climate will depend on committed warming caused by past anthropogenic emissions, as well as future anthropogenic emissions and natural climate variability (IPCC, 2014). The purpose of this chapter is to assess and quantify projections of possible future climate change from different climate models. A background of concepts used to assess climate change experiments is presented in different section which includes results from ensembles of several categories of future climate change experiments, factors that contribute to the response of those models, changes in variability and changes in extremes. Regional information derived in some way from global models (including results from embedded regional high-resolution models, downscaling, etc.) now appears in this chapter.

Anthropogenic rise in greenhouse concentrations is causing significant anomalies in climate at global and regional scales (IPCC, 2014). General Circulation Model (GCM) predictions have warned about frequency and severity of these changes in future (Wilby *et. al*., 2002; Nasim *et. al*., 2016a) and their profound biological, societal, and environmental impacts (Easterling *et. al*., 2000; Patz *et. al*., 2005; Rosenzweig *et. al*., 2008; Hautier *et. al*., 2015; Hertel, 2016; Nasim *et. al*., 2016b). These impacts are largely felt as the changes in the risks of extreme events, maximum and minimum temperature variations, and precipitations have caused floods (Porter *et. al*., 2014). Climatic predictions should be used for the future adaptations on the risks of climatic extremes and changes in their rate of occurrence and strength over time (Amin *et. al.*, 2016). Bangladesh is one of the examples from these events. In this context, in Bangladesh, these events should be tackling by integrated models and tools. Climate change adaptation assessments are essential that can help to link the gap between the management and technology in order to reduce these risks (Amin *et. al.,* 2016). The information of spatial scale used as a base to investigate the impact of changing climate on various sectors in our society can also affect the magnitude and sometimes even the sign of the potential change and corresponding impacts (Kueppers *et. al*., 2005; Amin *et. al*., 2015). Many scientists have proposed different changes for the implementation of climate modeling (Kravitz *et. al*., 2013). One of the most effective approaches for the climate modeling recommended by Intergovernmental Panel on Climate Change (IPCC) is global circulation models (GCMs) in representative greenhouse gas concentration pathway RCPs (IPCC, 2014). Spatial resolution of global climate models is still insufficient to adequately describe many regional climate processes (Amin *et. al.,* 2016). In order to determine better estimates for regional climate parameters, high-resolution regional climate models (RCMs) are frequently used (Warrick, 2009). This approach has been comprehensively employed in recent European research projects also including an ensemble approach, by designing series of coordinated experiments using multiple models to pursue different research questions (Bao *et. al*., 2015; Christensen *et. al*., 2008). RCM has higher resolution for the specific regions of the globe than a GCM which have resolutions 100 to 300 km for all over the globe (Katzav and Parker, 2015). RCMs were used within global model to access more specific simulations for a particular region or location (Warrick, 2009).

8.2 Important tools of SimCLIM Systems

An open framework modeling software SimCLIM can be used to study the impacts and adaptation strategies to climate change and climatic extremities (Warrick *et. al.*, 2012). CLIMPACTS was the basic origin of SimCLIM from New Zealand (Warrick, 2009), with different other countries and regions of the world (for example, it also develops a data pack for Bangladesh initially for mean, minimum, maximum temperature, and precipitation for climatic projections for specific region). SimCLIM 2013 is a computer-based modeling system for examining the spatiotemporal variability in climatic conditions and their impacts. It has a top down approach to deal with global, regional, and local models, and we can manipulate data for the study of impacts on human health, agricultural, and natural resource management for that specific region (Yin *et. al.,* 2013). At the basic scale, SimCLIM contains scenario generator which were developed by pattern scaling methods (Warrick, 2009) that deals with different patterns of climate change from complex GCMs which show time variant projections of global climate change. These variations are used to perturb the time series data to develop the climate scenarios for different sites or time scales as shown in (Figure 71). SimCLIM 2013 follows the fifth assessment report (AR5) of IPCC (IPCC, 2014). SimCLIM provides the facility to select the GCM patterns for the development of suitable global projections (AR5) of sensitivity values and future.

SimCLIM is one of the most useful and integrated model tools that can be used to examine the impacts and adaptations to climate change and extreme climatic events. Different tools of SimCLIM are used for the spatiotemporal analysis of spatial and site time series analyses. Basic feature of the SimCLIM is to deal with risk-based climate impact assessment by its greenhouse gas (GHG) concentration pathways generator and extreme event analyzer. In SimCLIM

Bangladesh data set, estimates of the return periods for predicted extreme events (e.g. mean temperature, maximum temperature, minimum temperature and precipitation) can be used to assess the current and future climate scenarios of climate change (Yin *et. al.,* 2013). This study was conducted to present and utilize features of the climate projection-integrated SimCLIM, CLIMsystems for the assessment of site-specific climatic events (precipitation, minimum and maximum temperature) and to study the variation associated with different time scales. Different features of the SimCLIM can be used to perform the site-specific climate analysis of maximum and minimum temperature and precipitation (Bao *et. al.,* 2015). In this study was to assess the past climate changes and compute the projected changes in Bangladesh, for the years 2025, 2050, 2075 and 2100 using regional and global climate models. In view of these changes, vulnerabilities of region may be assessed.

8.3 Selection of Climate Model

To project the future climate for local or regional scale is important to select suitable GCMs (Pierce *et. al.,* 2009; Bao *et. al.,* 2015). For a specific site, average of 40 GCMs (ensemble) should be used for suitable projections as single GCM projection has very limited scope (Hulme *et. al.,* 2000). GCM evolutions are accepted for specific site, and if these projected the current climate accurately, then these will project the accurate future climate (Coquard *et. al.,* 2004). According to this perspective, any climate change scenario consisted on single GHG emission rate and/or role of individual GCM output is ineffective for climate modeling purposes, because it cannot effectively provide the information associated with its projection, while other study claims that selection of proper GCM should be based on quality of predicted regional climate (Pierce *et. al.,* 2009).

In the (Figure 8.1) shows that the global mean temperature based on RCP mid sensitivity emission scenario. A SimCLIM simulation baseline 1995 that the global min temperature shows that lowest temperature was -44.52 ^{0}C while the height temperature was 30.27 ^{0}C. From north to south, middle area was the height temperate zone and Bangladesh is situated in 23 and ½^{0} north latitude. In the (Figure 8.2) shows that the global precipitation based on RCP mid sensitivity emission scenario. It shows that the lowest precipitation 311.66 mm and height precipitation 7182.60 mm. Bangladesh located in the tropical region that's why in monsoon season faced the height record of rainfall (see chapter 7). In (Figure 8.3 and 8.4) represent that the RCP 2.6, 4.5, 6.0 and 8.5 (GHG) concentration pathway time table 2015, 2040, 2080 and 2100 respectively. Using this SimCLIM tools Bangladesh climate change is assessed.

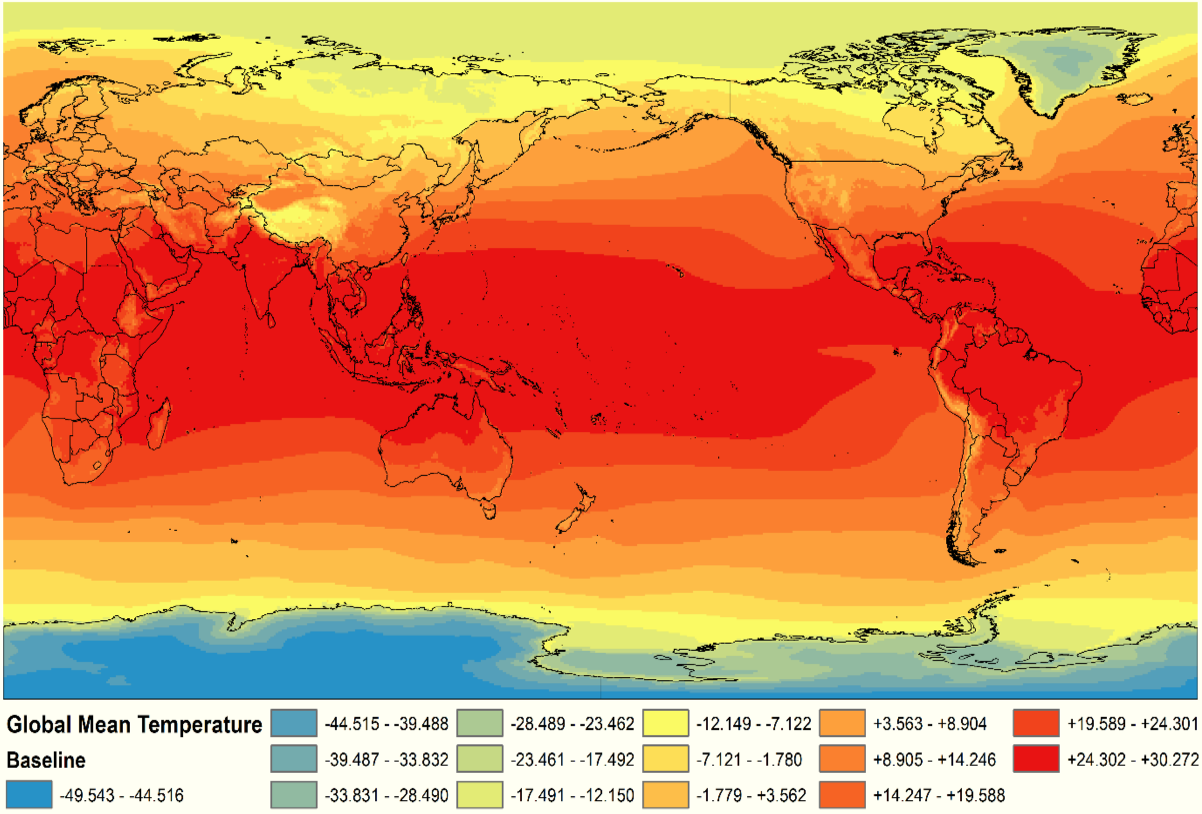

Figure 8.1: Global mean temp (^{0}C) mid sensitivity from SimCLIM simulation, baseline 1995

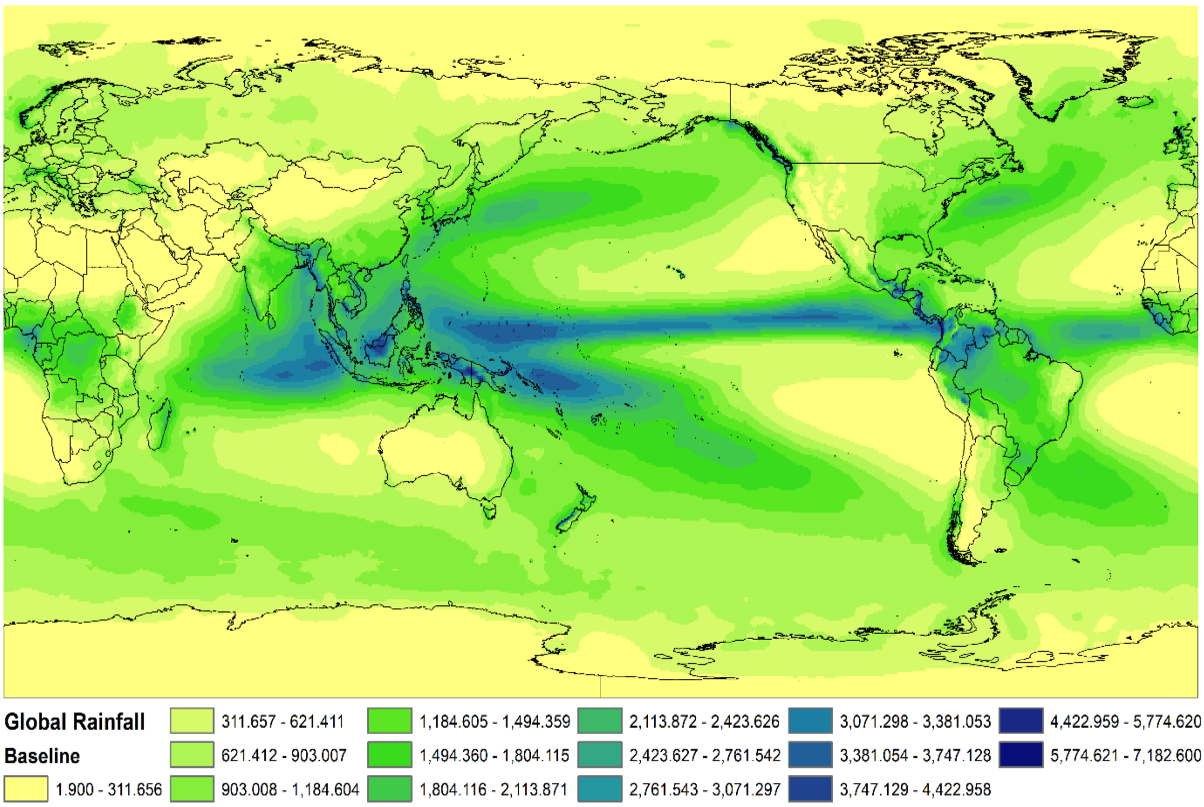

Figure 8.2: Global rainfall (mm) mid sensitivity from the SimCLIM simulation, baseline 1995

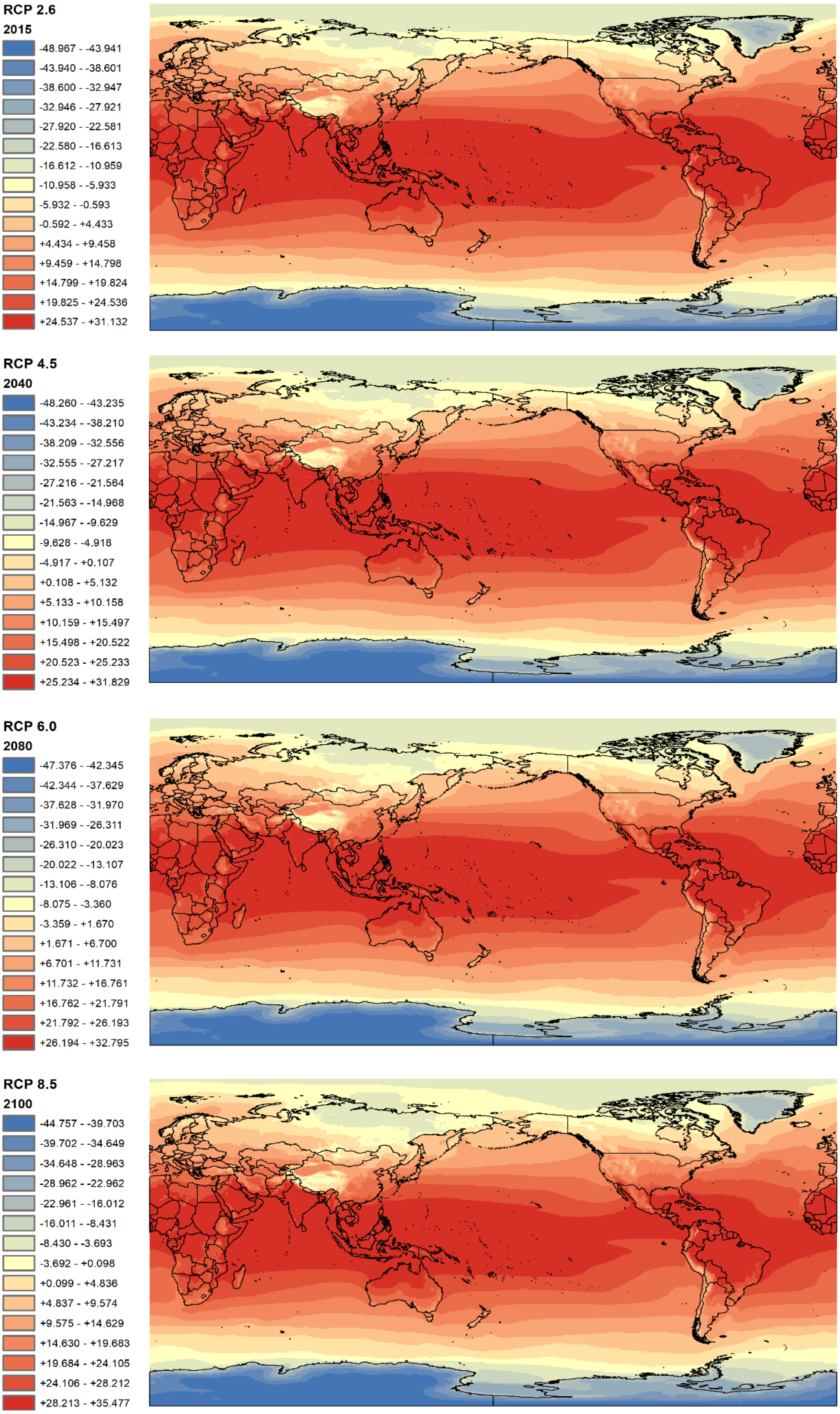

Figure 8.3: Global mean temp (^{0}C) mid sensitivity from the SimCLIM simulation different RCPs

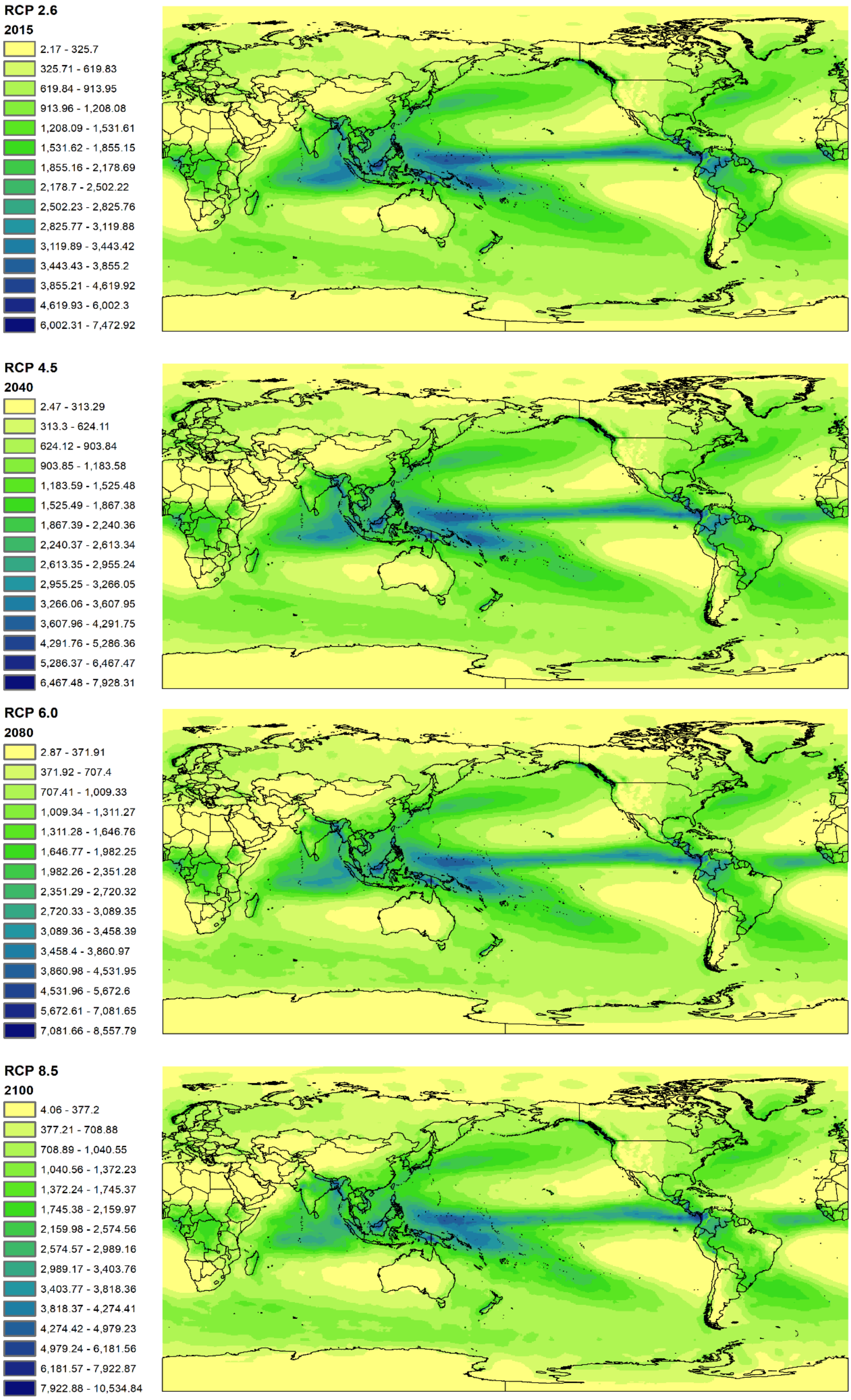

Figure 8.4: Global rainfall (mm) mid sensitivity from the SimCLIM simulation different RCPs

8.4 Simulation of Baseline (1995-2014) Climate

The regional climate has been simulated over the Bangladesh domain using SimCLIM for RCP4.5 with low and RCP6.0 with mid represents a middle range future global change scenario and RCP8.5 with high bounded low and high uncertainty range. Simulation was conducted from 1995-2100 using lateral boundary condition data. However, the period from 1995 to 2014 has been taken as baseline period as suggested by the fifth assessment report of IPCC. Using the daily minimum temperature, maximum temperature, mean temperature and precipitation spatial distribution maps of baseline climatic conditions are developed over Bangladesh.

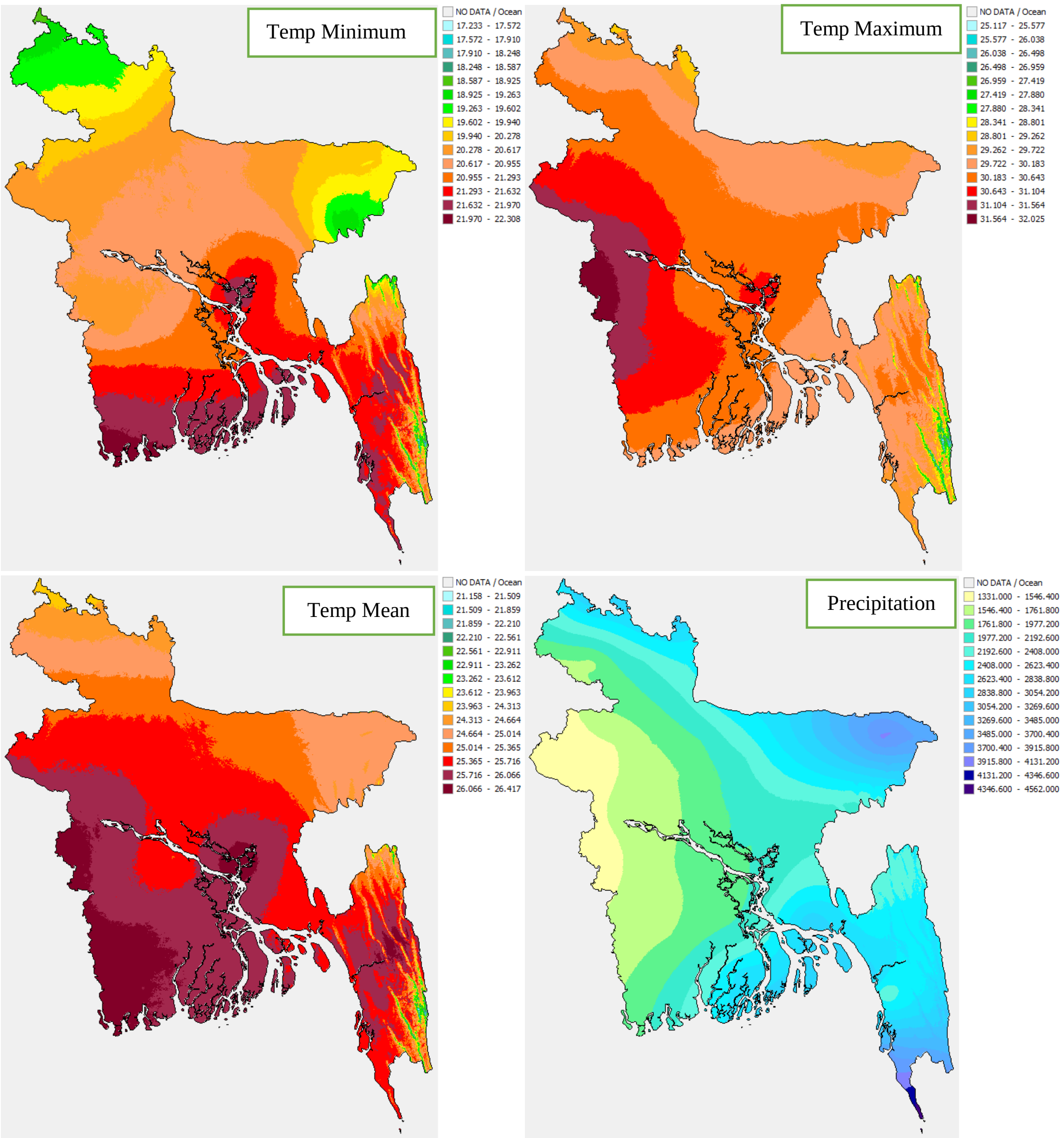

Figure 8.5: Spatial pattern, time-slice analysis e.g. minimum, maximum, mean temperature and precipitation change, baseline (1995-2014) over Bangladesh

8.5 Future Climate

In order to summarize climate response behavior, 40-model ensemble (median) was used to predict the climate change for 2025, 2050, 2075 and 2100 by SimCLIM. Monthly minimum, maximum, mean temperature and precipitation data shows (Table 8.1, 8.2, 83 and 8.4) huge variation, on the other hand for projection, data also the same scenario. For minimum, maximum and mean temperature for baseline varied 12.20-26.20, 25.80-34.40 and 19.00-29.10 ^{0}C respectively and in precipitation 7.00-381.00 mm.

Table 8.1: Minimum monthly temperature for Dhaka station from baseline, 2025, 2050, 2075 and 2100 year using median scenario

Month	Minimum Temperature (^{0}C)				
	Baseline	**2025**	**2050**	**2075**	**2100**
January	12.20	13.03	13.79	14.57	15.34
February	14.70	15.59	16.41	17.24	18.07
March	19.20	20.03	20.78	21.56	22.32
April	23.30	24.02	24.68	25.35	26.02
May	24.80	25.46	26.06	26.68	27.29
June	25.90	26.52	27.08	27.66	28.23
July	26.10	26.67	27.18	27.72	28.24
August	26.20	26.76	27.27	27.46	28.32
September	25.90	26.54	27.11	27.71	28.30
October	23.80	24.54	25.20	25.89	26.57
November	18.40	19.18	19.89	20.63	21.35
December	13.70	14.58	15.38	16.21	17.03

Table 8.2: Maximum monthly temperature for Dhaka station from baseline, 2025, 2050, 2075 and 2100 year using median scenario

Month	Maximum Temperature (^{0}C)				
	Baseline	**2025**	**2050**	**2075**	**2100**
January	25.80	26.64	27.40	28.18	28.95
February	28.50	29.21	29.86	30.53	31.19
March	32.40	33.09	33.80	34.54	35.26
April	34.40	35.09	35.72	36.38	37.01
May	33.40	34.01	34.56	35.13	35.69
June	31.90	32.49	33.02	33.57	34.11
July	31.20	31.72	32.20	32.69	33.17
August	31.60	32.08	32.52	32.97	33.42
September	31.80	32.47	32.95	33.51	34.06
October	31.30	31.96	32.55	33.16	33.76
November	29.20	29.94	30.60	31.29	31.97
December	26.50	27.24	27.92	28.62	29.31

Table 8.3: Mean monthly temperature for Dhaka station from baseline, 2025, 2050, 2075 and 2100 year using median scenario

Month	Mean Temperature (^{0}C)				
	Baseline	**2025**	**2050**	**2075**	**2100**
January	19.00	19.80	20.53	21.29	22.03
February	21.60	22.40	23.13	23.89	24.63
March	25.70	26.50	27.23	27.99	28.73
April	28.80	29.48	30.10	30.74	31.37
May	29.10	29.74	30.32	30.92	31.51
June	28.90	29.46	29.96	30.48	30.99
July	28.60	29.13	29.62	30.11	30.61
August	28.90	29.44	29.92	30.09	30.92
September	28.80	29.39	29.93	30.49	31.03
October	27.50	28.16	28.75	29.37	29.98
November	23.80	24.53	25.20	25.88	26.56
December	20.10	20.91	21.65	22.42	23.17

Table 8.4: Mean monthly precipitation for Dhaka station from baseline, 2025, 2050, 2075 and 2100 year using median scenario

Month	Precipitation (mm)				
	Baseline	**2025**	**2050**	**2075**	**2100**
January	7.00	6.54	6.13	5.70	5.28
February	21.00	22.57	23.36	24.52	25.66
March	56.00	58.98	61.67	64.46	67.21
April	135.00	133.43	132.00	130.52	129.07
May	272.00	287.29	301.15	315.47	329.58
June	369.00	392.92	414.61	437.01	459.09
July	381.00	397.27	412.01	427.25	442.26
August	315.00	327.22	338.30	349.75	361.02
September	270.00	282.35	293.54	305.11	316.50
October	159.00	165.90	172.15	178.61	184.97
November	32.00	31.03	30.15	29.23	28.34
December	7.00	6.81	5.64	6.46	6.28

Data set of Bangladesh Meteorological Department (BMD) station from Dhaka consisting of monthly minimum, monthly maximum, monthly mean temperatures and total precipitation for the baseline period (1995-2014) was used to compare (Figure 8.6) with SimCLIM base line climate data (temperature and precipitation) trends, both data shows similarities with slight difference. It appears that, local weather station data a little bit higher than the SimCLIM projected data but both data have the same similar readings all month during 1995-2014.

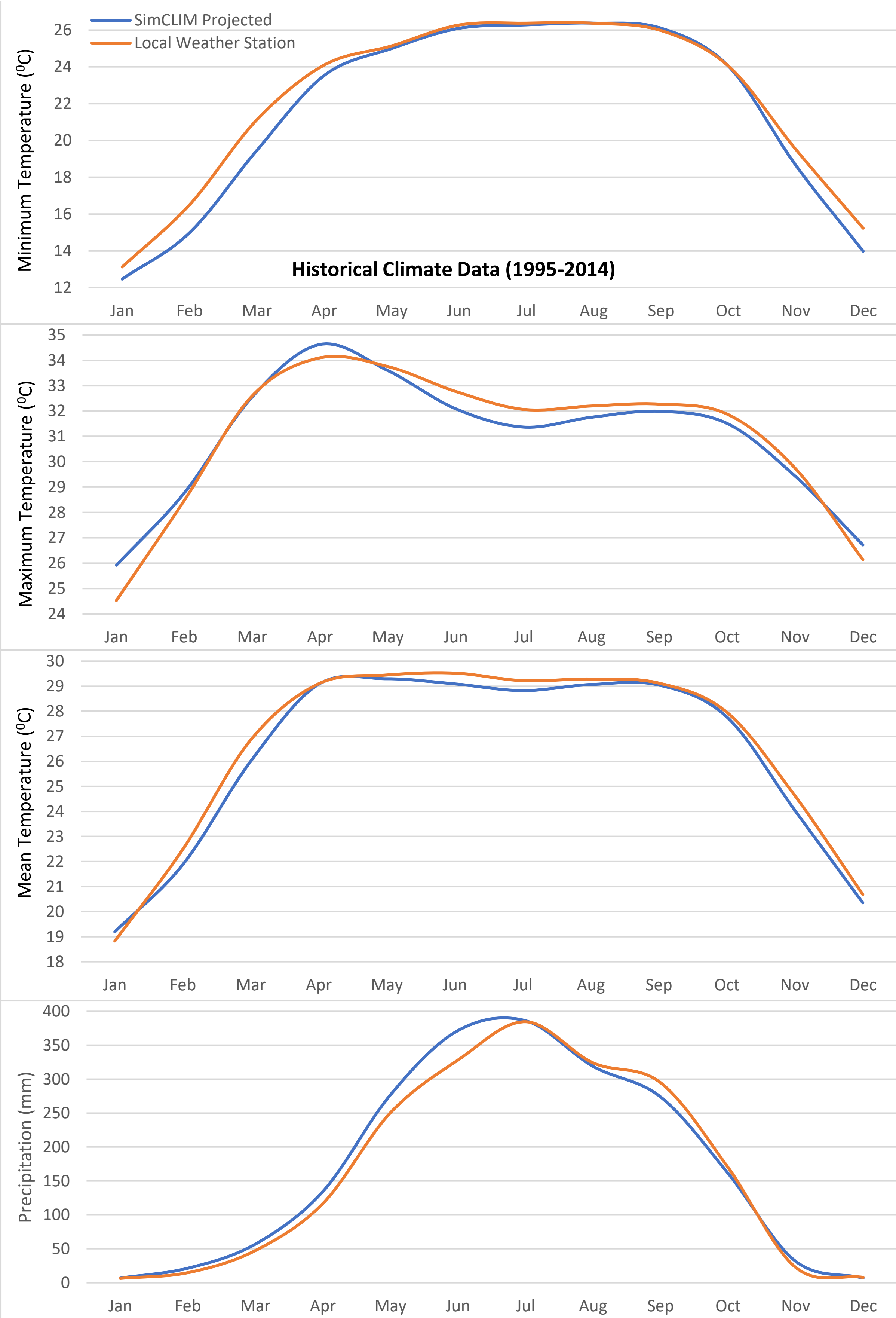

Figure 8.6: Timescale evaluation for historical climatic data (1995-2014) between local weather station (Dhaka) data and SimCLIM projected data with RCP4.5 (using 40 GCM ensemble)

8.6 Projected Future Climate

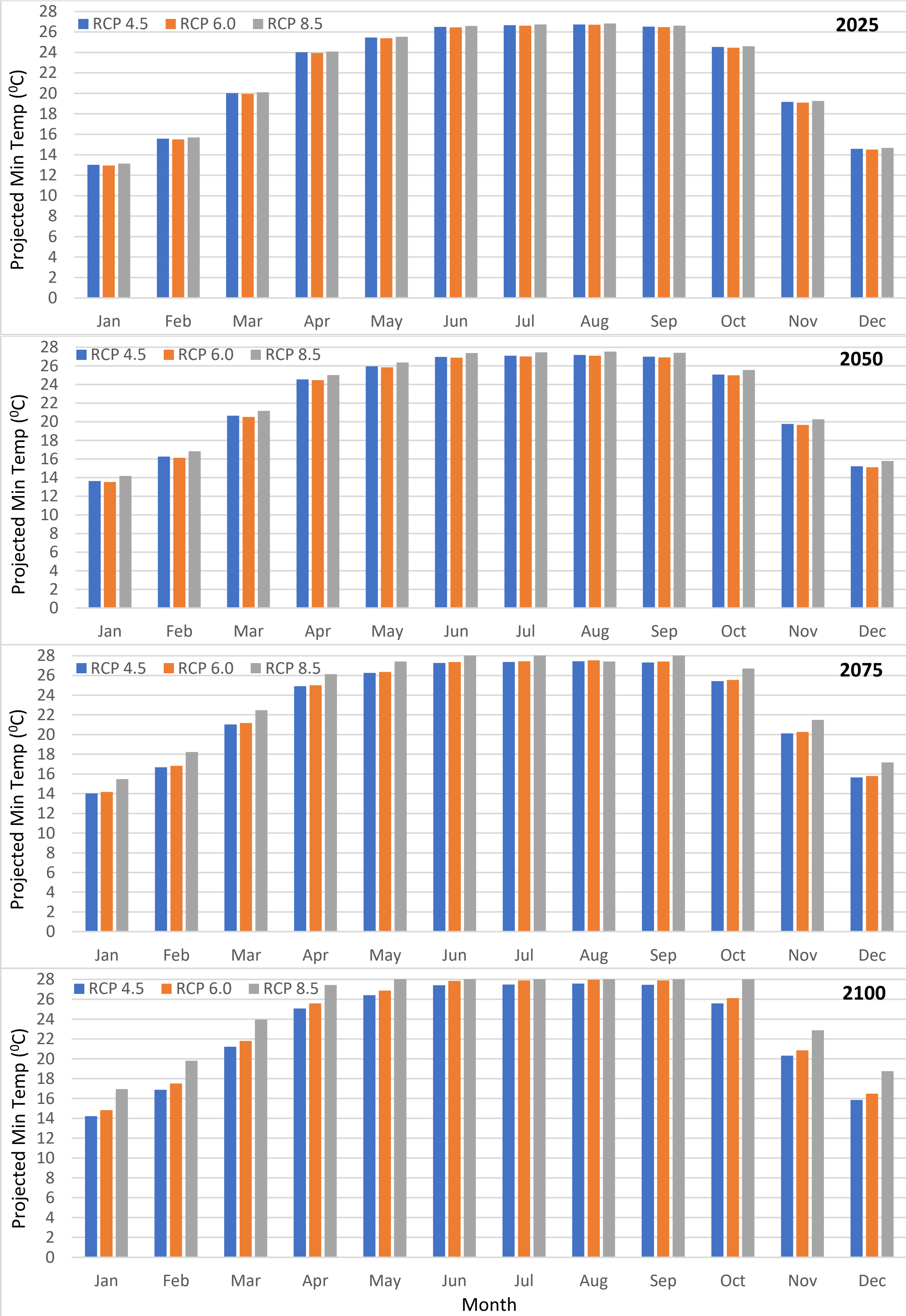

Figure 8.7: Projected min temperature by ensemble 40 GCMs with RCP4.5, 6.0, and 8.5 for station (Dhaka)

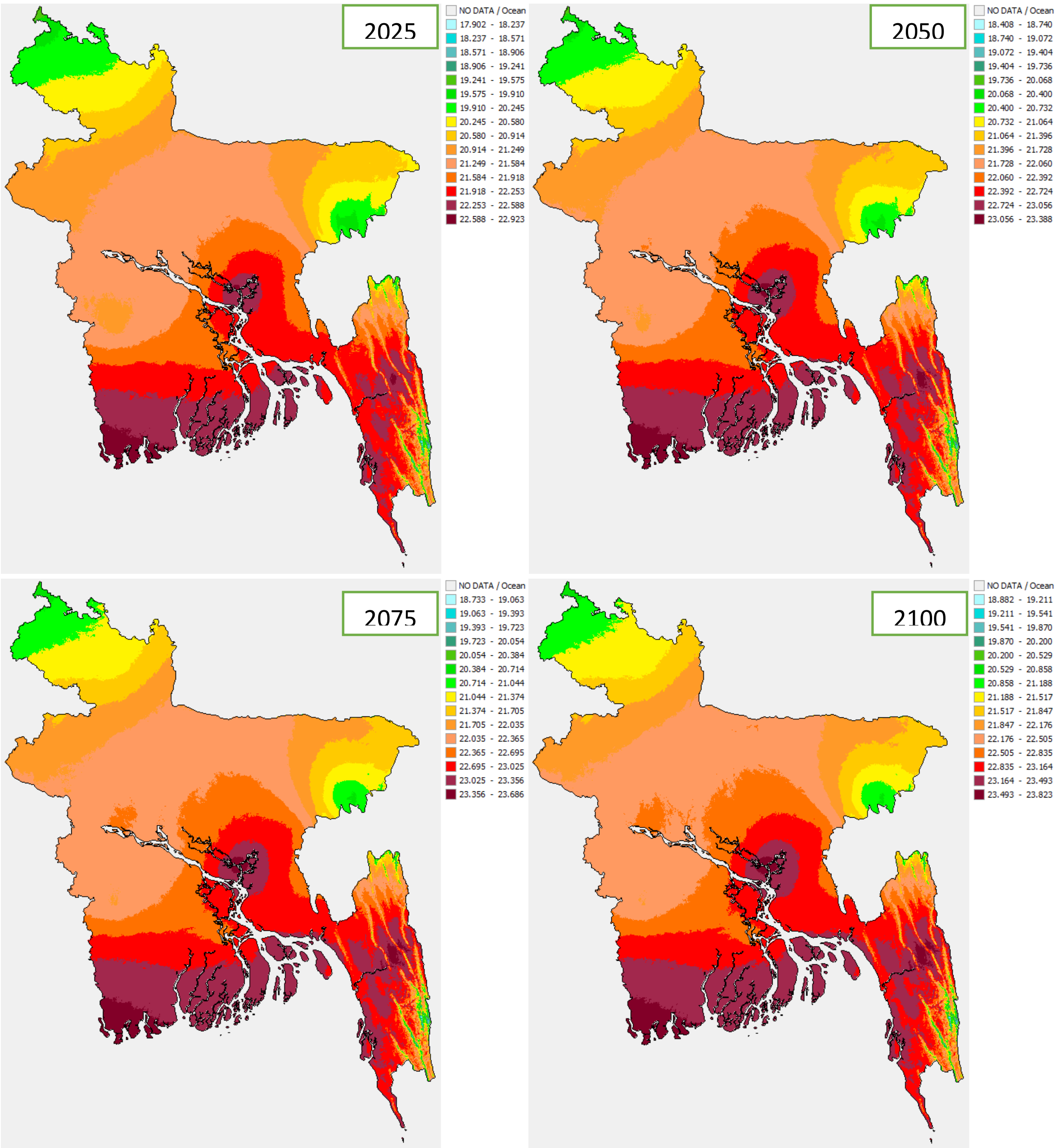

Figure 8.8: Projected min temperature by ensemble 40 GCMs with RCP4.5 mid sensitivity for Bangladesh

In terms of annual average minimum temperature for observed and model projected values for baseline, 2025, 2050, 2075 and 2100 are 21.18 (baseline), {21.90 (RCP4.5), 21.84 (RCP6.0) and 21.91 (RCP8.5)}, {22.44 (RCP4.5), 22.25 (RCP6.0) and 22.91 (RCP8.5)}, {22.79 (RCP4.5), 22.91 (RCP6.0) and 23.97 (RCP8.5)}, {22.96 (RCP4.5), 23.47 (RCP6.0) and 25.34 (RCP8.5)} ^{0}C respectively. All minimum temperature RCPs mid sensitivity show different readings in 2025, 2050, 2075 and 2100 in (Figure 8.7). In (Figure 8.8) is generated based on RCP4.5 with mid sensitivity. Above maps show 2025, 2050, 2075 and 2100 lowest and highest temperature 17.90-18.27 to 22.59-2292, 18.41-18.74 to 23.06-23.39, 18.73-19.06 to 23.36-23.69 and 18.88-19.21 to 23.49-23.82 ^{0}C respectively.

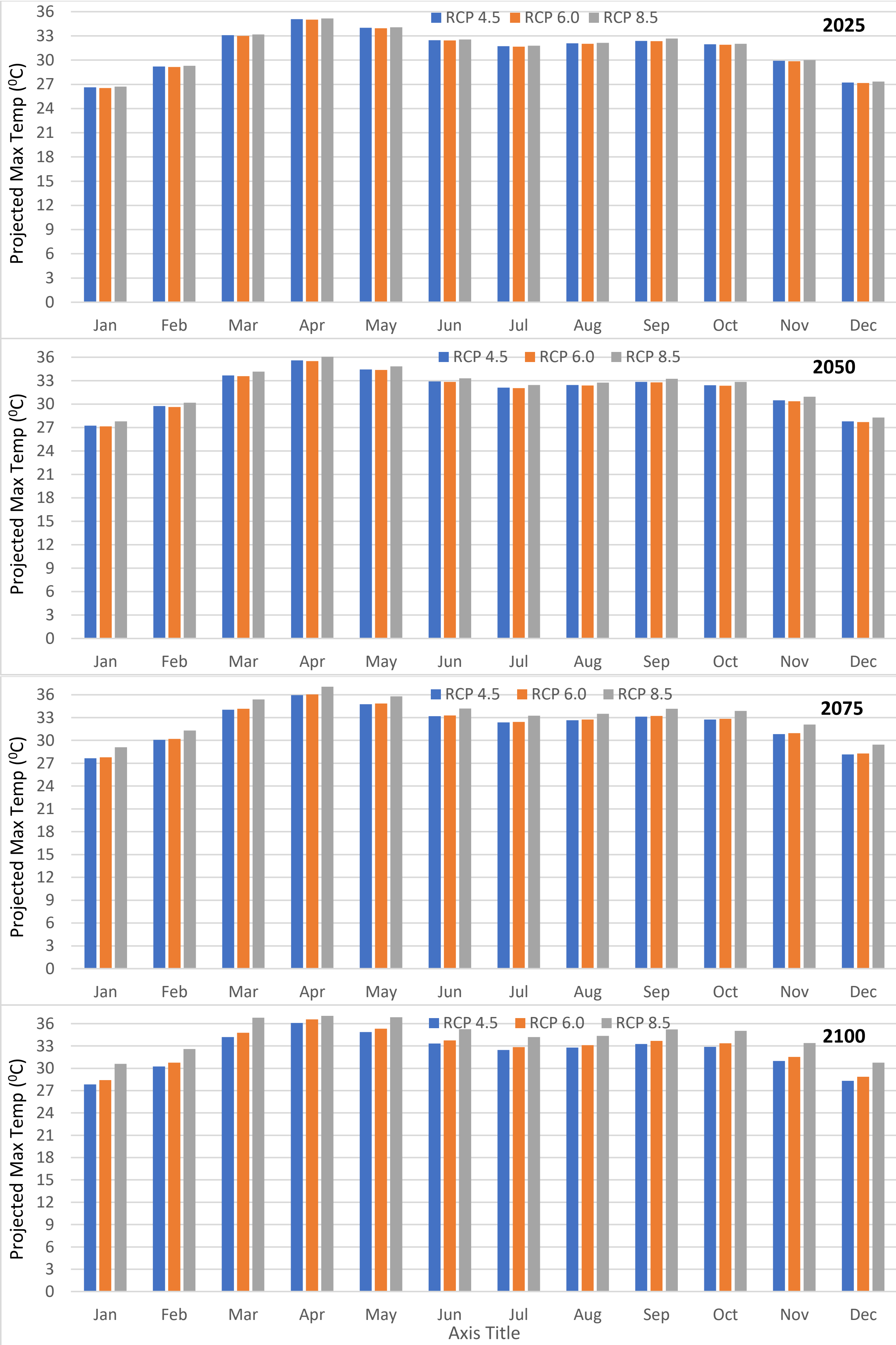

Figure 8.9: Projected max temperature by ensemble 40 GCMs with RCP4.5, 6.0, and 8.5 for station (Dhaka)

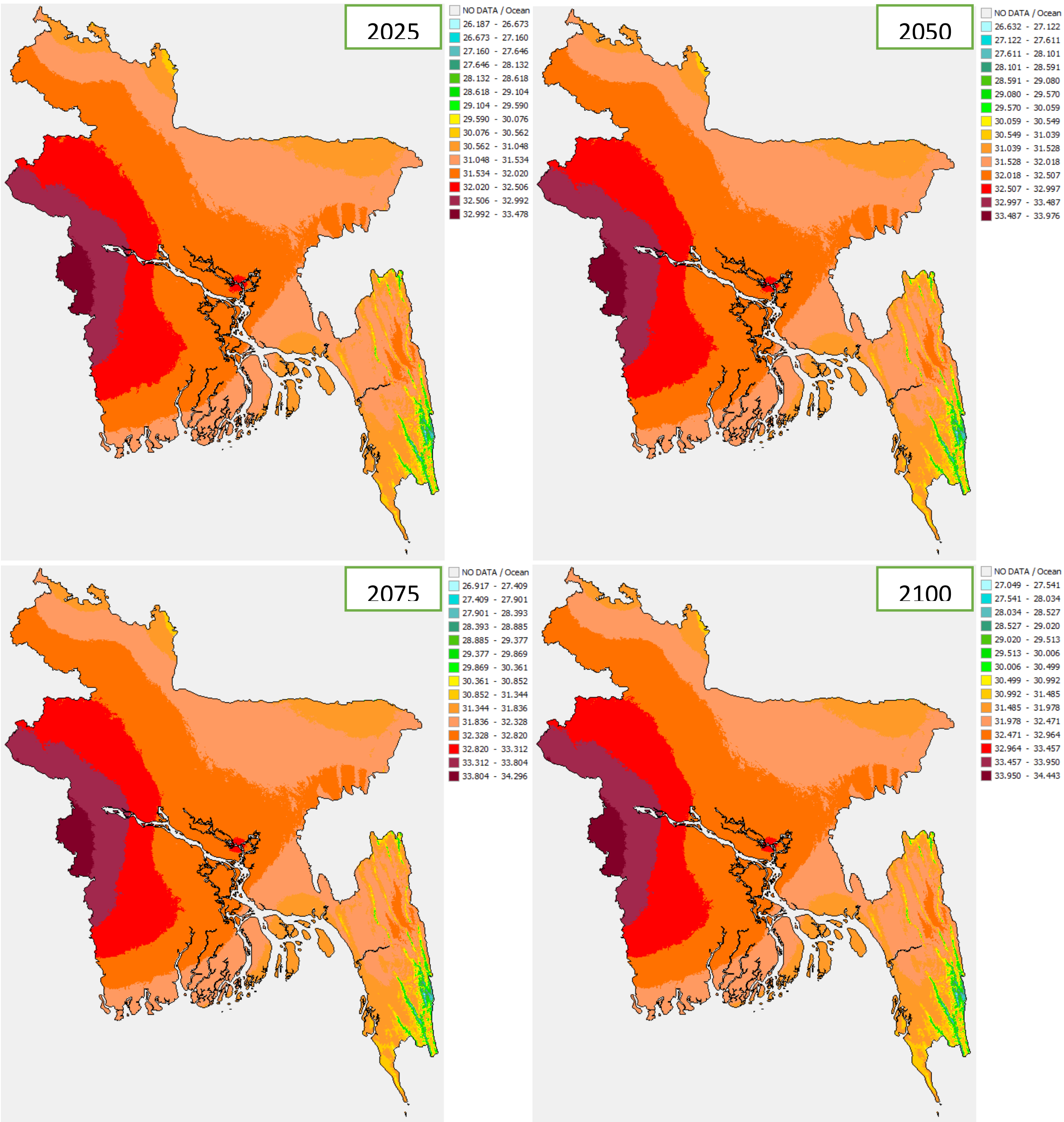

Figure 8.10: Projected max temperature by ensemble 40 GCMs with RCP4.5 mid sensitivity over Bangladesh

Simulation was not possible for RCPs February and December though data was generated from minimum and mean value but not in map. Annual average maximum temperature for observed and model projected values for baseline, 2025, 2050, 2075 and 2100 are 30.67 (baseline), {31.31 (RCP4.5), 31.25 (RCP6.0) and 31.42 (RCP8.5)}, {31.81 (RCP4.5), 31.73 (RCP6.0) and 32.24 (RCP8.5)}, {32.13 (RCP4.5), 32.24 (RCP6.0) and 33.28 (RCP8.5)}, {32.27 (RCP4.5), 32.75 (RCP6.0) and 34.46 (RCP8.5)} ^{0}C respectively. All maximum temperature RCPs mid sensitivity show different readings in 2025, 2050, 2075 and 2100 in (Figure 8.9). In (Figure 8.10) is generated based on RCP4.5 with mid sensitivity. Above maps show 2025, 2050, 2075 and 2100 lowest and highest temperature 26.19-26.67 to 32.99-33.48, 26.63-27.12 to 33.49-33.98, 26.92-27.41 to 33.80-34.30 and 27.05-27.54 to 33.95-34.44 ^{0}C respectively.

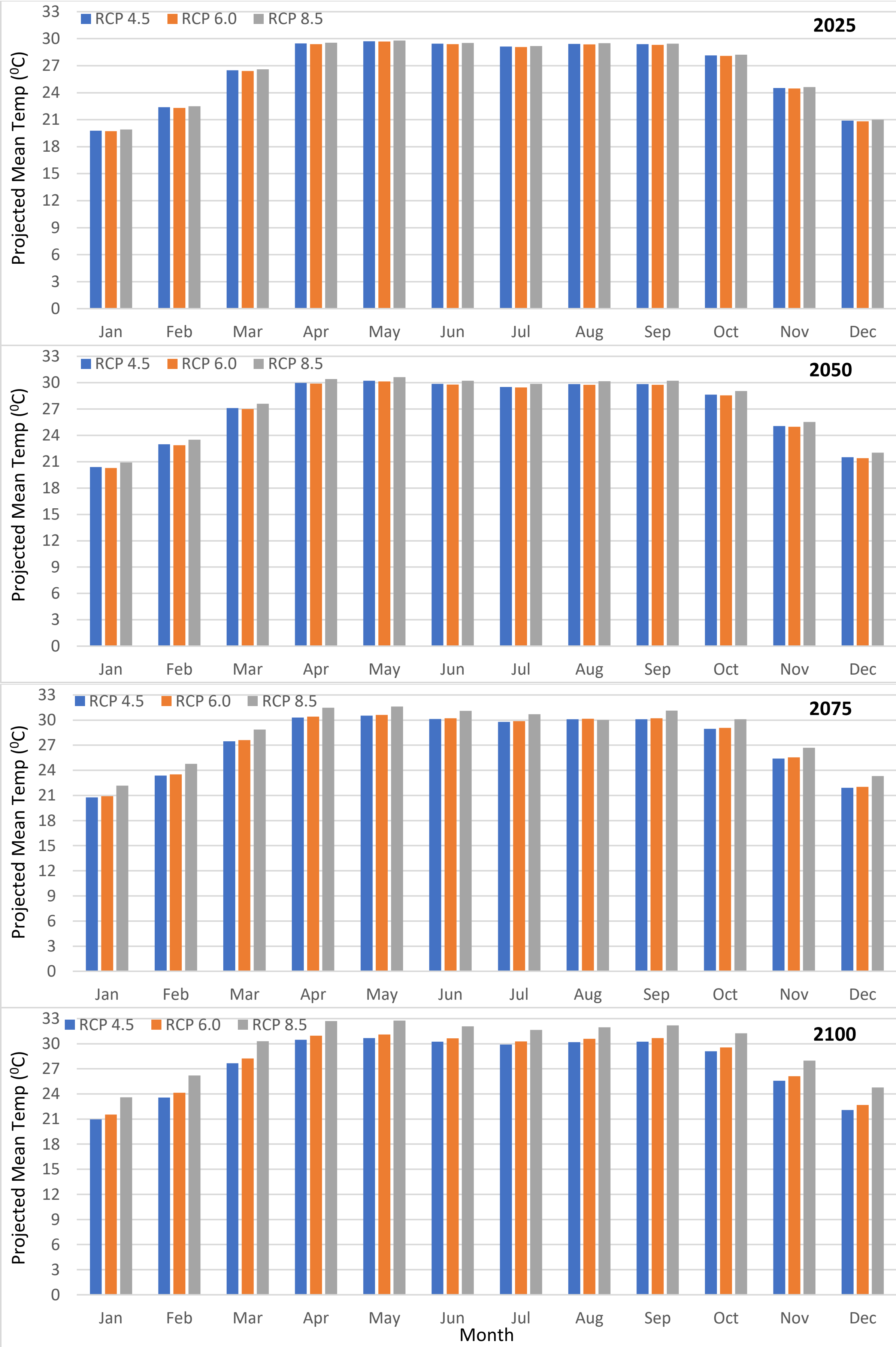

Figure 8.11: Projected mean temperature by ensemble 40 GCMs with RCP4.5, 6.0, and 8.5 for station (Dhaka)

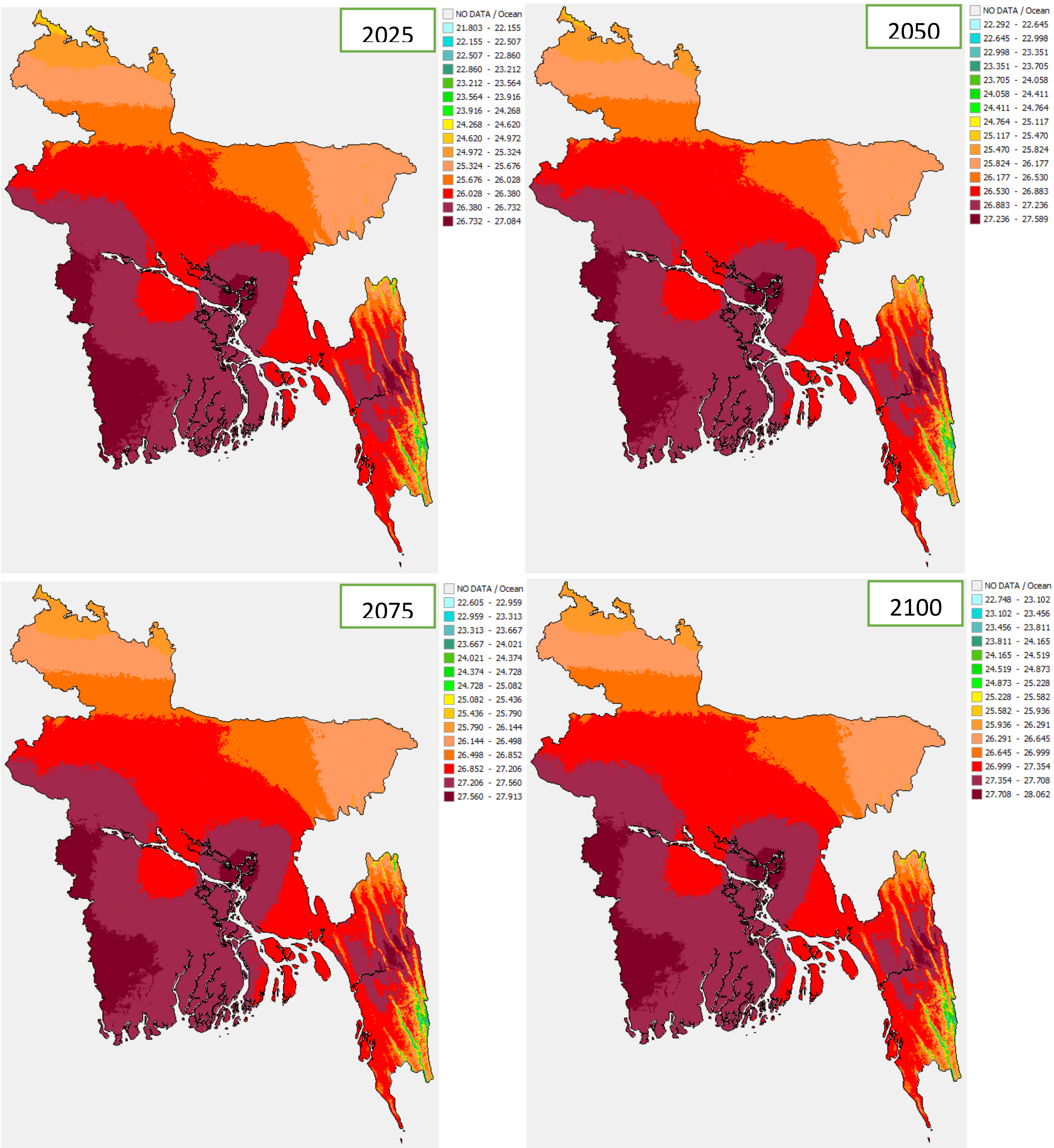

Figure 8.12: Projected mean temperature by ensemble 40 GCMs with RCP4.5 mid sensitivity over Bangladesh

In terms of annual average mean temperature for observed and model projected values for baseline, 2025, 2050, 2075 and 2100 are 25.90 (baseline), {26.57 (RCP4.5), 26.51 (RCP6.0) and 26.66 (RCP8.5)}, {27.08 (RCP4.5), 26.99 (RCP6.0) and 27.52 (RCP8.5)}, {27.41 (RCP4.5), 27.51 (RCP6.0) and 28.50 (RCP8.5)}, {27.55 (RCP4.5), 28.04 (RCP6.0) and 29.79 (RCP8.5)} ^{0}C respectively. All maximum temperature RCPs mid sensitivity show different readings in 2025, 2050, 2075 and 2100 in (Figure 8.11). In (Figure 8.12) is generated based on RCP4.5 with mid sensitivity. Above maps show 2025, 2050, 2075 and 2100 lowest and highest temperature 21.80-22.16 to 26.73-27.08, 22.29-22.65 to 27.24-27.59, 22.61-22.96 to 27.56-27.91 and 22.79-23.10 to 27.71-28.06 ^{0}C respectively.

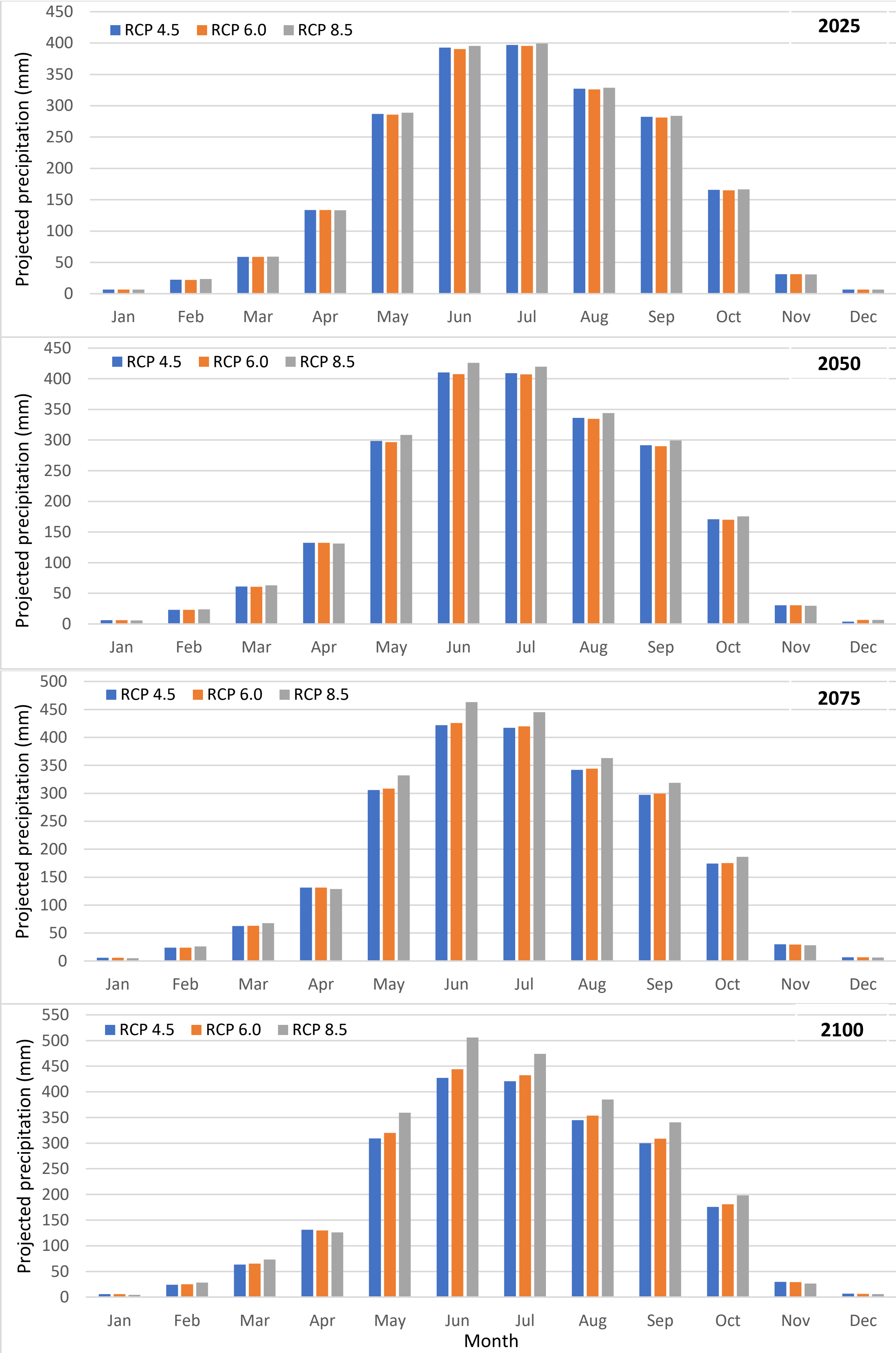

Figure 8.13: Projected precipitation by ensemble 40 GCMs with RCP4.5, 6.0, and 8.5 for station (Dhaka)

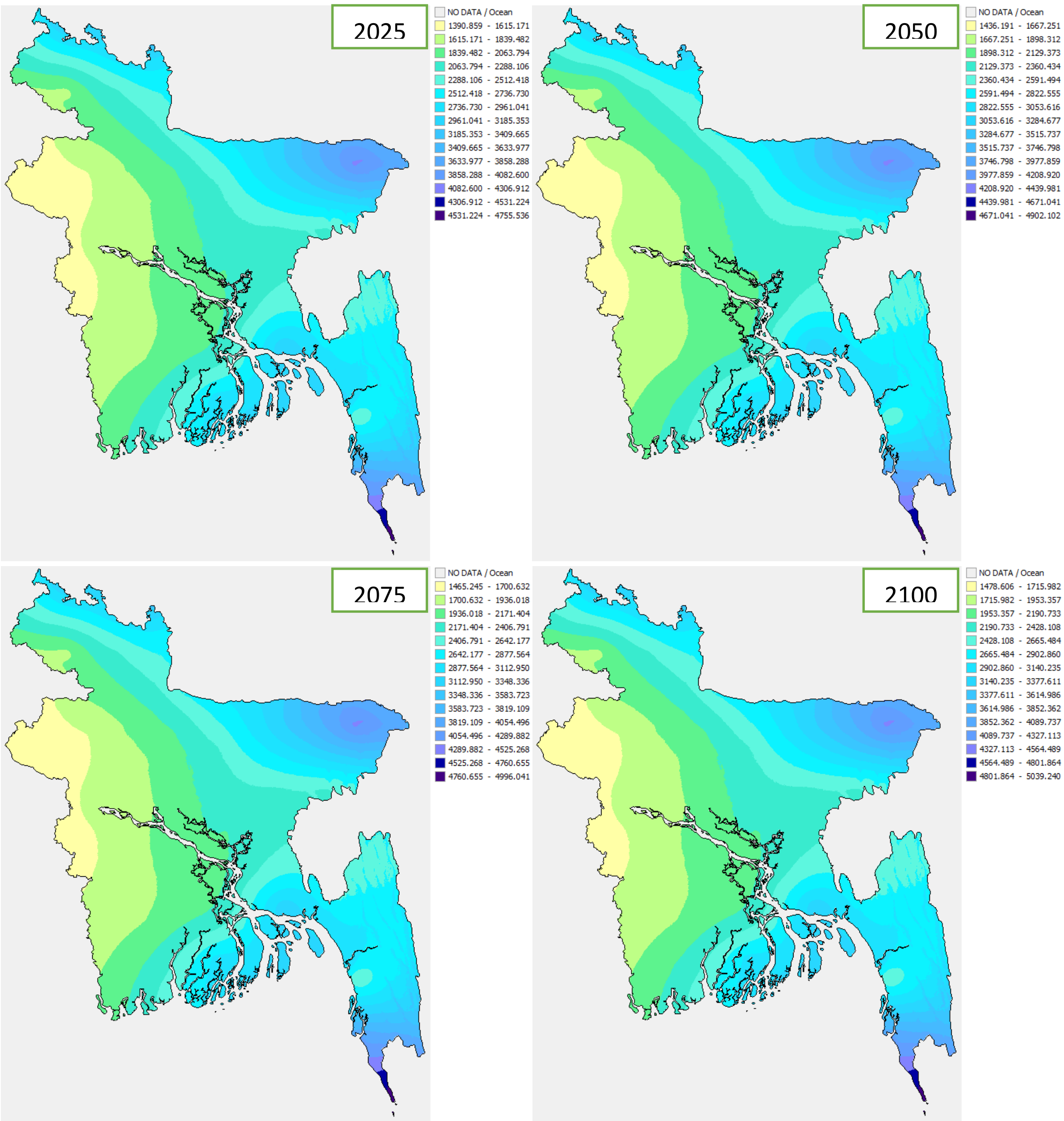

Figure 8.14: Projected precipitation by ensemble 40 GCMs with RCP4.5 mid sensitivity over Bangladesh

In terms of annual total precipitation for observed and model projected values for baseline, 2025, 2050, 2075 and 2100 are 2024.00 (baseline), {2110.79 (RCP4.5), 2103.17 (RCP6.0) and 2122.94 (RCP8.5)}, {2173.52 (RCP4.5), 2165.47 (RCP6.0) and 2233.08 (RCP8.5)}, {2218.64 (RCP4.5), 2232.78 (RCP6.0) and 2370.84 (RCP8.5)}, {2238.01 (RCP4.5), 2300.75 (RCP6.0) and 2527.07 (RCP8.5)} mm respectively. All total precipitation RCPs mid sensitivity show different readings in 2025, 2050, 2075 and 2100 in (Figure 8.13). In (Figure 8.14) is generated based on RCP4.5 with mid sensitivity. Above maps show 2025, 2050, 2075 and 2100 lowest and highest precipitation 1390.86-1615.17 to 4531.22-4755.54, 1436.19-1667.25 to 4671.04-4902.10, 1465.25-1700.63 to 4760.66-4996.04 and 1478.61-1715.98 to 4801.86-5039.24 mm respectively.

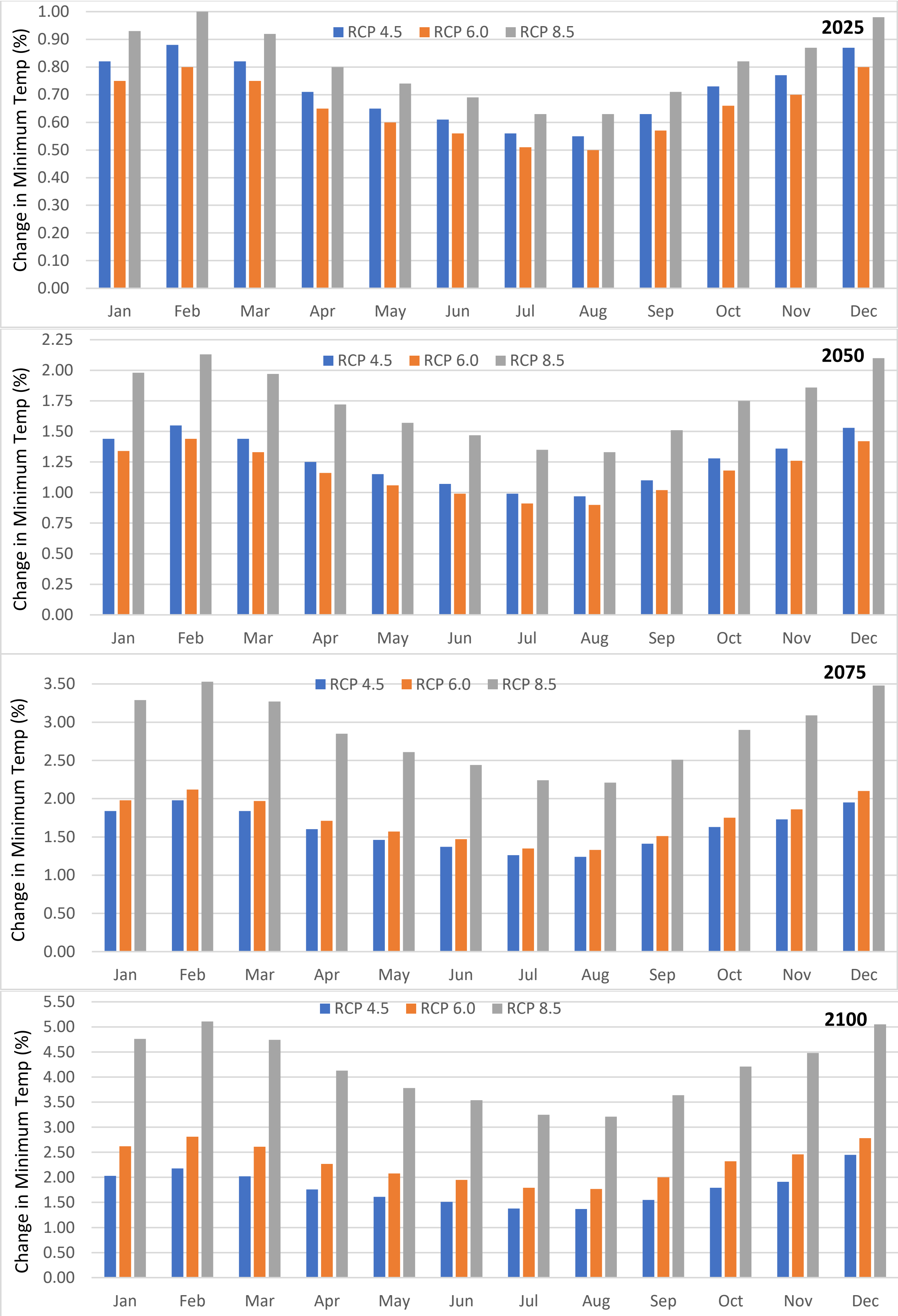

Figure 8.15: Percentage change in minimum temperature from baseline (1995-2014) for 2025, 2050, 2075 and 2100 by using (ensemble) 40 GCMs with RCP45, 6.0, and 8.5 for station (Dhaka)

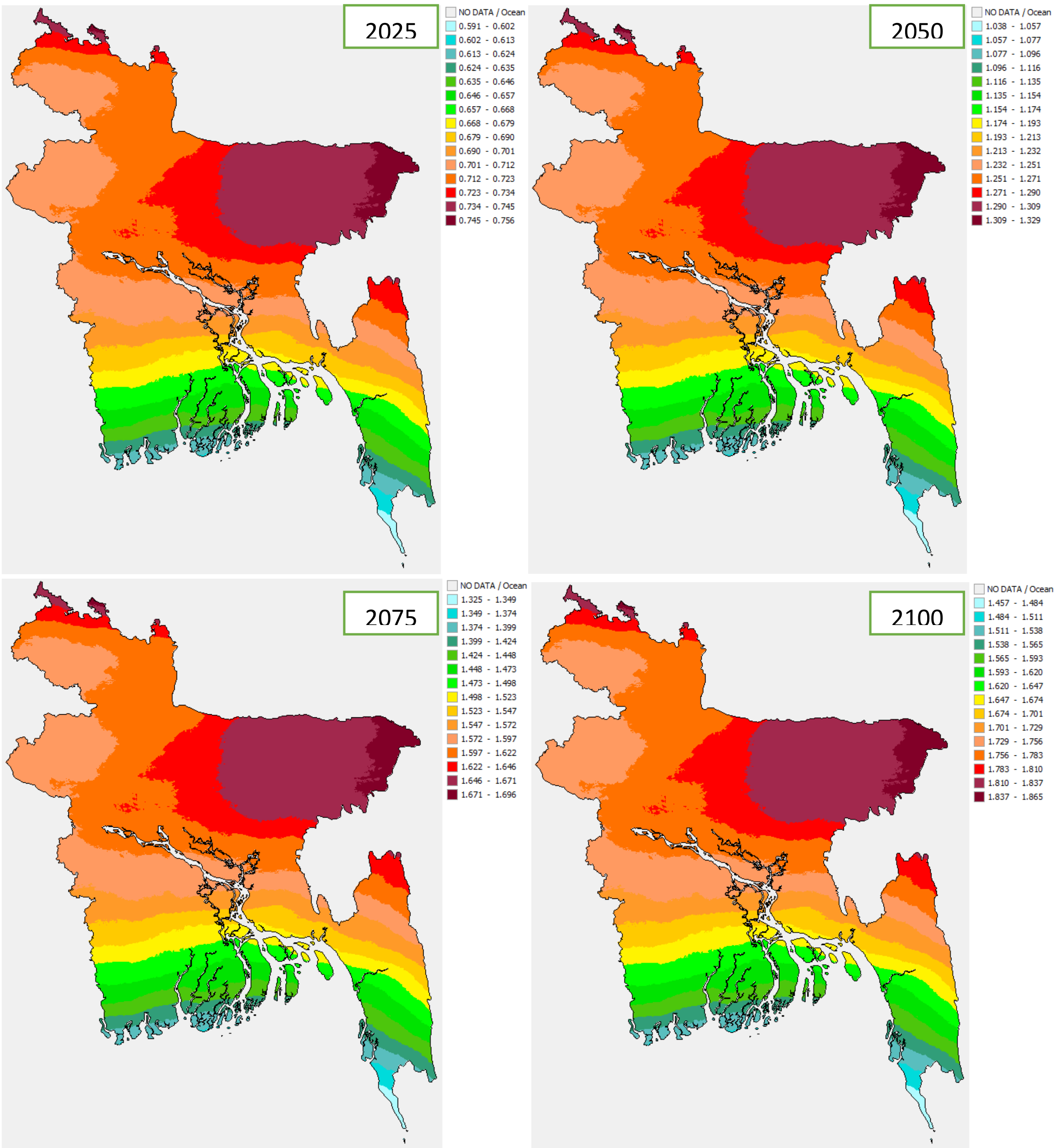

Figure 8.16: Percentage change in minimum temperature from baseline (1995-2014) for 2025, 2050, 2075 and 2100 using (ensemble) 40 GCMs with RCP4.5 over Bangladesh

Different climate models for Asian regions showed a temperature increase 0.5-2 ^{0}C by 2030 and 1-7 ^{0}C by 2070 (IPCC, 2007). Temperature ranges are more rapidly raising in the arid or semi-arid regions of India, western China, and northern Pakistan (Zahid and Rasul, 2011; IPCC, 2013). Projections showed increasing variability in minimum temperature among different years 2025, 2050, 2075 and 2100 are 0.59-0.60 to 0.75-0.76, 1.04-1.06 to 1.31-1.33, 1.33-1.35 to 1.67-1.70 and 1.46-1.48 to 1.84-1.87 % respectively (Figure 8.16). In (Figure 8.15) RCP4.5, 6.0 and 8.5 for 2025, 2050, 2075 and 2100 increasing variability are (0.72, 1.26, 1.61 and 1.80), (0.65, 1.17, 1.73 and 2.29) and (0.81, 1.73, 2.87 and 4.16) % respectively from baseline.

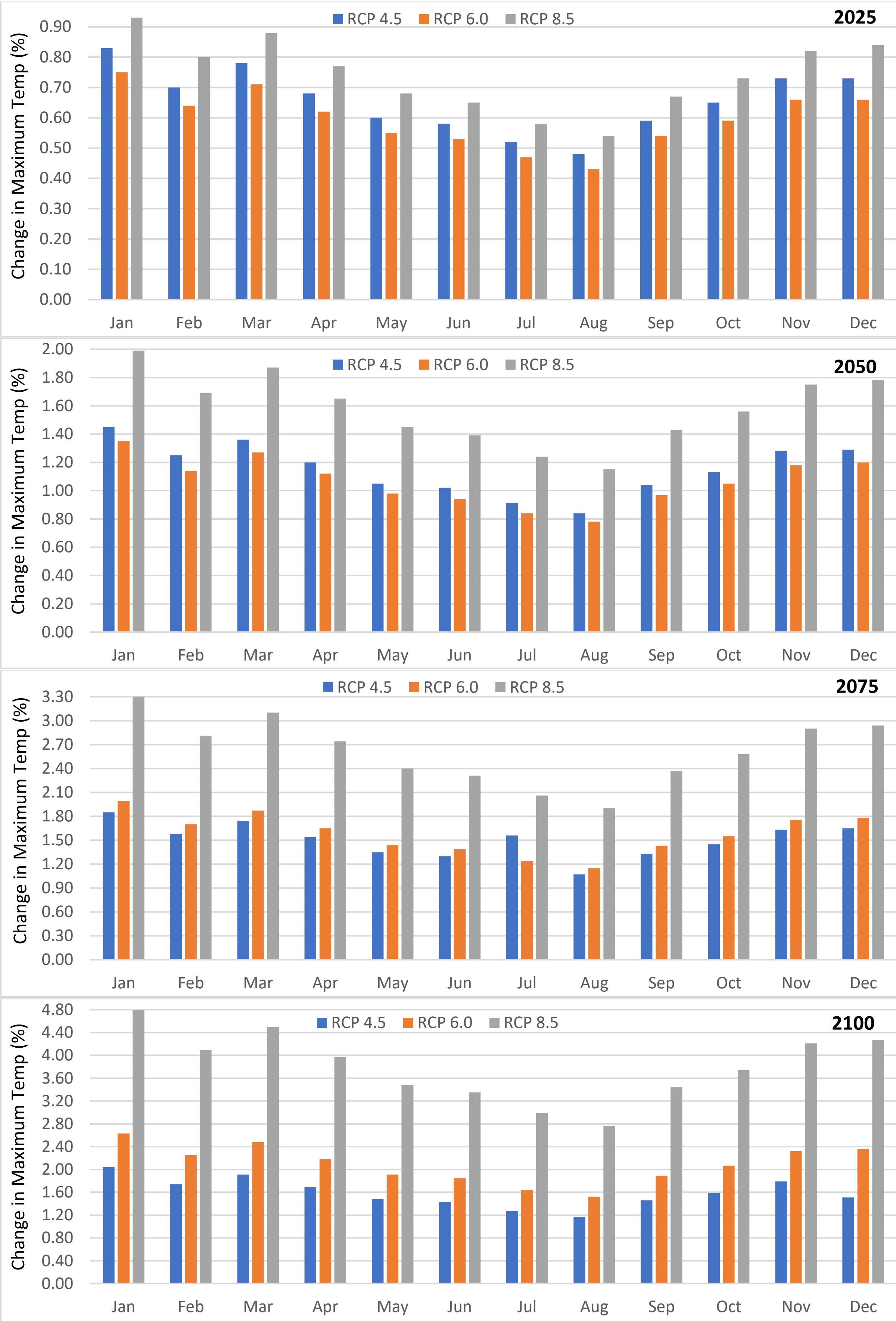

Figure 8.17: Percentage change in maximum temperature from baseline (1995-2014) for 2025, 2050, 2075 and 2100 by using (ensemble) 40 GCMs with RCP4.5, 6.0, and 8.5 for station (Dhaka)

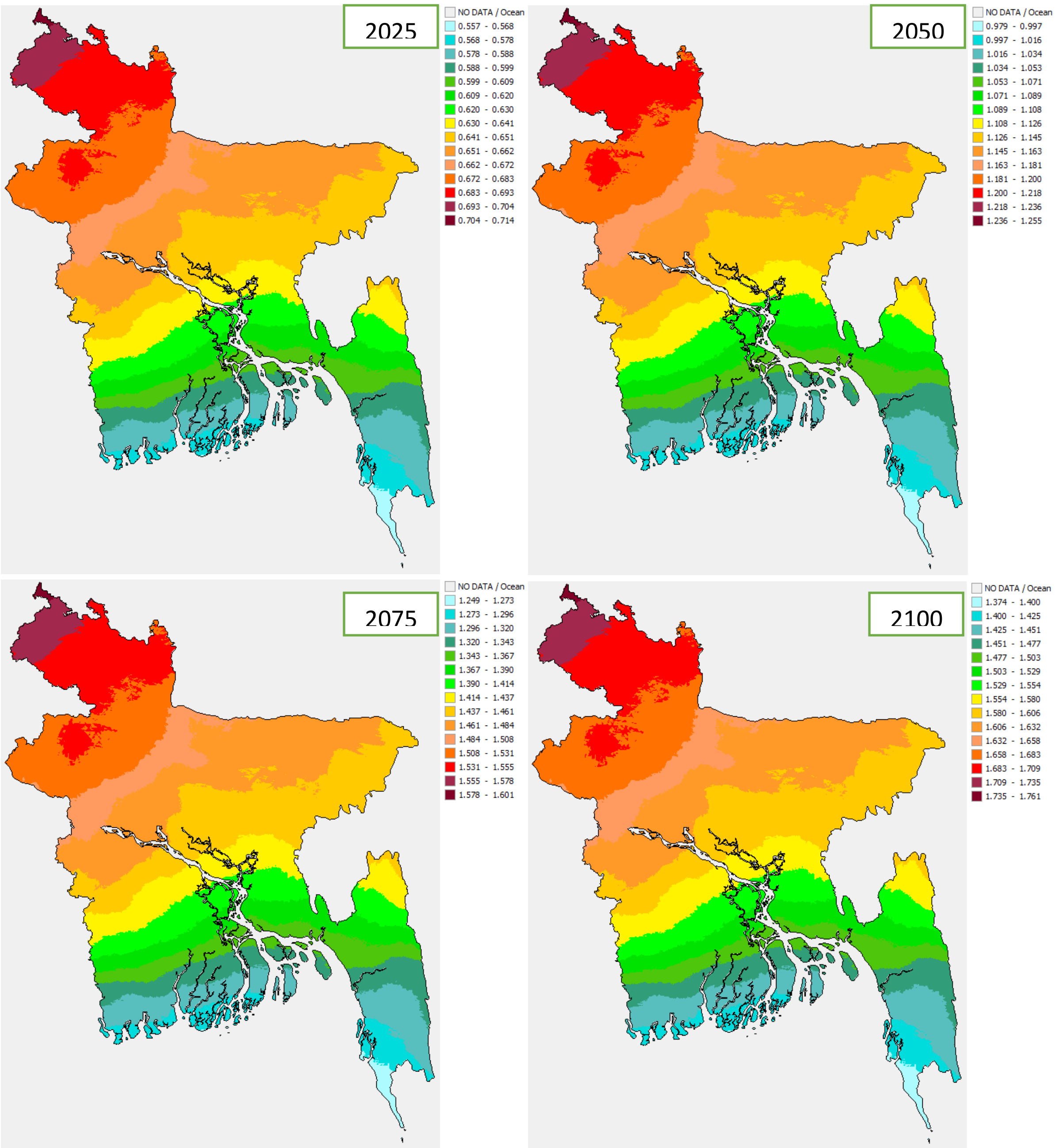

Figure 8.18: Percentage change in maximum temperature from baseline (1995-2014) for 2025, 2050, 2075 and 2100 by using (ensemble) 40 GCMs with RCP4.5 over Bangladesh

RCPs were used to estimate the high, medium, and low climatic uncertainty range for projected years (IPCC, 2014). Trends in projection showed increasing trend in maximum temperature for future as predicted by previous studies (Jones and Moberg, 2003). Projections showed increasing variability in maximum temperature among different years 2025, 2050, 2075 and 2100 are 0.56-0.57 to 0.70-0.71, 0.98-1.00 to 1.24-1.26, 1.25-1.27 to 1.58-1.60 and 1.37-1.40 to 1.74-1.76 % respectively (Figure 8.18) from baseline. In (Figure 8.17) RCP4.5, 6.0 and 8.5 for 2025, 2050, 2075 and 2100 increasing variability are (0.66, 1.15, 1.50 and 1.59), (0.60, 1.07, 1.58 and 2.09) and (0.74, 1.58, 2.62 and 3.80) % respectively from baseline.

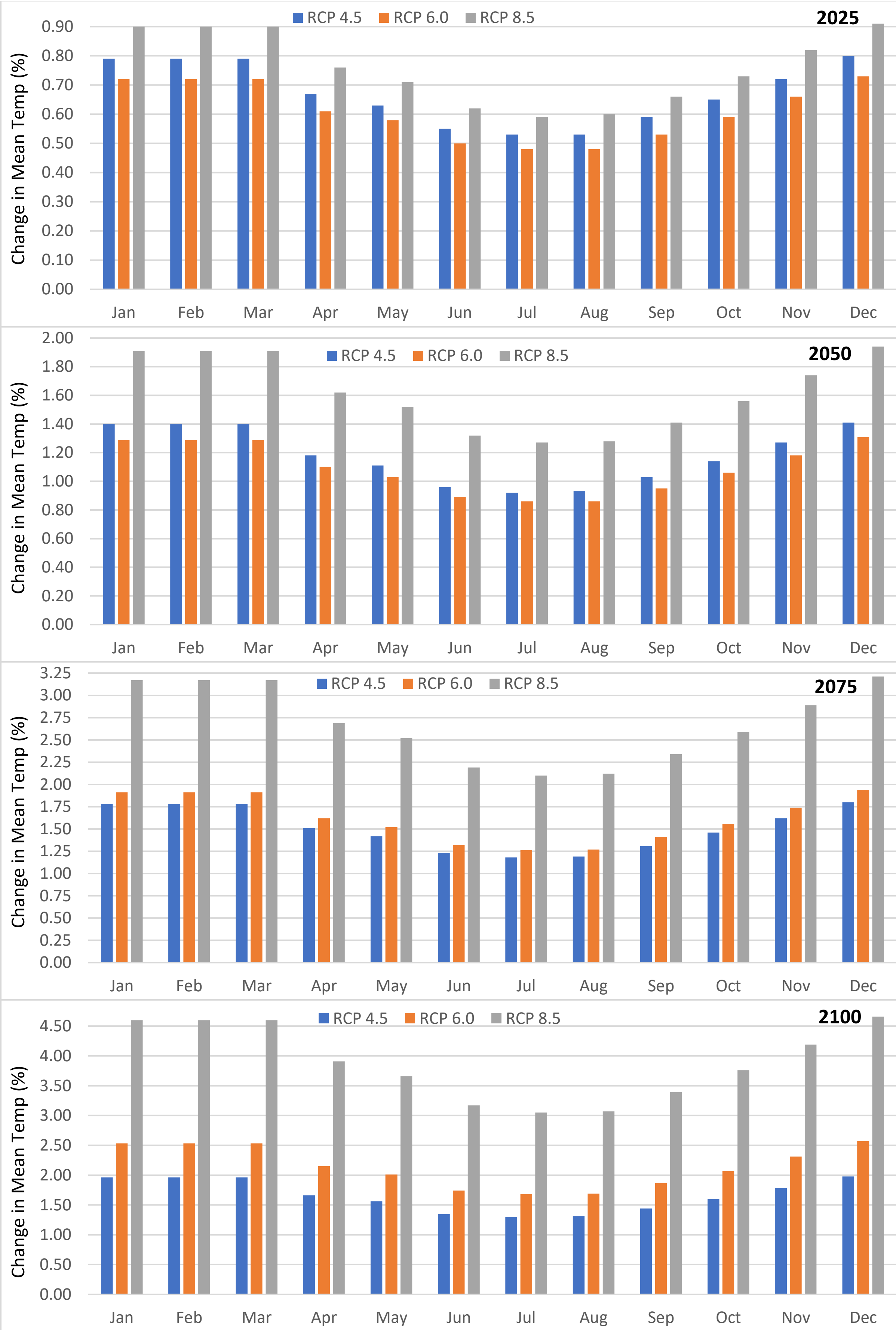

Figure 8.19: Percentage change in mean temperature from baseline (1995-2014) for 2025, 2050, 2075 and 2100 using (ensemble) 40 GCMs with RCP4.5, 6.0, and 8.5 for station (Dhaka)

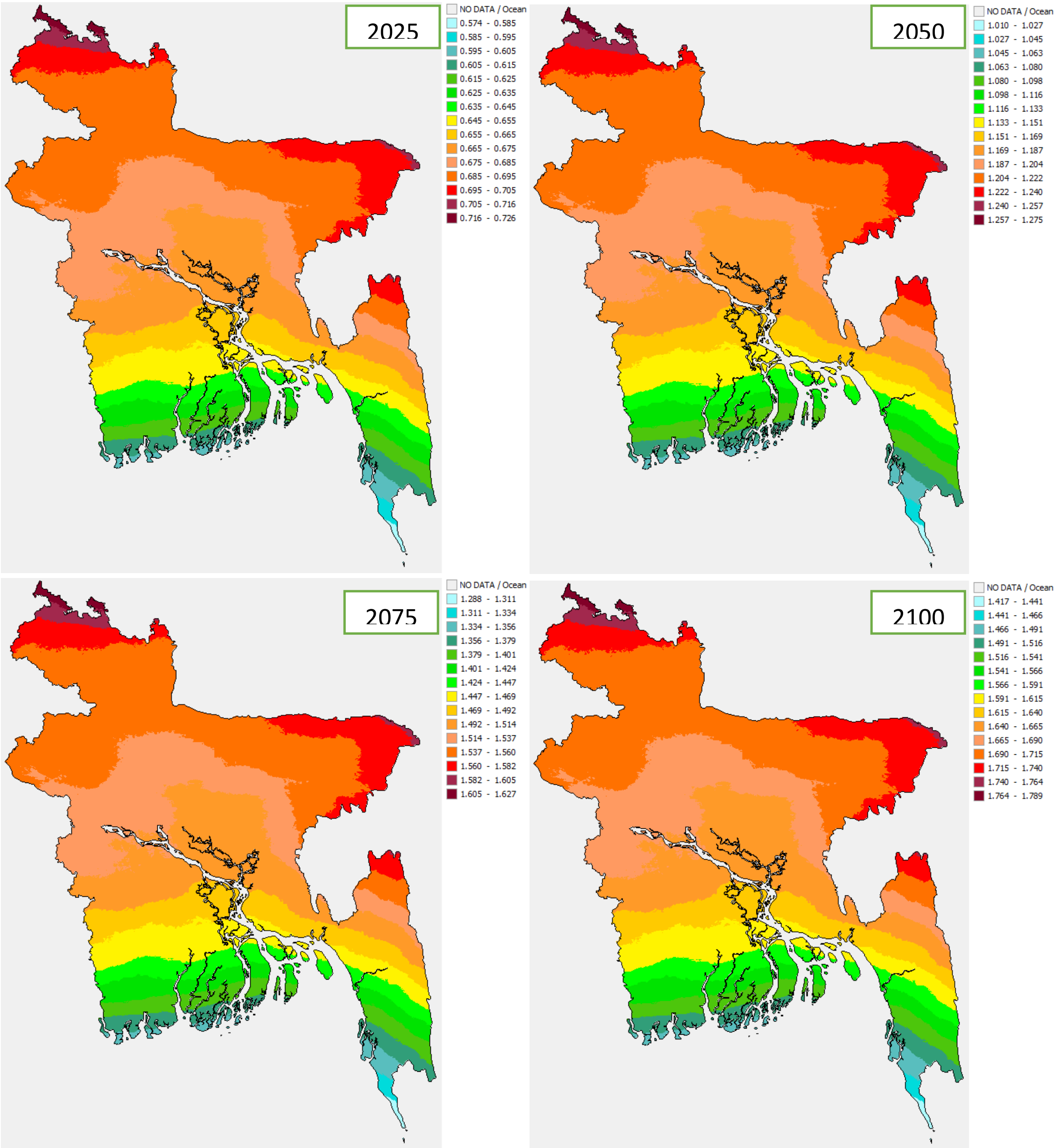

Figure 8.20: Percentage change in mean temperature from baseline (1995-2014) for 2025, 2050, 2075 and 2100 by using (ensemble) 40 GCMs with RCP4.5 over Bangladesh

Global temperature will increase by 1.8-4.0 ^{0}C with an overall average increase of 2.8 ^{0}C in temperature (IPCC, 2007). Historical data analysis in different studies showed that climatic extremes for most of the areas of the globe (Peterson and vose, 1997; New *et. al*., 2001; Hansen *et. al*., 2001; Marengo *et. al.* 2009; Safeeq *et. al.*, 2012; Abbas *et. al*., 2013; Abbas *et. al*., 2013). Projections showed increasing variability in mean temperature among different years 2025, 2050, 2075 and 2100 are 0.57-0.59 to 0.72-0.73, 1.01-1.03 to 1.26-1.28, 1.29-1.31 to 1.61-1.63 and 1.42-1.44 to 1.76-1.79 % respectively (Figure 8.20) from baseline. In (Figure 8.19) RCP4.5, 6.0 and 8.5 for 2025, 2050, 2075 and 2100 increasing variability are (0.67, 1.18, 1.51 and 1.66), (0.61, 1.09, 1.61 and 2.14) and (0.76, 1.62, 2.68 and 3.89) % respectively from baseline.

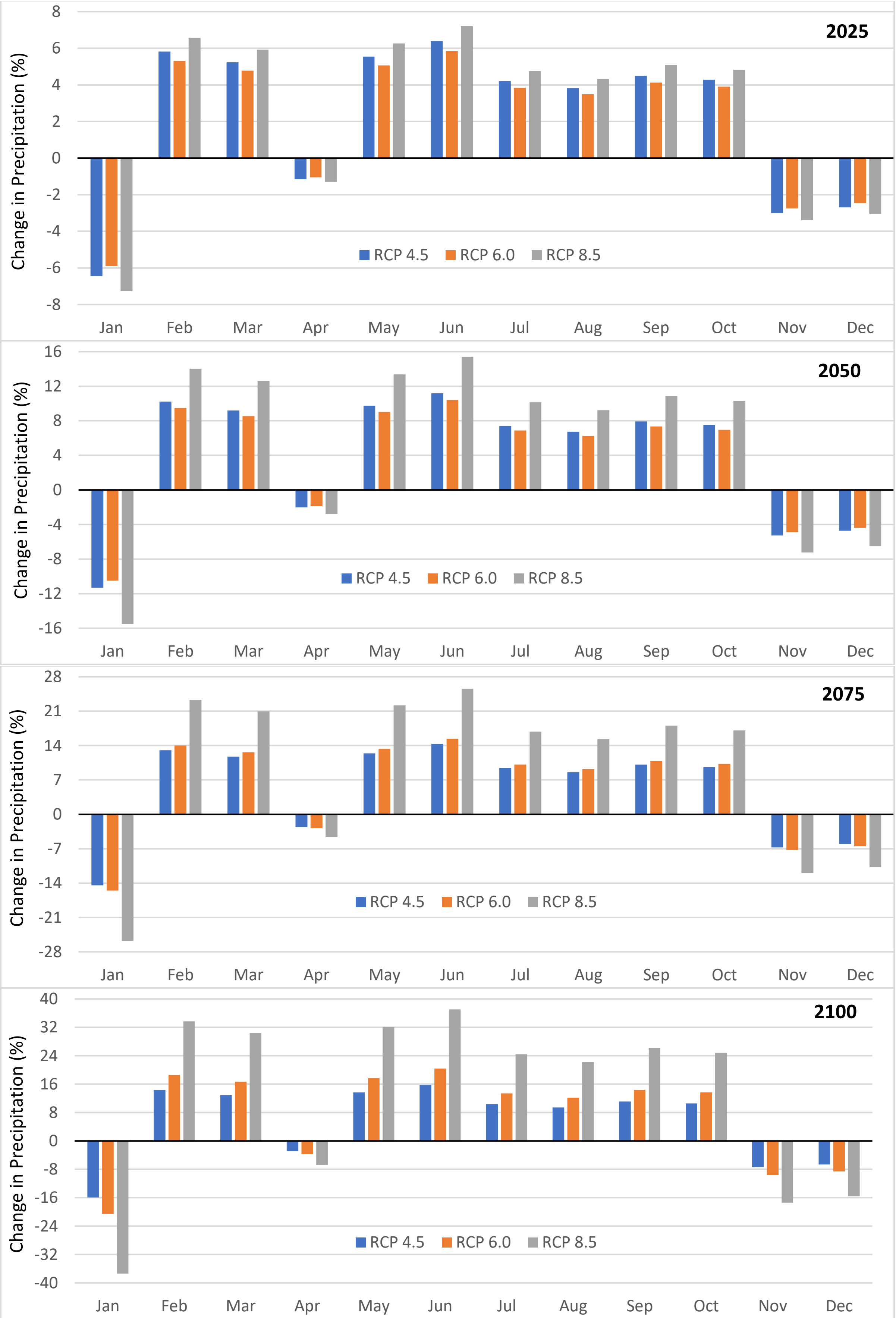

Figure 8.21: Percentage change in precipitation from baseline (1995-2014) for 2025, 2050, 2075 and 2100 by using (ensemble) 40 GCMs with RCP4.5, 6.0, and 8.5 for station (Dhaka)

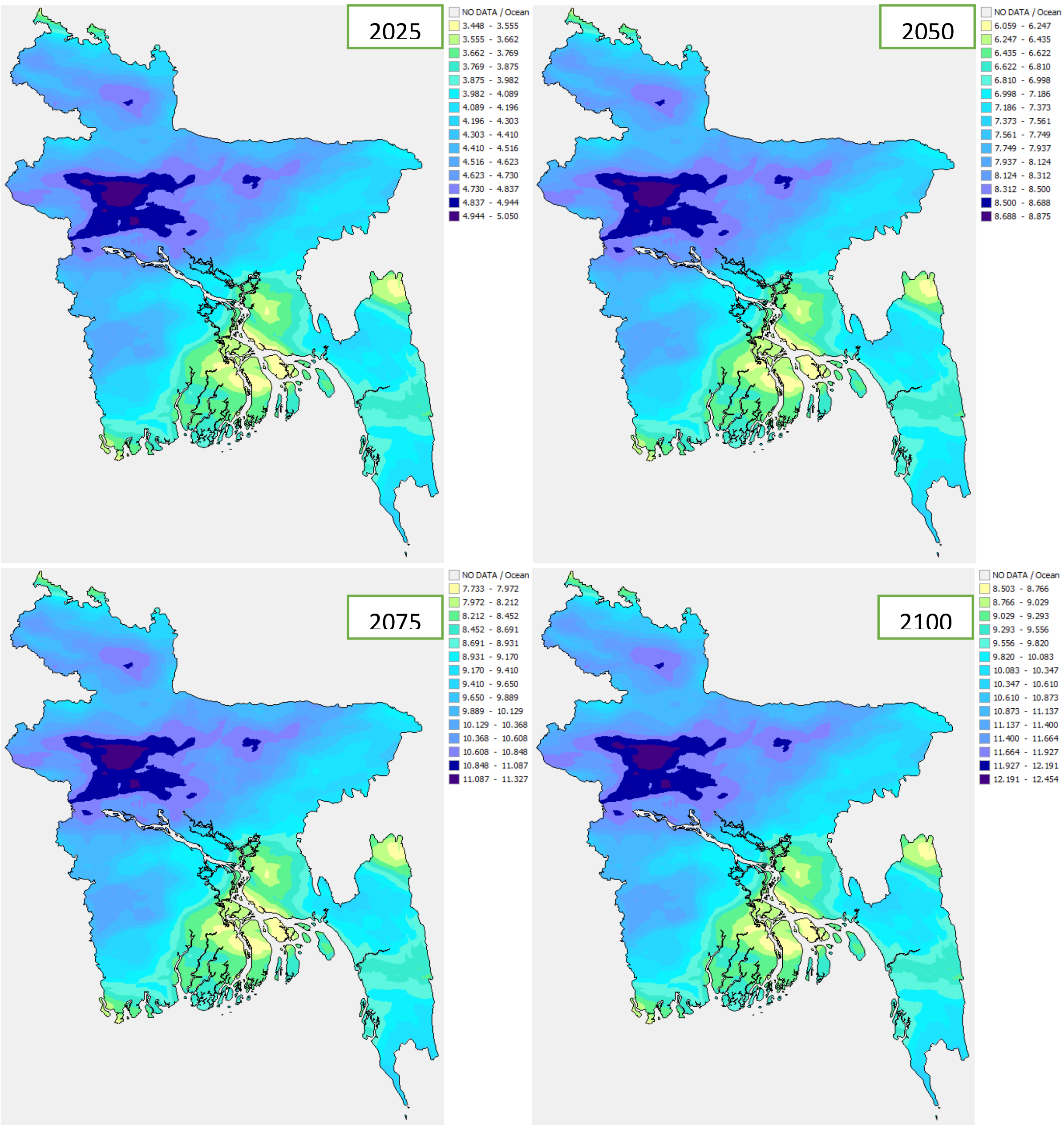

Figure 8.22: Percentage change in precipitation from baseline (1995-2014) for 2025, 2050, 2075 and 2100 by using (ensemble) 40 GCMs with RCP4.5 over Bangladesh

A study conducted in North America revealed the positive trends in the precipitation extreme indices (Griffiths and Bradley, 2007; Abbas *et. al.*, 2013). The overall increase in average precipitation for future projections while discussing the inter RCP variability (IPCC Fifth Assessment Report AR5) with present climate situations. Projections showed increasing and decreasing variability in total precipitation among different years 2025, 2050, 2075 and 2100 are 3.45-3.56 to 4.94-5.05, 6.06-6.25 to 8.69-8.88, 7.73-7.97 to 11.09-11.33 and 8.50-8.77 to 12.19-12.45 % respectively (Figure 8.22) from baseline. In (Figure 8.21) RCP4.5, 6.0 and 8.5 for 2025, 2050, 2075 and 2100 increasing variability are (2.21, 3.89, 4.96 and 5.46), (2.02, 3.61, 5.32 and 7.06) and (2.50, 5.33, 8.84 and 12.83) % respectively from baseline.

From the (Figure 8.21) projection showed both positive and negative change. February, March, May, June, July, August, September and October are positive change where RCP4.5, 6.0 and 8.5 for 2025, 2050, 2075 and 2100 increasing variability are (4.98, 8.75, 11.17 and 12.28), (4.54, 8.11, 11.98 and 15.88) and (5.62, 12.00, 19.90 and 28.87) % respectively. January, April November and December are negative change where RCP4.5, 6.0 and 8.5 for 2025, 2050, 2075 and 2100 decreasing variability are (-3.32, -5.84, -7.45 and -8.19), (-3.03, -5.41, -7.99 and -10.59) and (-3.75, -8.00, -13.28 and -19.25) % respectively.

8.7 Coastal District Future Climate Projection

All below graphs (Figure 8.23, 8.24, 8.25 and 8.26) showed 19 coastal district climate change scenarios. Latitude and longitude are considered district headquarters as individual district but not Bangladesh Meteorological Department (BMD) stations. All location selected from google earth imagery and data calculated from SimCLIM simulation to show the twentieth, twenty first and twenty second century from the baseline to future climate change scenario in the coastal zone. Minimum, maximum, mean temperature and precipitation are simulated low, mid and high sensitivity with GHG emission scenario. Shariatpur, Chandpur, Narail, Jessore, Gopalganj, Feni, Lakshmipur, Noakhali, Khulna, Satkhira, Barisal, Bhola, Bagerhat, Jhalokati, Pirojpur, Patuakhali, Chittagong, Barguna and Cox's Bazar were calculated.

SimCLIM provides a high regulation Regional Climate Model (RCM) to develop a site-specific climate change scenario. 19 individual coastal district headquarters selected by researcher as a coastal station. The comparison among minimum temperature, maximum temperature, mean temperature and precipitation in individual districts shows that, every station is increasing in nature in future scenario. This scenario also indicate that other districts of the country are the same in nature, though those are not listed in this chapter.

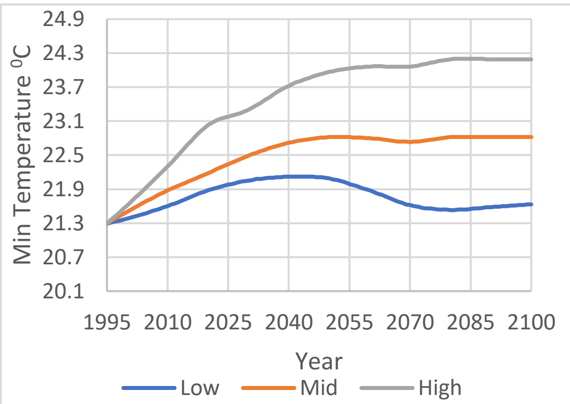

Shariatpur

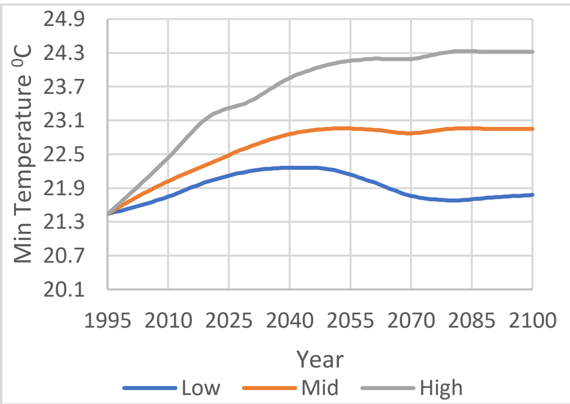

Chandpur

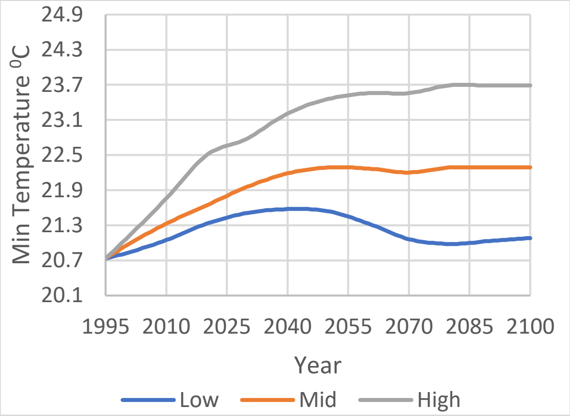

Narail

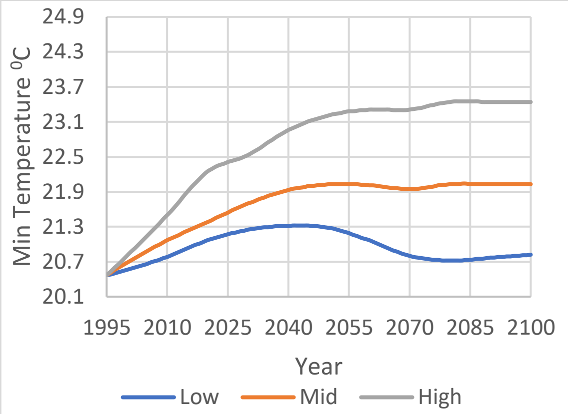

Jessore

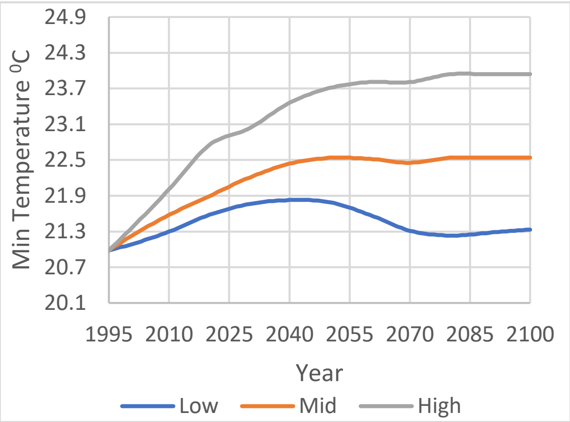

Gopalganj

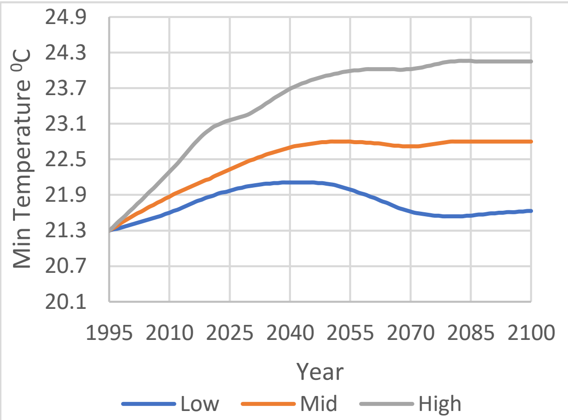

Feni

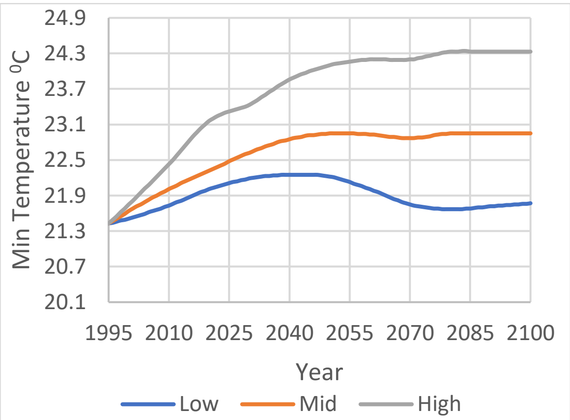

Lakshmipur

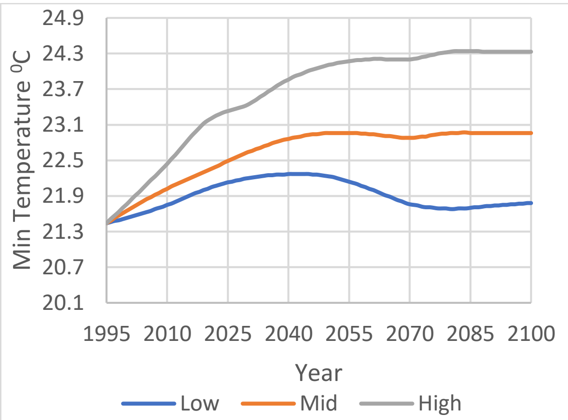

Noakhali

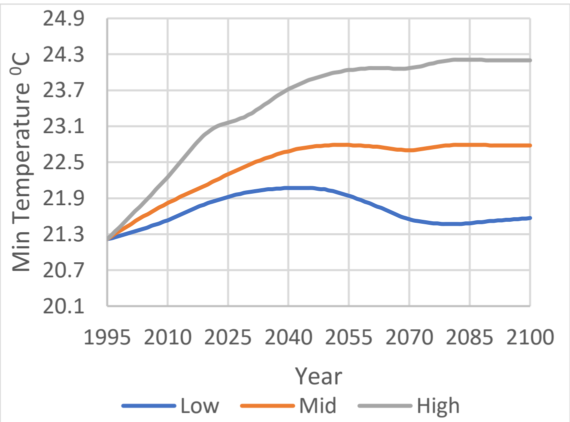

Khulna

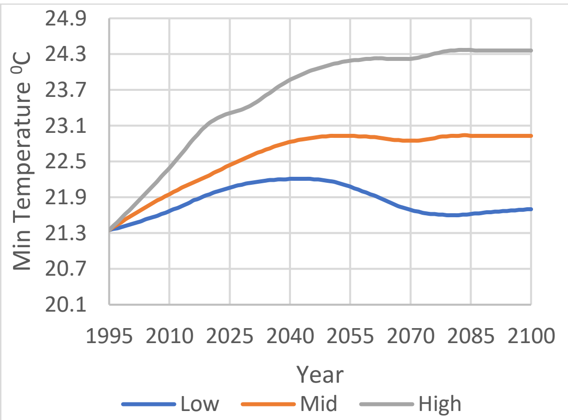

Satkhira

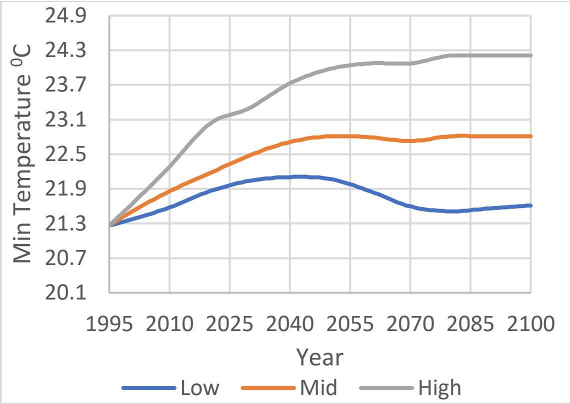

Barisal

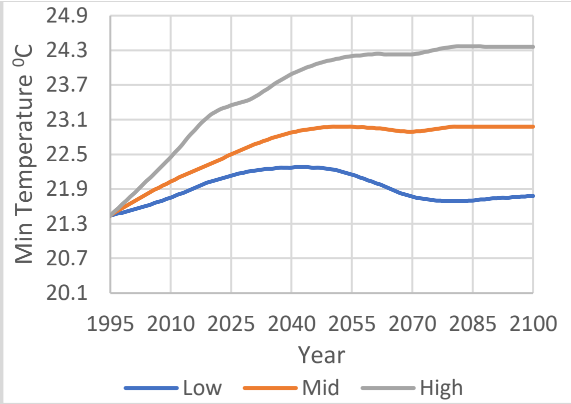

Bhola

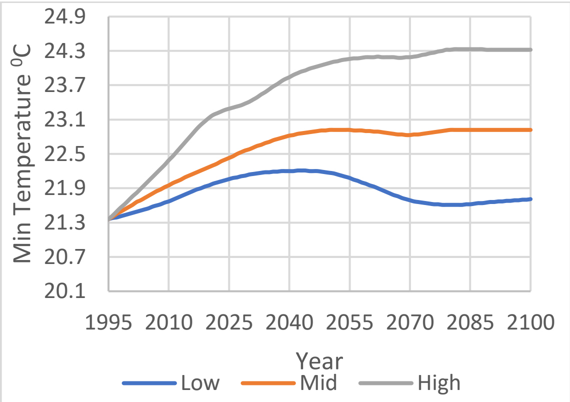

Bagerhat

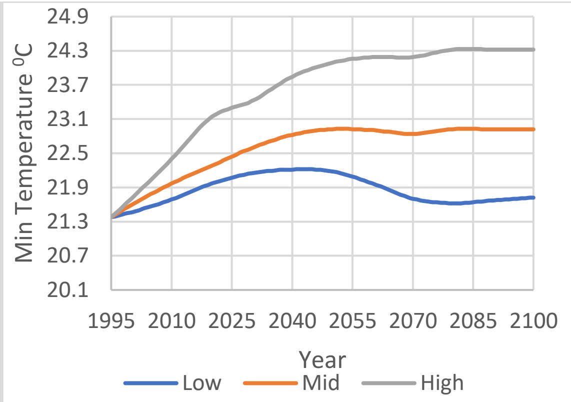

Jhalokati

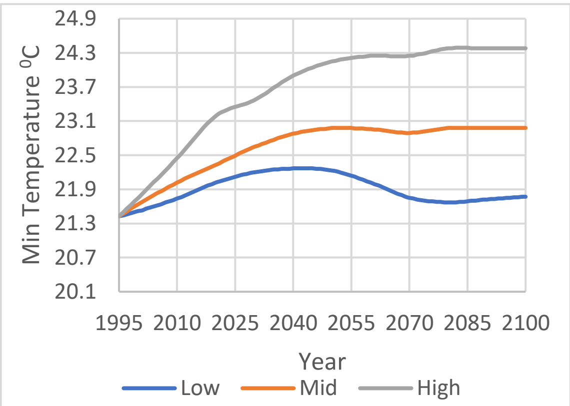

Pirojpur

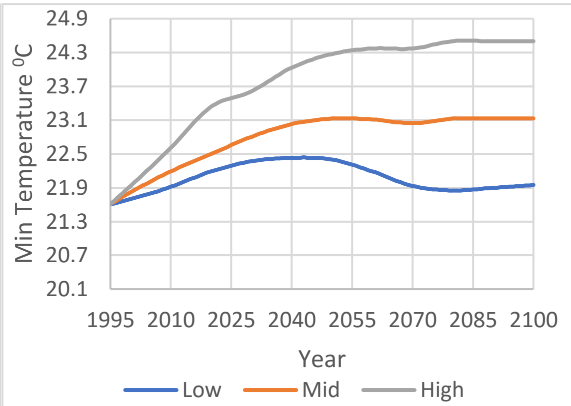

Patuakhali

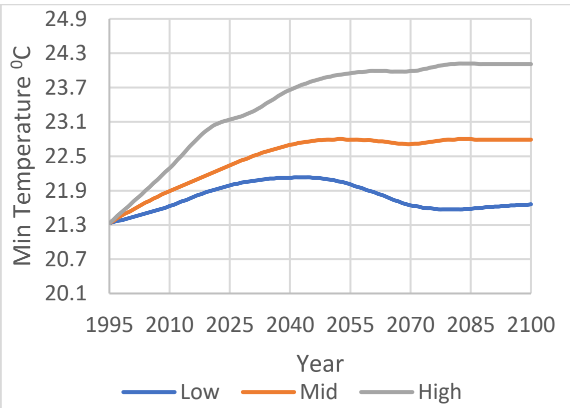

Chittagong

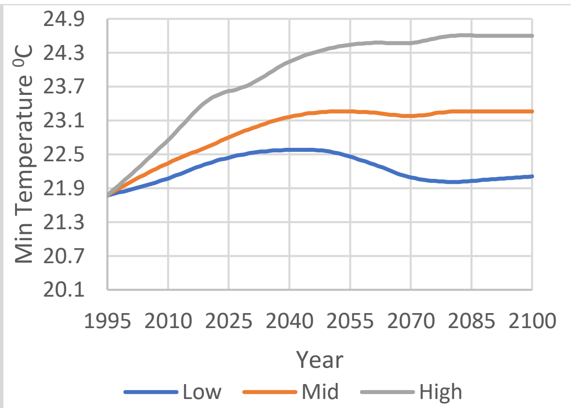

Barguna

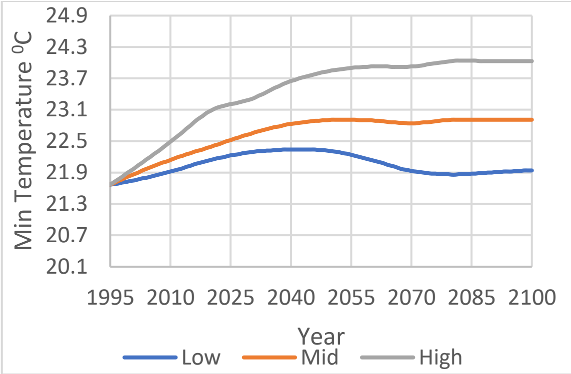

Cox's Bazar

Figure 8.23: Future climate scenario for minimum temp in coastal district from baseline 1995 to 2100

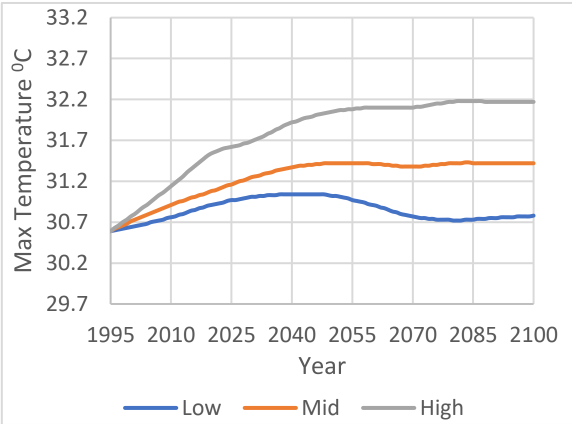

Shariatpur

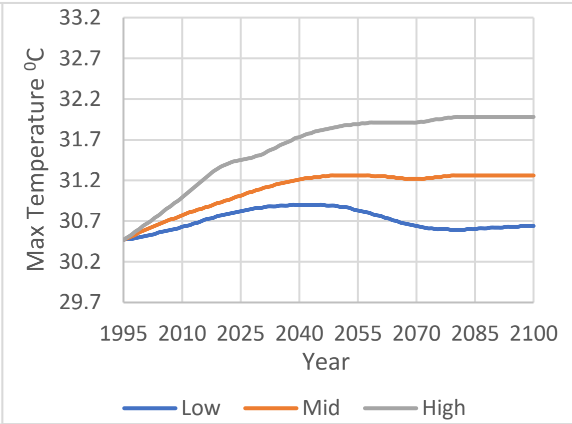

Chandpur

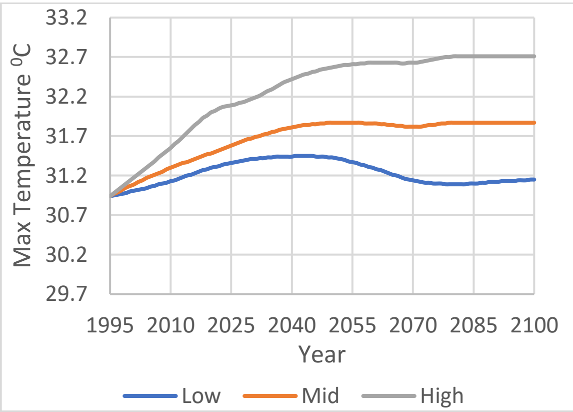

Narail

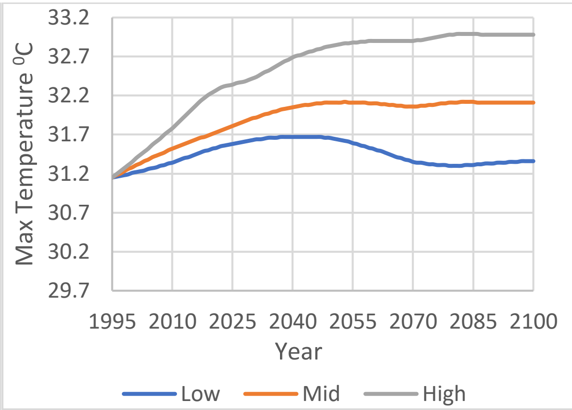

Jessore

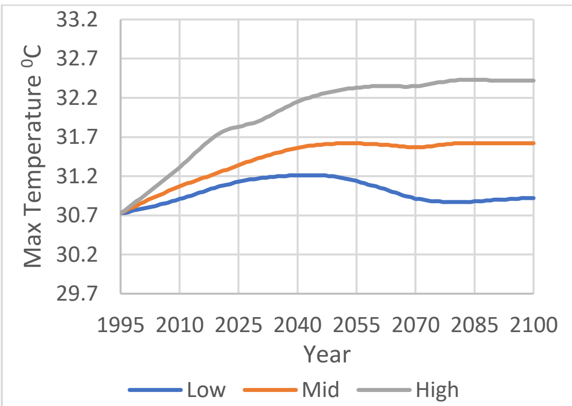

Gopalganj

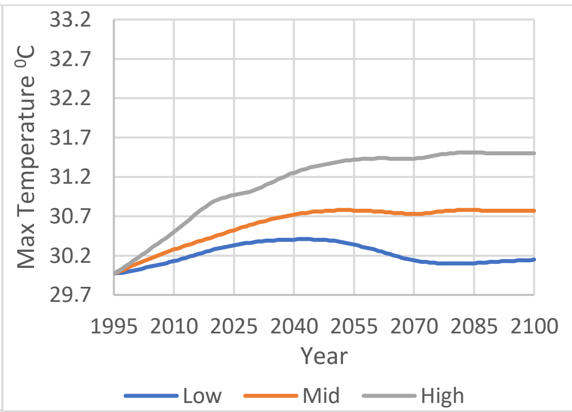

Feni

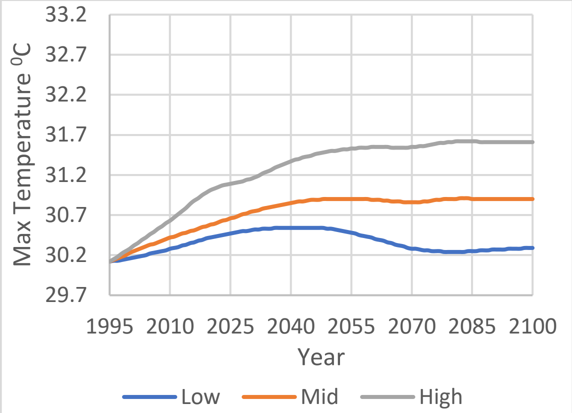

Lakshmipur

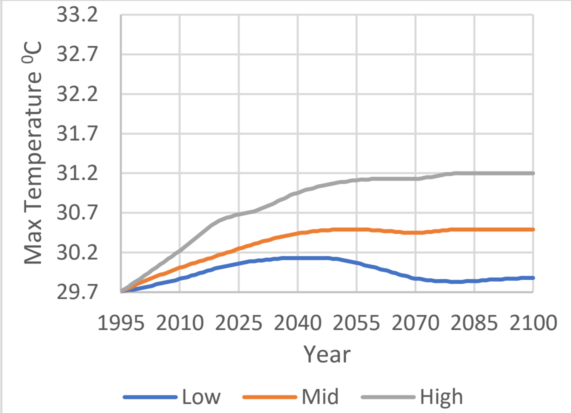

Noakhali

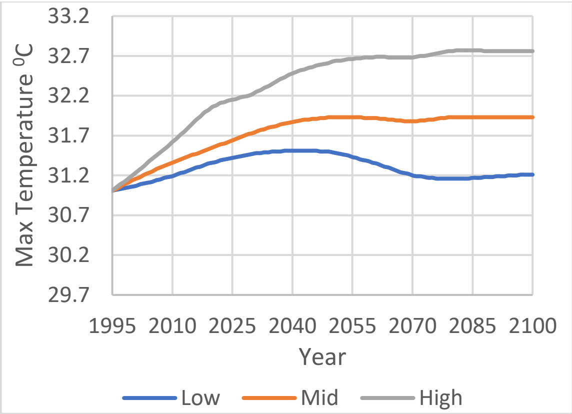

Khulna

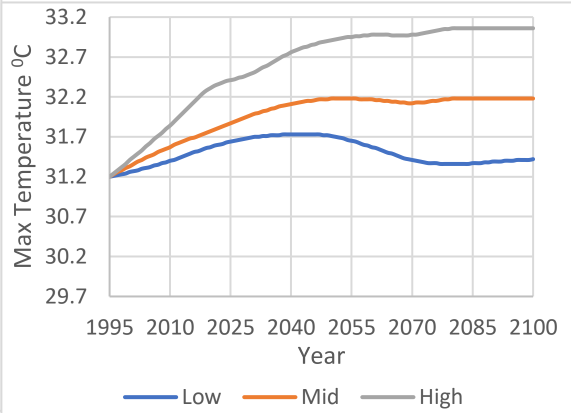

Satkhira

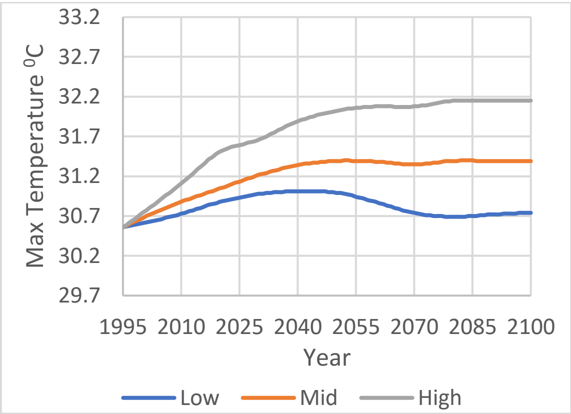

Barisal

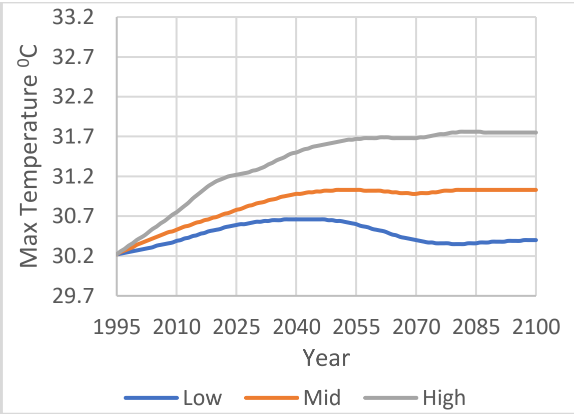

Bhola

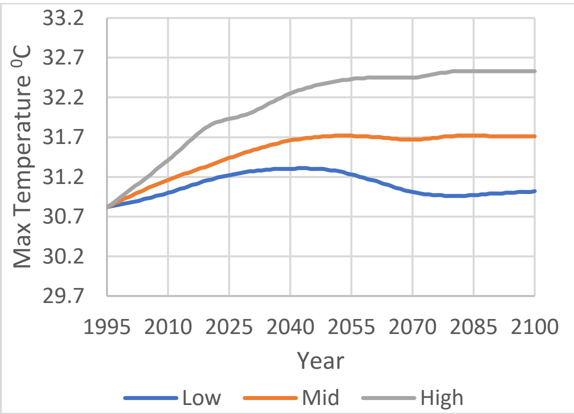

Bagerhat

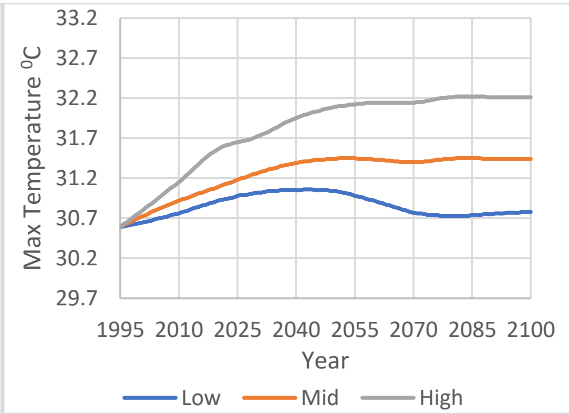

Jhalokati

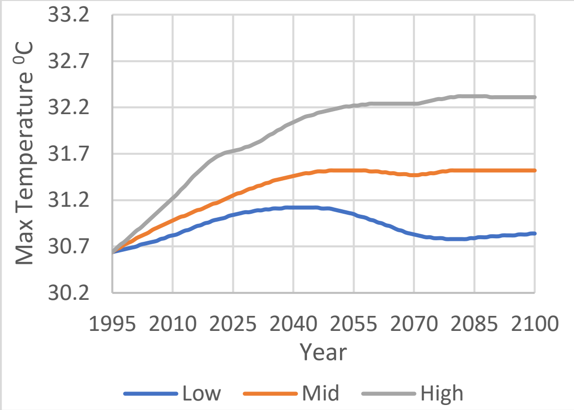

Pirojpur

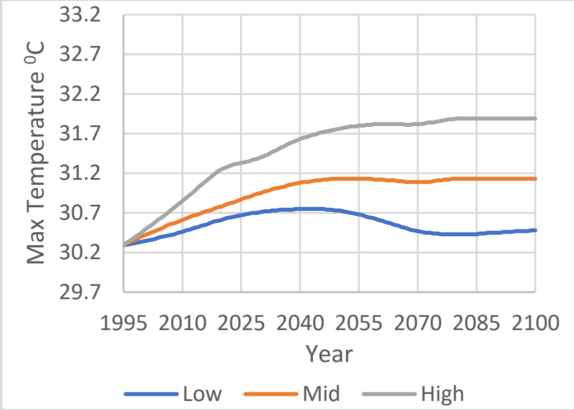

Patuakhali

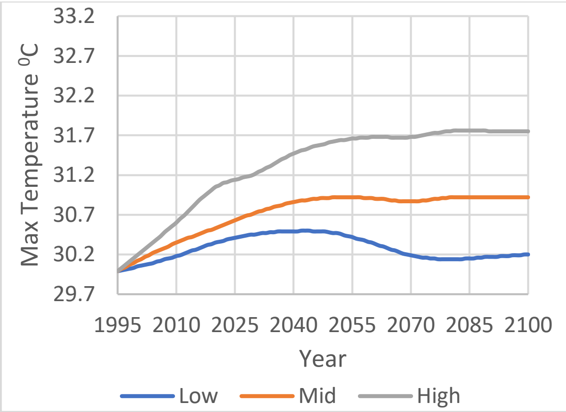

Chittagong

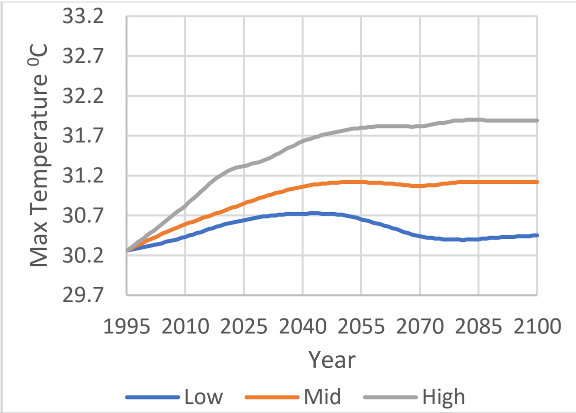

Barguna

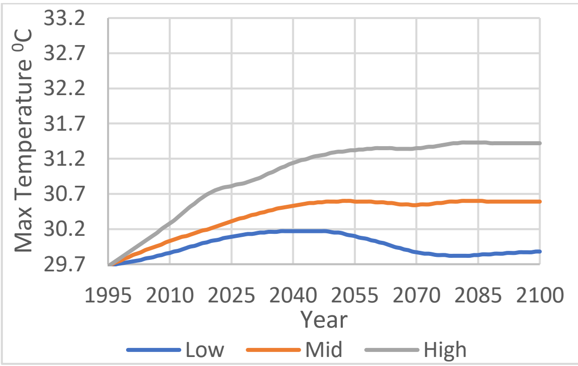

Cox's Bazar

Figure 8.24: Future climate scenario for maximum temp in coastal district from baseline 1995 to 2100

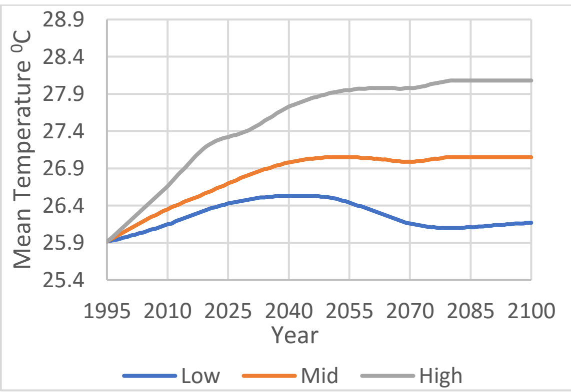

Shariatpur

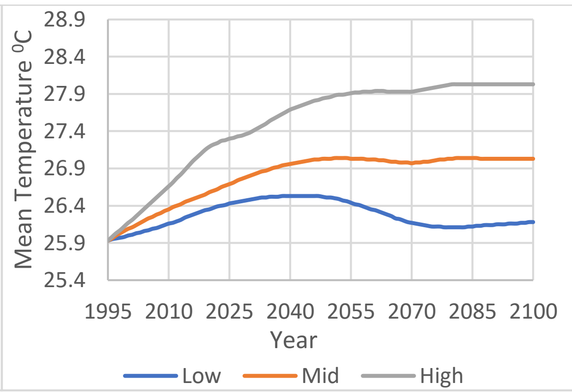

Chandpur

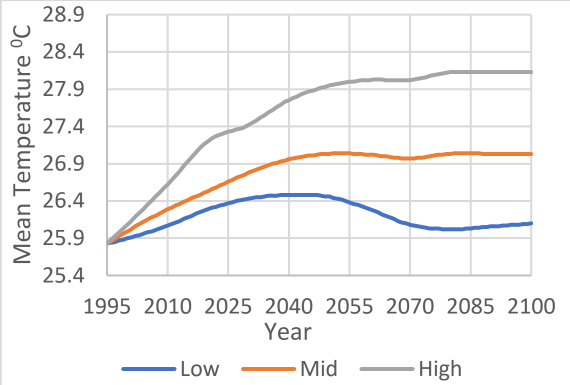

Narail

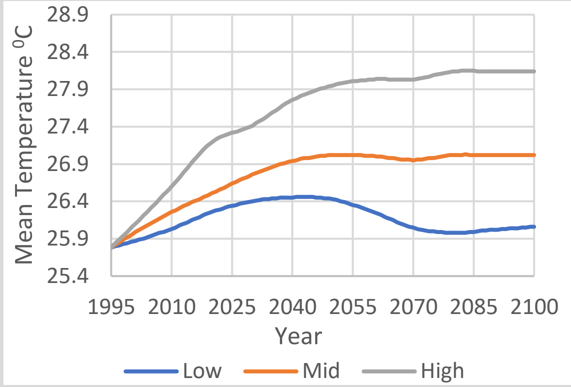

Jessore

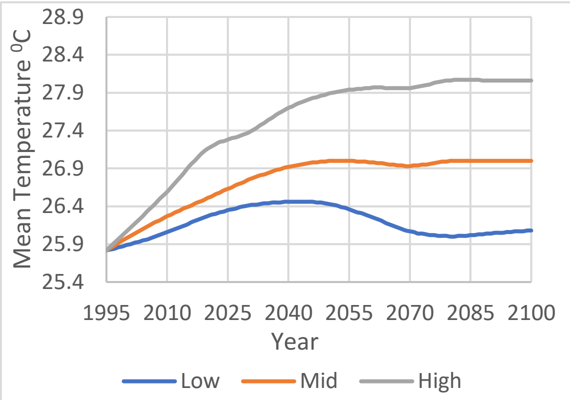

Gopalganj

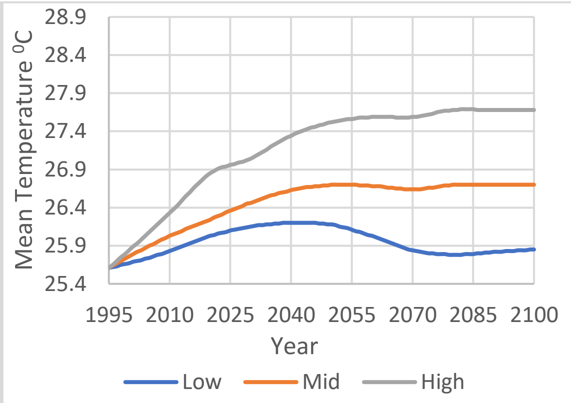

Feni

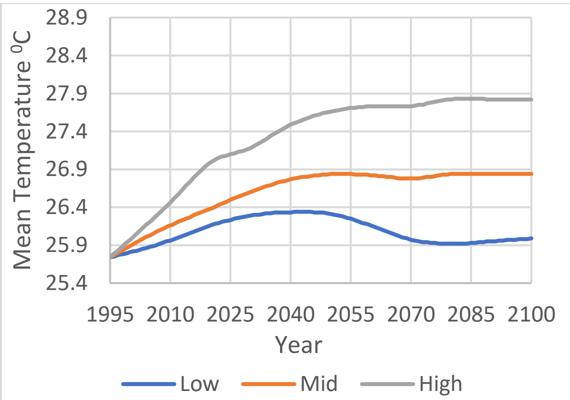

Lakshmipur

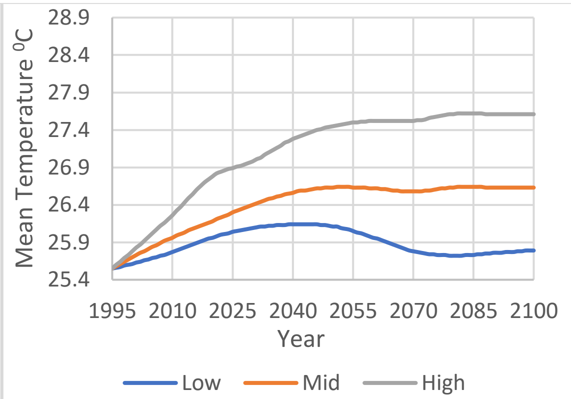

Noakhali

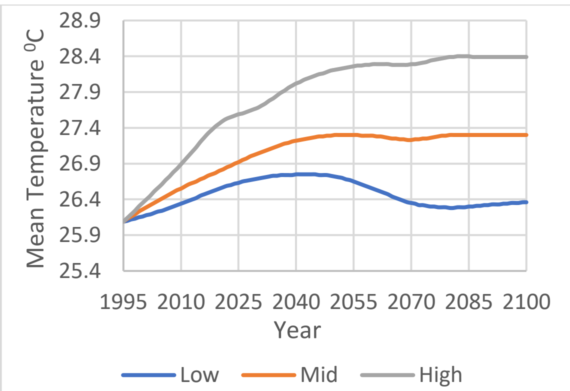

Khulna

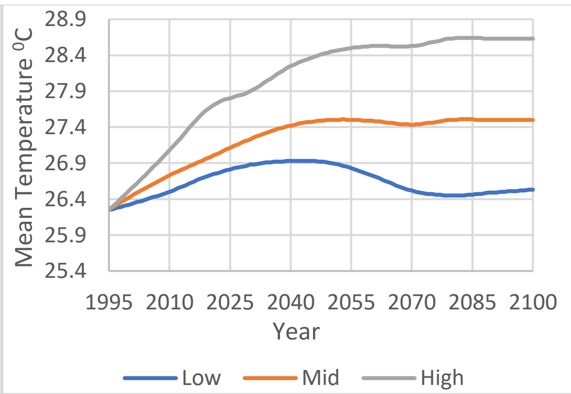

Satkhira

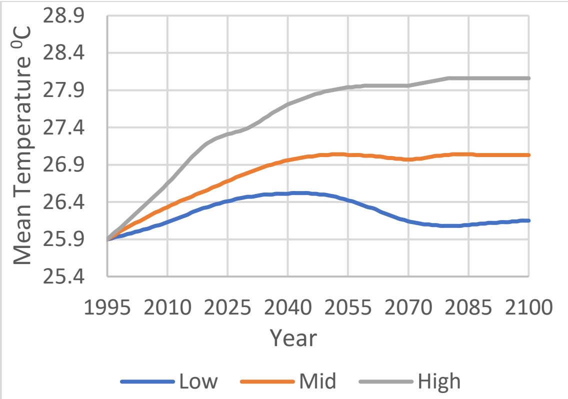

Barisal

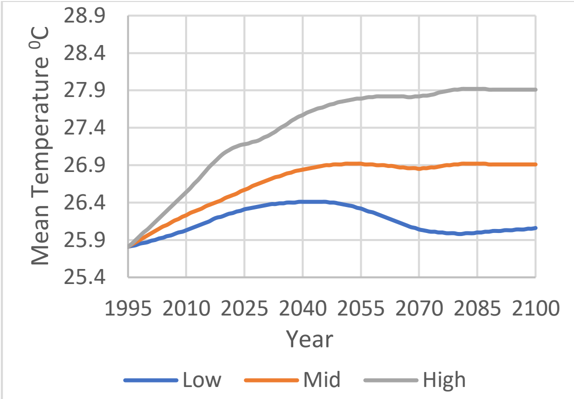

Bhola

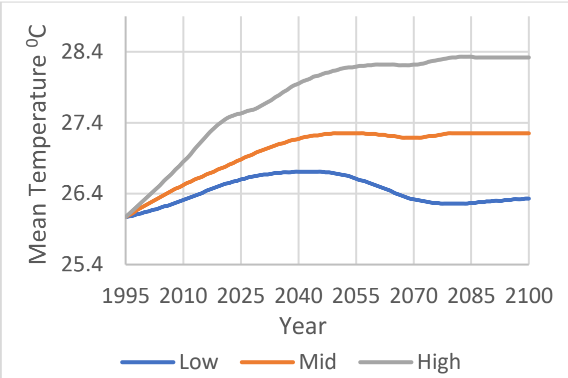

Bagerhat

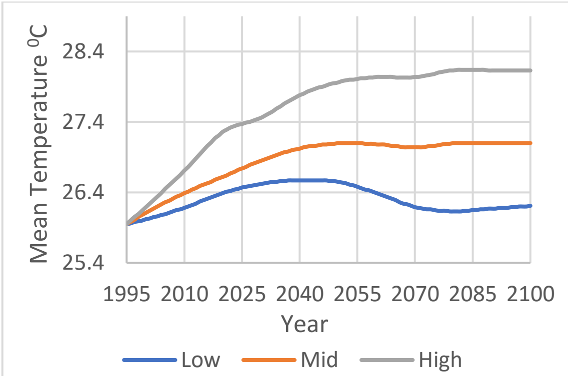

Jhalokati

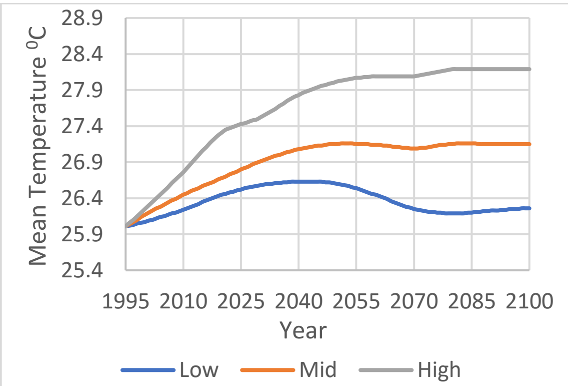

Pirojpur

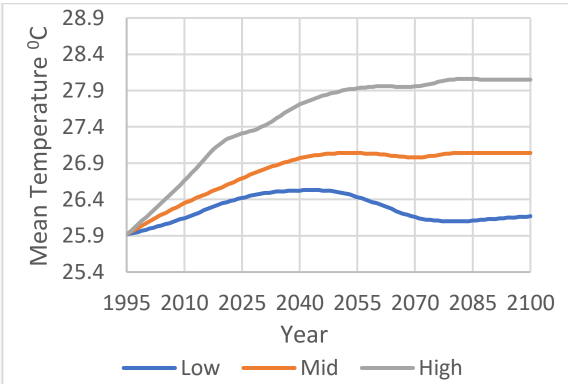

Patuakhali

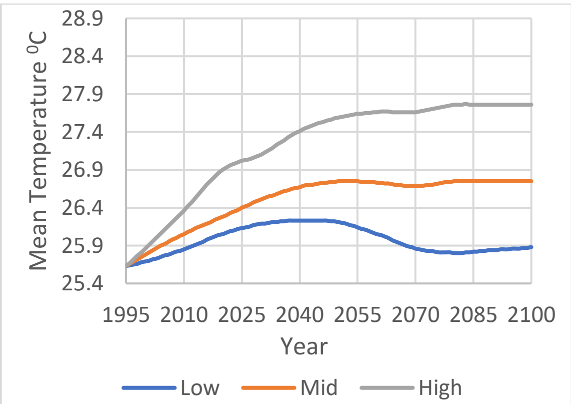

Chittagong

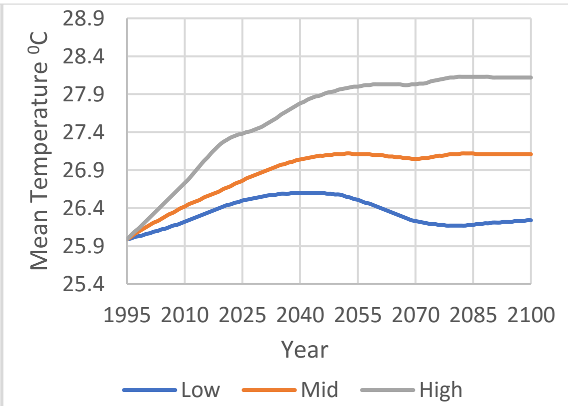

Barguna

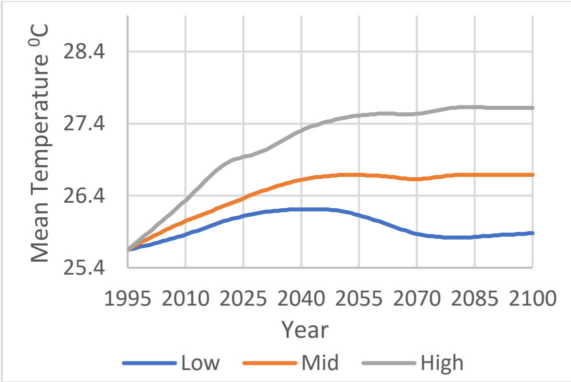

Cox's Bazar

Figure 8.25: Future climate scenario for mean temp in coastal district from baseline 1995 to 2100

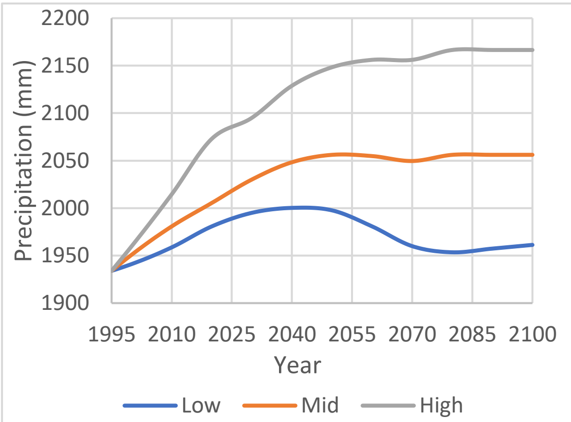

Shariatpur

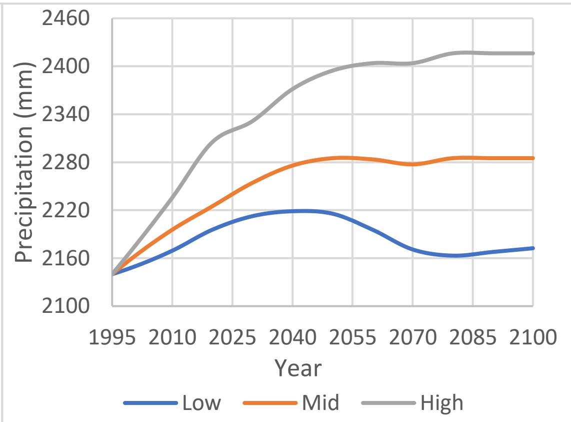

Chandpur

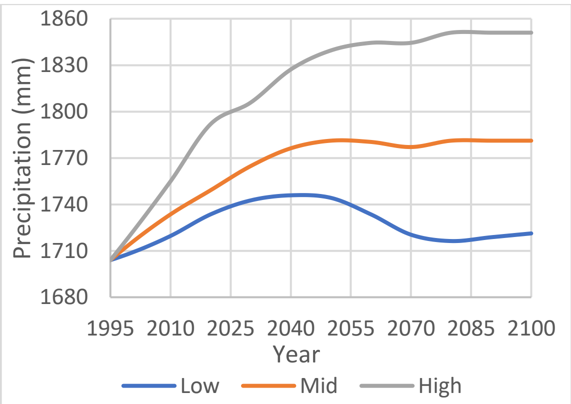

Narail

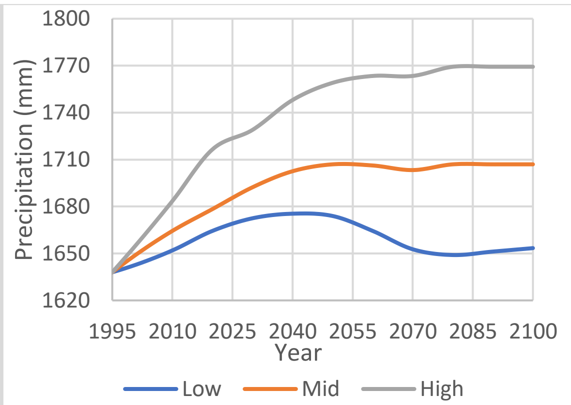

Jessore

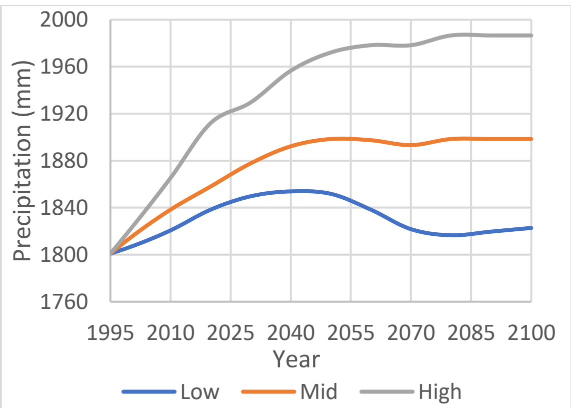

Gopalganj

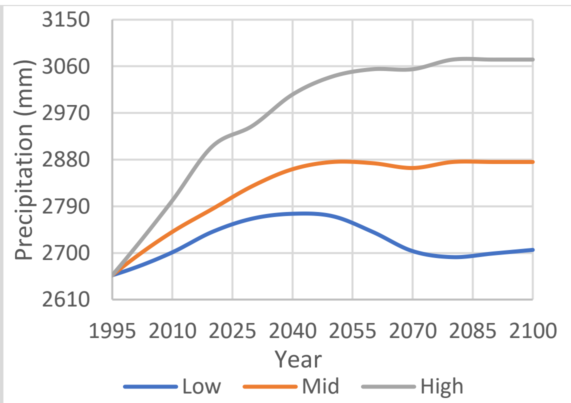

Feni

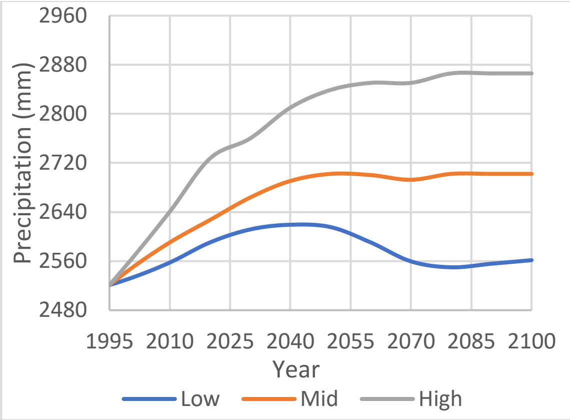

Lakshmipur

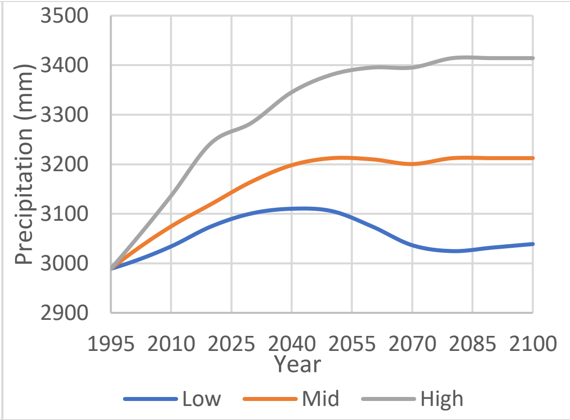

Noakhali

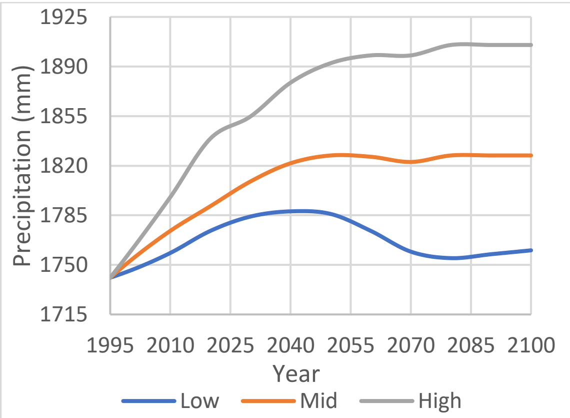

Khulna

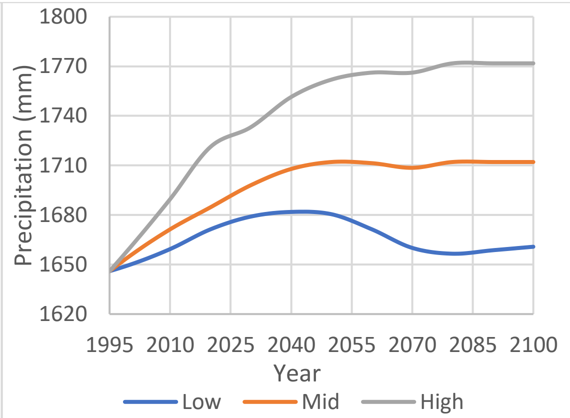

Satkhira

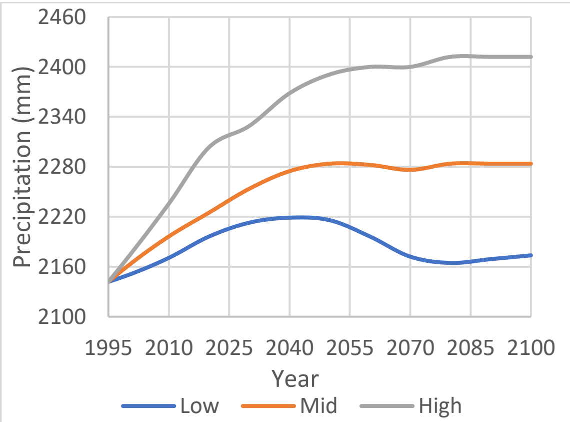

Barisal

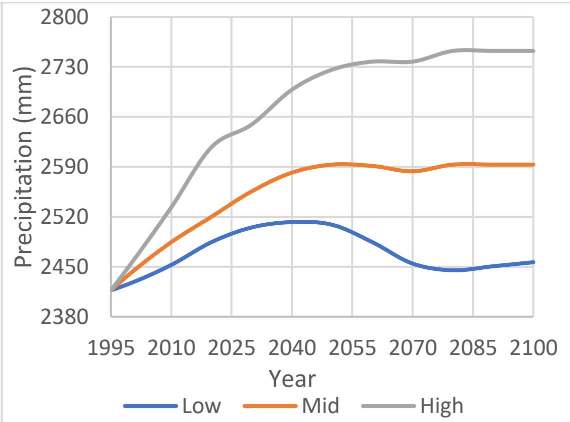

Bhola

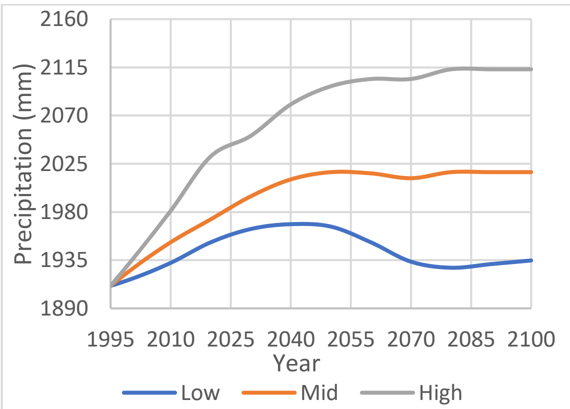

Bagerhat

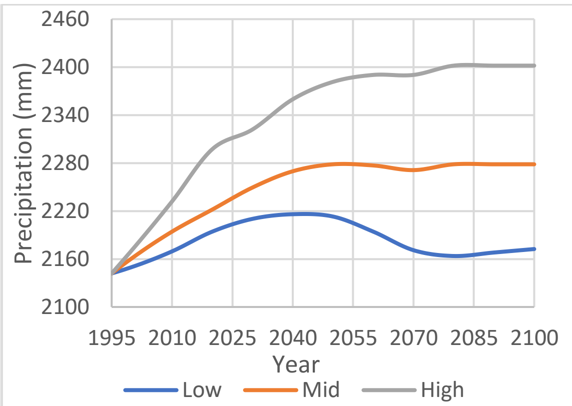

Jhalokati

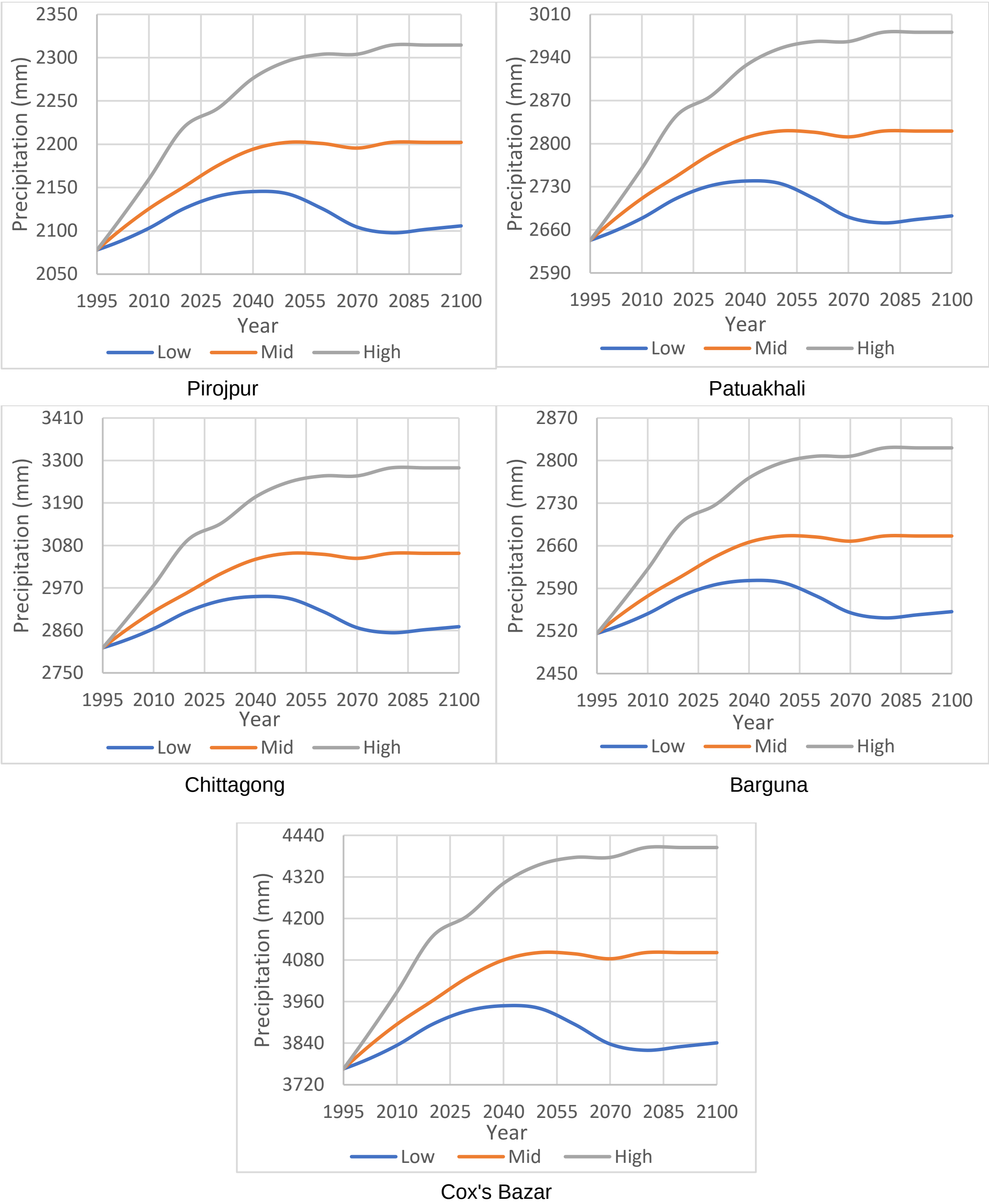

Figure 8.26: Future climate scenario for precipitation in coastal district from baseline 1995 to 2100

Overall conditions in this area shows that in the year of 2040s are the pick point for minimum, maximum, mean and precipitation. Though high sensitivity shows increasing in nature, but mid sensitivity is stable and low sensitivity decreasing in nature. Above all in the year of 2100 all three sensitivity are stable on their own stage. All three-sensitivity influencing based on increasing and decreasing of Green House Gas (GHG) emission scenario. This simulation fixing base year of 1995-2014 and researchers suggested that this situation going on in future as same.

Chapter Nine

Bangladesh Coastal Dynamics and Shoreline Change Detection

9.1 Introduction

Bangladesh coastal zone is one of the most disaster-prone area of the world. Its coastal zone is very much dynamics on its various character like, imbalance between the loss of sediment due to offshore transport and the decrease of the longshore transport, which results in a negative sediment budget. Tropical cyclone create short term erosion and seasonal fluctuation may not be stable to create long term coastal erosion. Several projects have been implemented to protected coastal erosion and moderate the long-term coastal erosion rate, wave attack and reduce the flooding damage. Sometimes this implementation influences the littoral transport (dam, embankment, dredging, groyne, breakwater etc.) modifies this balance. Proper system boundaries or not considering a super-system may cause huge damage in shoreline. The interaction between the waves and the bottom is due primarily to second order shallow water phenomena, such as the wave drift (which is responsible for mass transport) and the radiation stress, which is associated with the longshore current for obliquely incoming waves (Benassai, 2006). Shoreline changes due to sediment shifting are known as morpho-dynamics (Schwartz, 2005). The coastal zone of Bangladesh covers an area of 47,201 km^2 (WARPO, 2006).

9.2 Shoreline Change Analysis

To calculate a shoreline change, there are twelve sets of shorelines is used in this chapter for coastal zone of Bangladesh. Four sets of shorelines produced from historical topographic images ware acquired for four different decades: 1910s, 1940s, 1950s and 1960s from British Library, Texas Library and Survey of Bangladesh. Eight sets of Landsat imagery were acquired for eight different years: 1974, 1980, 1990, 1995, 2000, 2005, 2010 and 2015 from the USGS glovis (https://glovis.usgs.gov) and Earth Explorer (https://earthexplorer.usgs.gov) database (see Table 2.2 and 2.3).

It would be possible to extract shorelines a single operator digitize/manually from the satellite images (Dewan *et. al.*, 2017a and White *et. al.*, 1999). Although a Band ratio would be possible to extract shorelines to be an efficient approach to automated shoreline identification (Alesheikh *et. al.*, 2007). Modified Normalized Difference Water Index (MNDWI) or Normalized Difference Water Index (NDWI) for Landsat 8 OLI and TIRS (Green Band-3 is divided by SWIR Band-6 for MNDWI or Green Band-3 is divided by NIR Band-5 for NDWI), Landsat 7

ETM+ (Green Band-2 is divided by SWIR Band-5 for MNDWI or Green Band-2 is divided by NIR Band-4 for NDWI), Landsat 4-5 TM (Green Band-2 is divided by SWIR Band-5 for MNDWI or Green Band-2 is divided by NIR Band-4 for NDWI), Landsat 1-3 MSS (Green Band-4 is divided by NIR Band-6/7 for NDWI) and Landsat 4-5 MSS (Green Band-1 is divided by NIR Band-3/4 for NDWI) respectively using the Band Math tool in ENVI® 5.1. In Landsat 1-3 MSS and Landsat 4-5 MSS, there were no any SWIR band for calculating MNDWI. This calculation results three classes: water, land and high reflective land where a pixel value of zero (0) indicate water, pixel value of 1-127 indicate land and pixel value 127-255 indicate highly reflective land. Some researchers have adopted Band-4 for discrimination of shorelines, or a combination of bands; for example, Benny (1980) used band-7 of the Landsat MSS for shoreline definition and Marafai *et. al.* (2008) used Band-4 of MSS and Band 5 of ETM for shoreline mapping in Semarang, Indonesia. However, use of Band 5 has been shown to produce up to 96.9% accuracy (Frazier and Page, 2000) and was the preferred method adopted in this study.

The simplified band-ratio image was opened in ENVI 5.1 and ArcMap 10.5 then transformed by auto-threshold difference raster into three thresholding classes using Otsu's thresholding method, though there were four thresholding method (Otsu's, Tsai's, Kapur's and Kittler's) but Otsu's method was appropriate in my study area and then converted into a vector. The shoreline (land-water separation) was converted into polylines using the polygon to line tool. Small polygons in the land area that probably represented water bodies, such as ponds or small lakes, were eliminated by editing in ArcMap 10.5 and the mouths of rivers and tidal creeks were connected by straight lines to provide a single shoreline for the entire coastal zone. This approach was used to extract the 1974 shoreline from the earlier images and the 2015 shorelines from the most recent images in terms of five years interval. Both computers based automated shoreline and single operator digitize/manually shoreline were tested but single operator digitize/manually created shoreline is used in this study because from Meghna mouth to Feni river, Island areas of coastal zone and where mudflat present were not possible to calculated auto-threshold difference raster, mainly in Landsat MSS and/or Landsat TM/OLI (60 and/or 30 m resolution). Mudflat areas mislead/misguide whether it is land or water. That's why digitize/manually produced shoreline in every sets of temporal date. Ever year Ganges-Padma river carry huge amount of sediment and create *char* land, these are not stable.

Much of the coast of Bangladesh experiences a large tidal range, reaching up to 6 m or more at Sandwip Island (Barua, 1997). Large errors in shoreline change could result if one image was acquired at low tide and the other at high tide, particularly on an intertidal substrate of gentle gradient as characteristic of much of the Bay of Bengal (Jimenez *et. al.*, 1997). In order to minimize such shoreline-change error in the both images, the time of the image capturing was noted and tidal conditions at that time determined from tidal records held with the Bangladesh Inland Water Transport Authority (BIWTA). Landsat satellite captured images more or less at local time of 9.00 am to 10.30 am when mean tide was found.

9.3 Digital Shoreline Analysis System (DSAS)

After identifying the shorelines, the rates of shoreline change along different parts of the coast were calculated using Digital Shoreline Analysis System (DSAS) version 4.3 extension in ArcGIS 10.5 (Himmelstoss, 2009). The End Point Rate (EPR) is the most appropriate of the different statistical approaches available within DSAS for measuring the rate of shoreline change when calculated from only two shoreline positions in time. Shoreline change is calculated relative to a baseline, which can be either a user-defined line or a buffer generated relative to an existing shoreline. In this study a baseline was inserted manually and transects were created orthogonal to it, at 500 m intervals.

Bangladesh coastal zone is divided into three block (a) Eastern zone, (b) Central Zone and (d) Western zone. A total of 1,488 transects were generated. DSAS calculates the distance of each shoreline from the baseline, and then derives Net Shoreline Movement (NSM), End Point Rate (EPR) and Liner Regression Rate (LRR). Dividing the NSM by the number of intervening years to determine shoreline change in m/yr. Accretion is presented in positive numbers and erosion by a negative number in the DSAS calculation. A copy of the transect file can be clipped to this span for display purposes (Figure 9.1).

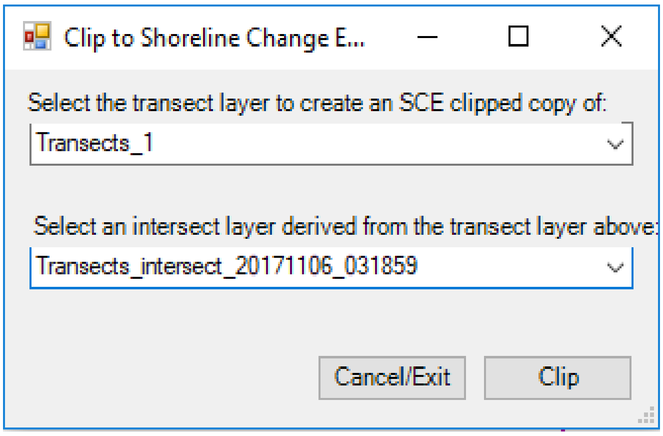

Figure 9.1: Screenshot of clip to Shoreline Change Envelope window example of required parameters

9.4 Statistical Analysis

Each method used to calculate shoreline rates of change is based on measured differences between shoreline positions through time. The reported rates are expressed as meters of change along transects per year. When the user-selected rate-change calculations have finished processing, DSAS merges the individual module calculations, and the output is made available as a table in ArcMap. The rate-change statistics provided with DSAS have the standardized field headings listed in the first column (Table 9.1).

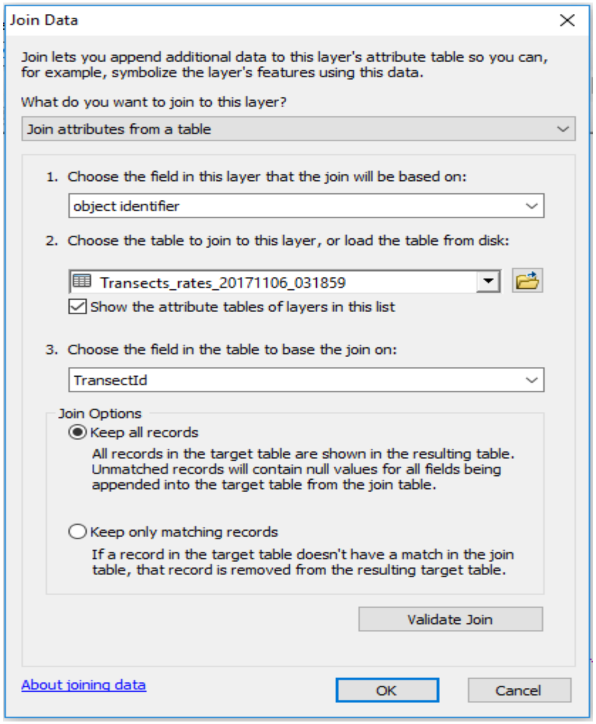

Figure 9.2: Screenshot of Join Data window in ArcMap

The (Table 9.2) of statistical results is joined to the transect feature class by the field they share in common. The values in the TransectID field of the results table are equal to the object identifier field ObjectID in the transect feature class. Completing a join allows the rates to be used as a value field to change the symbology of the transect feature class.

The clip to Shoreline Change Envelope (SCE) function will create a copy of the original transects clipped to the SCE extent. The Clip to SCE dialog requires the user to specify which transect layer is used. A new intersect file is generated (with time stamp) every time rate calculation is run (prior to DSAS 4.3, the intersect file was overwritten for each run). In addition to the transect-shoreline intersections used in the rate calculations, the intersect file also contains the information necessary to clip the data to the SCE extent; a separate SCE calculation is not required for the tool to function. The clipping process will create a copy of the specified transect file, cropped to the greatest extent between shorelines. Users can then join the rate calculation table to the clipped transects file and modify the symbology to generate a spatial display of the calculated shoreline change rates.

Table 9.1: Table of standardized field headings provided by DSAS for change calculations. The third column provides examples illustrating how the user-selected confidence interval is specified

NSM	Net Shoreline Movement	
SEC	Shoreline Change Envelope	
EPR	End Point Rate	
ECI	Confidence of End Point Rate	
LRR	Linear Regression Rate	
LSE	Standard Error of Linear Regression	
LCI	Confidence Interval of Linear Regression	*LCI95, LCI90
LR2	R-squired of Linear Regression	
WLR	Weighted Linear Regression Rate	
WSE	Standard Error of Weighted Linear Regression	
WCI	Confidence Interval of Weighted Linear Regression	*WCI95, WCI90
WR2	R-squired of Linear Regression	
LMS	Least Median of Squares	

Note: *LCI and WCI was used for 95% confidence interval in three blocks in coastal zone of Bangladesh

The end point rate is calculated by dividing the distance of shoreline movement by the time elapsed between the oldest and the most recent shoreline. The major advantages of the EPR are the ease of computation and minimal requirement of only two shoreline dates. The major disadvantage is that in cases where more data are available, the additional information is ignored. Changes in sign (for example, accretion to erosion), magnitude, or cyclical trends may be missed (Crowell *et. al.*, 1997; Dolan *et. al.*, 1991).

The shoreline change envelope reports a distance, not a rate. The SCE is the distance between the shoreline farthest from and closest to the baseline at each transect. This represents the total change in shoreline movement for all available shoreline positions and is not related to their dates. The NSM is associated with the dates of only two shorelines. It reports the distance between the oldest and youngest shorelines for each transect. This represents the total distance between the oldest and youngest shorelines.

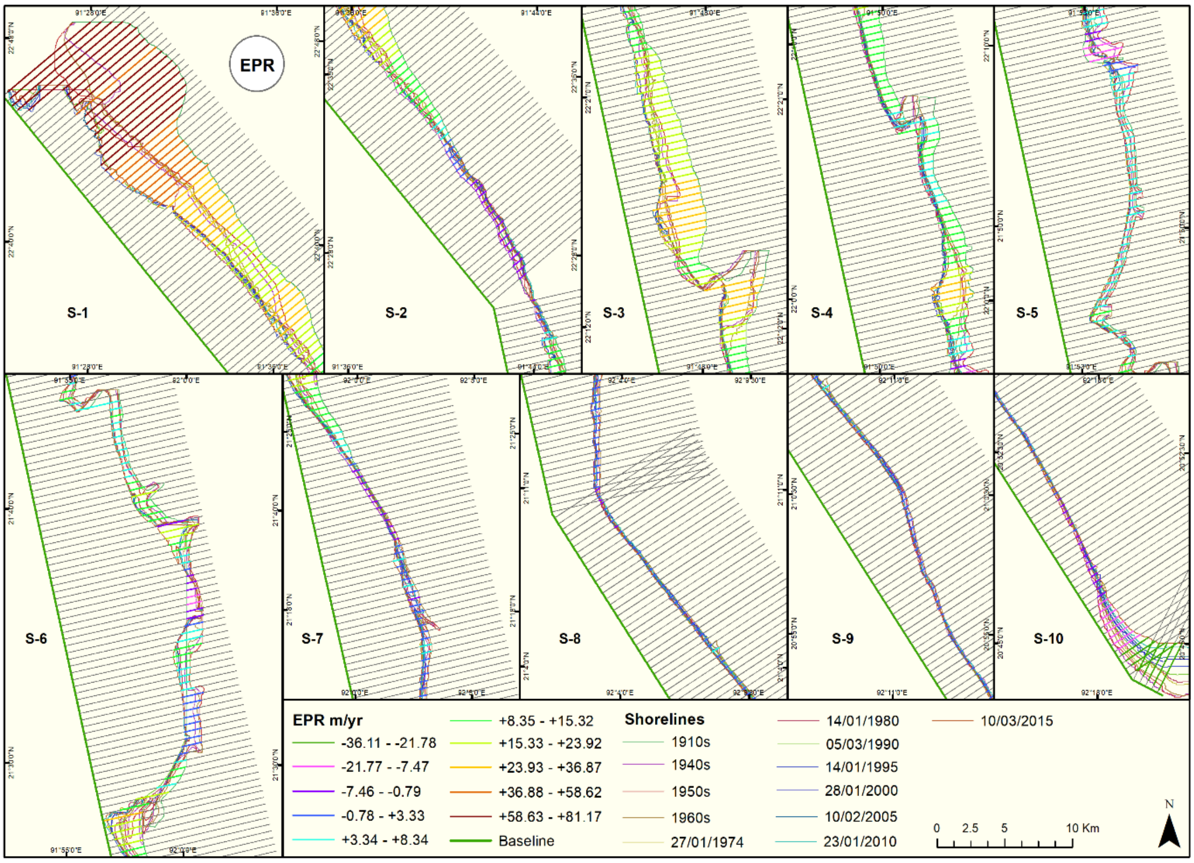

Figure 9.3: End Point Rate (EPR) in block 1 coastal zone of Bangladesh

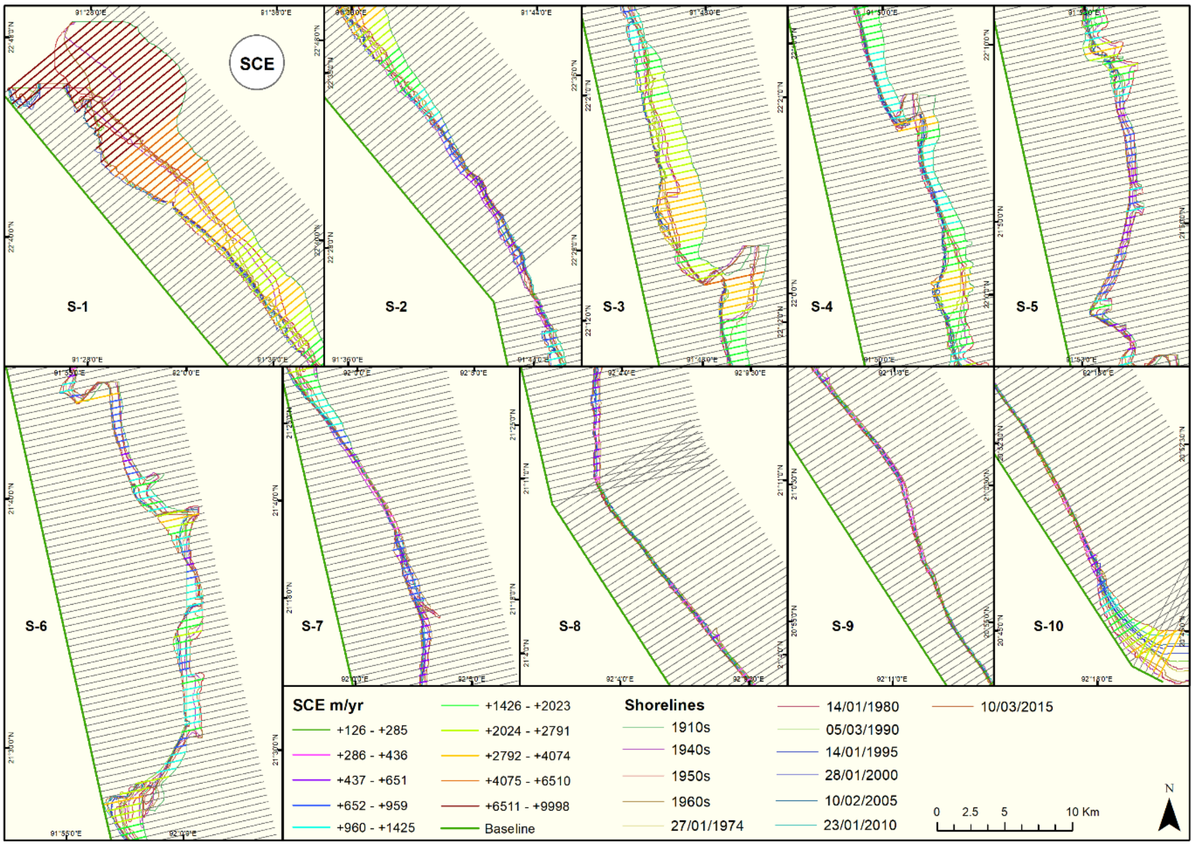

Figure 9.4: Shoreline Change Envelope (SCE) in block 1 coastal zone of Bangladesh

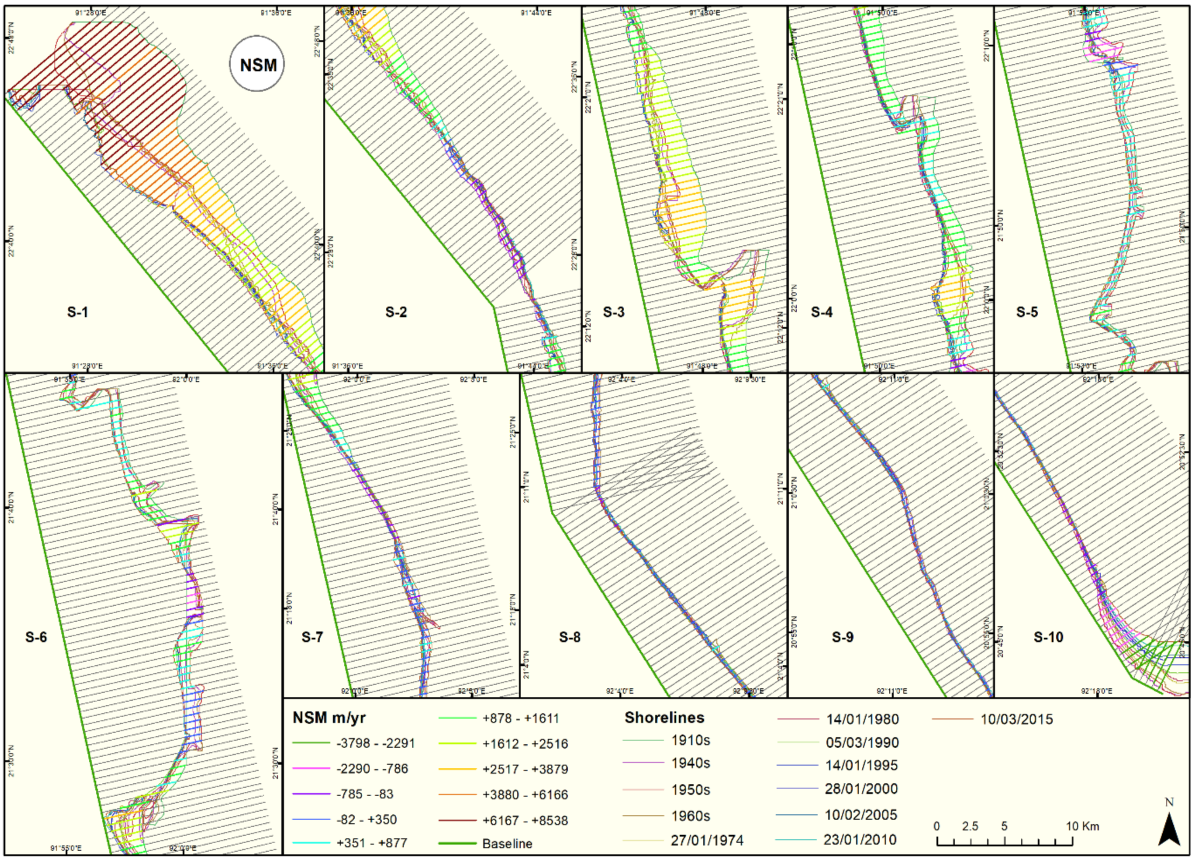

Figure 9.5: Net Shoreline Movement (NSM) in block 1 coastal zone of Bangladesh

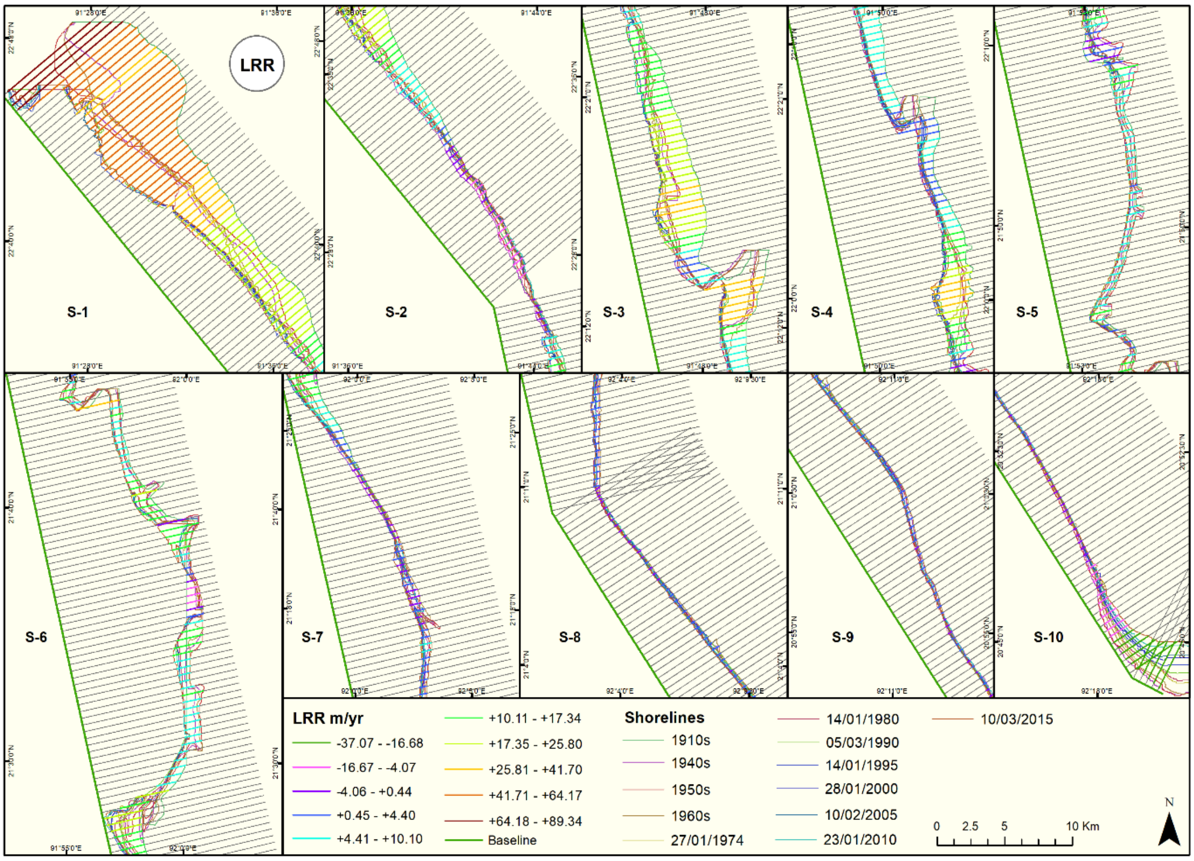

Figure 9.6: Liner Regression Rate (LRR) in block 1 coastal zone of Bangladesh

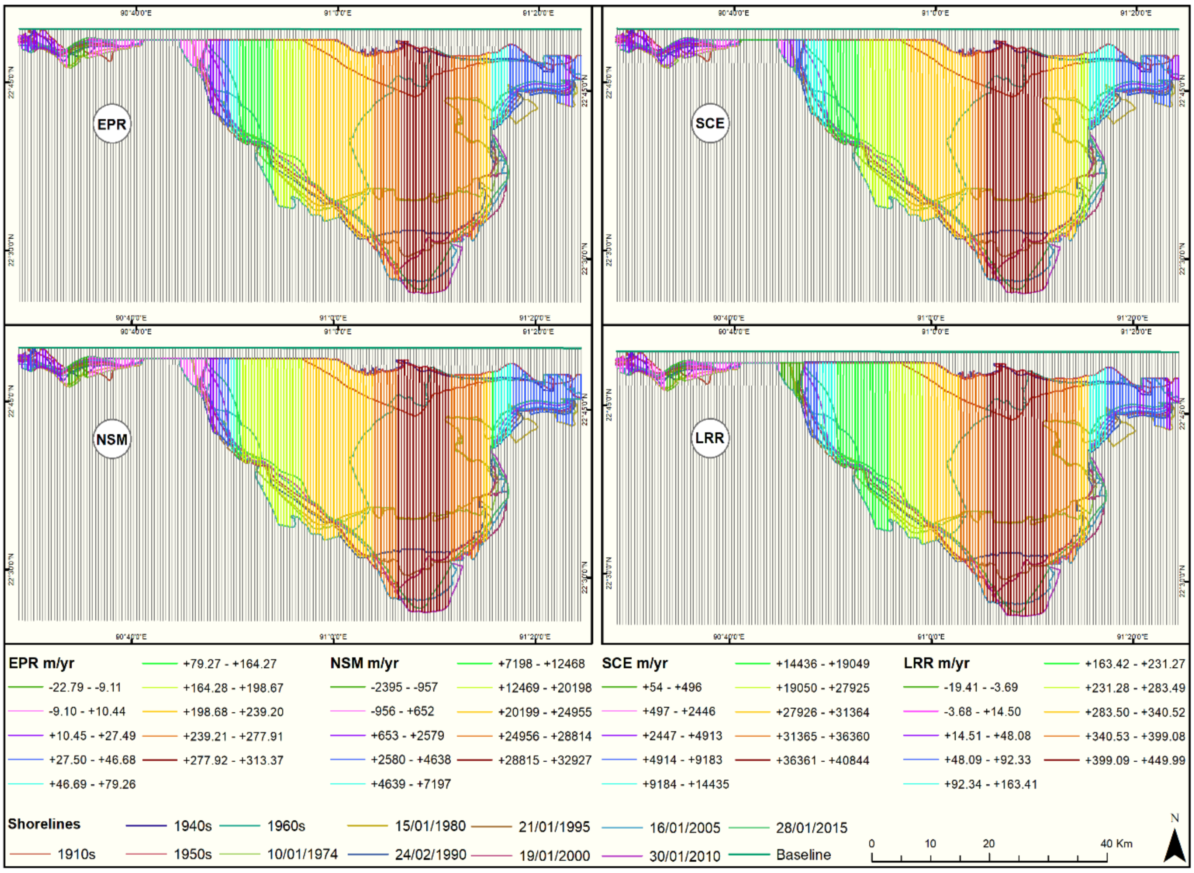

Figure 9.7: EPR, SCE, NSM and LRR in block 2 coastal zone of Bangladesh

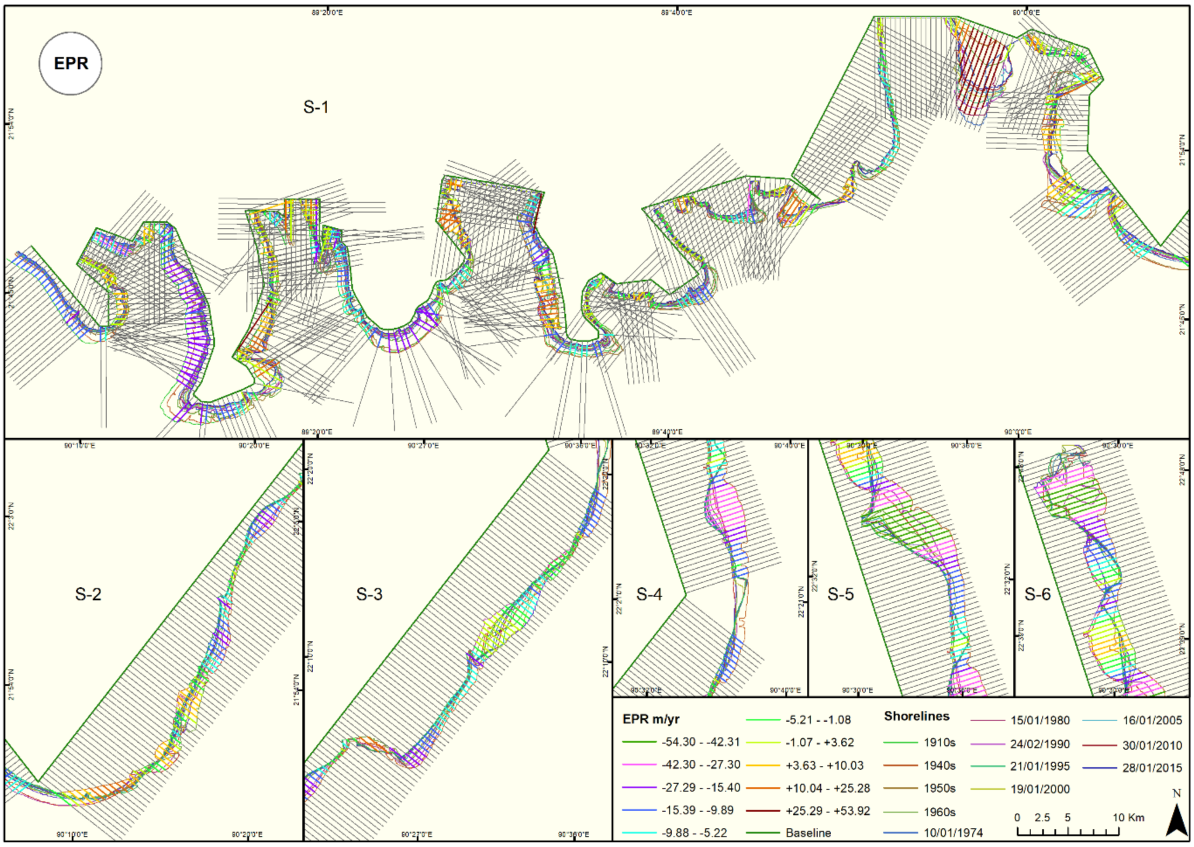

Figure 9.8: End Point Rate (EPR) in block 3 coastal zone of Bangladesh

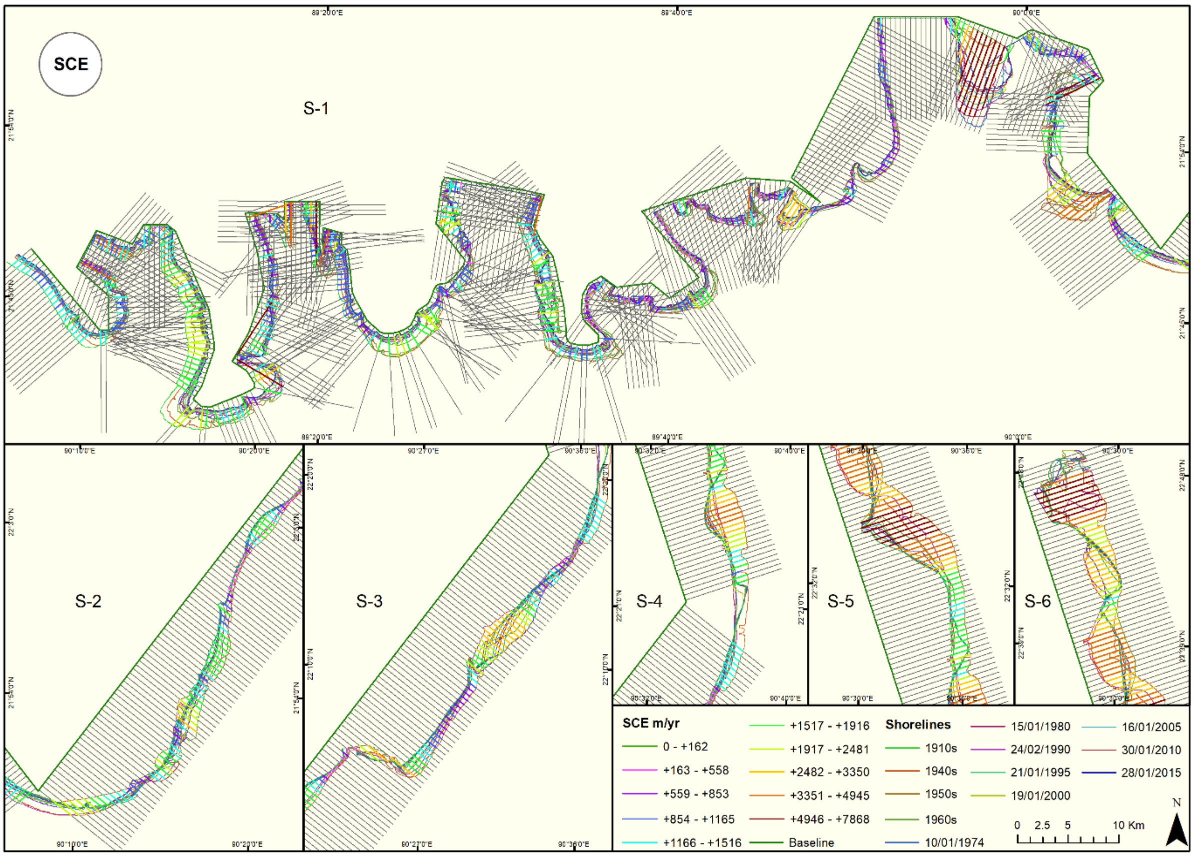

Figure 9.9: Shoreline Change Envelope (SCE) in block 3 coastal zone of Bangladesh

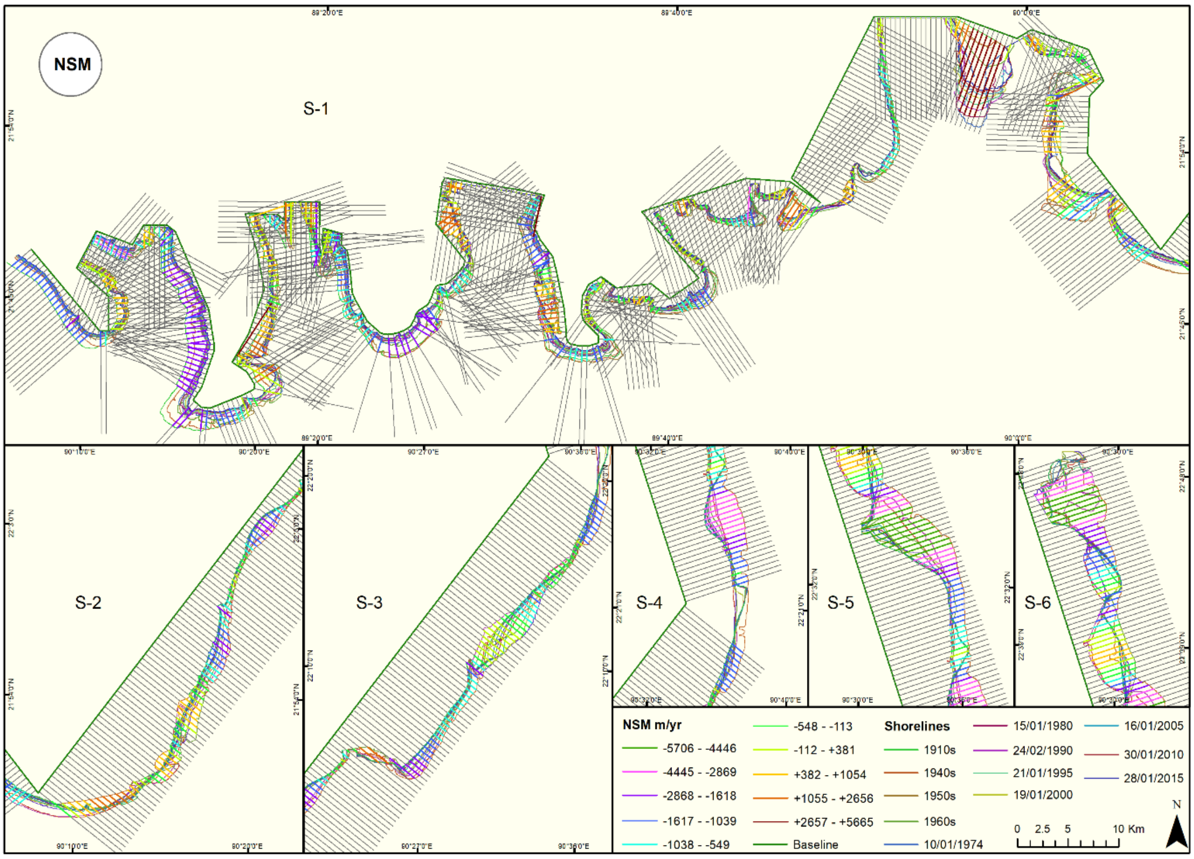

Figure 9.10: Net Shoreline Movement (NSM) in block 3 coastal zone of Bangladesh

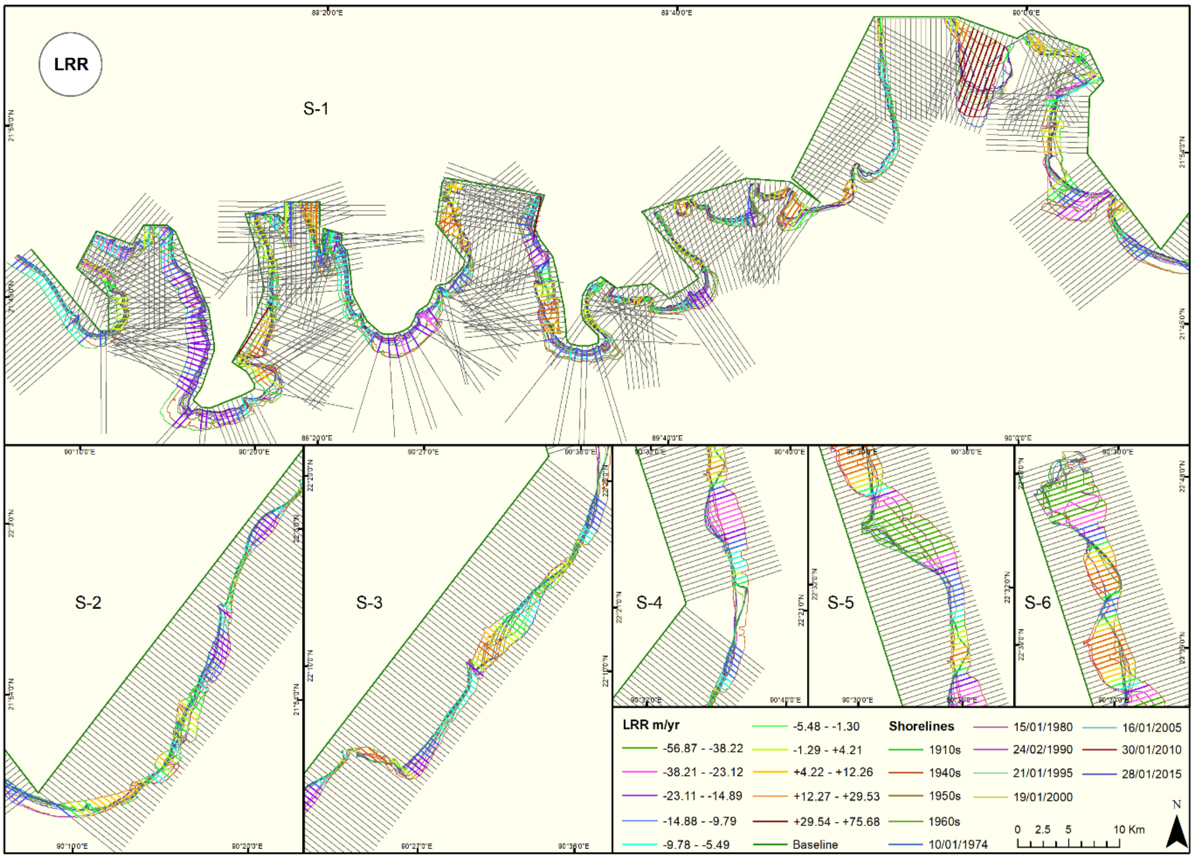

Figure 9.11: Liner Regression Rate (LRR) in block 3 coastal zone of Bangladesh

In block 1 there were 10 segments created (Figure 9.3-9.6) and transects were started from left to right. This block ranges from Feni river to Teknaf where 505 transects were generated. In block 2 there were no segments created (Figure 9.7) and transects were started from left to right. This block is ranges from Tentulia river to Feni River where 192 transects were generated. In block 3 there were 6 segments created (Figure 9.8-9.11) and transects were started from left to right. This block ranges from Bangladesh-India border to Tentulia river where 791 transects were generated but 23 transects with 0 ID were dropped because of no calculation was operate here. In every block transects ID was created 500 m interval. For calculation various types of statistics are generated and most useful statistics are used in this chapter.

9.5 End Point Rate (EPR)

In block 1 End Point Rate (EPR) (Figure 9.3 and 9.12) there were 99 transects in negative rate movement (erosion) and 406 transects in positive rate movement (accretion) where highest negative rate movement was -36.11 m/yr and lowest negative rate movement was -0.03 m/yr on the other hand highest positive rate movement was 81.17 m/yr and lowest positive rate movement was 0.06 m/yr. The average negative and positive rate movement were -5.79 m/yr and 13.15 m/yr respectively. The slope of End Point Rate is -0.0766 m/yr.

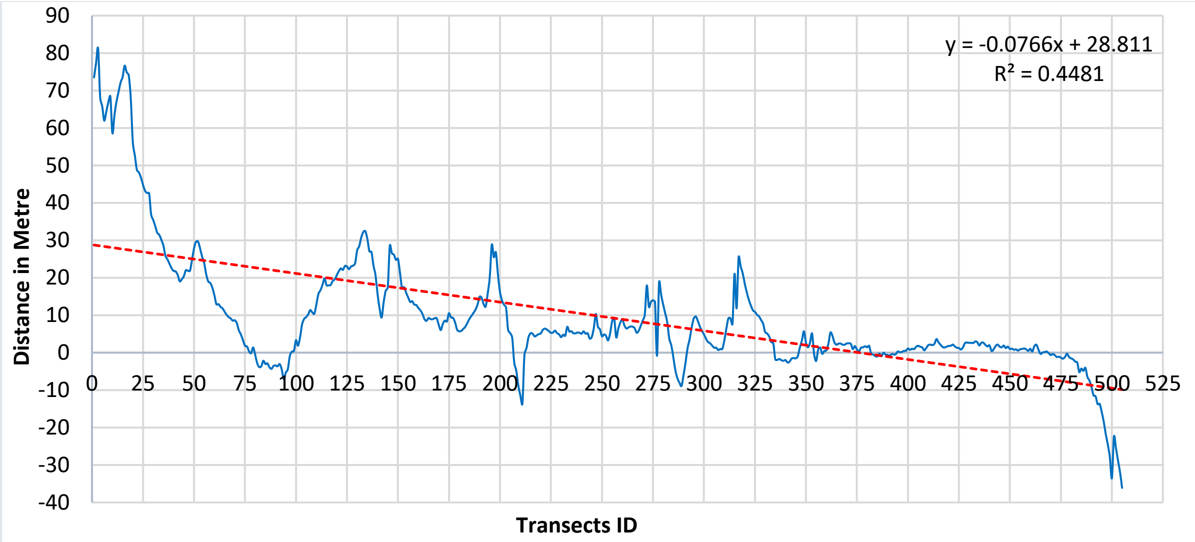

Figure 9.12: End Point Rate (EPR) Block 1 in coastal zone

In block 2 End Point Rate (EPR) (Figure 9.7 and 9.13) there were 30 transects in negative rate movement (erosion), 160 transects in positive rate movement (accretion) and 2 transects no change where highest negative rate movement was -22.79 m/yr and lowest negative rate movement was -0.01 m/yr on the other hand highest positive rate movement was 313.37 m/yr and lowest positive rate movement was 0.01 m/yr. The average negative and positive rate movement were -4.06 m/yr and 135.96 m/yr respectively. The slope of End Point Rate is 0.9995 m/yr.

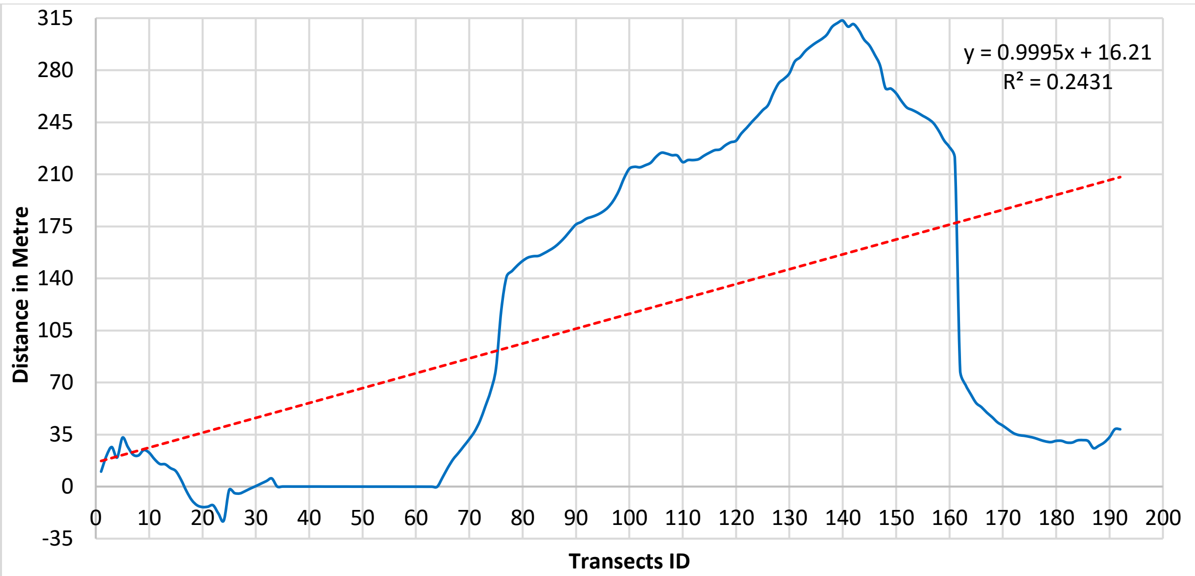

Figure 9.13: End Point Rate (EPR) Block 2 in coastal zone

In block 3 End Point Rate (EPR) (Figure 9.8 and 9.14) there were 488 transects in negative rate movement (erosion), 406 transects in positive rate movement (accretion) and 50 transects no change where highest negative rate movement was -54.30 m/yr and lowest negative rate movement was -0.01 m/yr on the other hand highest positive rate movement was 53.92 m/yr and lowest positive rate movement was 0.01 m/yr. The average negative and positive rate movement were -11.45 m/yr and 7.52 m/yr respectively. The slope of End Point Rate is -0.0111 m/yr. Though this calculation based on two dates shoreline movement by the time elapsed between the oldest and the most recent shoreline, but overall result is that there is positive rate movement (accretion) at present.

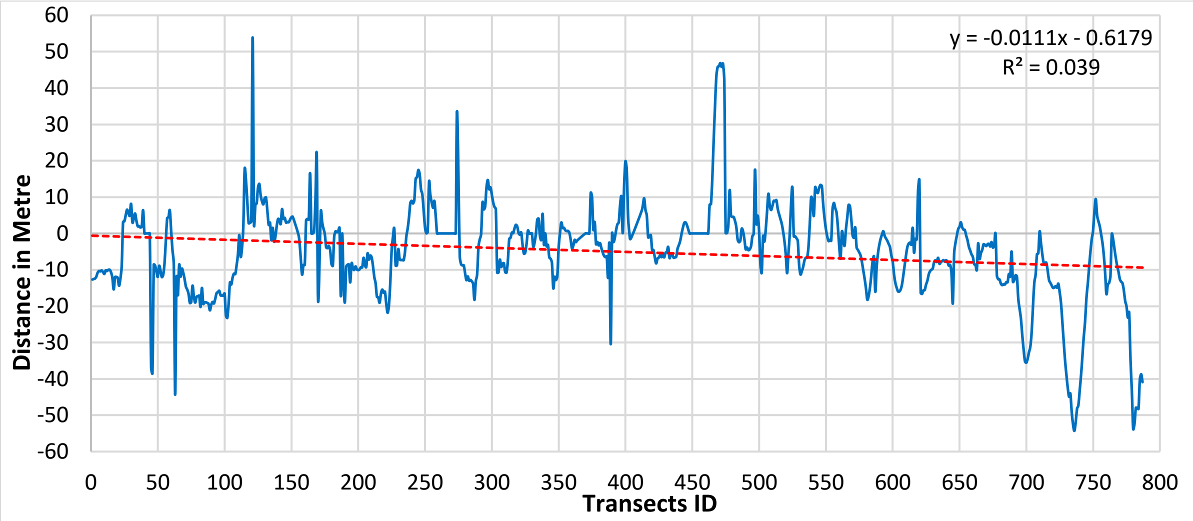

Figure 9.14: End Point Rate (EPR) Block 3 in coastal zone

9.6 Shoreline Change Envelope (SCE)

From Shoreline Change Envelope (SCE) (Figure 9.4, 9.7, 9.9 9.15, 9.16 and 9.17) from block 1, 2 and 3 was identified that the farthest transect was 9998.29, 40843.89 and 7867.75 m/yr on the other hand closest transect was 126.19, 54.22 and 0.00 m/yr the average distance was 1530.40, 16435.59 and 1526.86 m/yr and slope is -6.8345, 123.71 and 1.61.31 m/yr to the baseline respectively.

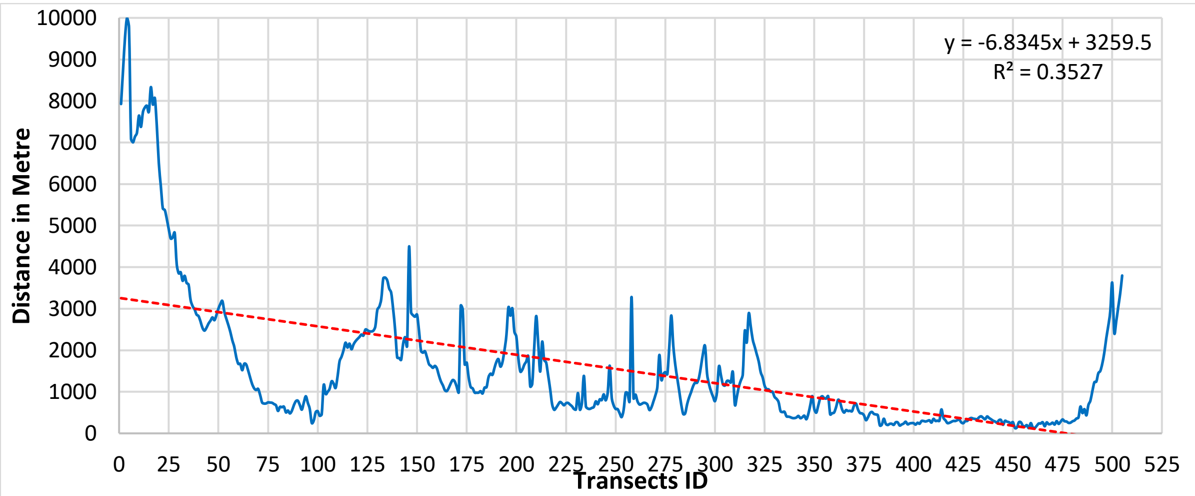

Figure 9.15: Shoreline Change Envelope (SCE) Block 1 in coastal zone

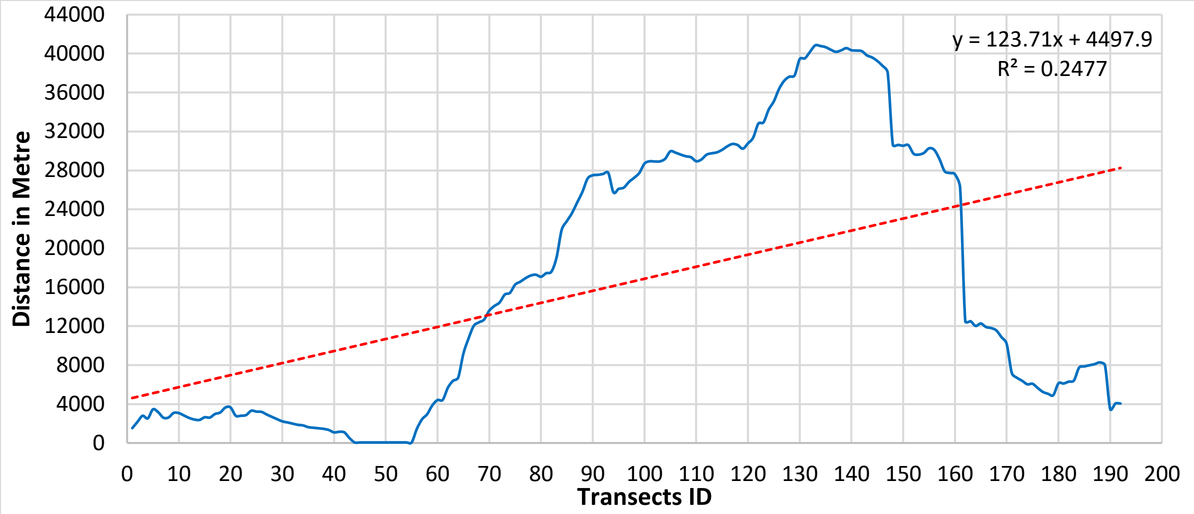

Figure 9.16: Shoreline Change Envelope (SCE) Block 2 in coastal zone

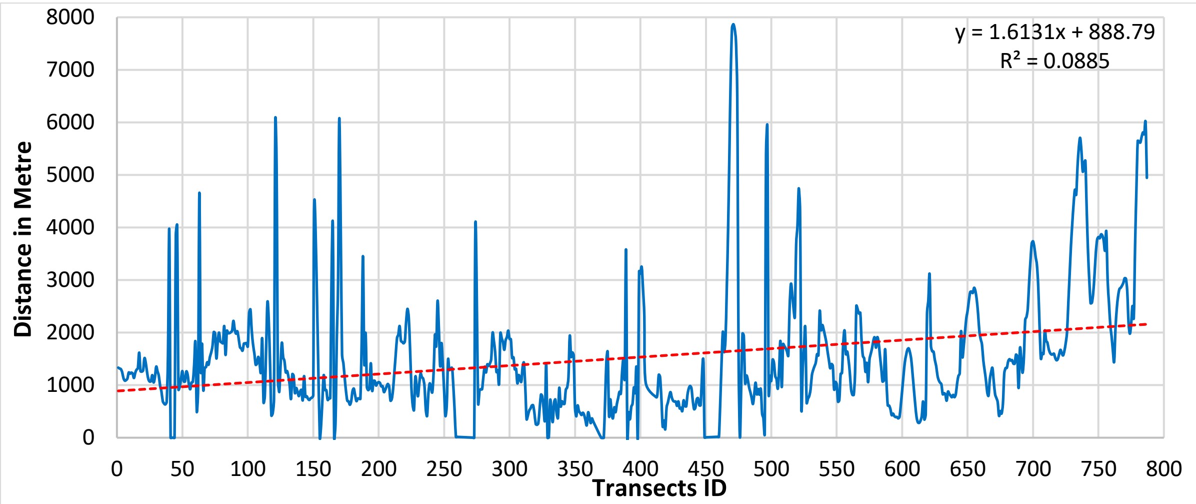

Figure 9.17: Shoreline Change Envelope (SCE) Block 3 in coastal zone

9.7 Net Shoreline Movement (NSM)

The Net Shoreline Movement (NSM) reports a distance not a rate. In block 1 total Net Shoreline Movement found 501029.81 m/yr where 99 transects in negative movement (erosion) that was -60328.95 m/yr and 406 transects in positive movement (accretion) that was 561358.76 m/yr. The highest negative movement was -3798.03 m/yr in 505 no. transect ID and lowest negative movement was -2.75 m/yr in 388 no. transect ID on the other hand highest positive movement was 8537.93 m/yr in 3 no. transect ID and lowest positive movement was 5.85 m/yr in 466 no. transect ID. The average negative and positive movement were -609.38 m/yr and 1382.66 m/yr respectively and slope is -8.0569 m/yr. In block 2 total Net Shoreline Movement found 2272922.72 m/yr where 31 transects in negative movement (erosion) that was -12783.94 m/yr and 161 transects in positive movement (accretion) was 2285706.66 m/yr. The highest negative movement was -2395.01 m/yr in 24 no. transect ID and lowest negative movement was -0.21

m/yr in 47 no. transect ID on the other hand highest positive movement was 32926.65 m/yr in 140 no. transect ID and lowest positive movement was 0.17 m/yr in 46 no. transect ID. The average negative and positive movement were -412.39 m/yr and 14196.94 m/yr respectively and slope is 105.02 m/yr. In block 3 total Net Shoreline Movement found -405577.37 m/yr where 496 transects in negative movement (erosion) that was -587298.48 m/yr and 161 transects in positive movement (accretion) was 181721.11 m/yr but 41 transects which have no movement. The highest negative movement was -5705.52 m/yr in 736 no. transect ID and lowest negative movement was -0.01 m/yr in 40 no. transect ID on the other hand highest positive movement was 5665.46 m/yr in 121 no. transect ID and lowest positive movement was 0.06 m/yr in 155 no. transect ID. The average negative and positive movement were -1184.07 m/yr and 786.67 m/yr respectively and slope is -1.171 m/yr (Figure 9.5, 9.7, 9.10, 9.18, 9.19 and 9.20).

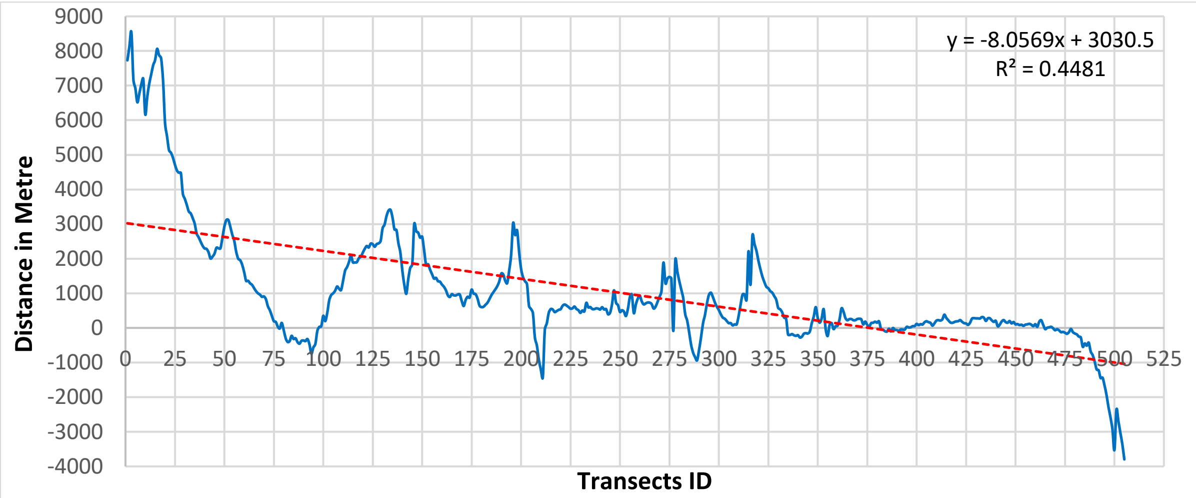

Figure 9.18: Net Shoreline Movement (NSM) Block 1 in coastal zone

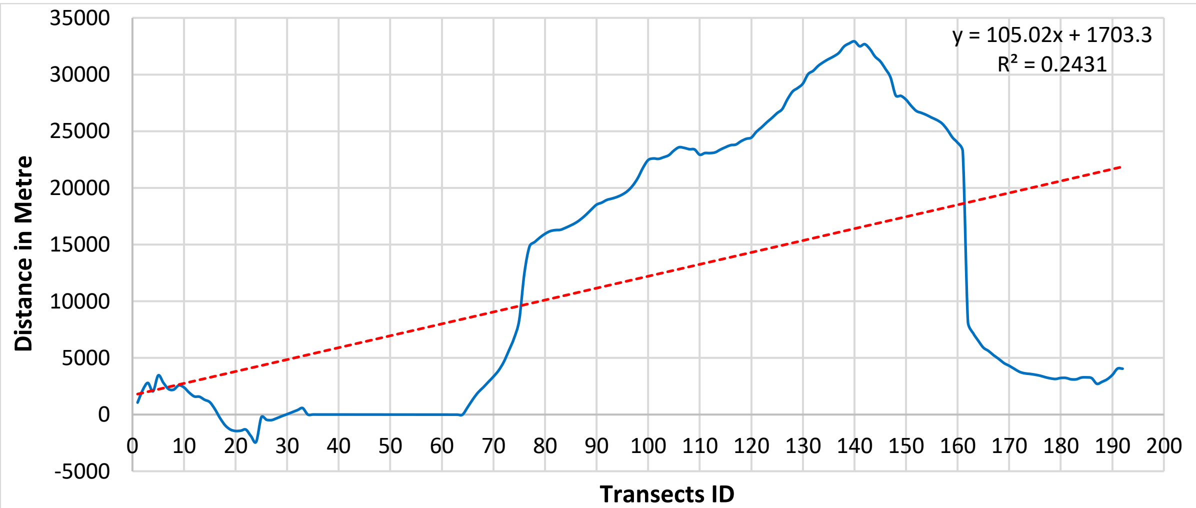

Figure 9.19: Net Shoreline Movement (NSM) Block 2 in coastal zone

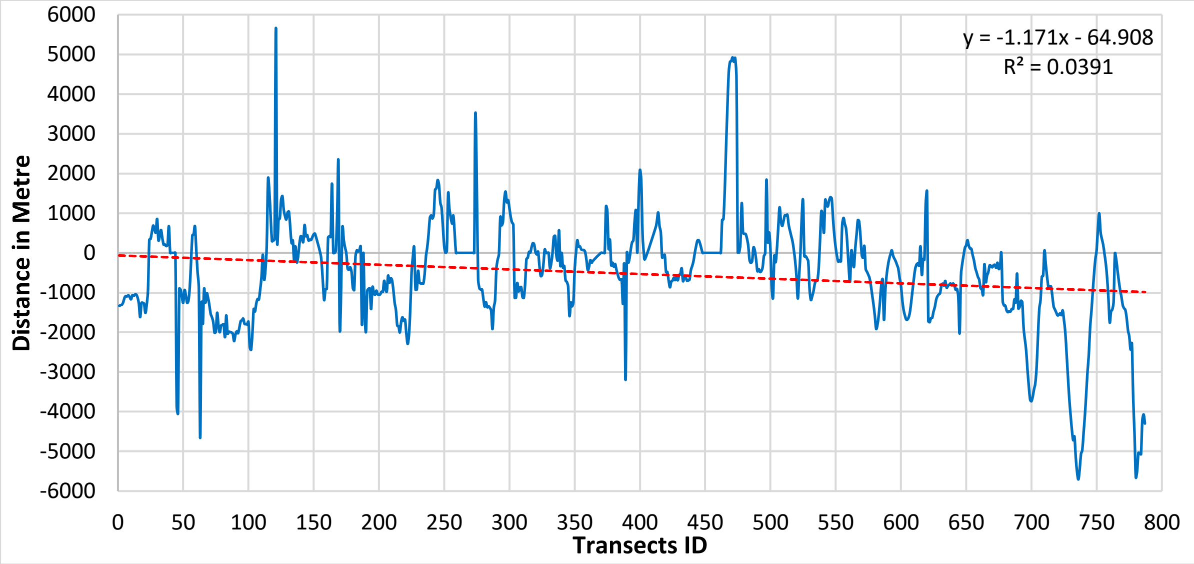

Figure 9.20: Net Shoreline Movement (NSM) Block 3 in coastal zone

9.8 Liner Regression Rate (LRR)

A linear regression rate-of-change statistic can be determined by fitting a least-squares regression line to all shoreline points for a particular transect (Figure 9.6, 9.7, 9.11 9.21, 9.22 and 9.23) and rate in Block 1, block 2 and block 3 is -0.0685, 1.5044, -0.0046 and slope is -0.0685, 1.5044 and -0.0046 m/yr respectively. The regression line is placed so that the sum of the squared residuals (determined by squaring the offset distance of each data point from the regression line and adding the squared residuals together) is minimized. The linear regression rate is the slope of the line. The method of linear regression includes these features: (1) All the data are used, regardless of changes in trend or accuracy, (2) The method is purely computational, (3) The calculation is based on accepted statistical concepts, and (4) The method is easy to employ (Dolan *et. al.*, 1991).

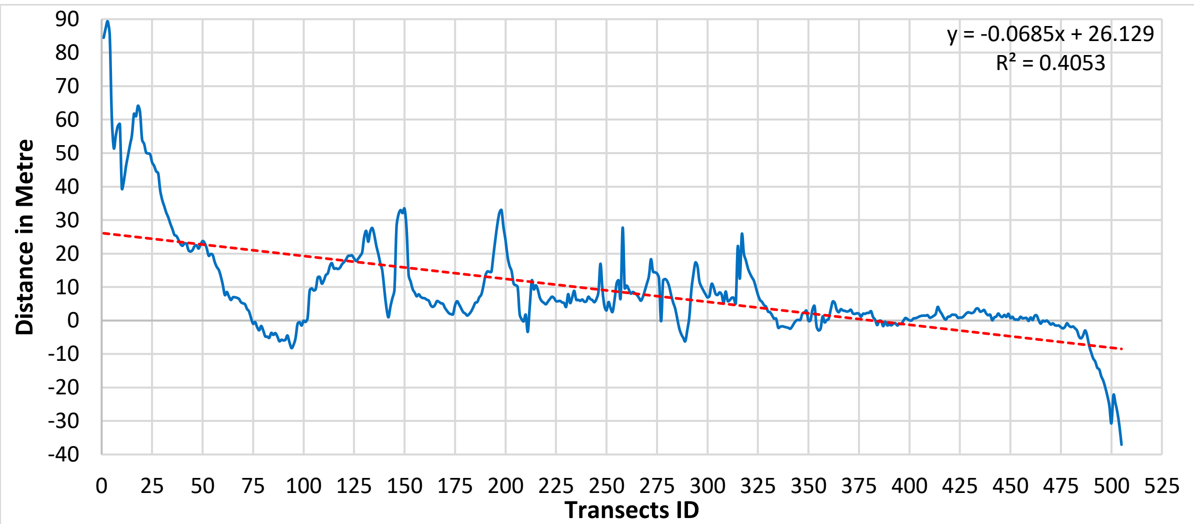

Figure 9.21: Liner Regression Rate (LRR) Block 1 in coastal zone

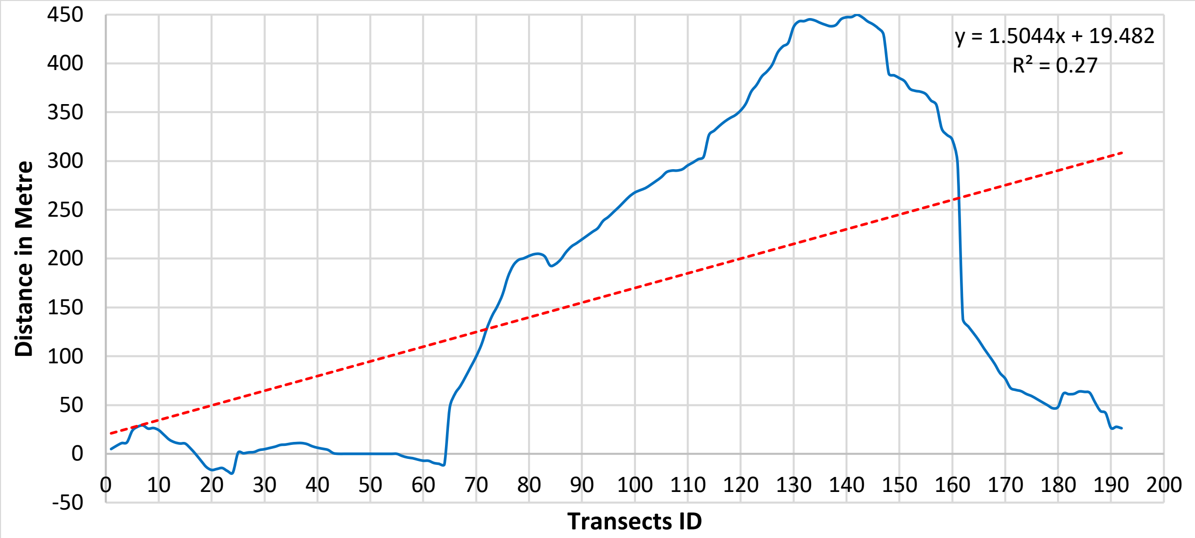

Figure 9.22: Liner Regression Rate (LRR) Block 2 in coastal zone

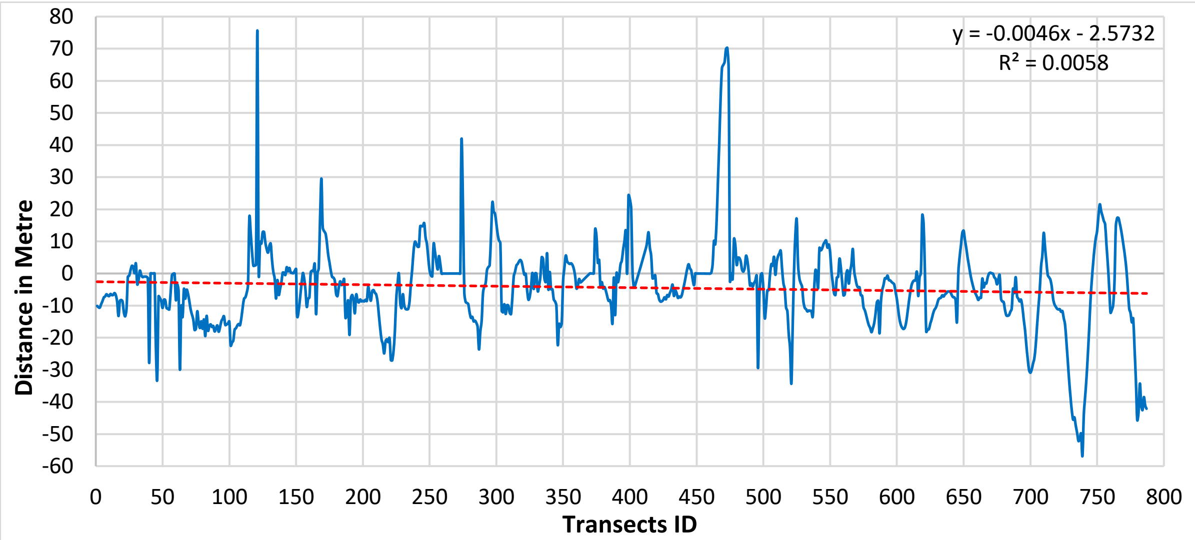

Figure 9.23: Liner Regression Rate (LRR) Block 3 in coastal zone

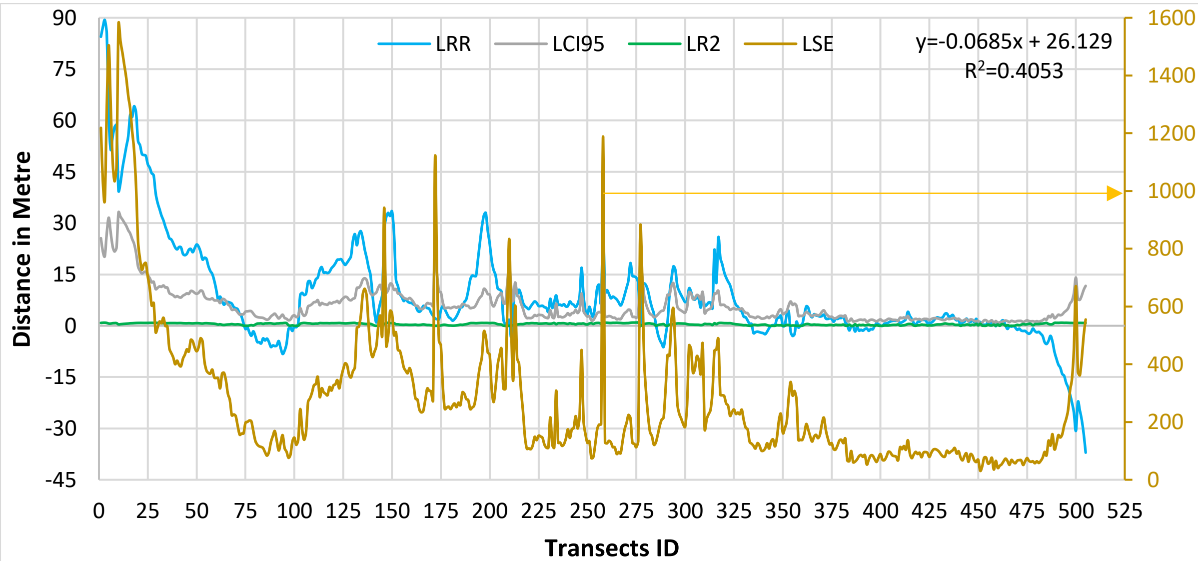

Figure 9.24: The slope of the LRR equation describing line is the rate (-0.0685 m/yr), block 1

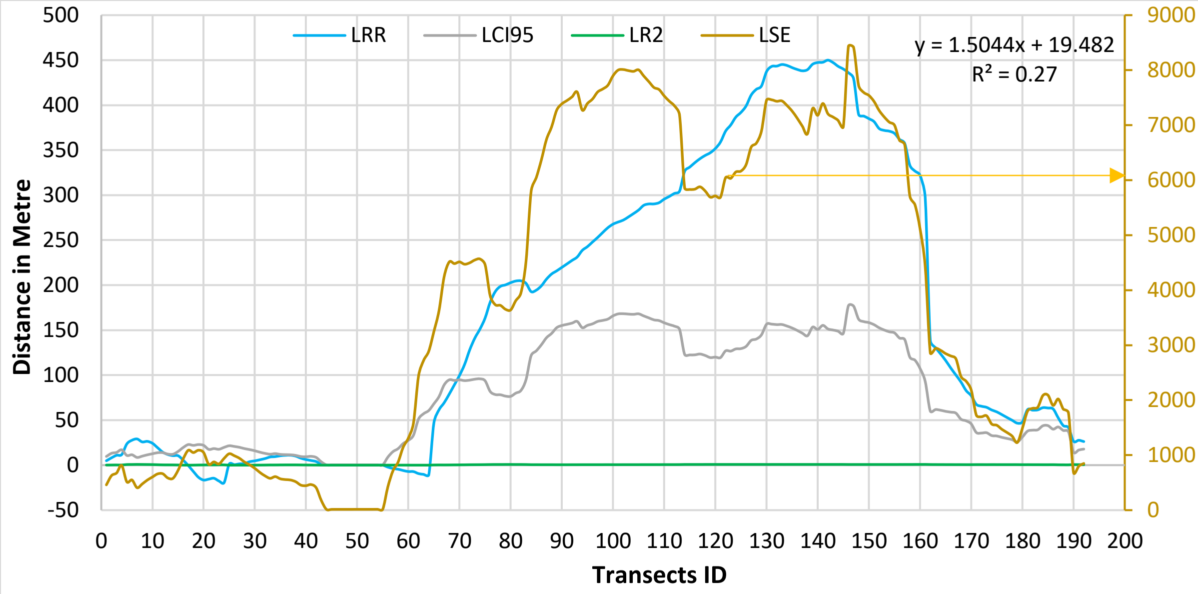

Figure 9.25: The slope of the LRR equation increasing line is the rate (1.5044 m/yr), block 2

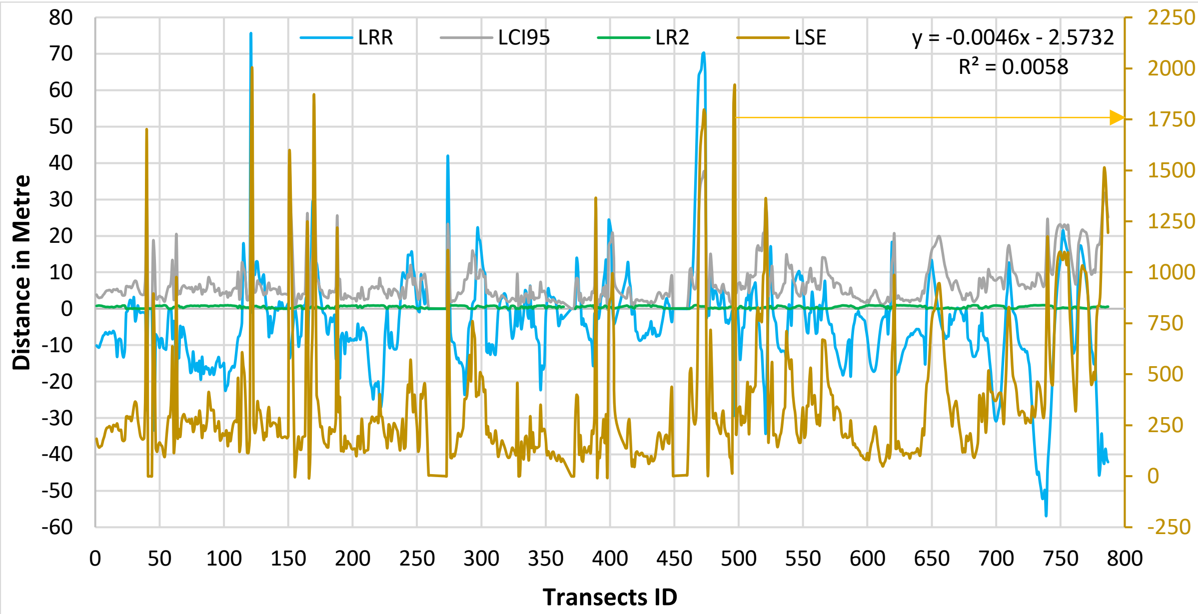

Figure 9.26: The slope of the LRR equation decreasing line is the rate (-0.0046 m/yr), block 3

However, the linear regression method is susceptible to outlier effects and also tends to underestimate the rate of change relative to other statistics, such as EPR (Dolan *et. al.*, 1991; Genz *et. al.*, 2007). In conjunction with the linear regression rate, the standard error of the estimate (LSE), the standard error of the slope with user-selected confidence interval (LCI), and the R-squared value (LR2) are reported (Figure 9.24, 9.25 and 9.2). Linear Regression Rate was determined by plotting the shoreline positions with respect to Transects and calculating the linear regression equation of block 1, block 2 and block 3 are y = - 0.0685x + 26.129, y = 1.5044x + 19.428 and y = - 0.0046x - 2.5732 respectively (Figure 9.24, 9.25 and 9.26). Here, 95% liner confidence interval and 15% shoreline uncertainty were used.

9.9 Weighted Linear Regression (WLR)

In a weighted linear regression, more reliable data are given greater emphasis or weight towards determining a best-fit line. In the computation of rate-of-change statistics for shorelines, greater emphasis is placed on data points for which the position uncertainty is smaller. The weight (*w*) is defined as a function of the variance in the uncertainty of the measurement (*e*) (Genz *et. al.*, 2007):

$w = 1 / (e^2)$

where,

e = shoreline uncertainty value

The uncertainty field of the shoreline feature class is used to calculate a weight. In conjunction with the weighted linear regression rate, the standard error of the estimate (WSE), the standard error of the slope with user-selected confidence interval (WCI), and the R-squared value (WR2) are reported (Figure 9.27, 9.28 and 9.29). Weighted Linear Regression Rate was determined by plotting the shoreline positions with respect to Transects; these data are exactly the same as in the linear regression example. The shoreline measurement points with smaller positional-uncertainty values had more influence in the regression calculation because of the weighting component in the algorithm in block 1, block 2 and block 3 are y = -0.0684x + 26.115, y = 1.5046x + 19753 and y = -0.0047x – 2.5604 respectively (Figure 9.27, 9.28 and 9.29). Here, 95% weighted liner confidence interval and 15% shoreline uncertainty were used.

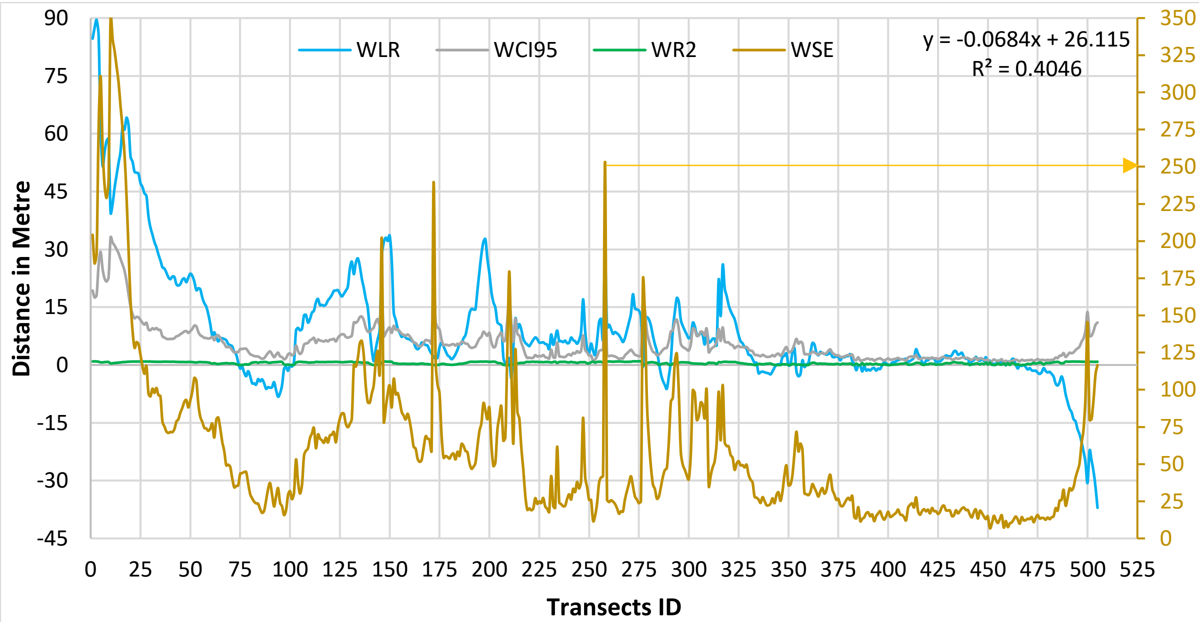

Figure 9.27: The slope of the WLR equation decreasing line is the rate (-0.0684 m/yr), block 1

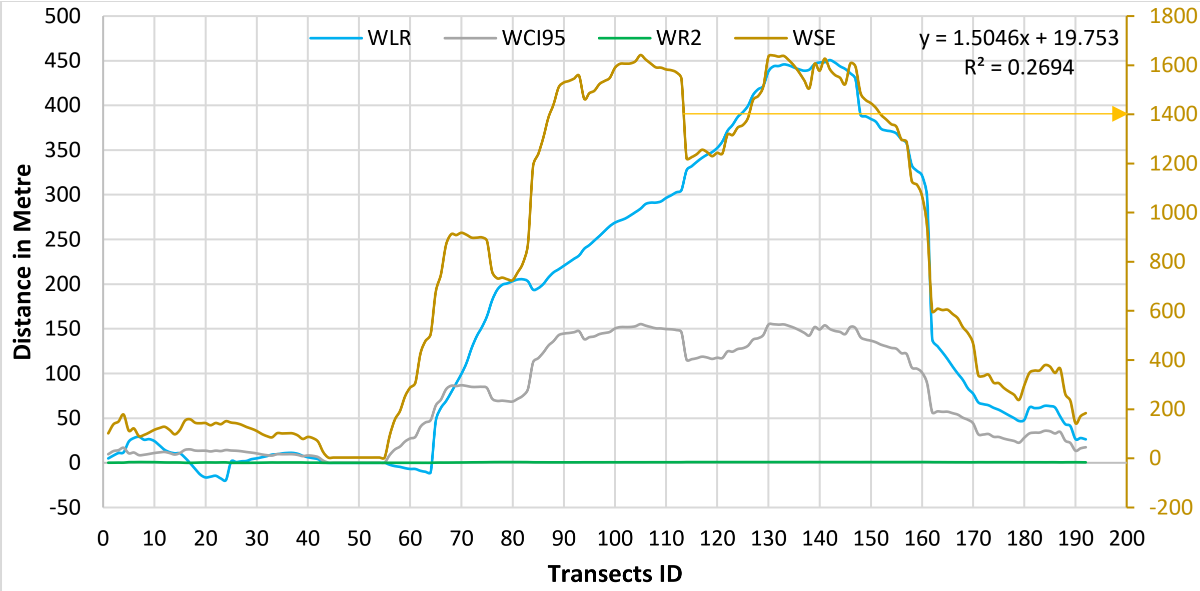

Figure 9.28: The slope of the WLR equation decreasing line is the rate (1.5045 m/yr), block 2

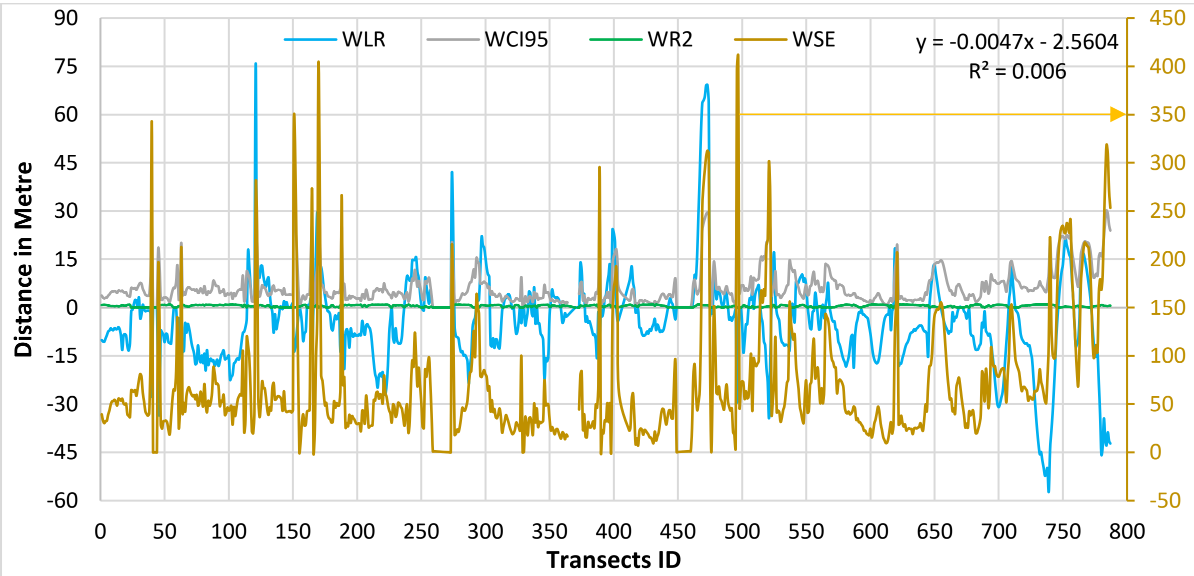

Figure 9.29: The slope of the WLR equation decreasing line is the rate (-0.0047 m/yr), block 3

9.10 Standard Error of the Estimate (LSE and WSE)

The predicted or estimated values of *y* (the distance from baseline) are computed for each shoreline point by using the values of *x* (the shoreline date) and solving the equation for the best-fit regression line:

$y = mx + b$

where,

y = predicted distance from baseline,

m = slope (the rate of change),

b = y-intercept (where the line crosses the y-axis)

The standard error of the estimate measures the accuracy of the predicted values of ***y*** by comparing them to known values from the shoreline point data. It is defined as (LSE for ordinary linear regression and WSE for weighted linear regression):

$$\frac{LSE}{\text{or}}{WSE} = \sqrt{\frac{\Sigma(y-y')^2}{n-2}}$$

Where,

y = known distance from baseline for a shoreline data point

y′ = predicted value based on the equation of the best-fit regression line

n^{-2} = number of degrees of freedom

The total number of shoreline points (*n*) along the DSAS transect is subtracted by 2 because 2 of the parameters in the regression line are being estimated (the slope and the intercept). The predicted *y*-values are subtracted from the known *y*-values to compute the residuals (*y*-*y′*). The residual is squared, and then the squared residuals (for each shoreline point) are added (along the DSAS transect) to get the sum of the squares of the residuals (which is the numerator in the equation above). This sum is divided by the number of degrees of freedom, and then the square root of the quotient is taken to compute the standard error of the estimate. The standard error of the estimate assesses the accuracy of the best-fit regression line in predicting the position of a shoreline for a given point in time. The equation describing the best-fit regression line is used to predict values *(y)* at given dates *(x)*. The residuals (actual values of *y* minus predicted values of *y*) are used to compute the standard error of the estimate (LSE) in block 1, block 2 and block 3 (Figure 9.29, 9.30 and 9.31).

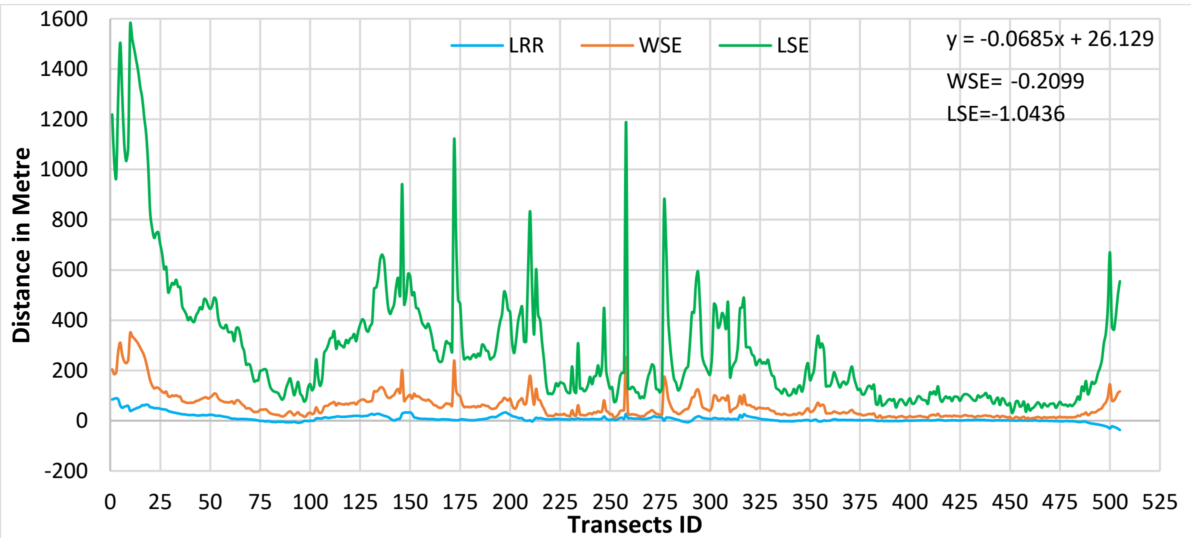

Figure 9.30: The standard error evaluates the accuracy of the best-fit regression line in predicting the position of a shoreline for a specific date, block 1

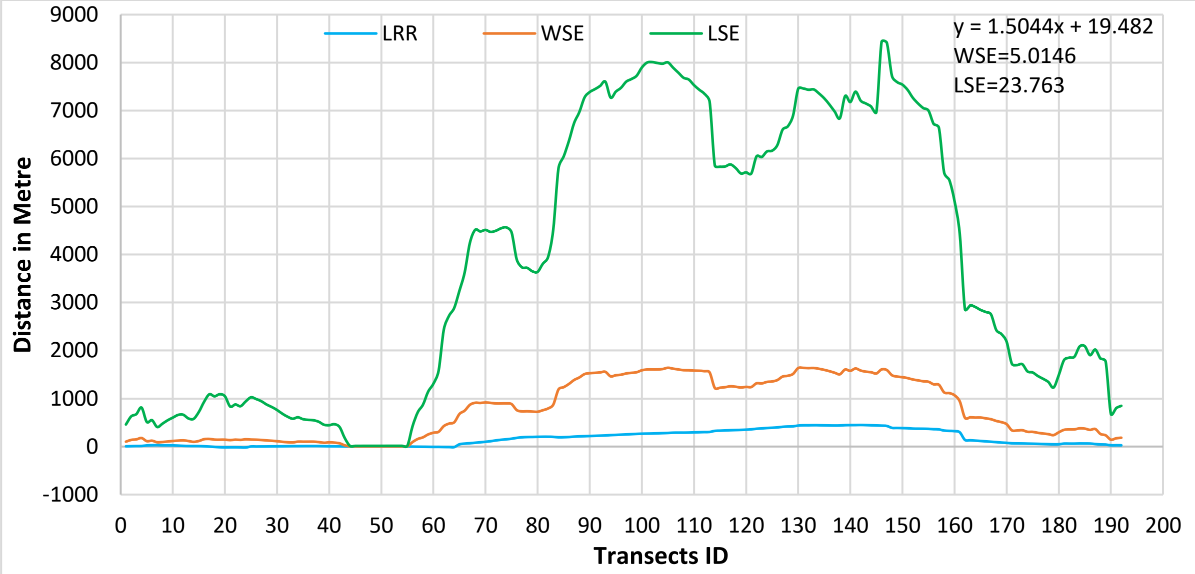

Figure 9.31: The standard error evaluates the accuracy of the best-fit regression line in predicting the position of a shoreline for a specific date, block 2

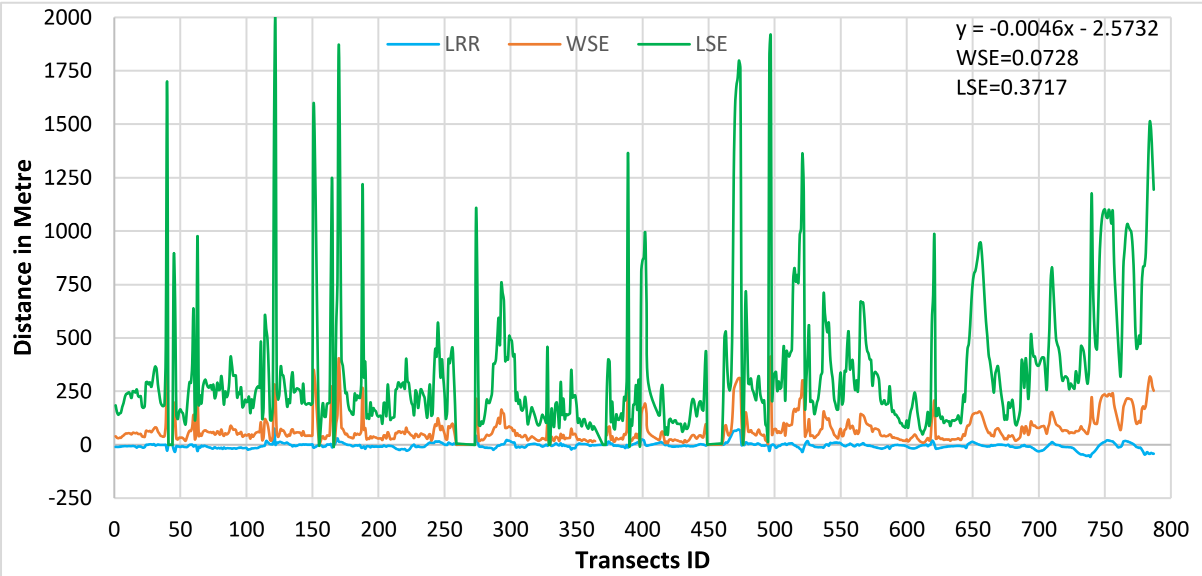

Figure 9.32: The standard error evaluates the accuracy of the best-fit regression line in predicting the position of a shoreline for a specific date, block 3

Overall conditions in coastal zone is positive change from 1910s to 2015. All the figure and table describe about the positive change but here noticeable matter is that only block 2 mainly in Meghna mouth to Feni river is increasing. Block 1 and 3, Moheskhali island, Sandwip Teknaf, Bhola island and Sundarbans have also decreasing its area. Meghan estuary is so much dynamic area where land or island come up or submerge is a routine work. But new *char* land or island come up forward and huge siltation and deposition create a possibility to new land form. May be near future we will be acquire a vast land or island area in Bay of Bengal.

9.11 Coastal Dynamics in Bangladesh

Shoreline changes due to sediment shifting are known as morpho-dynamics (Schwartz, 2006). Coastal zones are the most complex systems in the world with a large number of both living and non-living organisms (Aedla *et. al.,* 2015). Climate change and sea-level rising are the current issue in all over the world, especially in Bangladesh which is the worst affected and is facing early impacts of climate change (Sikder, 2010). Bangladesh is at extreme risk of floods, tropical cyclones, sea level rise and drought, all of which could bound millions of people to migrate (IPCC, 2014). A report by UN scientists has projected that rising sea levels will inundate 17% of Bangladesh by 2050, making about 30 million people homeless (Dummett, 2008). During years of severe flooding in 1987, 1988 and 1998 the country was transformed by intermittent inland seas that occupied as much as 60% of its land surface (Werle *et. al.*, 2000).

In an extreme-case scenario, Bangladesh could lose almost 25 percent of its 1989 land area by around 2100 (Alam and Uddin, 2013). According to the vulnerability index (Islam *et. al.,* 2015), about 57 km of the entire coast is under very high-risk and another more than 75 km is under high risk, about 67 km shoreline is at moderate risk and 63 km shoreline is at low risk. The most vulnerable coastal regions are found mainly along the western coast of *Char* Fasson and northern and southwestern coast of Bhola Sadar of Bhola Island (Islam *et. al.*, 2015). Islands in the Meghna estuary were especially dynamic; Hatiya Island accreted along some of its shoreline by 50 km between 1989 and 2009, but has lost 65 km^2 through erosion elsewhere, resulting in the island is moving southward (Sarwar and Woodroffe, 2013). The areal extent of Urir *Char* Island gets larger during the monsoon compared to the post monsoon and winter which is expanding at a very high rate of about 3.4 km^2 per year (Taguchi *et. al.*, 2013). The Sandwip Island has gained 25 km^2 and lost about 64 km^2 through 1980-2014-time period and the net shoreline has shifted by 3.1 km in this time period (Emran *et. al.,* 2016). Natural threats, such as erosion, water logging and increase in water and soil salinity, risks from climate change like sea-level rise, and cyclone have adversely affected the morphology of coastal zone and reduced the pace of social, economic and infrastructure developments in this region (Shibly and Takewaka, 2012). The impacts of this rise are wide-ranging encompassing coastal biological, physical and socio-economic realms such as loss of coastal wetlands, coastal flooding, coastal erosion, salinization of water resources, destroy of usual coastline shield, alteration and loss of coastal biodiversity, decline in fishing stocks, decrease in coastal land area and the migration of human population from the coastline are just some of these example (Blankespoor *et. al.* 2014).

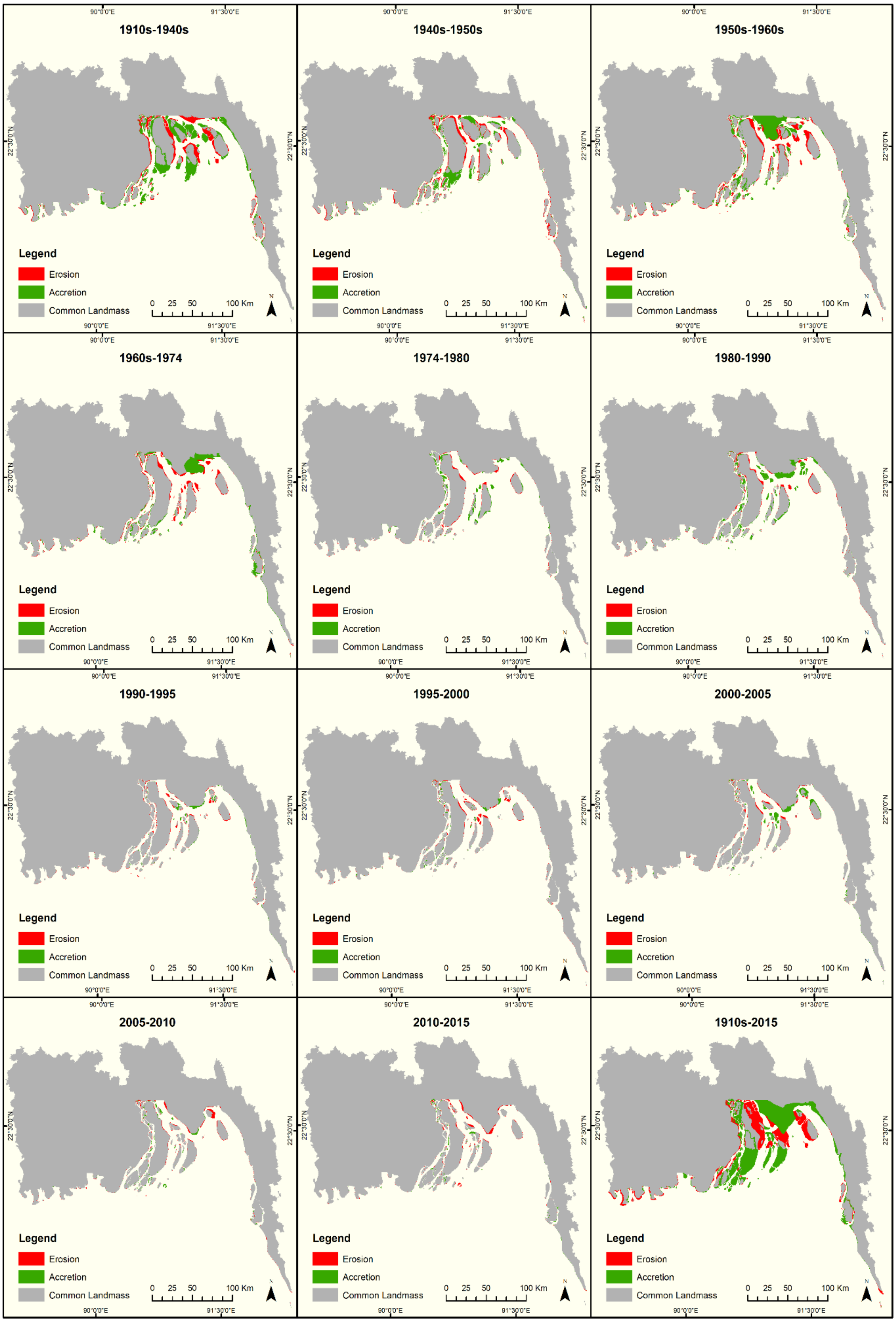

Figure 9.33: Erosion and Accretion (1910s-2015) in coastal zone of Bangladesh

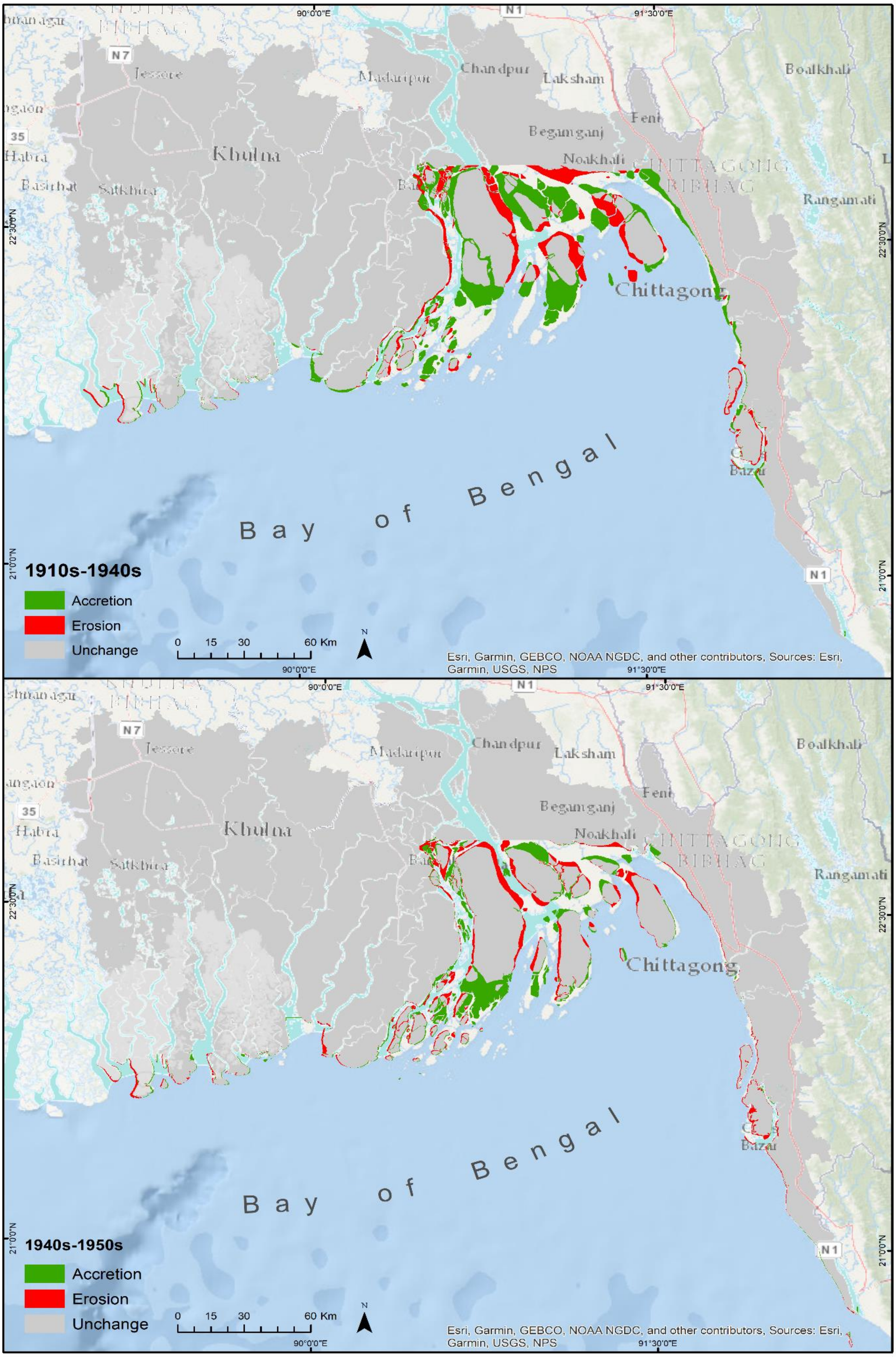

Figure 9.34: Erosion and Accretion (1910s-1940s and 1940s-1950s)

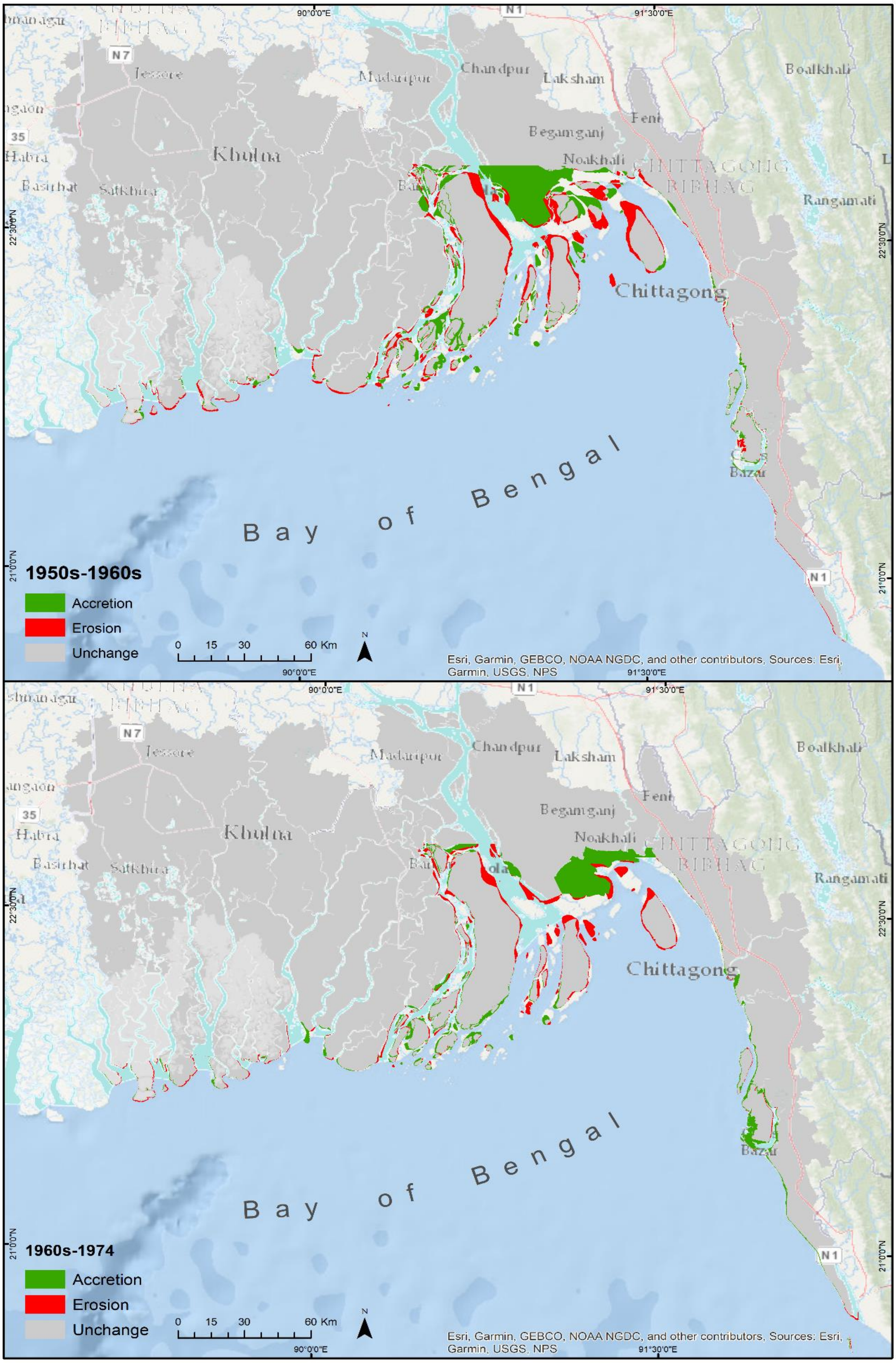

Figure 9.35: Erosion and Accretion (1950s-1960s and 1960s-1974)

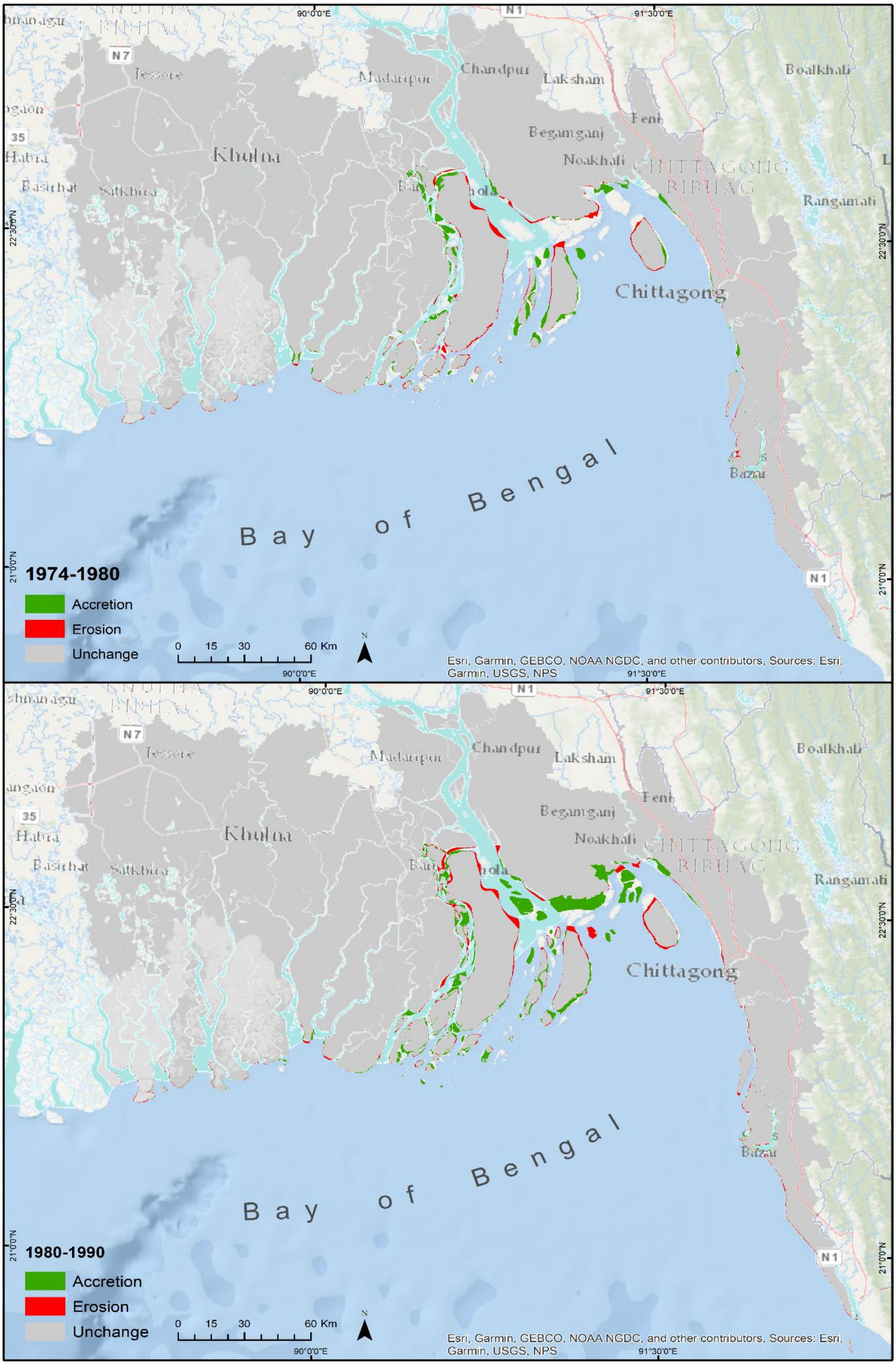

Figure 9.36: Erosion and Accretion (1974-1980 and 1980-1990)

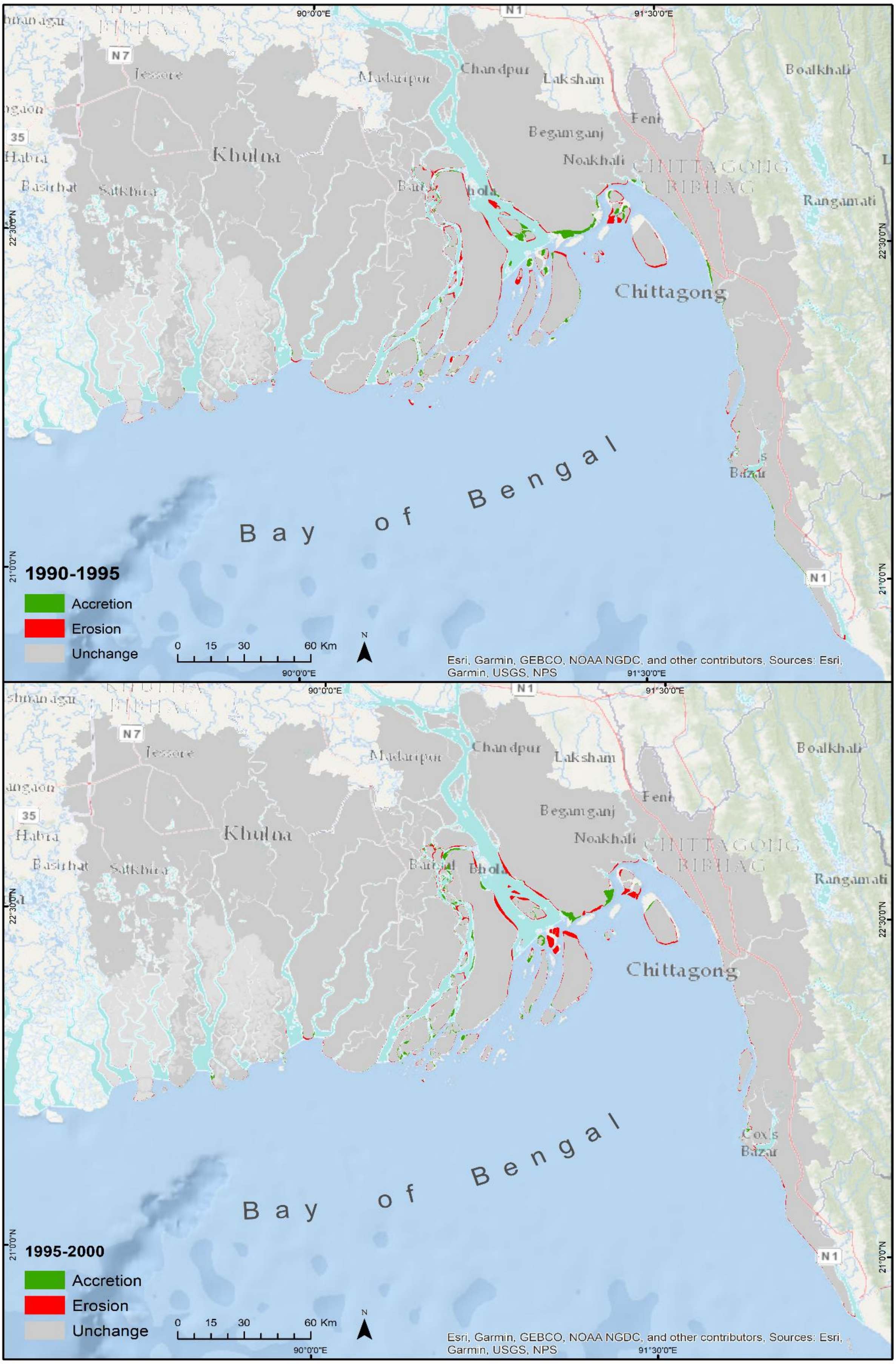

Figure 9.37: Erosion and Accretion (1990-1995 and 1995-2000)

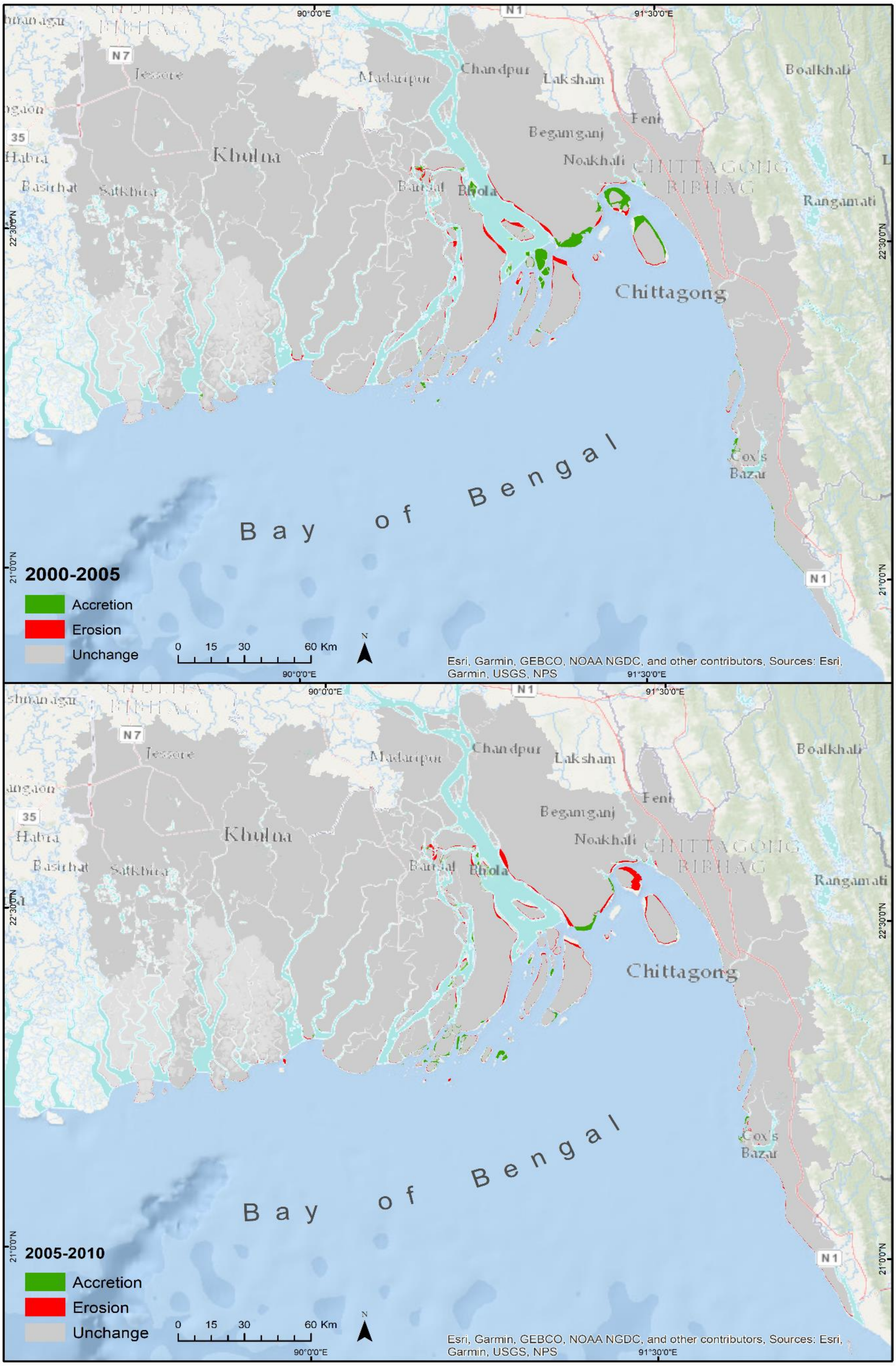

9.38: Erosion and Accretion (2000-2005 and 2005-2010)

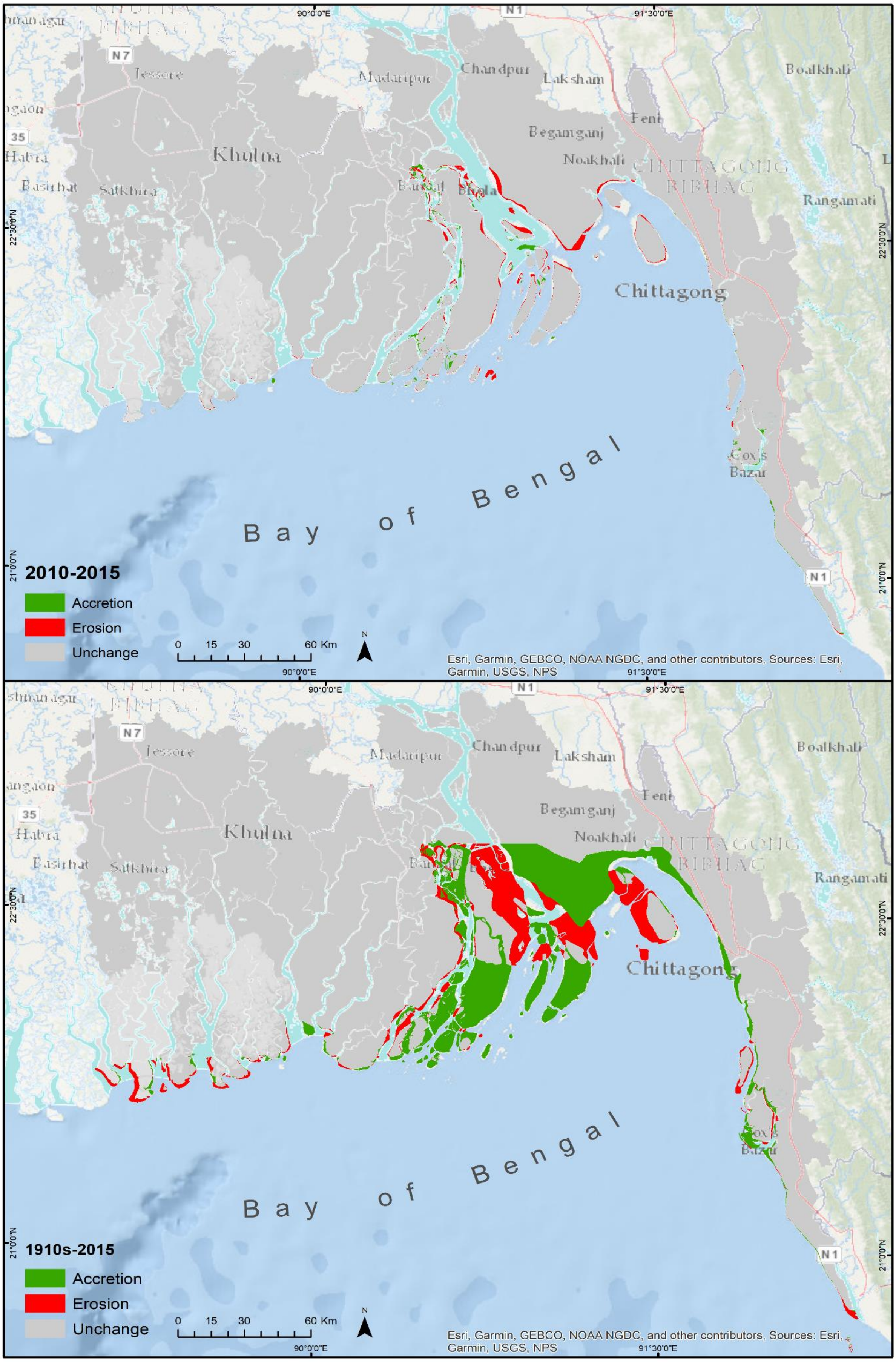

Figure 9.39: Erosion and Accretion (2010-2015 and 1910s-2015)

Table 9.2: Highest observed erosion and accretion rates along different coastal zone, block wise from 1910s-2015

Coastal Zone	Erosion (m/yr)		Accretion (m/yr)		Eroding Transects	Accreting Transects	No. Change	Total Transects
	Highest	Average	Highest	Average				
Block 1	-3798.0	-609.4	8537.9	1382.7	99	406	0	505
Block 2	-2395.0	-412.4	32926.7	14196.9	31	161	0	192
Block 3	-5705.5	-1184.1	5665.5	786.7	496	231	64	791
Total	-	-	-	-	626	798	64	1488

Based on transects intersect, block 3 was the highest eroded block and block 2 was the height accreted block compare to the others. Here, total 1488 transects is designed for calculating to measure the erosion rate per year. Five-hundred-meter interval transects equal distance in individual block carried out how much shoreline shifted every year from 1910s to 2015. In block 1, block 2 and block 3 each transects was drawn 12000, 45000 and 10000 meters in length and total transects was created 505, 192 and 791 respectively (Figure 9.4-9.11). This table describe that overall accretion much higher than erosion where total eroding transects was 626 and accreting transects was 798 though in block 3 there were 64 transects with no change.

Table 9.3: Mainland Shoreline length along different coastal blocks from 1910s to 2015

Year	Block 1 (km)	Block 2 (km)	Block 3 (km)	Total Length (km)
1910s	404.57	146.91	665.59	1217.08
1940s	434.65	137.15	691.20	1263.01
1950s	431.87	143.66	710.64	1286.17
1960s	420.04	207.94	689.19	1317.17
1974	370.81	208.24	663.21	1242.26
1980	367.49	227.57	651.30	1246.35
1990	379.36	188.70	668.86	1236.91
1995	387.75	199.14	649.42	1236.31
2000	384.68	202.53	647.60	1234.81
2005	385.40	201.33	646.13	1232.86
2010	380.45	197.35	629.74	1207.54
2015	383.12	187.44	631.72	1202.29

In the year interval, none of the shoreline length was static but dynamic its length. It cannot be said with the relation to erosion and accretion rate that if erosion and accretion rate is higher or lower then shoreline length that reduce or increase on its length that doesn't depend on erosion or accretion rather than its zigzag, straight or meandering shape. In Sundarbans and Meghna mouth shoreline measurement is a tough job for meandering as well as *Char* land which frequently come up or submerge, create another problem measuring actual shoreline. Above (Table 9.2 and 9.3) shows the same but precaution is that, it is not an alarming rate for decreasing in length. Block 1 in 1960s, block 2 in 1980, block 3 in 1950s was the height length year based on block wise and temporal date.

Table 9.4: Mainland and Island Shoreline length along coastal zone from 1910s to 2015

Year	Mainland		Island	
	Area (km^2)	Shoreline (km)	Area (km^2)	Shoreline (km)
1910s	36231.30	1217.08	3196.32	2028.67
1940s	36212.70	1263.01	4047.09	2298.44
1950s	36144.90	1286.17	4237.88	2822.99
1960s	36778.00	1317.17	3635.28	2515.72
1974	37340.60	1242.26	3238.42	1616.77
1980	37377.00	1246.35	3364.19	1816.19
1990	37529.40	1236.91	3679.63	2449.25
1995	37552.30	1236.31	3574.56	2390.83
2000	37526.70	1234.81	3472.92	2334.15
2005	37545.50	1232.86	3575.77	2497.15
2010	37488.30	1207.54	3548.47	2580.34
2015	37409.80	1202.29	3485.08	2607.87

Above (Table 9.4 and Figure 9.33-9.38) shows that mainland and island shoreline total length were acquired from 1910s to 2015. For example, 1940s mainland area decreased by 18.60 km^2 from 1910s but shoreline increased 45.93 km, inverted situation went to 1940s but 1950s area and length both were increased. 1960s to 1974 where area increased but shoreline decreased. In island same example as 2005 to 2010 and 2010 to 2015 where area decreased but shoreline increased respectively.

Table 9.5**:** Net Loss/Gain and Change in length along the shoreline of Bangladesh, 1910s to 2015

Year Range	Mainland Shoreline Net Loss/Gain (km)	% Change	Island Shoreline Net Loss/Gain (km)	% Change
1910s-1940s	45.93	3.77	269.77	13.30
1940s-1950s	23.16	1.83	524.55	22.82
1950s-1960s	31.00	2.41	-307.27	-10.88
1960s-1974	-74.91	-5.69	-898.95	-35.73
1974-1980	4.09	0.33	199.42	12.33
1980-1990	-9.44	-0.76	633.06	34.86
1990-1995	-0.60	-0.05	-58.42	-2.39
1995-2000	-1.50	-0.12	-56.68	-2.37
2000-2005	-1.95	-0.16	163.00	6.98
2005-2010	-25.32	-2.05	83.19	3.33
2010-2015	-5.25	-0.43	27.53	1.07
1910s-2015	-14.79	-1.22	579.20	28.55

Calculating net loss/gain is the sum of every couple year where every old date minus from near recent date. From 1910s to 2015 net loss/gain equal to sum of individual couple year from 1910s-1940s to 2010-2015 (Table 9.5 and Figure 9.33-9.38). Here, overall mainland shoreline and island shoreline net loss/gain were -14.79 and 579.20 km respectively. From the above table found that island shoreline bigger than mainland shoreline and mainland shoreline found negative value where island shoreline found positive value.

Table 9.6: Mainland Erosion, Accretion and Net Loss/Gain area from 1910s to 2015

Year Range	Total Area (km^2)	Unchanged (km^2)	Erosion (km^2)	Accretion (km^2)	Net Loss/Gain (km^2)
1910s-1940s	36539.46	35904.40	326.81	308.25	-18.56
1940s-1950s	36311.31	36046.20	166.46	98.65	-67.81
1950s-1960s	36940.39	35982.40	162.45	795.54	633.09
1960s-1974	37487.61	36630.90	147.03	709.68	562.65
1974-1980	37448.40	37269.20	71.40	107.80	36.40
1980-1990	37640.98	37265.40	111.63	263.95	152.32
1990-1995	37611.35	37470.40	58.98	81.97	22.99
1995-2000	37602.92	37476.10	76.22	50.60	-25.62
2000-2005	37613.87	37458.30	68.39	87.18	18.79
2005-2010	37581.84	37451.90	93.57	36.37	-57.20
2010-2015	37514.67	37383.50	104.83	26.34	-78.49
1910s-2015	37776.45	35864.60	366.65	1545.20	1178.55

Above (Table 9.6) shows that height eroded year is 1910s-1940s and it is 326.81 km^2, height accreted year is 1950s-1960s and it is 795.54 km^2 at the same time height net loss/gain year is 2010-2015 and 1950s-1960s and they are -78.49 km^2 and 633.09 km^2 respectively. Overall erosion and accretion are 366.65 km^2 and 1545.20 km^2 respectively. So, it can be said that 1910s to 2015 about 105 years in mainland area total net gain was accreted and that is 1178.55 km^2.

Table 9.7: Island Erosion, Accretion and Net Loss/Gain area from 1910s to 2015

Year Range	Total Area (km^2)	Unchanged (km^2)	Erosion (km^2)	Accretion (km^2)	Net Loss/Gain (km^2)
1910s-1940s	4773.87	2469.55	726.78	1577.54	850.76
1940s-1950s	4871.85	3413.12	633.97	824.76	190.79
1950s-1960s	4859.75	3013.41	1224.47	621.87	-602.60
1960s-1974	3952.92	2920.78	714.50	317.64	-396.86
1974-1980	3525.79	3076.81	161.61	287.37	125.76
1980-1990	3892.55	3151.28	212.91	528.36	315.45
1990-1995	3776.85	3477.35	202.29	97.21	-105.08
1995-2000	3680.78	3366.69	207.86	106.23	-101.63
2000-2005	3744.71	3303.98	168.94	271.79	102.85
2005-2010	3712.98	3411.26	164.51	137.21	-27.30
2010-2015	3650.93	3382.62	165.85	102.46	-63.39
1910s-2015	5162.27	1519.14	1677.19	1965.94	288.75

From the above (Table 9.7) shows that height eroded year is 1950s-1960s and it is 1224.47 km^2, height accreted year is 1910s-1940s and it is 1577.54 km^2 at the same time height net loss/gain year is 1950s-1960s and 1910s-1940s and they are -602.60 km^2 and 850.76 km^2 respectively. Overall erosion and accretion are 1677.19km^2 and 1965.94 km^2 respectively. So, it can be said that 1910s to 2015 about 105 years in island area total net gain was accreted and that is 288.75 km^2. Overall Bangladesh coastal zone obtain 1467.30 km^2 area in the year of 1910s to 2015. So, overall conditions from above scenario coastal zone area is accreted over time.

Chapter Ten

Correlation with Temperature and Sea Level Rise: Future Perspectives

10.1 Introduction

Global mean sea level increase is known as the sea level rise (SLR). Sea level rise is a common phenomenon nowadays. Sea level rise is usually attributed to global climate change by thermal expansion of the oceans water and melting of ice sheets and glaciers over land (Shennan, 2013). Floating ice shelves melting and icebergs at sea would raise sea levels only by about 4 cm (Noerdlinger and Brower, 2007). In global average sea level rise is not same but more or less equal in a specific location in the world. Local factors might include tectonic effects, subsidence of the land, tides, currents, storms, etc. (Fischlin *et. al.*, 2007). Present centuries is expected to continue to sea level rise. Because of long response times for parts of the climate system, it has been estimated that we are already committed to a sea level rise within the next 2000 years of approximately 2.3 meters (7.5 ft) for each degree Celsius of temperature rise (Anders *et. al.*, 2013). The International Panel on Climate Change (IPCC) Summary for Policymakers, AR5, 2014, predicts that the global mean sea level rise will continue during the 21st century, very likely at a faster rate than observed from 1971 to 2010 (IPCC, 2014). Projected rates and amounts vary one place to another. A January 2017 NOAA report suggests a range of GMSL rise of 0.3-2.5 meters possible during the 21st century (NOAA, 2017).

Hansen *et. al.* (1981), published the study Climate impact of increasing atmospheric carbon dioxide and predicted that anthropogenic carbon dioxide warming and its potential effects on climate in the 21st century could cause a sea level rise of 5 to 6 meters, from melting of the West Antarctic ice-sheet alone. In 2007 Fourth Assessment Report (IPCC 4) projected century-end sea levels using the Special Report on Emissions Scenarios (SRES) (IPCC, 2007). SRES developed emissions scenarios to project climate change impacts (Karl *et. al.*, 2009). The projections based on these scenarios are not predictions (IPCC, 2007), but reflect plausible estimates of future social and economic development (e.g., economic growth, population level) (Morita *et. al.*, 2001). The six SRES "marker" scenarios projected sea level to rise by 18 to 59 cm (7.1 to 23.2 in) (IPCC, 2007). Their projections were for the time period 2090-2099, with the increase in level relative to average sea level over the 1980-1999 period (IPCC, 2007). This estimate did not include all of the possible contributions of ice sheets. Hansen (2007), assumed an ice sheet contribution of 1 cm for the decade 2005-2015, with a potential ten-year doubling time for sea level rise, based on a nonlinear ice sheet response, which would yield 5 meters this century. Research from 2008 observed rapid declines in ice-mass balance from both Greenland and Antarctica and concluded that sea level rise by 2100 is likely to be at least twice as large as that presented by IPCC AR4, with an upper limit of about two meters (Allison *et. al.,* 2009).

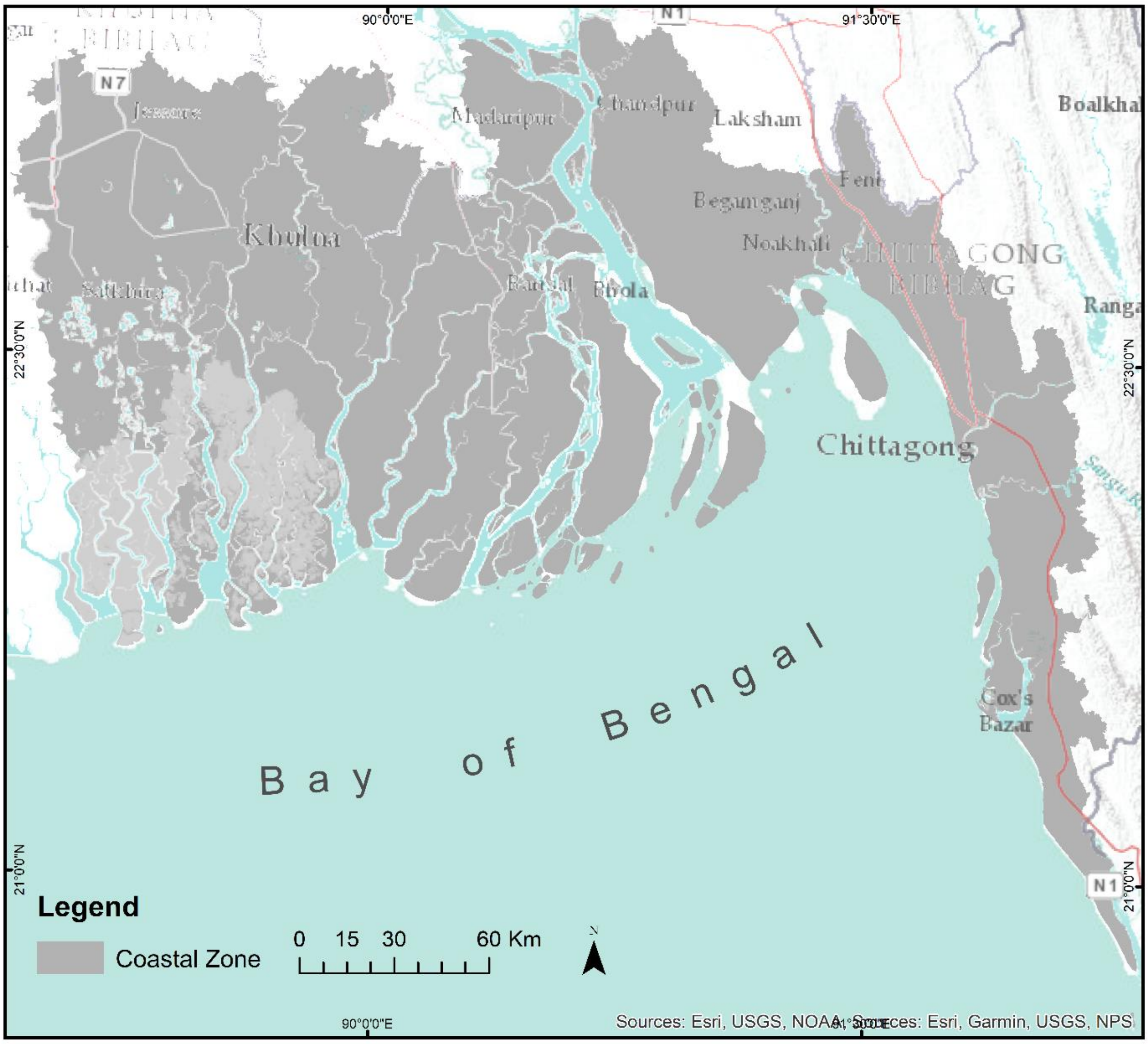

Figure 10.1: Coastal zone of Bangladesh

In IPCC Fifth Assessment Report (2013), the IPCC found that recent observations of global average sea level rise at a rate of 3.2 (2.8 to 3.6) mm per year is consistent with the sum of contributions from observed thermal ocean expansion due to rising temperatures 1.1 (0.8 to 1.4) mm per year, glacier melt 0.76 (0.39 to 1.13) mm per year, Greenland ice sheet melt 0.33 (0.25 to 0.41) mm per year, Antarctic ice sheet melt 0.27 (0.16 to 0.38) mm per year and changes to land water storage 0.38 (0.26 to 0.49) mm per year (IPCC, 2013). The report had also concluded that if emissions continue to keep up with the worst-case IPCC scenarios, global average sea level could rise by nearly 1 meter by 2100 (0.52-0.98 meters from a 1986-2005 baseline). If emissions follow the lowest emissions scenario, then global average sea level is projected to rise by between 0.28-0.6 meters by 2100 (compared to a 1986-2005 baseline) (Churchs and Clark, 2015). The Third National Climate Assessment (NCA), released May 6, 2014, projected a sea level rise of 1 to 4 feet (30-120 cm) by 2100. Decision makers who are particularly susceptible to risk may wish to use a wider range of scenarios from 8 inches to 6.6 feet (20-200 cm) by 2100 (NCA, 2014).

10.2 Global CO_2 Emission Scenario

Carbon dioxide (CO_2), greenhouse gases and human activities are accumulated in the earth's atmosphere, resulting in climate change. Rising temperature in the ocean caused thermal expansion of water it melts mass volume of ice of the polar region and the Antarctic ocean. Wigley and Raper (1987), comment that the relative contributions of thermal expansion and ice melting to this sea level rise are uncertain and estimates vary widely, from a small expansion effect through roughly equal roles for expansion and ice melting to a dominant expansion effect. Burning fossil fuels is the human activity mainly responsible for global warming and sea level rise. Cutting hill forest and deforestation is another human activity, responsible for decreasing the CO_2 sink. Miller (2004) states that, 75% of the human caused emissions of CO_2 since 1980 are due to fossil fuel burning and the remainder is the result of deforestation, agriculture, and other human changes in the land use. Hundreds of thousands of gasoline-burning motors vehicles, coal-burning power and industrial plants are the main human factor to increase CO_2 create earth's atmosphere temperature. Emissions of CO_2 from U.S. coal burning power and industrial plants alone exceeded the combined CO_2 emissions of 146 nations, which contain 75% of the world's people (Miller, 2004).

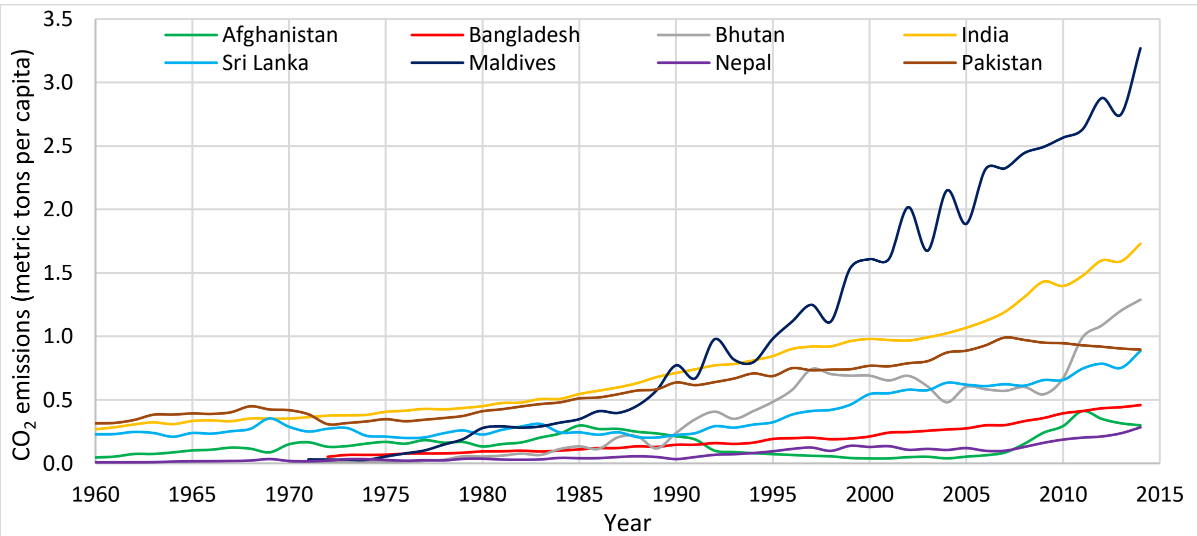

Figure 10.2: South Asia per capita Carbon dioxide (CO_2) mt emission scenario

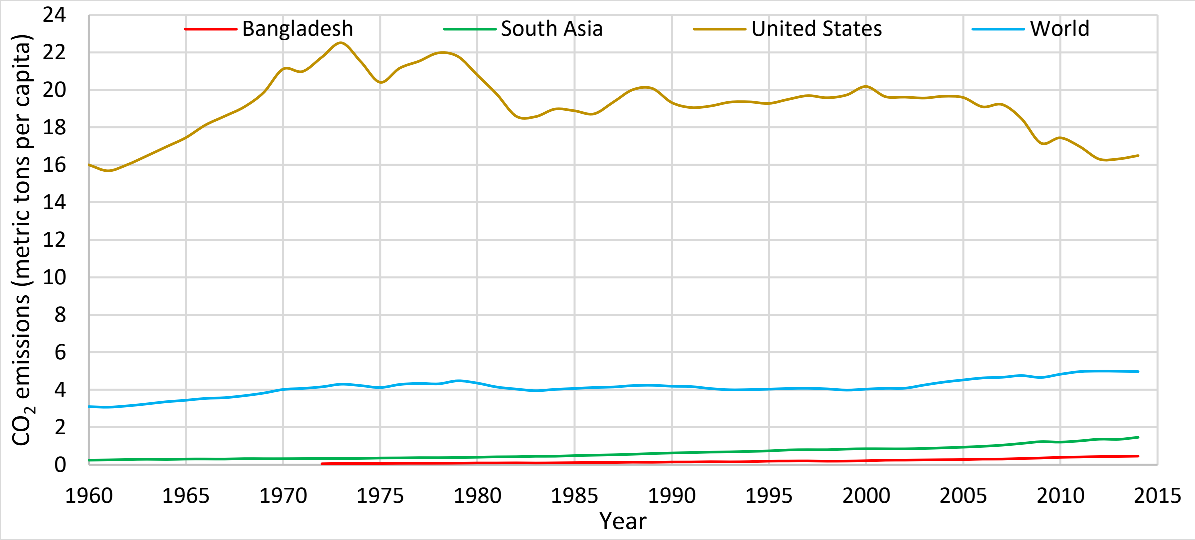

Figure 10.3: Region wise per capita Carbon dioxide (CO_2) mt emission scenario

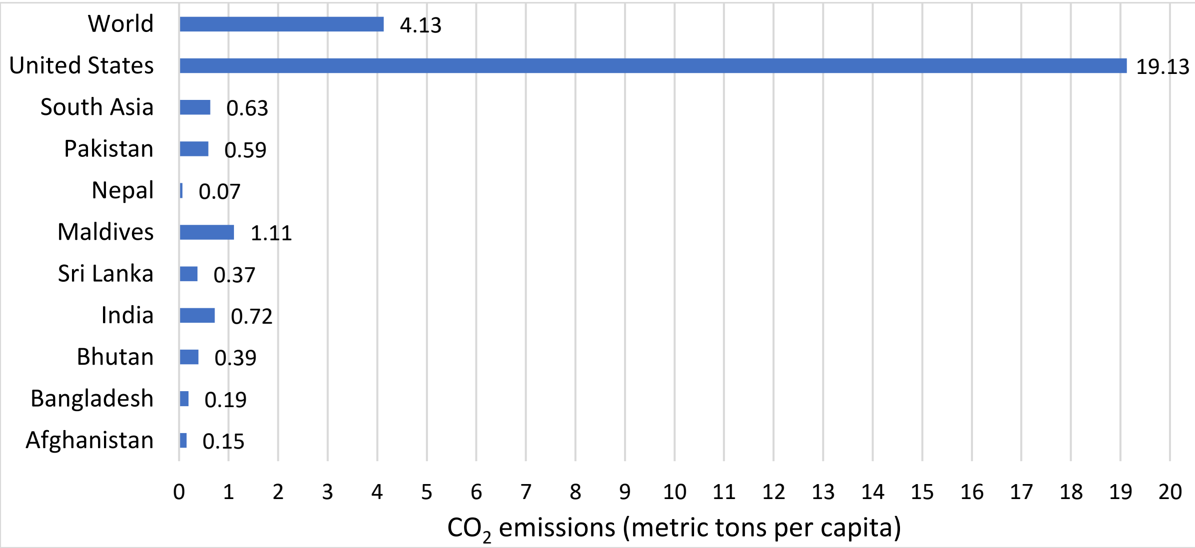

Figure 10.4: Worldwide per capita Carbon dioxide (CO_2) mt emission scenario

According to the World Bank and Carbon Dioxide Information Analysis Center (2014), per capita CO_2 emission in Bangladesh is 0.19 ton per year. But the above figures show that south Asia, United states and world average are 0.63, 19.13 and 4.13 tons respectively (Figure 10.2, 10.3 and 10.4). In south Asia, Maldives is the height CO_2 emission country where Pakistan, Nepal, Sri Lanka, India, Bhutan and Afghanistan are only 0.59, 0.07, 0.37, 0.72, 0.39 and 0.15 ton respectively. The south Asian countries, representing nearly three-quarters of the world population, are responsible for less than one-quarter of the fossil-fuel carbon emissions. The OECD countries, with about 15% of the world population, account for around 44% of the total emission. USA is solely responsible for 23% of the total yearly fossil-fuel carbon emission to the atmosphere where, Bangladesh contributes a minuscule 0.06% (Warrick *et al.*, 1993).

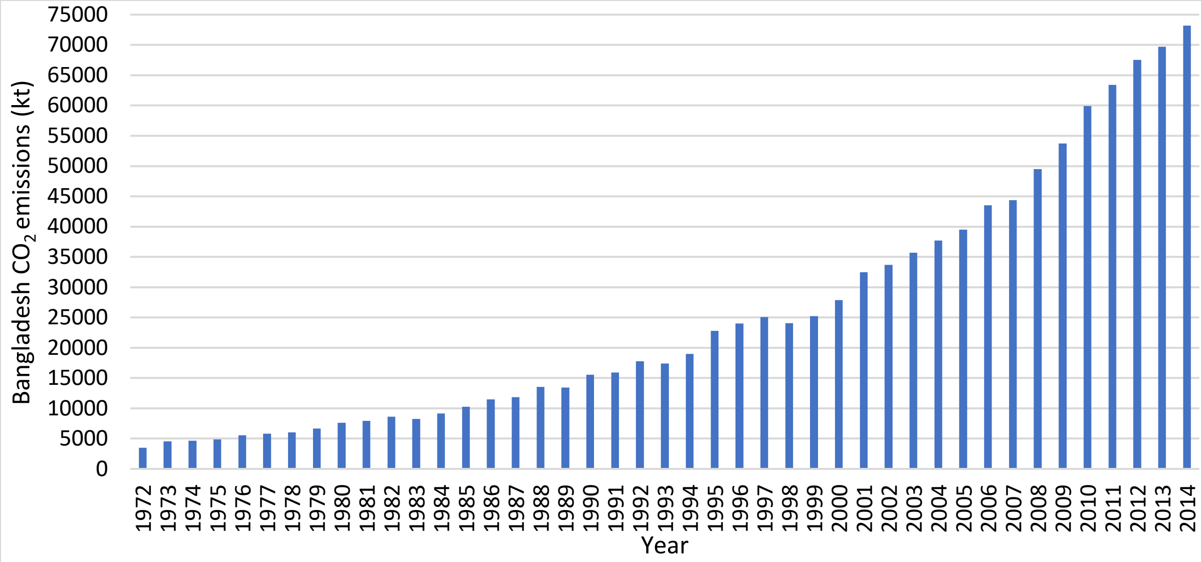

Figure 10.5: Bangladesh Carbon dioxide (CO_2) kt emission scenario

10.3 Global CO_2 Concentration and Temperature Scenario

Since the pioneering work of Callender (1938), many studies have been made on the climatic impact of an anthropogenic increase in the CO_2 concentration in the atmosphere. Earlier studies of this topic (Plass, 1956; Kondratiev and Niilisk, 1960; Kaplan, 1960; Miller, 1963) contain an evaluation of the temperature change at the earth's surface in response to an increase of the CO_2 concentration based upon the consideration of the surface radiation balance. One of the basic shortcomings of this approach is that it cannot properly incorporate the influence of the atmospheric heat balance upon the temperature change of the earth's surface. As was demonstrated by Miller (1963), this approach leads to rather unreliable results. There is good evidence that higher global temperatures will promote a rise of greenhouse gas level, implying a positive feedback which will increase the effect of anthropogenic emissions on global temperatures (Scheffer *et. al.*, 2006).

There is no evidence to measure previous 1000 years of global temperature record except supporting climate proxy record with recent 150 years in global scale. Intergovernmental Panel on Climate Change (IPCC) Fourth Assessment Report of 2007 concluded that "Average Northern Hemisphere temperatures during the second half of the 20th century were very likely higher than during any other 50-year period in the last 500 years and likely the highest in at least the past 1300 years." Some individual proxy record like as densities used in dendroclimatology and tree ring widths are the proxy calibrated record. In the 2017 edition of Germanwatch's Climate Risk Index, Bangladesh was judged to be the sixth hardest hit by climate calamities of 180 nations during the period 1996-2015.

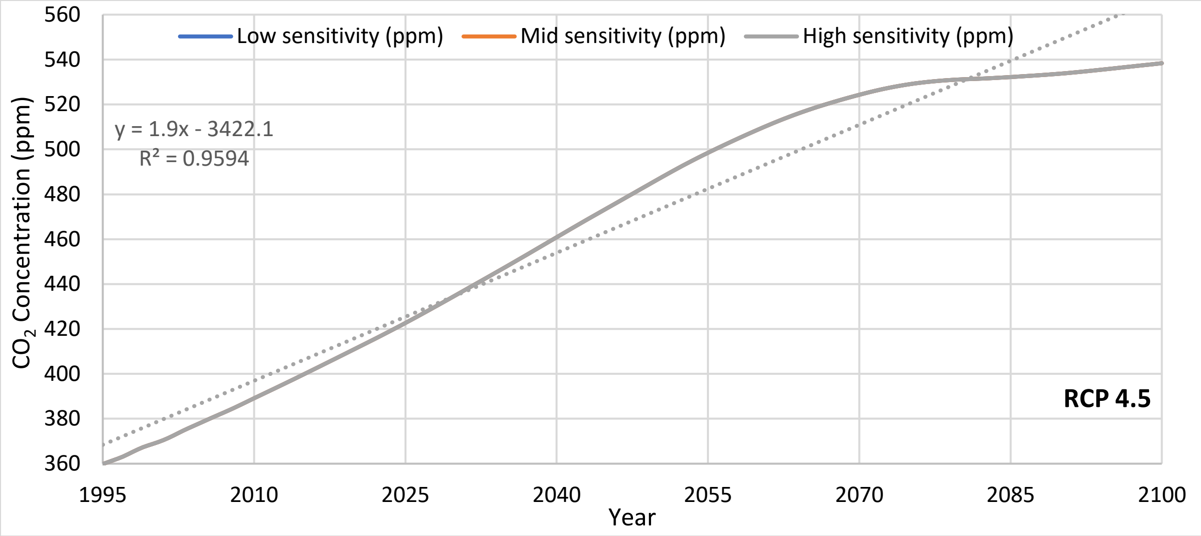

Figure 10.6: Global CO_2 concentration (ppm) low, mid and high sensitivity with RCP 4.5 scenario

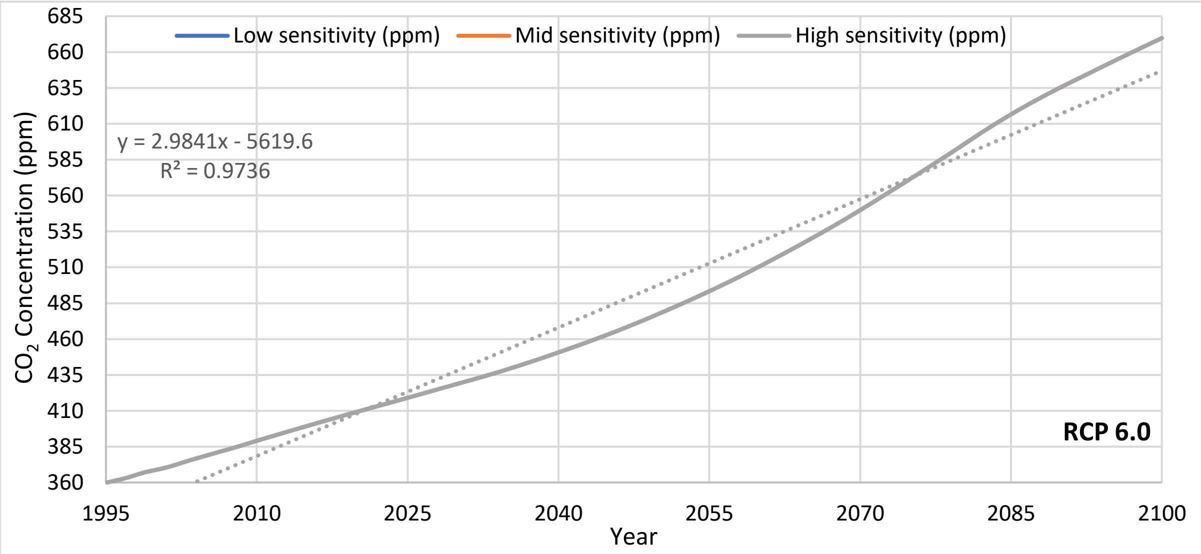

Figure 10.7: Global CO_2 concentration (ppm) low, mid and high sensitivity with RCP 6.0 scenario

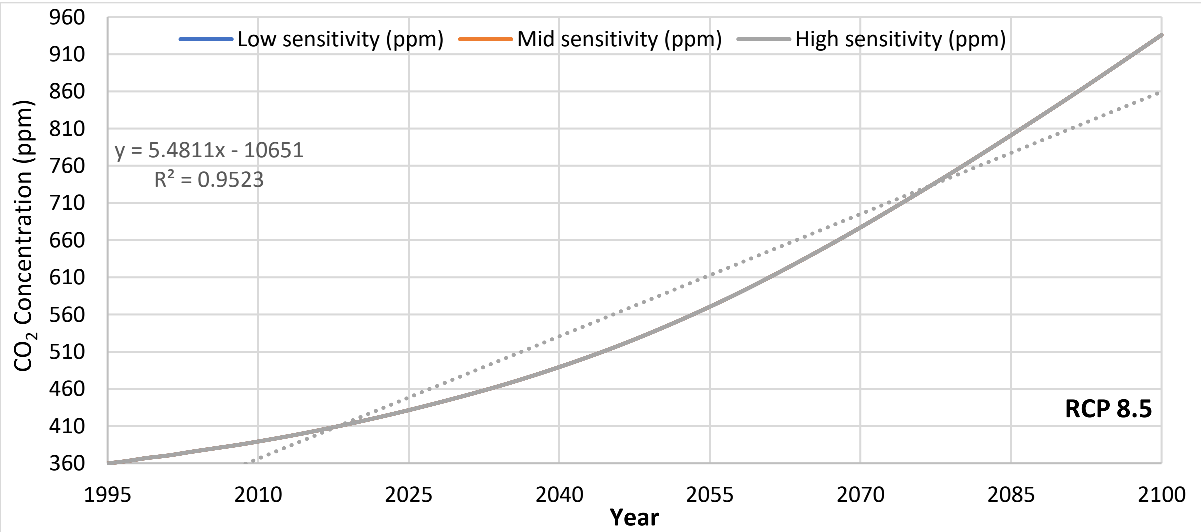

Figure 10.8: Global CO_2 concentration (ppm) low, mid and high sensitivity with RCP 8.5 scenario

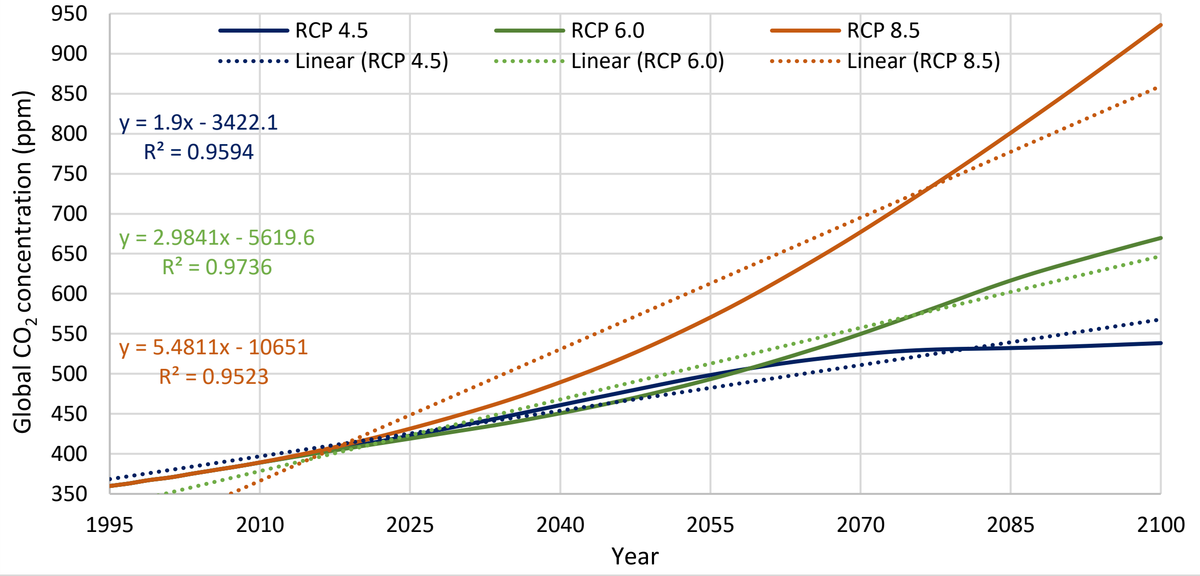

Figure 10.9: Global CO_2 concentration (ppm) (1995-2100) average RCPs

Table 10.1: Global CO_2 concentration (ppm) (1995-2100) RCP 4.5, 6.0 and 8.5

Year	RCP 4.5				RCP 6.0				RCP 8.5			
	Low	**Mid**	**High**	**Mean**	**Low**	**Mid**	**High**	**Mean**	**Low**	**Mid**	**High**	**Mean**
2025	422.7	422.7	422.7	422.7	419.0	419.0	419.0	419.0	431.5	431.5	431.5	431.5
2050	486.5	486.5	486.5	486.5	477.7	477.7	477.7	477.7	540.5	540.5	540.5	540.5
2075	529.0	529.0	529.0	529.0	571.7	571.7	571.7	571.7	717.0	717.0	717.0	717.0
2100	538.4	538.4	538.4	538.4	669.7	669.7	669.7	669.7	935.9	935.9	935.9	935.9

Above figures try to reveal that Global Circulation Model (GCM) by RCP 4.5, 6.0 and 8.5 in low, mid and high sensitivity in ppm for global CO_2 concentration. All three RCPs are the same value for low, mid and high sensitivity from baseline 1995 to 2100 (Figure 10.6, 10.7 and 10.8). The World Bank (2014), provides carbon dioxide (CO_2) data for Bangladesh from 1972 to 2014. The average value for Bangladesh during that period was 25171 kt with a minimum of 3509 kt in 1972 and a maximum of 73190 kt in 2014 (Figure 10.8). According to the World Bank (2014), Bangladesh was stand 44 in global rankings from the carbon dioxide (CO_2) emissions scenario. In 2016, CO_2 emissions per capita for Bangladesh was 0.46 metric tons (World Data Atlas, 2016). CO_2 emissions per capita of Bangladesh increased from 0.18 metric tons in 1997 to 0.46 metric tons in 2016 growing at an average annual rate of 5.17 % (World Data Atlas, 2016). In the (Figure 10.9 and Table 10.1) show that average RCP 4.5 (422.7, 486.5, 529.0 and 538.4) ppm, RCP 6.0 (419.0, 477.7, 571.7 and 669.7) ppm and RCP 8.5 (431.5, 540.5, 717.0 and 935.9) ppm on the other hand concentration increase rate RCP 4.5 (1.90) ppm, RCP 6.0 (2.98) ppm and RCP 8.5 (5.48) ppm will be rise by 2025, 2050, 2075 and 2100.

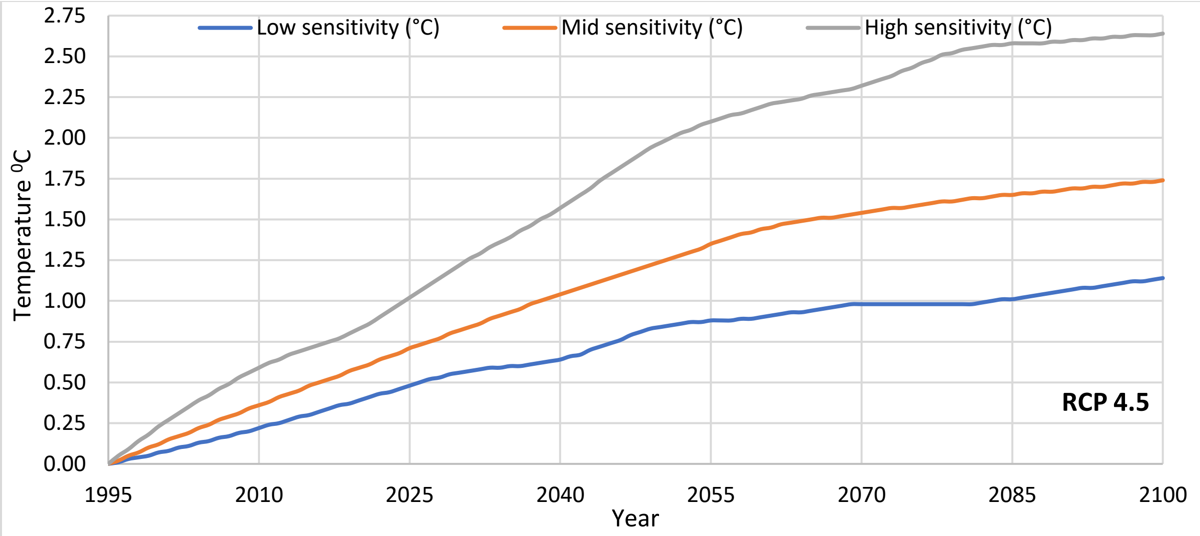

Figure 10.10: Global temperature (^{0}C) low, mid and high sensitivity with RCP 4.5 scenario

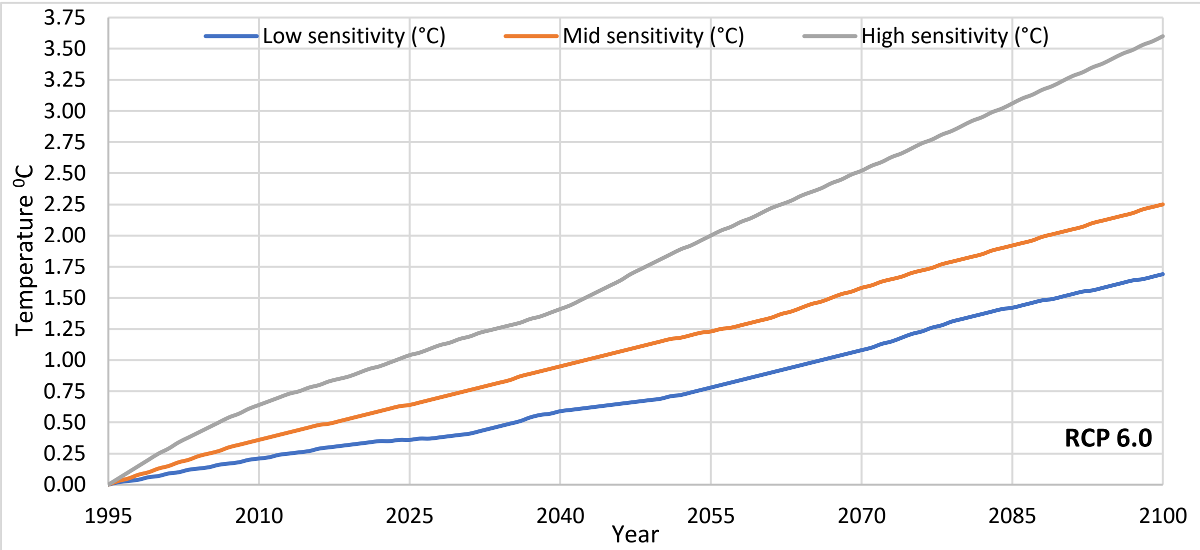

Figure 10.11: Global temperature (^{0}C) low, mid and high sensitivity with RCP 6.0 scenario

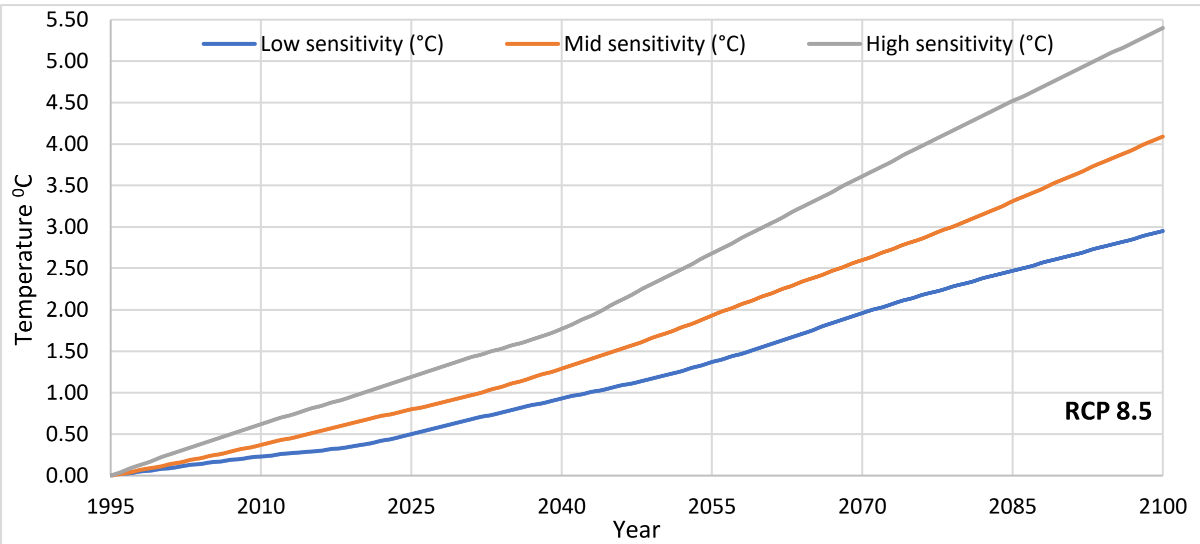

Figure 10.12: Global temperature (^{0}C) low, mid and high sensitivity with RCP 8.5 scenario

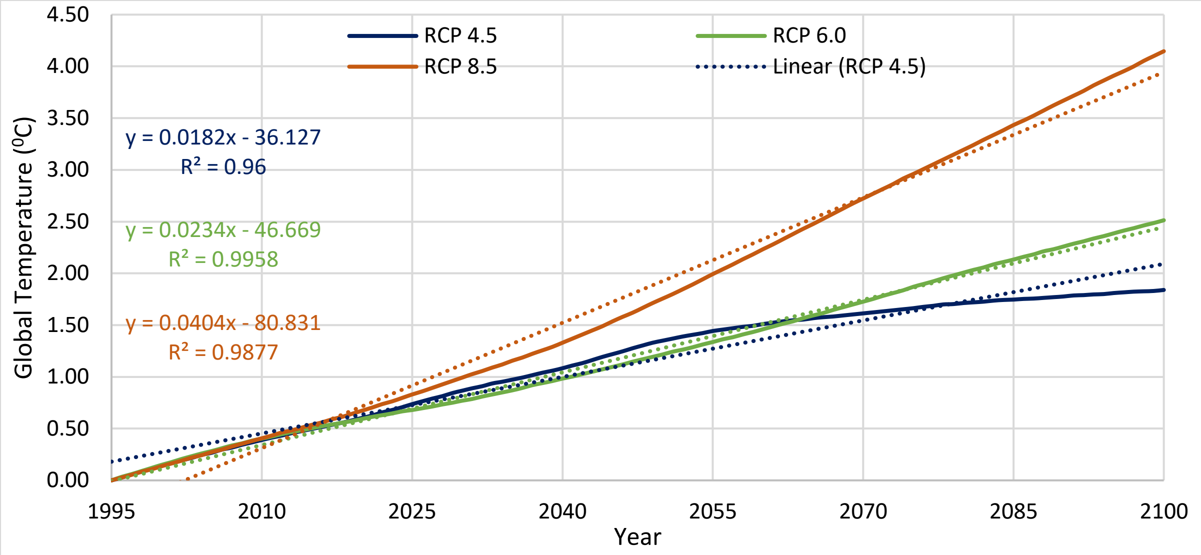

Figure 10.13: Global Temperature (^{0}C) (1995-2100) average RCPs

Table 10.2: Global Temperature (^{0}C) (1995-2100) RCP 4.5, 6.0 and 8.5

Year	RCP 4.5				RCP 6.0				RCP 8.5			
	Low	Mid	High	Mean	Low	Mid	High	Mean	Low	Mid	High	Mean
2025	0.48	0.71	0.02	0.74	0.36	0.64	1.04	0.68	0.5	0.8	1.19	0.83
2050	0.84	1.24	1.97	1.35	0.69	1.15	1.81	1.22	1.20	1.70	2.37	1.76
2075	0.98	1.58	2.43	1.66	1.21	1.70	2.70	1.87	2.14	2.82	3.92	2.96
2100	1.14	1.74	2.64	1.84	1.69	2.25	3.60	2.51	2.95	4.09	5.40	4.15

Global temperature from Global Circulation Model (GCM) in different RCPs varied, it depends on global carbon emission pattern. Different sensitivity measure what probability would be in the future, though carbon concentration is equal for low, mid and high sensitivity for each RCPs (Figure 10.6, 10.7 and 10.8). In the (Figure 10.13 and Table 10.2) show that average RCP 4.5 (0.74, 1.35, 1.66 and 1.84) ^{0}C, RCP 6.0 (0.68, 1.22, 1.87 and 2.51) ^{0}C and RCP 8.5 (0.83, 1.76, 2.96 and 4.15) ^{0}C on the other hand temperature increase rate RCP 4.5 (0.018) ^{0}C, RCP 6.0 (0.023) ^{0}C and RCP 8.5 (0.040) ^{0}C will be rise by 2025, 2050, 2075 and 2100.

10.4 Global Sea Level Rise Scenario

Intergovernmental Panel Climate Change (IPCC, 1990) estimated that a 3.3 ^{0}C rise in the global temperature under mid sensitivity by 2100 with a range of uncertainty of 2.2 to 4.9 ^{0}C. IPCC's estimation of global sea level rise was 1.0 to 2.0 mm/yr over the last century. With the high increasing rate of global temperature, sea level will rise at a faster rate of 2-6 times than the present rate (Kausher *et. al*., 1993). Wigley and Raper (1987) estimated that, the greenhouse-gas-induced thermal expansion contribution to sea-level rise between 1880 and 1985 was 2-5 cm and for the period 1985-2025 the estimate of greenhouse-gas-induced warming was estimated to 0.6-1.0 ^{0}C. The resulting concomitant oceanic thermal expansion would raise sea level by 4-8 cm. Nicholls *et. al.*, (1999) estimated that by the 2080s, sea-level rise could cause the loss of up to 22% of the world's coastal wetlands. When combined with other losses due to direct human action, up to 70% of the world's coastal wetlands could be lost by the 2080s. IPCC estimated that sea level rise would be 66 cm under mid sensitivity by 2100 with a range of uncertainty of 13 to 110 cm (Table 10.34).

Table 10.3: Global Worming (GW) and Sea Level Rise scenario

Model Assumption	**GW Scenario by year (^{0}C)**				**SLR Scenario by year (cm)**			
	2010	**2030**	**2050**	**2100**	**2010**	**2030**	**2050**	**2100**
Low	0.3	0.7	1.2	2.2	4	8	15	31
Mid	0.5	1.1	1.7	3.3	8	18	30	66
High	0.7	1.5	2.5	4.9	13	29	48	110
Source	Bretherton et. al., 1990; Cited in Warrick et. al., 1993				Warrick and Oerlemans, 1990; Cited in Warrick et. al., 1993			

Nowadays there are two important approaches to projecting future sea level rise: process-based models are the most important known as computer-based simulation processes and another one is empirical statistical based models that is apply to the observed relationship between temperature forcing and the sea level height on the other hand in the past and extrapolate feature that describe its future scenario. With the large uncertainties both approaches produce a spread of results, which results generate future sea-level rise. For the enhanced understanding of the contributions to recent sea level rise, process-based models projected future sea levels which has increased confidence in the use of process-based models. The limited number of available simulations with process-based models indicate GMSL rise by 2300 to be less than 1 m for greenhouse gas concentrations that do not exceed 500 ppm CO_2 equivalent but 1-3 m for concentrations above 700 ppm CO_2-equivalent (European Environmental Agency[11]).

For measuring Global Mean Sea Level (GMSL) RCP 4.5, RCP 6.0 and RCP 8.5 used to detect low, mid and high sensitivity and generate future forecasting data (Figure 10.14, 10.15 and 10.16). All figure show that sea level rise gradually though uncertainty is a very fact. If in future world tackle or reduce CO_2 like carbon sink or carbon sequestration then temperature will be steady, bellow figures show the same with different tail. Previous study (Table 10.3) show that Low 2.2 ^{0}C Mid 3.3 ^{0}C and High4.9 ^{0}C by 2100. Comparatively RCP 8.5 provides high reflectivity (Figure 10.16) compared to RCP 4.5 and RCP 6.0.

[11] https://www.eea.europa.eu/data-and-maps/indicators/sea-level-rise-3/assessment

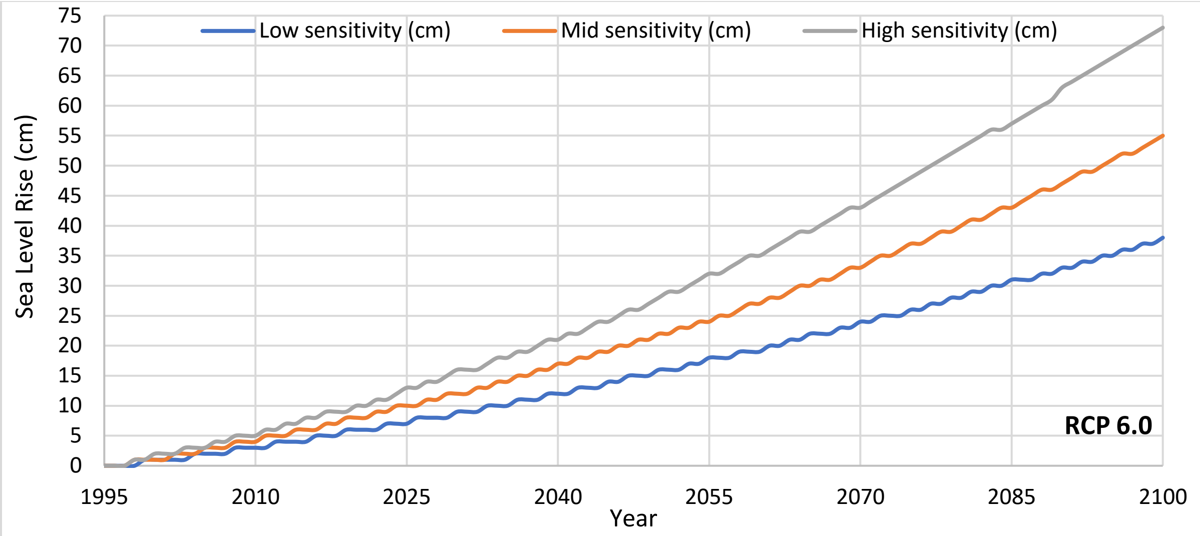

Figure 10.14: Global sea level rise (cm) low, mid and high sensitivity with RCP 6.0 scenario

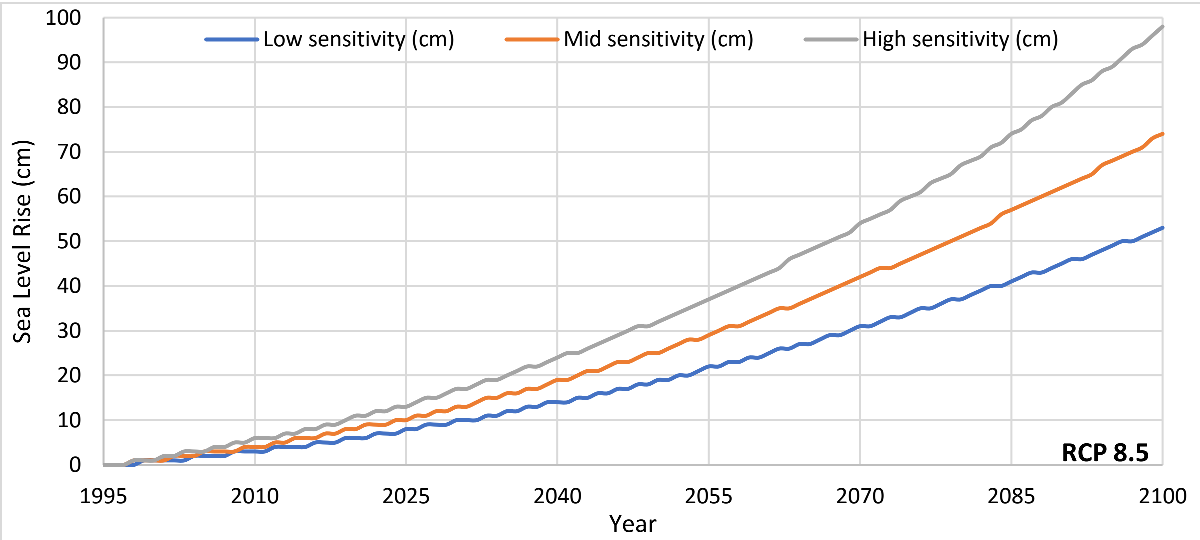

Figure 10.15: Global sea level rise (cm) low, mid and high sensitivity with RCP 8.5 scenario

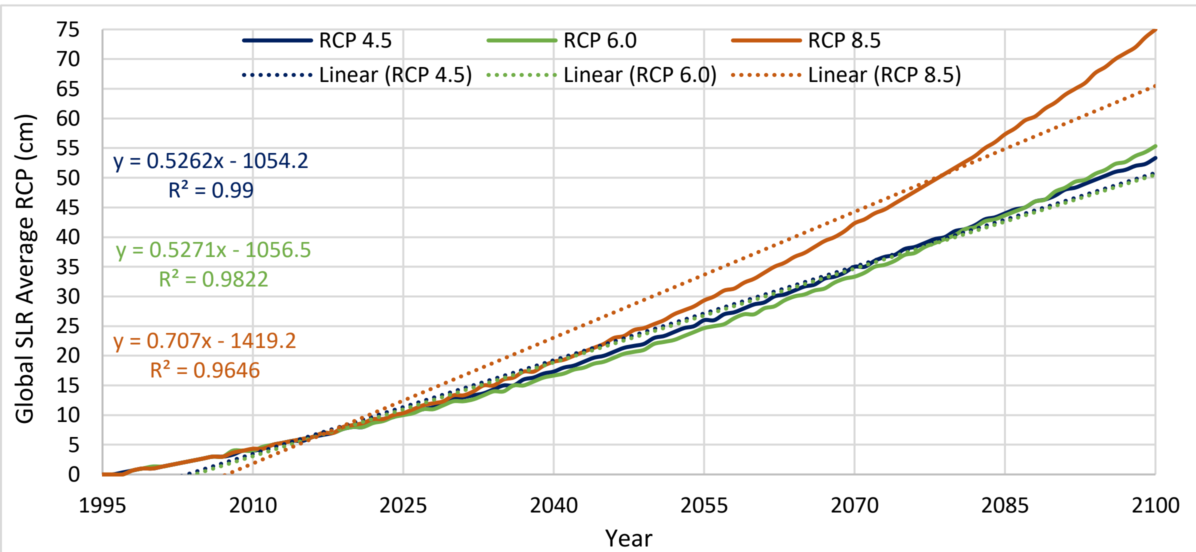

Figure 10.16: Global Sea Level Rise scenario (cm) (1995-2100) average RCP

Table 10.4: Global Sea Level Rise scenario (cm) (1995-2100) RCP 4.5, 6.0 and 8.5

Year	RCP 4.5				RCP 6.0				RCP 8.5			
	Low	Mid	High	Mean	Low	Mid	High	Mean	Low	Mid	High	Mean
2025	8	10	13	10.33	7	10	13	10.00	8	10	13	10.33
2050	17	23	29	23.00	16	22	28	22.00	19	25	32	25.33
2075	27	38	49	38.00	26	37	48	37.00	34	46	60	46.67
2100	36	53	71	53.33	38	55	73	55.33	53	74	98	75.00

The rise in Global Mean Sea Level (GMSL) for the period of 2025-2100, based on process-based models is likely to be in the range 10.33-53.33 cm for RCP 4.5, 10.00-55.33 cm for RCP 6.0 and 10.00-75.00 for RCP 8.5. Currently there is no sufficient evidence to evaluate the probability of specific levels above the likely range. If the carbon dioxide concentration CO_2 level decrease worldwide then mid, low and high sensitivity also be decrease and will be stand in a sensible level. The period of this model is designed 1995-2014 and predicted up to 2100 (Table 10.4), so it is statistically true that the sea level rise probability should be in this way.

10.5 Correlation with Temperature and Sea level Rise in Bangladesh

For the comparative analysis in temperature and sea level rise, bellow figure uses two axes vertically temperature and sea level rise. This (Figure 10.17) shows the relationship between temperature and sea level rise that how much temperature is responsible for sea level rise. On the passage of time temperature and sea level rise indicate increasing in rate. Comparison of temperature with sea level rise assume that when temperature (RCP 8.5) rise by 4.5 ^{0}C SLR (RCP 8.5) also be rise by 75 cm in 2100. This is the height proximity globally if the temperature rises according this scenario.

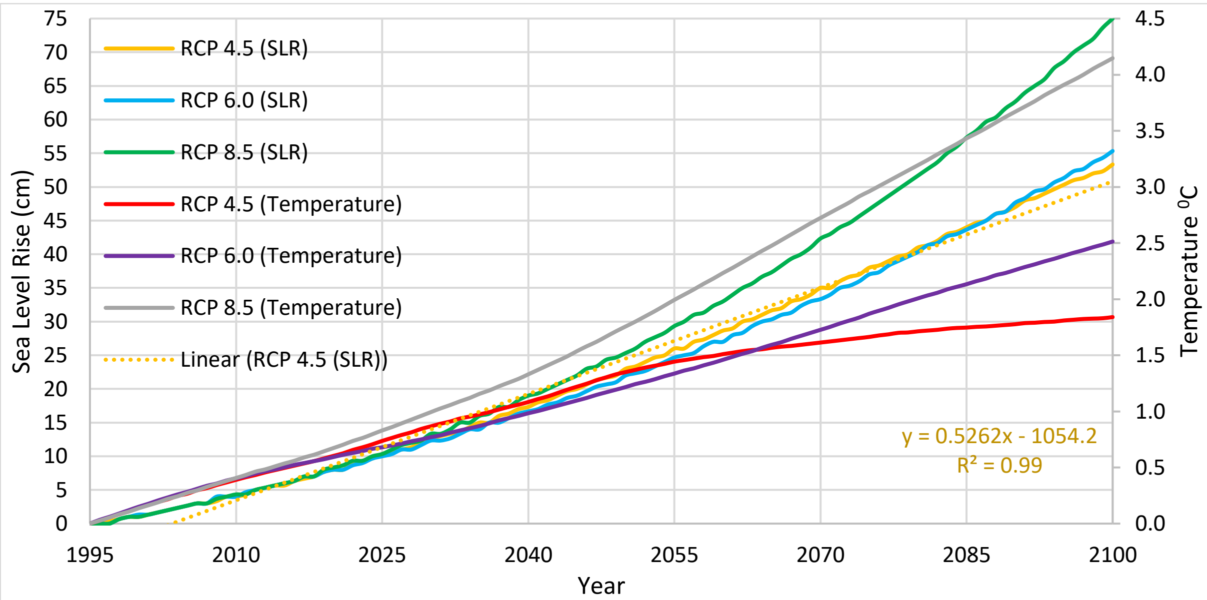

Figure 10.17: Comparative analysis between Temperature and Sea Level Rise with different RCPs

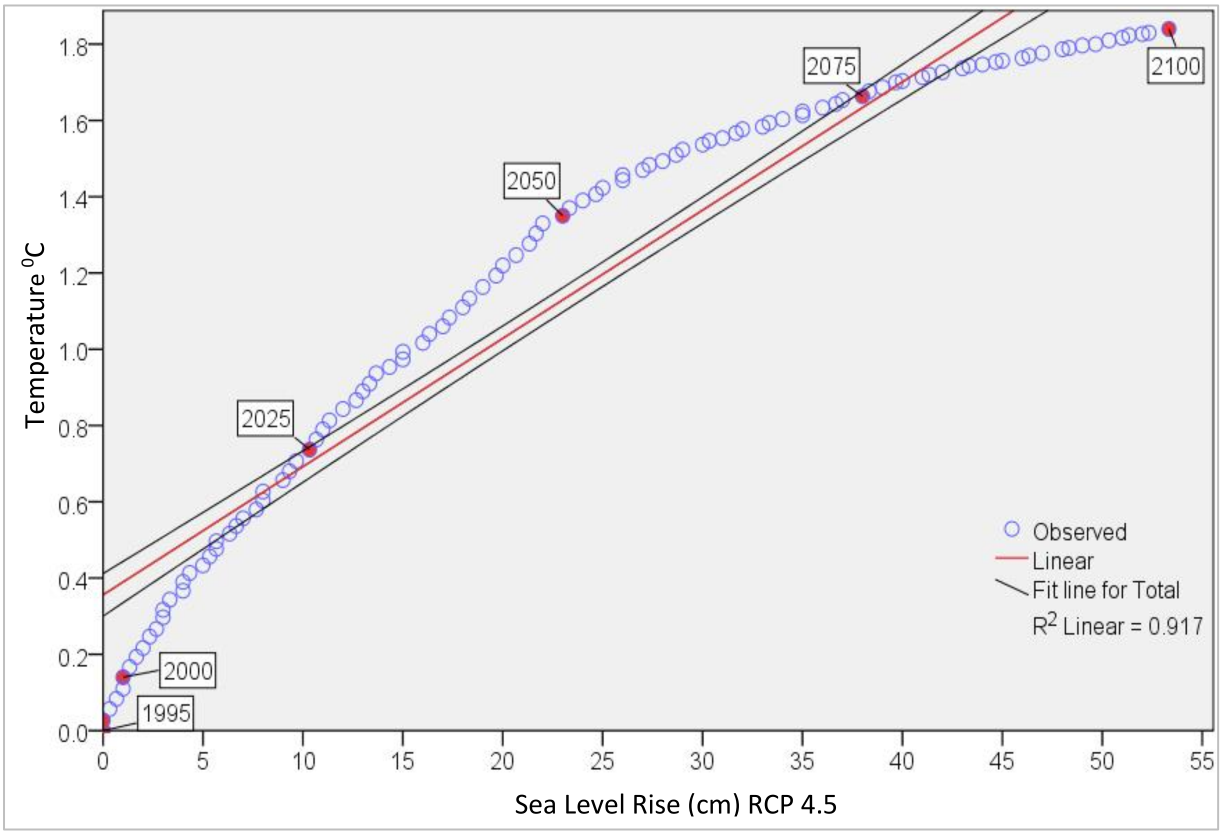

Figure 10.18: Regression best fit line analysis in Temperature and Sea Level Rise, RCP 4.5

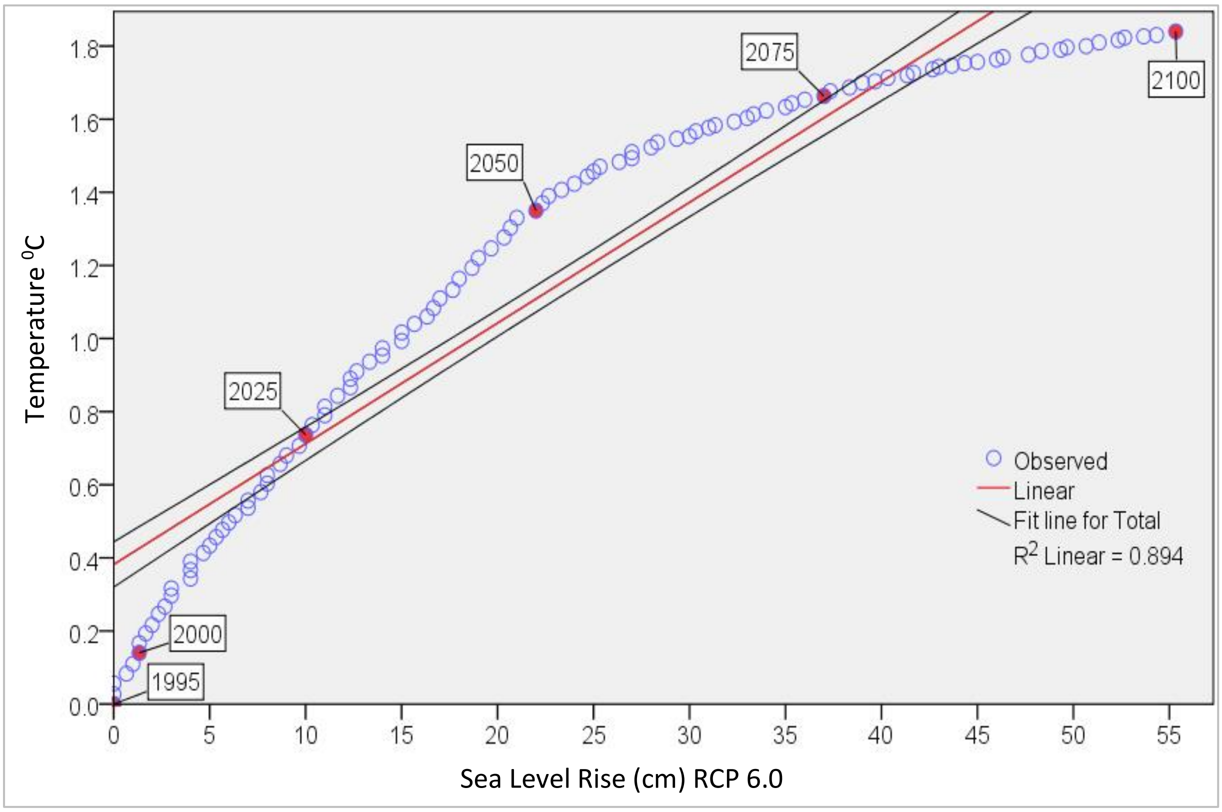

Figure 10.19: Regression best fit line analysis in Temperature and Sea Level Rise, RCP 6.0

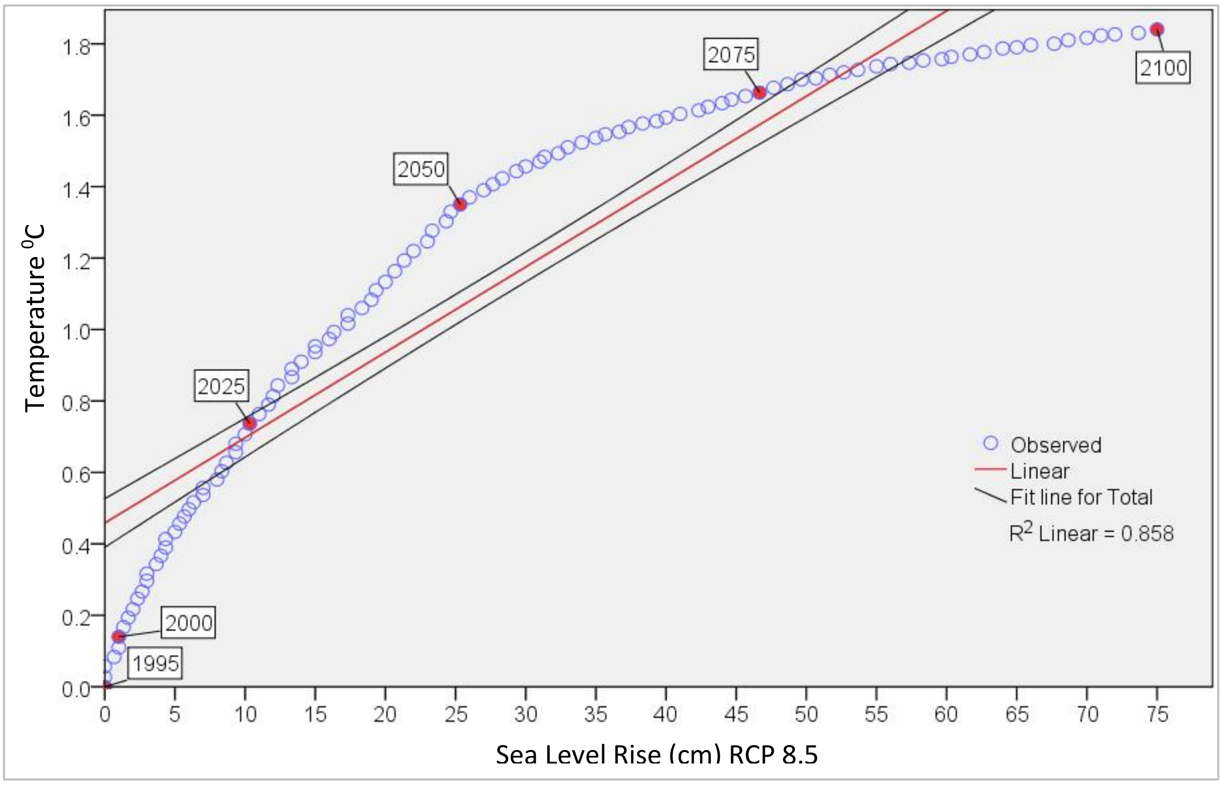

Figure 10.20: Regression best fit line analysis in Temperature and Sea Level Rise, RCP 8.5

Table 10.5: Sea Level Rise changing pattern based on rising Temperature, RCP 4.5, 6.0 and 8.5

Year	**Temperature ^{0}C***	**Sea Level Rise (cm)**		
		RCP 4.5	**RCP 6.0**	**RCP 8.5**
2000	0.14	0.93	1.30	1.01
2025	0.74	10.29	9.95	10.24
2050	1.35	22.92	21.97	25.28
2075	1.66	37.90	36.91	46.60
2100	1.84	53.33	55.31	75.00

Note: *Temperature always constant for RCP 4.5, 6.0 and 8.5

To evaluate the condition of the correlation of temperature and sea level rise regression analysis, the best fit line represents the R^2 value (Figure 10.18, 10.29 and 10.20 and Table 10.5). This table produced from the regression best fit line using SPSS Statistics 17.0. Here, temperature assume always constant for RCP 4.5, 6.0 and 8.5. In SPSS Statistics 17.0 correlation regression, figure need to specified dependent and independent variable, for the scientific calculation and measurement of SLR is selected for the independent variable that is changed or controlled by the effects of dependent variable (temperature). Above (Table 10.5) shows that the temperature increased 0.14 ^{0}C and sea level rise increased 0.93 (RCP 4.5) cm, 1.30 (RCP 6.0) cm and 1.01 (RCP 8.5) cm by 2000. The projection shows that, RCP 4.5 is the best fit correlation regression with temperature and sea level rise, the $R^2 = 0.917$ value found from this correlation in Bangladesh from global perspective (Figure 10.18).

10.5.1 Sea level Rise in Bangladesh

The Northern Indian Ocean, which includes the Bay of Bengal, has also been reported to experience a relatively high rate of SLR compared to other oceans globally (Han *et. al.,* 2010; Unnikrishnan and Shankar, 2007). Based on global sea level data and modelling, Ericson *et. al.,* (2006) have estimated that, the SLR of the Bay of Bengal is the world's highest, at 10 mm/yr. In this study also reflect the same result 0.93 cm/yr (9.3 mm/yr) in 2000 in RCP4.5. But it will be increase 10.29, 22.92, 37.90 cm/yr and 55.33 by 2025, 2050, 2075 and 2100 respectively (Table 10.5).

Bangladesh is a low laying with densely populated coastal country of smooth relief comprising broad and narrow ridges and depressions (Brammer *et. al.,* 1993). World Bank (2000) showed 10 cm, 25 cm and 1 m rise in sea level by 2020, 2050 and 2100; affecting 2%, 4% and 17.5% of total land mass respectively, which is almost similar scenario in this study (Table 10.5). Milliman *et. al.,* (1989; cited in Frihy, 2003) reported 1.0 cm per year sea level rise in Bangladesh. UNEP (1989), showed 1.5 m sea level rise in Bangladesh coast by 2030, affecting 22,000 km^2 (16% of total landmass) area with a population of 17 million (15% of total population) affected. A study by SAARC Meteorology Research Centre (SMRC, cited in Alam, 2003) found that tidal level in Hiron Point, *Char* Changa and Cox’s Bazar raised 4.0 mm/yr, 6.0 mm/yr and 7.8 mm/yr respectively. However, Sing (2002) mentioned that, the difference is mainly due to land subsidence.

Table 10.6: Increase of tidal level in ten coastal stations of Bangladesh’s coast

Stations	**Lon**	**Lat**	**Region**	**Data Source**	**Year Range**	**Year**	**Average (mm)**	**Trend (mm/yr)**	**RMSE (mm)**
Hatiya	91.11	22.42	Central	BWDB	1979-2008	30	2522.77	0.86	329.34
Sonapur	91.49	22.89	Central	BWDB	1982-2008	37	3960.59	-11.59	501.29
Moheshkhali	91.98	21.65	Eastern	BWDB	1968-2008	32	2052.66	-7.40	381.10
Rayenda	89.86	22.31	Western	BWDB	1979-2008	30	2218.16	0.63	233.42
Charchanga	91.05	22.22	Central	BIWTA	1979-2000	22	2113.68	7.60	88.88
Cox’s Bazar	91.83	21.45	Eastern	BIWTA	1978-2006	26	2067.46	1.02	108.14
Hiron Point	89.47	21.78	Western	BIWTA	1977-2003	27	1821.67	5.22	67.87
Khepupara	89.83	21.83	Western	BIWTA	1977-2000	24	2122.48	13.32	132.33
Chittagong*	-	-	Eastern	SOB	1993-2015	23	5441.76	4.97	92.97
Teknaf	92.30	20.88	Eastern	BIWTA	1983-1988	5	2363.93	12.59	299.41
Average	**-**	**-**		**-**	**-**	**-**	**2668.52**	**2.72**	**223.48**

Note: *Tidal station name (Chittagong, Rangadia) have no latitude/longitude

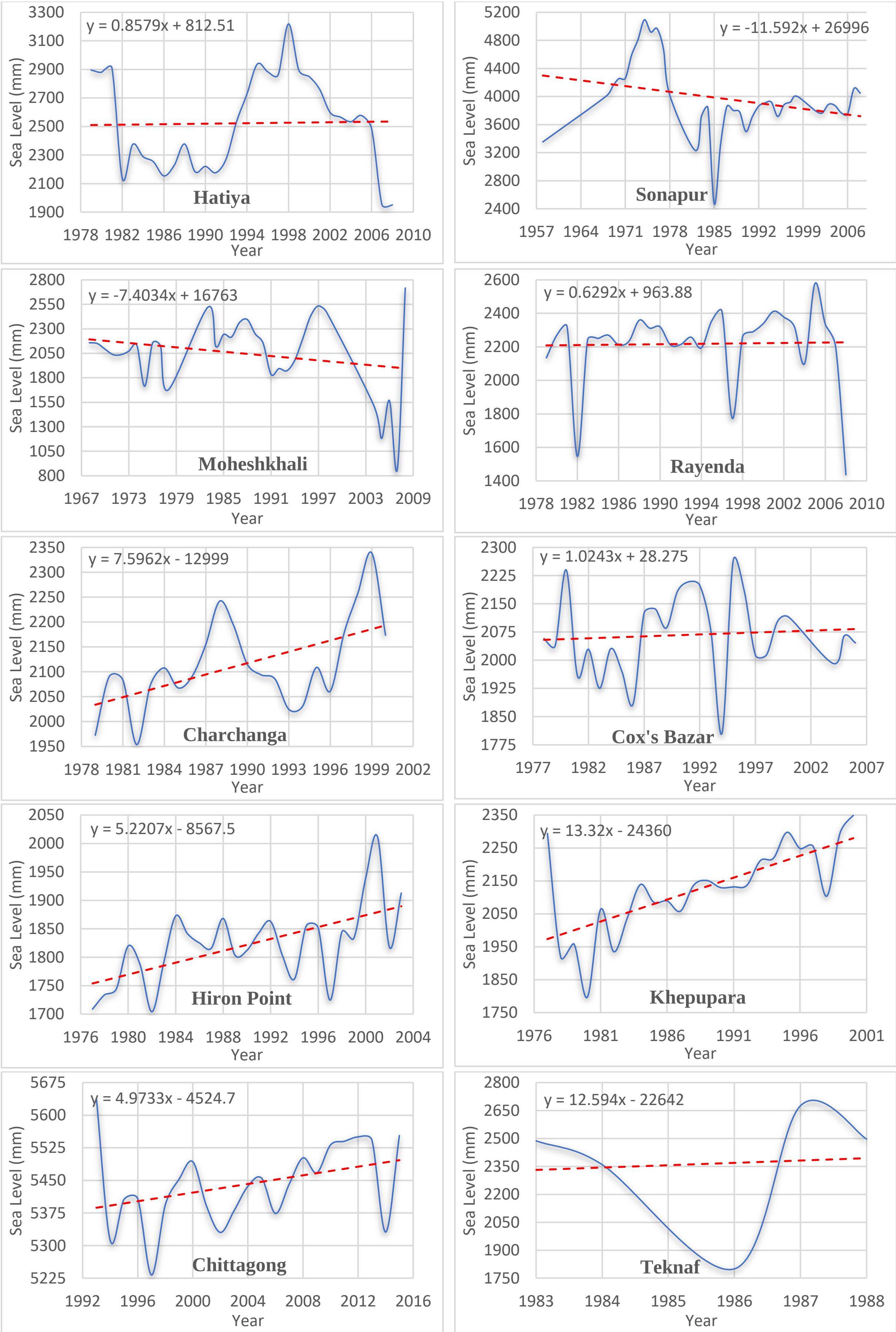

Figure 10.21: Trend of sea level rise at different tide guage stations along the coastal zone

In the (Table 10.6) is more update than SMRC report where latest data were included up to 2015. Though same temporal date was not used in individual stations but reflect more reliable because of recent data used. The average sea level rise rate found in coastal zone of Bangladesh is 2.72 mm/yr where global average found 5.87 mm/yr which is about two times more than Bangladesh average. Khepupara is the height rate increasing 13.32 mm/yr and Sonapur is the lowest rate decreasing -11.59 mm/yr. Three regions, Eastern rate is 2.80 mm/yr, Central rate is -1.04 mm/yr and Western rate is 6.39 mm/yr. Eastern and Western region is higher rate than Central region where Central region is negative in trend (Figure 10.21). Except Teknaf, the trend in Bangladesh average only 1.63 mm/yr, this rate is very little compare to the global average. The Ministry of Environment and Forests (MoEF, 2009) has prepared NAPA as a response to the decision of the Seventh Session of the Conference of the Parties (COP7) of the United Nations Framework Convention on Climate Change (UNFCCC). The observed trend in sea level rise used in that document was cited from the study conducted by the SAARC Meteorology Research Centre in 2003. The study (SMRC, 2003) found that the tidal level in Hiron Point, *Char* Changa and Cox's Bazar rose by 4.0 mm/yr, 6.0 mm/yr and 7.8 mm/yr respectively, observing tidal gauge record of 22 years from 1977-1998.

10.6 Projection of Future Sea Level Rise

Bangladesh sea level rise trend is half of global average, but it has a great importance for its low laying country. Previous study and current state of knowledge is not a negligible measurement. If we encompass that 2015 is the example year for its trend analysis and go through the same rate in the year of 2025, 2050, 2075 and 2100 then we will reach 27.20 mm, 95.20 mm, 163.20 mm and 231.20 mm SLR respectively. On the other hand, if we calculate the global rate, in the year of 2025, 2050, 2075 and 2100 then world will reach 63.90 mm 223.65 mm, 383.40 mm and 543.15 mm SLR respectively. For this calculation some anomalies like discontinuous of year, year gap, variety source of data, tidal surge, tsunami and seasonal flood level are not considered here, this anomaly unevenly may increase or imbalance tidal level around all the tidal stations. Above all, this scenario represent that Bangladesh will face a critical circumstance in next century. According to the (BBS, 2011) census track, without river - coastal area had 39937.80 km^2 area. Subtracting the Shuttle Radar Topography Mission (SRTM) Digital Elevation Model (DEM) satellite imagery by 2011 census track, sea level rise data were measured eventually. Hypothetically if the sea level rise 1 to 5 meter, then what will be the scenario in coastal area ! Using this measurement five sets of maps produced to visualize the future condition about sea level rise or coastal inundation.

Table 10.7: Increase of Sea Level Rise in future year in coastal area (2011 is the pop^n census)

Year	SLR (mm)	Inundated (km^2)	Area %	People Affected
2011	2.72	156.92	0.39	175068
2025	38.08			
2050	106.08			
2075	174.08			
2100	242.08			

Note: Inundated, area% and affected people were measured by BBS population census, 2011[12]

Table 10.8: 1 to 5-meter increase of Sea Level Rise in future; 2011 is the base year

SLR	Inundated (km^2)	Area %	People Affected* (m)
1 meter	1038.76	2.60	1.16
2 meters	2544.35	6.37	2.84
3 meters	5266.78	13.19	5.88
4 meters	9235.76	23.13	10.30
5 meters	13699.7	34.30	15.28

Note: Inundated, area% and affected people were measured by BBS population census, 2011

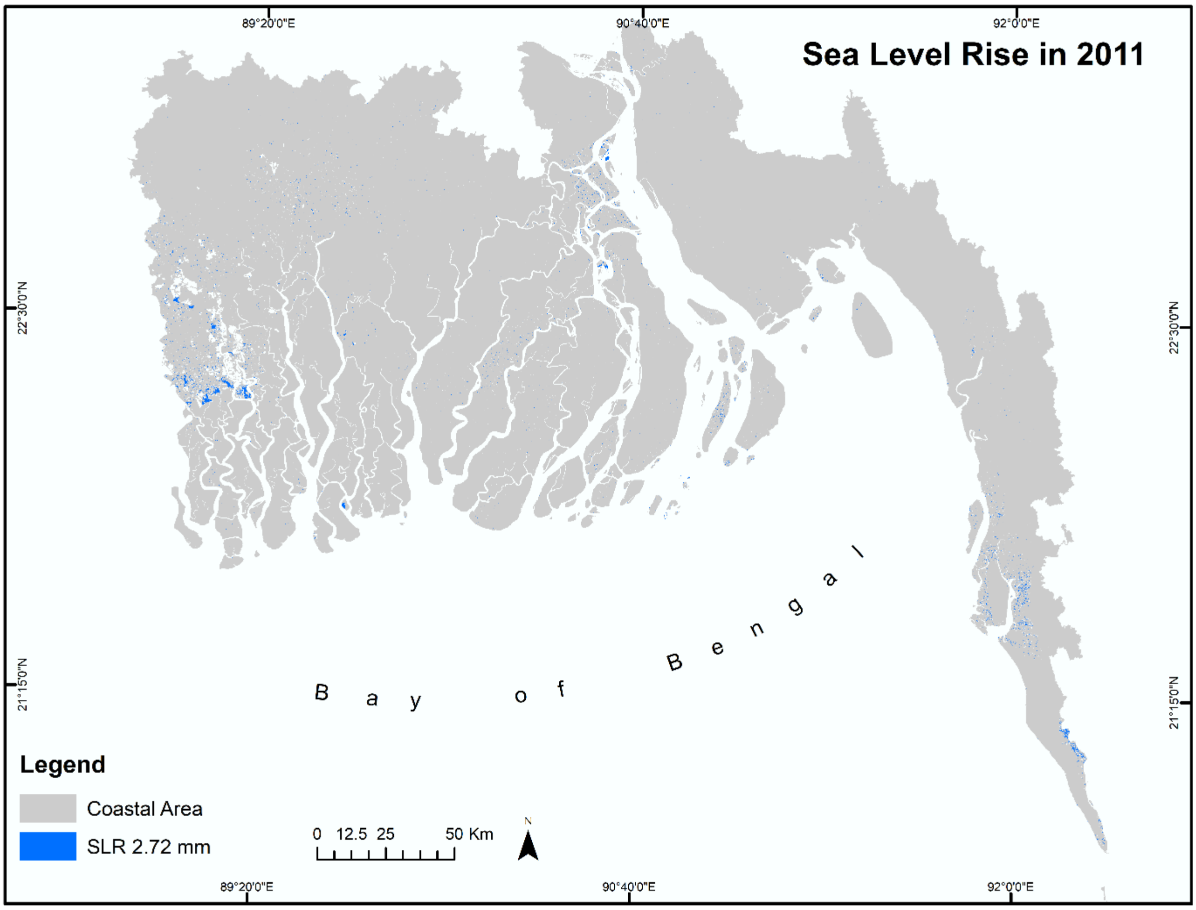

Figure 10.22: Sea Level Rise 2.72 mm in the year of 2011 (baseline)

[12] Probability were measured by (BBS, 2011) from SRTM DEM, 2011 do not reflect or change in (mm) SLR through 2100. SRTM DEM (3 arc second) data could not produce inundated area, until it reached a meter unit range (Figure 10.22-10.24).

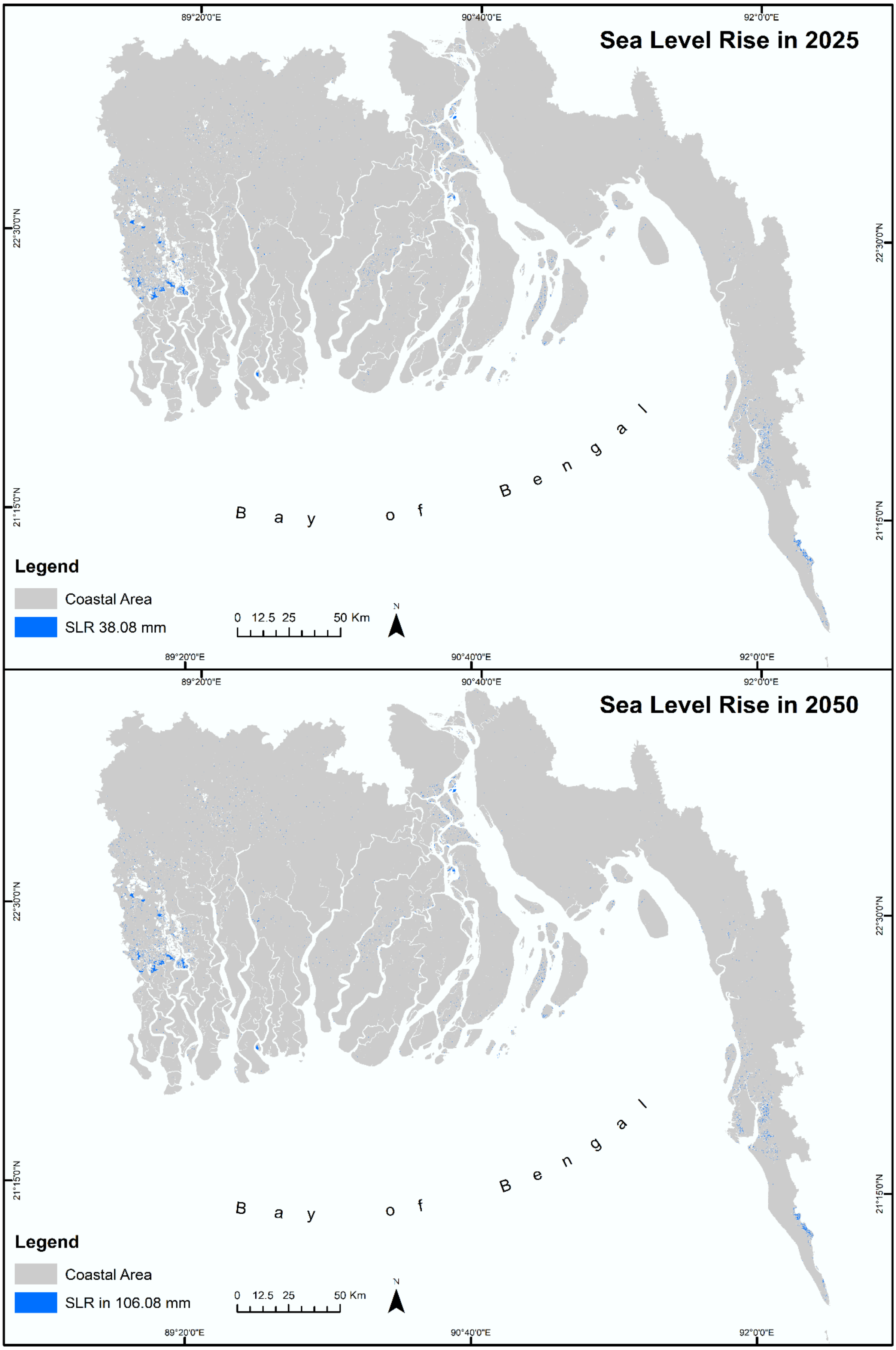

Figure 10.23: Sea Level Rise 38.08 and 106.08 mm in the year of 2025 and 2050

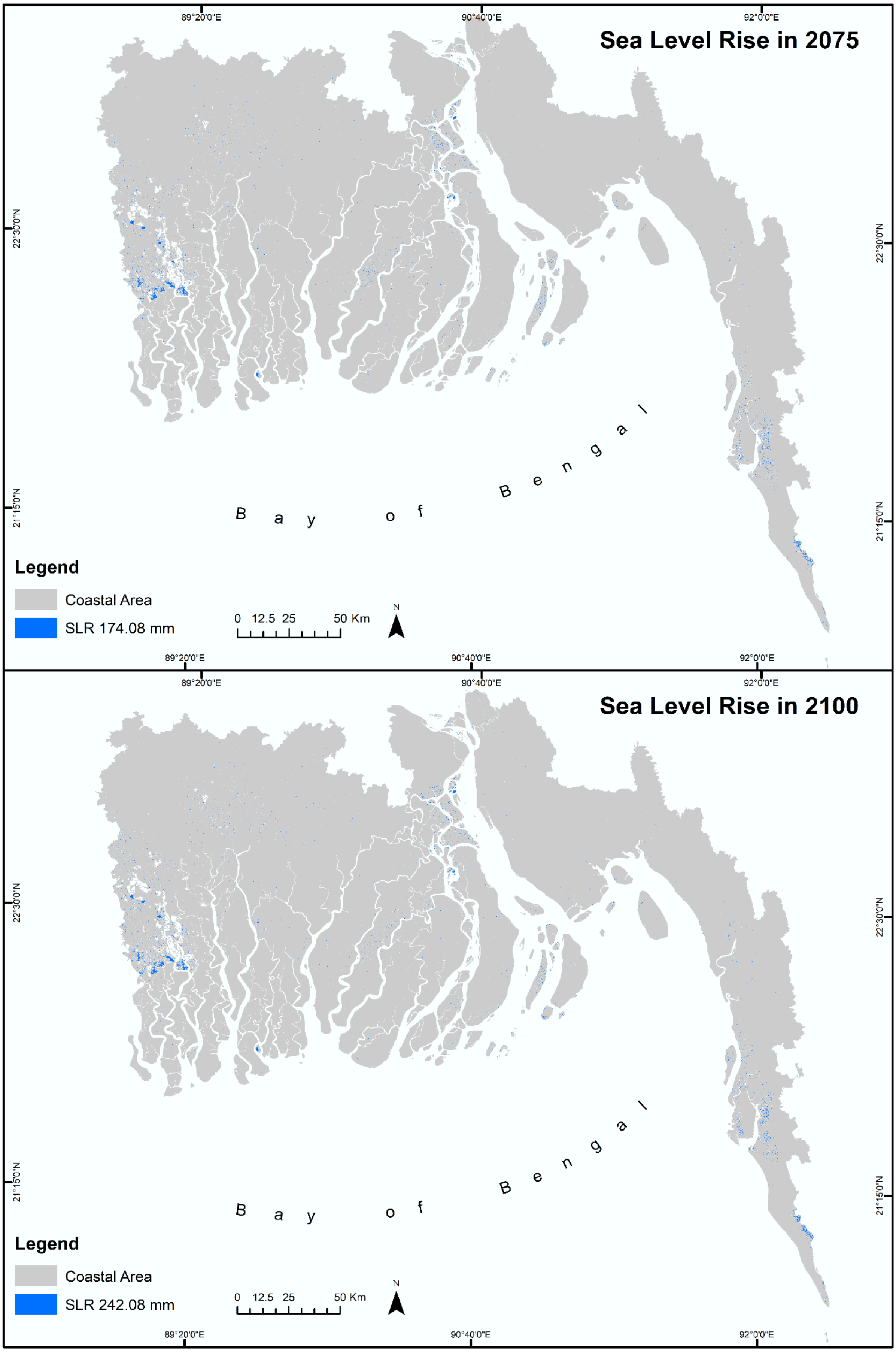

Figure 10.24: Sea Level Rise 174.08 and 242.08 mm in the year of 2075 and 2100

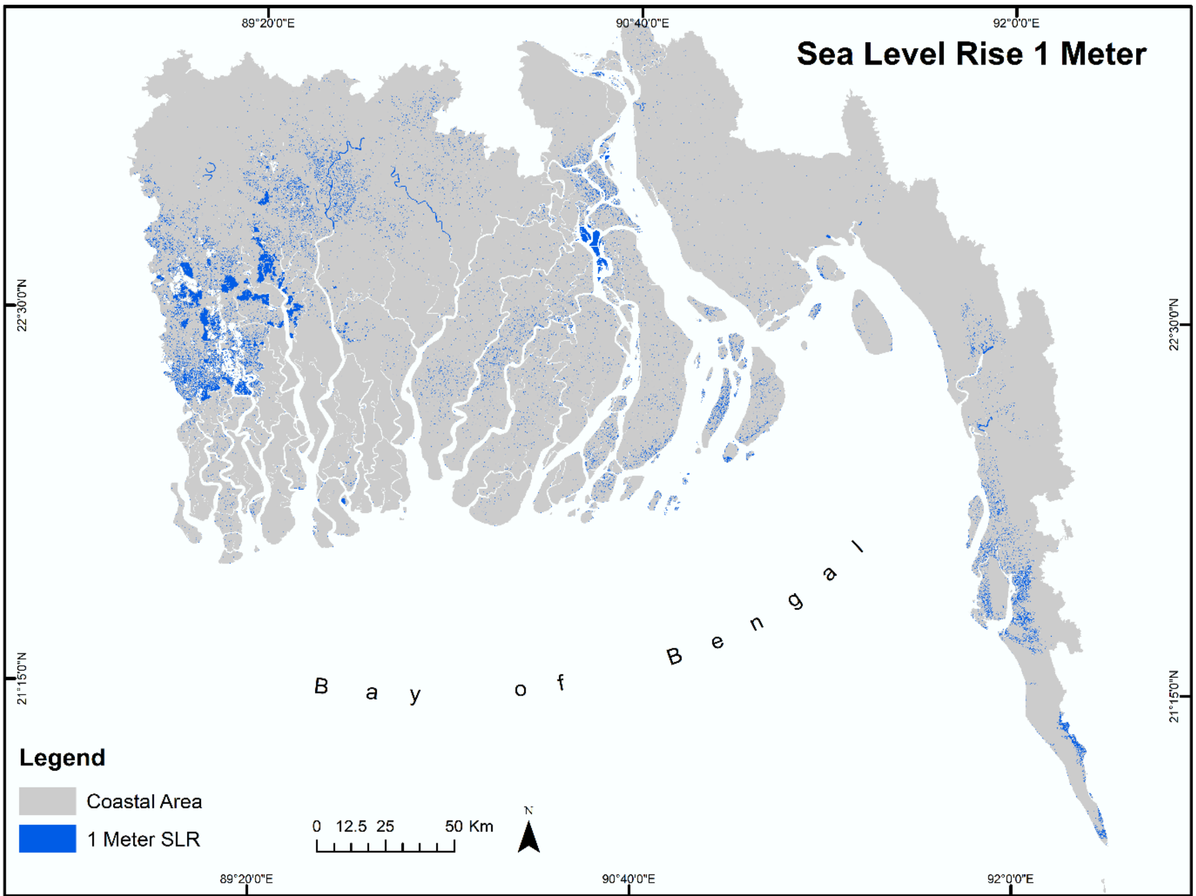

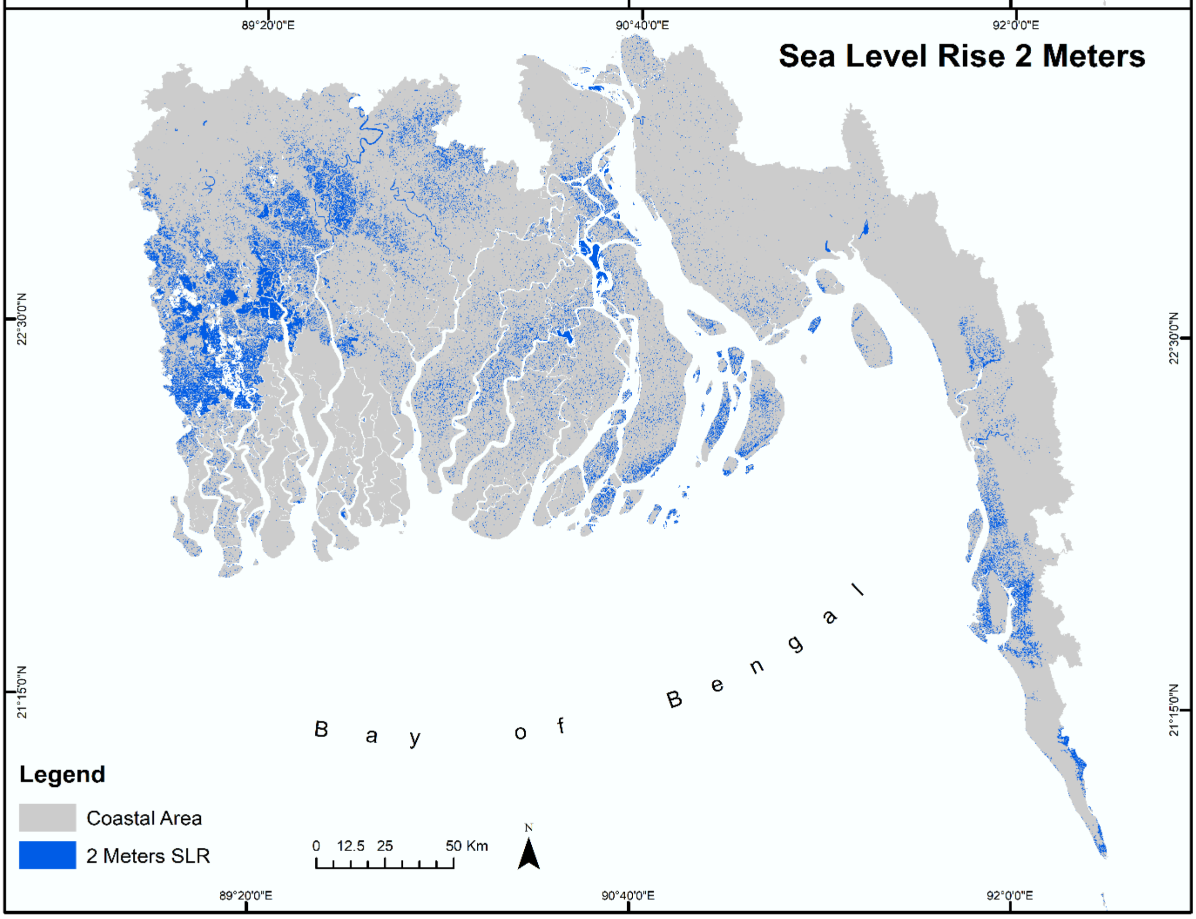

Figure 10.25: Sea Level Rise 1 meter and 2 meters in coastal zone of Bangladesh

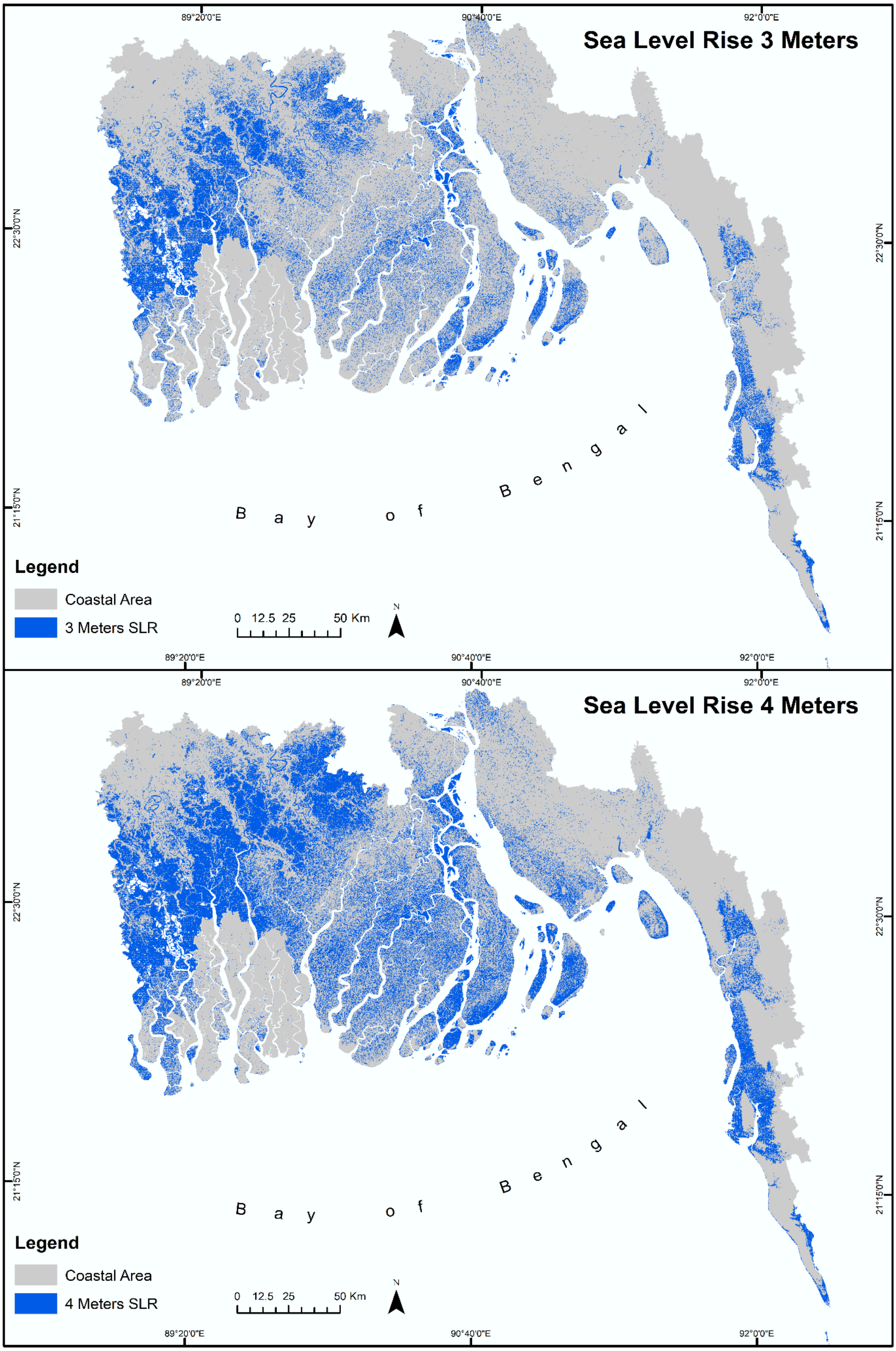

Figure 10.26: Sea Level Rise 3 meters and 4 meters in coastal zone of Bangladesh

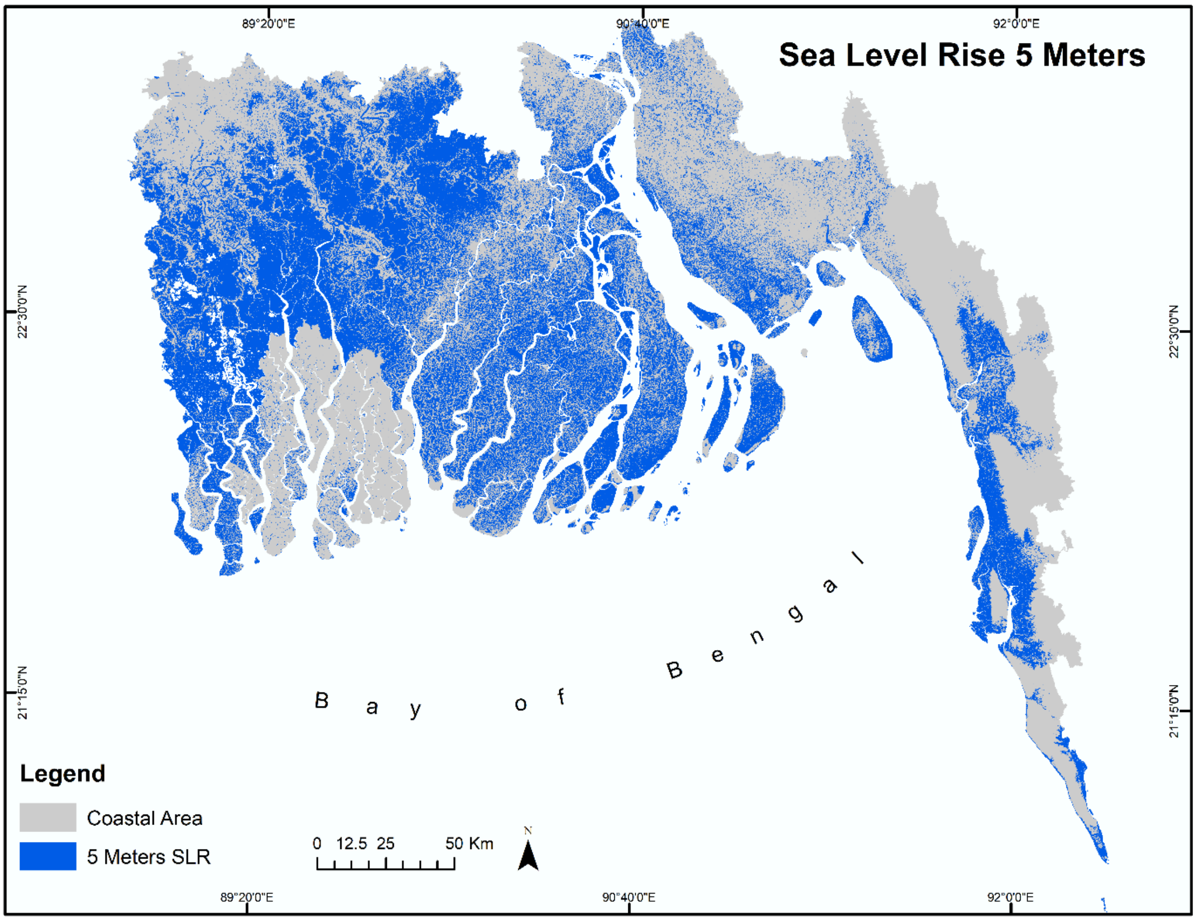

Figure 10.27: Sea Level Rise 5 meters in coastal zone of Bangladesh

From the above discussion, in the year of 2380 we will be reach 1-meter sea level rise. So, if we want to see 5 meters sea level rise we must wait 362 years from now. However, all the forecast is predicted rationally (Figure 10.22-10.27) but it will not be wise to think that sea level will not rise at all. If the global worming or Green House Gas (GHG) emission reduced near future, then this scenario will be change. This is the caution not only for Bangladeshi people but also the global people because it is not our local issue, who have contained coastal territory in the globe must have to remember that this scenario will also be happened to the other territory.

10.7 Affecting Future Sea Level Rise due to Land Subsidence

Much of the Ganges delta is underlain by Holocene, Pleistocene and Tertiary sandy sediments that are not subject to compaction with water abstraction; and Holocene peat layers underlying large parts of the tidal floodplain have remained saturated since their formation and so have not shrunk by drying out (except locally where water has been abstracted under Khulna city) (Brammer, 2014). It seems probable that most of such subsidence as is occurring is due to-

Table 10.9: Land subsidence rates on the Ganges Tidal Floodplain calculated from radio-carbon-dated buried organic material[13]

Site No	Material	Depth (m)	Radio Carbon Age	Calendar age (years BP)	Depth/calendar age (mm/yr)
6BP48	Buried tree	1.5	455 ± 45	614 ± 14	2.4
19BS98	Marine shell	1.4	1200 ± 30	730 ± 50	1.9
7BS99	Wood	0.7	90 ± 40	227 ± 48	3.1
7BS99	Crab claw	2.2	127 ± 7	309 ± 8	7.1
12BS99	Peat	1.5	570 ± 50	584 ± 64	2.6
BVS16	Peat	1.1	910 ± 50	820 ± 111	1.3
12BS99	Peat	3.2	2300 ± 40	2378 ± 29	1.3
12BS99	Peat	5.8	2690 ± 40	3192 ± 17	1.8

Note: Data in columns 1-5 from Allison *et. al.*, (2003). Cited in Brammer (2014).

tectonic subsidence of the Bengal Basin within which the region lies, possibly complicated by folds and faults within the basin (Stanley and Hait, 2000; Steckler *et. al.*, 2008). Elsewhere, large areas were reported to have subsided in Noakhali District (in the south-west of Subregion) and south of Chittagong in the 1762 Arakan earthquake (Khan, 1977; Cummins, 2007).

All the calculation, table, figure or output will try to reveal that, the circumstances about the present and future condition of sea level rise in the coastal area of Bangladesh. People who have no idea about the sea level rise must be understand that it is a slow process and take a long time to happen this scenario over the globe. Bangladesh is one of the most disastrous vulnerable country in the world. Seasonal flood, tidal surge and tropical cyclone is the most dangerous calamity in our country. Tropical cyclone increased tidal level 2-3 meters in general because of delta shape in the coast, so sea level rise will be a curse if it will rise the same rate as mention above.

[13] 1. That table includes coordinates of the sites sampled.
2. Column 6: depth (col. 3) divided by calibrated calendar age (col. 5) = annual change in land levels relative to mean sea-level.

Chapter Eleven
Conclusion and Recommendation

11.1 Introduction

Natural hazards and climate change risk is common phenomenon or interface in Bangladesh. To measure or calculate this calamity we must depend sometimes third-party source in the world. Some of the high configured instrument or devise are inadequate who measure or analyze this type of hazardous or climatic change risk or information. Long term and credible information very much depend the quality of the research, thesis or hypothesis. Climate change and sea level rise extremely involve over there each other. Sea level rise data and climatic data acquisition is a complex task in our country. Extreme price, permission, time consume delivery and lacking data consistency is a major problem everywhere. Maximum temperature, minimum temperature, mean temperature and precipitation data were used for measuring climatic condition and ten sets of tidal station from BWDB used for sea level rise. Bangladesh Meteorological Department (BMD), Permanent Service for Mean Sea Level (PSMSL), University of Hawaii Sea Level Center (UHSLC), Bangladesh Inland Water Transport Authority (BIWTA), United States geological Survey (USGS) for Landsat and STRM satellite imagery, SimCLIM 40 ensemble Global Circulation Model (GCM) and Regional Climate Model (RCM) were the main data source for measuring to predict future climate in this research.

11.2 Uses of Applications in the Research

Different types of tests, maps, graphs, charts were produced in ENVI 5.1, ERDAS Imagine 2015, ArcGIS 10.5, QGIS 3.0.0, Surfer 10, TerrSet, SimCLIM 3.4.0.0, SPSS Statistics 17.0, ILWIS 3.8.5, Microsoft Excel 2016, Microsoft access 2016, XLSTAT 2016 and web GIS. The main purpose of this study is to measure how much climate change struck over our country and how much this climate change is responsible for the sea level rise. What will be the future climate scenario, coastal shoreline and coastal people. This process is a complex task and statistically significant so, vast method and analytical conceptualization is important to analyze all the data. Spatial trend analysis, pattern scaling for prediction of future climate, shoreline assessment and measuring sea level rise are the main purpose in this research. Various literature review, information collection, field observation, researcher's opinion is also very much important to know the state of the knowledge. State of the art, quality journals, books, thesis papers, unpublished thesis papers, various national dailies, conference, symposium, web site, forums etc. are the main source for the literature review and finding the research gap.

11.3 Findings

11.3.1 Findings in Temperature and Rainfall

Climatic data analysis and prediction of its trend in local level like Bangladesh territory depends on Bangladesh meteorological Department (BMD). Though its long-term data is a major part for analyzing climate trend but sometimes credibility of continuous data and missing value may change its nature a little bit. But we must depend this data because of lacking availability of data source. Temperature variation follows in different seasons like pre-monsoon (March-May), monsoon (June-September), post-monsoon (October-November) and winter (December-February) trends.

On an average the trend in mean, minimum and maximum temperature is 0.82 ^{0}C, 1.41 ^{0}C and 0.96 ^{0}C per century respectively. The corresponding pre-monsoon, monsoon, post-monsoon and winter are (0.13, 1.07, 1.28 and 0.86 ^{0}C), (1.55, 0.97, 1.13 and 1.97 ^{0}C) and (0.06, 1.77, 2.33 and 0.02 ^{0}C) per century respectively. The magnitude at individual stations varied between -0.15% to 0.25% of normal annual mean temperature, -0.12% to 0.24% of normal annual minimum temperature and -0.06% to 0.24% of normal annual maximum temperature per year. It was seen from the calculation that the northern part of the country has a higher rate of increase in mean temperatures compared to the mid and mid-western and south eastern hilly regions. The north-eastern part of the country has a higher rate of increase and middle to Meghna estuary has a higher rate of decrease in minimum temperatures. The north and south-eastern and central part of coastal zone of the country has a higher rate of increase in maximum temperatures compared to the mid to mid-western and mid northern part.

All-Bangladesh annual normal rainfalls were 1068.17, 1460.57, 1845.10 and 2215.20 mm during 1948-1976, 1957-1986, 1967-1996, 1977-2006 respectively. It thus appears that the annual normal rainfalls have changed in Bangladesh. It was seen from the calculation that the rainfalls increased gradually over the first six decades and then decreased. The highest rainfall was observed during the 1997-2006. The seasonal rainfall like the monsoon (June-September), post-monsoon (October-November) and winter (December-February) normal rainfalls have increased and the pre-monsoon (March-May) normal rainfall has increased in the last four periods and then decreased over the five-time periods. However, these changes in rainfalls in different seasons would be statistically significant. The increasing trend in the pre-monsoon, monsoon, post-monsoon and winter were found to be about 5.21, 20.93, 2.61 and 0.39 mm/year respectively with significant at 95% level of confidence whereas, annual rate was 29.13. The calculation showed that the rainfalls in the months of December 0.08 mm, January 0.07 mm and February 0.24 mm in the winter season have nearly stable in trends. The month of March (pre-monsoon) about to same as winter, like 0.47 mm and the months of April and May (pre-monsoon) have slightly increasing trends with 1.13 and 3.61 mm respectively. The months of June, July, August and September (monsoon) have a higher increasing trend with 5.27, 6.56, 4.84 and 4.27 mm respectively.

However, in October (post-monsoon) also slightly increasing trend 2.27 mm and November (post-monsoon) was found to be nearly stable trend with 0.34 mm. The variability in rainfalls in the months of January, February, March, April, May, June, August and October have increased, while that in the months of July and September have decreased. It thus appears that the interannually variability in rainfalls in most months has increased. This indicates that the rainfall is becoming increasingly more uncertain and unpredictable.

11.3.2 Findings in GCM and RCM

In this research one of the most powerful software SimCLIM was used for calculating Regional Climate Model (RCM) and General Circulation Model (GCM). SimCLIM 2013 is a computer-based modeling system for examining the spatiotemporal variability in climatic conditions and their impacts. Here, 40 GCMs were ensemble and produced verities maps, graphs, figures and predicted future climate scenarios. SimCLIM 2013 follows the fifth assessment report (AR5) of IPCC (IPCC, 2014). SimCLIM provides the facility to select the GCM patterns for the development of suitable global projections (AR5) of sensitivity values and future. A SimCLIM simulation based on baseline temperature 1995 showed that, the global lowest temperature was -44.52 ^{0}C while the height was 30.27 ^{0}C. In Bangladesh minimum, maximum and mean temperature for baseline varied 12.20 ^{0}C - 26.20 ^{0}C, 25.80 ^{0}C - 34.40 ^{0}C and 19.00 ^{0}C - 29.10 ^{0}C respectively and precipitation was 7.00 mm - 381.00 mm.

11.3.3 Findings in Regional Climate Model and Projection

Bangladesh Meteorological Department (BMD) and the SimCLIM climate model (temperature and precipitation) both data shows similarities with slight difference. It appears that, local weather data a little bit higher than the SimCLIM projection but both have the similar in nature during 1995-2014. Annual average minimum temperature for observed and model projected values for baseline (1995), 2025, 2050, 2075 and 2100 were 21.18 ^{0}C (baseline), 21.88 ^{0}C, 22.53 ^{0}C, 23.22 ^{0}C and 23.92 ^{0}C respectively. Annual average maximum temperature for observed and model projected values for baseline (1995), 2025, 2050, 2075 and 2100 were 30.67 ^{0}C (baseline), 31.33 ^{0}C, 31.93 ^{0}C, 32.55 ^{0}C and 33.16 ^{0}C respectively. Annual average mean temperature for observed and model projected values for baseline (1995), 2025, 2050, 2075 and 2100 were 25.90 ^{0}C (baseline), 26.58 ^{0}C, 27.20 ^{0}C, 27.81 ^{0}C and 28.46 ^{0}C respectively.

In terms of annual total precipitation for observed and model projected values found in baseline, 2025, 2050, 2075 and 2100 were 2024.00 mm (baseline year) whereas, {2110.79 mm (RCP4.5), 2103.17 mm (RCP6.0) and 2122.94 mm (RCP8.5)}, {2173.52 mm (RCP4.5), 2165.47 mm (RCP6.0) and 2233.08 mm (RCP8.5)}, {2218.64 mm (RCP4.5), 2232.78 mm (RCP6.0) and 2370.84 mm (RCP8.5)}, {2238.01 mm (RCP4.5), 2300.75 mm (RCP6.0) and 2527.07 mm (RCP8.5)} respectively. Calculation showed that, lowest and highest precipitation of 2025, 2050, 2075 and 2100 were (1390.86 - 1615.17) mm to (4531.22 - 4755.54) mm; (1436.19 - 1667.25) mm to (4671.04 - 4902.10) mm; (1465.25 - 1700.63) mm to (4760.66 - 4996.04) mm and (1478.61 - 1715.98) mm to (4801.86 - 5039.24) mm respectively.

Projection showed that the percentage of the increasing variability in minimum temperature among different years 2025, 2050, 2075 and 2100 were (0.59 - 0.60) ^{0}C to (0.75 - 0.76) ^{0}C; (1.04 - 1.06) ^{0}C to (1.31 - 1.33) ^{0}C; (1.33 - 1.35) ^{0}C to (1.67 - 1.70) ^{0}C and (1.46 - 1.48) ^{0}C to (1.84 - 1.87) ^{0}C respectively from the baseline year. RCP4.5, 6.0 and 8.5 for 2025, 2050, 2075 and 2100 showed that the percentage of the increasing variability were (0.72 ^{0}C, 1.26 ^{0}C, 1.61 ^{0}C and 1.80 ^{0}C), (0.65 ^{0}C, 1.17 ^{0}C, 1.73 ^{0}C and 2.29 ^{0}C) and (0.81 ^{0}C, 1.73 ^{0}C, 2.87 ^{0}C and 4.16 ^{0}C) respectively from the baseline.

Projection showed that the percentage of the increasing variability in maximum temperature among different years 2025, 2050, 2075 and 2100 were (0.56 - 0.57) ^{0}C to (0.70 - 0.71) ^{0}C; (0.98 - 1.00) ^{0}C to (1.24 - 1.26) ^{0}C; (1.25 - 1.27) ^{0}C to (1.58 - 1.60) ^{0}C and (1.37 - 1.40) ^{0}C to (1.74 - 1.76) ^{0}C respectively from the baseline year. RCP4.5, 6.0 and 8.5 for 2025, 2050, 2075 and 2100 showed that the percentage of the increasing variability were (0.66 ^{0}C, 1.15 ^{0}C, 1.50 ^{0}C and 1.59 ^{0}C), (0.60 ^{0}C, 1.07 ^{0}C, 1.58 ^{0}C and 2.09 ^{0}C) and (0.74 ^{0}C, 1.58 ^{0}C, 2.62 ^{0}C and 3.80 ^{0}C) respectively from baseline.

Projection showed that the percentage of the increasing variability in mean temperature among different years 2025, 2050, 2075 and 2100 were (0.57 - 0.59) ^{0}C to (0.72 - 0.73) ^{0}C; (1.01 - 1.03) ^{0}C to (1.26 - 1.28) ^{0}C; (1.29 - 1.31) ^{0}C to (1.61 - 1.63) ^{0}C and (1.42 - 1.44) ^{0}C to (1.76 -

1.79) ^{0}C respectively from baseline. RCP4.5, 6.0 and 8.5 for 2025, 2050, 2075 and 2100 showed that the percentage of the increasing variability were (0.67 ^{0}C, 1.18 ^{0}C, 1.51 ^{0}C and 1.66 ^{0}C), (0.61 ^{0}C, 1.09 ^{0}C, 1.61 ^{0}C and 2.14 ^{0}C) and (0.76 ^{0}C, 1.62 ^{0}C, 2.68 ^{0}C and 3.89 ^{0}C) respectively from baseline.

Projection showed that the percentage of the increasing and decreasing variability in total precipitation among different years 2025, 2050, 2075 and 2100 were (3.45 - 3.56) mm to (4.94 - 5.05) mm; (6.06 - 6.25) mm to (8.69 - 8.88) mm; (7.73 - 7.97) mm to (11.09 - 11.33) mm and (8.50 - 8.77) mm to (12.19 - 12.45) mm respectively from baseline. RCP4.5, 6.0 and 8.5 for 2025, 2050, 2075 and 2100 showed that the percentage of the increasing variability were (2.21 mm, 3.89 mm, 4.96 mm and 5.46 mm), (2.02 mm, 3.61 mm, 5.32 mm and 7.06 mm) and (2.50 mm, 5.33 mm, 8.84 mm and 12.83 mm) respectively from baseline.

11.3.4 Findings in Shoreline Change

Twelve sets of shorelines were used in the shoreline change analysis for coastal zone of Bangladesh. Four sets of shorelines produced from historical topographic images and eight sets of Landsat. In 1940s mainland area decreased by 18.60 km^2 from 1910s but shoreline increased 45.93 km, inverted situation went to 1940s and 1950s whereas, area and shoreline both were increased, 1960s-1974 area were increased but shoreline decreased. In island, same example as 2005-2010 and 2010-2015 whereas, area decreased but shoreline increased respectively.

From 1910s-2015, net loss/gain equal to sum of individual couple year from 1910s-1940s to 2010-2015. Overall mainland shoreline and island shoreline net loss/gain were -14.79 and 579.20 km respectively. Island shoreline bigger than mainland shoreline and mainland shoreline found negative value whereas, island shoreline was positive value and in mainland height eroded year found 1910s-1940s and it was 326.81 km^2. Height accreted year found 1950s-1960s and it was 795.54 km^2, at the same time height net loss/gain year found 2010-2015 and 1950s-1960s and they were -78.49 km^2 and 633.09 km^2 respectively. Overall erosion and accretion were 366.65 km^2 and 1545.20 km^2 respectively.

It is clear that, in 105 years (1910s-2015) the mainland area, total net gain was accreted and found 1178.55 km^2. On the other hand, height eroded year found 1950s-1960s and it was 1224.47 km^2, height accreted year found 1910s-1940s and it was 1577.54 km^2, at the same time height net loss/gain year found 1950s-1960s and 1910s-1940s and they were -602.60 km^2 and

850.76 km^2 respectively. Overall erosion and accretion were 1677.19km^2 and 1965.94 km^2 respectively. So, it can be said that 1910s to 2015 about 105 years in island area total net gain accreted by 288.75 km^2. Overall Bangladesh coastal zone obtain 1467.30 km^2 area in the year of 1910s to 2015. Overall conditions from above discussion the scenario in the coastal zone accreted over time.

11.3.5 Findings in Sea Level Rise

Long response times for parts of the climate system, it has been estimated that we are already committed to a sea level rise within the next 2000 years of approximately 2.3 meters (7.5 ft) for each degree Celsius of temperature rise (Anders *et. al.,* 2013). The International Panel on Climate Change (IPCC) Summary for Policymakers, AR5 (2014), predicts that the global mean sea level rise will continue during the 21st century, very likely at a faster rate than observed from 1971 to 2010. In IPCC Fifth Assessment Report (2013), the IPCC found that recent observations of global average sea level rise at a rate of 3.2 (2.8 to 3.6) mm per year is consistent with the sum of contributions from observed thermal ocean expansion due to rising temperatures 1.1 (0.8 to 1.4) mm per year, glacier melt 0.76 (0.39 to 1.13) mm per year.

Greenland ice sheet melt 0.33 (0.25 to 0.41) mm per year, Antarctic ice sheet melt 0.27 (0.16 to 0.38) mm per year and changes to land water storage 0.38 (0.26 to 0.49) mm per year (IPCC, 2013). The report had also concluded that if emissions continue to keep up with the worst-case IPCC scenarios, global average sea level could rise by nearly 1 m by 2100 (0.52-0.98 m from a 1986-2005 baseline). If emissions follow the lowest emissions scenario, then global average sea level is projected to rise by between 0.28-0.6 m by 2100 (compared to a 1986-2005 baseline) (Churchs and Clark, 2015). Intergovernmental Panel on Climate Change (IPCC, 1990) estimated that a 3.3 ^{0}C rise in the global temperature under mid sensitivity by 2100 with a range of uncertainty of 2.2 to 4.9 ^{0}C. IPCC's estimation of global sea level rise was 1.0 to 2.0 mm/yr over the last century.

11.3.5.1 Major Findings in Sea Level Rise (Local Data)

The average sea level rise rate found in Bangladesh is 2.72 mm/yr whereas, global average found 5.87 mm/yr which was about two times more than Bangladesh average. Khepupara was the height increasing rate by 13.32 mm/yr and Sonapur was the lowest decreasing rate by -11.59 mm/yr. Three regions, Eastern rate 2.80 mm/yr, Central rate -1.04 mm/yr and Western rate 6.39 mm/yr found. Eastern and Western region were higher rate than Central region whereas, Central region found negative in trend (Figure 10.21).

Except Teknaf, the trend in Bangladesh average only 1.63 mm/yr, this rate was very little compare to the global average. The Ministry of Environment and Forests (MoEF, 2009) has prepared NAPA as a response to the decision of the Seventh Session of the Conference of the Parties (COP7) of the United Nations Framework Convention on Climate Change (UNFCCC). The observed trend in sea level rise used in that document was cited from the study conducted by the SAARC Meteorology Research Centre in 2003. The study (SMRC, 2003) found that the tidal level in Hiron Point, *Char* Changa and Cox's Bazar rose by 4.0 mm/yr, 6.0 mm/yr and 7.8 mm/yr respectively, observing tidal gauge record of 22 years from 1977-1998.

In this study the rise in Global Mean Sea Level (GMSL) for the period of 2025-2100, based on process-based models is likely to be in the range of 10.33-53.33 cm for RCP 4.5, 10.00-55.33 cm for RCP 6.0 and 10.00-75.00 for RCP 8.5. Currently there is no enough evidence to evaluate the probability of specific levels above the likely range. If the carbon dioxide concentration CO_2 level decrease worldwide then mid, low and high sensitivity also be decrease and will be stand in a sensible level. World Bank (2000) showed 10 cm, 25 cm and 1 m rise in sea level by 2020, 2050 and 2100; affecting 2%, 4% and 17.5% of total land mass respectively, which is almost similar in global scenario (Table 10.5). Milliman *et al.*, (1989; cited in Frihy, 2003) reported 1.0 cm per year sea level rise in Bangladesh. UNEP (1989) showed 1.5 m sea level rise in Bangladesh coast by 2030, affecting 22,000 km^2 (16% of total landmass) area with a population of 17 million (15% of total population) affected.

11.3.5.2 Projection of Future Sea Level Rise (RCM Data)

Bangladesh sea level rise trend is half of global average, but it has a great importance for its low laying country. Previous study and current state of knowledge is not a negligible measurement. If we contain that 2015 is the base year and its trend go through the same rate then in the year 2025, we will be reached 27.20 mm from 2015, and 2050, 2075 and 2100 will be raised by 95.20 mm, 163.20 mm and 231.20 mm respectively. On the other hand, if we calculate the global rate, in the year 2025 world will be reached 63.90 mm from 2015, and 2050, 2075 and 2100 will be raised by 223.65 mm, 383.40 mm and 543.15 mm respectively. For this calculation some anomalies like discontinuous of year, year gap, variety source of data, tidal surge, tsunami and seasonal flood level were not considered here, this anomaly unevenly may increase or imbalance tidal level around all the tidal stations. Above all, this scenario represent that Bangladesh will face a critical circumstance in the next century. According to the (BBS,

2011) census track, without river coastal area had 39937.80 km^2 area. Subtracting the Shuttle Radar Topography Mission (SRTM) Digital Elevation Model (DEM) satellite imagery by 2011 census track, sea level rise data were measured hypothetically if sea level rise 1 to 5 meter then what scenario will be in the coastal area. Using this measurement five sets of maps produced to visualize the future condition about sea level rise. Calculation showed that, in the year 2380 we will be reached 1 m sea level rise, and if we want to see 5 meters sea level rise in Bangladesh, we should have to wait 362 years from now.

Though all the forecast is predicted by simulation, but it will not be wise to think that sea level will not rise at all. If the global worming or greenhouse gas (GHG) emission will not be reduced near future, then this scenario will be unchanged. This change is not only the precaution for Bangladeshi people but also the global people because it is not our local issue now, who have contained coastal territory in the globe must have to remember that this scenario will also be happened to the other territory equally.

11.4 Recommendations

Constructing measures in relation to sea level rise is important in order to comprehensive analysis depends on geographic, physical and economic condition in coastal area of Bangladesh. Bangladesh country level institutions are the focus level to ensure the factual level of measurement to provide state of art, knowledge and information. Bangladesh need to update surveyed materials, instruments and methods carried out more reliable information. Such surveys will need to be followed by relevant studies to identify, test and cost appropriate intervention measures for individual areas, including institutional and political measures that might be needed to implement and support identified measures (Brammer, 2010). Government must provide more budgets to implement local level stations with relation to the local people. Engaging local people and provide updated information for them to ensure the gap which can be provide the acceleration about the update information. Brammer (2004) state that, the geographical diversity and complexity of Bangladesh’s coastal zone and the multidisciplinary nature of many of the mitigation measures identified suggest that a comprehensive Integrated Coastal Zone Management Plan (ICZMP) is needed, along the lines of the Dutch delta management plan, with appropriate staffing to prepare, operate and oversee it.[14]

[14] Ideally, a comprehensive regional water management plan for the Ganges-Brahmaputra-Meghna (GBM) catchment area is needed. However, to-date, India has not been prepared to support such a plan or to share hydrological data with Bangladesh, and Bangladesh has needed to prepare flood protection plans independently Brammer (2004)

Government even though already made much embank along the riverside, adjoining to the inland margin such barriers should be built for upcoming sea level rise, as well as saline water tolerable tree plantation like Sundarbans. Future sea-level rise and climate change (Brammer, 2013) merely add urgency to the existing need for a national plan to implement relevant measures to safeguard, maintain and accelerate economic and social development in the country in pace with its growing population and its exposure to existing environmental hazards (Brammer, 2010). The range of studies needed in order to formulate such an integrated development plan in Bangladesh the country in which intervention to meet current and future development needs is perhaps most urgently required could provide a model for such planning in other countries with low-lying coastal areas (Brammer, 2014). Climate change and sea level rise is not only the problem in Bangladesh but a global problem. Government should keep in mind that this problem will continue in future so, they should train up to avoid this situation in local and community level for upcoming or uncertain event and other hazards.

References

"Sea Level Rise Key Message Third National Climate Assessment". National Climate Assessment. (accessed on 25-06-2014)

Aedla, R., Dwarakish, G.S. and Reddy, D.V., 2015. Automatic shoreline detection and change detection analysis of netravati-gurpurrivermouth using histogram equalization and adaptive thresholding techniques. Aquatic Procedia, 4: 563-570.

Agrawala, S., Ota, T., Ahmed, A.U., Smith, J., Aalst, M.V., 2003. Development and Climate Change in Bangladesh: Focus on Coastal Flooding and the Sundarbans. OECD Publication COM/ENV/EPOC/DAC (2003)3/FINAL.

Ahmad, Q.K., Warrick, R.A., Ericksen, N.J. and Mirza, M.M.Q., 1996. The implications for climate change for Bangladesh: A synthesis, In R.A. Warrick and Q.K. Ahmad (eds.), The implications of climate and sea-level change for Bangladesh, Kluwer Academic Publishers, Dordrecht, The Netherlands.

Ahmed, A.U., 2005a. Adaptation Options for Managing Water-Related Extreme Events Under Climate Change Regime: Bangladesh Perspectives. In Mirza, M.M.Q., and Ahmad, Q.K. (eds). Climate Change and Water Resources in South Asia. Pp. 255-278. A.A. Balkema Publishers, Leiden, The Netherlands.

Ahmed, A.U., 2005b. Toward integrating adaptation to climate change in current policy regime: perspectives on Bangladesh's water resources and associated sectors. Asia Pacific Journal on Environment and Development. Vol. 12, No.1, Pp. 35 -54.

Ahmed, S.M.U., Hoque, M.M. and Hussain, S., 1992. Floods in Bangladesh: A hydrological analysis, Final Report No. R01/92, IWFM, BUET.

Alam, M.S. and Uddin, K., 2013. A Study of Morphological Changes in the Coastal Areas and Offshore Islands of Bangladesh Using Remote Sensing. American Journal of Geographic Information System. 2(1): 15-18.

Allison; et al., 2009. "The Copenhagen Diagnosis, 2009: Updating the World on the Latest Climate Science".

Anders Levermann, Peter U. Clark, Ben Marzeion, Glenn A. Milne, David Pollard, Valentina Radic, and Alexander Robinson, 2013. "The multimillennial sea-level commitment of global warming". doi:10.1073/pnas.1219414110.

Anders, F.J., and Byrnes, M.R., 1991. Accuracy of shoreline change rates as determined from maps and aerial photo-graphs: Shore and Beach, v. 59, pp. 17-26. Apl Technical Digest. 21(1): 148-154.

Bagdanaviciut e, I., Kelpsaite, L., Soomere, T., 2015. Multi-criteria evaluation approach to coastal vulnerability index development in micro-tidal low-lying areas. Ocean. Coast. Manag. 104, 124e135.

Bhattacharyya, G.K. and Johnson, R.A., 1977. Statistical concepts and methods, John Wiley, New York.

Bird, E.C.F., 1993. Submerging Coasts: The Effects of a Rising Sea Level on Coastal Environments. John Wiley & Sons Ltd., Chichester. Boruff, B.J., Emrich, C., Cutter, S.L., 2005. Erosion hazard.

Blankespoor, B., S. Dasgupta and B. Laplante, 2014. Sea-level rise and coastal wetlands. Ambio, 43(8): 996-1005.doi:10.1007/s13280-014.

Boruff, B.J., Emrich, C., Cutter, S.L., 2005. Erosion hazard vulnerability of US coastal counties. J. Coast. Res. 21, 932e942.

Brammer, H., 1989. Monitoring the Evidence of the Greenhouse effect and its Impact on Bangladesh. In Moudud, H. J., Rashid, H. E., Rahman, A. A., Hossain, M., (eds). The Greenhouse Effect and Coastal Area of Bangladesh. Proceedings of an International Conference held in Dhaka, Bangladesh, 5th March 1989.

Brammer, H., Asaduzzaman, M., Sultana, P., 1996. Effects of Climate and Sea-Level Changes on the Natural Resources of Bangladesh. In Warrik, R.A. and Ahmad, Q.K. (eds). The Implications of Climate and Sea-Level Change for Bangladesh. Pp. 143-204. Kluwer Academic Publishers. The Netherlands.

Brammer, H., 2004. Can Bangladesh be Protected from Floods? University Press Ltd, Dhaka.

Brammer, H., 2010. After the Bangladesh Flood Action Plan: looking to the future. Environ. Hazards 9 (1), 118-130.

Brammer, H., 2012. The Physical Geography of Bangladesh. University Press Ltd, Dhaka.

Brammer, H., 2013. Climate Change, Sea-level Rise and Development in Bangladesh, University Press Ltd, Dhaka.

Brammer, H., 2014. Bangladesh's dynamic coastal regions and sea-level rise. Climate Risk Management (1), 51-62.

Broadus, J. et. al., 1986. 'Rising Sea Level and Damming of Rivers: Possible Effects in Egypt and Bangladesh', in Titus, J. (ed.), Effects of Changes in Stratospheric Ozone and Global Climate Volume 4: Sea Level Rise, United Nations Environment Program and the U.S. Environmental Protection Agency, pp. 165-189.

Bryan, G.H., 1907. Thermodynamics. An Introductory Treatise dealing mainly with First Principles and their Direct Applications, B.G. Teubner, Leipzig, page 3.

Callender, G.S., 1938. The artificial production of carbon dioxide and its influence on temperature. Quart. J. Roy. Meteorol. Soc., 64, 223-240.

Carbon Dioxide Information Analysis Center, Environmental Sciences Division, Oak Ridge National Laboratory, Tennessee, United States. Available from https://data.worldbank.org/indicator/EN.ATM.CO2E.PC?contextual=region&end=2014&locations=BD&start=1960&type=shaded&view=chart

Carter, R.W.G., 1988. Coastal Environment: An Introduction to the Physical, Ecological and Cultural Systems of Coastlines. Academic Press, London.

Chander, G., B.L. Markham and D.L. Helder, 2009. Summary of current radiometric calibration coefficients for Landsat MSS, TM, ETM+, and EO-1 ALI sensors. Remote Sensing of Environment 113: 893-903.

Churchs, John; Clark, Peter. "Chapter 13: Sea Level Change-Final Draft Underlying Scientific-Technical Assessment". climatechange2013.org. IPCC Working Group I. Retrieved January 21, 2015.

Clarke, L. et. al., 2007. Scenarios of Greenhouse Gas Emissions and Atmospheric Concentrations. Sub-report 2.1A of Synthesis and Assessment Product 2.1 by the U.S. Climate Change Science Program and the Subcommittee on Global Change Research. Department of Energy, Office of Biological & Environmental Research, Washington, 7 DC., USA, 154 pp.

IPCC, 2014. Climate Change 2014 Synthesis Report Fifth Assessment Report, AR5 (Report).

Climate Change Cell, 2009. Characterizing long-term changes of Bangladesh climate in context of agriculture and irrigation, Department of Environment, Dhaka.

CMIP5 Coupled Model Intercomparison Project. WCRP World Climate Research Program. (IPCC AR5 WGI, page 22).

Coleman, J.M., 1981. Deltas: processes of deposition and models for exploration (2nd ed). Minneapolis: Burgess.

Coppin, P.; Jonckheere, I.; Nackaerts, K.; Muys, B.; Lambin, E., 2004. Digital change detection methods in ecosystem monitoring: A review. Int. J. Remote Sens. 25, 1565-1596.

Crowell, M., Leatherman, S.P., and Buckley, M.K., 1991. Historical shoreline change-Error analysis and mapping accuracy: Journal of Coastal Research, v. 7, pp. 839-852.

Devoy, R.J., 2008. Coastal vulnerability and the implications of sea-level rise for Ireland. J. Coast. Res. 325e341.

Dewan, A., Corner, R., Saleem, A., Rahman, M.M., Haider, M.R., Rahman, M.M. and Sarker, M.H., 2017a. Assessing channel changes of the Ganges-Padma River system in Bangladesh using Landsat and hydrological data. Geomorphology, 276, 257-279.

Dewan, A., Hossain, M.F., Rahman, M.M., Yamane, Y., and Holle, R.L., 2017b. Recent Lightning-Related Fatalities and Injuries in Bangladesh. Weather Clim Soc 9:575–589. https://doi.org/10.1175/WCAS-D-16-0128.1

Dewan, A., Ongee, E.T., Rafiuddin, M., Rahman, M.M. and Mahmood, R., 2017c. Lightning activity associated with precipitation and CAPE over Bangladesh. Int. J. Climatol. doi:10.1002/joc.5286.

Dewan, A., Ongee, E.T., Rahman, M.M., Mahmood, R. and Yamane, Y., 2017d. Spatial and temporal analysis of a 17-year lightning climatology over Bangladesh with LIS data Theor Appl Climatol. https://doi.org/10.1007/s00704-017-2278-3.

DOE, 1993. Assessment of the Vulnerability of Coastal Areas to Sea Level Rise and Other Effects of Global Climate Change, Pilot Study Bangladesh. Department of Environment, Government of Bangladesh.

Doukakis, E., 2005. Coastal vulnerability and risk parameters. Eur.Water 11/12, 3e7. Dube, S.K., Sinha, P.C., Roy, G.D., 1986. Numerical simulation of storm surges in Bangladesh using a bay-river coupled model. Coast. Eng. 10, 85e101.

Dummett, M., 2008. Bangladesh landmass 'is growing'. Dhaka: BBC. Retrieved August 12, 2016. Available from http://news.bbc.co.uk/2/hi/south_asia/7532949.stm

Emran, A., Rob, M.A., Kabir, M.H. and Islam, M.N., 2016. Modelling spatio-temporal shoreline and areal dynamics of coastal island using geospatial technique. Modelling Earth System Environment. 2(4): 1-11.

Ericson, J.P., C.J. Vörösmarty, S.L. Dingman, L.G. Ward and M. Meybeck, 2006. "Effective sea-level rise and deltas: Causes of change and human dimension implications." Global and Planetary Change 50(1): 63-82.

European Environmental Agency. Available from https://www.eea.europa.eu/data-and-maps/indicators/sea-level-rise-3/assessment (Access on 10-08-2018)

Fischlin; et al., 2007. "Section 4.4.9: Oceans and shallow seas-Impacts", in IPCC AR4 WG2 2007, Chapter 4: Ecosystems, their Properties, Goods and Services, p. 234.

Fitzgerald A., 2012. Methodological Approach and Design. In: Fitzgerald A. (eds) Science in Primary Schools. Sense Publishers, Rotterdam. from Satellite Images. Proceedings of Coastal Engineering. JSCE. 3: 41-45.

Fujino, J., R. Nair, M. Kainuma, T. Masui, Y. Matsuoka, 2006. Multi-gas mitigation analysis on stabilization scenarios using AIM global model. Multigas Mitigation and Climate Policy. The Energy Journal Special Issue.

NOAA, 2017. Global and regional sea level rise scenarios for the united states (NOAA technical report nos co-ops 083 ed.) (accessed on 25-01-2017).

Gore, A., 2009. An Inconvenient Truth. Rabowsky, London.

Gornitz, V.M., 1990. Vulnerability of the East Coast, USA to future sea level rise. J. Coast. Res. 9, 201e237.

Gornitz, V.M., Daniels, R.C., White, T.W., Birdwell, K.R., 1994. The development of a coastal risk assessment database: vulnerability to sea-level rise in the U.S. southeast. J. Coast. Res. 327e338.

Hale, S.R.; Rock, B.N., 2003. Impact of topographic normalization on land-cover classification accuracy. Photogramm. Eng. Remote Sens. 69, 785-791.

Han, W., G.A. Meehl, B. Rajagopalan, J.T. Fasullo, A. Hu, J. Lin, W.G. Large, J.-w. Wang, X.-W. Quan and L. L. Trenary, 2010. "Patterns of Indian ocean sea-level change in a warming climate." Nature Geoscience 3(8): 546-550.

Hanebuth, T.J.J., Kudrass, H.R., Linstädter, J., Islam, B., Zander, A.M., 2013. Rapid coastal subsidence in the Central Ganges–Brahmaputra Delta (Bangladesh) since the 17th century deduced from submerged salt-producing kilns. Geology 41, 987-990.

Hansen, J. et al., 1981. "Climate impact of increasing atmospheric carbon dioxide". Science. 231: 957-966. doi:10.1126/science.213.4511.957.

Hapke, C.J., and Reid, D., 2007. National Assessment of Shoreline Change, part 4-Historical coastal cliff retreat along the California coast: U.S. Geological Survey Open-File Report 2007-1133. Available from http://pubs.usgs.gov/of/2007/1133

Hapke, C.J., Reid, D., Richmond, B.M., Ruggiero, P., and List, J., 2006. National Assessment of Shoreline Change part 3- Historical shoreline change and associated coastal land loss along sandy shorelines of the California coast: U.S. Geological Survey Open-File Report 2006-1219. Available from http://pubs.usgs.gov/of/2006/1219

Hegde, A.V., Reju, V.R., 2007. Development of coastal vulnerability index for Mangalore coast, India. J. Coast. Res. 23, 1106e1111.

Helsel, D.R. and Hirsch, R.M., 2002. Statistical methods in water resources, U.S.G.S.

Hirt, C.; Filmer, M.S.; Featherstone, W.E., 2010. "Comparison and validation of recent freely-available ASTER-GDEM ver1, SRTM ver4.1 and GEODATA DEM-9S ver3 digital elevation models over Australia". Australian Journal of Earth Sciences. 57 (3): 337-347. Bibcode:2010AuJES.57.337H. doi:10.1080/08120091003677553.

Houghton, J., 2009. Global Warming. CUP, Cambridge.

http://amsglossary.allenpress.com/glossary/ (accessed on 17-11-2017).

http://badc.nerc.ac.uk/view/badc.nerc.ac.uk_ATOM_ACTIVITY_3ec0d1c6-4616-11e2- 9a3-00163e251233 (accessed on 10-08-2017).

https://en.wikipedia.org/wiki/Subsidence (accessed on 10-08-2018).

http://disc.sci.gsfc.nasa.gov/daac-bin/FTPSubset.pl (accessed on 01-01-2017).

http://en.banglapedia.org/index.php?title=Rainfall (accessed on 10-08-2017).

http://glossary.ametsoc.org/wiki/Mean_temperature (accessed on 10-08-2017).

http://spatial-analyst.net/ILWIS/htm/ilwisapp/correlation_matrix_functionality.htm (accessed on 15-05-2017).

http://www.climsystems.com (installed 05-07-2016)

http://www.hse.gov.uk/temperature/law.htm (accessed on 21-08-2018).

http://www.psmsl.org/data/ (accessed on 01-01-2017).

https://earthexplorer.usgs.gov (accessed on 01-01-2017).

https://glovis.usgs.gov (accessed on 01-01-2017).

https://uhslc.soest.hawaii.edu/data/?rq#uh138a (accessed on 01-01-2017).

https://www.alzheimer-europe.org/Research/Understanding-dementia-research/Types-of-research/The-four-main-approaches (accessed on 21-08-2018).

Hurrell, J.W., J.J. Hack, D. Shea, J.M. Caron, and J. Rosinski, 2008. A New Sea Surface Temperature and Sea Ice Boundary Dataset for the Community Atmosphere Model. J. Climate, 21, 5145–5153. doi: 10.1175/2008JCLI2292.1.

IPCC, 2007. AR4, Glossary P-Z: "Projection", in IPCC AR4 WG1.

IPCC, 2007. Topic 3, Section 3.2.1: 21st century global changes, p. 45, in IPCC AR4 SYR.

IPCC, 2014. The IPCC Fifth Assessment Report: What's in it for South Asia. Retrieved August 12, 2016. Available from http://cdkn.org/wp-content/uploads/2014/04/CDKN-IPCC-Whats-in-it-for- South-Asia-AR5.pdf

Islam M.A., Mitra D., Dewan A. and Akhter S.H., 2016. Coastal multi-hazard vulnerability assessment along the Ganges deltaic coast of Bangladesh-A geospatial approach, Ocean & Coastal Management 127,1-15.

Islam, M. A., M. S. Hossain and S. Murshed, 2015. Assessment of Coastal Vulnerability Due to Sea Level Change at Bhola Island, Bangladesh: Using Geospatial Techniques. Journal of Indian Society of Remote Sensing. 43(3): 625-637. doi:10.1007/s12524-014-0426-0.

Islam, T. and Neelim, A., 2010. Climate Change in Bangladesh: A closer look into temperature and rainfall data, The University Press Limited.

J E Hansen, 2007. "Scientific reticence and sea level rise". Environmental Research Letters. IOPScience. 2: 024002. doi:10.1088/1748-9326/2/2/024002.

Kaplan, L. D., 1960. The influence of carbon dioxide variations on the atmospheric heat balance, Tellus, 12, 204-208.

Karim M.F, Mimura N., 2008. Impacts of climate change and sea-level rise on cyclonic storm surge floods in Bangladesh. Glob Environ Chang 18:490-500.

Karl, TR; et al., eds., 2009. Global Climate Change Impacts in the United States. 32 Avenue of the Americas, New York, NY 10013-2473, USA: Cambridge University Press. pp. 22-24. ISBN 978-0-521-14407-0. Retrieved 2011-04-28.

Kausher, A., Kay, R.C., Asaduzzaman, M., Paul, S., 1993. Climate Change and Sea-level Rise: The Case of the Coast. Briefing Ducument No. 6, Bangladesh Unnayan Parishad (BUP), Dhaka.

Khan, N.I. (Ed.), 1977. Bangladesh District Gazetteers: Noakhali. Gov't press, Dhaka.

Cummins, P.E., 2007. The potential for giant tsunamigenic earthquakes in the northern Bay of Bengal. Nature 449 (6), 75-78.

Kondratiev, K., and H. I. Niilisk, 1960. On the question of carbon dioxide variation in the atmosphere, Geofis Pura. Appl., 46, 216-230.

Kreft, Sönke; David Eckstein, David; Melchior, Inga, 2016. Global Climate Risk Index 2017. Bonn: Germanwatch e.V. ISBN 978-3-943704-49-5.

Kuehl, S.A., Hariu, T.M, and Moore, W.S., 1989. Shelf sedimentation off the Ganges-Brahmaputra river system: Evidence for sediment bypassing to the Bengal Fan. Geology 17: 1132-1135.

Kumar, A., Narayana, A.C., Jayappa, K.S., 2010a. Shoreline changes and morphology of spits along southern Karnataka, west coast of India: A remote sensing and statistics-based approach. Geomorphol. Geomor. 120, 133e152.

Kumar, A.A., Kunte, P.D., 2012. Coastal vulnerability assessment for Chennai, east coast of India using geospatial techniques. Nat. Hazards 64, 853e872.

Kumar, T.S., Mahendra, R.S., Nayak, S., Radhakrishnan, K., Sahu, K.C., 2010b. Coastal Vulnerability Assessment for Orissa State, East Coast of India. J. Coast. Res. 263, 523e534.

Kunte, P.D., Jauhari, N., Mehrotra, U., Kotha, M., Hursthouse, A.S., Gagnon, A.S., 2014. Multi-hazards coastal vulnerability assessment of Goa, India using geospatial techniques. Ocean. Coast. Manag. 95, 264e281.

Mahapatra, M., Ramakrishnan, R., Rajawat, A.S., 2015. Coastal vulnerability assessment using analytical hierarchical process for South Gujarat coast, India. Nat. Hazards 76, 139e159.

Makarau, A.; Richter, R.; Müller, R.; Reinartz, P., 2014. Haze detection and removal in remotely sensed multispectral imagery. IEEE Trans. Geosci. Remote Sens. 52, 5895-5905.

Markham, B.L., S. Goward, T. Arvidson, J. Barsi and P. Scaramuzza, 2006. Landsat-7 long-term acquisition plan radiometry-Evolution over time. Photogrammetric Engineering and Remote Sensing 72:1129-1135.

Mart´ınez, M.D., Serra, C., Burgue~no, A., Lana, X., 2009. Time trends of daily maximum and minimum temperatures in Catatonia (NE Spain) for the period 1975-2004. Int. J. Climatol. 30 (2), 267-290. Available from http://dx.doi.org/10.1002/ joc.1884.

McFeeters, S. K., 1996. The use of Normalized Difference Water Index (NDWI) in the delineation of open water features. International Journal of Remote Sensing 17(7):1425-1432.

Meehl, G.A. et. al., 2007. Global climate projections. In: Solomon, S. et. al., (Eds.), Climate Change 2007: The Physical Science Basis, Contribution of Working Group I to the Fourth

Assessment Report of the Intergovernmental Panel on Climate Change. Cambridge University Press, Cambridge, UK.

Miller, F., 1963. On the influence of changes in air on the radiation balance of the earth's Surface and on the climate, J. Geophys Res., 68, 3877-3886.

Miller, G. T., 2004. Living in the Environment. Brooks/ Cole-Thomson Learning, USA.

Milliman, J. D., Rutkowski, C., and Meybeck, M., 1995. River discharge to the sea: a global river index (GLORI). Texel: NIOZ, 125 pp.

Minimum Temperature. A Dictionary of Plant Sciences. Available from http://www.encyclopedia.com (accessed on 17-11-2017).

Mitchell, T.D., 2003. Pattern Scaling: An Examination of the Accuracy of the Technique for Describing Future Climates. Climatic Change, 60(3), 217-242. 10.1023/a:1026035305597.

MoEF, 2005. National adaptation program of action. Final Report, Ministry of Environment and Forest, Government of Bangladesh.

MoEF, 2009. Bangladesh Climate Change Strategy and Action Plan 2009, Ministry of Environment and Forests, Government of the People's Republic of Bangladesh, Dhaka, Bangladesh. Xviii+76pp.

Mondal, M.S. and Wasimi, S.A., 2004. Impact of climate change on dry season water demand in the Ganges Delta of Bangladesh, In Contemporary Environmental Challenges.

Mondal, M.S., Nasrin, F., Zaman, S. and Hossain, M.M.A.H., 2009. Long-term changes in bright sunshine duration in Bangladesh and its effects on crop evapotranspiration, Proceedings of the second International Conference on Water and Flood Management, Organized by Institute of Water and Flood Management, held during 15-17 March, Dhaka, pp. 185-194.

Moore, L.J., 2000. Shoreline mapping techniques: Journal of Coastal Research, v. 16, pp. 111-124.

Morita et al., 2001. Chap. 2: Greenhouse Gas Emission Mitigation Scenarios and Implications, Section 2.2.1: Introduction to Scenarios, in IPCC TAR WG3 2001.

Morton, R.A., and Miller, T.L., 2005. National Assessment of Shoreline Change-part 2 Historical shoreline changes and associated coastal land loss along the U.S. southeast Atlantic coast: U.S. Geological Survey Open-file Report 2005-1401. Available from http://pubs.usgs.gov/of/2005/1401.

Morton, R.A. et. al., 2004. National Assessment of Shoreline Change- part 1 Historical shoreline changes and associated coastal land loss along the U.S. Gulf of Mexico: U.S. Geological Survey Open-File Report 2004-1043. Available from http://pubs.usgs.gov/of/2004/1043.

Moss, M., et al., 2010. The next generation of scenarios for climate change research and assessment, Nature, doi:10.1038/nature08823.

Murali, R.M., Ankita, M., Amrita, S., Vethamony, P., 2013. Coastal vulnerability assessment of Puducherry coast, India, using the analytical hierarchical process. Nat. Hazards. Earth Syst. Sci. 13, 3291e3311.

Nageswara Rao, K., Subraelu, P., Venkateswara, Rao T., Hema Malini, B., Ratheesh, R., Bhattacharya, S., Rajawat, A.S., Ajai, 2008. Sea-level rise and coastal vulnerability: an assessment of Andhra Pradesh coast, India through remote sensing and GIS. J. Coast. Conserv. 12, 195e207.

Nasrin, F. and Mondal, M.S., 2011. Long-term changes in climatic variables in Bangladesh and their combined effects on irrigation water requirement in the dry season, Proceedings of the Third International Conference on Water and Flood Management, Organized by Institute of Water and Flood Management, held during 8-10 January, Dhaka, pp. 899-906.

Nicholls, R.J., Hoozemans, F.M.J., Marchand, M., 1999. Increasing flood risk and wetland losses due to global sea-level rise: regional and global analyses, Global Environmental Change 9, S69-S87.

Noerdlinger, P.D. and Brower, K.R., 2007. The melting of floating ice raises the ocean level. Geophysical Journal International, 170(1), 145-150.

Pendleton, E.A., Thieler, E.R., Williams, S.J., 2004. Coastal Vulnerability Assessment of Cape Hettaras National Seashore (CAHA) to Sea Level Rise. USGS Open File Report 2004-1064. Available from http://pubs.usgs.gov/of/2004/1064/images/pdf/caha.pdf (accessed on 30-08-2013).

Pippard, A.B. 1957/1966, p. 18.

Plass, G.N., 1956. The influence of 15-micron carbon dioxide band on the atmospheric infrared cooling rate, Quart. J. Roy. Meteorol., Soc., 82, 310-324.

PSMSL (Permanent Service for Mean Sea Level). Available from https://www.psmsl/data/obtaining

Rahman, A. and Alam, M., 2003. Mainstreaming adaptation to climate change in Least Developed Countries (LDCs), Working Paper 2: Bangladesh Country Case Study, IIED, London, UK.

Rahman, M.M., 2013. Temporal Change Detection of Vegetation Coverage in Patuakhali Coastal Area of Bangladesh Using GIS & Remotely Sensed Data, International Journal of Geomatics and Geosciences, 4(1): 36-46. Available from http://www.ipublishing.co.injggsarticlesvolfourEIJGGS4005.pdf

Rahman, M.R., Salehin, M. and Matsumoto, J., 1997. Trend of monsoon rainfall pattern in Bangladesh, Bangladesh J. Water Resour. Resear., 14-18, 121-138.

Raper, S.C.B., Gregory, J.M., and Osborn, T.J., 2001. Use of an upwelling-diffusion energy balance climate model to simulate and diagnose A/OGCM results. Climate Dynamics, 17(8): 601-613. 10.1007/pl00007931.

Rasid, H., and Paul, B.K., 1987. Flood problems in Bangladesh: Is there an indigenous solution? Environ Manage 11(2): 155-173.

Riahi K, Gruebler A, Nakicenovic N., 2007. Scenarios of long-term socio-economic and environmental development under climate stabilization. Technol Forecast Soc Chang 74(7): 887-935.

Rogelj, J. et. al., 2012. Global warming under old and new scenarios using IPCC climate sensitivity range estimates, 2012, Nature Climate Change, DOI: 10.1038/NCLIMATE1385.

Roy, D.P. et. al., 2014. Landsat-8: Science and product vision for terrestrial global change research. Remote Sensing of Environment 145: 154-172.

Ruosteenoja, K., Tuomenvirta, H., & Jylhä, K., 2007. GCM-based regional temperature and precipitation change estimates for Europe under four SRES scenarios applying a super-ensemble pattern-scaling method. Climatic Change, 81(0): 193-208. 10.1007/s10584-006-9222-3.

Sarker, M.H., Choudhury, G.I., Akter, J., Hore, S.K., 2013. Bengal Delta Not Subsiding at a Very High Rate. Available from http://www.cegisbd.com/pdf/bengaldelta.pdf

Sarwar, M.M. and C. Woodroffe, 2013. Rates of shoreline change along the coast of Bangladesh. Journal of Coastal Conservation. 17: 515-526.

Savage, R.J., Foster, E.R., 1989. Historical shoreline changes in southeast Florida. In: Magoon, O.T., Converse, H., Miner, D., et al. (Eds.), Coastal Zone'89, American Society of Civil Engineers 5, pp. 4406e4433.

Savage, R.J., Foster, E.R., 1989. Historical shoreline changes in southeast Florida. In: Magoon, O.T., Converse, H., Miner, D., et al. (Eds.), Coastal Zone'89, American Society of Civil Engineers 5, pp. 4406e4433.

Scheffer, M., V. Brovkin, and P. Cox, 2006. Positive feedback between global warming and atmospheric CO_2 concentration inferred from past climate change, Geophys. Res. Lett., 33 L10702, doi: 10.1029/2005GL025044.

Schwartz, M. (Ed.), 2006. Encyclopedia of coastal science. Springer Science & Business Media.

Shahid, S., 2010. Rainfall variability and the trends of wet and dry periods in Bangladesh. Int. J. Climatol., 30: 2299–2313. doi:10.1002/joc.2053.

Shaw, J., Taylor, R.B., Forbes, D.L., Ruz, M.-H., Solomon, S., 1998. Sensitivity of the Canadian coast to sea-level rise. Geol. Surv. Can. Bull. 505 Available from http://dx.doi.org/10.4095/210075

Shennan, I., 2013. Sea Level Studies: Overview. In: Elias SA, Mock J (eds) Encyclopedia of Quaternary Science (Second Edition). Elsevier, Amsterdam, Netherlands, pp 369-376. ISBN 978-0-444-53643-3.

Shibly, A. M. and S. Takewaka, 2012. Morphological Changes along Bangladesh Coast Derived from Satellite Images. Proceedings of Coastal Engineering. JSCE. 3: 41-45.

Sidker, T., 2010. September. The impacts of climate change on the coastal belt of Bangladesh: An investigation of risks & adaptations on agricultural sector. In Proceedings of international conference on environmental aspects of Bangladesh (ICEAB10).

Smith, S.J. and T.M.L. Wigley, 2006. Multi-Gas Forcing Stabilization with the MiniCAM. Energy Journal (Special Issue #3) pp 373-391.

SMRC, 2003. The vulnerability assessment of the SAARC Coastal Region due to sea level rise: Bangladesh case study. Dhaka, SAARC Meteorological Research Center.

Song, C.; Woodcock, C.E.; Seto, K.C.; Lenney, M.P.; Macomber, S.A., 2001. Classification and change detection using Landsat TM data: When and how to correct atmospheric effects? Remote Sens. Environ. 75, 230-244.

Stanley, D.J., Hait, A.K., 2000. Holocene depositional patterns, neotectonics and Sundarban mangroves in the western Ganges–Brahmaputra delta. J. Coastal Res. 16 (1), 26-39.

Steckler, M.S., Akter, S.H., Seeber, L., 2008. Collision of the Ganges-Brahmaputra delta with the Burma arc: implications for earthquake hazard. Earth Planet. Sci. Lett. 273, 367-378.

Syvitski, J.P.M. et. al., 2009. Sinking deltas due to human activities. Nat. Geosci. 2, 681-686.

Szlafsztein, C., Sterr, H., 2007. A GIS-based vulnerability assessment of coastal natural hazards, state of Par_a, Brazil. J. Coast Conserv. 11, 53e66.

Taguchi, Y., et. al., 2013. Detecting Recent Coastline Changes Around the Urir Char Island at the Eastern Part of Meghna Estuary Using PALSAR Images. In: Proceedings of the 4th International onference on Water and Flood Management.

Tan, B.; Masek, J.G.; Wolfe, R.; Gao, F.; Huang, C.; Vermote, E.F.; Ederer, G., 2013. Improved forest change detection with terrain illumination corrected Landsat images. Remote Sens. Environ. 136, 469-483.

Thieler, E.R., and Danforth, W.W., 1994. Historical shore-line mapping (1)-Improving techniques and reducing positioning errors: Journal of Coastal Research, v. 10, p. 549-563.

Thieler, E.R., Hammer-Klose, E.S., 1999. National Assessment of Coastal Vulnerability to Sea-level Rise: Preliminary Results for the U.S. Atlantic Coast. United States Geological Survey (USGS), Woods Hole, Massachusetts.

Thieler, E.R., Himmelstoss, E.A., Zichichi, J.L., and Ergul, Ayhan, 2009. Digital Shoreline Analysis System (DSAS) version 4.0-An ArcGIS extension for calculating shoreline change: U.S. Geological Survey Open-File Report 2008-1278. *current version 4.3.

Unnikrishnan, A.S. and Shankar D., 2007. Are sea-level-rise trends along the coasts of north Indian Ocean coasts consistent with global estimates? Global and Planetary Change, 57, 301-307.

van Beers, W.C.M. and Kleijnen, J.P.C., 2004. Kriging interpolation in simulation: A survey, Proceedings of the 2004 Winter Simulation Conference, 5-8 December, Washington DC.

van Vuuren, D. et. al., 2007. Stabilizing greenhouse gas concentrations at low levels: an assessment of reduction strategies and costs. Climatic Change, doi:10.1007/s/10584-006-9172-9.

Vanonckelen, S.; Lhermitte, S.; Van Rompaey, A., 2013. The effect of atmospheric and topographic correction methods on land cover classification accuracy. Int. J. Appl. Earth Observ. Geoinf. 24, 9-21.

Warrick, R.A., Bhuiya, A.H., Mirza, M.Q., 1993. Climate Change and Sea-level Rise: The Case of the Coast. Briefing Document No. 6, Bangladesh Unnayan Parishad (BUP), Dhaka.

Warrick, R.A., Bhuiya, A.H., Mitchell, W.M., Murty, T.S., Rasheed, K.B.S., 1996. Sea level changes in the Bay of Bengal. In: Warrick, R.A., Ahmad, Q.K. (Eds.), The Implications of Climate and Sea-level Change for Bangladesh. Kluwer Academic Publishers, Dordrecht.

Werle, D., T. Martin and K. Hasan, 2000. Flood and Coastal Zone Monitoring in Bangladesh with Radarsat Scan SAR: Technical Experience and Institutional Challenges. Johns Hopkins.

Whetton P.H., K.L. McInnes, R.N. Jones, K.J. Hennessy, R. Suppiah, C.M. Page, J. Bathols, and P.J. Durack, 2005: Australian Climate Change Projections for Impact Assessment and Policy Application: A Review. Climate Impact Group, CSIRO Marine and Atmospheric Research, Aspendale, Victoria, Australia.

Wigley, T.M.L., Raper, S.C.B., 1987. Thermal expansion of sea water associated with global warming, Nature 357, pp.293-300.

Wigley, T.M.L., Raper, S.C.B., 1987. Thermal expansion of sea water associated with global warming, Nature 357, pp.293-300.

World Data Atlas, 2016. Available from: https://knoema.com/atlas/Bangladesh/CO2-emissions-per-capita.

Xie and Arkin, 1997. Global Precipitation: A 17-year monthly analysis based on gauge observations, satellite estimates, and numerical model outputs, Bulletin of the American Meteorological Society, 78, 2539-2558.

Xu, H., 2006. Modification of normalized difference water index (NDWI) to enhance open water features in remotely sensed imagery. International Journal of Remote Sensing 27:3025-3033.

Yin, J., Yin, Z., Wang, J., Xu, S., 2012. National assessment of coastal vulnerability to sea-level rise for the Chinese coast. J. Coast. Conserv. 16, 123e133.

Zaman, S. and Mondal, M.S., 2011. Dimming in sunshine duration of Bangladesh and its impact on rice evapotranspiration and production, Proceedings of the Third International Conference on Water and Flood Management, Organized by Institute of Water and Flood Management, held during 8-10 January, Dhaka, pp. 857-864.

Appendix

Monthly Minimum Temperature: (HAD CM3) baseline temperature (1995), Normalized GCM* Value (% ^{0}C)

Month	Sha	Cha	Nar	Jes	Gop	Fen	Lak	Noai	Kh	Sat	Bar	Bho	Bag	Jha	Piro	Pat	Chi	Bar	Cox
GCM*	1.62	1.61	1.65	1.66	1.65	1.59	1.62	1.62	1.67	1.68	1.64	1.63	1.66	1.65	1.65	1.62	1.55	1.58	1.32
Jan	12.50	12.80	11.40	10.80	11.90	13.10	12.90	13.30	12.10	12.30	12.30	12.90	12.40	12.50	12.50	13.10	13.50	13.30	14.60
Feb	14.90	15.30	13.80	13.40	14.40	15.40	15.40	15.60	14.70	15.30	15.20	15.50	15.10	15.30	15.30	15.90	15.80	16.20	16.40
Mar	19.70	19.90	19.10	18.90	19.50	20.10	20.20	20.20	19.80	20.20	20.20	20.30	20.00	20.30	20.30	20.60	20.30	20.90	20.20
Apr	23.50	23.70	23.20	23.20	23.30	23.50	23.80	23.70	23.40	24.10	23.70	23.80	23.60	23.80	23.70	24.00	23.60	24.20	23.80
May	24.90	25.00	24.70	24.90	24.80	24.70	25.00	24.90	24.90	25.50	25.20	25.20	25.10	25.20	25.20	25.50	24.90	25.60	25.00
Jun	25.80	25.80	25.60	25.80	25.50	25.30	25.60	25.30	25.80	26.10	25.70	25.70	25.80	25.70	25.80	25.70	25.20	25.90	24.90
Jul	25.90	25.80	25.60	25.50	25.60	25.20	25.60	25.30	25.80	25.90	25.60	25.60	25.80	25.60	25.70	25.60	25.00	25.70	24.80
Aug	26.00	26.00	25.80	25.60	25.80	25.30	25.60	25.40	26.00	26.00	25.60	25.60	25.90	25.70	25.80	25.70	25.00	25.80	24.80
Sep	25.80	25.70	25.60	25.40	25.60	25.20	25.60	25.40	25.80	25.80	25.50	25.60	25.80	25.70	25.80	25.60	25.00	25.60	24.80
Oct	23.90	24.00	23.40	23.10	23.70	24.00	24.10	24.20	24.00	23.70	23.90	24.00	24.00	24.00	24.00	24.00	23.80	24.20	24.00
Nov	18.70	19.00	17.80	17.00	18.40	19.20	19.00	19.30	18.80	18.10	18.50	18.90	19.00	18.70	19.00	19.20	19.10	19.40	20.50
Dec	13.90	14.30	12.80	12.00	13.30	14.60	14.30	14.70	13.50	13.20	13.80	14.20	13.80	14.00	14.00	14.40	14.80	14.50	16.20
Ann	21.29	21.44	20.73	20.47	20.98	21.30	21.43	21.44	21.22	21.35	21.27	21.44	21.36	21.38	21.43	21.61	21.33	21.78	21.67

Monthly Minimum Temperature: (40 GCM Ensemble) mean temperature, Normalized GCM* Value (% ^{0}C)

Month	Sha	Cha	Nar	Jes	Gop	Fen	Lak	Noai	Kh	Sat	Bar	Bho	Bag	Jha	Piro	Pat	Chi	Bar	Cox
GCM*	1.62	1.61	1.65	1.66	1.65	1.59	1.62	1.62	1.67	1.68	1.64	1.63	1.66	1.65	1.65	1.62	1.55	1.58	1.32
Jan	1.13	1.13	1.13	1.13	1.12	1.12	1.11	1.11	1.10	1.11	1.08	1.08	1.09	1.08	1.08	1.05	1.05	1.03	0.95
Feb	1.21	1.22	1.20	1.20	1.19	1.21	1.19	1.19	1.18	1.17	1.16	1.16	1.16	1.16	1.15	1.12	1.13	1.09	0.99
Mar	1.13	1.13	1.14	1.15	1.13	1.14	1.12	1.12	1.12	1.13	1.09	1.09	1.10	1.09	1.09	1.06	1.09	1.04	0.97
Apr	1.03	1.04	1.05	1.06	1.03	1.03	1.01	1.00	1.01	1.02	0.98	0.97	0.99	0.98	0.98	0.95	0.98	0.93	0.91
May	0.92	0.92	0.91	0.92	0.91	0.93	0.91	0.92	0.90	0.90	0.89	0.89	0.89	0.89	0.88	0.87	0.91	0.86	0.86
Jun	0.84	0.84	0.85	0.85	0.84	0.84	0.84	0.84	0.85	0.85	0.84	0.83	0.84	0.84	0.84	0.83	0.83	0.82	0.81
Jul	0.79	0.80	0.78	0.78	0.79	0.80	0.80	0.80	0.78	0.78	0.79	0.80	0.79	0.79	0.79	0.79	0.80	0.79	0.77
Aug	0.78	0.78	0.77	0.76	0.77	0.79	0.78	0.78	0.77	0.76	0.77	0.77	0.77	0.77	0.77	0.77	0.78	0.76	0.75
Sep	0.86	0.86	0.86	0.86	0.86	0.87	0.86	0.86	0.85	0.85	0.85	0.85	0.85	0.85	0.84	0.83	0.85	0.82	0.79
Oct	1.00	1.01	0.99	0.99	0.99	1.00	0.99	0.98	0.97	0.97	0.97	0.96	0.96	0.96	0.96	0.94	0.94	0.92	0.86
Nov	1.09	1.09	1.08	1.08	1.07	1.10	1.08	1.07	1.06	1.05	1.05	1.05	1.05	1.05	1.04	1.02	1.04	1.00	0.93
Dec	1.16	1.17	1.17	1.17	1.15	1.16	1.14	1.14	1.14	1.14	1.12	1.12	1.12	1.12	1.11	1.08	1.09	1.06	0.99
Ann	1.00	1.00	1.00	1.00	0.99	1.00	0.98	0.98	0.98	0.98	0.97	0.96	0.97	0.96	0.96	0.94	0.96	0.93	0.88

Monthly Minimum Temperature: (40 GCM Ensemble) median temperature, Normalized GCM* Value (% ^{0}C)

Month	Sha	Cha	Nar	Jes	Gop	Fen	Lak	Noai	Kh	Sat	Bar	Bho	Bag	Jha	Piro	Pat	Chi	Bar	Cox
GCM*	1.62	1.61	1.65	1.66	1.65	1.59	1.62	1.62	1.67	1.68	1.64	1.63	1.66	1.65	1.65	1.62	1.55	1.58	1.32
Jan	1.16	1.20	1.12	1.11	1.13	1.17	1.17	1.15	1.09	1.09	1.10	1.14	1.08	1.09	1.09	1.09	1.08	1.07	0.97
Feb	1.29	1.28	1.26	1.24	1.23	1.24	1.21	1.21	1.25	1.22	1.19	1.17	1.20	1.18	1.17	1.11	1.13	1.07	1.02
Mar	1.06	1.05	1.14	1.11	1.10	1.09	1.04	1.08	1.09	1.09	1.01	1.02	1.05	1.02	1.04	1.04	1.07	1.01	0.98
Apr	0.96	0.96	1.01	1.03	0.97	0.96	0.93	0.93	0.97	1.00	0.91	0.90	0.95	0.91	0.93	0.89	0.96	0.90	0.91
May	0.90	0.88	0.94	0.96	0.89	0.91	0.86	0.87	0.89	0.91	0.84	0.85	0.87	0.85	0.85	0.85	0.86	0.85	0.83
Jun	0.84	0.85	0.87	0.88	0.86	0.85	0.83	0.83	0.86	0.86	0.83	0.83	0.86	0.83	0.85	0.82	0.84	0.83	0.79
Jul	0.81	0.80	0.76	0.77	0.78	0.78	0.79	0.79	0.77	0.76	0.79	0.78	0.78	0.79	0.78	0.78	0.75	0.77	0.75
Aug	0.79	0.79	0.78	0.77	0.78	0.80	0.80	0.80	0.77	0.75	0.78	0.79	0.77	0.78	0.78	0.77	0.77	0.76	0.72
Sep	0.88	0.88	0.84	0.84	0.84	0.87	0.86	0.86	0.84	0.84	0.84	0.85	0.84	0.84	0.83	0.83	0.84	0.81	0.77
Oct	0.96	0.97	0.94	0.93	0.91	0.93	0.92	0.91	0.90	0.91	0.90	0.89	0.87	0.89	0.87	0.86	0.91	0.84	0.85
Nov	1.05	1.05	1.04	1.04	1.02	1.05	1.03	1.03	1.00	1.01	1.00	1.01	1.00	1.01	1.00	0.97	0.96	0.93	0.88
Dec	1.19	1.19	1.20	1.20	1.17	1.16	1.14	1.13	1.16	1.16	1.12	1.11	1.14	1.12	1.13	1.08	1.06	1.07	0.99
Ann	1.00	1.00	0.98	0.96	0.97	0.98	0.97	0.96	0.96	0.93	0.94	0.94	0.95	0.93	0.93	0.90	0.93	0.89	0.85

Monthly Minimum Temperature: (40 GCM Ensemble) 10% low percentile temperature, Normalized GCM* Value (% ^{0}C)

Month	Sha	Cha	Nar	Jes	Gop	Fen	Lak	Noai	Kh	Sat	Bar	Bho	Bag	Jha	Piro	Pat	Chi	Bar	Cox
GCM*	1.62	1.61	1.65	1.66	1.65	1.59	1.62	1.62	1.67	1.68	1.64	1.63	1.66	1.65	1.65	1.62	1.55	1.58	1.32
Jan	0.66	0.68	0.65	0.70	0.67	0.64	0.66	0.63	0.70	0.74	0.66	0.64	0.69	0.66	0.67	0.64	0.61	0.66	0.66
Feb	0.87	0.87	0.89	0.89	0.87	0.85	0.84	0.83	0.85	0.86	0.82	0.81	0.83	0.82	0.82	0.79	0.78	0.79	0.74
Mar	0.78	0.80	0.76	0.75	0.77	0.81	0.76	0.77	0.76	0.77	0.75	0.73	0.75	0.76	0.77	0.74	0.79	0.75	0.76
Apr	0.68	0.69	0.67	0.66	0.64	0.74	0.71	0.73	0.64	0.64	0.70	0.70	0.64	0.70	0.69	0.68	0.72	0.66	0.70
May	0.61	0.63	0.60	0.59	0.61	0.69	0.66	0.68	0.62	0.62	0.66	0.67	0.64	0.66	0.67	0.66	0.70	0.66	0.70
Jun	0.61	0.62	0.60	0.56	0.64	0.64	0.66	0.66	0.67	0.65	0.68	0.68	0.69	0.69	0.69	0.69	0.65	0.67	0.63
Jul	0.60	0.61	0.62	0.61	0.63	0.62	0.62	0.62	0.62	0.61	0.65	0.63	0.64	0.65	0.64	0.64	0.64	0.64	0.64
Aug	0.56	0.57	0.56	0.57	0.56	0.56	0.56	0.57	0.58	0.58	0.58	0.58	0.58	0.58	0.59	0.58	0.58	0.59	0.57
Sep	0.65	0.64	0.67	0.67	0.66	0.68	0.64	0.66	0.67	0.66	0.66	0.67	0.67	0.66	0.67	0.67	0.67	0.67	0.67
Oct	0.56	0.56	0.56	0.56	0.56	0.66	0.59	0.65	0.57	0.60	0.59	0.62	0.58	0.60	0.60	0.66	0.66	0.68	0.72
Nov	0.46	0.48	0.51	0.53	0.50	0.58	0.50	0.56	0.56	0.62	0.53	0.51	0.58	0.55	0.58	0.60	0.71	0.66	0.68
Dec	0.73	0.72	0.71	0.71	0.72	0.85	0.77	0.82	0.72	0.74	0.70	0.73	0.71	0.69	0.69	0.67	0.78	0.68	0.72
Ann	0.81	0.82	0.82	0.82	0.82	0.82	0.81	0.81	0.83	0.84	0.82	0.81	0.83	0.82	0.83	0.78	0.78	0.78	0.76

Monthly Minimum Temperature: (40 GCM Ensemble) 90% high percentile temperature, Normalized GCM* Value (% ^{0}C)

Month	Sha	Cha	Nar	Jes	Gop	Fen	Lak	Noai	Kh	Sat	Bar	Bho	Bag	Jha	Piro	Pat	Chi	Bar	Cox
GCM*	1.62	1.61	1.65	1.66	1.65	1.59	1.62	1.62	1.67	1.68	1.64	1.63	1.66	1.65	1.65	1.62	1.55	1.58	1.32
Jan	1.59	1.57	1.56	1.56	1.61	1.53	1.51	1.48	1.59	1.53	1.45	1.43	1.54	1.44	1.47	1.39	1.36	1.36	1.28
Feb	1.54	1.56	1.56	1.58	1.52	1.57	1.54	1.54	1.50	1.51	1.47	1.47	1.48	1.46	1.45	1.40	1.44	1.36	1.22
Mar	1.47	1.51	1.50	1.52	1.44	1.52	1.48	1.52	1.47	1.49	1.49	1.49	1.49	1.48	1.48	1.46	1.49	1.40	1.15
Apr	1.44	1.48	1.32	1.33	1.33	1.38	1.40	1.38	1.28	1.30	1.29	1.30	1.26	1.25	1.22	1.18	1.17	1.10	1.06
May	1.28	1.28	1.25	1.25	1.22	1.27	1.31	1.29	1.18	1.17	1.23	1.26	1.15	1.20	1.15	1.13	1.13	1.08	1.07
Jun	1.06	1.05	1.04	1.09	1.03	1.08	1.01	1.01	1.03	1.04	0.99	0.98	1.03	0.99	1.03	1.03	1.08	1.02	1.04
Jul	1.02	1.03	0.99	0.99	0.97	1.04	1.03	1.02	0.95	0.93	0.98	0.99	0.94	0.97	0.95	0.96	1.01	0.96	0.93
Aug	0.97	0.96	0.98	0.98	0.96	1.02	0.96	0.99	0.96	0.95	0.95	0.95	0.95	0.96	0.96	0.96	1.00	0.94	0.91
Sep	1.03	1.03	1.04	1.04	1.06	1.06	1.01	1.05	1.06	1.05	1.05	1.04	1.06	1.05	1.05	1.01	1.03	0.99	0.94
Oct	1.29	1.31	1.27	1.26	1.29	1.31	1.28	1.27	1.27	1.26	1.26	1.26	1.27	1.26	1.27	1.19	1.14	1.15	1.02
Nov	1.56	1.60	1.53	1.52	1.52	1.60	1.56	1.54	1.46	1.44	1.47	1.48	1.44	1.45	1.43	1.39	1.54	1.35	1.21
Dec	1.59	1.60	1.58	1.57	1.55	1.55	1.53	1.54	1.53	1.50	1.46	1.45	1.52	1.47	1.49	1.40	1.50	1.37	1.28
Ann	1.18	1.18	1.19	1.20	1.16	1.22	1.18	1.20	1.14	1.14	1.14	1.16	1.13	1.13	1.13	1.12	1.16	1.08	1.05

Monthly Maximum Temperature: (HAD CM3) baseline temperature (1995), Normalized GCM* Value (% ^{0}C)

Month	Sha	Cha	Nar	Jes	Gop	Fen	Lak	Noai	Kh	Sat	Bar	Bho	Bag	Jha	Piro	Pat	Chi	Bar	Cox
GCM*	0.88	0.85	0.99	1.02	0.95	0.86	0.84	0.83	0.98	1.04	0.89	0.85	0.96	0.91	0.93	0.89	0.99	0.91	0.98
Jan	25.80	26.00	25.60	25.70	25.60	25.80	25.80	25.70	26.10	26.00	25.80	25.90	26.00	25.80	25.80	25.80	26.40	25.80	26.40
Feb	28.60	28.70	28.60	28.70	28.60	28.10	28.20	28.00	28.90	28.80	28.40	28.20	28.70	28.40	28.50	28.20	28.70	28.20	28.20
Mar	32.60	32.20	33.30	33.40	33.00	31.50	31.80	31.10	33.40	33.30	32.40	31.80	32.90	32.50	32.60	31.90	31.30	31.90	30.50
Apr	34.10	33.70	35.20	35.90	34.50	32.50	33.00	32.20	34.60	35.00	33.70	33.10	34.10	33.80	33.80	33.10	32.00	33.00	31.80
May	33.90	33.40	34.60	35.10	34.40	32.30	33.10	32.20	34.40	34.90	35.20	34.00	34.60	35.10	34.80	34.70	32.10	34.30	32.10
Jun	31.80	31.60	32.30	32.60	32.00	30.90	31.10	30.60	32.40	33.10	31.70	31.30	32.10	31.80	31.90	31.40	30.70	31.50	30.20
Jul	30.90	30.70	31.40	31.40	31.10	30.30	30.40	30.10	31.40	31.60	30.60	30.40	31.20	30.70	30.80	30.30	30.10	30.40	29.60
Aug	31.10	31.00	31.40	31.60	31.10	30.60	30.60	30.20	31.30	31.80	30.80	30.50	31.10	30.80	30.90	30.50	30.30	30.50	29.60
Sep	31.60	31.40	32.00	32.10	31.70	31.10	31.10	30.80	31.90	32.00	31.40	31.20	31.80	31.50	31.60	31.20	31.10	31.10	30.60
Oct	31.20	31.10	31.50	31.70	31.40	31.00	31.00	30.70	31.70	31.80	31.30	31.10	31.50	31.30	31.40	31.10	31.10	31.20	30.90
Nov	29.10	29.20	29.20	29.20	29.10	29.00	28.90	28.70	29.50	29.50	29.00	28.90	29.40	29.00	29.20	29.00	29.20	29.00	29.30
Dec	26.40	26.60	26.20	26.40	26.20	26.50	26.40	26.20	26.50	26.60	26.40	26.30	26.40	26.40	26.40	26.30	26.90	26.20	26.90
Ann	30.59	30.47	30.94	31.15	30.73	29.97	30.12	29.71	31.01	31.20	30.56	30.23	30.82	30.59	30.64	30.29	29.99	30.26	29.68

Monthly Maximum Temperature: (40 GCM Ensemble) mean temperature, Normalized GCM* Value (% ^{0}C)

Month	Sha	Cha	Nar	Jes	Gop	Fen	Lak	Noai	Kh	Sat	Bar	Bho	Bag	Jha	Piro	Pat	Chi	Bar	Cox
GCM*	0.88	0.85	0.99	1.02	0.95	0.86	0.84	0.83	0.98	1.04	0.89	0.85	0.96	0.91	0.93	0.89	0.99	0.91	0.98
Jan	1.14	1.13	1.14	1.14	1.12	1.09	1.10	1.08	1.10	1.10	1.08	1.07	1.09	1.08	1.07	1.04	1.02	1.01	0.95
Feb	1.09	1.08	1.10	1.11	1.08	1.05	1.05	1.04	1.06	1.07	1.04	1.03	1.04	1.03	1.03	1.00	1.00	0.98	0.93
Mar	1.01	1.00	1.03	1.04	1.01	0.99	0.97	0.98	0.99	1.00	0.96	0.95	0.97	0.96	0.96	0.94	0.96	0.92	0.92
Apr	0.94	0.94	0.97	0.98	0.94	0.94	0.91	0.92	0.93	0.93	0.89	0.89	0.91	0.89	0.89	0.87	0.93	0.85	0.89
May	0.87	0.87	0.87	0.86	0.86	0.90	0.87	0.88	0.85	0.84	0.85	0.85	0.85	0.85	0.85	0.84	0.90	0.83	0.86
Jun	0.77	0.77	0.76	0.76	0.76	0.76	0.77	0.77	0.77	0.77	0.77	0.77	0.77	0.77	0.77	0.78	0.76	0.77	0.76
Jul	0.76	0.77	0.74	0.73	0.75	0.76	0.77	0.76	0.74	0.74	0.76	0.76	0.75	0.76	0.75	0.76	0.74	0.76	0.73
Aug	0.74	0.75	0.69	0.67	0.70	0.74	0.74	0.73	0.69	0.67	0.72	0.73	0.69	0.71	0.70	0.71	0.71	0.70	0.70
Sep	0.84	0.85	0.80	0.79	0.81	0.83	0.84	0.82	0.79	0.78	0.81	0.82	0.80	0.81	0.80	0.80	0.79	0.78	0.75
Oct	0.86	0.87	0.81	0.79	0.82	0.86	0.86	0.86	0.80	0.79	0.84	0.85	0.81	0.83	0.82	0.83	0.84	0.81	0.82
Nov	0.99	1.00	0.97	0.96	0.96	0.98	0.97	0.97	0.94	0.93	0.94	0.94	0.93	0.94	0.93	0.91	0.93	0.89	0.89
Dec	1.08	1.08	1.10	1.10	1.08	1.05	1.05	1.04	1.07	1.07	1.04	1.03	1.05	1.04	1.04	1.00	1.00	0.99	0.95
Ann	0.92	0.93	0.91	0.91	0.91	0.91	0.91	0.90	0.90	0.89	0.89	0.89	0.89	0.89	0.88	0.87	0.88	0.86	0.85

Monthly Maximum Temperature: (40 GCM Ensemble) median temperature, Normalized GCM* Value (% ^0C)

Month	Sha	Cha	Nar	Jes	Gop	Fen	Lak	Noai	Kh	Sat	Bar	Bho	Bag	Jha	Piro	Pat	Chi	Bar	Cox
GCM*	0.88	0.85	0.99	1.02	0.95	0.86	0.84	0.83	0.98	1.04	0.89	0.85	0.96	0.91	0.93	0.89	0.99	0.91	0.98
Jan	1.11	1.13	1.11	1.14	1.10	1.10	1.10	1.10	1.10	1.11	1.06	1.08	1.08	1.05	1.05	1.02	1.02	0.99	0.93
Feb	1.15	1.14	1.15	1.16	1.13	1.11	1.11	1.10	1.12	1.13	1.10	1.09	1.10	1.09	1.09	1.04	1.01	1.02	0.97
Mar	1.04	1.03	1.09	1.10	1.05	1.04	1.00	1.01	1.06	1.10	0.99	0.98	1.04	1.00	1.00	0.98	0.96	0.97	0.89
Apr	0.93	0.92	1.00	1.03	0.97	0.94	0.90	0.91	0.95	0.94	0.88	0.85	0.90	0.87	0.87	0.81	0.87	0.80	0.80
May	0.86	0.81	0.92	0.94	0.89	0.82	0.80	0.81	0.90	0.90	0.84	0.81	0.89	0.85	0.87	0.83	0.85	0.83	0.81
Jun	0.79	0.79	0.83	0.84	0.81	0.75	0.76	0.75	0.83	0.83	0.79	0.77	0.82	0.80	0.81	0.79	0.79	0.80	0.78
Jul	0.70	0.70	0.73	0.75	0.72	0.72	0.72	0.71	0.74	0.77	0.72	0.73	0.73	0.71	0.73	0.73	0.74	0.75	0.72
Aug	0.72	0.71	0.74	0.74	0.73	0.71	0.71	0.71	0.73	0.72	0.71	0.71	0.72	0.71	0.72	0.70	0.71	0.72	0.71
Sep	0.82	0.82	0.81	0.80	0.80	0.78	0.80	0.79	0.78	0.77	0.79	0.79	0.78	0.79	0.77	0.76	0.76	0.75	0.72
Oct	0.90	0.91	0.85	0.85	0.85	0.87	0.88	0.87	0.84	0.81	0.87	0.87	0.84	0.86	0.84	0.85	0.82	0.80	0.81
Nov	0.99	1.00	1.00	0.98	0.98	0.98	0.97	0.95	0.95	0.95	0.94	0.92	0.94	0.94	0.93	0.90	0.90	0.89	0.88
Dec	1.09	1.13	1.06	1.08	1.06	1.12	1.10	1.09	1.04	1.05	1.07	1.08	1.05	1.06	1.06	1.04	1.05	1.02	0.94
Ann	0.91	0.91	0.90	0.91	0.90	0.91	0.90	0.90	0.89	0.89	0.89	0.88	0.88	0.89	0.87	0.86	0.86	0.84	0.81

Monthly Maximum Temperature: (40 GCM Ensemble) 10% low percentile temperature, Normalized GCM* Value (% ^{0}C)

Month	Sha	Cha	Nar	Jes	Gop	Fen	Lak	Noai	Kh	Sat	Bar	Bho	Bag	Jha	Piro	Pat	Chi	Bar	Cox
GCM*	0.88	0.85	0.99	1.02	0.95	0.86	0.84	0.83	0.98	1.04	0.89	0.85	0.96	0.91	0.93	0.89	0.99	0.91	0.98
Jan	0.70	0.69	0.71	0.68	0.72	0.66	0.68	0.69	0.70	0.63	0.67	0.66	0.69	0.67	0.67	0.74	0.77	0.68	0.68
Feb	0.53	0.53	0.56	0.56	0.57	0.59	0.57	0.59	0.58	0.58	0.59	0.59	0.59	0.57	0.60	0.63	0.68	0.65	0.70
Mar	0.31	0.32	0.24	0.23	0.31	0.44	0.42	0.48	0.36	0.35	0.44	0.47	0.42	0.44	0.45	0.57	0.53	0.59	0.59
Apr	0.25	0.26	0.31	0.32	0.30	0.38	0.34	0.39	0.38	0.37	0.40	0.41	0.40	0.41	0.42	0.47	0.58	0.54	0.65
May	0.20	0.26	0.22	0.21	0.21	0.38	0.32	0.37	0.26	0.30	0.31	0.35	0.27	0.31	0.30	0.39	0.57	0.43	0.62
Jun	0.21	0.23	0.21	0.17	0.20	0.29	0.35	0.37	0.32	0.27	0.35	0.35	0.33	0.35	0.35	0.40	0.39	0.44	0.53
Jul	0.52	0.53	0.44	0.43	0.48	0.47	0.55	0.53	0.45	0.45	0.48	0.56	0.47	0.46	0.47	0.51	0.54	0.49	0.59
Aug	0.41	0.46	0.36	0.36	0.36	0.48	0.46	0.47	0.33	0.35	0.35	0.45	0.35	0.35	0.34	0.37	0.53	0.36	0.53
Sep	0.58	0.58	0.47	0.47	0.51	0.57	0.56	0.57	0.50	0.50	0.58	0.56	0.57	0.57	0.57	0.61	0.58	0.60	0.59
Oct	0.49	0.51	0.22	0.19	0.35	0.53	0.50	0.51	0.32	0.29	0.48	0.50	0.39	0.46	0.38	0.50	0.57	0.50	0.63
Nov	0.52	0.53	0.46	0.47	0.46	0.61	0.57	0.59	0.48	0.50	0.55	0.57	0.50	0.55	0.52	0.55	0.63	0.55	0.65
Dec	0.64	0.64	0.63	0.63	0.63	0.68	0.66	0.67	0.64	0.62	0.65	0.66	0.65	0.66	0.66	0.68	0.68	0.68	0.72
Ann	0.53	0.57	0.45	0.45	0.47	0.62	0.59	0.61	0.47	0.46	0.57	0.59	0.49	0.55	0.51	0.64	0.66	0.63	0.69

Monthly Maximum Temperature: (40 GCM Ensemble) 90% high percentile temperature, Normalized GCM* Value (% ^{0}C)

Month	Sha	Cha	Nar	Jes	Gop	Fen	Lak	Noai	Kh	Sat	Bar	Bho	Bag	Jha	Piro	Pat	Chi	Bar	Cox
GCM*	0.88	0.85	0.99	1.02	0.95	0.86	0.84	0.83	0.98	1.04	0.89	0.85	0.96	0.91	0.93	0.89	0.99	0.91	0.98
Jan	1.72	1.68	1.80	1.85	1.72	1.49	1.56	1.51	1.68	1.75	1.55	1.51	1.64	1.55	1.56	1.47	1.33	1.42	1.23
Feb	1.52	1.50	1.54	1.56	1.51	1.42	1.43	1.41	1.49	1.49	1.41	1.37	1.44	1.40	1.39	1.31	1.30	1.26	1.12
Mar	1.67	1.68	1.64	1.65	1.56	1.56	1.57	1.53	1.55	1.55	1.43	1.45	1.44	1.42	1.39	1.31	1.37	1.30	1.26
Apr	1.59	1.57	1.65	1.62	1.61	1.60	1.52	1.52	1.59	1.61	1.48	1.43	1.49	1.44	1.39	1.30	1.31	1.25	1.20
May	1.53	1.52	1.42	1.41	1.41	1.39	1.44	1.41	1.37	1.33	1.37	1.40	1.35	1.34	1.29	1.25	1.23	1.17	1.13
Jun	1.30	1.36	1.28	1.25	1.24	1.20	1.27	1.17	1.21	1.19	1.15	1.19	1.16	1.13	1.13	1.05	1.04	1.02	0.99
Jul	1.08	1.09	1.11	1.12	1.08	1.02	1.04	1.02	1.04	1.00	1.02	1.02	1.05	1.02	1.04	1.01	0.97	1.00	0.95
Aug	1.08	1.13	1.11	1.14	1.07	1.05	1.06	1.02	1.04	1.02	1.02	1.00	1.00	1.01	0.99	0.99	0.96	0.98	0.90
Sep	1.25	1.26	1.19	1.19	1.19	1.16	1.18	1.12	1.17	1.14	1.15	1.12	1.14	1.14	1.12	1.07	1.02	1.05	0.94
Oct	1.22	1.22	1.19	1.18	1.19	1.20	1.21	1.19	1.15	1.14	1.18	1.18	1.14	1.16	1.14	1.12	1.11	1.08	0.99
Nov	1.43	1.42	1.44	1.45	1.40	1.35	1.38	1.33	1.38	1.39	1.34	1.33	1.34	1.31	1.31	1.25	1.24	1.23	1.15
Dec	1.49	1.45	1.60	1.62	1.53	1.38	1.40	1.36	1.48	1.52	1.40	1.37	1.43	1.41	1.41	1.33	1.22	1.30	1.17
Ann	1.28	1.25	1.27	1.29	1.23	1.18	1.19	1.17	1.20	1.20	1.15	1.14	1.17	1.16	1.15	1.10	1.09	1.05	0.99

Monthly Mean Temperature: (HAD CM3) baseline temperature (1995), Normalized GCM* Value (% ^{0}C)

Month	Sha	Cha	Nar	Jes	Gop	Fen	Lak	Noai	Kh	Sat	Bar	Bho	Bag	Jha	Piro	Pat	Chi	Bar	Cox
GCM*	1.21	1.17	1.29	1.32	1.25	1.16	1.16	1.15	1.28	1.33	1.21	1.18	1.26	1.22	1.22	1.19	1.19	1.19	1.10
Jan	19.10	19.40	18.50	18.20	18.70	19.40	19.30	19.50	19.10	19.10	19.00	19.40	19.20	19.10	19.20	19.40	19.90	19.50	20.50
Feb	21.70	22.00	21.20	21.00	21.50	21.70	21.80	21.80	21.80	22.00	21.80	21.80	21.90	21.80	21.90	22.00	22.20	22.20	22.30
Mar	26.10	26.00	26.20	26.10	26.20	25.80	26.00	25.60	26.60	26.70	26.30	26.00	26.40	26.40	26.40	26.20	25.80	26.40	25.30
Apr	28.80	28.70	29.20	29.50	28.90	28.00	28.40	27.90	29.00	29.50	28.70	28.40	28.80	28.80	28.80	28.50	27.80	28.60	27.80
May	29.40	29.20	29.60	30.00	29.60	28.50	29.00	28.50	29.60	30.20	30.20	29.60	29.80	30.10	30.30	30.10	28.50	29.90	28.50
Jun	28.80	28.70	28.90	29.20	28.70	28.10	28.30	27.90	29.10	29.60	28.70	28.50	28.90	28.70	28.80	28.50	27.90	28.70	27.50
Jul	28.40	28.20	28.50	28.40	28.30	27.70	28.00	27.70	28.60	28.70	28.10	28.00	28.50	28.10	28.20	27.90	27.50	28.00	27.20
Aug	28.50	28.50	28.60	28.60	28.40	27.90	28.10	27.80	28.60	28.90	28.20	28.00	28.50	28.20	28.30	28.10	27.60	28.10	27.20
Sep	28.70	28.50	28.80	28.70	28.60	28.10	28.30	28.10	28.80	28.90	28.40	28.40	28.80	28.60	28.50	28.40	28.00	28.30	27.70
Oct	27.50	27.50	27.40	27.40	27.50	27.50	27.50	27.40	27.80	27.70	27.60	27.50	27.70	27.60	27.60	27.50	27.40	27.70	27.40
Nov	23.90	24.10	23.50	23.10	23.70	24.10	23.90	24.00	24.10	23.80	23.70	23.90	24.20	23.80	24.00	24.10	24.10	24.20	24.90
Dec	20.10	20.40	19.50	19.20	19.70	20.50	20.30	20.40	20.00	19.90	20.10	20.20	20.10	20.20	20.10	20.30	20.80	20.30	21.50
Ann	25.92	25.93	25.83	25.78	25.82	25.61	25.74	25.55	26.09	26.25	25.90	25.81	26.07	25.95	26.01	25.92	25.63	25.99	25.65

Monthly Mean Temperature: (40 GCM Ensemble) mean temperature, Normalized GCM* Value (% ^{0}C)

Month	Sha	Cha	Nar	Jes	Gop	Fen	Lak	Noai	Kh	Sat	Bar	Bho	Bag	Jha	Piro	Pat	Chi	Bar	Cox
GCM*	1.21	1.17	1.29	1.32	1.25	1.16	1.16	1.15	1.28	1.33	1.21	1.18	1.26	1.22	1.22	1.19	1.19	1.19	1.10
Jan	1.10	1.09	1.10	1.11	1.09	1.08	1.07	1.07	1.07	1.08	1.05	1.05	1.06	1.05	1.04	1.02	1.02	1.00	0.94
Feb	1.11	1.11	1.12	1.12	1.10	1.11	1.09	1.09	1.08	1.09	1.07	1.06	1.07	1.06	1.06	1.03	1.05	1.01	0.95
Mar	1.03	1.03	1.05	1.05	1.03	1.04	1.01	1.02	1.02	1.02	0.99	0.99	1.00	0.99	0.99	0.97	1.01	0.96	0.94
Apr	0.95	0.95	0.97	0.98	0.95	0.96	0.93	0.94	0.93	0.94	0.91	0.91	0.92	0.91	0.90	0.89	0.94	0.87	0.89
May	0.88	0.88	0.87	0.87	0.87	0.90	0.88	0.89	0.86	0.85	0.86	0.86	0.85	0.86	0.85	0.85	0.90	0.84	0.85
Jun	0.80	0.80	0.80	0.80	0.80	0.79	0.80	0.80	0.80	0.81	0.80	0.80	0.80	0.80	0.80	0.80	0.80	0.80	0.79
Jul	0.77	0.77	0.75	0.75	0.76	0.77	0.77	0.77	0.76	0.75	0.77	0.77	0.76	0.77	0.77	0.77	0.77	0.77	0.76
Aug	0.74	0.75	0.72	0.71	0.72	0.76	0.75	0.75	0.72	0.71	0.73	0.74	0.72	0.73	0.73	0.73	0.74	0.73	0.73
Sep	0.84	0.84	0.81	0.81	0.82	0.84	0.83	0.83	0.81	0.80	0.82	0.82	0.81	0.81	0.81	0.80	0.81	0.79	0.77
Oct	0.91	0.92	0.89	0.88	0.89	0.93	0.91	0.91	0.88	0.87	0.89	0.90	0.88	0.89	0.88	0.87	0.89	0.86	0.84
Nov	1.01	1.02	1.00	0.99	0.99	1.02	1.00	1.00	0.98	0.97	0.98	0.98	0.97	0.97	0.97	0.95	0.98	0.93	0.91
Dec	1.09	1.09	1.10	1.10	1.08	1.08	1.07	1.07	1.07	1.07	1.05	1.05	1.06	1.05	1.04	1.02	1.03	1.00	0.96
Ann	0.93	0.94	0.93	0.93	0.92	0.94	0.93	0.93	0.91	0.91	0.91	0.91	0.91	0.91	0.90	0.89	0.91	0.88	0.86

Monthly Mean Temperature: (40 GCM Ensemble) median temperature, Normalized GCM* Value (% ^{0}C)

Month	Sha	Cha	Nar	Jes	Gop	Fen	Lak	Noai	Kh	Sat	Bar	Bho	Bag	Jha	Piro	Pat	Chi	Bar	Cox
GCM*	1.21	1.17	1.29	1.32	1.25	1.16	1.16	1.15	1.28	1.33	1.21	1.18	1.26	1.22	1.22	1.19	1.19	1.19	1.10
Jan	1.13	1.12	1.10	1.11	1.10	1.14	1.12	1.13	1.09	1.07	1.11	1.09	1.09	1.10	1.09	1.05	1.05	1.02	0.96
Feb	1.14	1.16	1.11	1.10	1.11	1.16	1.15	1.16	1.09	1.08	1.12	1.12	1.10	1.12	1.11	1.09	1.09	1.05	0.97
Mar	1.08	1.06	1.14	1.15	1.11	1.06	1.04	1.03	1.09	1.12	1.04	1.01	1.06	1.05	1.04	1.00	1.00	1.00	0.96
Apr	0.92	0.93	0.97	1.00	0.92	0.98	0.92	0.95	0.92	0.95	0.89	0.89	0.90	0.89	0.89	0.87	0.94	0.86	0.85
May	0.89	0.88	0.92	0.91	0.91	0.90	0.87	0.88	0.89	0.89	0.88	0.86	0.90	0.89	0.89	0.87	0.89	0.86	0.84
Jun	0.78	0.79	0.79	0.80	0.79	0.80	0.80	0.79	0.80	0.82	0.79	0.79	0.78	0.79	0.79	0.80	0.82	0.81	0.79
Jul	0.74	0.73	0.74	0.75	0.73	0.74	0.74	0.74	0.76	0.77	0.75	0.74	0.75	0.75	0.75	0.75	0.73	0.76	0.72
Aug	0.75	0.75	0.74	0.73	0.74	0.76	0.75	0.75	0.73	0.73	0.73	0.74	0.74	0.73	0.73	0.73	0.74	0.72	0.71
Sep	0.82	0.83	0.79	0.79	0.80	0.83	0.80	0.81	0.80	0.79	0.80	0.81	0.80	0.80	0.79	0.80	0.80	0.77	0.73
Oct	0.86	0.87	0.89	0.90	0.87	0.90	0.86	0.87	0.87	0.87	0.85	0.85	0.86	0.86	0.86	0.83	0.86	0.82	0.82
Nov	1.02	1.03	1.04	1.03	1.01	1.01	1.00	1.00	1.00	0.99	0.99	0.98	0.98	0.98	0.97	0.93	0.93	0.90	0.85
Dec	1.16	1.14	1.12	1.11	1.14	1.12	1.10	1.10	1.09	1.09	1.08	1.07	1.08	1.08	1.07	1.05	1.06	1.02	0.98
Ann	0.91	0.91	0.92	0.93	0.90	0.92	0.91	0.91	0.89	0.90	0.89	0.89	0.89	0.89	0.89	0.88	0.90	0.86	0.84

Monthly Mean Temperature: (40 GCM Ensemble) 10% low percentile temperature, Normalized GCM* Value (% ^{0}C)

Month	Sha	Cha	Nar	Jes	Gop	Fen	Lak	Noai	Kh	Sat	Bar	Bho	Bag	Jha	Piro	Pat	Chi	Bar	Cox
GCM*	1.21	1.17	1.29	1.32	1.25	1.16	1.16	1.15	1.28	1.33	1.21	1.18	1.26	1.22	1.22	1.19	1.19	1.19	1.10
Jan	0.71	0.68	0.72	0.70	0.72	0.65	0.66	0.64	0.70	0.67	0.71	0.66	0.69	0.72	0.72	0.69	0.72	0.68	0.67
Feb	0.79	0.79	0.79	0.77	0.79	0.82	0.78	0.81	0.76	0.77	0.78	0.78	0.77	0.77	0.77	0.74	0.78	0.73	0.74
Mar	0.58	0.57	0.64	0.66	0.62	0.64	0.59	0.63	0.65	0.65	0.60	0.60	0.64	0.60	0.61	0.70	0.70	0.69	0.69
Apr	0.58	0.56	0.60	0.60	0.60	0.62	0.57	0.59	0.62	0.63	0.57	0.55	0.60	0.58	0.58	0.66	0.70	0.65	0.67
May	0.48	0.50	0.47	0.44	0.49	0.57	0.54	0.56	0.52	0.50	0.54	0.55	0.54	0.55	0.55	0.61	0.65	0.63	0.68
Jun	0.41	0.44	0.42	0.41	0.45	0.47	0.47	0.50	0.51	0.53	0.54	0.54	0.54	0.56	0.56	0.58	0.53	0.59	0.58
Jul	0.56	0.56	0.54	0.53	0.55	0.57	0.57	0.57	0.55	0.54	0.57	0.57	0.56	0.57	0.57	0.60	0.60	0.60	0.63
Aug	0.52	0.54	0.49	0.48	0.50	0.56	0.55	0.55	0.49	0.49	0.49	0.54	0.49	0.49	0.49	0.52	0.54	0.52	0.57
Sep	0.63	0.63	0.61	0.61	0.63	0.64	0.63	0.64	0.63	0.63	0.63	0.63	0.63	0.64	0.64	0.64	0.64	0.64	0.63
Oct	0.56	0.56	0.52	0.52	0.53	0.55	0.57	0.56	0.54	0.54	0.59	0.58	0.55	0.60	0.60	0.63	0.65	0.61	0.72
Nov	0.57	0.60	0.64	0.62	0.65	0.67	0.62	0.64	0.64	0.62	0.65	0.62	0.64	0.66	0.66	0.65	0.71	0.65	0.68
Dec	0.79	0.79	0.80	0.78	0.79	0.76	0.78	0.78	0.75	0.74	0.75	0.74	0.76	0.74	0.74	0.70	0.73	0.73	0.73
Ann	0.71	0.71	0.65	0.66	0.70	0.72	0.71	0.71	0.68	0.68	0.69	0.70	0.69	0.69	0.69	0.70	0.72	0.70	0.72

Monthly Mean Temperature: (40 GCM Ensemble) 90% high percentile temperature, Normalized GCM* Value (% ^{0}C)

Month	Sha	Cha	Nar	Jes	Gop	Fen	Lak	Noai	Kh	Sat	Bar	Bho	Bag	Jha	Piro	Pat	Chi	Bar	Cox
GCM*	1.21	1.17	1.29	1.32	1.25	1.16	1.16	1.15	1.28	1.33	1.21	1.18	1.26	1.22	1.22	1.19	1.19	1.19	1.10
Jan	1.53	1.52	1.59	1.59	1.53	1.45	1.44	1.42	1.48	1.52	1.41	1.39	1.45	1.41	1.40	1.32	1.35	1.30	1.18
Feb	1.42	1.40	1.46	1.47	1.42	1.39	1.37	1.36	1.41	1.44	1.33	1.33	1.36	1.33	1.32	1.28	1.36	1.25	1.16
Mar	1.42	1.39	1.40	1.43	1.37	1.39	1.35	1.35	1.33	1.37	1.33	1.30	1.30	1.32	1.31	1.25	1.32	1.20	1.15
Apr	1.28	1.31	1.34	1.38	1.23	1.26	1.25	1.23	1.23	1.26	1.16	1.17	1.19	1.16	1.15	1.12	1.19	1.08	1.14
May	1.31	1.32	1.30	1.29	1.22	1.21	1.23	1.18	1.20	1.20	1.16	1.14	1.14	1.17	1.15	1.12	1.23	1.07	1.11
Jun	1.18	1.20	1.15	1.16	1.13	1.13	1.15	1.11	1.10	1.10	1.11	1.10	1.08	1.09	1.08	1.02	0.99	0.98	0.93
Jul	1.01	1.02	0.98	0.97	0.99	0.99	0.99	0.97	0.97	0.97	0.97	0.96	0.97	0.97	0.97	0.97	0.96	0.96	0.91
Aug	0.97	0.97	0.97	0.97	0.96	0.99	0.97	0.97	0.95	0.95	0.95	0.95	0.95	0.96	0.95	0.94	0.95	0.93	0.89
Sep	1.07	1.07	1.08	1.08	1.06	1.03	1.02	0.99	1.03	1.01	1.00	0.99	1.01	1.00	0.99	0.95	0.97	0.96	0.91
Oct	1.22	1.24	1.18	1.18	1.18	1.23	1.22	1.21	1.16	1.14	1.18	1.18	1.15	1.17	1.16	1.13	1.12	1.10	1.02
Nov	1.40	1.39	1.39	1.39	1.40	1.42	1.41	1.42	1.36	1.33	1.33	1.36	1.34	1.31	1.30	1.29	1.32	1.24	1.17
Dec	1.43	1.42	1.40	1.43	1.36	1.35	1.35	1.32	1.32	1.34	1.31	1.28	1.33	1.31	1.29	1.26	1.30	1.24	1.22
Ann	1.12	1.16	1.21	1.21	1.16	1.16	1.13	1.13	1.13	1.11	1.11	1.11	1.10	1.10	1.09	1.04	1.08	1.02	1.02

Monthly Rainfall: (HAD CM3) baseline rainfall (1995), Normalized GCM* Value (% mm)

Month	Sha	Cha	Nar	Jes	Gop	Fen	Lak	Noai	Kh	Sat	Bar	Bho	Bag	Jha	Piro	Pat	Chi	Bar	Cox
GCM*	6.72	7.21	4.82	4.48	5.76	8.75	7.64	7.95	5.27	4.27	7.05	7.75	5.91	6.78	6.36	7.14	9.25	6.77	9.48
Jan	8	7	10	11	10	9	6	9	12	11	10	3	12	11	12	12	6	12	7
Feb	21	15	19	19	21	17	18	18	19	17	20	24	21	22	22	27	15	24	11
Mar	51	47	42	40	46	61	46	53	40	28	44	40	43	46	45	51	48	44	23
Apr	130	148	90	76	102	123	132	115	87	61	106	132	90	100	93	100	125	87	107
May	237	256	187	167	202	265	272	283	180	130	208	267	189	208	200	242	226	214	251
Jun	357	398	327	313	341	553	493	591	333	294	417	505	366	416	402	533	586	502	836
Jul	368	441	322	303	349	564	539	675	359	344	432	489	398	440	436	582	753	571	1060
Aug	332	369	293	293	311	519	467	599	309	320	380	421	344	386	378	496	529	480	785
Sep	247	268	235	248	235	303	318	373	224	271	290	310	250	286	275	347	262	332	346
Oct	143	146	143	132	146	192	175	209	143	136	182	171	157	177	169	196	204	194	248
Nov	33	38	28	28	30	47	47	52	29	28	42	49	33	40	37	47	50	46	72
Dec	7	7	8	8	8	4	8	12	6	6	11	6	8	10	9	10	11	10	20
Ann	1934	2140	1704	1638	1801	2657	2521	2989	1741	1646	2142	2417	1911	2142	2078	2643	2815	2516	3766

Monthly Rainfall: (40 GCM Ensemble) mean rainfall, Normalized GCM* Value (% mm)

Month	Sha	Cha	Nar	Jes	Gop	Fen	Lak	Noai	Kh	Sat	Bar	Bho	Bag	Jha	Piro	Pat	Chi	Bar	Cox
GCM*	6.72	7.21	4.82	4.48	5.76	8.75	7.64	7.95	5.27	4.27	7.05	7.75	5.91	6.78	6.36	7.14	9.25	6.77	9.48
Jan	-4.39	-4.47	-3.48	-3.21	-3.51	-4.32	-3.91	-3.80	-2.86	-2.42	-3.15	-2.97	-2.71	-2.97	-2.63	-1.94	-1.86	-1.41	0.81
Feb	13.88	13.39	16.53	17.50	15.72	12.47	13.32	13.24	16.91	17.98	14.51	13.92	16.55	15.13	16.21	15.52	9.16	15.95	8.32
Mar	13.69	13.37	14.38	14.44	14.05	11.82	12.81	12.05	13.89	14.27	13.07	12.60	13.57	13.24	13.38	12.41	9.26	11.84	7.84
Apr	2.62	2.43	2.45	2.32	3.52	1.44	3.09	2.18	4.41	4.29	5.13	4.27	5.01	5.41	5.18	4.84	1.37	4.93	5.98
May	6.56	6.56	7.14	7.80	7.75	6.72	7.48	7.11	9.21	10.82	9.68	8.86	9.50	10.06	9.86	10.31	6.31	10.87	7.15
Jun	12.59	12.11	14.48	15.15	13.36	12.30	11.65	11.85	13.37	14.24	11.87	11.45	12.73	12.09	12.42	11.85	11.85	11.62	9.80
Jul	6.31	6.20	6.96	7.08	6.71	6.28	5.99	6.07	6.91	7.07	6.09	6.02	6.74	6.19	6.53	6.28	5.80	6.51	5.67
Aug	5.53	5.46	6.02	6.20	5.94	5.34	5.56	5.52	6.19	6.28	6.10	6.02	6.32	6.27	6.49	6.96	5.81	7.23	7.06
Sep	6.83	6.67	7.59	7.75	7.41	6.82	6.81	7.02	7.68	7.84	7.15	7.08	7.62	7.28	7.55	7.57	7.26	7.81	7.61
Oct	6.99	6.92	6.75	6.49	6.90	7.55	6.80	7.17	6.88	6.57	6.82	6.67	6.95	6.87	6.96	6.94	7.51	7.10	7.39
Nov	0.60	1.14	-0.92	-1.40	0.13	1.95	2.17	2.34	0.19	-0.63	2.35	2.96	1.14	2.29	2.05	3.75	2.76	3.62	3.26
Dec	7.36	6.96	8.97	9.32	8.13	7.40	6.39	6.54	8.37	9.54	6.46	5.92	7.61	6.75	7.19	6.39	6.13	6.55	3.86
Ann	7.37	7.15	8.20	8.47	8.01	7.38	7.27	7.30	8.32	8.53	7.83	7.67	8.24	8.02	8.21	8.20	7.17	8.29	7.23

Monthly Rainfall: (40 GCM Ensemble) median rainfall, Normalized GCM* Value (% mm)

Month	**Sha**	**Cha**	**Nar**	**Jes**	**Gop**	**Fen**	**Lak**	**Noai**	**Kh**	**Sat**	**Bar**	**Bho**	**Bag**	**Jha**	**Piro**	**Pat**	**Chi**	**Bar**	**Cox**
GCM*	6.72	7.21	4.82	4.48	5.76	8.75	7.64	7.95	5.27	4.27	7.05	7.75	5.91	6.78	6.36	7.14	9.25	6.77	9.48
Jan	-9.87	-8.45	-8.49	-8.07	-9.45	-7.50	-7.27	-6.86	-8.79	-8.69	-8.80	-7.45	-8.49	-8.78	-8.51	-6.84	-4.43	-5.99	-5.40
Feb	6.75	7.67	6.43	7.35	6.09	6.90	8.15	7.26	5.84	5.79	7.73	9.35	6.97	7.73	7.20	8.01	0.31	6.21	0.29
Mar	6.01	5.37	11.53	13.03	9.21	6.31	6.06	6.13	10.89	12.34	7.25	6.16	7.64	7.77	7.61	5.88	3.83	4.06	1.07
Apr	-2.37	-1.81	-0.07	0.33	-0.85	-1.79	-2.27	-2.27	1.75	2.93	-2.46	-3.37	0.09	-2.22	-1.64	-3.89	-3.19	-3.39	5.28
May	7.00	7.02	7.40	6.67	7.24	5.11	5.90	5.08	6.64	6.01	5.82	5.45	6.13	5.62	5.04	4.31	6.92	5.28	6.90
Jun	9.82	8.43	9.85	10.73	8.90	10.79	8.29	10.07	10.04	11.47	7.81	8.22	7.96	7.75	7.69	7.78	9.58	7.57	7.68
Jul	5.59	5.95	5.92	5.85	5.60	5.38	5.49	4.71	5.43	5.25	4.12	4.27	5.22	4.45	4.91	4.43	4.50	4.35	3.99
Aug	5.23	4.42	5.52	5.14	5.84	4.43	4.24	3.76	5.90	5.23	4.76	5.40	5.46	4.60	4.96	5.96	4.69	5.84	5.48
Sep	4.91	5.26	6.73	7.03	6.07	5.34	4.31	5.38	7.59	7.21	6.36	5.99	7.49	6.71	7.19	7.80	5.81	7.35	6.75
Oct	5.61	5.54	6.08	5.47	4.87	5.57	5.34	4.64	5.32	4.94	4.34	3.77	4.92	4.42	4.65	4.08	4.90	3.56	4.19
Nov	-4.00	-3.47	-7.31	-7.95	-3.51	-0.81	-1.83	0.10	-2.87	-5.56	-0.71	0.31	-1.36	-0.60	-0.62	2.96	3.39	3.59	4.64
Dec	-4.95	-5.14	-5.90	-5.91	-7.10	-0.80	-4.07	-0.87	-6.16	-6.00	-5.65	-4.78	-5.67	-5.58	-5.63	-5.80	-1.45	-5.15	-2.34
Ann	5.62	5.37	6.36	6.43	5.89	5.84	5.11	5.33	6.46	6.44	5.00	5.15	5.73	5.11	5.32	5.43	5.50	5.33	5.55

Monthly Rainfall: (40 GCM Ensemble) 10% low percentile rainfall, Normalized GCM* Value (% mm)

Month	Sha	Cha	Nar	Jes	Gop	Fen	Lak	Noai	Kh	Sat	Bar	Bho	Bag	Jha	Piro	Pat	Chi	Bar	Cox
GCM*	6.72	7.21	4.82	4.48	5.76	8.75	7.64	7.95	5.27	4.27	7.05	7.75	5.91	6.78	6.36	7.14	9.25	6.77	9.48
Jan	-27.71	-28.28	-27.45	-27.78	-27.08	-28.09	-28.35	-28.82	-27.27	-26.92	-28.12	-28.76	-27.17	-27.95	-27.72	-28.89	-28.02	-29.03	-27.19
Feb	-12.23	-11.78	-12.38	-12.27	-11.54	-10.85	-11.09	-10.99	-12.68	-9.76	-13.62	-11.44	-11.00	-13.05	-10.20	-12.50	-19.46	-13.97	-24.02
Mar	-15.80	-16.08	-16.69	-17.99	-16.12	-17.03	-17.14	-17.47	-16.92	-18.59	-17.81	-18.03	-17.70	-17.99	-18.18	-19.22	-16.58	-20.13	-17.40
Apr	-21.77	-20.19	-24.44	-25.23	-23.03	-19.16	-20.08	-19.13	-23.19	-24.56	-20.45	-19.58	-21.49	-20.64	-20.40	-20.15	-15.31	-21.56	-16.80
May	-18.85	-17.64	-18.03	-17.00	-17.99	-14.79	-18.16	-16.30	-19.20	-19.75	-20.55	-18.81	-19.14	-20.63	-20.21	-22.27	-15.98	-23.10	-16.60
Jun	-6.41	-5.41	-5.37	-7.58	-4.83	-4.10	-5.61	-4.92	-7.11	-5.47	-6.36	-6.17	-6.63	-6.51	-6.07	-6.34	-3.10	-6.67	-5.41
Jul	-2.02	-3.17	-3.43	-4.05	-2.98	-3.45	-3.29	-3.46	-3.41	-4.49	-3.77	-3.92	-3.17	-3.65	-3.26	-4.63	-3.82	-4.63	-6.10
Aug	-2.67	-3.00	-3.34	-2.50	-2.55	-3.30	-2.14	-1.33	-2.33	-1.66	-0.22	-0.84	-2.18	-0.26	-0.48	-0.78	-2.51	-0.60	-1.93
Sep	-5.69	-5.20	-4.23	-3.61	-4.49	-5.10	-4.24	-4.03	-4.38	-3.99	-4.54	-4.44	-4.21	-4.53	-4.15	-4.26	-1.79	-4.27	-2.79
Oct	-10.70	-12.48	-10.65	-11.62	-9.06	-10.72	-12.52	-11.60	-8.84	-12.66	-9.92	-11.21	-8.30	-9.29	-8.51	-8.56	-8.52	-9.25	-7.33
Nov	-24.36	-25.21	-23.37	-23.78	-24.92	-24.01	-25.49	-24.07	-24.11	-24.00	-25.25	-24.28	-24.78	-25.19	-25.14	-26.19	-25.98	-26.90	-26.75
Dec	-26.02	-28.13	-23.58	-24.14	-23.65	-29.77	-31.04	-31.45	-22.98	-25.22	-30.79	-33.03	-24.63	-29.15	-26.96	-31.21	-26.71	-29.20	-24.55
Ann	-8.49	-8.25	-8.20	-8.32	-7.79	-6.97	-7.64	-6.62	-8.11	-7.51	-7.78	-7.76	-7.68	-7.67	-7.27	-7.65	-5.90	-7.72	-6.51

Monthly Rainfall: (40 GCM Ensemble) 90% high percentile rainfall, Normalized GCM* Value (% mm)

Month	Sha	Cha	Nar	Jes	Gop	Fen	Lak	Noai	Kh	Sat	Bar	Bho	Bag	Jha	Piro	Pat	Chi	Bar	Cox
GCM*	6.72	7.21	4.82	4.48	5.76	8.75	7.64	7.95	5.27	4.27	7.05	7.75	5.91	6.78	6.36	7.14	9.25	6.77	9.48
Jan	15.82	15.87	23.27	26.74	21.42	17.19	18.73	19.29	26.86	29.72	23.66	22.67	27.22	26.02	27.68	26.34	19.44	25.69	28.59
Feb	33.31	33.94	41.33	46.99	37.30	34.65	31.43	32.63	39.41	45.49	33.64	32.04	37.26	34.59	35.70	33.00	29.61	33.38	36.86
Mar	48.07	52.42	43.01	41.87	48.33	61.59	55.12	57.37	51.24	46.57	56.77	58.83	55.27	56.82	57.59	60.83	51.46	63.20	43.74
Apr	27.15	25.97	25.24	25.80	26.36	26.22	25.74	27.17	29.39	32.80	27.10	26.94	32.37	28.95	31.28	28.28	22.34	28.51	37.36
May	20.50	19.06	25.15	27.23	27.02	18.35	19.83	19.65	29.48	32.88	25.16	24.05	28.49	26.34	27.71	28.32	22.32	30.33	28.61
Jun	30.72	30.16	35.06	39.13	33.36	30.44	28.47	28.09	34.40	37.90	29.90	28.93	33.53	31.51	32.76	31.19	25.21	29.93	21.61
Jul	13.19	12.59	20.02	22.75	15.80	15.43	13.57	14.86	17.90	21.27	15.03	15.15	16.54	15.77	16.68	18.38	18.46	20.42	19.45
Aug	15.69	16.59	16.19	14.72	17.43	16.12	17.93	17.35	15.08	14.99	17.60	18.89	15.80	18.21	16.63	18.10	16.13	16.59	18.68
Sep	16.48	16.60	15.57	14.96	15.36	16.72	16.33	16.87	15.86	16.72	15.94	16.79	15.31	16.08	17.58	20.38	18.01	22.96	19.74
Oct	28.55	29.30	24.84	24.33	27.31	32.00	31.64	32.30	27.45	24.28	31.26	30.59	30.21	31.64	32.04	36.03	35.94	36.50	28.46
Nov	38.56	41.56	33.45	31.17	35.45	43.32	42.13	41.99	34.20	32.85	39.39	39.61	36.20	38.28	35.28	35.48	33.11	37.27	24.40
Dec	33.25	36.42	48.77	59.24	44.65	45.25	34.49	39.08	57.19	75.65	33.41	33.34	52.56	39.13	47.09	35.45	41.31	41.40	53.67
Ann	21.90	21.52	24.05	25.09	23.71	22.55	21.70	21.82	24.32	24.99	23.11	23.05	24.21	23.92	24.48	25.14	22.11	25.57	22.00

Data Inventory of Minimum Temperature, Maximum Temperature, Mean Temperature and Rainfall (Available Data)

Station Name	Available Year	Year Gap	Total Year	Month Gap (First Two Digit Year*)	Missing Monthly Data (***)	Missing Rainy Days
Dhaka	1953-2014	-	-	*66(3), 71(1), 73(1)	***	Same as Month Gap
Tangail	1987-2014	-	-	-	-	"
Mymensingh	1948-2014	1949	1	66(1), 69(1), 71(7), 73(5), 74(4)	***	"
Faridpur	1948-2014	-	-	65(1), 71(4)	***	"
Madaripur	1977-2014	1979	-	81(5)	***	"
Srimangal	1948-2014	1960-61, 1981	3	48(1), 54(1), 65(1), 71(3), 72(1), 74(2), 75(2), 76(4), 77(1), 78(2), 84(1), 85(3)	***	"
Sylhet	1956-2014	1973	1	56(1), 61(2), 66(3), 71(2), 75(2), 79(1)	***	"
Bogra	1948-2014	-	-	48(2), 49(3), 64(1), 71(3), 77(6), 78(3)	***	"
Dinajpur	1948-2014	1973-80	8	52(1), 71(4), 72(2)	***	"
Ishurdi	1961-2014	-	-	61(2), 67(7), 71(9), 72(1), 78(1)	***	"
Rajshahi	1964-2014	1969-70	2	71(2)	***	"
Rangpur	1954-2014	1968,1974	2	58(6), 71(3), 72(1), 77(3), 81(3)	***	"
Sydpur	1991-2014	-	-	-	-	"
Chuadanga	1989-2014	-	-	-	-	"
Jessore	1948-2014	1978	1	48(8), 71(6)	***	"
Khulna	1948-2014	1956, 1967, 1975	3	62(1), 63(1), 66(4), 72(6), 73(5), 74(1), 77(2), 83(1)	***	"
Mongla	1991-2014	-	-	-	-	"
Satkhira	1948-2014	1955	1	52(1), 65(1), 67(7), 69(1), 70(1), 71(2), 72(2), 73(2), 74(1), 75(1), 76(1), 80(1)	***	"
Barisal	1949-2014	1952, 1955	2	58(1), 75(3)		"
Bhola	1966-2014	-	-	73(3)	***	"
Khepupara	1974-2014	-	-	79(3), 82(1), 83(1), 88(1)	***	"
Patuakhali	1973-2014	1974, 1980	2	73(7), 76(7), 77(1), 79(2)	***	"
Chandpur	1964-2014	1965, 1971-72, 1978, 1980	5	64(1), 76(1), 77(4), 79(1)	***	"
Ambagan (Ctg)	1999-2014	-	-	-	-	"
Chittagong	1949-2014	2004-07	4	66(1), 68(1), 71(1), 72(2), 76(1), 81(1), 91(1)	***	"
Comilla	1948-2014	1963, 1978	2	67(1), 68(1), 70(1), 71()2	***	"
Cox's Bazar	1948-2014	-	-	49(2), 71(1), 78(1), 79(1), 80(2)	***	"
Feni	1973-2014	-	-	73(10), 74(4), 83(1), 05(1)	***	"
Hatiya	1966-2014	1972, 1981, 1995-98	6	70(3), 71(8), 73(4), 83(1), 94(4)	***	"

Note: Table Continued………

Station Name	Available Year	Year Gap	Total Year	Month Gap (First Two Digit Year*)	Missing Monthly Data (***)	Missing Rainy Days
Kutubdia	1977-2014	1978, 1981-84	5	-	***	“
M.Court	1952-2014	1976-77	2	51(8), 63(1), 66(1), 71(1), 72(2), 78(8), 95(1)	***	“
Rangamati	1957-2014	1967-68	2	74(2), 81(3)	***	“
Sandwip	1966-2014	1975, 2003	2	66(4), 69(1), 91(1), 02(4)	***	“
Sitakunda	1977-2014	-	-	77(4)	***	“
Teknaf	1977-2014	-	-	83(1)	***	“

Missing Months of Minimum Temperature, Maximum Temperature, Mean Temperature and Rainfall

Stations	Year	Month ID	Month
Barisal	1958	3	March
Barisal	1975	3	March
Barisal	1975	4	April
Barisal	1975	9	September
Bhola	1973	6	June
Bhola	1973	9	September
Bhola	1973	10	October
Bogra	1978	11	November
Bogra	1978	12	December
Bogra	1948	1	January
Bogra	1948	6	June
Bogra	1949	5	May
Bogra	1949	6	June
Bogra	1949	9	September
Bogra	1964	5	May
Bogra	1971	4	April
Bogra	1971	5	May
Bogra	1971	6	June
Bogra	1977	1	January
Bogra	1977	2	February
Bogra	1977	3	March
Bogra	1977	4	April
Bogra	1977	5	May
Bogra	1977	6	June
Bogra	1978	2	February
Chandpur	1964	5	May
Chandpur	1976	8	August
Chandpur	1977	4	April
Chandpur	1977	5	May
Chandpur	1977	6	June
Chandpur	1977	7	July
Chandpur	1979	8	August
Chittagong	1966	4	April
Chittagong	1968	12	December
Chittagong	1971	11	November
Chittagong	1972	1	January
Chittagong	1972	9	September
Chittagong	1976	7	July
Chittagong	1981	12	December
Chittagong	1991	4	April
Chuadanga	1989	11	November
Feni	1979	9	September

Stations	Year	Month ID	Month
Comilla	1967	1	January
Comilla	1968	12	December
Comilla	1970	12	December
Comilla	1971	4	April
Comilla	1971	12	December
Cox's Bazar	1949	1	January
Cox's Bazar	1949	2	February
Cox's Bazar	1971	12	December
Cox's Bazar	1978	12	December
Cox's Bazar	1979	11	November
Cox's Bazar	1980	9	September
Cox's Bazar	1980	10	October
Dhaka	1966	1	January
Dhaka	1966	2	February
Dhaka	1966	3	March
Dhaka	1971	12	December
Dhaka	1973	7	July
Dinajpur	1952	3	March
Dinajpur	1971	4	April
Dinajpur	1971	5	May
Dinajpur	1971	6	June
Dinajpur	1971	7	July
Dinajpur	1972	4	April
Dinajpur	1972	5	May
Faridpur	1971	3	March
Faridpur	1971	4	April
Faridpur	1971	5	May
Faridpur	1971	6	June
Faridpur	1965	8	August
Feni	1973	1	January
Feni	1973	2	February
Feni	1973	3	March
Feni	1973	4	April
Feni	1973	5	May
Feni	1973	6	June
Feni	1973	7	July
Feni	1973	8	August
Feni	1973	9	September
Feni	1973	10	October
Feni	1979	7	July
Feni	1979	8	August
Ishurdi	1978	8	August

Stations	Year	Month ID	Month
Feni	1979	10	October
Feni	1983	7	July
Feni	2005	3	March
Hatiya	1970	1	January
Hatiya	1970	11	November
Hatiya	1970	12	December
Hatiya	1971	1	January
Hatiya	1971	2	February
Hatiya	1971	3	March
Hatiya	1971	4	April
Hatiya	1971	5	May
Hatiya	1971	10	October
Hatiya	1971	11	November
Hatiya	1971	12	December
Hatiya	1973	1	January
Hatiya	1973	2	February
Hatiya	1973	3	March
Hatiya	1973	4	April
Hatiya	1983	7	July
Hatiya	1994	9	September
Hatiya	1994	10	October
Hatiya	1994	11	November
Hatiya	1994	12	December
Ishurdi	1961	1	January
Ishurdi	1961	2	February
Ishurdi	1967	1	January
Ishurdi	1967	2	February
Ishurdi	1967	4	April
Ishurdi	1967	5	May
Ishurdi	1967	6	June
Ishurdi	1967	9	September
Ishurdi	1967	12	December
Ishurdi	1971	2	February
Ishurdi	1971	3	March
Ishurdi	1971	4	April
Ishurdi	1971	5	May
Ishurdi	1971	6	June
Ishurdi	1971	9	September
Ishurdi	1971	10	October
Ishurdi	1971	11	November
Ishurdi	1971	12	December
Ishurdi	1972	1	January
M.Court	1995	1	January

Stations	Year	Month ID	Month
Jessore	1948	4	April
Jessore	1948	5	May
Jessore	1948	6	June
Jessore	1948	7	July
Jessore	1948	10	October
Jessore	1971	3	March
Jessore	1971	4	April
Jessore	1971	5	May
Jessore	1971	10	October
Jessore	1971	11	November
Jessore	1971	12	December
Jessore	1948	1	January
Jessore	1948	2	February
Jessore	1948	3	March
Khepupara	1979	10	October
Khepupara	1979	11	November
Khepupara	1979	12	December
Khepupara	1982	12	December
Khepupara	1983	7	July
Khepupara	1988	6	June
Khulna	1962	7	July
Khulna	1963	3	March
Khulna	1966	9	September
Khulna	1966	10	October
Khulna	1966	11	November
Khulna	1966	12	December
Khulna	1972	6	June
Khulna	1972	8	August
Khulna	1972	9	September
Khulna	1972	10	October
Khulna	1972	11	November
Khulna	1972	12	December
Khulna	1973	1	January
Khulna	1973	2	February
Khulna	1973	3	March
Khulna	1973	10	October
Khulna	1973	11	November
Khulna	1974	1	January
Khulna	1977	7	July
Khulna	1977	10	October
Khulna	1983	7	July
M.Court	1978	12	December
Patuakhali	1973	6	June

Stations	Year	Month ID	Month
M.Court	1951	1	January
M.Court	1951	2	February
M.Court	1951	3	March
M.Court	1951	4	April
M.Court	1951	5	May
M.Court	1951	6	June
M.Court	1951	7	July
M.Court	1951	11	November
M.Court	1963	9	September
M.Court	1966	8	August
M.Court	1971	4	April
M.Court	1972	1	January
M.Court	1978	1	January
M.Court	1978	2	February
M.Court	1978	7	July
M.Court	1978	8	August
M.Court	1978	9	September
M.Court	1978	10	October
M.Court	1978	11	November
Madaripur	1981	8	August
Madaripur	1981	9	September
Madaripur	1981	10	October
Madaripur	1981	11	November
Madaripur	1981	12	December
Mymensingh	1966	2	February
Mymensingh	1969	6	June
Mymensingh	1971	1	January
Mymensingh	1971	2	February
Mymensingh	1971	3	March
Mymensingh	1971	4	April
Mymensingh	1971	5	May
Mymensingh	1971	6	June
Mymensingh	1971	7	July
Mymensingh	1973	3	March
Mymensingh	1973	9	September
Mymensingh	1973	10	October
Mymensingh	1973	11	November
Mymensingh	1973	12	December
Mymensingh	1974	5	May
Mymensingh	1974	6	June
Mymensingh	1974	11	November
Mymensingh	1974	12	December
Sandwip	1966	4	April

Stations	Year	Month ID	Month
Patuakhali	1973	7	July
Patuakhali	1976	6	June
Patuakhali	1976	7	July
Patuakhali	1976	8	August
Patuakhali	1976	9	September
Patuakhali	1976	10	October
Patuakhali	1976	12	December
Patuakhali	1977	9	September
Patuakhali	1979	4	April
Patuakhali	1979	5	May
Patuakhali	1973	1	January
Patuakhali	1973	2	February
Patuakhali	1973	3	March
Patuakhali	1973	4	April
Patuakhali	1973	5	May
Patuakhali	1976	11	November
Rajshahi	1971	3	March
Rajshahi	1971	4	April
Rangamati	1974	4	April
Rangamati	1974	5	May
Rangamati	1981	1	January
Rangamati	1981	2	February
Rangamati	1981	3	March
Rangpur	1958	7	July
Rangpur	1958	8	August
Rangpur	1958	9	September
Rangpur	1958	10	October
Rangpur	1958	11	November
Rangpur	1958	12	December
Rangpur	1971	3	March
Rangpur	1971	4	April
Rangpur	1971	5	May
Rangpur	1972	8	August
Rangpur	1977	2	February
Rangpur	1977	3	March
Rangpur	1977	11	November
Rangpur	1981	7	July
Rangpur	1981	8	August
Rangpur	1981	9	September
Sandwip	1966	1	January
Sandwip	1966	2	February
Sandwip	1966	3	March
Srimangal	1976	2	February

Stations	Year	Month ID	Month
Sandwip	1969	10	October
Sandwip	1991	4	April
Sandwip	2002	8	August
Sandwip	2002	9	September
Sandwip	2002	10	October
Sandwip	2002	11	November
Satkhira	1952	2	February
Satkhira	1965	5	May
Satkhira	1967	6	June
Satkhira	1967	7	July
Satkhira	1967	8	August
Satkhira	1967	9	September
Satkhira	1967	10	October
Satkhira	1967	11	November
Satkhira	1967	12	December
Satkhira	1969	3	March
Satkhira	1970	10	October
Satkhira	1971	4	April
Satkhira	1971	8	August
Satkhira	1972	9	September
Satkhira	1972	12	December
Satkhira	1973	1	January
Satkhira	1973	3	March
Satkhira	1974	1	January
Satkhira	1975	8	August
Satkhira	1976	6	June
Satkhira	1980	7	July
Sitakunda	1977	1	January
Sitakunda	1977	2	February
Sitakunda	1977	3	March
Sitakunda	1977	4	April
Srimangal	1948	8	August
Srimangal	1954	11	November
Srimangal	1965	9	September
Srimangal	1971	4	April
Srimangal	1971	5	May
Srimangal	1971	6	June
Srimangal	1972	6	June
Srimangal	1974	8	August
Srimangal	1974	9	September
Srimangal	1975	2	February
Srimangal	1975	8	August

Stations	Year	Month ID	Month
Srimangal	1976	3	March
Srimangal	1976	5	May
Srimangal	1976	11	November
Srimangal	1977	7	July
Srimangal	1978	2	February
Srimangal	1978	4	April
Srimangal	1984	1	January
Srimangal	1985	4	April
Srimangal	1985	5	May
Srimangal	1985	6	June
Sylhet	1956	1	January
Sylhet	1961	1	January
Sylhet	1961	2	February
Sylhet	1966	5	May
Sylhet	1966	11	November
Sylhet	1966	12	December
Sylhet	1971	4	April
Sylhet	1971	12	December
Sylhet	1975	6	June
Sylhet	1975	12	December
Sylhet	1979	1	January
Teknaf	1983	7	July